

GEOLOGICAL SURVEY OF WESTERN AUSTRALIA

BULLETIN 119

THE IRON FORMATIONS OF
THE PRECAMBRIAN
HAMERSLEY GROUP
WESTERN AUSTRALIA

WITH SPECIAL REFERENCE TO
THE ASSOCIATED CROCIDOLITE



1970

GEOLOGICAL SURVEY OF WESTERN AUSTRALIA

BULLETIN 119

THE IRON FORMATIONS OF THE PRECAMBRIAN HAMERSLEY GROUP WESTERN AUSTRALIA

WITH SPECIAL REFERENCE TO
THE ASSOCIATED CROCIDOLITE

by

A. F. TRENDALL, B.Sc. (Hons.), Ph.D., A.R.C.S.
and J. G. BLOCKLEY, B.Sc. (Hons.)



1970

Issued under the authority of the Hon. A. F. GRIFFITH, M.L.C., Minister for Mines

(1)—64439

PREFATORY NOTE

Since exploration commenced in the Hamersley Iron Province of the North West of Western Australia, the Geological Survey has been active in unravelling the geology. All of the 1:250,000 geological sheets have been mapped and published and a Bulletin (No. 117) has been issued describing the general geology and the nature of the iron ores of the Province.

After the completion of the above regional studies, the Australian Blue Asbestos Company, which was then operating the crocidolite mine at Wittenoom, requested the Survey in 1964 to investigate the geological controls of crocidolite growth with a view to forecasting occurrences where there is no surface indication. An effort was to be made also to assess the economic potential of crocidolite in the Hamersley Iron Province. The Company suggested that five years were available to complete the study but unfortunately mining operations ceased at the end of 1966.

To pursue the objectives of this project it was found necessary to carry out a detailed structural and petrological investigation of the iron formations of the Hamersley Group in which the crocidolite occurs. In addition, large areas of this Group were mapped and examined in closer detail than in the initial regional survey.

The results of the work suggest that a better grade of crocidolite is not likely to be found, and the known occurrences cannot be developed until economic conditions alter. Nevertheless the geological information gained from these studies will be of great interest to both economic and academic workers in many fields and should stimulate further research throughout the world into many facets of this interesting Group.

The format of the Bulletins of the Geological Survey has remained unchanged for many years. It has now been modernised and we hope that the new form presented here will be found more acceptable to the reader.

22nd August, 1969.

J. H. LORD,
Director.

CONTENTS

SUMMARY	Page 15
CHAPTER 1. INTRODUCTION	
Purposes, scope and progress of study	19
Arrangement of this Bulletin	19
Location, communication, industries, settlement and services	20
Physiography	22
Climate and vegetation ..	24
Water supply	24
Nomenclature	25
Previous work	27
Acknowledgements	28
CHAPTER 2. OUTLINE OF REGIONAL GEOLOGY	
General	30
Evidence for age	31
Regional geology of the Hamersley Group	31
Regional extent, correlations and continuity	31
The Fortescue Group in relation to the Hamersley Group	33
The Wyloo Group in relation to the Hamersley Group	33
Structure ..	34
CHAPTER 3. HAMERSLEY GROUP STRATIGRAPHY	
Formal stratigraphic nomenclature in relation to sedimentation	36
Note on order of description	41
Brockman Iron Formation	41
Dales Gorge Member	41
Definition and type section	41
Lithology	43
Scales of banding	43
Mesoband classification, thicknesses and abundance in BIF macrobands	44
Further classification of chert mesobands	51
Mesoband sequence in BIF macrobands: the Calamina cyclothem	55
Reassessment of chert mesoband classification	60
Field assessment of BIF lithology	61
Macrobands S1-16	61

	Page
Lateral stratigraphic continuity	65
General statement	65
Macrobands and mesobands	66
Thickness variation	68
Topographic expression	72
Whaleback Shale Member	72
Previous references	72
Definition and type section	73
Lithology	73
Lateral stratigraphic continuity and thickness variation	74
Topographic expression	74
Joffre Member	75
Previous references	75
Definition and type section	75
Lithology	75
General description	75
Mesoband sequence: the Knox Cyclothem and other regularity	78
Lateral stratigraphic continuity and thickness variation	80
Topographic expression	80
Yandicoogina Shale Member	80
Marra Mamba Iron Formation	82
Definition and type area	82
Lithology	82
Subdivision	83
Lateral stratigraphic continuity	84
Thickness variation	84
Topographic expression	84
Wittenoom Dolomite	85
Mount Sylvia Formation	86
Mount McRae Shale	86
Definition and type section	86
Subdivision	87
Lithology	88
Lateral stratigraphic continuity	88
Thickness variation	88
Topographic expression	89
Weeli Wolli Formation	89
Redefinition	89
Lithology	90
Lateral stratigraphic continuity and thickness variation	91
Topographic expression	92
Woongarra Volcanics	92
Boolgeeda Iron Formation	93

CHAPTER 4. PETROGRAPHY AND MINERALOGY OF THE IRON FORMATION

	Page
Introduction	94
Petrography of the main mesoband types	94
Microbanded chert	94
Definition and characteristics of microbanding	94
Textural and compositional variation	95
Multiple microband grouping	100
Marginal and internal microband relationships	102
Lateral continuity of microbanding	106
Non-microbanded chert	108
Chert-matrix	108
Magnetite	108
Stilpnomelane	109
Carbonate	109
Miscellaneous	110
Iron formation without mesobanding ..	110
Petrography of S macrobands of the Dales Gorge Member and some related rocks	111
Shale	111
Chert-siderite	115
Mineralogy	117
Quartz	117
Carbonate minerals	118
Hematite	121
Magnetite	123
Sheet silicates	124
Apatite	125
Pyrite	125
Feldspar	127
Carbon	127
Barite	127
Notes on paragenetic evidence	127
Introduction	127
Notes	129

CHAPTER 5. CHEMICAL COMPOSITION OF THE IRON FORMATION

General	133
Analyses of iron formation (Table 11)	133
Complete analyses of individual mesobands from the Dales Gorge Member of the Brockman Iron Formation (Table 12)	138
Partial analyses of individual chert mesobands from the Dales Gorge Member of the Brockman Iron Formation (Table 13) ..	144
Analyses of riebeckite (including crocidolite) (Table 14)	147
Analyses of shales (Table 15)	147
Miscellaneous analyses directed mainly towards mineral identification (Table 16)	150

CHAPTER 6. STRUCTURES IN THE IRON FORMATION		Page
Introduction	153
Chert podding, and related structures	..	153
Definitions and classification	153
Random podding	154
Cross-podding and related types	..	155
Other types of podding	158
Petrography of pods: concentric and septarian structure	158
Small spheroidal nodules	..	159
Macules	160
Pseudofossils	162
Northeast and duplicate structures: regional orientation	162
Regional rippling	164
Slumping and related collapse structures	167
Minor folds with fibrous minerals in the north	169
Minor folding in the south	172
Vertical veins	172

CHAPTER 7. RIEBECKITE (INCLUDING CROCIDOLITE) IN THE IRON FORMATIONS		
Introduction	174
Forms of riebeckite occurrence	174
Vertical and lateral stratigraphic distribution of the two main forms of riebeckite		175
General note	175
Vertical distribution of riebeckite	176
Total riebeckite: riebeckite zones	176
Massive riebeckite	178
Crocidolite: crocidolite seams and horizons	183
Definition, nomenclature and stratigraphic relationship	183
Marra Mamba Riebeckite Zone	185
Vivash Riebeckite Zone	186
Yampire Riebeckite Zone	186
Junction Gorge Riebeckite Zone	187
Yandicoogina Crocidolite Horizon	188
Lateral distribution of riebeckite	188
Massive riebeckite	188
Crocidolite	189
Regional distribution: provinces and sub-provinces	189
Local distribution: enrichments and deposits	..	190
Distributional inter-relationship between the two main forms of riebeckite and other stratigraphic features	191
Petrography and textural relationships of riebeckite forms	192
Massive riebeckite	..	192
Spatial relationship to iron formation	192
Petrography	195
Crocidolite	..	196
Spatial relationship to iron formation	196
Structural petrography	199

	Page
Minor concordant forms of riebeckite	207
Acicular riebeckite	207
Forms gradational to massive riebeckite	209
Other riebeckite forms	210
Cross-cutting occurrences of riebeckite	211
Slip-fibre riebeckite	211
Regional orientation of structures in crocidolite and other fibrous forms	212
Details of crocidolite deposits ..	212
Assay methods	212
Description of deposits	213
Wittenoom Sub-Province	213
Wittenoom Gorge	213
Yampire Gorge ..	220
Dales Gorge	226
Bee Gorge	229
Range Gorge	229
Calamina Gorge	230
Asbestos Gorge ..	230
Miller's Gorge	231
Junction Gorge ..	231
Coondiner Gorge	233
Marillana prospect	234
Lamb Creek	234
Minor occurrences	235
Marra Mamba Sub-Province	237
Marra Mamba deposits ..	237
Kungarra Gorge prospect	239
Vivash Gorge deposits ..	241
Other occurrences in the Marra Mamba Sub-Province	241
Crocidolite occurrences outside the two sub-provinces	243
Jimmawurrada Creek	243
Mt. Nicholson	243
Fish Pool	243
Juna Downs	243
Summary of relationship between crocidolite and structure	243

CHAPTER 8. CROCIDOLITE MINING IN WESTERN AUSTRALIA

History of mining	245
Mining methods ..	248
Surface mining methods	250
Underground mining methods	251
Health hazards ..	254

CHAPTER 9. ORIGIN OF THE IRON FORMATION

Introduction	255
Review of the problems ..	255
Significance of microbands	257
Relationship of mesoband types: the basic hypothesis	257

	Page
Significance of mesobanding	259
Iron/silica relationship in the basic hypothesis	263
The control of compaction	265
Physical state of the precipitate	266
Chemical composition and evolution of the precipitate: a modified hypothesis	268
Mineralogy of diagenesis	272
Derivation of the iron	273
Significance of chert-siderite	276
Summary	276

CHAPTER 10. DEVELOPMENT OF THE HAMERSLEY BASIN

The beginning of the basin	278
Depositional environment of the Hamersley Group ..	279
Thickness control of iron formation	279
Size, shape, and structure of the basin	280
Depth, circulation, and iron content of the water	282
Possibility of an algal raft	283
Was the basin closed or open?	284
Vulcanicity	285
Conditions on the surrounding land	286
Composition of the atmosphere	287
Controls of stratigraphy	287
Post-depositional effects of basin development	292
Early structures in the iron formation	292
Thermal history of the Hamersley Group	294
The end of the basin	294
Material balance in the basin	295
Sinking rate and time span of the basin	298

CHAPTER 11. ORIGIN OF RIEBECKITE (INCLUDING CROCIDOLITE) IN THE IRON FORMATIONS

Review of the problems	299
Massive riebeckite	299
Basic argument for genetic process	299
Evidence from time relationships	300
Chemical evidence	303
Distributional controls	304
Crocidolite	307
Basic argument for genetic process	307
Chemical evidence for iron derivation	309
Evidence for time relationships	310
The stress-reversal hypothesis for crocidolite growth	310
Distributional controls	313
Some consequences of the hypotheses proposed	317
Application of the hypotheses outside the Wittenoom Sub-Province	319
Comparison with South African crocidolite occurrence	320

CHAPTER 12. ECONOMIC APPLICATIONS OF THIS STUDY										Page
Exploration	323
Principles	323
Exploration of new areas	325
Exploration in areas with known deposits	325
Areas recommended for further exploration	326
Evaluation of deposits	328
Methods	329
Reliability of diamond drilling results	329
Crocidolite resources	334
GLOSSARY										334
LIST OF UNPUBLISHED PLANS										339
REFERENCES										342
INDEX										347

PLATES

Plate	Facing page
1. Regional geological map showing setting of the Mount Bruce Supergroup. Scale 1:6,000,000	30
2. Regional geological map of the Hamersley Group. Scale 1:2,500,000	38
3. Isopach map of the Dales Gorge Member, showing minor structures within the Hamersley Group and outcrop of the Brockman Iron Formation. Scale 1:1,000,000	72
4. Geological map of the Hamersley Crocidolite Province. Scale 1:750,000	192
5. Geological map of main crocidolite-bearing area, Hamersley Range. Scale 1:200,000	212
6. Geological map of Wittenoom Gorge, showing structural contours and fibre concentrations. Scale 1:50,000	214
7. Plan of Colonial mine, showing fibre grades and structural contours of the Upper seam. Scale 1 inch to 600 feet	220
8. Plan of Yampire Gorge showing crocidolite workings. Scale: 1:25,000	224
9. Plan of Yampire mine area, showing localities of diamond drillholes, structural contours and fibre enrichments. Scale 1:8,000	226
10. Geological map of Junction Gorge, showing outcrop of Aspinall Seam. Scale 1:40,000	232
11. Geological plan, Marra Mamba crocidolite area. Scale 1:50,000	238
12. Geological map, Kungarra Gorge area. Scale 1:60,000	240

FIGURES

Figure	Page
1. Photograph of Dales Gorge, showing physiographic features of the Hamers- ley Range	23
2. Comparative stratigraphic columns of the Mount Bruce Supergroup in different parts of the Hamersley Range area	32
3. Stratigraphic columns, to scale, of the Hamersley Group and the Dales Gorge Member of the Brockman Iron Formation	37
4. Photograph showing the macrobands of the Dales Gorge Member at Wittenoom Gorge	42
5. Photograph of part of the type section of the Dales Gorge Member (Plate 29 of original description)	45
6. Photograph of part of the type section of the Dales Gorge Member (Plate 35 of original description)	46
7. Photograph of 3 pieces of core from the type section of the Dales Gorge Member, illustrating features of chert mesobands	48

Figure	Page
8. A. T plotted against t for 34 nominal primitive and 121 nominal flat-modified cherts.	
B. T plotted against t for 145 unclassified cherts	51
9. T frequency distribution for 300 microbanded chert mesobands of the Dales Gorge Member	53
10. t frequency distribution for 300 microbanded chert mesobands of the Dales Gorge Member	54
11. n frequency distribution for 300 microbanded chert mesobands of the Dales Gorge Member	55
12. n frequency distribution for two groups of microbanded chert mesobands arbitrarily divided by t	56
13. Photographs showing different expressions of the Calamina cyclothem in the Dales Gorge Member	57
14. Comparative lithology within macrobands S1-S16 of the Dales Gorge Member	63
15. Photographs showing lateral mesoband correlation in selected cherts within the BIF0 macroband of the Dales Gorge Member	67
16. Isopach map of the lowermost part of the Dales Gorge Member in the central part of the Hamersley Range area	71
17. Isopach map of the middle part of the Dales Gorge Member in the central part of the Hamersley Range area	71
18. Isopach map of the uppermost part of the Dales Gorge Member in the central part of the Hamersley Range area	72
19. Photographs showing the field expression of various kinds of cyclicity in the Brockman Iron Formation	77
20. Photography showing the characteristic topographic expression of the lower and central parts of the Hamersley Group	81
21. Photomicrographs showing microband textures typical of coarsely and finely microbanded cherts	96
22. Photomicrographs showing typical microbanding in chert of chert-siderite in the Dales Gorge Member and in the Whaleback Shale Member	97
23. Photomicrographs of microbanded cherts from the Joffre Member and from the Boolgeeda Iron Formation	98
24. Photographs showing microbanded cherts from the Dales Gorge Member and Woongarra Volcanics	100
25. Photomicrographs showing microbanding in the striped facies of the Weeli Wolli Formation	101
26. Photomicrographs showing microbanding in iron formation transitional between striped facies to mesoband iron formation	102
27. Photomicrographs showing continuity of microbands between chert pods and their adjacent chert-matrix	103
28. Photomicrographs showing continuity of microbanding between chert and chert-matrix	104
29. Photomicrographs showing behaviour of laminations within microbands at transitions from chert to chert-matrix, and other textures possibly related	105

Figure	Page
30. Photomicrographs illustrating correlation of microbrands using widely separated samples of the same chert mesoband	107
31. Photographs and photomicrographs showing selected petrographic features of Hamersley Group shales	113
32. Photomicrographs showing selected petrographic features of magnetite and carbonate occurrence in iron formations	116
33. Triangular diagram illustrating the calculated compositions of carbonate minerals in analysed samples of cherts and iron formation	119
34. Photomicrographs of cellular hematite in incident light	122
35. Photomicrographs of varied types of apatite occurrences in the Dales Gorge Member	126
36. Photomicrographs showing stilpnomelane pseudomorphs after carbonate, and post-carbonate compaction in the Dales Gorge Member	128
37. Photomicrograph showing selected paragenetic relationships in the Dales Gorge Member	130
38. Photographs showing random podding in the Dales Gorge Member	154
39. Photographs showing cross-podding in the Dales Gorge Member	156
40. Photomicrographs showing concentric textures in chert pods	159
41. Photomicrographs and photograph showing small spheroidal nodules in the Dales Gorge Member	160
42. Photographs of macules in the Dales Gorge Member	161
43. Photographs of regional rippling in the Dales Gorge Member	165
44. Photograph and photomicrographs of slump structures and related features in the Weeli Wolli Formation and the Dales Gorge Member	166
45. Photomicrographs showing stratigraphically restricted brecciation of microbanding in microbanded chert	168
46. Photographs of minor folds with fibrous quartz from Mt. Bruce	170
47. Photomicrographs of stress-reversal in regional rippling of the Dales Gorge Member	171
48. Stratigraphic columns of crocidolite-bearing parts of the Hamersley Group, with positions and nomenclature of crocidolite horizons and riebeckite zones	177
49. Distribution of massive riebeckite mesobands in BIF2 and BIF3 in 35 drillholes in the Wittenoom and Yampire areas	179
50. Histogram summarising the information in Figure 49	181
51. Comparison of massive riebeckite occurrence in the same three consecutive Calamina cyclothems of BIF2, transected in 9 different drillholes in the Wittenoom and Yampire areas	182
52. Stratigraphic columns about the main crocidolite horizons of the Marra Mamba and Brockman Iron Formations	184
53. Photograph showing riebeckite swells and associated structures at Dales Gorge	194
54. Photograph showing the lateral transition from iron formation to massive riebeckite at Dales Gorge	196
55. Photographs showing the typical occurrence of crocidolite in the Dales Gorge Member	197

Figure	Page
56. A. Photomicrograph of massive riebeckite. B. Photograph showing the typical surface structure of a crocidolite meso- band	201
57. Photographs illustrating details of a cone structure at the margin of a crocidolite mesoband	202
58. Photomicrographs of fibrous quartz at the edge of a crocidolite mesoband with kink bands	205
59. Photographs and photomicrographs of crocidolite folded after growth at Marra Mamba	206
60. Photomicrographs showing selected features of riebeckite petrography ..	208
61. Photomicrographs showing riebeckite relationships in chert mesobands ..	209
62. Vertical north-south cross-section showing geological structure of the Hamersley Range at Wittenoom	214
63. Scatter diagram showing grade relationship between vertically superimposed samples of the Upper Seam and Lower Seam in the Colonial mine at Wittenoom Gorge	218
64. Histogram showing distribution of assay values in the Upper Seam at the Colonial mine	219
65. Map of crocidolite workings at Dales Gorge	228
66. Map of crocidolite prospects at Junction Gorge	232
67. Sections through Kungarra Gorge crocidolite deposit	240
68. Photograph showing abandoned surface bench working of crocidolite at Snell Gorge	250
69. Photograph of the Colonial mine at Wittenoom Gorge	252
70. Cross-section of part of the Colonial mine, showing layout of workings ..	253
71. Diagram illustrating the possible cyclic climatic control of mesobanding ..	260
72. Graph showing iron/microband relationship in chert mesobands of the Dales Gorge Member	264
73. Diagram illustrating suggested movement of silica during diagenesis of iron formation	270
74. Diagrammatic cross-sections showing suggested relationship of the Hamersley Group and Wyloo Group deposition	296
75. Diagrammatic stratigraphic relationship of massive riebeckite and iron formation, and three theoretically possible sequences in its development ..	300
76. Diagram illustrating the stress-reversal hypothesis of crocidolite growth ..	311
77. Diagrams illustrating structural control of crocidolite growth	314
78. Diagrams showing theoretical inter-relationships of vertically superimposed crocidolite enrichments	318
79. Curves showing the chance of one drill-hole intersecting a value of less than some specified threshold grade in any seam averaging between 2 and 5 inches of crocidolite	331

TABLES

Table	Page
1. Proportions of lithological types in the Hamersley Group	39
2. Proportions of lithological types in the Hamersley Group: revised estimate for the eastern part of the Hamersley Range area	39
3. Comparative lithological proportions in the upper and lower parts of the Hamersley Group	40
4. Relative abundances, by mesoband numbers and total volume, mean thicknesses, and thickness ranges of mesoband types in BIF macrobands of the Dales Gorge Member	50
5. Means and ranges of thickness (T), microband thickness (t) and number of microbands (n) in 300 microbanded chert mesobands from the Dales Gorge Member, subjectively grouped	52
6. Type section footage limits and thicknesses in feet of conspicuous examples of the Calamina cyclothem	58
7. Type section footage limits and thicknesses in feet of less conspicuous expressions of the Calamina cyclothem	60
8. Summary of strength of expression of the Calamina cyclothem in the BIF macrobands of the Dales Gorge Member	62
9. Thickness variations in Dales Gorge Member macrobands	70
10. Comparison of calculated and measured carbonate proportions in ten chert mesobands of the Dales Gorge Member	120
11. Analyses of iron formation of the Hamersley Group	134
12. Complete analyses of individual mesoband types from the Dales Gorge Member of the Brockman Iron Formation	139-141
13. Partial analyses of individual chert mesobands from the Dales Gorge Member of the Brockman Iron Formation	143-145
14. Analyses of riebeckite (including crocidolite) from the Hamersley Group	146
15. Analyses of eleven shales from the Hamersley Group and one shale from the Fortescue Group	148
16. Miscellaneous analyses directed mainly towards mineral identification	151
17. Miscellaneous calculated compositions	152
18. Summary of results of diamond drilling in the Wittenoom Gorge area	221-223
19. Details of diamond drilling at Yampire Gorge	227
20. Annual production of crocidolite in Western Australia	248
21. Comparison of microband interval and total iron content of 22 chert mesobands of the Dales Gorge Member	265
22. Silica content per microband in some cherts and in chert-matrix	272
23. Total original metal and silicon content of Hamersley Group sediments, and comparison with equivalent content of average Precambrian crust	275
24. Primary control of various orders of stratification in Hamersley Group iron formations	291
25. Comparison of stratigraphically equivalent BIF and massive riebeckite	303
26. Chance of overlooking an ore body of average grade about 3.23 inches by ignoring single assays less than specified threshold values	331
27. Estimated Western Australian crocidolite reserves and resources	333

Summary

CHAPTER 1. This bulletin reports results of a 4-year study of Precambrian iron formations of the Hamersley Range area (roughly 22°—23°S and 116° 30'—119° 30'E). Much of the country of rough, semi-arid and sparsely inhabited, with population centred on a few important iron-mining towns. It is all covered by recent mapping (mainly published) at a scale of 1:250,000 by the Geological Survey. BIF is the preferred abbreviation of banded iron formation.

CHAPTER 2. The three constituent groups of the Mount Bruce Supergroup are (oldest first): Fortescue, Hamersley, and Wyloo. The Fortescue Group, with a maximum thickness of 14,000 feet, unconformably overlies Archaean (3,000 m.y.) rocks; it contains mainly basic lava and tuff, sandstone and shale. The conformably overlying Hamersley Group, about 8,000 feet thick, is characterised by abundant BIF; interstratified acid lava is 2,000 m.y. old. The Wyloo Group has mixed clastic sediments with locally important dolomite and basalt; it is up to 30,000 feet thick and locally discordant. In the northern part of the outcrop, dips are gentle and southward; the central part has broad open folding about east-west axes, while in the south, folding in the same direction steadily intensifies. The important Hamersley Range Synclinorium runs east-west for some 150 miles to define the Hamersley Range itself.

CHAPTER 3. The eight constituent formations of the Hamersley Group, with usual thicknesses in feet, are (oldest first): Marra Mamba Iron Formation (600), Wittenoom Dolomite (500), Mount Sylvia Formation (100), Mount McRae Shale (300), Brockman Iron Formation (2,000), Weeli Wolli Formation (1,500), Woongarra Volcanics (2,400) and Boolgeeda Iron Formation (700). The Brockman Iron Formation is further subdivided into four members: Dales Gorge Member (500), Whaleback Shale Member (200), Joffre Member (1,200), Yandicoogina Shale Member (200). Stratigraphic and petrographic attention has been concentrated on the Dales Gorge Member. It is divided into 33 numbered macrobands (BIF0-16 alternating with S1-16) which are up to 82 feet thick and recognisable in the field. They allow accurate regional thickness measurements; 31 such sections give an isopach map showing, with local complexity, an ovoid pattern over the existing outcrop area. Within the BIF macrobands there are mesobands, with an average thickness less than an inch, which consist of chert, chert-matrix (fine-grained quartz, carbonate, iron oxides), magnetite, stilpnomelane, carbonate and miscellaneous types; the first three make up over 90 per cent of the BIF. Most chert mesobands are internally laminated, or microbanded (Chapter 4), with a usual interval about 1 mm. At some levels, regular alternation over about 6 inches of chert mesobands with different microband intervals (among other characters) define the Calamina cyclothem. Macrobands and mesobands have basin-wide continuity. The BIF of the other four main levels (Marra Mamba IF, Joffre Member, Weeli Wolli Formation, Boolgeeda IF) is conveniently described by comparison with the Dales Gorge Member; each of these five main BIF levels of the Hamersley Group has individual and internally consistent characteristics which allow field recognition without reference to stratigraphic sequence.

CHAPTER 4. Microbanding within chert mesoband is defined by regularly alternating iron-rich and iron-poor laminae within a fine-grained (20 microns) quartz mosaic. The iron-bearing minerals involved are variously ankerite, hematite, magnetite and stilpnomelane.

Microbands vary in thickness from about 4 mm downwards, and show wide variety in textural and compositional detail. At the lateral terminations of chert pods (see Chapter 6) microbands pass continuously, but with thinning of about 7:1, into the enclosing chert-matrix. In parts of the Weeli Wolli Formation the iron formation is finely microbanded although not mesobanded. The microband interval increases and decreases systematically to define regular stripes. Microbanding within correlated chert mesobands has been correlated over 185 miles. The minerals in Hamersley Group BIF are: quartz, carbonate, hematite, magnetite, sheet silicates (riebeckite: Chapter 7), apatite, pyrite, feldspar, carbon and barite, in observed order of abundance. Ankerite, 'siderite', dolomite, and calcite all occur, and may be identified by analysis and staining; 'siderite' includes highly magnesian types. Stilpnomelane is the most abundant sheet silicate, and has a characteristic composition in each main IF unit.

CHAPTER 5. Sixty-seven new analyses (48 complete, 19 partial) are reported, consisting of: 12 of BIF, 19 complete of separate mesobands, 17 partial of separate mesobands, 2 of riebeckite, 12 of shale, and 7 miscellaneous. The calculated average composition of BIF from mesoband proportions is consistent with direct analysis. The total iron content of lithologically different BIF units varies little: it is 24 to 34 per cent.

CHAPTER 6. Although the banding (mesobanding) of BIF can mostly be considered as geometrically ideal planar layering, lateral discontinuity in chert mesobands defines several types of spatially confined chert body; these include random pods, cross-pods, small spheroidal nodules and macules. Cross-pods are linear structures consistently elongate in a northeast direction, and are one of a family of related structures which include duplicate corrugations, riebeckite swells, and cross-podding troughs and ridges. Slumping and other minor collapse structures are present, together with regional rippling, a persistent asymmetric puckering of banding surfaces with an east-west axial trend. On both the north and south sides of the Hamersley Range Synclinorium the axial planes of regional ripples dip north; small folds associated with fibrous mineral growth also found on both limbs of this synclinorium have their axial planes dipping inwards towards its central axis.

CHAPTER 7. Riebeckite occurs in Hamersley Group iron formation in two main forms: (1) massive riebeckite mesobands made up of a felted mass of interlocking fibres, and (2) crocidolite, the commercial blue asbestos, which occurs in discontinuous mesobands mainly $\frac{1}{2}$ to 2 inches thick with the fibres perfectly parallel and at a high angle to the plane of the banding. Minor riebeckite forms include slip-fibre, like crocidolite but in thinner bands, in which the fibres lie at a low angle to the banding. Riebeckite is confined to the Marra Mamba, Brockman and Boolgeeda Iron Formations, and abundant occurrence is restricted to four narrow *riebeckite zones*: The Marra Mamba and Vivash Riebeckite Zones of the Marra Mamba IF and the Yampire and Junction Gorge Riebeckite Zones of the Dales Gorge Member of the Brockman Iron Formation. Massive riebeckite is the most abundant riebeckite form in these zones; in any one area a zone *may not* contain riebeckite, but *if* riebeckite is locally present it is *always* within one or other of them. With one exception crocidolite is restricted between narrower limits within the riebeckite zones: these are the Mackay, Dun and Foxall Crocidolite Horizons of the Marra Mamba Riebeckite Zone, the Third Seam, Knapping Seam, Lower Seam, Upper Seam and Yampire C Crocidolite Horizons of the Yampire Riebeckite Zone, and the Yampire B, Aspinall and Yampire A Crocidolite Horizons of the Junction Gorge Riebeckite Zone. As with massive riebeckite, each of these horizons may or may *not* locally bear crocidolite; if mineable crocidolite is present the horizon locally forms a seam. There is a general, but not exact, association between the areal distribution of massive riebeckite and crocidolite. In the horizons of the Dales Gorge Member, crocidolite is largely restricted to the northern Hamersley Range, to define the Wittenoom Sub-Province of the Hamersley Crocidolite Province; in the Marra

Mamba IF, crocidolite is confined to the west-central Hamersley Range area to define the Marra Mamba Sub-Province. Massive riebeckite may pass laterally into groups of chert and magnetite mesobands with complete stratigraphic equivalence. Crocidolite mesobands pinch out laterally, and have no non-riebeckite stratigraphic equivalent. Summary accounts are given of all known crocidolite occurrences in the Hamersley Range area.

CHAPTER 8. Crocidolite was first reported from the Hamersley Range in 1908 but there was official reluctance to accept the report until 1930. Small-scale surface mining began in 1933 and continued sporadically until 1946. Underground mining at Wittenoom began in 1943 and continued until 1966, most crocidolite being won from the Upper Seam Horizon. A long-wall stoping method with stopes 7 feet high instead of the previously employed bord and pillar system with stopes 40 inches high is proposed should mining recommence. A total long tonnage of 152,467 tons was produced from the whole Hamersley Crocidolite Province.

CHAPTER 9. Microbands are believed to be annual seasonal varves. It is argued that mesobands of chert-matrix were initially varved like those of microbanded chert, but that extreme compaction has destroyed the varving and simultaneously increased the iron content of chert-matrix by expelling silica. Magnetite mesobands result from further progress of the same process. Mesobanding probably developed during diagenesis as the result of differential response to compaction of varve groups with slight (unknown) initial differences controlled by rhythmic environmental (climatic) changes. Neither the physical nor chemical state of the original precipitate is certain, but the bulk composition of existing BIF probably corresponds closely with that of the precipitate, except for such mobile constituents as H_2O , CO_2 and Na_2O . An estimate of the total weight of metals in the Hamersley Group makes their derivation without an appeal to a volcanic source virtually inconceivable.

CHAPTER 10. The name Hamersley Basin is here applied to the depositional basin of the Mount Bruce Supergroup. It began with gentle depression of an erosion surface cut across Archaean rocks over an ovoid area of about 100,000 square kilometres. Depression was initially erratic but later was greatest about a central east-west axis, with progressively less sinking towards the margins. During Fortescue Group time the resultant basin was filled largely by vulcanicity, and during Hamersley Group time by chemical precipitation of volcanically (fumarolically) derived iron and silica; much of the vulcanicity was probably along the western basin edge. During neither of these periods was there complementary elevation of adjacent crust to form high surrounding country. During BIF deposition water depth was probably 50 to 250 metres over most of the basin, with a shallower marginal shelf; there may have been connection with open ocean to the northwest. Iron content of the basin water was probably in the range 10 to 20 ppm. Currents were less than 1 metre/sec, and there was a desert climate, with high evaporation, and negligible run-off; the BIF is an evaporitic deposit. Many of the unusual chert structures (Chapter 6) were formed by stress due to continued sinking of the basin during diagenesis; the soft gelatinous precipitates were highly sensitive to the small slopes developed. Between the base of the Fortescue Group and the top of the Hamersley Group probably about 100 to 200 m.y. elapsed, with an average sinking rate about 4,000 years per foot. At the end of Hamersley Group time the basin was 'full' in the sense (of Dallmuis) that the basal unconformity of its infilling sediments was planar, not geoidal. Continuation of the (unknown) deep primary cause of depression led to the final deposition of the Wyloo Group in an arcuate trough in the south.

CHAPTER 11. Massive riebeckite developed, during diagenesis, from previously existing banded material which was the common parent of the riebeckite and its stratigraphically equivalent BIF. The slight chemical difference between the two is almost entirely in Na_2O .

Its distributional controls are largely conjectural, but no appeal to unusual temperatures is necessary. Crocidolite grew later by splitting and dilation of magnetite mesobands in BIF as a relief from balanced compression from two sides in particular structural situations, where gravitational sliding opposed 'tectonic' stress. This stress-reversal hypothesis is supported by small-scale evidence in minor structures. All the material for crocidolite growth was derived from adjacent BIF, not from previously existing riebeckite. Exact quantitative correlation of crocidolite with its controlling structure must be empirical; pure theory cannot forecast the existence of ore but can set limits on expected enrichment. Exceptional bonanzas of crocidolite in known areas are unlikely. The hypotheses put forward appear to apply to South African (Cape Province) crocidolite.

CHAPTER 12. Further surface discovery of crocidolite in the Hamersley Range area is most unlikely, and occurrences outside the described stratigraphic levels (Chapter 7) cannot be expected. Drilling for blind ore bodies away from known areas of crocidolite is not justified. Further exploration of several locations in previously known areas of crocidolite occurrence would be worthwhile if the relative selling price of blue asbestos increased or if the cost of mining, milling and transport were reduced by improved techniques. Drillhole intersection assays should be used with great caution. Indicated and inferred crocidolite reserves are just over 400,000 tons, with the largest known deposit containing 225,000 tons at an average grade of 2.8 inches. These reserves could be profitably worked only after a favourable change in the total economy of mining in the area.

CHAPTER 1

Introduction

PURPOSES, SCOPE, AND PROGRESS OF STUDY

This bulletin reports the results of an investigation of blue asbestos, or crocidolite, in the Hamersley Range area, in the northwestern part of Western Australia, which was carried out by the Geological Survey between 1964 and 1967. The study began with two main objectives:

1. to assess the economic potential of crocidolite deposits in the Hamersley area, and
2. to determine the geological controls of crocidolite growth, if possible with sufficient accuracy to enable the forecasting of crocidolite ore bodies where there is no surface indication.

It was evident at the start that the asbestos could not be studied in isolation from its iron formation host rock, and that a thorough study of the iron formation necessarily involved an examination of all evidence relevant to the deposition and subsequent modification of the stratigraphic group, the Hamersley Group, to which the iron formation is confined. That the study progressed so far towards the achievement of both primary objectives is due to this broadly based research approach.

In May, 1964, Mr. G. R. Ryan, who was to have taken charge throughout, began the first field season and was supported for a few weeks by Mr. L. E. de la Hunty. During the second field season, from April to October, 1965, Mr. Ryan was joined by Mr. J. G. Blockley. Dr. A. F. Trendall, who had given petrological support to the investigation from the outset, assumed full responsibility when Mr. Ryan resigned from the Survey in December, 1965. Mr. Blockley was assisted by Mr. P. Muhling during the 1966 field season. During the period September to December, 1966, Dr. Trendall visited the Lake Superior, Ontario, and Labrador areas of North America, and the Cape Province and Transvaal areas of South Africa to make a direct field assessment of the comparative results of the investigation before the preparation of this bulletin in co-operation with Mr. Blockley during 1967 and 1968.

ARRANGEMENT OF THIS BULLETIN

This bulletin follows closely an account of the iron deposits of the Hamersley Range area which includes a full description of the general geology of the Hamersley Group (MacLeod, 1966). We have avoided unnecessary duplication

by referring appropriately to the earlier bulletin, but at the same time we have retained sufficient general geology for this to be read and used independently.

As far as possible Chapters 2 to 8 record uninterpreted geological data, while Chapters 9 to 12 assess and interpret these data from different viewpoints; the only exceptions are at various points where description of textures or structures can be made only artificially without reference to their obvious commonsense or conventionally accepted time-sequence interpretation.

After a broad survey of the regional geological setting in Chapter 2, each formation of the Hamersley Group is described separately in Chapter 3, and some detailed information is given for rocks other than the iron formations; those petrographic, chemical, and structural features which are common to the iron formations are dealt with separately in greater detail in Chapters 4, 5, and 6. Chapter 7 is concerned with the geology of all forms of riebeckite; the mining and economics of crocidolite are the subject of Chapter 8.

In discussing the origin and diagenesis of the iron formations in Chapter 9, two principles are followed: firstly the evidence relevant to the many separate problems involved is, as far as possible, separately presented and discussed, and secondly, reference to evidence from outside the Hamersley area is kept to a minimum. The same principles are used in Chapters 10 and 11, which deal respectively with the broader aspects of the Hamersley basin and with crocidolite growth. Finally, in Chapter 12, information from all preceding chapters is assessed from the point of view of the possible future exploitation of crocidolite resources in the Hamersley area.

The Glossary on page 334 includes new terms initially introduced both here and in preliminary publications; it covers also a few terms used by us in senses possibly more restricted or more general than is usual. The final list of plans is included as a guide for future students of the Hamersley Group.

Those interested in the commercial exploitation of blue asbestos represent one of the several different categories of reader for whom this bulletin is intended. For these we emphasize that our concern is with the *geology* of crocidolite. In Chapter 8 we deal with crocidolite mining in Western Australia insofar as it is necessarily affected by or related to geology; but except for some general considerations of economics in Chapter 12, our concern with the ore ceases as it leaves the mine. Those interested in practical production and marketing of blue asbestos should seek information elsewhere on milling methods, mining and milling costs, world production of blue asbestos, and its industrial utilisation.

LOCATION, COMMUNICATIONS, INDUSTRIES, SETTLEMENT, AND SERVICES

The Hamersley Range (Plate 2) runs for some 250 miles in a west-northwest to east-southeast direction in the North-West Division of Western Australia, roughly between latitude 22° and 23°S and longitude 116° 30' and 119° 30'E, some 700 miles north of Perth. We use the loosely defined term 'Hamersley

Range area' to apply to an area including the Hamersley Range itself, the Ophthalmia Range, which is its eastern extension, and all the contiguous topographically comparable country corresponding roughly to the outcrop of the early Precambrian iron formations with which the bulletin is concerned, together with their contemporaneous sediments and volcanics.

Access from the southern part of the State is gained by either the Great Northern Highway through Meekatharra and Mundiwindi, or the North West Coastal Highway through Carnarvon and Onslow. The Great Northern Highway passes through the eastern end of the area and is linked to Wittenoom Gorge on the northern edge of the Hamersley Range by a road branching off near Roy Hill Station. The North West Coastal Highway skirts the western end of the range, and is linked to Wittenoom by roads branching at Yarraloola and Roebourne. Wittenoom Gorge is also connected to Port Hedland by road and at present a road is being constructed to provide a direct route from Wittenoom to Onslow. Mount Tom Price, in the central part of the Hamersley Range area, is connected to Dampier on the coast by about 170 miles of standard gauge railway and a well-made dirt road. Another railway is under construction linking Mount Whaleback in the Ophthalmia Range with Port Hedland. A few minor roads serving the pastoral stations in the ranges have been supplemented in recent times by tracks made by mining companies searching for iron ore; though many of the roads constructed during the peak period of iron exploration in 1962-3 are no longer usable. The increasing interest in the Hamersley Range being shown by tourists has caused a few roads to be made into the more scenic spots. Despite the greater number of roads, many parts of the Hamersley Range, and its contiguous ranges, are still hard to reach on the ground, and helicopters have been used by mining companies working in the area.

Until recently, the chief industry in the area was crocidolite mining at Wittenoom Gorge. This situation changed suddenly when the asbestos mine closed down at the end of 1966. Iron ore mining, which started at Mount Tom Price in mid-1966, is now, and is likely to be for many years, the main industry of the area. Had the blue asbestos mine stayed in production, it would soon have been overshadowed by the new industry. Other than mining, the only industry in the Hamersley Range area is ranch-style stock grazing. The valleys of the Fortescue and Ashburton Rivers, north and south of the ranges, support important sheep properties. However, in the ranges themselves, only a few scattered cattle stations exist and much of the more hilly country is not grazed at all.

There are three towns in the area of the Hamersley Range: Wittenoom, Tom Price, and Newman. Wittenoom, the oldest of the three, formerly had a population of about 1,000, but now houses fewer than 200 people. Since the crocidolite mine closed, Wittenoom is little more than a tourist centre and supply depot for some of the pastoralists. Tom Price, built in 1966 to house the work-force of the Mount Tom Price iron ore mine, now has a population of about 1,000. Newman is the new townsite for the Mount Whaleback iron-ore mine, near the Ophthalmia

Range. All towns have airstrips capable of taking the largest planes used in internal services and are connected by radio to the telegraph and telephone network of the Commonwealth. All supplies, such as fuel and building material, and most of the food consumed, are brought in from the south, either by ship to the coastal ports, or by road.

The pastoral stations support small communities of from one to a dozen people. Many have an airstrip able to take light airplanes and most are connected to the Royal Flying Doctor Service radio network which provides a means of sending and receiving telegrams as well as for calling emergency medical services.

PHYSIOGRAPHY

The Hamersley Range was named in 1861 by Gregory, who applied the name only to the prominent range forming the southern edge of the Fortescue River valley. His account (Gregory and Gregory, 1884) shows that he considered himself through the range (that is, on the south side of it) when he reached the plains of Hamersley Station, and did not include the numerous but less continuous ridges farther south. The eastern extension of all these ranges is now generally called the Ophthalmia Range, although this name should be restricted to the one ridge which includes Giles Point and Mount Newman.

The shapes and distributions of the hills in both the Hamersley and Ophthalmia Ranges are controlled very closely by the structure of the underlying strata. In the northern part, where the beds dip gently, the highlands are broad dissected plateaux in broad, open synclines. Farther south, where the rocks are more folded, the iron formations crop out as hog-backed strike-ridges trending in a general easterly direction. Within the sedimentary rocks, the rivers and creeks are controlled mainly by the disposition of the less resistant beds, and especially of the dolomite units. Joints and faults have exercised a smaller, but still important control, and many gorges follow such structures. Within the outcrops of the volcanic rocks below the sediments geology has less influence on the drainage pattern.

The Hamersley Range is a large plateau, 250 miles long by 20 to 40 miles wide, extending from Deepdale in the west to Coondiner Creek in the east. On top it consists of ranges of rounded and dome-shaped hills separated by broad scree-filled valleys. Many of the hills are between 3,000 and 3,500 feet above sea level, and the general elevation of the intervening valleys is about 2,500 feet. Most streams on the plateau flow north to the Fortescue River, and as a result, the northern edge is very dissected. In contrast, the southern edge is but little eroded, and for stretches of many miles it forms an unbroken scarp 1,000 feet high.

South of the Hamersley Range, the country is broken and rough, with many prominent ranges of iron formation rising 1,500 to 2,000 feet above the general level. Many peaks on these ranges approach 4,000 feet, and one, Mount Meharry, at 4,104 feet above sea level, is the highest point in Western Australia. This belt

of high country forms the watershed between the drainage basins of the Fortescue and Ashburton Rivers. The northern and eastern parts of the ranges are drained by tributaries of the Fortescue River, and the southwestern part by streams flowing southwards to the Ashburton River.

In many places the creeks are actively cutting down into a more mature landscape generally taken to be of Tertiary age: the Hamersley surface of MacLeod (1966). The old surface is best seen on the plateau of the Hamersley Range, where it can often be traced by eye for distances of several miles. The smooth, duricrust-covered hills and intervening scree-filled valleys are part of the old surface. At present this surface is being eroded in two ways: waterfalls on the main streams are cutting backwards to leave steep-sided ravines such as Wittenoom Gorge and Dales Gorge, and the edges of the rounded hills are being cut back by the headwaters of numerous small gullies to form irregular cliffs. Figure 62 shows a typical section of the plateau, and a general view of the Hamersley surface is shown in Figure 1.

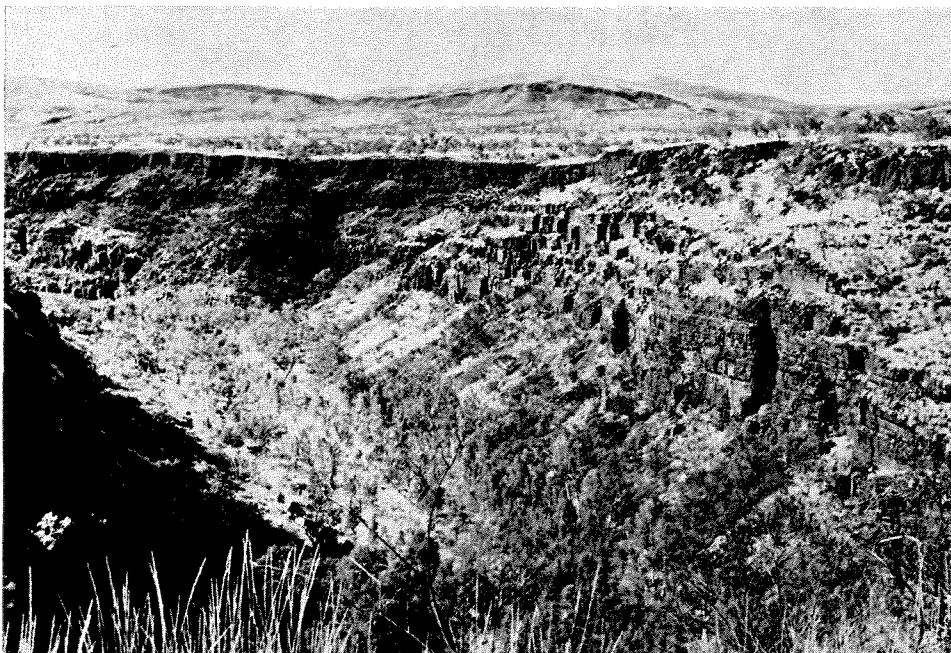


Figure 1. View looking southeast over Dales Gorge just downstream from The Gordon Falls (Figure 65). The laterite-covered Hamersley surface, with very slight relief, is sharply transected by the gorge, and stretches evenly up to the distant rounded hills formed by the Joffre Member of the Brockman Iron Formation. The top of the Mount McRae Shale crops out at creek level, and the macrobands of the Dales Gorge Member are characteristically exposed in the steep walls of the gorge (compare Figure 4). Thus the smooth development of the Hamersley surface was here evidently assisted by the flat-lying Whaleback Shale Member, between the Dales Gorge Member and the Joffre Member.

Many of the ridges south of the Hamersley Range, and rising to the same height, are capped by remnants of the Hamersley surface. However, it may not have extended continuously to these outliers, for in many of the intervening valleys there are deposits of pisolitic limonite and calcrete possibly of equivalent age to the duricrust of the old surface. In other places the caps of duricrust grade into deposits of cemented scree, which extend down the sides of the hills and almost reach the level of the valleys. It seems likely that the broad physiographic outline of the Hamersley Range area was already established in the Tertiary, if not earlier; the present creeks are flowing in the same valleys which then ran between hills little different in position and relief from those seen today, although with smoother and more rounded outlines.

CLIMATE AND VEGETATION

The Hamersley Range area is typical of semi-arid steppes found on the western sides of continents at corresponding latitudes. The average rainfall varies from about 14 inches in the northwest end to about 10 inches at the eastern end. Most of the rain falls in the summer, from January to March, and is associated with tropical thunderstorms and cyclones coming in from the Indian Ocean. At times, during the winter months, intense depressions in the southern part of the State extend their influence far enough northwards to bring short spells of heavy rain to the area. The rate of evaporation is very high and for most of the year there is little surface water to be found.

During the summer, daytime temperatures commonly rise above 100°F, and the nights are warm and sultry. In contrast, the winter climate is pleasant, with temperatures of 80 to 90°F by day and 40 to 50°F at night. In the higher parts of the ranges, frosts are common in the winter.

The stony hills of the Hamersley Range grow little vegetation other than spinifex, stunted trees such as snappy gum (*Eucalyptus brevifolia*), and a few xerophytic shrubs. The deeper soils in the valleys support dense stands of mulga trees (*Acacia spp.*), which grow to around 15 feet in height, and a variety of flowering herbs and shrubs. The only big trees in the area grow along the larger water courses. They include cajeput (*Melaleuca leucadendron*) and river gum (*Eucalyptus camaldulensis*). Cypress pines and a species of wild fig grow in the rocky cliffs of some of the sheltered gorges. There is little timber suitable either for construction or fuel in the area.

WATER SUPPLY

None of the rivers in the Hamersley Range area flows permanently, although some, such as the Fortescue River, have an appreciable underflow. Where such a river passes over a bar of impermeable rock, the underflow emerges as springs which may form large pools. Examples of such pools are seen at Millstream on the Fortescue River, and at Weeli Wolli Spring. These springs, together with

rock-holes and claypans which hold rainwater, constitute the only surface water in the area for much of the year. Consequently, the towns and pastoral stations rely entirely on underground supplies. The most commonly tapped aquifers are the unconsolidated accumulations of scree and alluvium in the valleys. Many bores in these deposits yield from 1,000 to 3,000 gallons a day, but available reserves are little known. Where the aquifer is replenished by the underflow of a large creek, higher yields can be expected. The Town Bore at Wittenoom, fed by the underflow of Joffre Creek, gives about 700 gallons per hour. Of the consolidated rocks, the Tertiary calcrete of the Oakover Formation provides by far the best aquifers. Unfortunately most outcrops of this rock are away from habitation, and the capabilities of the unit as an aquifer have never been tested fully. Whincup (1968) notes that some calcrete areas occupy high ground in the present topography, and are unfavourable for recharge. Some stock bores sunk in calcrete yield 400 to 500 gallons per hour and all exceed 1,000 gallons per day.

There seems little likelihood of artesian water being obtained from the Proterozoic rocks, most of which are of low permeability and porosity. Only the dolomite and the coarser clastic rocks have any significant permeability, and these only in their near-surface weathered parts. Good supplies can sometimes be obtained from bores in such weathered rocks; the Hamersley Iron Ltd. company has three bores along the Hardey River drawing 12,000 gallons an hour from goethite developed in weathered shale and siltstone. However recharge must be adequate for long-term supply on this scale.

Although supplying little water itself, the Wittenoom Dolomite has had a profound effect upon the hydrology of the Hamersley Range area. Its outcrops have weathered to give large valleys filled by permeable detritus. Its lime content has been the raw material for the calcrete deposits many of which overlie the dolomite. Most of the successful bores in the Hamersley Range area are underlain by dolomite, their water coming mainly from the upper layers of gravel or calcrete, but in part from the weathered bedrock.

NOMENCLATURE

During the course of the work for this bulletin a number of new terms were introduced and defined in preliminary publications (Trendall, 1965a; 1966a). It also became desirable to accept closer definitions of existing terms that had been used loosely in the past. Nomenclature is discussed at several appropriate points within this bulletin, but to assist rapid clarification of any nomenclatural difficulty a comprehensive glossary is provided on page 334. In this are included not only terms used or introduced in Western Australia, but equivalent terms in use elsewhere in the general field of iron formation studies, together with page references, where necessary, to fuller definitions in the text.

At this point it is appropriate to discuss our usage of the terms iron formation, banded iron formation, and jaspilite.

The name jaspilite was first proposed by M. E. Wadsworth (1880, p. 76) for "all the acidic eruptive rocks, whose physical and chemical constitution carries them above the rhyolites" associated with the iron ores of the Lake Superior region. He was referring to the rocks now known in that area as iron-formation. These are usually more basic, in the classical sense of igneous petrology, than rhyolites, which is probably why N. H. Winchell (1900, p. 997) later described one type of iron-bearing rock as "a jaspilite, or silicified basic rhyolitic lava". Wadsworth coined the name because he objected to the name jasper, which was then commonly applied to these rocks, but it is not clear whether the supposed eruptive origin or the common lack of red colouring (or both) was the basis of his objection. Not long afterwards both terms were in more or less synonymous use, and Van Hise and Leith (1911, p. 461) were able to write that "the iron-bearing formations of the Lake Superior region consist essentially of interbanded layers, in widely varying proportions of iron oxides, silica, and combinations of the two" . . . "called jasper or jaspilite, where anhydrous and crystalline". At that time these rocks were recognised as sedimentary. A red colour, due to ferric oxide, seems to have been necessary for either name to be applied throughout the Lake Superior literature. One common distinction between them was that jasper was homogeneous and jaspilite was banded. This still continues, and a reasonable definition of jaspilite as currently used in the Lake Superior area is: iron-formation with interbanded black crystalline hematite and jasper (*red* chert).

The 'iron-bearing formation' of Van Hise and Leith, in the quotation given above, is now contracted to 'iron-formation', firstly strictly defined by James (1954, p. 239) as "a chemical sediment, typically thin-bedded or laminated, containing 15 per cent or more iron of sedimentary origin, commonly but not necessarily containing layers of chert"; LaBerge (1966a, p. 147) prefers to make the presence of chert a defining character.

In Western Australia the term jaspilite, at first used with proper regard for earlier definition (Ellis, 1939, p. 81) was gradually applied to a wider variety of iron-rich or cherty rocks, and is now often used roughly synonymously with the term iron-formation in the Lake Superior area. Before its introduction most of the ferruginous cherty rocks of the older Precambrian were called jaspers and were regarded as a type of shear or fault infilling (e.g. Feldtmann, 1921). In view of the confusing origin of the name jaspilite and the advantages of a common nomenclature at least between Australia and America the following definitions have been adopted on this Survey:

1. *iron formation*: a lithological term applied to a chemical sedimentary rock with a high iron content; in addition to banded iron formation (defined below) it includes the high-iron shales, slates, carbonate rocks, and mixed oolitic rocks frequently associated with Precambrian banded iron formations, as well as Phanerozoic chamositic sediments.

2. *banded iron formation* (BIF): a lithological term applied to a chemical sedimentary rock consisting in its least metamorphosed state of successive thin layers (mesobands) of fine-grained quartz, iron oxides, carbonates, and silicates

in various proportions. Some non-defining characteristics are: (1) there is usually a wide range between the relatively low iron content of quartz-rich (chert) mesobands and the high iron content of adjacent magnetite-rich or hematite-rich mesobands; (2) the total iron content of samples taken cross the banding over widths about 10 times the average mesoband thickness is often in the range 15 to 35 per cent; (3) almost all banded iron formation is Precambrian.

3. *Iron Formation*: a formal lithostratigraphic term capitalised when coupled with its local place-name qualifier, as in Brockman Iron Formation. The word 'Formation' here is part of the lithological term 'Iron Formation', and is *not* equivalent to the same word in, for example, 'Mount Sylvia Formation', where it has formal stratigraphic significance; 'Iron Formation' in 'Brockman Iron Formation' is equivalent to 'Shale' in 'Mount McRae Shale'. This somewhat legalistic point is both confusing and unsatisfactory, and is probably in part why iron formation is usually (but not always!) hyphenated in north America. We regret, but currently accept, the possibility of confusion.

4. *jaspilite*: a lithological term applied to rock with alternating thin bands of jasper (red chert) and some other material, usually either black iron oxides or chert of another colour. We prefer to restrict this term to rocks in which the colouring is not due to recent surface weathering.

Although jaspilite can normally be regarded as a special type of banded iron formation, many of the older Precambrian (> 2,500 m.y.) jaspilites of Western Australia have a very low iron content; the well known 'jasper bar' at Marble Bar is an example. There is a case for following James (1954) in setting a strict lower limit of 15 per cent iron for iron formation, and calling the cherty rocks below it ferruginous cherts, but at present we prefer to avoid setting up definitions so strict that chemical analysis is necessary before a rock can be properly named. The banded iron formation of the Hamersley area has much more than 15 per cent iron, and there is no present problem of nomenclature.

PREVIOUS WORK

It is not necessary to repeat MacLeod's (1966, p. 24-25) recent account of general geological investigation in the Hamersley area. We give a history of crocidolite mining in Chapter 8, and note here: firstly, the few previous publications directly concerned with crocidolite; secondly, the regional mapping of the Hamersley area by the Geological Survey, without which our own investigation could not have been accomplished, and on which most of the maps in this bulletin are based; and thirdly, the preliminary publications stemming from our own work.

The brief notes of Woodward and Montgomery (1917) and Wilson (1922) are the earliest published records of the existence of crocidolite in the Hamersley Range area. Simpson (1930) later gave analyses by J. N. Grace of two crocidolite samples from an unstated source. Brief field examinations of crocidolite workings were made by Forman (1938) and Foxall (1939), and a more thorough report was prepared by Finucane (1939). Miles (1942) gave good petrographic

descriptions of a group of samples of crocidolite and its host iron formation collected mainly by H. W. B. Talbot (of the Geological Survey) in 1914 and by K. J. Finucane in 1938. Foxall (1942) reassessed the economic potential of the crocidolite at that time. N. A. Trueman (1963) published a description of crocidolite samples provided by Australian Blue Asbestos Pty. Limited in connection with an investigation of milling properties of the ore. Finucane (1964; 1965) revised his earlier account of the mining geology of Hamersley crocidolite in the light of his experience as geological consultant to Australian Blue Asbestos Pty. Limited during the preceding years.

During the several years preceding our investigations the Hamersley Range area had been the object of a systematic programme of regional mapping at a scale of 1:250,000 by the Geological Survey. This programme was in part directed specifically towards the provision of a firm geological background for iron ore exploitation (MacLeod, 1966) and was in part a continuing programme of general geological mapping. The joint result was the availability of all 1:250,000 map sheets (1° latitude by $1\frac{1}{2}^{\circ}$ longitude) on which rocks of the Mount Bruce Supergroup crop out. The positions of most of these sheets are shown on Plate 4, and those now published are: SF/50-2* and SF/50-1, Dampier and Barrow Island (Kriewaldt, 1964); SF/50-3, Roebourne (Ryan, 1966); SF/50-4, Port Hedland (Low, 1965); SF/51-1, Yarrie (Wells, 1959); SF/50-6, Yarraloola (Williams, 1965); SF/50-7, Pyramid (Kriewaldt and Ryan, 1967); SF/50-8, Marble Bar, and SF/51-4, Nullagine (Noldart and Wyatt, 1962); SF/50-10, Wyloo (Daniels and Halligan, 1968); SF/50-11, Mount Bruce (de la Hunty, 1965); SF/50-12, Roy Hill (MacLeod and de la Hunty, 1966); and SF/50-16, Newman (Daniels and MacLeod, 1965).

Progress reports of the investigation recorded in this bulletin have been published by Trendall (1965a, 1966a), Ryan and Blockley (1965), and Blockley (1967); and Trendall and Blockley (1968) have separately published some detailed stratigraphic information. We have tried to include a sufficient summary of all these publications, so that the average reader is not forced to refer to them in order to follow any part of the bulletin; on the other hand readers with a special interest in some aspects of the iron formations will find detailed information in them which we have not repeated.

ACKNOWLEDGEMENTS

We are grateful to the management of the former Australian Blue Asbestos Pty. Limited company, and particularly its geologists at Wittenoom, for their co-operation throughout this investigation. Many colleagues of the Geological Survey, especially those at times actively collaborating in the work, must be thanked for much patient discussion which preceded the preparation of this bulletin. Mr. L. H. Fimmell, laboratory supervisor, prepared most of the photographs. All the chemical analyses reported were carried out by staff of the Government

* International Index numbers.

Chemical Laboratories; the Geological Mapping Section of the Surveys and Mapping Branch, Mines Department, prepared all the maps and line drawings used in the Plates and Figures. Among the staff of several iron mining and exploration companies from whom we have received friendly co-operation, special mention should be made of the persistence of Messrs. J. Baldwin and N. Herriman, of Hamersley Exploration Pty. Limited, in correctly identifying the macrobands of the Dales Gorge Member at Seven Mile Creek, after we had both made the same misinterpretation of the section there.

Outline of regional geology

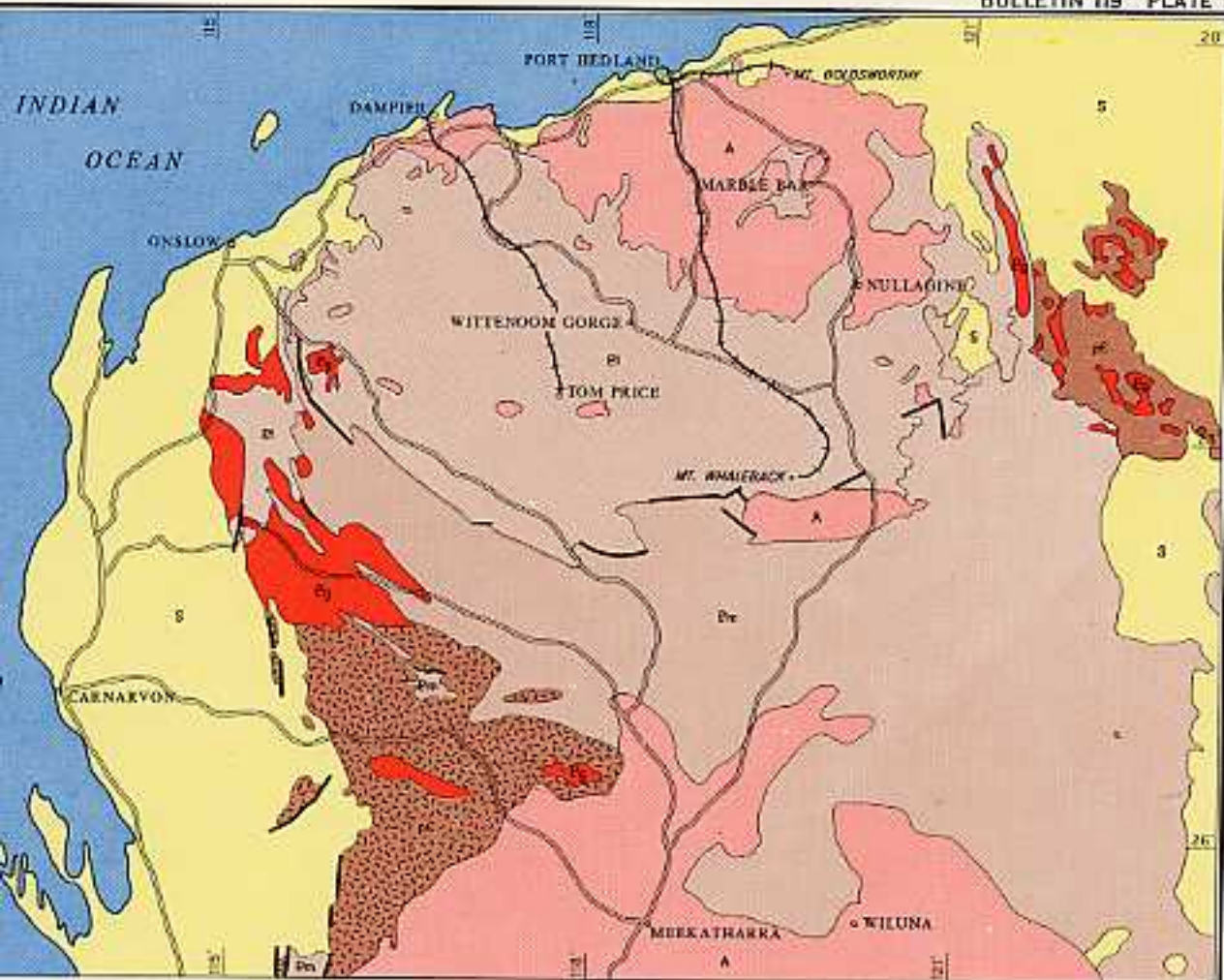
GENERAL

The outcrop area of the Mount Bruce Supergroup is shown on Plate 1. It has three constituent groups: the Fortescue Group, Hamersley Group, and Wyloo Group, in ascending stratigraphic order. Their outcrop areas appear on Plate 2. The Fortescue Group has a maximum thickness of 14,000 feet and consists largely of basic lava, pyroclastic rocks, sandstone, and shale. The Hamersley Group is about 8,000 feet thick, and is defined by an abundance of iron formations, which are interstratified with shale, dolomite and acid lava, and are at some levels intruded by thick dolerite sills. It is perfectly conformable with the Fortescue Group. The Wyloo Group consists of mixed clastic sediments with thick local developments of dolomite and basalt; it reaches 30,000 feet in thickness. Its relationship with the underlying Hamersley Group is broadly conformable, but locally discordant or equivocal. Generalised stratigraphic columns of all three groups in different parts of our area appear in Figure 2.

In the northern part of its outcrop the Fortescue Group dips gently south and overlies with marked angular unconformity the older (Pilbara System) rocks of the Pilbara block (Ryan, 1964). These include deep synclinal keels of metasedimentary and metavolcanic rocks separated by broad domes of granite and gneiss. The erosion surface on which the Fortescue Group rests is mostly of low relief. Further south the Fortescue Group, with the overlying Hamersley and Wyloo Groups, is at first gently and then increasingly tightly folded, until along the southern margin of its outcrop the basal unconformity either dips steeply, is overturned, or is sharply faulted out. Archaean rocks are locally re-exposed in anticlinal cores within the main Mount Bruce Supergroup outcrop. The Wyloo Group is itself intruded by later diapiric granites.

In this southern, folded, area the Mount Bruce Supergroup is itself overlain unconformably by the younger Precambrian Bresnahan, Bangemall, Mount Minnie, and Manganese Groups. These rocks extend southwards to overlie unconformably the northern edge of the main southwestern area of Archaean rocks in Western Australia. They are comparatively gently folded, and consist mainly of mixed clastic sediments, with associated carbonates and cherts.

By the end of Precambrian time all of the Precambrian rocks so far mentioned had jointly acquired the status of a single stable structural block. During



GEOLOGICAL SURVEY OF WESTERN AUSTRALIA
REGIONAL GEOLOGICAL MAP
SHOWING
SETTING OF MOUNT BRUCE SUPERGROUP

REFERENCE

S	Phanerozoic sediments
Dm	Bangerell, Breckenridge and Mount Minnie Groups
B	Mount Bruce Supergroup
A	Archaean
U	Undetermined (Precambrian)
G	Proterozoic Granite

SYMBOLS

Area of high grade metamorphism	
Geological boundary (unconformity or intrusive contact)	
Geological boundary (folded)	
Road	
Railway	

the Phanerozoic steady uplift and erosion was accompanied by a complementary sinking of the Canning Basin to the east and of the Carnarvon Basin to the west.

EVIDENCE FOR AGE

Earlier isotopic dating in the area was summarised by Leggo, Compston, and Trendall (1965) in a paper reporting age determinations for the Wyloo Group and its intrusive granite, volcanics of the Hamersley Group, and granite of the Pilbara System. Subsequent work (Compston and Arriens, 1968) has modified these results, and the current position may be summarised thus:

1. The granites of the Pilbara System are about 3,000 m.y. old.
2. The Woongarra Volcanics of the Hamersley Group have been extensively studied, as a result of which an age close to 2,000 m.y. is preferred to the earlier 2,100 m.y.
3. A reliable date for the Fortescue Group has not yet been obtained, but an age of about 2,200 m.y. is given by unsatisfactory material.
4. The previously reported age of 1,850 m.y. for a Wyloo Group siltstone is now thought unsatisfactory, and the only reliable younger limit on the Wyloo Group is set by the intrusive granites at about 1,700 m.y.
5. Bangemall Group shales give an age of about 1,100 m.y.

All these figures are subject to modification before final publication, but their general order of magnitude is not likely to be altered. All are the result of total-rock Rb-Sr analyses.

REGIONAL GEOLOGY OF THE HAMERSLEY GROUP

REGIONAL EXTENT, CORRELATIONS, AND VARIATION

MacLeod and others (1963) defined the Fortescue, Hamersley, and Wyloo Groups on the basis of their mapping of the central Hamersley Range area during 1962. The nomenclature was carried outwards to the surrounding map sheets during contemporaneous and later mapping by the Geological Survey (see 'Previous work', Chapter 1). However, correlative rocks had already been systematically mapped to the east and northeast of the Hamersley Iron Province, with which MacLeod and others (1963) and MacLeod (1966) were concerned. Our representation of the regional extent of the Hamersley Group on Plate 2 differs somewhat from that of MacLeod (1966), especially east of the 120° meridian, along the rough line of which the Fortescue River flows northwards to Roy Hill before turning west-northwestwards along the main part of its valley. We have followed MacLeod and de la Hunty (1966, Table 1) in correlating the lowest two formations of the Hamersley Group, the Marra Mamba Iron Formation and Wittenoom Dolomite, with the upper part of the Lewin Shale and the Carawine Dolomite respectively as mapped by de la Hunty (1964) in the Balfour Downs area, and we have then extrapolated this correlation over the adjoining sheets.

In this general area of Hamersley Group outcrop (east and north of the upper Fortescue River) only these two lowest formations of the Hamersley Group are present, iron formation is poorly developed, and no crocidolite occurs. Consequently we have not worked in this area, and in later discussion we rely on MacLeod and de la Hunty's (1966) interpretation of the mapping there.

Almost throughout the outcrop area of the Mount Bruce Supergroup the Hamersley Group either is present with all its formations recognisable or is

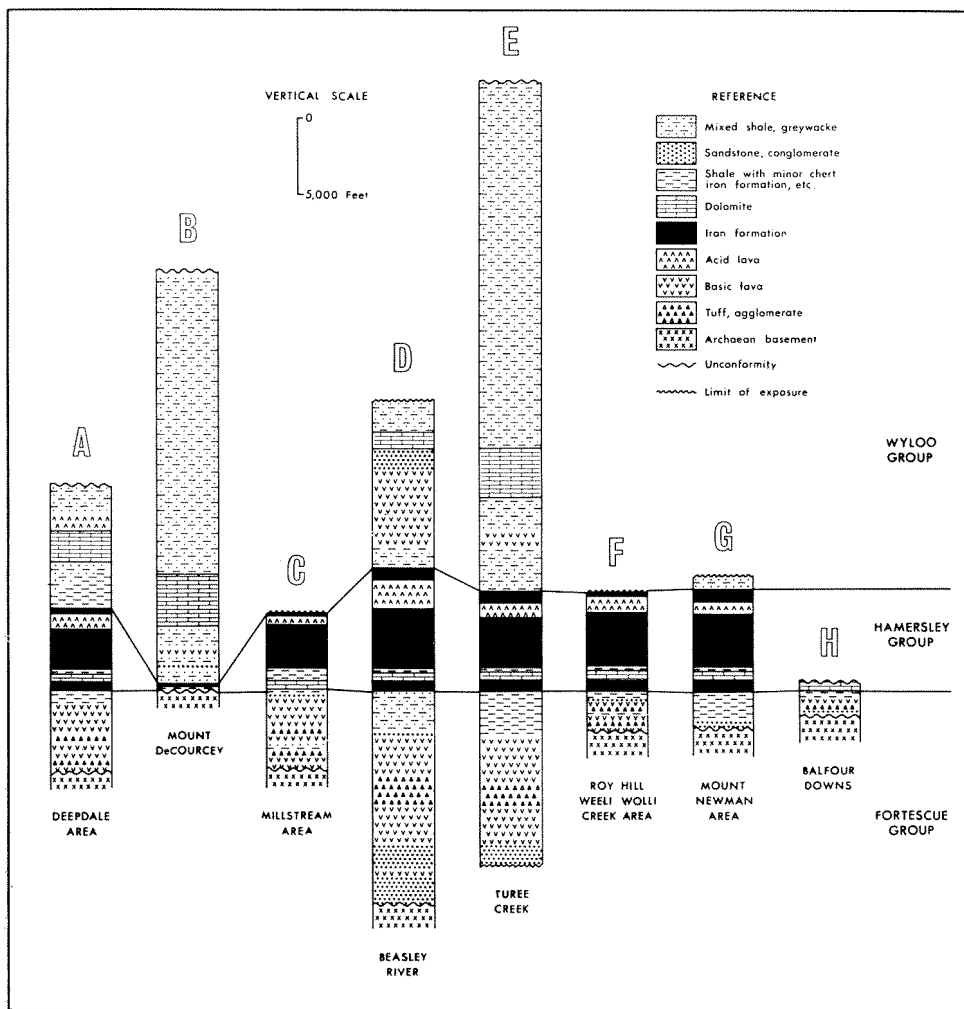


Figure 2. Comparative stratigraphic columns, to scale, of the Mount Bruce Supergroup in different parts of the Hamersley Range area. Published authorities of the columns are as follows: (A) Williams, 1965. (B) Daniels and Halligan, 1968. (C) Kriewaldt and Ryan, 1967. (D) Daniels and Halligan, 1968. (E) Daniels, 1967. (F) MacLeod and de la Hunty, 1966. (G) Daniels and MacLeod, 1965. (H) de la Hunty, 1964. In some columns, modifications have been made based on our observations.

incompletely represented because some level within it represents the youngest uneroded rock (Figure 2 C, F, and H). The only exception to this is in the area of the Wyloo Anticline (Plates 2 and 4; Figure 2 B; see also Daniels and Halligan, 1968). At the eastern end of this structure the Hamersley Group is fully represented, but it thins quickly, and its formations become progressively less easily distinguishable as it is traced westwards along both the north and south limbs of the anticline. The westernmost outcrops of the group on the Wyloo Anticline comprise isolated remnants of iron formation scattered along the contact between the Fortescue Group below and the Wyloo Group above. In the south-western corner of the area of Plate 4 the Wyloo Group appears to lie directly on the Fortescue Group for about 20 miles. The contact is often faulted, and the relationship between the two groups is uncertain. However, the Hamersley Group is certainly absent, and it seems more likely that it was either not deposited or was eroded before the deposition of the Wyloo Group, rather than that faulting should have effectively concealed it over so great a distance.

Only in this Wyloo Anticline area do gross changes affect any formations of the Hamersley Group. The more subtle regional variations in thickness and lithology of individual formations are described in the following chapter.

THE FORTESCUE GROUP IN RELATION TO THE HAMERSLEY GROUP

The regional extent of the Fortescue Group is shown on Plate 2. Variations in lithology and thickness are summarised by Figure 2, from which it is apparent that, compared with the Hamersley Group, the Fortescue Group shows great lateral variation in both respects. Because of this, and also because its mapping was started in separate areas by different workers at different times, the formal stratigraphic nomenclature of the Fortescue Group is confused, and has yet to be clearly set out in a single publication.

Throughout its outcrop area the Hamersley Group is perfectly conformable with the uppermost shale of the Fortescue Group—the Jerrinah Formation. This shale shows, in its lateral persistence, more affinity with the Hamersley Group than the Fortescue Group. In the central part of the Hamersley Range area (Figure 2 D) it is underlain by some 12,000 feet of mixed lavas, pyroclastic rocks and sediments; but it lies directly on Archaean rocks where Jimblebar Creek cuts the extension of the Ophthalmia Range (Figure 2 G). On the south side of the Wyloo Anticline, at Mount DeCoursey and Mount McGrath, the whole of the Hamersley and Fortescue Groups are represented by 200 to 300 feet of shale and iron formation resting on Archaean rocks.

It thus appears that, in spite of wide regional variations in lithology and thickness of the Fortescue Group, the stability which was to characterise Hamersley Group deposition was already established during deposition of the uppermost shale of the Fortescue Group.

THE WYLOO GROUP IN RELATION TO THE HAMERSLEY GROUP

The regional extent of the Wyloo Group is also shown on Plate 2, and representative stratigraphic columns appear in Figure 2. It is obvious that a major distributional character of the group is its restriction to the west and southwest parts of the area. As discussed in Chapters 10 and 11, the significance of this is uncertain.

The two groups are in most places assumed to be broadly conformable, because of the usual absence of any apparent structural or stratigraphic discontinuity about their mapped contact. But this is often poorly exposed, and perfect conformity can rarely be proved. However, the uppermost part of the Boolgeeda Iron Formation, at the top of the Hamersley Group, is lithologically gradational into green siltstone similar to that of the lower part of the Wyloo Group.

There is demonstrable discordance only in the Wyloo Anticline area. The two lowest formations of the Wyloo Group, the Turee Creek Formation and the Beasley River Quartzite, pinch out against the Hamersley Group in the south-eastern part of the structure. In one well-exposed section, where Hamersley Group stratigraphy is still discernible, the Beasley River Quartzite rests, via bouldery passage beds representing a disconformity, on lavas of the Wongarra Volcanics, with the uppermost Boolgeeda Iron Formation absent from the sequence. Farther west, on the western spur of Mount DeCoursey, the iron formation at the top of the Hamersley Group contains beds of intraformational breccia at or just below the contact with the overlying quartzite; but here the formations of the Hamersley Group are not recognisable, and it is uncertain how much is missing and how much has merely thinned. It has already been noted that the Wyloo Group rests directly on the Fortescue Group over much of the southern part of the Wyloo Anticline.

In the area between Red Hill and Mount Stuart, intercalations of banded iron formation occur locally within the Wyloo Group. Groups of several beds, each 6 to 15 feet thick, are separated by the mainly shaly and cherty sediments with carbonates of which the Wyloo Group here consists. Their lateral extent and precise position within the group are both uncertain.

STRUCTURE

The structure of the Hamersley Range area was well described by MacLeod (1966, p. 63), and the folding in the central part is clearly displayed on Plate 4. MacLeod's names for the major folds also appear on Plate 4, except for the term Hamersley Range Synclinorium, which is applied to the broad open synclinorium whose axis runs in an east-southeasterly direction from the Silver Grass Syncline, through the Hamersley Syncline to the Marillana Syncline; it includes these three structures as well as their associated subparallel folds within the

Hamersley Range, and is best defined on Plate 4 by the inward-dipping Wittenoom Dolomite along both the north and south sides of the range.

We add here only two notes to MacLeod's account of the structure, which are important for later discussion. Firstly, there is a characteristic lack of axial continuity in the folding, at all scales. On the broad regional scale the prolongation of the axial plane traces of major anticlines often pass directly into those of synclines along the structural strike, and vice versa. On Plate 4 the westward extension of the syncline forming The Governor (about $23^{\circ} 05'S$; $118^{\circ} 45'E$) passes within a few miles into an anticline. Similarly, a west-northwesterly extension of the Hardey Syncline passes directly into the Wyloo Anticline. It is for this reason that it is necessary to show axial plane traces of such folds as the Jeerinah Anticline with a sigmoid shape, since a smooth easterly prolongation of the western part of the Jeerinah Anticline would pass into the eastern part of the Brockman Syncline, and vice versa. It is this feature of the fold geometry which is expressed also by the presence of the Turner Syncline in the very centre of the broad dome occupying the south-central part of Plate 4, which is outlined by the diamond-shaped peripheral outcrop of the Jeerinah Formation. This rather erratic character of the folding is present on whatever scale structure is mapped in the Hamersley Range area.

The second structural point is concerned with the difficulty of describing structure accurately, especially within the Hamersley Group, without first defining and restricting the scale of description. In the iron formations particularly, and even in the open folds of the Hamersley Range Synclinorium itself, there is slight but continuous waviness of the bedding at any chosen scale of observation. Thus at whatever map scale is chosen to represent the structure of any part of the Hamersley Range, anticlines and synclines could be inserted at a convenient separation for representation, while smaller folds on their limbs would be too numerous to be shown. This point is important for later discussion (Chapter 11).

Hamersley Group stratigraphy

FORMAL STRATIGRAPHIC NOMENCLATURE IN RELATION TO SEDIMENTATION

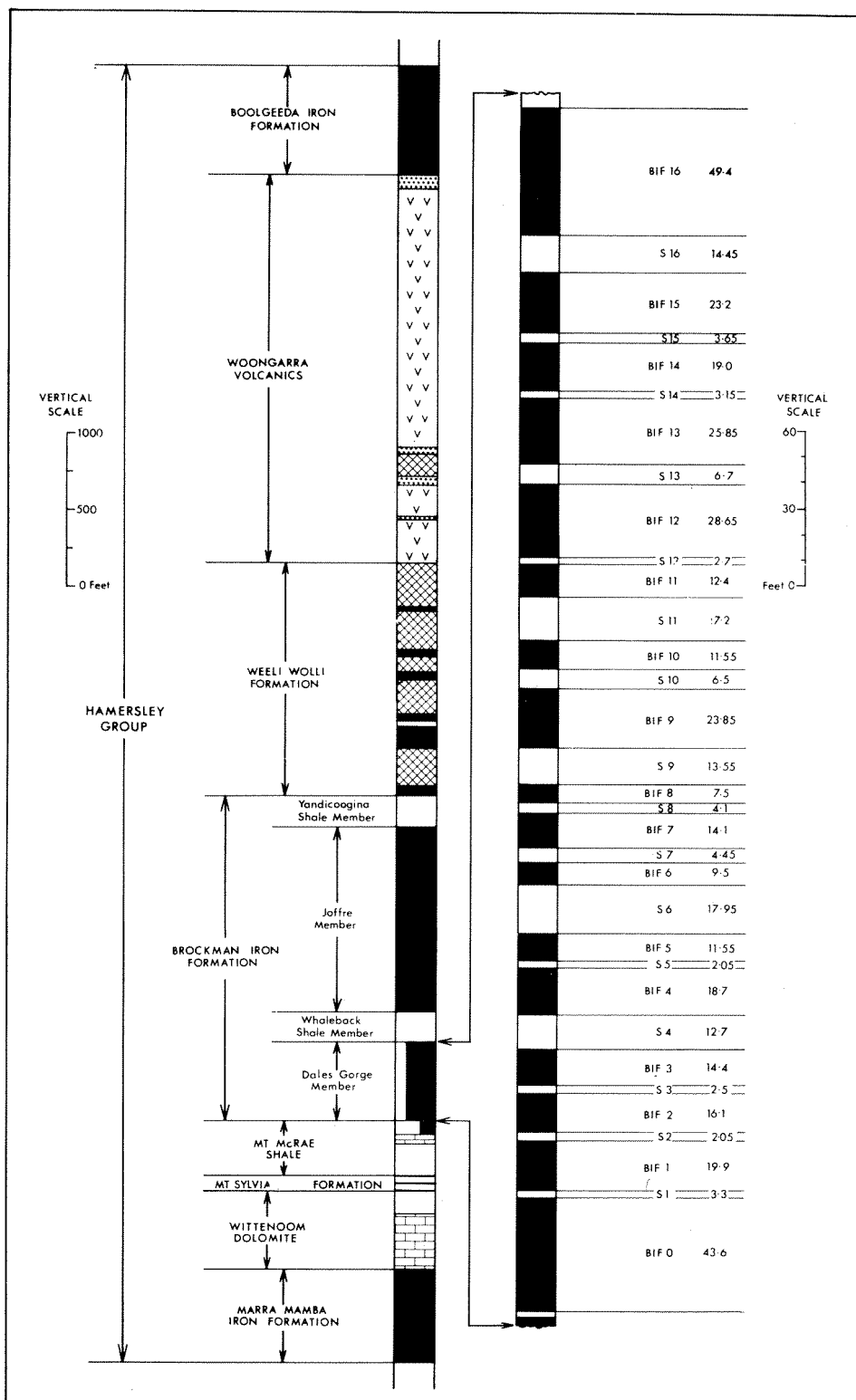
The Hamersley Group was formally defined by MacLeod and others (1963), with the following 8 formations:

- Boolgeeda Iron Formation
- Woongarra Dacite
- Weeli Wolli Formation
- Brockman Iron Formation
- Mount McRae Shale
- Mount Sylvia Formation
- Wittenoom Dolomite
- Marra Mamba Iron Formation

De la Hunty (1965, p. 15) subsequently re-named the Woongarra Dacite the Woongarra Volcanics. The relative thickness of these formations (rock units, or lithostratigraphic units) is shown in Figure 3, together with their generalised lithology and later subdivisions, which are described under appropriate headings of this chapter.

It is apparent from Figure 3 that there is a wide range in the thicknesses of the named formations. This is entirely in accordance with common practice and with the provisions of the Australian Code of Stratigraphic Nomenclature (Geological Society of Australia, 1964). This (Articles III, 4 & 5; IV, 17) makes it clear that named formations are stratigraphic units whose distinctive lithology enables them to be used in field mapping; if such units fulfil the basic

Figure 3 (opposite). Stratigraphic columns, to scale, of the Hamersley Group (left-hand column) and of the Dales Gorge Member of the Brockman Iron Formation (right-hand column), showing numbering and thicknesses in feet of the 33 macrobands in the type section. Formation thicknesses in the Hamersley Group are mainly those described by Ryan and Blockley (1965) from the west-central part of the area, except that the Woongarra Volcanics and the Weeli Wolli Formation are as re-measured by A. F. Trendall and J. G. Blockley respectively at Woongarra Gorge, while the member subdivision of the Brockman Iron Formation is new in this bulletin. Lithology is represented as follows: BIF—solid black; shale—white; dolerite—diagonal hatching; acid lava—v; tuff—stipple; dolomite—brick pattern. The vertical divisions in the Mount McRae Shale and Dales Gorge Member in the left-hand column indicate diagrammatically the approximate proportions of different components too closely mixed for clear representation at the scale used. Shale in the right-hand column includes chert-siderite.



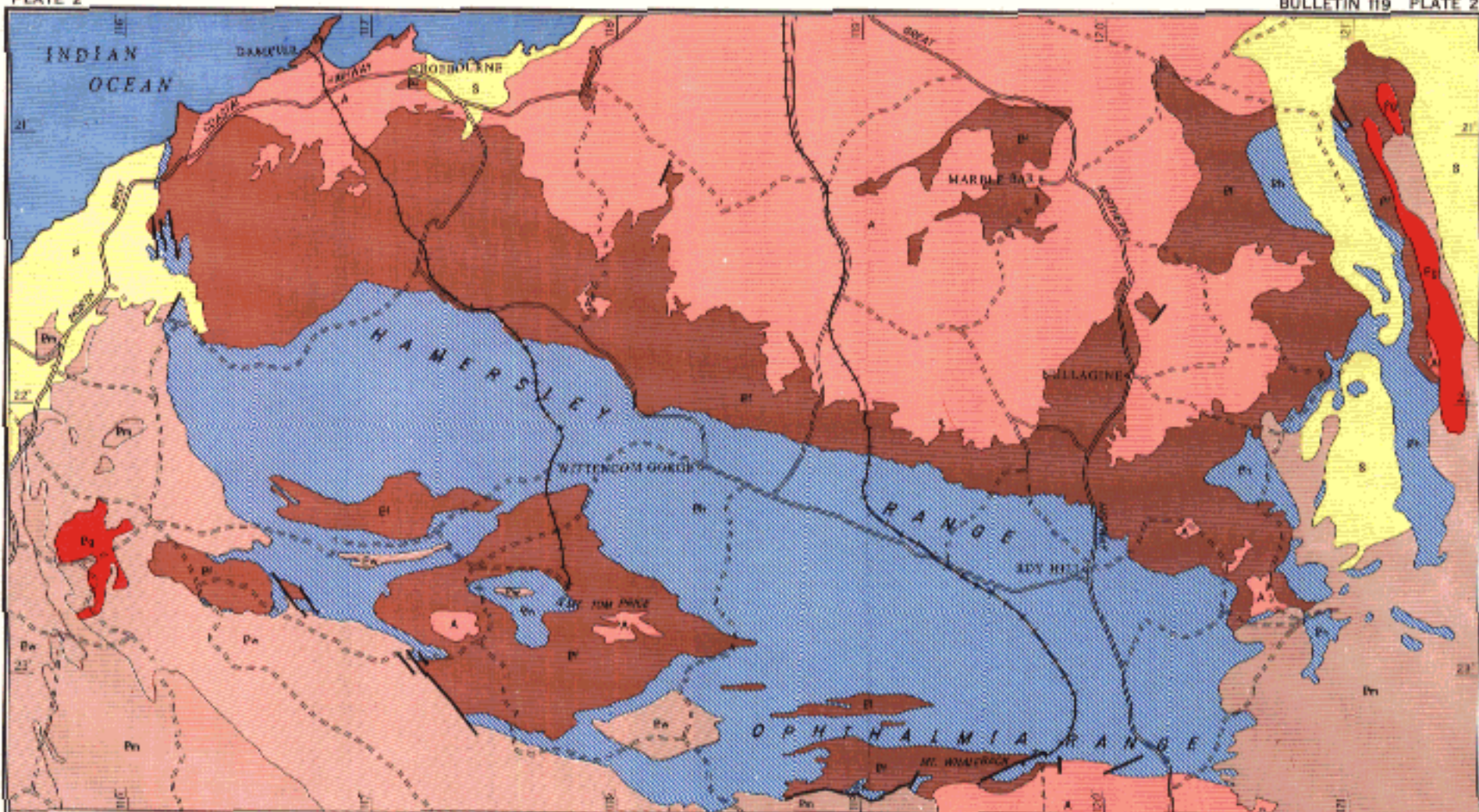
requirements that they consist wholly or mainly of one lithological type, and are marked at top and bottom by a change in lithology (Article IV, 18), then thickness is immaterial (Article IV, 8). However, it does not follow that all stratigraphic units satisfying these requirements will be equally useful for field mapping; and in practice the formal selection and naming of formations will depend upon accidents of physiographic development, the judgment of the mapping geologist, and the purpose and scale of the mapping. A thick sequence of mixed sediments may be acceptably subdivided and named in an almost infinite number of ways according to these factors, although some units may be so outstandingly distinctive as to appear in all variants.

Although we use the formally established stratigraphy of MacLeod and others (1963) as a basis for the headings within this chapter we first discuss the extent to which the eight named formations reflect the abundance and inter-relationships of the main lithologies of the group.

The problem is well exemplified (Figure 3) by the Mount Sylvia Formation and the Joffre Member of the Brockman Iron Formation. As MacLeod (1966, p. 42-44) pointed out, the 110-foot thick Mount Sylvia Formation owes its status to the presence within shale and dolomite of three thin iron formation beds which form a characteristic triad of low cliffs (*ibid.*, Fig. 11); these provided an invaluable marker for regional mapping. However, the utility of the formation in this way is out of all proportion to its sedimentational significance for the Hamersley Group, of whose thickness it forms only about one-eightieth part. On the other hand the nearly 1,200-foot thick Joffre Member of the Brockman Iron Formation is easily the thickest unit of uninterrupted iron formation in the group, if not in the world. But due to various factors it seldom forms cliffs, and its only good natural exposures are in gorges difficult of access. For these reasons, and because it less commonly acts as a host for iron ore, MacLeod and others (1963) found it unnecessary for their purpose to differentiate it from the Brockman Iron Formation, of whose thickness it forms about a half, and within which it forms a distinct lithological unit.

The proportions of the various rock types comprising the Hamersley Group, both for the whole group and with igneous rocks progressively removed, are given in Table 1. It is noteworthy that in the area of original definition over 40 per cent of the group consists of igneous rocks.

In fact, the average thicknesses of igneous rocks, in both the Woongarra Volcanics and the Weeli Wolli Formation, are probably rather lower than those used for Figure 3. Recalculated abundances using the measured sections of these two formations reported by MacLeod (1966, p. 52 and 55) from Kalgan Creek, near the eastern end of the Hamersley Range, are given in Table 2. It appears from these figures that although either real thickness variation or uncertainty of measurement (probably both) give widely different values for igneous rock and tuff proportions, the relative abundance estimates for the three main sedimentary types vary little, and in round figures are about 70, 20, and 10 per cent for iron formation, shale, and dolomite respectively.



REFERENCE

PHANEROZOIC	S	Mesozoic to Recent marine and continental sediments
MIDDLE PROTEROZOIC	Pa	Sangamit, Brecken, Mount Vennie and Manganoo Groups
LOWER PROTEROZOIC	Pa	Wylba Group
	Bn	Hamersley Group
	Fm	Fortescue Group
ARCHAEOAN	A	Werruwoona Series, Noogate Creek Series, and GEORGE CREEK FORMATION with granitic gneisses
IGNEOUS ROCKS	IV	Proterozoic granites intruding into Wylba Group

SYMBOLS

Geological boundary	—
Fault	—
Railway	—+—+—+—
Highway	—
Formal Road	—
Track	- - - - -

GEOLOGICAL SURVEY OF WESTERN AUSTRALIA
REGIONAL GEOLOGICAL MAP OF HAMERSLEY GROUP

SCALE 1:2,500,000

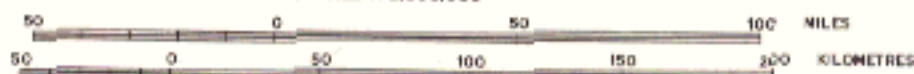


TABLE 1. PROPORTIONS OF LITHOLOGICAL TYPES IN THE HAMERSLEY GROUP, BASED ON FIGURE 3

Rock type	Thickness	Volume percentages		
		Total	without:	
			Dolerite	Dolerite, lava, and tuff
	feet			
Iron formation	3,360	40.2	47.4	70.5
Acid lava	2,160	25.9	30.5	
		41.1		
Dolerite (sills)	1,265	15.2		
Shale	995	11.9	14.0	20.9
Dolomite....	410	4.9	5.8	8.6
Tuff	160	1.9	2.3	
Total	8,350			

TABLE 2. PROPORTIONS OF LITHOLOGICAL TYPES IN THE HAMERSLEY GROUP; REVISED ESTIMATE FOR THE EASTERN PART OF THE HAMERSLEY RANGE AREA

Rock type	Thickness	Volume percentages		
		Total	without:	
			Dolerite	Dolerite, lava, and tuff
	feet			
Iron formation	3,879	57.7	63.3	73.1
Acid lava	800	11.9	13.1	
		20.8		
Dolerite (sills)	600	8.9		
Shale	1,021	15.2	16.7	19.2
Dolomite....	410	6.1	6.7	7.7
Tuff	15	0.2	0.2	
Total	6,725			

When sequence is taken into account, the most obvious imbalance in the Hamersley Group not immediately revealed from the stratigraphic nomenclature is that between the upper and lower parts. Taking the top of the Brockman

Iron Formation as the dividing line, the lower and upper parts have the lithological proportions shown in Table 3. From these figures, between a half and three-quarters of the upper part of the Hamersley Group consists of igneous rocks, and variations in this proportion are largely controlled by variations in the thickness of these, rather than of the sediments.

The most evident regularity in the arrangement of sedimentary lithologies is a large-scale alternation between shale, or shale and dolomite, and iron formation, with or without subordinate shale. In these terms the natural sedimentation units below the Woongarra Volcanics and extending down into the top of the Fortescue Group would be:

	Approximate thickness in feet
8. Weeli Wolli Formation	600
7. Yandicoogina Shale Member of Brockman Iron Formation	200
6. Joffre Member of Brockman Iron Formation	1,200
5. Whaleback Shale Member of Brockman Iron Formation	200
4. Dales Gorge Member of Brockman Iron Formation + top of Mount McRae Shale	600
3. Wittenoom Dolomite + Mount Sylvia Formation + lower part of Mount McRae Shale	850
2. Marra Mamba Iron Formation	600
1. Jeerinah Formation of Fortescue Group	500-1,000

TABLE 3. COMPARATIVE LITHOLOGICAL PROPORTIONS IN THE UPPER AND LOWER PARTS OF THE HAMERSLEY GROUP

Rock type	Lower part of group*		Upper part of group			
			Based on Figure 3		Eastern Hamersley Range	
	Total thickness	Volume	Total thickness	Volume	Total thickness	Volume
	feet	per cent	feet	per cent	feet	per cent
Iron formation	2,275	62.3	1,085	23.1	1,450	50.7
Acid lava	2,160	46.0	800	27.9
				72.9		48.8
Dolerite	1,265	26.9	600	20.9
Shale	965	26.5	30	0.6
Dolomite	410	11.2
Tuff	160	3.4	15	0.5
Total	3,650		4,700		2,865	

* The lower part of the group in the eastern Hamersley Range area would be slightly different, owing to our redefinition of the top of the Brockman Iron Formation, but the magnitude of the differences does not justify crowding extra data into this table.

The problem of the significance of this broad alternation is discussed in a wider context in Chapter 10. In the preceding discussion we have simply emphasized the necessity to differentiate between formal stratigraphic nomenclature and sedimentational significance. It is noteworthy that each of the numbered iron formation units in this sequence (2, 4, 6, 8) is lithologically distinct from the others, as well as from the top-most Boolgeeda Iron Formation, which is not included. These distinctions appear in the following descriptions.

NOTE ON ORDER OF DESCRIPTION

The Dales Gorge Member of the Brockman Iron Formation (Trendall and Blockley, 1968) has in several inter-related ways played a unique part in our study: it is the main host for crocidolite; it has many subdivisions whose characteristic topographic expression makes them easy to follow in the field; and from it drilling and mining have provided magnificent fresh material for petrographic studies. As one consequence, several new terms were introduced to describe it, and we therefore depart from the normal stratigraphic practice of dealing with the rocks in depositional order. In the following description of the Hamersley Group the Brockman Iron Formation is taken first, and its members are described in order of deposition; subsequently other formations of the group follow, also in depositional order. In this way the Dales Gorge Member serves as an example for the initial clarification of nomenclature, and as a standard for much comparative reference in later description.

BROCKMAN IRON FORMATION

DALES GORGE MEMBER

DEFINITION AND TYPE SECTION

The composite type section of the Dales Gorge Member was formally designated by Trendall and Blockley (1968) as the core between 856.95 and 1,298.6 feet drilling depth in Hole 47A (lat. 22° 20'S, long. 118° 14'E) of the Australian Blue Asbestos Pty. Limited company's drilling at Wittenoom Gorge, continuing down from 303.5 to 328.75 feet in Hole Y1 (lat. 22° 25'S, long. 118° 27'E) at Yampire Gorge; except that because of broken core the parts of Hole 47A from 1,052.9 to 1,063.0 feet and 1,227.65 to 1,230.25 feet were replaced by 375.6 to 385.25 feet and 540.8 to 543.3 feet respectively of the core of Hole EC10 (lat. 22° 19'S, long. 118° 20'E). The core forming the 466.25 feet of this type section was completely illustrated by Trendall and Blockley at an approximate scale of x1/5, and they recommended that all future work on the Dales Gorge Member be specified in feet and tenths (or if necessary twentieths) by reference to the ascending scale of feet marked on the published photographs.

Selected parts of the published type section are reproduced here at a reduced scale as Figures 5 and 6.

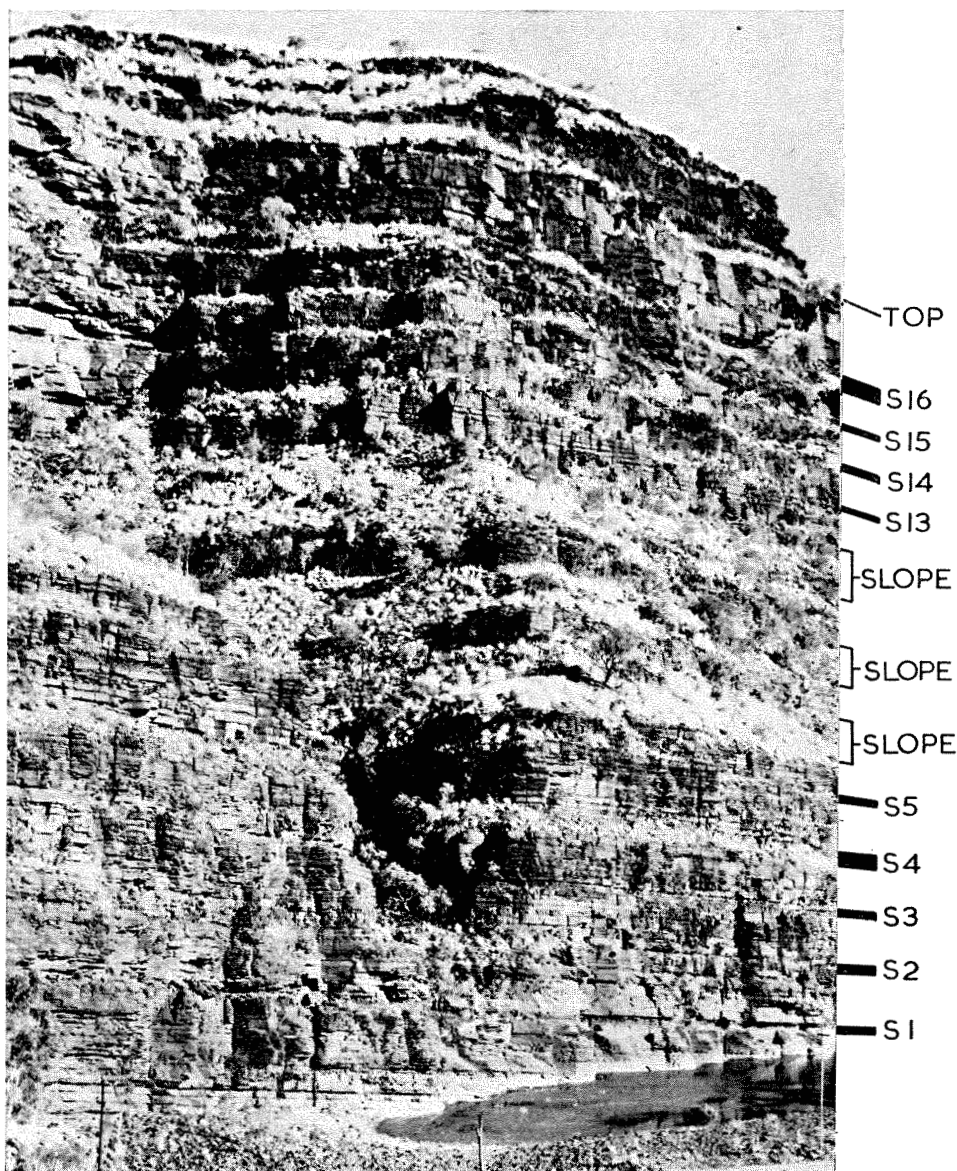


Figure 4. View of the eastern side of Wittenoom Gorge immediately north of the old Wittenoom mine buildings (see Plate 6), showing the macrobands of the Dales Gorge Member. The base of the cliff is at about the mid-point of BIF0, and the S macroband sequence up the cliff is marked. As may be expected from the right-hand column of Figure 3, the groups S6 and S7, S8 and 9, and S10, 11 and 12 tend to merge into single grassy slopes, which are marked. See also Figures 1, 20 and 69 for illustrations of surface macroband expression.

LITHOLOGY

Although a description of the lithology of a sedimentary rock usually carries some immediate broad implication of origin or facies, the present condition of the Dales Gorge Member cannot be simply or self-evidently interpreted in terms of either deposition or diagenesis. Because we have elected to separate factual description from genetic hypotheses this lithological account is confined to those compositional and textural characters of the Dales Gorge Member which appear in core or field exposure; finer details of many of the same features, which are best studied in the laboratory, though not necessarily with a microscope, are given separately in Chapter 4, and the interpretation of our data is delayed until Chapter 9.

We do not describe in detail here a number of structures which are defined principally by irregularities in the sequence of mesobands (defined below the following heading). They are dealt with instead in Chapter 6, partly because some are common to several of the iron formations, and partly because we believe (Chapters 9 and 10) that all represent post-depositional modifications of an originally undisturbed mesoband sequence. For this reason we emphasize here that in this present description of lithology the banding of the Dales Gorge Member is taken to be closer to a geometrically ideal model than is normal in field exposures.

SCALES OF BANDING

Trendall (1965a, p. 56) first defined three scales on which the iron formation of the Dales Gorge Member could be described as banded:

1. Coarse *macrobanding*: major alternation between two contrasted lithologies, banded iron formation and 'shale'. Trendall and Blockley (1968) abandoned the provisional and unsatisfactory term 'shale' and proposed an extension of Trendall's numbering system for the 33 macrobands into which they divided the Dales Gorge Member: macrobands BIF0 to BIF16 are made up of iron formation and alternate with macrobands S1 to S16, which are generally thinner and consist of shale, chert, and siderite. Macroband thicknesses and sequence are shown in Figure 3, and the field expression of macrobanding appears in Figure 4; Figure 12 of MacLeod (1966) is a fine photograph of macrobanding from just above the top of S13 to a level slightly above the middle of BIF16.

2. Medium-scale *mesobanding*: the conspicuous striped succession of internally consistent bands of different composition, with an average thickness of less than an inch, which is clearly displayed within the banded iron formation macrobands in Figures 5 and 6, and which is shown at a larger scale in Figure 7.

3. Small-scale *microbanding*: an alternation, typically within chert mesobands only, of regularly repetitive laminae of even thickness, usually in the range 0.3 to 1.7 mm and defined by a varying content of some iron-bearing mineral within the chert; microbanding is clearly visible to the naked eye as a

light and dark colour alternation (Figure 7). Most chert mesobands are internally microbanded (Table 4).

In spite of difficulties in precise definition, which are discussed below, we retain these three terms as a basis for this description of lithology, in which Trendall's (1965a) earlier descriptions are amplified, and his classification and nomenclature of mesobands are initially revised.

MESOBAND CLASSIFICATION, THICKNESSES, AND ABUNDANCE IN BIF MACROBANDS

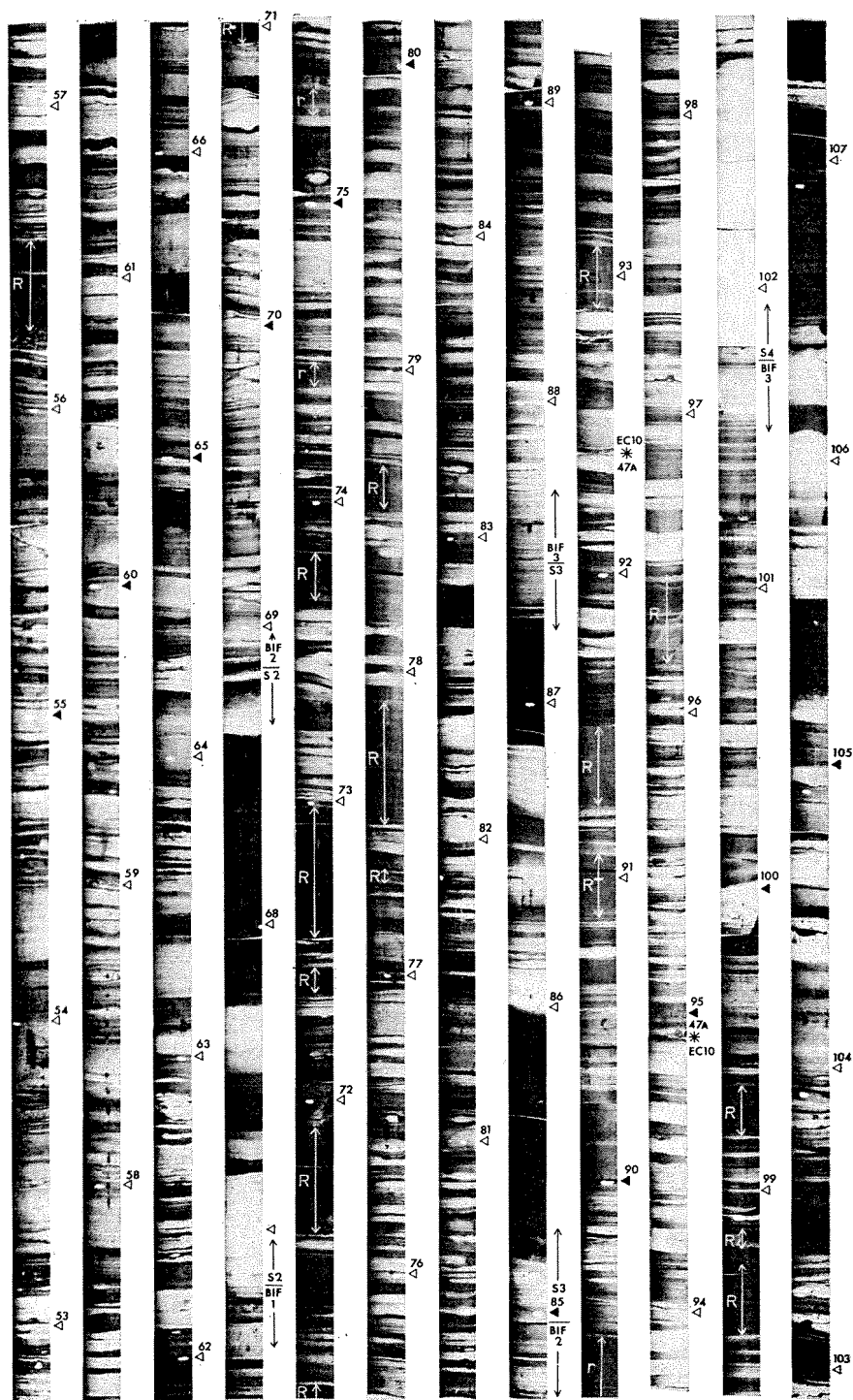
Trendall (1965a) pointed out that a qualitative compositional classification of mesobands, based on all possible combinations of the minerals known to occur, would involve an impossibly large number of types; but that in practice the following classification, based simply on the principal mineral constituent of each mesoband, was adequate:

1. Chert
2. Quartz-iron oxide (abbreviated to QIO)
3. Magnetite
4. Stilpnomelane
5. Carbonate
6. Riebeckite

We retain this form of classification, with two amendments. Firstly, since the occurrence of riebeckite is examined in a later chapter this is replaced, for the purposes of the following summaries of the main macroscopic characters of each type, by a new category: miscellaneous. Secondly, we replace Trendall's term QIO by the new term 'chert-matrix', for reasons which are explained under this heading (2) below.

1. *Chert*. Chert mesobands are pale buff, grey or pink in fresh core. Weathered cherts are usually yellow-stained, but may be dark brown, red or green; in the field they resist weathering and stand out in cliff faces. By definition here cherts have over 50 per cent of quartz by volume, but most have more than 60 per cent; the remaining material consists variously, in fresh rock, of magnetite, hematite, stilpnomelane, and carbonates. Most chert mesobands have internal

Figure 5 (opposite page; reduced from Plate 29 of Trendall and Blockley, 1968). Part of the type section of the Dales Gorge Member, from 52.75 to 107.5 feet. The core runs stratigraphically upwards from lower left to upper right, and the footage marks to the right of each column indicate feet above the base of the member (which is also that of the Brockman Iron Formation). Arbitrary macroband boundaries based on the appearance of magnetite are also marked. The dark green or black shale of the S macrobands and the bright blue of massive riebeckite are indistinguishable on these photographs, and massive riebeckite mesobands are therefore marked by a white R; the letter r indicates that sufficient riebeckite is present within a chert mesoband to give a perceptible blue colour. The three chert mesobands in the chert-siderite within S3 (see Figure 14) have basin-wide continuity. The figures between the 92 and 93 footage marks, and immediately below the 95-foot mark, show the drillhole numbers of the core used in the type section. The adit roof riebeckite (Trendall and Blockley, 1968) is at 77.5 to 77.95 feet.



microbanding, but some are structureless. Chert thicknesses, and a subdivision into types, are discussed under the next heading.

Although most cherts are laterally continuous, with either straight or wavy margins (Figure 7) a common feature of some chert mesobands is apparent lateral pinching out or 'podding'. Although chert podding is described fully later (Chapter 6) it may here be noted that the commonest form has, in plan, a randomly reticulate amoeboid appearance which causes, in vertical section, an apparent discontinuity of parts of chert mesobands which are in fact connected in a single sheet (Figure 38).

2. *Chert-matrix*. This is the characteristic enclosing material of chert pods, and the common dark separating material between successive chert mesobands. It is dark grey, greenish, or brown when fresh but usually black or dark rusty red when weathered; it is more susceptible to weathering than chert. Chert-matrix is fine-grained material which lacks the regular microbanding of chert and has instead an irregular striping due to variations in magnetite content. This striping has ill-defined margins and is highly variable in thickness. By comparison with the clarity and regularity of chert microbanding the striping of chert-matrix is vaguely defined and ghost-like. There is very rarely any difficulty in deciding whether any mesoband should be classified as chert or chert-matrix. Chert-matrix in the Dales Gorge Member typically contains 30 to 40 per cent of quartz and 30 to 50 per cent of magnetite, with smaller and variable amounts of hematite, carbonates, and stilpnomelane. For this reason it was originally called 'quartz-iron oxide' or 'QIO' (Trendall, 1965a). However, material with equivalent textural (and probably genetic) relationship with chert mesobands in other iron formations of the Hamersley Group often consists of mineral combinations such as quartz-stilpnomelane or stilpnomelane-hematite. It seems better now to use one term for all such material regardless of composition, rather than to introduce a family of confusing terms (e.g. QS, SH, and so on) which would need thin-section examination before they could be properly applied.

3. *Magnetite*. Mesobands consisting mainly of magnetite usually have a small proportion of quartz, hematite, or stilpnomelane. They are typically black, with no internal structure. By increase in the quartz and hematite contents, in particular, there is complete gradation between magnetite and chert-matrix mesobands, and judgment between them outside the laboratory is subjective.

4. *Stilpnomelane*. Mesobands consisting mainly of stilpnomelane are usually black or greenish and brittle in core, and deeply weathered to yellow clay in the field. They usually have no internal structure, but a faint colour

Figure 6 (opposite page; reduced from Plate 35 of Trendall and Blockley, 1968). Part of the type section of the Dales Gorge Member, from 385.0 to 441.3 feet. Symbols are explained in the caption of Figure 5. Refer to Table 6 for the positions of two Calamina cyclothem sequences, in macrobands BIF15 and BIF16.

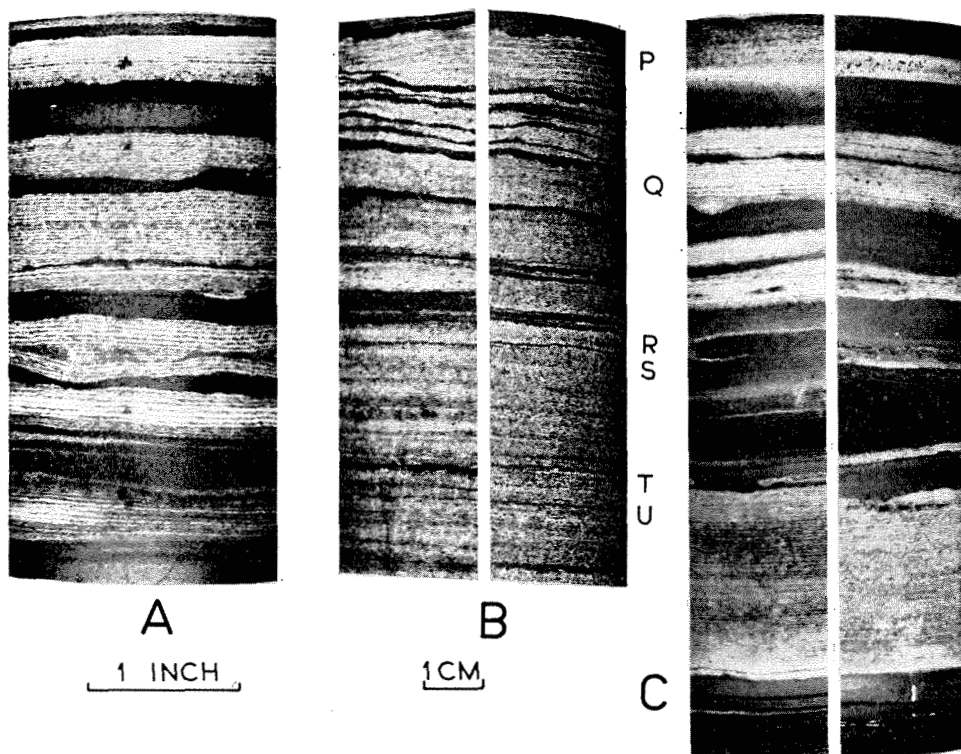


Figure 7. A. Part of the type section core from BIF0 of the Dales Gorge Member at 36.2 to 36.5 feet rephotographed at a larger scale to show details of the microbanding within chert mesobands, which are separated by chert-matrix. Note that the side of the core shown is not precisely that in Plate 28 of Trendall and Blockley (1968). There is only slight variation of microband interval within any one mesoband, and the microbanding is generally concordant with mesoband edges; apparent discordance, as at the base of the second chert from the top, is discussed further in Chapter 4, as is also the internal microband discontinuity in the chert just below the centre.

B. Cores of part of the BIF12 macroband of the Dales Gorge Member, representing 297.3 to 297.6 feet on the type section; this is the upper part of the chert-magnetite group of a Calamina cyclothem in a part of the member where this cyclothem is particularly well developed (see Table 6, Figure 13A, and Trendall and Blockley, 1968, Plate 33). The left-hand half is from Hole 51 at Wittenoom Gorge (see Plate 6) and the right-hand half is part of the type section itself, from Hole 47A. The two holes are 4.1 miles (6,614 metres) apart, and the close similarity, both in the details of mesoband sequence and in minor irregularities within the thick lowest chert, is self-evident. The letters P-U are used during discussion in the text.

C. Cores of part of the BIF2 macroband of the Dales Gorge Member, representing 77.0 to 77.4 feet on the type section (see Figure 5), just below the adit roof riebeckite (Chapter 7). The left-hand half is from Hole JG1 at Junction Gorge and the right-hand half from Hole 40 at Wittenoom Gorge; these two holes are 51 miles apart. While the mesoband sequences match less exactly than in B there is no difficulty in recognizing the correlation. In the core itself this is made simpler by the colouring; for example, the dark

striping is sometimes present. The petrography of stilpnomelane mesobands is discussed later (page 109).

5. *Carbonate*. Carbonate mesobands are not abundant within the banded iron formation. They are usually thin, internally structureless, and deeply weathered in outcrop. Carbonate mineralogy is discussed later (page 118).

6. *Miscellaneous*. In this category are placed various unusual types that do not fit into the five previous categories either because they consist of mixtures of two or more minerals in nearly equal proportions or because they consist mainly of some unusual mineral. They may be mixtures of magnetite and stilpnomelane, carbonate, and stilpnomelane, or quartz and carbonate, or may consist largely of apatite. Some unusual mesobands described later, are placed here because they have structures not typical of any of the foregoing categories.

Although a first glance at the iron formation as a whole (Figures 5 and 6), and at such clearly defined mesobands as those of Figure 7A, suggest that precise specification of mesoband thickness should be simple, the task is surprisingly difficult. In Figure 7B the top of the chert mesoband which forms the lowest part of the core may appear to be exactly defined (at R), but this really depends whether the magnetite-rich layer at S is allowed mesoband status. In this case it seems more reasonable to call S a thicker microband, but whatever judgement be made it is obvious that there is complete downward gradation in magnetite mesoband thickness (for example, from P to Q to T to S to U) to a point where, in systematic measurement, an arbitrary limit must be drawn. The point at which this limit is set can radically affect the result, since it is also the point at which the two mesobands adjacent to the one immediately affected by the judgement are counted as two or as one.

Trendall (1965a, p. 62) noted that no properly measured estimates of the relative abundance of mesoband types had been made. In an effort to do this, a count was made of all mesobands within six stratigraphic intervals spread throughout the type section. A lower limit of one millimetre was set and all mesobands of, or above, this thickness were measured and classified. The six sections ranged from about one foot to about five feet in thickness. Each was chosen to show as wide a variation of mesoband proportions as possible, and all were free from riebeckite. Chert mesobands were subdivided into microbanded and non-microbanded types. The results are set out in Table 4 for the total 6,789 millimetres measured.

The data in this Table must be read with the difficulties both of objective mesoband identification and of setting an arbitrary lower thickness limit in mind. In general, Trendall's (1965a, p. 62) estimate of about 90 per cent for chert, magnetite, and chert-matrix (QIO) and about 80 per cent for chert and chert-matrix are confirmed, but mean thicknesses for all mesobands are surprisingly

mesoband just below the mid-point on both sides is a bright green stilpnomelane-rich mesoband, while most of the remaining material between the cherts is grey chert-matrix. The relatively thick and evenly microbanded chert in the lower part is also illustrated in part in Figure 30.

TABLE 4. RELATIVE ABUNDANCES, BY MESOBAND NUMBERS AND TOTAL VOLUME, MEAN THICKNESSES, AND THICKNESS RANGES OF MESOBAND TYPES IN BIF MACROBANDS* OF THE DALES GORGE MEMBER. ALL MEASUREMENTS IN MILLIMETRES

	Chert		Chert-matrix	Magnetite	Stilpnomelane	Carbonate	Miscellaneous	Total
	Micro-banded	Non-micro-banded						
Number of mesobands	282	82	138	278	24	15	41	860
Mean thickness	8.3	7.7	10.4	3.2	6.5	4.7	10.7	7.9
Range of thickness	1-80	1-39	1-37	1-13	1-20	1-26	1-41	1-80
Percent of total thickness	46.5	9.3	21.1	13.3	2.3	1.0	6.5	100
	55.8							
	76.9							
	90.2							

* Approximate type section footages 32-37 feet (BIF0), 60-65 feet (BIF1), 187-192 feet (BIF7), 220-222 feet (BIF9), 294-299 feet and 319-320 feet (BIF12).

low; this point is taken up again below in connection with the Calamina cyclothem. Complete data for each of the six measured levels are not given separately; they mostly show a small scatter in both thickness and bulk volume, and much of the variation can be attributed to subjectivity in identification. For example, the six readings for total chert percentages are, in stratigraphic order: 59.9, 44.1, 56.4, 44.5, 67.9, 67.3. Although the equivalent figures for magnetite are 17.3, 11.6, 14.7, 17.8, 9.8, and 2.9, the last figure is associated with a chert-matrix percentage of 29.8, while the highest, 17.8, is associated with 16.4 per cent of chert-matrix. More variation between the six measured levels is present in the minor than in the major mesoband types. Thus stilpnomelane ranges between 0 and 8.4 per cent, carbonate between 0 and 4.7 per cent, and miscellaneous between 0 and 11.4 per cent. One real difference, indicated by the Table is the tendency for magnetite mesobands to be thinner than others; although magnetite and microbanded chert mesobands are of equal numerical abundance,

magnetite has less than a third of the volume of microbanded chert. The thickness frequency distribution of the microbanded cherts measured for Table 4 is shown in histogram in Figure 9.

FURTHER CLASSIFICATION OF CHERT MESOBANDS

Trendall's (1965a, p. 63) hypothesis for the diagenetic development of various kinds of microbanded chert mesoband (modified and extended in Chapter 9 of this bulletin) was closely integrated with a nomenclatural distinction between: 'primitive chert', with relatively coarse microbanding defined by alternate ankerite and stilpnomelane in quartz; 'flat-modified chert', with relatively fine microbanding defined by hematite in quartz; and 'pod chert', similar to primitive chert but stratigraphically discontinuous. It was noted (*ibid.*, p. 64) that "the commonest type of primitive chert . . . is about half an inch thick with ten microband pairs", while "flat-modified cherts up to 5 inches thick occur with about 350 microbands". Trendall (1966a) later retained this nomenclature, but it was never clearly specified which, or what combination, of the four implied criteria (mineralogy, microband width, thickness of mesoband, number of micro-

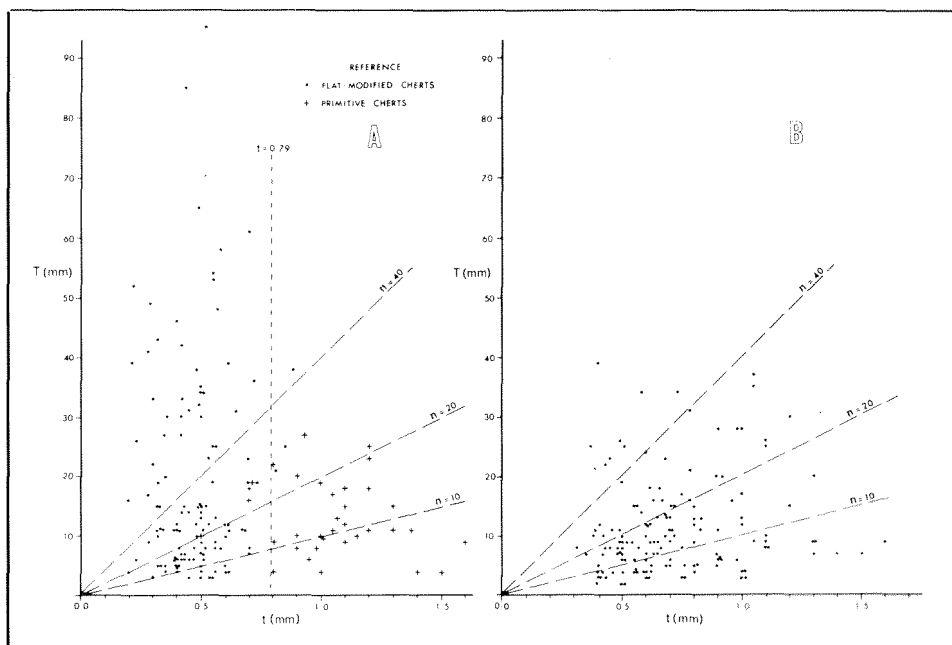


Figure 8. The relationship between mesoband thickness and microband interval in microbanded cherts of the Dales Gorge Member.

A. T plotted against t for 34 nominal primitive and 121 nominal flat-modified cherts.

B. T plotted against t for 145 unclassified cherts. The line $t = 0.79$ in A has all but three flat-modified cherts to the left and all but three primitive cherts to the right. Lines of constant n are included for ease of comparison. Although 'primitive' and 'flat-modified' cherts are clearly differentiated in A, the area in B occupied by unclassified cherts spreads indiscriminately among and between these, and destroys their 'usefulness as a practical classification.

bands) for differentiating primitive and flat-modified cherts was diagnostic and defining, rather than descriptive. Although we have found the nomenclature useful it is necessary now to examine more closely both its objective validity and its completeness as a chert classification.

Since a classification involving microband mineralogy would be applicable only after microscopic examination this criterion is initially excluded. There remain three quantitative parameters for any microbanded chert mesoband: total mesoband thickness (T), mean microband thickness (t), and number of microbands ($n = T/t$). The mean microband thickness is likely to be a useful parameter only if the variation within mesobands is comparatively small. Our immediate subjective judgement is that microband width variation with any chert mesoband is small compared with that between different chert mesobands; this is illustrated in Figure 7A. However, there is certainly some internal width variation, which is discussed further in Chapter 4 (Lateral microband continuity). We measured* these for 300 microbanded cherts in six 5-foot intervals and one 6-foot interval of the type section, chosen for absence of riebeckite, and varied lithology. The intervals used (Table 5) duplicate in part those used for the total mesoband sample, but more core was needed to obtain a sample with 300 microbanded cherts. Very thin cherts, and cherts whose microbanding was too vague, or too fine to be measured without a microscope, were excluded. Before measurement a subjective classification was made of each chert into

* Refer to Appendix A, under T, t, and n, for notes on measurement techniques and errors.

TABLE 5. MEANS AND RANGES OF THICKNESS (T), MICROBAND THICKNESS (t), AND NUMBER OF MICROBANDS (n) IN 300 MICROBANDED CHERT MESOBANDS FROM THE DALES GORGE MEMBER*, SUBJECTIVELY GROUPED. ALL MEASUREMENTS IN MILLIMETRES

		'Primitive' cherts	'Flat-modi- fied' cherts	Unclassified cherts	Total
Number of cherts in group		34	121	145	300
T {	mean	12.9	18.9	11.5	14.6
	range	4-27	2-85	2-39	2-85
t {	mean	1.06	0.47	0.71	0.65
	range	0.50-1.60	0.20-0.88	0.31-1.60	0.20-1.60
n {	mean	13	44	18	28
	range	3-29	5-236	4-98	3-236

* This table includes all cherts with measurable T and t in the type section of the Dales Gorge Member within the following approximate intervals: 31-36 feet (BIF0), 60-65 feet (BIF1), 136-141 feet (BIF5), 186-191 feet (BIF7), 251-256 feet (BIF10), 308-313 feet (BIF12), and 360-366 feet (BIF14).

primitive, flat-modified, or unclassified. The number in each of these divisions, together with mean values and ranges for T, t, and n, are shown in Table 5.

The differences between the means for T, t, and n for primitive and flat-modified cherts are clearly significant, and the two types occupy distinct areas in Figure 8A. However, this merely shows that the relevant parameters can be subjectively estimated with adequate accuracy for distinction. The real point at issue here is whether there is a continuous gradation and overlap of any or all of the possible distinguishing criteria in the total chert population, or whether a bimodal frequency distribution of any of them supports a valid natural subdivision. Since about half of the cherts are not subjectively classifiable, and these overlap (Figure 8B) the two fields of Figure 8A, there is clearly a need for some objective criteria if Trendall's (1965a) nomenclature is to remain useful.

The smoothed frequency distribution for T is shown in Figure 9. The equivalent distribution for the 282 microbanded cherts used in the course of total mesoband measurement, as reported under the preceding heading, is shown in the same figure; this illustrates the exclusion of cherts too thin for effective t measurement and suggests also that the minor maxima at 7 and 12 millimetres

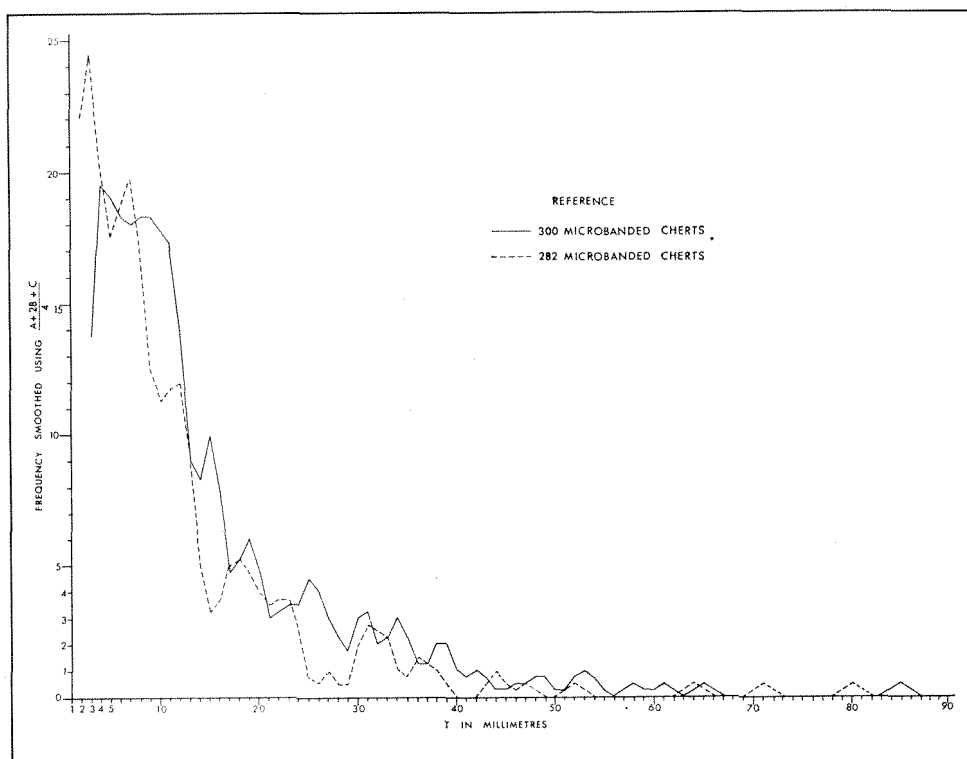


Figure 9. T frequency distribution for 300 microbanded chert mesobands of the Dales Gorge Member.

on the 282-chert frequency distribution pattern are probably not significant. There is no evidence supporting subdivision here.

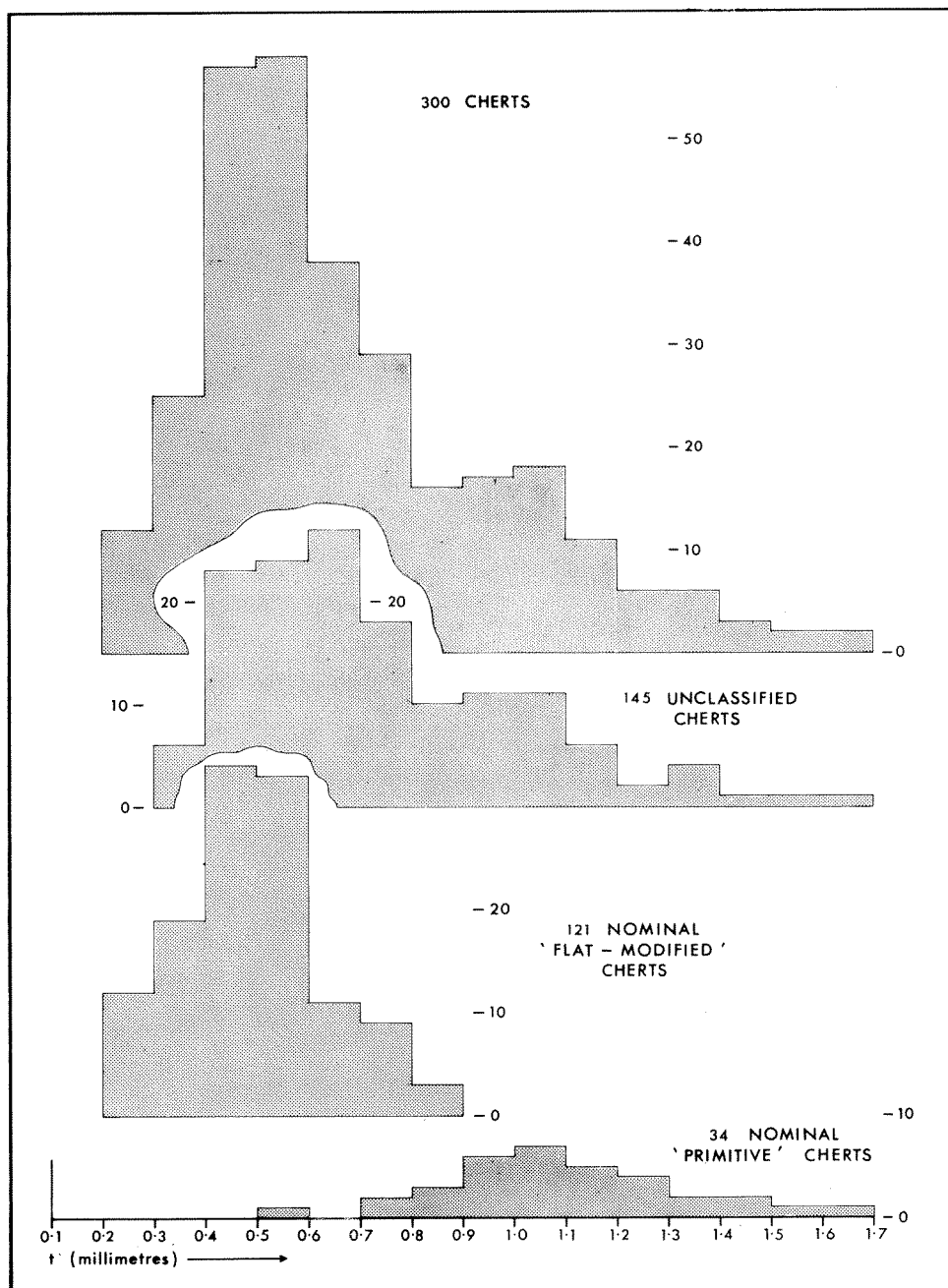


Figure 10. t frequency distribution for 300 microbanded chert mesobands of the Dales Gorge Member.

The smoothed frequency distribution for t appears in Figure 10 for all 300 cherts as well as by nominal classes. A bimodal t distribution is suggested here, with modes at approximately 0.5 and 1.0 mm, but there is a very large overlap.

In Figure 11 smoothed frequency distributions for n are shown for nominal classes as well as for all 300 cherts. Here it appears, subjectively, that the distributions of unclassified and flat-modified cherts are different and (particularly the flat-modified cherts) of an irregular pattern. The maxima at 7, 14-15, and 27 in the total frequency distribution show an interesting numerical relationship.

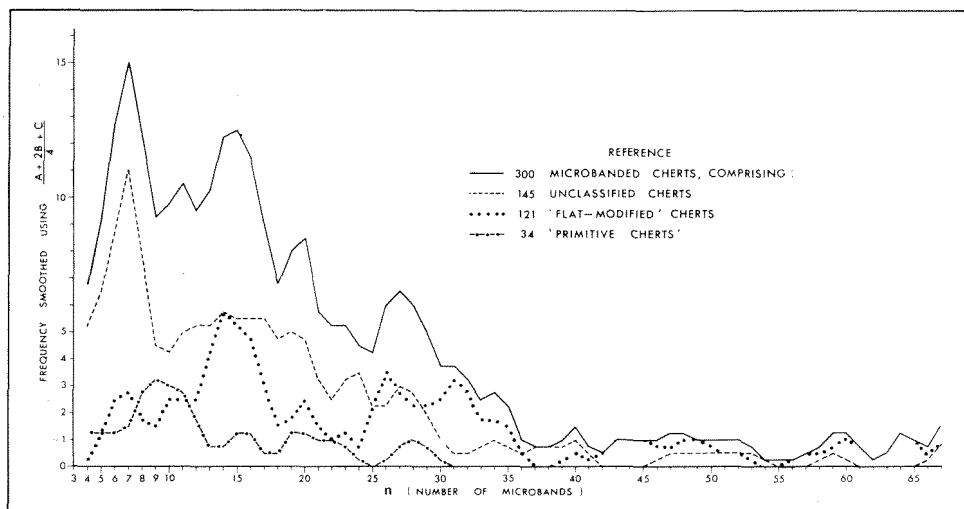


Figure 11. n frequency distribution for 300 microbanded chert mesobands of the Dales Gorge Member.

In order to test whether the possible bimodality of the t distribution is related to a difference in n distribution, further n frequency distribution diagrams were prepared for cherts selected by t interval on the basis of Figure 10A. In Figure 12 comparative n frequencies for 219 cherts with $t < 0.8$ mm and 65 with $t \geq 0.9$ mm are given (cherts with $t = 0.8$ are omitted to emphasize any correlation present). The differences in pattern are striking, and strongly suggestive of some significance for chert classification; however, nothing of immediate practical applicability is likely to come from such a relatively subtle means of differentiation, applicable only to cherts in groups, and attention is more profitably turned to the significance of mesoband sequence in chert differentiation.

MESOBAND SEQUENCE IN BIF MACROBANDS: THE CALAMINA CYCLOTHEM

Although Trendall's earlier (1965a, p. 62) estimates of mesoband proportions correspond accurately with the measurements of Table 4, the mean mesoband thickness, and particularly the mean microbanded chert thickness, of this Table are lower than Trendall's descriptions suggest. He (Trendall, 1965a, p. 62) noted cherts up to 5 inches thick, with thicknesses of $\frac{1}{2}$ to 2 inches common; of

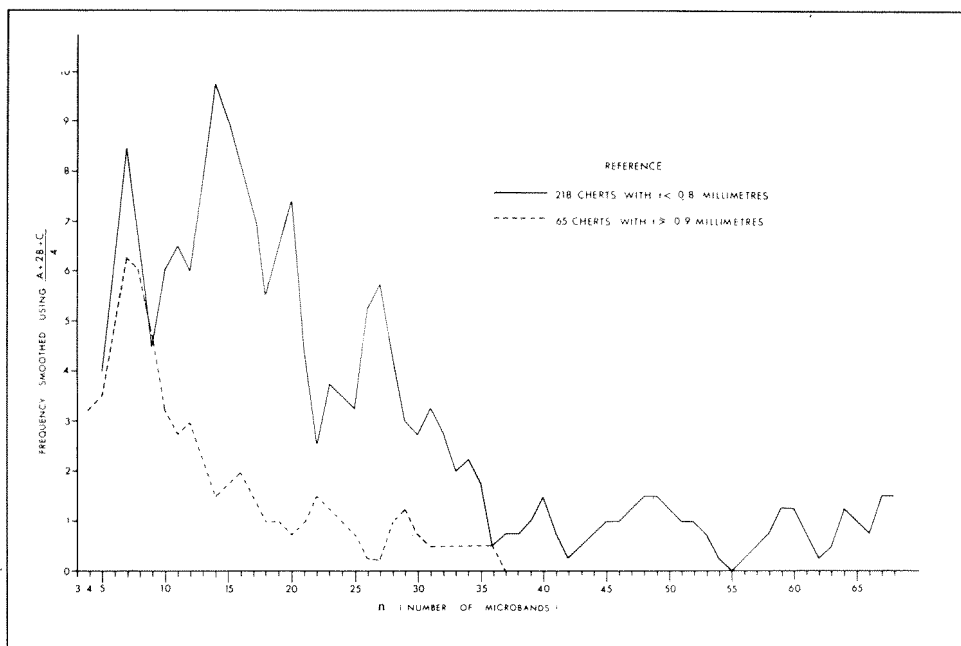


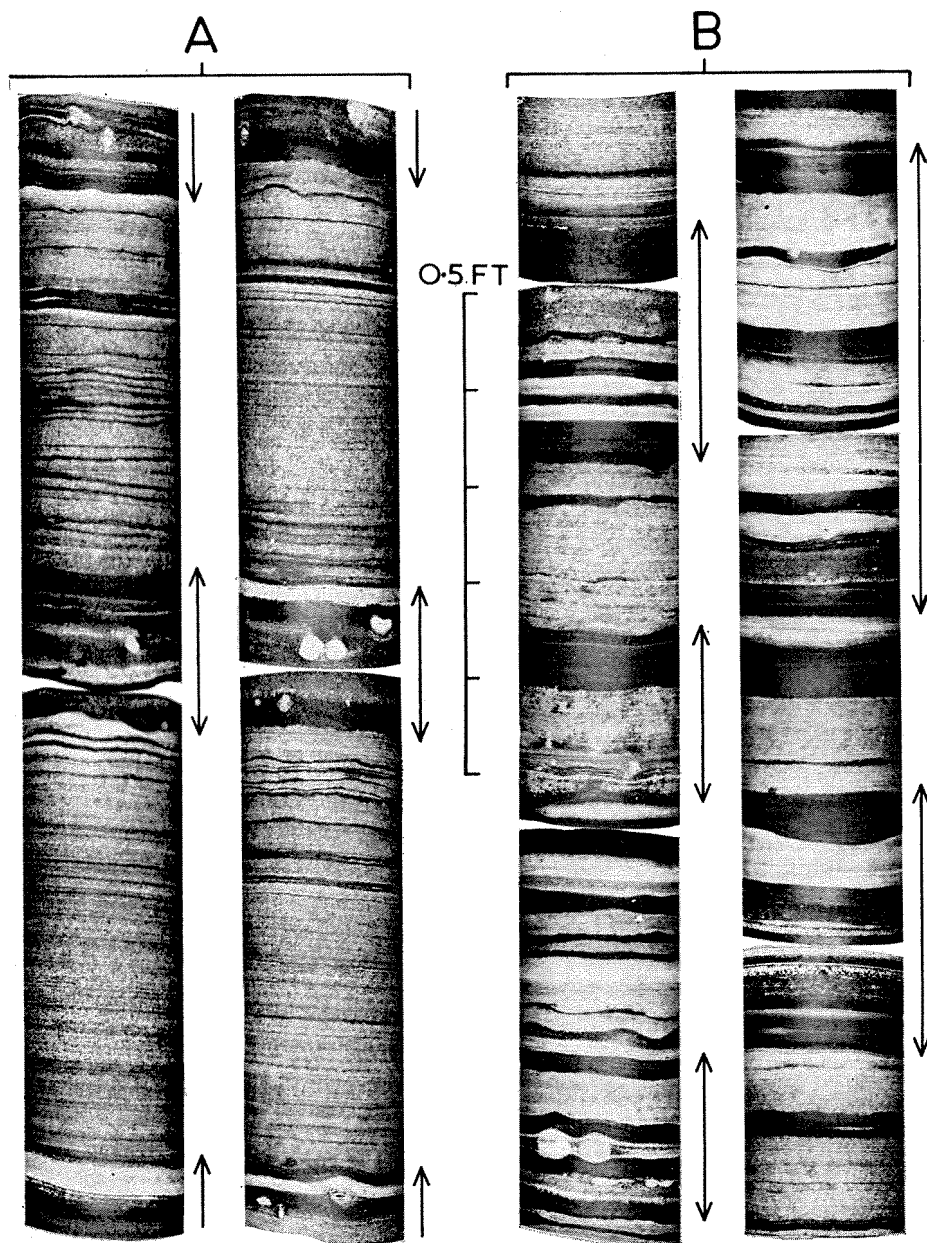
Figure 12. n frequency distribution for two groups of microbanded chert mesobands arbitrarily divided by t .

the 282 microbanded chert mesobands measured for Table 4, 205 are 12 mm or less thick ($\frac{1}{2}$ inch = 12.7 mm). The resolution of this anomaly lies partly in the definition of a mesoband and partly in the existence of a characteristic mesoband sequence which is here described and named the Calamina cyclothem. It was referred to briefly by Trendall and Blockley (1968) and previously, but not by name, by Trendall (1965a, p. 60; 1966b, p. 76 and Plate 39).

The Calamina cyclothem is defined as a common cyclic sequence of mesoband types in the BIF macrobands of the Dales Gorge Member, in which either a single thick chert mesoband with fine microbanding, or a group of such cherts separated by thin magnetite mesobands, alternates repeatedly at regular intervals with a mixed mesoband group of chert-matrix, magnetite, and comparatively thin and coarsely microbanded cherts. These two parts of the cyclothem are referred to below as the chert-magnetite group and the mixed group.

Figure 13 (opposite). Differing expressions of the Calamina cyclothem in the Dales Gorge Member.

A. Part of the type section core of BIF12, from 296.0 to 298.2 feet. A different side of the core from that illustrated by Trendall and Blockley (1968, Plate 33) is shown in this larger-scale photograph. The core runs stratigraphically upwards from lower left to upper right, and includes four complete Calamina cyclothems, taking the start and finish of a cyclothem as the centre of the mixed group. Mixed groups are marked by adjacent double-headed arrows, the unmarked parts are the chert-magnetite groups, previously called 'flat-modified' cherts. Note the variation of mesoband subdivisibility in the chert-magnetite



groups, and the virtual absence of chert mesobands and presence of small spheroidal nodules (Chapter 6) in the mixed groups. The field appearance of a similar sequence in BIF16 is shown in Figure 19A.

B. Part of the type section core of BIF0, from 33.2 to 35.4 feet. Parts of five Calamina cyclothems are illustrated, and marked as in A. By comparison with A note the wide thickness variation in successive cyclothems, the equal abundance of cherts (differently coloured) in both groups, and the incipient development of small spheroidal nodules in only the mixed groups.

TABLE 6. TYPE SECTION FOOTAGE LIMITS AND THICKNESSES IN FEET OF CONSPICUOUS EXAMPLES OF THE CALAMINA CYCLOTHEM

Type section footage limits	Thickness	Type section footage limits	Thickness	Type section footage limits	Thickness
BIF16		BIF16		BIF15	
451·5	0·7	435·0	0·75	384·5	0·60
450·8	0·7	434·25	0·65	383·9	0·55
450·1	0·6	433·6	0·75	383·35	0·50
449·5	0·7	432·85	0·95	382·85	0·50
448·8	0·5	431·9	0·8	382·35	0·54
448·3	0·65	431·1	0·7	Mean	
447·65	0·65	430·4	0·65	BIF12	
447·0	0·6	429·75	0·75	300·9	0·60
446·4	0·6	Mean		300·3	0·45
445·8	0·45	BIF15		229·85	0·60
445·35	0·70	389·65	0·55	299·25	0·50
444·65	0·62	389·1	0·50	298·75	0·55
Mean		388·6	0·55	298·2	0·55
		388·05	0·45	297·65	0·60
		387·6	0·55	297·05	0·50
		387·05	0·50	296·55	0·55
		386·55	0·60	296·0	0·60
		385·95	0·53	295·4	0·55
		Mean		Mean	

The limits and thicknesses of 39 of the most clearly defined cyclothems on the type section, in macrobands BIF12, BIF15, and BIF16, are given in Table 6. The sequences from 385.95 to 389.65 feet and 429.75 to 435.0 feet are illustrated in Figure 6, while the individual cyclothems from 296.0 to 298.2 feet are shown at a greater scale in Figure 13A. All 39 cyclothems specified in Table 6 have a mean thickness of 0.60 feet. For the purposes of these measurements

the limits of a cyclothem are arbitrarily taken as the middle of the mixed group. However, boundaries between the two groups are gradational, and similar at top and bottom, so that there are no obvious breaks defining the natural beginning and end of each cyclothem for measurement or description. The chert-magnetite group usually occupies between a half and three-quarters of the total cyclothem thickness, and the whole group tends, on erosion, to stand out as a single unit bordered by the more deeply weathered mixed groups above and below (Figure 19A). The whole of such groups, including their magnetite mesobands 1 to 3 mm thick, were included in Trendall's (1965a, p. 60-62) flat-modified cherts, and gave rise to the descriptions of cherts 5 inches thick. It is unfortunate, but unavoidable, that an arbitrary lower limit of one millimetre for the objective measurement of mesobands in fresh core leads to a concept of a mesoband which does not correspond exactly with that given by the effect of erosion on the mesoband sequence of the Calamina cyclothem, but so long as this is understood there is no danger in this slight imprecision in mesoband definition; as with many definitions, more precise limitation would decrease the usefulness of the term.

In the conspicuous examples of the Calamina cyclothem given in Table 6 there is some variety in the composition of the mixed groups between the chert-magnetite groups. Mixed groups usually have a generally darker tone in core and may consist of material gradational between chert-matrix and magnetite which is not mesobanded at all, for example the cyclothem in BIF15 from 387.05 to 388.6 feet (Figure 6). Alternatively there may be several thin and coarsely microbanded cherts closely packed in this part of the cyclothem, as in the cyclothem between 429.75 and 435.0 feet (also Figure 6); cherts in this position are very commonly podded (e.g. 432.9 to 433.0 feet) whereas the finely microbanded cherts in the chert-magnetite part of the cyclothem are only partially podded, if podding occurs at all. The 'primitive' cherts of the earlier classification invariably form part of the mixed groups. Another characteristic feature of mixed groups is the presence of small spheroidal nodules (Figure 13A). These are further described in Chapter 6. Stilpnomelane is very abundant in the mixed group of some Calamina cyclothem sequences (e.g. BIF1, 60 to 65 feet) but is present in only small quantities elsewhere.

Once its existence is recognised where it is conspicuously developed, the Calamina cyclothem can be followed at other levels where it is less apparent. Three examples of sequences of decreasing strength are given in Table 7. That of BIF0, in particular, could not be detected from the photographs alone, and reference to the core is necessary. It is illustrated by Figure 13B.

TABLE 7. TYPE SECTION FOOTAGE LIMITS AND THICKNESSES IN FEET OF LESS CONSPICUOUS EXPRESSIONS OF THE CALAMINA CYCLOTHEM

Type section footage limits	Thickness	Type section footage limits	Thickness	Type section footage limits	Thickness
BIF6		BIF14		BIF0	
168·9	0·6	370·45	0·35	34·5	0·4
168·3	0·5	370·1	0·4	34·1	0·5
167·8	0·55	369·7	0·75	33·6	0·4
167·25	0·75	368·95	0·5	33·2	0·4
166·5	0·6	368·45	0·4	32·8	0·35
Mean		368·05	0·35	32·45	0·41
		367·7	0·3	Mean	
		367·4	0·44		
		Mean			

REASSESSMENT OF CHERT MESOBAND CLASSIFICATION

It now appears both that: (1) alternation of mesoband groups with cherts of two types (a main difference being relatively coarse and fine microbanding) defines the Calamina cyclothem, and (2) the Calamina cyclothem can be used to define the chert types comprising it. This is not a circular argument; it is simply that the microbanding in the cherts of the chert-magnetite groups of one succession of Calamina cyclothem, although fine relative to that in the cherts of its associated mixed groups, may be coarser than the microbanding in the cherts of the mixed groups of another succession of Calamina cyclothem in a different part of the type section, although the microbanding of these cherts will be coarser again than that of the cherts of their associated chert-magnetite groups. Any attempt to set absolute values of *t* in classifying cherts throughout the Dales Gorge Member, without reference to the Calamina cyclothem, is therefore unlikely to be practically useful. A study of *t* in microbanded cherts based on departure from a locally restricted running average, would probably yield useful results, but for present purposes we propose simply to discontinue the names 'flat-modified' and 'primitive' cherts and to use instead unequivocal non-genetic descriptive terms where it is necessary to specify a class of chert mesoband with restricted characteristics.

FIELD ASSESSMENT OF BIF LITHOLOGY

Ryan and Blockley (1965, p. 21-22) distinguished two lithologies of banded iron formation in the Dales Gorge Member: 'even-bedded' and 'wavy-bedded'. This distinction is largely dependent on the degree of regularity of the Calamina cyclothem and the extent to which cherts are developed in the mixed groups, good development of the cyclothem giving very even bedding, and vice versa. It is very rarely that the Calamina cyclothem cannot be seen at all. The two main types of departure from any sign of adherence to it are firstly where there is a complete absence of clear chert-magnetite groups throughout the macroband, and secondly in intervals about 2 feet thick in which there is a close but rather wavy sequence of thin cherts separated by only thin mesobands of magnetite or chert-matrix. In the brief summary of BIF macroband lithology of Table 8 in terms of Calamina cyclothem development, this is referred to as a close-packed chert sequence.

MACROBANDS S1-16

In the type section (Trendall and Blockley, 1968) these macrobands vary in thickness between 2.05 and 17.95 feet (S2 and S5; S6). In thickness alone there seems to be a possible division into nine 'thin' macrobands (S1, 2, 3, 5, 7, 8, 12, 14, 15; mean 3.1 feet; range 2.05 to 4.45 feet) and five 'thick' macrobands (S4, 6, 9, 11, 16; mean 15.2 feet; range 13.55 to 17.95 feet), with S10 and S13 falling into neither group.

Although each of these macrobands is typically expressed in the field as a single erosional unit (Figure 4) it is convenient to describe their lithology in terms of two main components: shale proper and chert-siderite. This division was first made by Trendall (1966b); it still seems valid and useful, although, as we discuss in Chapter 10, we doubt whether the division is as simple or as sharp as was first thought. The following descriptions are largely based on core samples, since clean fresh field exposures are rare. The distribution of these two main types in each of the S macrobands appear in Figure 14, together with that of other minor constituents noted in the following paragraphs. Together they comprise some 94 per cent of the total S macroband thickness, with chert-siderite contributing a slightly greater thickness than shale. There is a broad alternation of the two types rather than close interlamination.

Chert-siderite (see Figures 5 and 6, in conjunction with 14A) has mesobanding on the same scale as that of the BIF macrobands, with microbanded chert mesobands usually between 2 and 6 cm thick separated by dark green sideritic material. The microbanding in these cherts is usually between 1 and 2 mm wide, but no detailed measurements have been made as for those of the BIF macrobands. The microbanding has a number of characteristic features which are described in the following chapter (Figure 22). The intervening sideritic material is either very finely laminated, more or less structureless, or thinly bedded with an evident clastic structure defined by colour variation in the uniformly fine-grained siderite. None of this material is ever fissile, whether

TABLE 8. SUMMARY OF STRENGTH OF EXPRESSION OF THE CALAMINA CYCLOTHEM IN THE BIF MACROBANDS OF THE DALES GORGE MEMBER, WITH NOTES OF GROSS DEPARTURES FROM THE CYCLOTHEM, AND OF OTHER SPECIAL FEATURES

BIF macroband	Expression of Calamina cyclothem	Additional notes
16	Strong (Table 6)	Close-packed cherts at centre (c. 438-440) and top (c. 456-459)
15	Strong (Table 6), weakening upwards	
14	Moderate; rather thin (Table 7)	
13	Moderate to weak	
12	Strong top and bottom (Table 6)	Close-packed cherts at centre (c. 304-306)
11	Strong in centre, weak at top	Close-packed cherts at base (c. 277-279)
10	Moderate to weak; rather thin	Close-packed cherts at base (c. 249-252). Stilpnomelane-rich
9	Moderate to weak; rather thin	Stilpnomelane-rich
8	Weak; thin	Close-packed cherts at base (c. 197-200)
7	Moderate	
6	Fairly strong (Table 7)	
5	Weak	
4	Very weak to absent	Close-packed cherts at base (c. 115-117)
3	Moderate to weak	
2	Moderate to weak	Close-packed cherts at base (c. 69-70.5) = Upper Seam
1	Moderate to weak	
0	Moderate to weak (Table 7)	

or not it is laminated. Some thin beds of clastic appearance are clearly graded over thickness of up to 2cm. We prefer not to extend the mesoband-microband nomenclature to cover the various scales of stratification in the siderite, which has the same textural relationship to the microbanded chert mesobands within it as has chert-matrix to the cherts of the BIF.

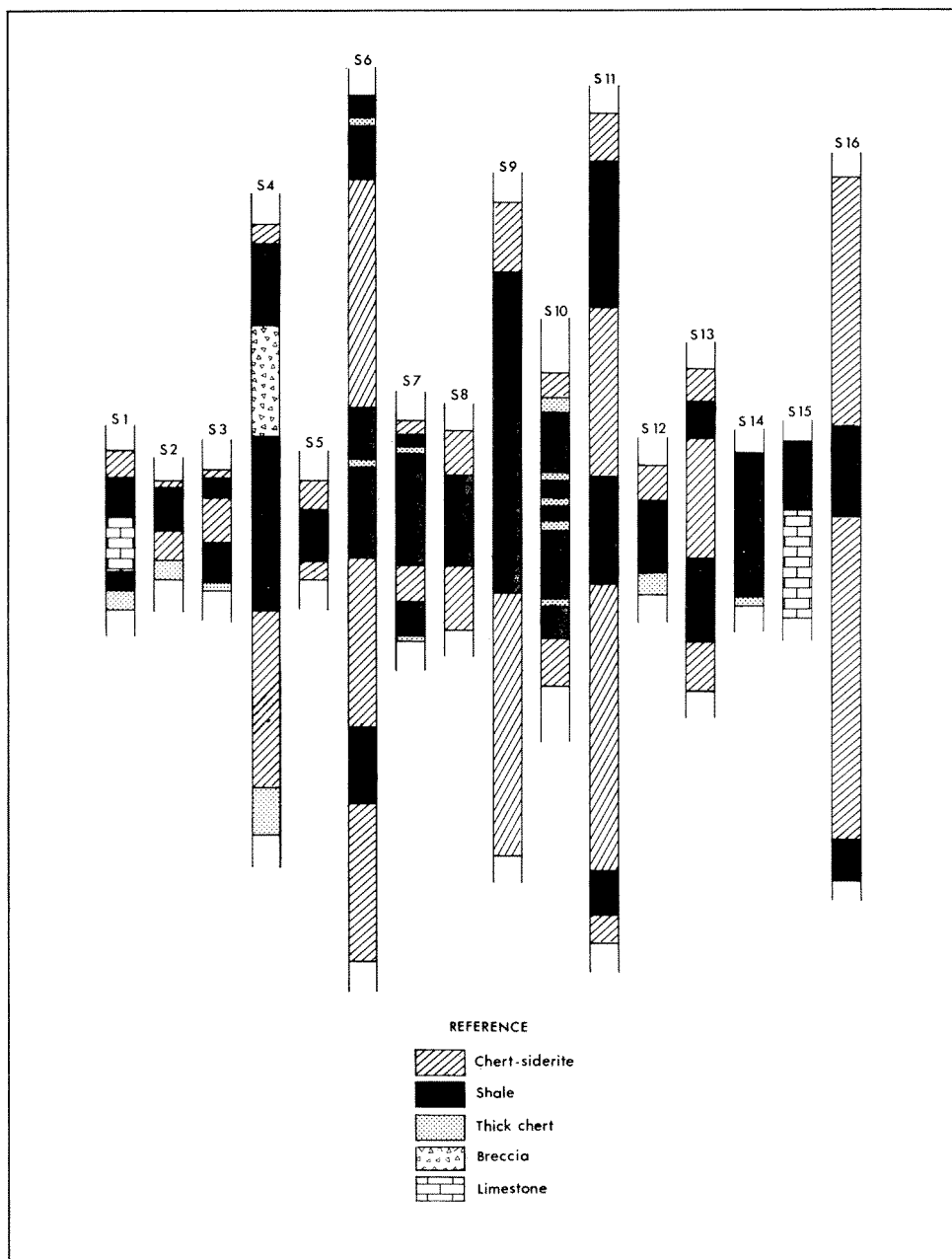


Figure 14. Comparative lithology within macrobands S1-S16 of the Dales Gorge Member.

The shale proper normally has no mesoband scale stratification within it, and forms intercalations mainly 1 to 4 feet thick within the S macrobands (Figure 14). The shale of S9, some 6.5 feet thick, is by far the thickest individual shale. Shale is rarely exposed in the field. In core it is dark green, dark grey, or black, and like the siderite of the chert-siderite it may either be finely laminated in shades of these colours or apparently structureless. One type of regular lamination, and the thin tuffaceous shard bands, are described in Chapter 4. In general it is massive or brittle rather than fissile but the shale of some S macrobands (e.g. S10) splits very finely and evenly in exposed core; this is never exposed in the field.

Some shales have intercalated beds with clastic texture defined by colour variations like that of the siderite, and, as in the siderite, graded beds may be thus defined. An exceptionally thick one is present in the type section at 410.5 to 410.7 feet (Figure 6). In S16, S7, and particularly in S4, these clastic textures are locally the most conspicuous lithological features present. A coarse breccia is intercalated within the higher part of S4 throughout the central and eastern parts of the Hamersley Range (type section 110.35 to 112.3 feet), and is well exposed in Wittenoom, Calamina, Yampire, and Dales Gorges. Its thickness varies between about 2 and 5 feet, and the base is certainly stratigraphically discordant; this is clearly demonstrable both from intersections in the available drillholes at Wittenoom and from the exposures at Calamina Gorge. It is not clear whether the upper contact of the breccia is similarly discordant. It consists of a jumbled mixture of rounded and angular fragments of shale and chert mostly varying in size from a few inches in diameter at the base to less than an inch at the top; occasional disproportionately larger pieces of shale and chert reach lengths of several feet, and all lie in a structureless green matrix. A curious feature of many of the largest chert pieces is that they lie at the top of the otherwise graded breccia, as though floating in the finer material.

Although in general chert mesobands do not occur within shales in the same way as in the chert-siderite there are occasional exceptions; chert mesobands, in thickness and microband interval similar to those of the chert-siderite, occur in the shale of S6, S7, and S10, and are marked in Figure 14. In several of the S macrobands an exceptionally thick and coarsely microbanded chert mesoband lies at or near the base; these are also shown in Figure 14, in S1, S2, S3, S4, S12, and S14.

S1 and S2 are frequently, S3 is rarely, and S15 is almost invariably, represented by limestone. For reasons given later (p. 114) this is believed to be a late diagenetic replacement. In core it is very pale grey and massive, but weathers to grey or yellowish brown in the field. Wherever it is well exposed the stratification of the parent shale is etched out more distinctly than in the original rock. In S1 at both Dales Gorge and Yampire Gorge, fine cross-bedding is thus revealed; no consistent orientation has been observed.

LATERAL STRATIGRAPHIC CONTINUITY

GENERAL STATEMENT

Some parts of the Hamersley Group exhibit a degree of lateral continuity in their lithostratigraphic detail unparalleled in the sediments of any other recorded depositional basin, of any age. The closest recorded approach to a similar order of correlation appears to be that of the Permian Zechstein evaporites of western Germany (Richter-Bernburg, 1960), but the thickness involved there is only about a metre. Within the group there are, ignoring microbanding, at least 100,000 lithostratigraphic (mesoband) boundaries available for attempted correlation. It is obviously a misuse of time, if not a physical impossibility, to observe and record these at every available exposure over an outcrop of 20,000 square miles. It is therefore appropriate to show first why some levels were chosen for particular attention, why we think other levels may be as well, or less well, correlatable as those in which correlation was tested, and why the examples illustrating this bulletin were selected. It is appropriate also to discuss here some of the general principles which have governed our acceptance or non-acceptance of the small-scale lithostratigraphic correlations with which we are concerned.

Our present knowledge of lateral continuity grew over a period of about five years. What started as a purely exploratory study in the first year had its objectives more sharply defined each year on the basis of the accumulated results. Thus the totality of presently available evidence does not necessarily correspond with that which would have been sought initially if the final result could have been foreseen. However, it is not necessary now to retrace the various steps in which our existing knowledge was acquired, and we list the following principles, which took form gradually over the whole period of the study, as though they were more consciously systematised and accepted from the start than was the case:

1. *Vertical restriction of effort.* We accept that, faced with the task of determining the full lateral extent of some 100,000 boundaries observably continuous in single exposures, it is best to determine the continuity of a selected few of these in detail.

2. *Successive scale reduction.* The levels chosen should form part of as numerous a hierarchy of stratigraphic orders as possible (e.g. formation-member-macroband-mesoband-microband) so that their small thicknesses can confidently be identified within a large scale framework before time is spent on detailed comparison.

3. *Greatest extent.* The levels chosen should be those likely to show greatest lateral correlation, since this is the most difficult limiting parameter to establish. No rules other than trial-and-error with subjective feedback can guide this choice.

4. *Subjective comparison.* Once the limited thickness for detailed comparison is identified by its relative position with a larger reference framework we accept subjective assessment of similarity as the only practicable means of

establishing distant correlation. The reliability of subjective comparison can be strengthened by consciously separate use of different scales. For example, two mesobands in different localities identified as occupying the same relative level within a macroband can be correlated by assessing the degree of similarity of their status in the mesoband sequence above and below; after this first judgment is made a separate comparison can then be made of any internal discontinuities or other characteristics.

5. *Extension of detailed study.* When the full areal extent of a small stratigraphic thickness is established, the applicability of these observations to other levels must be based on an assessment of the general similarity of the stratification between it and other levels. The confidence with which any belief about the lateral stratigraphic continuity of any level not observed in detail can be held is clearly proportional to the reliability of this assessment of similarity.

These principles may seem, wholly or partly, self-evident; we nevertheless think them worth setting out. The observed and inferred lateral stratigraphic continuity in the Hamersley Group is one of the most important results of our study for pure geology, and it is as well to establish clearly the status of our inferences. The principles explain also why there is an imbalance in our data between different formations; they indicate the necessity and scope for further work; and they show why in this chapter we express belief in the lateral continuity, or otherwise, of lithostratigraphic divisions which have not been worked on in detail. Above all they explain why the macrobanding of the Dales Gorge Member makes it (point '2', above) an obvious choice for internal selection of small thicknesses for detailed study. It remains to give examples of the degree of similarity which we require before accepting correlation, and to show, both under the next heading and in Chapter 4 (Lateral continuity of microbanding), some of the limitations on correlation.

MACROBANDS AND MESOBANDS

In our formal designation of the type section of the Dales Gorge Member (Trendall and Blockley, 1968) we asserted that all 33 macrobands are, given adequate exposure, easily distinguishable in the field over almost the entire outcrop area. The field expression of these macrobands is shown in Figure 4; there is no difficulty in relating the illustrated cliff to Figure 3. Nothing need be added to the earlier statement, except that those areas in which all the macrobands are not recognisable are noted under the following heading.

Examples of the standard of similarity which we require for confident mesoband correlation in BIF macrobands appear in Figure 7. The maximum separation in these is 51 miles, the longest distance available between boreholes. Figure 7C shows the subjective correlation of mesobands by equivalence of their status in the mesoband sequence, while Figure 7B shows also the correlation of discontinuities within a mesoband, and of bands at about the arbitrarily accepted lower limit of one millimetre for mesoband status.

Figure 15 shows the longer range correlation of the internal characteristics of a chert mesoband from BIF0, using surface material. There is sufficient similarity of internal features to support the initial correlation made quite independently by status in the mesoband sequence, followed downwards from the top of the macroband. There is no doubt that mesobands are, like macrobands, potentially correlatable over the whole outcrop area. It remains to note some limitations on mesoband correlation.

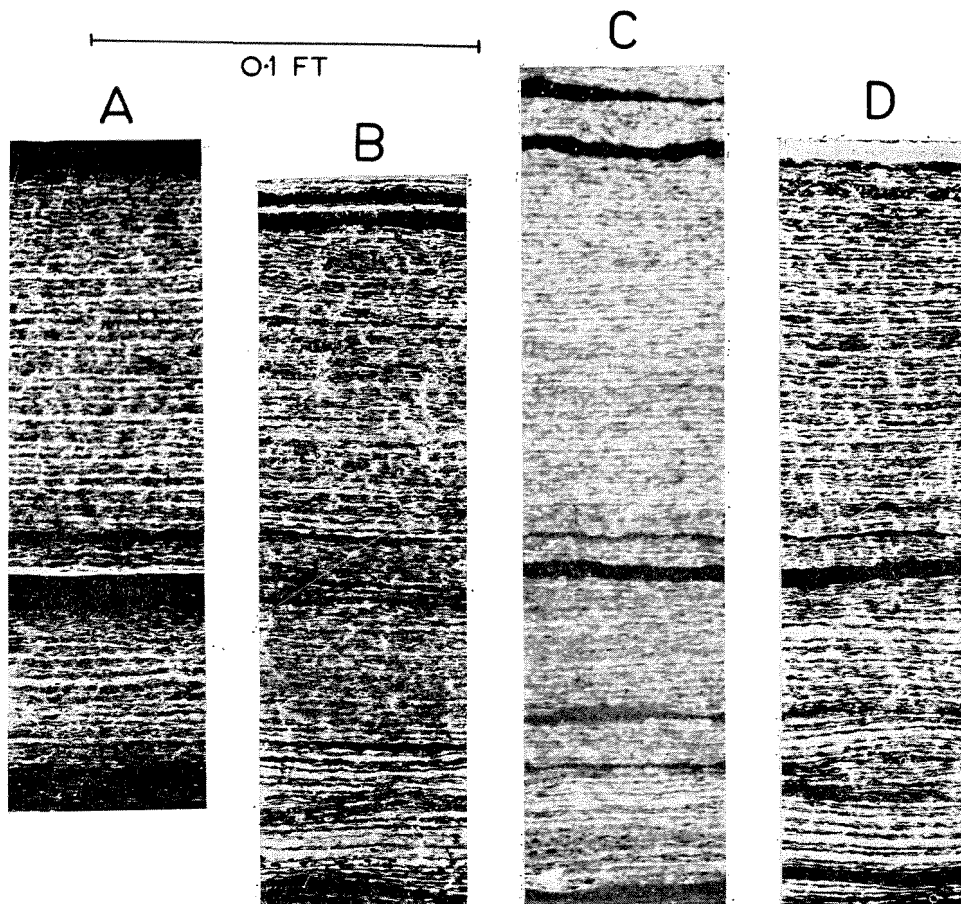


Figure 15. Comparison of the chert-magnetite group at about 36.6 to 36.85 feet in the type section of the Dales Gorge Member (BIF0; see Trendall and Blockley, 1968, Plate 28) at widely separated localities.

- A. Thin-section from Woongarra Gorge (lat. $22^{\circ} 52' 30''$ S., long. $117^{\circ} 07' 30''$ E).
- B. Thin-section from Point James (lat. $20^{\circ} 58'$ S., long. $116^{\circ} 10'$ E).
- C. Surface photograph of the type section core from Hole 47A at Wittenoom Gorge.
- D. Thin-section from Dales Gorge (lat. $22^{\circ} 28'$ S., long. $118^{\circ} 33'$ E). The localities A, B and D form a triangle with sides of length 92, 145 and 185 miles. C and D are, by comparison, only 19 miles apart. The lateral correlation of internal irregularities of the microbanding below mesoband scale is evident.

Firstly, the Calamina cyclothem can be a hindrance to correlation. Wherever the cyclothem is clearly and regularly expressed it is often difficult in the field to be certain of individual cyclothem correlation, since an offset of one or two cyclothem has little effect on apparent correlation. Internal structures must then be used if accurate correlation is needed (cf. Figures 13A and 7A).

Secondly, the variety of podded structures described in Chapter 6 (Figures 38 and 39) may ensure, particularly for the cherts of the mixed group of the Calamina cyclothem, that individual mesobands may not be correlatable in cores, or poor field exposures.

Lateral mesoband continuity within macrobands S1-16 is not as well known as that in the BIF macrobands. From assessment in single exposures we doubt whether most individual cherts in chert-siderite have as perfect continuity as the cherts of the chert-magnetite groups of the Calamina cyclothem in the BIF macrobands; however, 3 chert mesobands within S3 probably have a basin-wide distribution (Trendall and Blockley, 1968; Figure 5 of this bulletin). More work is desirable on continuity within the shale parts of the S macrobands, particularly of the shard bands, whose individual areal extent is not yet known.

THICKNESS VARIATION

In the early stages of the investigation, it was the practice to measure sections of the Dales Gorge Member wherever it contained crocidolite to correlate the various fibre horizons. This practice was extended to areas where it was hoped to use the newly-won stratigraphic knowledge to prospect for blue asbestos. Towards the end of the 1965 field season, it became apparent that there was an appreciable thickening of the member between the north and south sides of the Hamersley Plateau; the crocidolite apparently being confined to the thinner, northern part. The prospect of a paleogeographic, or basin-depth control, of crocidolite was attractive enough to warrant further thickness measurements being made. During the remainder of 1965 more measurements were made in the central part of the outcrop area, and the results were presented by Ryan and Blockley (1965) as an incomplete isopach map. In the 1966 field season, measurements were extended to the edges of the outcrop area of the Brockman Iron Formation.

The isopach map of Plate 3 was constructed from 31 measurements, ranging from 284 feet to 607 feet. The location and thickness of each measured section is shown on the map. Figures in brackets indicate that the section is a composite one compiled from two or more individually incomplete sections measured in the vicinity. The closer spacings of measurements in the northern and western parts of the area reflect the better outcrops there. In the eastern and southern parts, few sections of the Dales Gorge Member are sufficiently well exposed to be measurable.

The isopachs show that the member is thickest along a west-northwest trending axis passing through Mount Brockman, Mount Bruce and Mount Newman.

West of Hamersley Station, the isopachs have a regular elliptical pattern centred on Mount Brockman. East of Hamersley Station, the isopach pattern is more complex, the overall thinning to the north and south of the principal axis being interrupted by anomalously thin sections near Mount Frederick and Mount Lockyer, and by other irregularities between Juna Downs and Mount Newman. A single section measured at Mardie Station suggests that the isopachs are more widely spaced to the north of Mount Dempster. The isopachs are slightly more closely spaced on the southwestern side of the central axis than on the northeast.

A possible edge of the original sedimentary basin is preserved only in the southwestern part of the map area. Here the member thins rapidly on the Wyloo Anticline, and could not be identified in the remnants of Brockman Iron Formation preserved at Mount DeCoursey and Mount McGrath. The western edge has been faulted against the overlying Wyloo Group, while the northern and eastern edges have been removed by erosion. Interpretation of the southern edge is difficult, through the complex inter-relationship of the Hamersley and Wyloo Groups in that area. (Figure 74 and p. 295). At Point James, where the Hamersley Group disappears into the sea, the Dales Gorge Member is well developed but due to strike faults, could not be accurately measured. However, it seems to be at least 500 feet thick. The possible implications of this are discussed in Chapter 10 (p. 281).

Where possible, the thickness of each macroband of the Dales Gorge Member was recorded while measuring the sections. They showed great variation with respect both to their average thicknesses and to their proportions of the total thickness of the member. The results are summarized in Table 9, which gives the mean, standard deviation, and greatest and least thickness of each macroband. Macrobands with a low standard deviation are close to their mean thicknesses in most of the measured sections and have a uniform thickness over much of the outcrop area. Bands with a high standard deviation vary widely in thickness, and their means seldom represent the true thicknesses at any one spot. The S macrobands show more variation than the BIF macrobands. This may be due to their poorer outcrop, or, with thin bands, the practice of taking measurements to the nearest half foot. However, we think that the greater variation shown in the Table is valid in at least a qualitative way. The most variable BIF macrobands are 8 and 10, both of which have an unusually high chert content. Two very thick sections near the southern part of the outcrop contribute to the large variation shown by BIF15. If these are discounted, the unit varies by about the same amount as BIF14.

In an analysis of drill core at Wittenoom Trendall (1965a) showed that small variations of up to 10 per cent in thickness within the Dales Gorge Member can be accounted for by random changes in the thicknesses of the constituent macrobands. He concluded that an increase in the total thickness could be achieved if the hole contained more 'thick' macrobands than 'thin' macrobands, the terms 'thick' and 'thin' relating to comparisons with the local averages. A hole with a thick section could still contain some bands which were below the

TABLE 9. THICKNESS VARIATIONS IN DALES GORGE MEMBER MACROBANDS

Macroband	No. of Readings	Mean thickness	Standard deviation		Range of thickness	
			Value	% of Mean	From	To
		feet	feet		feet	feet
BIF16	31	46.2	16.4	35	27	82
BIF15	30	24.1	10.5	43	14.5	60
BIF14	29	21.5	5.1	24	13	34
BIF13	26	25.2	6.8	27	10	37.5
BIF12	29	26.7	8.3	31	9	43
BIF11	28	14.6	5.1	35	9	35
BIF10	24	13.9	7.3	52	5.5	35
BIF9	26	18.7	4.3	23	12	25.5
BIF8	28	12.5	6.3	50	6	30.5
BIF7	26	14.8	4.2	29	7	26
BIF6	28	9.7	2.3	24	5.5	17
BIF5	25	13.3	3.2	24	9	21.5
BIF4	28	17.8	3.1	18	8.5	24
BIF3	31	16.2	4.2	26	10.5	24
BIF2	32	17.2	3.3	19	8	24.5
BIF1	32	20.0	4.0	20	14	28.5
BIF0	30	44.6	4.9	11	28	55
S16	30	16.2	11.7	72	26	5
S15	29	2.3	1.1	42	1	6
S14	26	2.3	1.2	52	0	5
S13	27	4.1	2.7	66	1	10
S12	30	2.8	1.6	57	1	7
S11	24	10.4	4.0	39	2	18
S10	25	4.4	3.1	70	1	12
S9	27	8.3	3.9	47	1.5	15
S8	27	3.1	1.7	55	1	6
S7	26	4.6	1.6	35	1	6
S6	26	10.9	7.4	68	1.5	27
S5	27	2.4	1.4	58	1	7
S4	31	7.1	2.8	39	2.5	13
S3	33	2.1	0.8	39	0.7	4.5
S2	31	1.8	0.55	30	0.8	4
S1	32	1.5	0.6	40	0.5	3

average. In the larger regional variations in the Dales Gorge Member gross thickening of the member is accomplished by thickening in all of the macrobands, although the greatest increase usually takes place in the upper 5 BIF units. For example, in 15 sections ranging from 351 feet to 460 feet and averaging 414 feet, the macrobands above S12 make up 37 per cent of the total thickness of the member, while in 9 sections above 490 feet, averaging 536 feet, the same units

comprise 41 per cent of the total. Conversely, the macrobands below S4 constitute 25 per cent of the thinner sections and only 21 per cent of the thicker sections. Variations in the macrobands below the S7 and above S12 are usually consistent with the regional pattern, but in the units from S7 to S12, variations are more erratic and sometimes show little or no correspondence with overall thickening of the member. The changes in thickness of the Dales Gorge Member

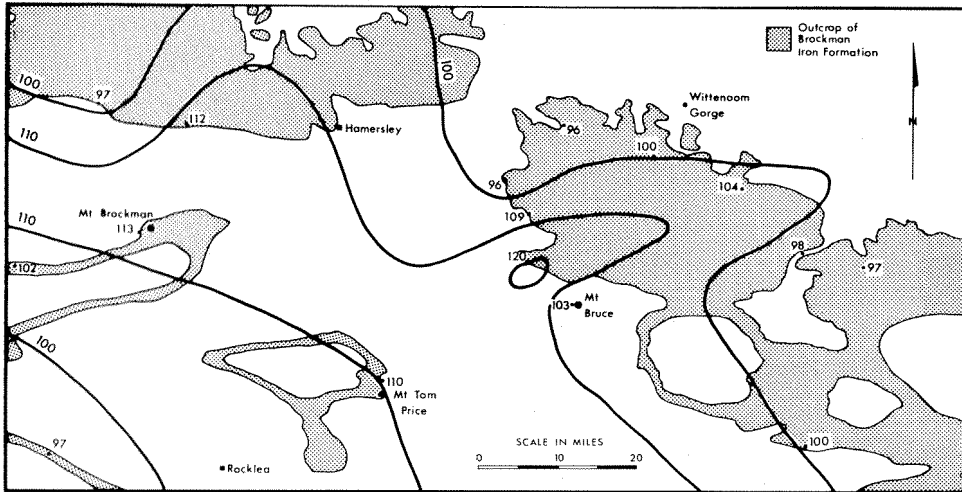


Figure 16. Isopach map of the lower part of the Dales Gorge Member (macrobands BIF0 to BIF3 inclusive) in the central part of the Hamersley Range area. Isopach values are expressed as percentages of the section at Wittenoom Gorge.

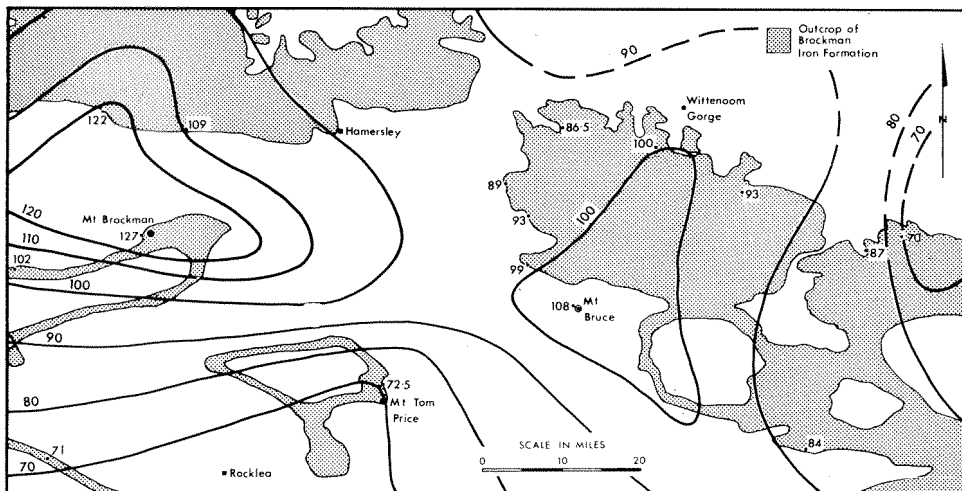


Figure 17. Isopach map of the middle part of the Dales Gorge Member (macrobands S4 to BIF11 inclusive) in the central part of the Hamersley Range area. Isopach values are expressed as percentages of the section at Wittenoom Gorge.

cannot be attributed to any one rock type. Calculations of the ratio of shale to BIF show that any increase is fairly evenly distributed between the two types.

Figures 16, 17, and 18 show separate isopachs of the lower, middle, and upper parts of the Dales Gorge Member respectively for the central northeast part of the area of Plate 3. They show that the marked thickening of the whole member along the central axis of its outcrop is contributed to most strongly by the upper part. The irregularities which disturb the simple pattern of axial thickening in the vicinity of Mount Frederick and Mount Lockyer are present in the lower part of the member. The middle section of the member seems to be mainly responsible for the saddle separating the two thickest parts of the thick central axis. These changing patterns are discussed in Chapter 10 (p. 280).

TOPOGRAPHIC EXPRESSION

The Dales Gorge Member is topographically the most prominent member of the Hamersley Group. Where it is flat dipping, it forms high, terraced cliffs (Figure 4) and, because of its resistance to erosion, it has produced escarpments many miles long. In areas where the beds have steeper dips, the member stands out as prominent, round-topped ridges, fronted by steep cliffs of the lower few macrobands.

WHALEBACK SHALE MEMBER PREVIOUS REFERENCES

MacLeod (1966, p. 103) referred to the "Mount Whaleback Shale Member" in his description of the Mount Whaleback iron deposit, where he recognized its value as a stratigraphic marker. In later usage (with which MacLeod agrees)

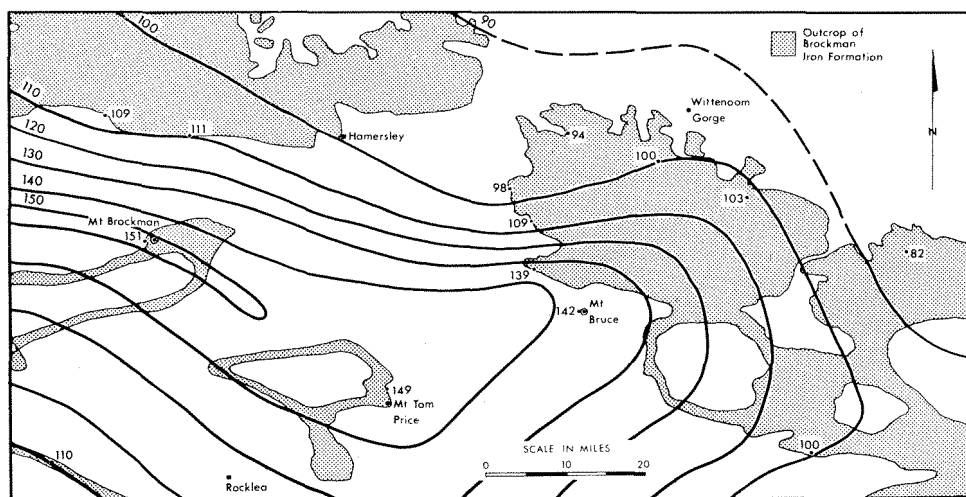


Figure 18. Isopach map of the upper part of the Dales Gorge Member (macrobands S12 to BIF16 inclusive) in the central part of the Hamersley Range area. Isopach values are expressed as percentages of the section at Wittenoom Gorge.

the prefix 'Mount' has been dropped, for brevity, and Trendall and Blockley (1968) used the shorter name 'Whaleback Shale Member'. The member is defined formally for the first time here.

DEFINITION AND TYPE SECTION

The type section of the Whaleback Shale Member is herein defined as the core between 642.2 feet and 856.95 feet drilling depths in hole 47A (lat. 22° 20'S; long. 118° 14'E) of the Australian Blue Asbestos Pty. Limited company's diamond drilling at Wittenoom Gorge. The name is derived from Mount Whaleback (lat. 23° 20'S; long. 119° 40'E), where the member was used as a marker bed in the geological mapping of the iron ore deposits. The Whaleback Shale Member conformably overlies the Dales Gorge Member and is in turn overlain with perfect conformity by the banded iron formation of the Joffre Member. It is the second member of the Brockman Iron Formation counting from the base. The core constituting the type section is preserved by the Geological Survey of Western Australia. Good field exposures of the member may be seen in the upper parts of Wittenoom Gorge and its tributary, Bismarck Gorge. A generalised log of the type section core measured upwards from the base is:

<i>From (feet)</i>	<i>To (feet)</i>	<i>Thickness (feet)</i>	<i>Lithology</i>
92.4	214.75	122.35	Interbedded shale and chert with shale predominant
88.2	92.4	4.2	Banded chert and shale
84.4	88.2	3.8	Interbedded shale and chert
82.8	84.4	1.6	Banded chert with some shale
80.2	82.8	2.6	Dark, banded shale
76.4	80.2	3.8	Banded chert with some shale
74.1	76.4	2.3	Dark, banded shale
55.0	74.1	19.1	Banded chert, siderite, and shale (cherty iron formation)
53.0	55.0	2.0	Dark, banded shale
49.5	53.0	3.5	Banded chert with shale
21.6	49.5	27.9	Dark banded shale with a few chert bands
10.7	21.6	10.9	Banded chert, carbonate, and shale
0.0	10.7	10.7	Interbedded chert and shale

LITHOLOGY

In lithology, the Whaleback Shale Member is similar to the thicker S macrobands of the Dales Gorge Member. It consists of shale, chert, and carbonate bands in varying proportions and combinations. Shale forms the major part of the member and two types are present; the first a finely banded rock with graded bedding and obvious clastic particles; and the second a black, massive, structureless rock consisting mainly of stilpnomelane. The chert beds are coarsely microbanded and most are from $\frac{1}{2}$ to 1 inch in thickness. Some cherts in the chert-siderite sections are podded, but most are of even thickness. Most chert beds contain carbonate rhombs. Carbonate bands are most common in the lower part of the member, where they are associated with the chert-rich sections. The rock so formed consists of banded chert, carbonate (usually siderite), and

stilpnomelane and may best be described as a cherty iron formation. It resembles the BIF8 macroband of the Dales Gorge Member. The bed of cherty iron formation between 55 feet and 74.1 feet in the type section forms a good marker in the field and is characterised by prominent undulations, with a wavelength of the order of 6 to 9 inches, of the top-most chert.

The upper part of the Whaleback Shale Member, about 122 feet in the type section, has a distinct cyclic repetition of chert and shale. Each cycle is made up of a chert pair or triplet separated by 4 to 6 inches of black, finely banded shale. A section of the member showing this cyclic banding was illustrated on Plate 44 of Trendall and Blockley (1968).

STRATIGRAPHIC CONTINUITY AND THICKNESS VARIATIONS

The Whaleback Shale Member has been recognized from Mount Whaleback to Point James, and as a unit is believed to have the same lateral continuity and distribution as the Dales Gorge Member. However, subdivisions within the member may not be persistent throughout the area. The prominent bed of cherty iron formation mentioned above has been seen in nearly all exposures, and is probably continuous throughout the extent of the member, but at times it is joined by a second, equally prominent chert bed which cannot be traced for more than a few miles at a time. In some sections there is a band of banded iron formation near the base of the member with the same lithology as the BIF16 macroband of the Dales Gorge Member. This band is absent in the type section and in many other places. It may in part be laterally equivalent to the cherty iron formation at 10.7 feet in the type section, but normally is too close to the base of the member for this to be likely. No attempts have been made to correlate mesobands within the Whaleback Shale Member, for lack of suitable exposures.

Owing to the difficulty of identifying the top of the member in weathered outcrops, there is little reliable information on the variations in its thickness. Measured sections range from 214 feet at Wittenoom to 180 feet at Woongarra Gorge and 160 feet in Yandicoogina Creek. MacLeod (1966) estimates a thickness of 150 feet at Mount Whaleback. The interval between the base of the member and the prominent band of cherty iron formation varies from about 25 feet to 60 feet.

TOPOGRAPHIC EXPRESSION

The Whaleback Shale Member usually weathers out to give areas of low relief amongst the surrounding iron formation. Where flat dipping, it forms broad steps separating cliffs of Dales Gorge Member below and steep hills of Joffre Member above (Figures 1 and 20). In more folded areas, its outcrop is in saddles or valleys between strike ridges of iron formation. The 20-foot band of cherty iron formation usually forms a low but prominent cliff within the outcrop.

JOFFRE MEMBER

PREVIOUS REFERENCES

Ryan and Blockley (1965) previously named this unit the Mindy Mindy Member in a form of publication not acceptable for formal stratigraphic definition by the Australian Code of Stratigraphic Nomenclature (Geological Society of Australia, 1964). The name Joffre Member is now preferred because the section at and downstream from Joffre Falls (lat. $22^{\circ} 24'S$; long. $118^{\circ} 16'E$), after which the member is named, is both more easily accessible and better exposed than the type section, although the uppermost part cannot be seen. Trendall (1965) tentatively used the name Joffre Member for the S15 macroband of the Dales Gorge Member, but the macroband numbering system now adopted has freed this name for its present more apposite application.

DEFINITION AND TYPE SECTION

The type section is on Yandicoogina Creek (lat. $22^{\circ} 49'S$; long. $119^{\circ} 10'E$), where the whole member is well exposed for 2 miles along a gorge. The member consists of about 1,100 (1,145 measured at the type section) feet of rather uniform banded iron formation with thin beds of stilpnomelane-rich shale and other material of tuffaceous origin. It overlies the Whaleback Shale Member and is overlain by the Yandicoogina Shale Member; both contacts are perfectly conformable. The lower boundary is clearly defined in the core of hole 47A, but it is often difficult to determine in the field, where the junction appears gradational over some tens of feet of shale and chert. In the Yandicoogina Syncline the top of the member is marked by an 8-foot thick bed of thick-banded cherty iron formation which locally contains crocidolite; a section about the upper contact appears in Figure 52.

Very detailed work would be needed to record the rather subtle lithological variations present through the measured type section in a form useful for practical correlation. The lithological description under the following heading may therefore be taken to apply to the whole thickness of the member. We record here only those levels in the type section at which beds of stilpnomelane-rich shale or other unusual material, between about 0.5 and 2 feet thick, cause stratigraphic discontinuity. Although it is not always possible to be sure of the identity of the controlling material, the following figures give the heights in feet above the base of the member, of the bases of the fifteen major discontinuities of this kind: 10.5, 71.0, 105.0, 141.5, 343.5, 395.5, 424.0, 468.5, 711.0, 797.0, 1020.5, 1121.5, 1127.5, and 1135.5.

LITHOLOGY

GENERAL DESCRIPTION

The lithology of the Joffre Member is conveniently described by comparison with that of the Dales Gorge Member. There is a clear general resemblance between the two, as would be expected in banded iron formation members of

close chemical similarity (Chapter 5). The resemblance is expressed lithologically in the Joffre Member by its possession of mesobanding on a similar scale to that of the BIF macrobands of the Dales Gorge Member, and also by the existence within the chert mesobands, which have the same order of thickness, of almost exactly similar microbanding; attention is now drawn to four ways in which different characters of the two members are reflected in general lithology.

Firstly, macrobanding is absent from the Joffre Member. It may well be that the rhythmic appearance of stilpnomelane tuffs at intervals of 2 to 5 feet (see under following heading, Figure 19C, and Chapter 10) is an analogous form of stratification above the mesoband scale, but this is irrelevant for lithology: the absence of more or less regular and radical lithological alternations on the macro-band scale is a striking difference from the Dales Gorge Member.

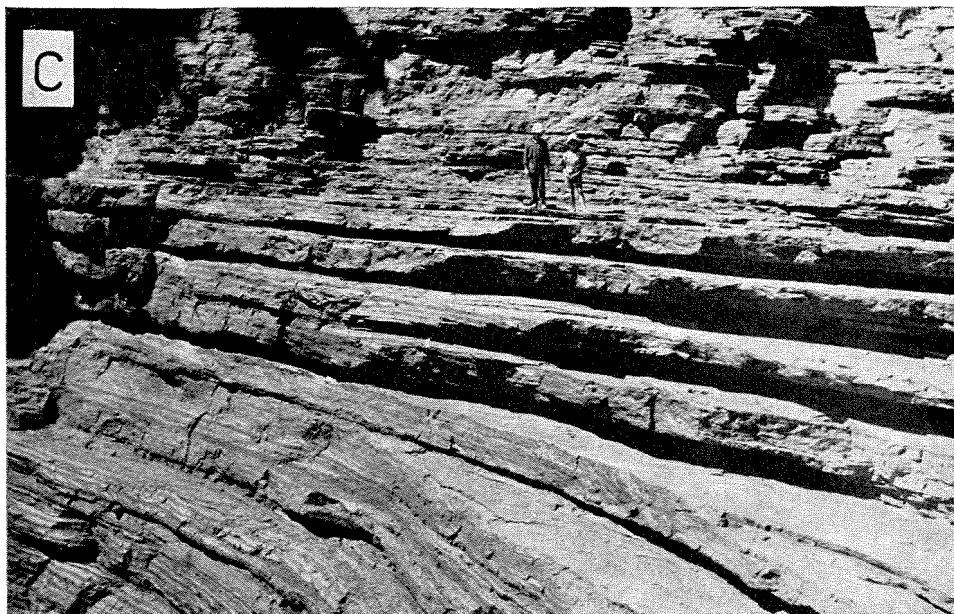
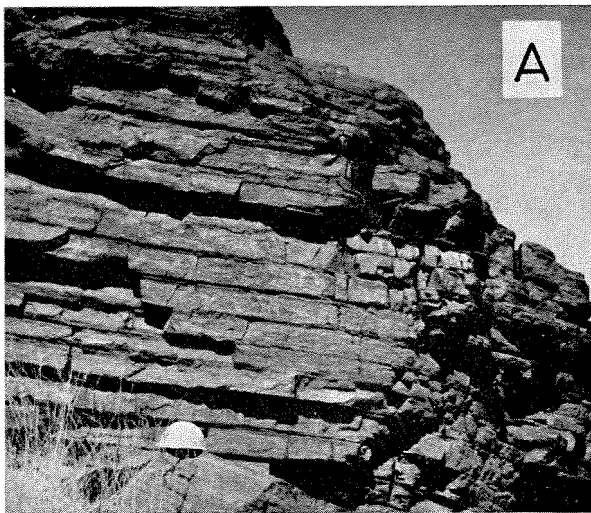
Secondly, there are several differences in the nature and proportions of the mesobands which collectively affect lithology. Although none of these has been quantitatively assessed in as systematic a way as for the Dales Gorge Member we have no doubt of the validity of the following subjective assessments. Apart from the thick stilpnomelane tuffs and black flinty mesobands described further below almost all the mesobands are either chert or chert-matrix. Thin magnetite mesobands occur rarely within the chert-matrix and are not clearly differentiated from it, and no carbonate mesobands are present. Chert and chert-matrix each make up about half of the total thickness; this is in sharp contrast with the Dales Gorge Member (Table 4). Thus there is a more regular alternation of chert and chert-matrix mesobands of even thickness. The chert-matrix is dark bluish grey to almost black in fresh exposures and (macroscopically) more homogeneous than that of the Dales Gorge Member; it varies little from mesoband to mesoband. Chert mesobands are more clearly divisible into two types than in the Dales Gorge Member; these (white cherts and red cherts) are described under the next heading. In summary, all these differences in mesobanding collectively give a darker, more 'shaly', less 'cherty', and more uniform appearance compared with the Dales Gorge Member, particularly in contrast to those parts of the Dales Gorge Member where the Calamina cyclothem is strongly developed, with thick chert-magnetite groups (Table 6).

A third characteristic difference between the Joffre and Dales Gorge Members, which strongly affects field assessment of lithology, is the distribution and strength of development of the various structures defined by mesoband irregularity,

Figure 19 (opposite). The field expression of various kinds of cyclicity in the Brockman Iron Formation.

A. The typical appearance of the well developed repetitions of the Calamina cyclothem, like those in the lower part of BIF12 of the Dales Gorge Member illustrated in Figure 13B, but here in BIF16 just south of Aspinall prospect at Junction Gorge. The hat brim is at a stratigraphic level of about 444 feet on the type section.

B. Exceptionally regular expression of the Knox cyclothem in the Joffre Member, exposed at the base of the western wall of Joffre Gorge about 1½ miles north of Joffre Falls, at the southern end of a long pool preventing dry passage of the gorge, and just north of a



dolerite dyke crossing the gorge and forming steep gullies on either side. The hammer has a total length of 15 inches; the head rests on the upper surface of a white chert mesoband and white cherts recur upwards at 3-inch intervals. Thin red cherts, not clearly discernible from chert-matrix in the photograph, are centrally grouped between the white cherts.

C. Four $2\frac{1}{2}$ -foot repetitions of thin stilpnomelane-rich tuffs in the Joffre Member well displayed on the east side of Joffre Falls below the ledge on which the boys are standing. These four units of massive BIF have a total thickness of nine feet, and the taller of the two boys is 4 ft 6 inches tall. In the lower left-hand corner of the picture the much thinner Knox cyclothem may be discerned as a white striping; each stripe consists of a double white chert, in contrast with the single white chert of B.

which are the subject of Chapter 6. Although, as with the Dales Gorge Member, it is more convenient to describe the lithology here in terms of geometrically ideal banding it should nevertheless be noted that local development of large and conspicuous random pods and cross-pods (Figure 39, A and D), some with shapes not elsewhere developed, is a characteristic feature of the Joffre Member. These involve mainly the white chert mesobands, but the red cherts are also affected wherever these structures are strongly developed.

Fourthly, and finally, although riebeckite is similarly not the concern of this chapter, it is very relevant for lithology that the more even distribution of riebeckite through all mesobands of the Joffre Member, in the Wittenoom area at least, is in marked contrast to its highly selective and erratic distribution in the Dales Gorge Member. Its presence gives the typical bluish grey colour of the chert-matrix, already noted. Further details of its distribution, in both members, are given in Chapter 7.

Two lithological types present in the Joffre Member do not form part of the ordinary mesoband sequence of the iron formation. Bands of stilpnomelane shale between about one inch and two feet thick appear as tough, black, blocky, and macroscopically homogeneous material; it breaks with difficulty with the hammer and gives a smooth conchoidal fracture. The distribution of this rock is noted under the next heading; an analysis appears in Table 16, and a petrographic description in Chapter 4. It is a tuff. Other bands, also 1 to 2 feet thick, and similarly black, tough and homogeneous, occur less frequently. These are more brittle than the stilpnomelane bands, and fracture like black flint; the name 'black porcelainite' seems appropriate (Table 16). They consist largely of potassic feldspar (p. 127), and may also represent tuffs. These two rocks jointly comprise the various discontinuities already recorded in the type section.

MESOBAND SEQUENCE: THE KNOX CYCLOTHEM, AND OTHER REGULARITY

Chert mesobands of the Joffre Member are of two types: white cherts and red cherts. White cherts are so named from their colour in clean fresh exposures of the standard of the cliffs at Joffre Falls. In general they are between 1 and 5 cm thick and are rather faintly and indistinctly microbanded, usually with an interval between 0.5 and 1.0 mm. In field exposures they often appear completely structureless, but in such cherts some traces of microbanding are usually present in thin-section. Red cherts have the same order of thickness as the white cherts, but share with the cherts of the chert-magnetite groups of the Calamina cyclothem in the Dales Gorge Member a tendency for a number of thin mesobands to be grouped closely together in such a way as to make exact mesoband definition arbitrary. These cherts vary in colour between pale reddish brown, bright brick red, and pink according partly to their state of weathering. Microband intervals vary between 0.5 and 1.0 mm, as in the white cherts, but in the red cherts the microbanding is very clearly expressed by colour variations, as in most cherts of the Dales Gorge Member.

In parts of the Joffre Member a cyclic alternation of these two chert types is apparent. A fine example is shown in Figure 19B, in which six white cherts of even thickness recur at intervals of just over 3 inches, with closely spaced groups of thinner red chert mesobands placed centrally in the five intervals thus created. Elsewhere a similar sequence is present with the same interval and the same cyclic regularity, but with a pair of white chert mesobands, separated by a chert-matrix mesoband with a thickness about equal to that of each of the cherts, instead of one. This type of regularity can be seen in the lower left-hand corner of Figure 19C, although the red cherts cannot be distinguished in the photograph.

We propose to call mesoband sequences such as these the Knox cyclothem, which we define as a common cyclic sequence of mesoband types in the Joffre Member, in which one or more white chert mesobands alternate repeatedly at regular intervals with one or more red chert mesobands, with all the cherts separated by chert-matrix. Like the Calamina cyclothem of the Dales Gorge Member the Knox cyclothem is apparently similar at top and bottom (Figure 19B), so that each cyclothem is symmetrical about the central plane of either of its component chert groups, and there is no naturally defineable beginning or end of each cyclothem. The interval from any arbitrary reference plane in the Knox cyclothem to its equivalent levels in adjacent cyclothem is usually between 3 and 4 inches. We have no type section for the Joffre Member for specification of the stratigraphic position of individual Knox cyclothem with the accuracy used for the Calamina cyclothem, but the localities of the examples in Figure 19, B and C), given in the caption, are sufficient for unguided relocation in the field.

Like the Calamina cyclothem, the Knox cyclothem, once recognised in its most regular expression, can be used as a basis for interpreting red and white chert sequences in parts of the member where no cyclicity is otherwise evident. Its depositional significance and its relationship to the Calamina cyclothem are discussed in Chapter 9.

In the well exposed Joffre Member in the cliffs at and below Joffre Falls stilpnomelane tuff bands 2 to 4 inches thick are distributed within the iron formation at remarkably regular intervals. The average separation is about $2\frac{1}{2}$ feet, with a range of about 2 to 5 feet. The stilpnomelane bands weather back to emphasize the regularity of their distribution. This is clearly illustrated in Figure 19C. This regularity is here superimposed on the Knox cyclothem, several of which are included between successive stilpnomelane bands. The possible significance of this larger-scale regularity is discussed in Chapters 9 and 10. It remains to note here that both it and the Knox cyclothem are well illustrated by Figure 13 of MacLeod (1966), which was taken looking north-north-eastwards obliquely across the first long pool below Joffre Falls: the $2\frac{1}{2}$ -foot succession of stilpnomelane tuffs including those shown in Figure 19C, appears in the distant cliffs between about $\frac{1}{2}$ and $1\frac{1}{2}$ inches above the climber's head, while the 3-inch Knox cyclothem is particularly well displayed in the closer cliffs in the upper right-hand corner of the photograph.

LATERAL CONTINUITY AND THICKNESS VARIATION

The Joffre Member forms the larger part of the Brockman Iron Formation and is seen in almost every locality in which that formation is exposed. Exceptions are at Point James, where the identity of the member is obscured by faulting, and in places on the Wyloo Anticline, where the whole Brockman Iron Formation is only about 250 feet thick and individual members are indistinguishable. The lack of any distinctive internal marker beds, and the small economic importance of the member has prevented any attempt at detailed correlations, although it is clear in the excellent exposures at Joffre Falls and the gorges downstream that mesoband continuity is not perceptibly less than that in the Dales Gorge Member over distances of a few hundreds of feet. We doubt whether mesoband continuity is any less perfect than in the BIF macrobands of the Dales Gorge Member.

Only three measurements of the thickness of the member were made: 1,120 feet at Mindy Mindy Creek, 1,145 feet at Yandicoogina Creek, and 1,080 feet at Woongarra Pool. Thicker sections could be expected in the Mount Brockman area, but poor outcrop there prevented any being measured. The only place in which the member is both recognisable and appreciably thinner than 1,100 feet is near Seven Mile Creek where a thickness of about 500 feet was estimated.

TOPOGRAPHIC EXPRESSION

The Joffre Member is not as resistant to erosion as the lower Dales Gorge Member, but it still forms spectacular cliffs where, as at Joffre Falls, it is being actively cut back. Its most typical expression is seen on the Hamersley Plateau (Figures 1 and 20), where it forms ranges of high domed hills, often flanked by irregular cliffs. In more folded areas, it forms rounded strike ridges, often in combination with the Dales Gorge Member.

YANDICOOGINA SHALE MEMBER

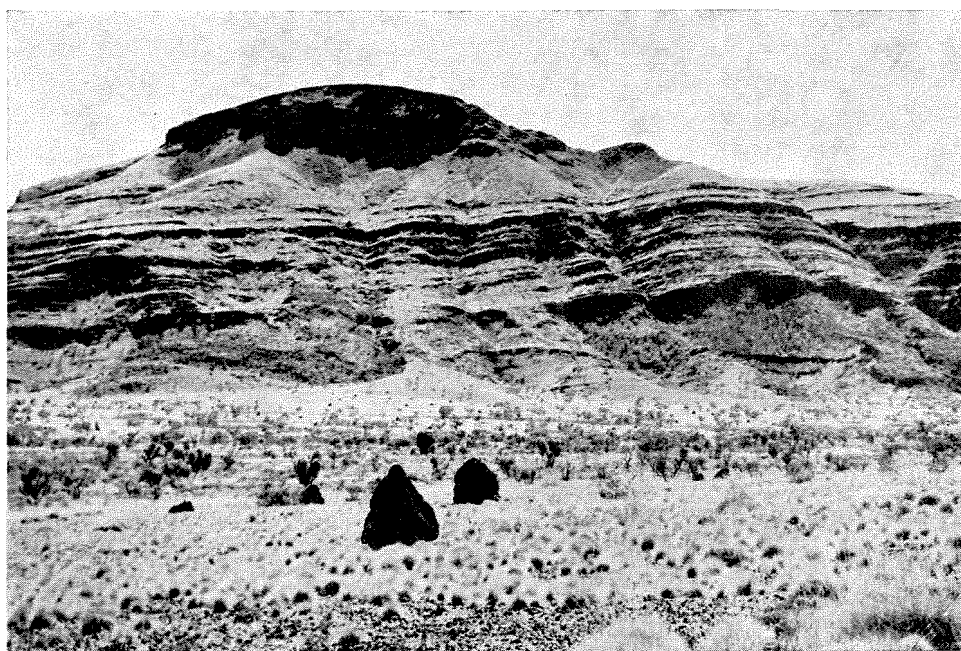
The 200-foot thick Yandicoogina Shale Member is named after Yandicoogina Creek, the drainage basin of which contains many good exposures of the member. The type section is at lat. 22° 49'S and long. 119° 11'E, on the main stream of

Figure 20. Mount Farquhar (lat. 22° 18'S., long. 116° 45'E), on the south side of the main Hamersley Range, seen from the southwest. The photograph was taken from the gentle northerly dip slope of the Marra Mamba Iron Formation, across the valley (Serpentine Creek) formed by the Wittenoom Dolomite, towards the abrupt escarpment forming the south side of the Hamersley Range Synclinorium. On the steep slopes of the escarpment two of the three thin BIF bands of the Mount Sylvia Formation are visible near the base on the right, and are succeeded upwards by the smooth slopes of the Mount McRae Shale, the conspicuous macrobands of the Dales Gorge Member, the grassy slopes of the Whaleback Shale Member, and finally, in the highest cliffs to the left of centre, the relatively unstepped cliffs of the Joffre Member.

Yandicoogina Creek. In this area there is a sharp contact between the shale member and the underlying iron formation of the Joffre Member, but in Woongarra Gorge, in the western part of the Hamersley Range area, the contact is gradational, and no sharp boundary can be placed between the two units. The Yandicoogina Shale Member is overlain by the Weeli Wolli Formation, and is the highest member of the Brockman Iron Formation.

Lithologically, the unit consists entirely of an alternation of thin chert and shale bands and is similar to the upper part of the Whaleback Shale Member. It contains no internal marker beds. At Woongarra Pool the shales of the member seem to be more ferruginous than in Yandicoogina Creek, but differences in local weathering conditions may account for this.

Typically the member forms a belt of low relief in the iron formations and good exposures of it are rare. Often its presence can only be assumed from its topographic expression. Thus the evidence for its continuity is not conclusive, but we think that it persists along the length of the Hamersley Range area from at least Mount Newman to the eastern end of the Wyloo Anticline. It was not recognised on Seven Mile Creek, but here it may be intruded by a dolerite sill, and may have been mistaken for the Weeli Wolli Formation. In the northern part of the Hamersley Range area, few exposures go high enough in the stratigraphic column to expose the member although it may underlie the wide area of colluvium and alluvium at the headwaters of Joffre Creek (Plate 5).



MARRA MAMBA IRON FORMATION

DEFINITION AND TYPE AREA

The Marra Mamba Iron Formation is the lowest unit of the Hamersley Group. It was first defined by MacLeod and others (1963), who gave the type area as Marra Mamba, the site of old crocidolite workings within the formation, and nominated a thickness of 600 feet for the unit where measured on the north limb of the Hardey Syncline. The formation overlies with perfect conformity the Roy Hill Shale Member of the Jeerinah Formation and is overlain in turn by the Wittenoom Dolomite. The lower contact is sharp and frequently well exposed in scarps formed by the resistant basal part of the unit, but at the upper boundary the iron formation grades into dolomite by way of a thin sequence of interbedded dolomitic shale and chert.

LITHOLOGY

Fresh exposures of this formation are confined to gorges in the Mount Wall—Duck Creek area. Four factors contribute jointly to its distinctive lithology: the distribution of shales within it, the characteristics of the mesobanding, the structures of the cherts, and to a lesser extent its mineralogy. Although only clearly observable in good exposures all these four control the weathering processes that lead to its easy recognition when concealed (see Topographic expression, below).

Massive bands of black stilpnomelane shale, weathered to friable grey clayey material in all but the finest exposures, are common. They vary from about 3 inches to 3 feet in thickness, and are mainly between 6 and 12 inches. Their distribution in parts of the formation appears in Figures 52 and 67, and was shown more completely by Blockley (1967, Plate 34). They are not, like the shale of the Dales Gorge Member, associated with chert-siderite, and more closely resemble the stilpnomelane tuffs of the Joffre Member (Figure 19C). However their normally greater abundance and proneness to weathering increases their effect on general lithology. In places their spacing recalls the macrobanding of the Dales Gorge Member, but they are usually thinner, more abundant and less regular, and we prefer at present to confine this term to the Dales Gorge Member.

Like that of the Joffre Member the BIF of the Marra Mamba Iron Formation consists almost exclusively of two mesoband types: chert and chert-matrix. Magnetite mesobands like those of the Dales Gorge Member are absent. The chert mesobands are rather thick (estimated mean 4 cm) and have very coarse microbanding (2 mm or above) which is often difficult to detect. It has only slight mineralogical expression, and is often best expressed on deeply weathered faces. The chert-matrix is characteristically finely laminated; the dark and light colouring by which this is expressed is related to magnetite laminae in a matrix of quartz and sheet silicate. This is in marked contrast to the uniformly drab grey and homogeneous chert-matrix of the Joffre Member.

Although we choose to deal with chert structures in Chapter 6 it must be noted here that the prevalence of erratic fluctuations of chert mesoband thickness, or the presence of irregularly rounded chert pods often arranged along the bedding like strings of potatoes, is a characteristic feature of this formation.

The abundance of minnesotaite (Chapter 4) in the Marra Mamba Iron Formation, rather than ferristilpnomelane (as in the Joffre Member) or ferrostilpnomelane (as in the Dales Gorge Member) is probably one important explanation of its susceptibility to weathering. Its breakdown also gives the cherts their characteristic yellow colouring in most types of exposure; the yellow colour often extends over the whole rock.

SUBDIVISION

Although the Marra Mamba Iron Formation is largely composed of alternating shale and BIF no attempt has been made to subdivide it in a similar way to the Dales Gorge Member. We believe that such a subdivision would be possible if good exposures were available, but in the existing weathered outcrops, individual shale bands are often leached out, making accurate identifications of sequence impossible. The lithology of the formation is monotonous, and reliable markers are absent from the section. The formation is broadly divisible into three members, two of more continuous BIF and one with a greater proportion of shale and chert. Ryan and Blockley (1965) named two of the members, but not in a form which complied with the requirements of the Australian Code of Stratigraphic Nomenclature (Geological Society of Australia, 1964). One of the names used was later found to be invalid under the rules of the code. We now believe that any attempt to set up formal members within the Marra Mamba Iron Formation should wait until drill core is available to permit accurate identifications of the member boundaries. At present, no consistently recognisable boundaries have been established between the three parts of the formation, and rather than propose formal members which may be subject to radical change at some future time, we shall refer to the three divisions informally as the lower BIF member, the middle shaly member, and the upper BIF member respectively. The lower BIF member is about 450 feet thick and consists of banded iron formation with numerous podded horizons and thin bands of shale, chert, and dolomite. The top of the member is marked by a prominent bed of chert with ovoid pods. It contains crocidolite and riebeckite at Marra Mamba and some other localities. The middle shaly member is rarely well exposed. At Mount Wall it is about 120 feet thick and consists of black stilpnomelane shale, chert, and banded iron formation with a few bands of dolomite. In many respects it is like the Whaleback Shale Member of the Brockman Iron Formation. The upper BIF member is well exposed in gorges at the west end of the Rocklea Dome and in a tributary of Duck Creek but elsewhere is usually covered by duricrust or colluvium. It is approximately 200 feet thick and is made up of banded iron formation with subordinate chert and shale.

LATERAL STRATIGRAPHIC CONTINUITY

Poor exposure, and scarcity of distinctive internal marker beds, makes correlation on less than formation scale uncertain. The three-fold subdivision can be recognised, where there is adequate exposure, in the area of the Jeerinah Anticline and the Brockman Syncline, but it has not been seen elsewhere. On a smaller scale the only successful lithostratigraphic correlation, apart from the crocidolite horizons described in Chapter 7, is of a sequence of thin alternations of shale and BIF which lie about the Dun Horizon, 260 feet above the base of the formation (Figure 48), and which were recognised at Marra Mamba, at Duck Creek, and on the western end of the Turner Syncline. Almost perfect exposure is needed before a confident identification of the sequence can be made. Some individual mesobands within this sequence can also be correlated.

Extending as it does over a greater area of the Hamersley basin (Chapter 2) the Marra Mamba Iron Formation provides a possible object for a future search for an even more extensive mesoband correlation than in the more restricted Dales Gorge Member. At present we have little evidence for judging the possibility of success in such a quest.

THICKNESS VARIATION

The Marra Mamba Iron Formation varies considerably in total thickness, but it is not possible to construct an isopach map without drill-hole data. Most of the sections measured during this investigation were in the western end of the Hamersley Range area where the formation ranges from 600 to 750 feet thick. Daniels and MacLeod (1965) give its thickness near Mount Newman as 300 to 400 feet, and say that it is thickening to the north. MacLeod and de la Hunty (1966) estimate its thickness to be 200 feet or more in the eastern part of the Chichester Range and 600 feet in the Weeli Wolli Anticline. Kriewaldt and Ryan (1965) measured thicknesses of about 50 feet near Coolawanyah Station while Williams (1965) gives its thickness as 500 feet near Millstream Station, decreasing rapidly to almost nothing to the northwest on Mardie Station. On the Wyloo Anticline, the formation thins, with the remaining formations of the Hamersley Group, from 600 feet to nothing within about 20 miles. However, at Seven Mile Creek, where the Brockman Iron Formation thins appreciably, the Marra Mamba Iron Formation is quite thick at 680 feet. Near Bee Hill, on the Davis River, at lat. 22° 05'S, long. 120° 45'E, on the Balfour Downs Sheet, the Marra Mamba Iron Formation is represented by about 20 feet of poddy cherts at the top of the Lewin Shale. In general, the thickness variations of the formation follow the same pattern as do those of the Dales Gorge Member, although the thickest part may lie a little south of Mount Brockman, and it may not thin out so rapidly to the south.

TOPOGRAPHIC EXPRESSION

Where it is better exposed in the western and southern parts of the Hamersley Range area, the Marra Mamba Iron Formation forms low ridges or cuestas flanking the abrupt escarpments of the Brockman Iron Formation (Figure 20).

In the eastern part of the Hamersley Range and in the area of the Ophthalmia Range, outcrops of the formation are reduced to low, rounded, gravelly rises with only scree of chert and BIF to indicate the underlying rock-type. Abundant weathered out chert pods are characteristic of this formation (Chapter 6). Creeks draining the Marra Mamba Iron Formation cut shallow ravines and usually these are the only places where the unit can be seen even in an oxidised state beneath its usual cover of duricrust.

WITTENOOM DOLOMITE

The Wittenoom Dolomite was first defined by MacLeod and others (1963), who gave its type area as the hills south of Wittenoom townsite. The formation consists of 500 to 600 feet of dolomite, chert, and shale. It is stratigraphically equivalent to the Carrawine Dolomite mapped to the east on the Nullagine and Balfour Downs 1:250,000 sheets (Noldart and Wyatt, 1962; de la Hunty, 1964). In the Hamersley Range area the dolomite conformably overlies the Marra Mamba Iron Formation and is in turn overlain by the Mount Sylvia Formation. The best exposures are along the northern face of the Hamersley Range, where the dolomite often forms the lower 500 feet or so of the escarpment. Dolomite crops out in the valley of the Fortescue River, and it is likely that the whole of this broad plain is underlain by the formation. If so, then its apparent thickness is probably increased by minor folding.

Many sections of the formation have been examined, but in most the base is obscured by scree from neighbouring iron formation outcrops. The lower part of the unit is composed of massive, medium to thin-bedded dolomite with rare beds of black chert. The upper part contains increasing amounts of shale, chert, and iron formation. Where fresh, the dolomite is finely crystalline and brown, pink or grey with faint colour banding. It contains sedimentary structures such as cross-beds and slumps, and diagenetic features such as stylolites, and chert nodules. Algal structures have been recognised in the Carrawine Dolomite at Woodie Woodie (lat. $21^{\circ} 34'S$; long. $121^{\circ} 12'E$) but no fossils are known from the Hamersley Range area. Some sections show sedimentary rhythms repeated at 5 to 6 inch intervals.

The Wittenoom Dolomite maintains a fairly consistent thickness and composition over most of the outcrop area of the Hamersley Group. Localities where appreciable variations are known are Point James, where the dolomite thins to nothing, Wyarma Spring (lat. $22^{\circ} 58'S$; long. $117^{\circ} 12'E$) where it is also missing, and Seven Mile Creek, where it is very thin and contains mostly shale.

In general, the Wittenoom Dolomite is very poorly exposed, but its presence can usually be inferred from its topographic expression of broad scree and alluvium filled valleys walled by ridges of Marra Mamba and Brockman Iron Formations. Calcrete deposits in the Hamersley Range area are largely restricted to areas underlain by dolomite, and serve to indicate the presence of the formation.

MOUNT SYLVIA FORMATION

The thin, but remarkably persistent Mount Sylvia Formation was defined by MacLeod and others (1963) at Mount Sylvia (lat. $22^{\circ} 18'S$; long. $117^{\circ} 37'E$), where it is 110 feet thick. Although consisting mainly of thin-bedded shale, chert, and dolomite, the formation contains three BIF bands which crop out prominently on the hill-sides as dark steps separated by smooth concave slopes (MacLeod, 1966, Figure 11; Figure 20 of this bulletin). The uppermost of these bands is colloquially called 'Bruno's Band' after Dr. Bruno Campana, who used it as a marker bed when mapping iron deposits in the Hamersley Range. The upper and lower boundaries of the formation are defined by the top of Bruno's Band and the base of the lowest BIF band respectively. The Mount Sylvia Formation conformably overlies the Wittenoom Dolomite and is overlain by the Mount McRae Shale.

The two lower BIF bands are about 6 and 10 feet thick respectively. They consist of green and brown banded ferruginous chert, rather like parts of the Marra Mamba Iron Formation. Bruno's Band differs from them in resembling the younger Dales Gorge Member. It has a dark purple-brown colour and is made up of thin, planar mesobands of chert, hematite, and chert-matrix. Fine microbands are common in the chert beds.

The rocks between the BIF bands comprise thin-bedded cream to yellow shale interspersed with grey, coarsely microbanded chert and thin beds of dolomite. A comparatively fresh section of the formation exposed in a rail cutting north of Hamersley Station shows the shales and cherts to be carbonaceous.

With its distinctive BIF bands the Mount Sylvia Formation forms a striking stratigraphic marker throughout the Hamersley Range area. In some places the shales near the two lower bands are indurated, and the BIF does not stand out so clearly on the hillsides, although the upper band is always conspicuous. Laterally, the formation extends throughout the Hamersley Range area, and Bruno's Band can be traced almost continuously from the Ophthalmia Range to Mount Dempster and has been recognised at Point James, where the Hamersley Group extends into the Indian Ocean. Only at the southern margin of the outcrop area of the Hamersley Group, at Wyarma Spring and Seven Mile Creek, is the formation absent.

Although the Mount Sylvia Formation is an excellent stratigraphic marker of great use to the mapping geologist, its thinness and narrow outcrop-widths preclude it being shown as a separate unit on most maps. We have included it with the Wittenoom Dolomite on Plates 4, 5, 6, 9, and 12.

MOUNT McRAE SHALE

DEFINITION AND TYPE SECTION

MacLeod and others (1963) named the Mount McRae Shale from Mount McRae (lat. $22^{\circ} 17'S$; long. $117^{\circ} 35'E$), where the formation is exposed on the southern scarp of the Hamersley Plateau. The type section is at Mount Sylvia,

3 miles east of Mount McRae. The base of the formation is defined by the top of the prominent Bruno's Band and the top by a massive black 20-inch thick shale bed which underlies the lowest (BIF0) macroband of the Dales Gorge Member. Immediately below this shale is a 3 to 4-foot thick band of BIF which, in weathered outcrops contains, 18 inches from its top, a 6-inch band with cavities formed by leaching of carbonate nodules. The pitted BIF, which is known as the 'bed of holes' overlies another thin shale band. It is a very good stratigraphic marker which indicates the base of the economically important Brockman Iron Formation.

SUBDIVISION

Where the Mount McRae Shale is best exposed, in gorges incised into the north side of the Hamersley Range, it can be subdivided into three members:

- Top 3.* iron formation member; predominantly cherty BIF with beds of shale and thick chert, thickness 50 to 90 feet;
2. dolomite member; dolomitic shale, dolomite, shale, and chert, thickness 70 to 130 feet; and
1. shale member; shale and dolomitic shale with chert and a thick bed of massive blue chert at the top, thickness 115 to 225 feet.

Generally this subdivision applies where the formation is thick and contains dolomite. In thinner sections such as those seen near Weeli Wolli Spring, and Mount Flora, the dolomite is absent, and the three-fold division does not apply. The only member which can be consistently recognised is the uppermost iron formation unit. This consists of a sequence of alternations of BIF and shale which are laterally continuous over a wide area and could be used, if necessary as a basis for further subdivision. A section of this member measured at Wittenoom Gorge is as follows:

<i>Thickness (feet)</i>	<i>Rock type</i>	<i>Thickness (feet)</i>	<i>Rock type</i>
Top			
1	Shale	1	Shale
$\frac{3}{4}$	Chert		
3	BIF with pitted horizon	$3\frac{1}{2}$	Ferruginous chert
$1\frac{1}{2}$	Shale	$1\frac{1}{2}$	Shale
$\frac{1}{2}$	Chert	3	BIF
10	BIF	$1\frac{1}{2}$	Shale
2	Shale	8	Cherty BIF
5	BIF	$\frac{1}{2}$	Shale
2	Shale	$\frac{1}{2}$	Chert
1	Chert	6	BIF
11	BIF	$\frac{1}{2}$	Shale
$\frac{1}{2}$	Shale	$3\frac{1}{2}$	Cherty BIF
3	BIF	$\frac{1}{2}$	Shale
2	Shale	$2\frac{1}{2}$	BIF
1	Chert		
1	Shale		
2	BIF		
		Total	<u>$79\frac{3}{4}$</u>

LITHOLOGY

The lithology of the lower shale member is very much like that of the Mount Sylvia Formation, although it lacks prominent BIF units. It comprises thin-bedded shale and chert with some dolomite or marl. In a fresh exposure near Mount Margaret, the shale is graphitic. The top of the member is marked by a 4 to 6-foot thick bed of blue or grey chert which often has quartz-lined vugs. The dolomite member consists of interbedded dolomitic shale and chert with one or two very prominent beds of brown dolomite each 5 to 10 feet thick. At Mount Margaret and elsewhere, these dolomite beds contain intraformational breccias. The upper BIF member is similar to the Dales Gorge Member of the Brockman Iron Formation, being composed of alternations of BIF and shale.

LATERAL STRATIGRAPHIC CONTINUITY

The Mount McRae Shale has been recognised within the Hamersley Group from Mount Whaleback to Point James, a distance of 280 miles. The only places where it does not form a distinct unit within the stratigraphic column are near the southern margin of the basin, at Wyarma Spring and Seven Mile Creek, and on the eastern part of the Wyloo Anticline.

Members of the formation vary in their persistence. The dolomite member can only be identified in the northern and central part of the outcrop area, but the upper BIF member, persists throughout the whole outcrop area. Some sequences within the BIF member can be correlated over wide areas and the uppermost three alternations of BIF and shale, which contain the 'bed of holes' has been seen in places as far apart as Giles Point, Fish Pool (lat. 23° 17'S; long. 118° 04'E), Seven Mile Creek, Duck Creek, and James Point. Correlations of mesobands have not been attempted, but the persistence of the 6-inch band with the rows of leached cavities suggests that correlation would be feasible on this scale. In the eastern and northern parts of the Hamersley Range area, the thick chert at the top of the shale member forms a prominent marker. A similar bed seen at Mount Brockman, Mount Flora, and on the southern scarp of the Hamersley Plateau, is probably the same one, but no definite correlation has been established.

THICKNESS VARIATION

The Mount McRae Shale varies appreciably in thickness throughout the Hamersley Range area. Its greatest known thicknesses are at Mount Margaret, Wittenoom Gorge, and Mount Brockman where sections of from 360 to 380 feet were measured. The thinnest section measured during the present work was west of Mardie Station and totalled only 145 feet. At Mount Flora, and near Weeli Wolli Spring, the formation is about 250 feet thick, while MacLeod (1966) states it to be only 50 feet thick in some sections in the Ophthalmia Range, where it may be thinned in folds.

TOPOGRAPHIC EXPRESSION

The typical topographic expression of the Mount McRae Shale is a concave, scree-covered slope separating the cliffs of the Dales Gorge Member from the prominent step of Bruno's Band (Figure 20). In places, the upper iron formation member forms cliffs immediately below those of the Dales Gorge Member, adding to the height of the scarp, but generally it is buried beneath scree. The concave slope is sometimes broken by low cliffs where resistant bands of chert and dolomite stand out, but more often lacks any outcrop.

WEELI WOLLI FORMATION

REDEFINITION

The Weeli Wolli Formation was defined by MacLeod and others (1963) as a thick succession of jaspilite, shale, and dolerite overlying the Brockman Iron Formation. The type locality was given as Weeli Wolli Spring and a type section measured near Woongarra Pool. At that early stage, the base of the formation was not accurately defined, but later MacLeod and de la Hunty (1966) stated "the base of the Weeli Wolli Formation is marked by a remarkably persistent concordant dolerite intrusion which can be followed for scores of miles within the ferruginous shales". In the type locality of the formation, this sill is intrusive into the top of the Yandicoogina Shale Member, but because it is slightly transgressive, may rise 20 to 60 feet above this position in other places. Where this occurs there is a sequence of BIF and shale between the sill and the Yandicoogina Shale Member. Ryan and Blockley (1965) in an unpublished report, named this unit the Coondiner Member of the Brockman Iron Formation, and Trendall (1966a) included it when he referred to five members of that formation. The name Coondiner Member is still informal, and it is here proposed to discard it and to incorporate the unit within the Weeli Wolli Formation, rather than formally define a member whose thickness, and very existence, depends more upon the vagaries of a dolerite sill than on stratigraphic logic. During the regional mapping of the Hamersley Group, the base of the Weeli Wolli Formation was often taken as the thick sill and the iron formation immediately below it as part of the Brockman Iron Formation. In such places then, the mapped contacts will not conform to our present definition of the boundary, but the discrepancy is seldom more than a few hundred feet. Due to this new definition of the base of the formation, 60 feet must be added to the type section of MacLeod and others (1963), and the thickness of the Brockman Iron Formation is reduced by 60 feet in the same area. Considering the great thicknesses of the two formations, and the errors inherent in the measurements, we feel that the changes are negligible.

A section of the formation, measured in the vicinity of Woongarra Pool, is:

Thickness (feet)	Description	Thickness (feet)	Description
Top			
60	Dolerite	20	Shaly BIF
2	BIF	225	Dolerite
55	Dolerite	35	BIF
3	BIF	30	Shale
160	Dolerite	75	Shaly BIF and shale
30	BIF	80	BIF
110	Dolerite	240	Dolerite
5	BIF	35	Shaly BIF
135	Dolerite	Base 25	BIF
35	BIF		
100	Dolerite	Total ...	1,485
25	BIF		

LITHOLOGY

Most exposures of the Weeli Wolli Formation are in the more deeply weathered parts of the Hamersley Range area. Consequently there are no uninterrupted exposures of clean fresh rock such as those of the Brockman Iron Formation in the gorges near Wittenoom. Fortunately the iron formation stands out as ridges on which there is some exposure, but the intervening shale and dolerite are rarely exposed at all. The BIF is characteristically red, in contrast with the usual yellow of the Marra Mamba Iron Formation and the grey of the Joffre Member. It is divisible into two types.

The first, and most common, is a dark red or red-brown, heavy rock, regularly and evenly laminated in stripes most obviously defined by variations in depth of colour. These stripes are usually between 2 and 5 mm thick (Figure 25) and in any one hand specimen vary little in thickness. In the more weathered exposures the rock is fissile, and splits into thin sheets, like slate. We call this the *striped facies* of the Weeli Wolli Formation. The stripes are made up of groups of very fine microbands, described in Chapter 4; but these are not normally distinguishable in the field.

In the second type of BIF, material resembling that of the striped facies, but either less conspicuously striped or not clearly striped at all, acts as chert-matrix for chert mesobands of the same order of thickness as those of the Dales Gorge Member. These cherts are, like those of the Joffre Member, either red or white. The red cherts are remarkable for their thick microbanding. Alternations of bright red and pale grey or buff within these cherts define the microbands, which are usually 2 to 5 mm thick; thus a chert mesoband a centimetre thick may contain only 2 or 3 microbands, a textural situation unknown outside the Weeli Wolli Formation. The white cherts are of the same order of thickness as the red cherts, but their microbanding is usually slightly thinner, although still well above the general microband thickness for the cherts of the Dales Gorge

or Joffre Members. It differs from that of the red cherts in being rather weakly defined, by thin dark lines in the conspicuously white body of the chert. In one exposure near Weeli Wolli Springs groups of white and red cherts were found to alternate in a manner reminiscent of the Knox cyclothem of the Joffre Member. A single example of this alternation contained a total of about 70 stripes or mesobands; the significance of this observation is suggested in Chapter 9, after further details of the striping are presented in Chapter 4.

We cannot relate the occurrence of these two BIF types to the field lithological assessment of the measured section given under the immediately preceding heading.

The sills which comprise the greater part of the thickness of the formation, consist of fine to medium-grained, deuterically altered dolerite. Because these sills extend for many miles with almost perfect conformity, it has been suggested that they are actually lava flows. The evidence which has now accumulated confirms the intrusive origin of the dolerites. Briefly it is as follows: the sills transgress the bedding of the host sediments in many localities; the upper margins of some sills show chilling and the adjacent sediments have been altered; rafts of iron formation lie in the dolerites; and near Kalgan Creek, the dolerite contains a xenolith of the overlying Woongarra Volcanics. The proportion of dolerite in the Weeli Wolli Formation is known to vary, but little precise information is available. At Woongarra Pool, dolerite makes up 75 per cent of the outcropping thickness of the formation, and at Kalgan Creek the proportion is over 50 per cent. Daniels and MacLeod (1965) state that the amount of dolerite decreases northwards from the Ophthalmia Range, while Kriewaldt and Ryan (1965) found only one sill in the formation where it is exposed in the Silvergrass Syncline. The field distinction of the formation as a mappable unit depends largely upon the existence of the dolerite sills; where they are absent, the formation is difficult to separate from the Brockman Iron Formation.

The Weeli Wolli Formation contains a little volcanic material in places. One 4-inch bed of blue-grey material found at Weeli Wolli Spring proved to be a tuff. Daniels (1967) records a possible volcanic ash near the top of the formation.

LATERAL DISTRIBUTION AND THICKNESS VARIATION

The Weeli Wolli Formation is best preserved in the central and southern parts of the Hamersley Range area. It is known from Ethel Gorge in the east to Mount Wall in the west, and in places, forms the southern margin of the outcrop of the Hamersley Group. On the Hamersley Plateau, it is well developed in the Yandicoogina Syncline, where the upper part is usually removed by erosion, and it has been recognised in the Silvergrass Syncline.

The large and variable thickness of dolerite in the formation makes the true thickness of the sediments difficult to determine. The section in Woongarra Gorge contains about 400 feet of sediments and one at Kalgan Creek, about 600 feet.

TOPOGRAPHIC EXPRESSION

Where it is flat dipping, the Weeli Wolli Formation forms conical buttes terraced by outcrops of BIF. Where inclined, the more resistant strata of BIF form cuestas or hog-backed ridges, while the dolerite sills and shaly beds weather out to troughs. The series of parallel ridges and troughs so formed often extends for many miles without interruption. The thick dolerite sill near the base of the formation forms a particularly prominent valley, which on the regional scale is a useful stratigraphic marker.

WOONGARRA VOLCANICS

MacLeod and others (1963) applied the name Woongarra Dacite to a succession of acid lavas and tuffs with interbedded iron formation lying stratigraphically between the Weeli Wolli Formation and the Boolgeeda Iron Formation. Later, the name was changed to Woongarra Volcanics (MacLeod, 1966) in recognition of the presence of rhyolite within the lavas. The formation was first noted in the Brockman Syncline; and Woongarra Pool, where good exposures of the lavas can be seen in the gorge of the Beasley River, was nominated as the type area.

Outcrops of the lavas extend along the length of the Hamersley and Ophthalmia Ranges, from Jimblebar Creek to Mount Wall and Deepdale. In the northern part of the Hamersley Range, erosion has removed most of the formation leaving the volcanics preserved only in a few structural basins. Contacts between the lavas and the adjacent sediments are always conformable. MacLeod (1966) gives a section of the formation measured near Kalgan Creek. A section measured at Woongarra Pool is as follows:

	<i>Thickness (feet)</i>	<i>Rock Types</i>
Top		
	80	Stratified tuffs, siltstones, and some microbanded cherts
	1,580	Flinty grey porphyritic rhyolite with brecciated bands
	20	Stratified green tuffs and BIF
	20	Brecciated lava
	280	Exposure gap thought to be occupied by a dolerite sill
	10	Stratified tuffs
	210	Non-porphyritic, grey-green dacite
	20	Stratified green tuffs
	150	Non-porphyritic grey-green rhyolite
Total	2,380	Base of exposure a little distance above top of Weeli Wolli Formation

Petrographic examination shows that most of the lavas can be classed as rhyolite but the green, chloritic dacite near the base of the section has been recognised over a wide area. It is a dense, green siliceous rock with a granularity which gives it the appearance of a quartzite. The rhyolites are blue-grey to black, dense porphyritic rocks containing crystals of quartz and potash feldspar set in

a glassy groundmass. The BIF unit in the formation has wide lateral persistence, and demonstrates that conditions necessary for the deposition of iron formation existed in the middle of a volcanic epoch. Although only 20 feet thick in Woongarra Gorge, the unit attains a thickness of 150 feet in the area of Kalgan Creek, and could well be classed as a separate formation within the Hamersley Group. Lithologically it resembles the iron formation in the Weeli Wolli Formation. Apart from the measured sections of 2,400 feet at Woongarra Pool, and 950 feet at Kalgan Creek, there is little information on the thickness variations of the volcanics. MacLeod (1966) estimates a thickness of 1,900 feet in the Brockman Syncline, 400 feet at Jimblebar Creek (lat. $23^{\circ} 20'S$, long. $120^{\circ} 10'E$) and 100 feet on the south side of the Turee Creek Syncline. Williams (1966) states that the thickness is around 1,000 feet in the northwest corner of the Hamersley Range and a similar figure is given by Kriewaldt and Ryan (1965) for the section on the Pyramid Sheet to the east.

BOOLGEEDA IRON FORMATION

This is the youngest formation of the Hamersley Group. With the exception of thin local iron formations in the Wyloo Group (p. 34) its top marks the end of banded iron formation deposition in Western Australia. MacLeod and others (1963) defined the type locality as Boolgeeda Creek (lat. $22^{\circ} 36'S$, long. $117^{\circ} 04'E$), where the formation is 700 feet thick. Its distribution appears on Plate 4.

With the usual exception of the Wyloo Anticline, and with the proviso that few measurements have been made, the Boolgeeda Iron Formation appears to retain its thickness and broad internal divisions in a degree at least equal to the underlying formations of the Hamersley Group. The uppermost and lowermost 300 feet consist of iron formation, while the middle part, which is very rarely exposed, is shaly.

We differ from MacLeod (1966, p. 56) in finding that the iron formation is distinctively different from that of any of the older formations of the Hamersley Group. It is a tough, fine-grained, finely laminated, heavy, dark greyish brown to black, flaggy rock which resembles the striped facies of the Weeli Wolli Formation but differs from it in being intensely magnetic, in its different colour, in breaking into thicker plates, and in lacking regular striping. In summary it is like much chert-matrix of the Dales Gorge Member without its associated chert mesobands. Occasional chert mesobands do occur and tend to be thicker, coarsely and faintly microbanded, and rather glassy in appearance. In the lower section at Woongarra Pool there are thin shaly partings at about 1-foot intervals. These partings, and the scattered cherts, are the only signs of stratification at a larger scale than the general fine lamination.

In the upper part of the formation at Woongarra Pool, the iron formation passes gradationally into the green siltstone and greywacke of the conformably overlying Turee Creek Formation of the Wyloo Group, by a gradual change of colour reflecting a gradual increase of clastic material.

CHAPTER 4

Petrography and mineralogy of the iron formation

INTRODUCTION

In the preceding chapter those compositional and textural features of the Hamersley Group iron formations which are conveniently studied in the field or in core were described, under the heading 'Lithology', separately for each stratigraphic formation and member. In this chapter more detailed descriptions are given of features best seen in the laboratory; the headings here are based on the described lithological features of the iron formation rather than on their stratigraphic divisions.

This chapter has three main parts. Under the heading 'Petrography of the main mesoband types' emphasis is placed on textures rather than composition. The section headed 'Mineralogy' is a summary of the occurrences of each of the minerals contributing to the textures described; it briefly synthesises and adds to the mineralogical information inevitably given in the course of the preceding textural descriptions. Finally, beneath the heading 'Notes on paragenetic evidence', all the evidence useful in interpreting the sequence of mineral growth is assembled.

Because we have chosen to discuss riebeckite in a separate chapter, it is not systematically treated here, but occasional references cannot be avoided.

PETROGRAPHY OF THE MAIN MESOBAND TYPES

MICROBANDED CHERT

DEFINITIONS AND CHARACTERISTICS OF MICROBANDING

The term microbanding is applied in this bulletin to regularly repeated laminae of even thickness, typically within chert mesobands, normally defined by a varying content of some iron-bearing mineral within the chert. Two successive laminae, one iron-poor and one iron-rich, together constitute a single microband; the *joint* thickness of such a pair of laminae is called the microband interval or thickness. The microband interval (t) throughout the Hamersley

Group is mainly within the range 0.5 to 1.2 mm (Figure 10 for Dales Gorge Member), but some examples of microbanding to be described below have intervals as small as 0.1 mm and as large as 5 mm. Thus thickness is not of itself a sufficient criterion for distinguishing microbanding from mesobanding; an essential feature of microbanding is the regular alternation of the two parts of each microband with almost the same thickness. In most sequences there is, apart from constant interval, also a precise replication in successive microbands of a number of textural and compositional details, which may differ markedly between the microbanding of different mesobands. In mesobanding, on the other hand, even in unusual situations where two mesoband types alternate repeatedly, there is usually a good deal of variation in thickness, composition or texture between alternations. This is true even where a cyclic alternation of types is present. Only in the striped facies of the Weeli Wolli Formation is there any possibility of confusion between mesobanding and microbanding when the criterion of regularity is used.

TEXTURAL AND COMPOSITIONAL VARIATION

It was shown in Chapter 3 that, for the Dales Gorge Member, the earlier distinction (Trendall, 1965a) into 'primitive' chert and 'flat-modified' chert mesobands was subjectively practicable for only about half of the total number of microbanded chert mesobands; and that for any chosen mesoband parameter (Figures 8 and 10) the remainder were distributed gradationally between the values typical of the two end-member types. It is nevertheless convenient to begin this account of microband variation with descriptions of the textural and compositional expression of microbanding in what would formerly have been described as primitive and flat-modified cherts of the Dales Gorge Member, before approaching the range of intergradational and variant types throughout the Hamersley Group iron formations. The following descriptions are therefore of microbanding in a typical coarsely microbanded chert from the mixed mesoband group of the Calamina cyclothem and of a typical finely microbanded chert from the chert-magnetite group of the Calamina cyclothem.

Figures 21A and C show the common features of microbanding in the coarsely microbanded chert. The microbands are defined, within an even-grained quartz mosaic of average grain diameter about 0.02 mm, by alternate layers of ankerite and stilpnomelane. The ankerite is in subhedral rhombs about 0.2 mm across in virtually continuous layers of roughly two rhombs thickness; it is not uncommon for ankerite rhombs to have 'hollow' (quartz-filled) centres. In the remainder of each microband pair ferro-stilpnomelane, in flakes about 0.01 mm across, is concentrated in central discontinuous streaks. These streaks characteristically die out and reappear laterally, and in their thicker parts are often made up of several separate laminae. In the mesoband illustrated a little hematite in fine platelets is associated with the stilpnomelane, and a few small magnetite octahedra are present.

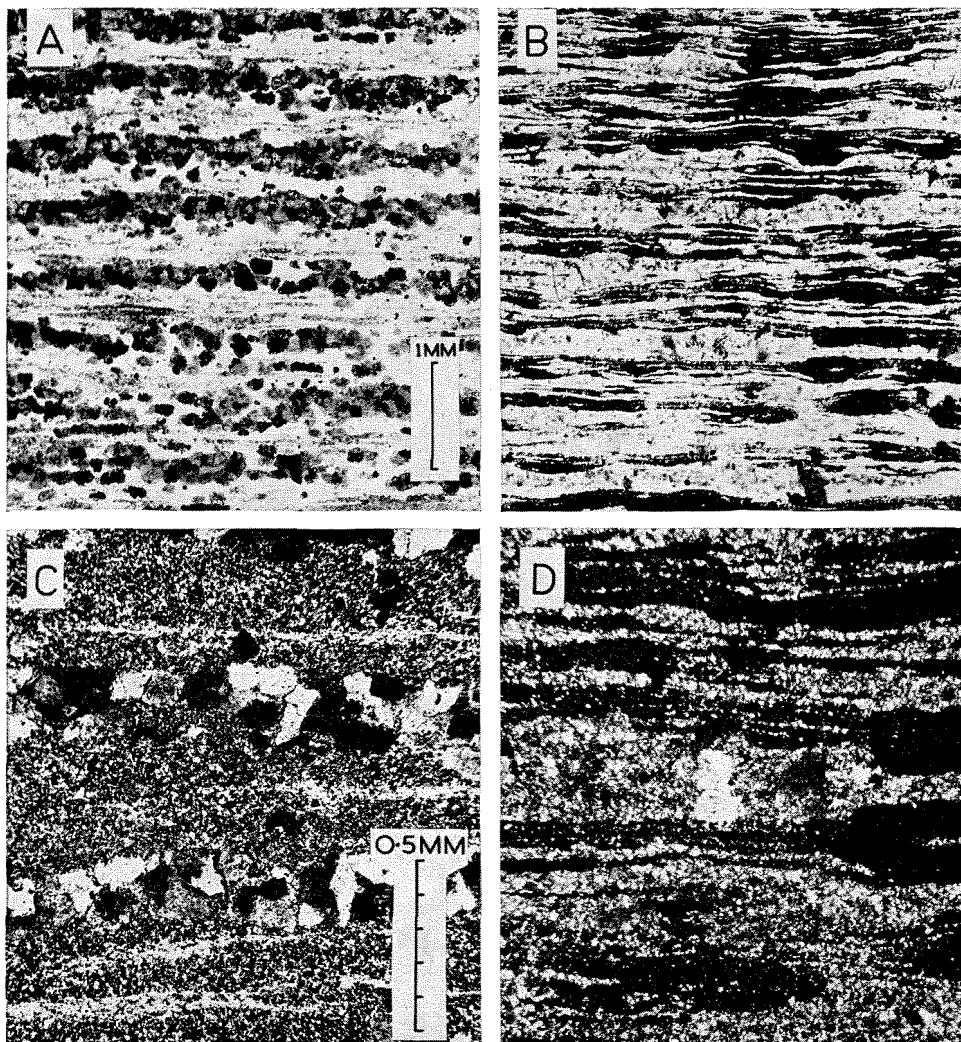


Figure 21. Typical microband textures in cherts of the Dales Gorge Member.

A and C. Photographs at different magnifications of a coarsely microbanded chert mesoband ($T = 5$ mm, $t = 0.55$ mm, $n = 9$) from the mixed group of a poorly defined Calamina cyclothem in BIF2 of the Dales Gorge Member. The chert illustrated is at 645 feet 5 inches in Hole 40 at Wittenoom Gorge, and is stratigraphically equivalent to the upper of the two thin chert mesobands at about 80.1 feet on the type section (Figure 5). The mineralogy and texture are described in the text. A detail of the immediately overlying magnetite mesoband appears in Figure 37C.

B and D. Photographs at different magnifications (equal to those of A and C respectively) of a finely microbanded chert mesoband ($T = 60$, $t = 0.28$, $n = 214$; t and n very approximate) from the chert-magnetite group of a poorly defined Calamina cyclothem in BIF2 of the Dales Gorge Member. The chert illustrated is at 647 feet 10 inches in Hole 40 at Wittenoom Gorge, and is stratigraphically equivalent to the adit roof riebeckite at 77.5 to 77.95 feet on the type section (Figure 5). The mineralogy and texture, particularly their contrast with A and C, are described in the text.

In the adjacent Figures 21B and D, which are at the same scale, the usual features of finely microbanded cherts are contrasted with those just described. Salient mesoband parameters are also contrasted in the caption. The microbanding is here defined, again within an even-grained quartz mosaic of average grain diameter about 0.02 mm, by hematite-rich layers, each composed of several thin laminae which thin and thicken laterally. A characteristic of this feature is that the thinner and thicker parts tend to be superimposed, so that lines joining, in section, the thinnest or thickest parts of successive laminae are vertical or steeply dipping (see also Figure 29A). The hematite consists variously of a solid interlocking mosaic, in the central part of the laminae, more loosely aggregated plates and blebs 0.005 to 0.1 mm across, and associated smaller 'dusty' platelets down to sub-micron size. There is more variation in successive

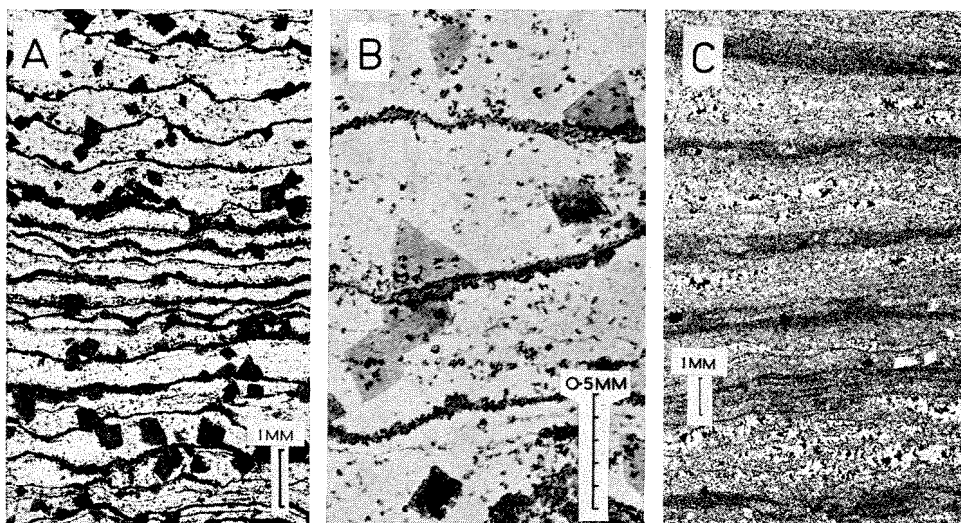


Figure 22. Textural and compositional expression of microbanding in chert-siderite of the Dales Gorge Member and the Whaleback Shale Member.

A and B. Photographs at different magnifications of microbanding in a microbanded chert ($T = 37$ mm, $t = 0.48$ mm, $n = 77$) from chert-siderite of the S13 macroband. The chert shown comes from 318 feet 6 inches in Hole 51 at Wittenoom Gorge, which is approximately equivalent to 326.0 feet on the type section. In A the rather undulating lines of siderite, with a much wider range of microband interval than is ever present in BIF cherts, are well displayed. B shows the details of the texture: each 'siderite' line has a concentration of small siderite rhombs along each edge, with stilpnomelane-rich chert between. Note the inclusion of small siderite rhombs within ankerite and the truncation of the ankerite crystals at the siderite lines; these features are referred to in later discussion.

C. Microbanding defined mainly by variations in grain-size of chert in a microbanded chert mesoband ($T = 37$ mm, $t = 2.5$ mm, $n = 15$) in the Whaleback Shale Member at 656 feet in Hole 47 at Wittenoom Gorge, close to the top of the member. Crossed nicols show up the unusually coarse chert; some ankerite rhombs are present, while finely flaky stilpnomelane is abundant in the darker parts of the microbands, and locally defines minor laminations.

microband intervals in this chert, and some of the hematite layers are so close that it is difficult to distinguish them clearly. Minor ankerite, siderite, magnetite, and riebeckite are also present in the illustrated chert.

The two types of microband expression contrasted in Figure 21 lie near the ends of a wide range of intermediate varieties. The proportions of hematite, magnetite, stilpnomelane, siderite, and ankerite appear in virtually every possible combination, and are combined with variations in microband interval and other characters so as to make the roughly 2,500 microbanded chert mesobands of the Dales Gorge Member divisible into almost as many classes, if sufficiently subtle differences are used as criteria. Some of these variations are illustrated or described in other sections of this chapter; it is necessary here only to select a few which, as will appear in later discussion, have special interest for genesis, or which are remarkable for extreme departure from normality.

The typical features of a microbanded chert from the chert-siderite facies of the S macrobands of the Dales Gorge Member are shown in Figures 22A and B. The irregular undulation of the thin siderite-rich layers which define the microbanding is characteristic of chert-siderite facies cherts of both the Dales

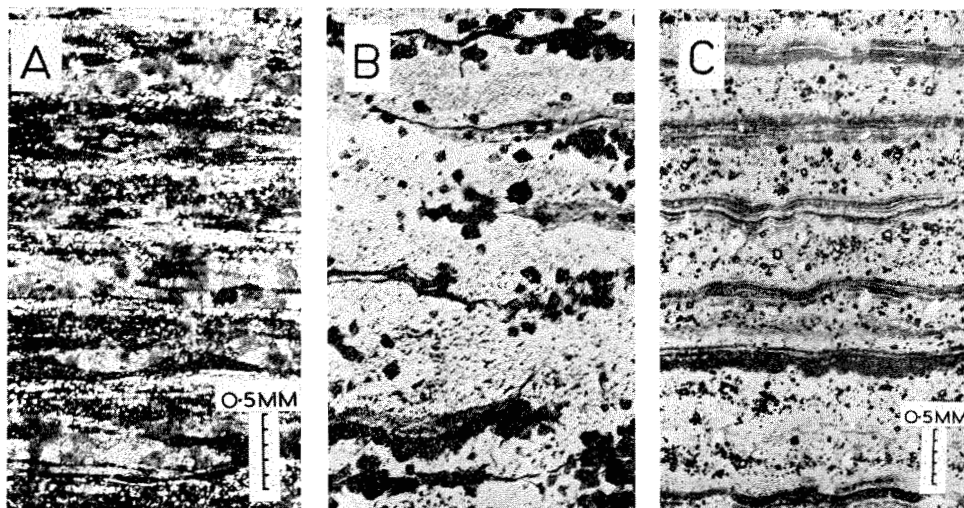


Figure 23. Textural and compositional expression of microbanding in red and white cherts of the Joffre Member and in a chert mesoband from the Boolgeeda Iron Formation.

A. Microbands defined by carbonate and stilpnomelane in a red chert ($T = 5$ mm, $t = 0.5$ mm, $n = 10$) of the Joffre Member, at 511 feet in Hole 47 at Wittenoom Gorge, about 131 feet above the base of the member.

B. Microbands defined mainly by siderite and stilpnomelane in a white chert ($T = 15$ mm, $t = 0.52$ mm, $n = 29$) of the Joffre Member, at 349 feet in Hole 47 at Wittenoom Gorge, about 293 feet above the base of the member. The dark grains are siderite rhombs, and the other dark lines and blotchiness in the chert are due to fine-grained ferristilpnomelane. A few small, feathery-ended prisms of riebeckite appear among the siderite (scale as in A).

C. Microbands defined by concentrations of finely granular hematite which are themselves made up of several continuous laminae. The illustrated chert mesoband ($T = 50$ mm, $t = 0.58$ mm, $n = 86$) is from near the base of the Boolgeeda Iron Formation about 6 miles east-southeast of Mt. Turner.

Gorge Member and the Whaleback Shale Member. A common variant of chert mesobands in this facies, especially where they are close to the associated stilpnomelane shale, is for a combination of stilpnomelane and variations in quartz grain-size jointly to define the microbanding. This is shown in Figure 22C.

The microbanding in a red chert of the Joffre Member which shows some characteristic and some most unusual features is shown in Figure 23A. The alternation of light and dark bands of about equal thickness and with rather flat boundaries is characteristic of many red cherts in both the Joffre Member and the Weeli Wolli Formation, as is the mottling of the dark bands; it is unusual, though, for this mottling to be expressed in ferristilpnomelane, as in the illustrated example, rather than fine hematite, and it is even more unusual for the light bands to consist of ankerite rather than chert. The microbanding of a white chert of the Joffre Member is contrasted with this in Figure 23B. It has some affinity with that of the cherts of the chert-siderite facies.

An unusual type of microbanding in a thick chert near the base of the Boolgeeda Iron Formation appears in Figure 23C. Each iron-rich part of the microband consists of several thin continuous laminae defined by concentrations of hematite granules about 1 to 5 microns across.

The macules of the Dales Gorge Member were described by Trendall (1966a), and are noted again in Chapter 6. One of their properties which is relevant here is the coarse microbanding of their cores; an example of this is illustrated in Figure 24A. Apart from its great width the striking textural feature here is the definition of the microbanding mainly by changes in abundance and composition of the virtually continuous sequence of streaky lenticles in the quartz matrix. Texturally similar microbanding is locally present in cherts of the Weeli Wolli Formation, in which chert mesobands 10 mm thick, with only two microband pairs, alternate with chert matrix mesobands 2 to 3 mm thick. Here is an instance where mesobands are thinner than adjacent microbands.

One characteristic of microbanding that has been emphasized elsewhere in this bulletin is the comparatively slight variation in microband interval in the microband sequence within any one mesoband. The examples illustrating this chapter mainly bear out this judgment, but an exception is shown in Figure 24B. In this chert, within tuffs at the top of the Woongarra Volcanics, the microband interval steadily increases towards the centre of the chert. The microbanding here is defined solely by textural (largely grain-size) variations in iron-free chert.

Although the symmetry of microbands is such that it is not possible to tell stratigraphic top and bottom from textural evidence, a few instances where this is not so have been found; two of these are illustrated in Figures 24C and 26C, from the Dales Gorge Member and the Weeli Wolli Formation respectively.

Where crocidolite occurs abundantly in the Dales Gorge Member in a close-packed chert sequence, as in the Upper Seam (page 183) the microbanding in these cherts is usually defined entirely by jaspery hematite platelets (page 122) and carbonate is almost absent, to make them distinctly reddish in macroscopic appearance.

MULTIPLE MICROBAND GROUPING

The striped facies of the Weeli Wolli Formation differs from any other part of the Hamersley Group in being continuously microbanded. Elsewhere in the iron formations microbanding is confined to cherts bounded by non-microbanded chert-matrix material; and few microbanded cherts have more than 100 consecutive microbands (Figure 17).

The striping of the striped facies is due to alternation of microband groups which, in aggregate, appear darker or lighter. This is shown in Figure 25A and B. The thin-section displayed in Figure 25A has about 565 consecutive microbands (470 of which appear in the Figure) in its thickness of 44 mm; they are arranged in fairly sharply defined light and dark groups. The numbers of

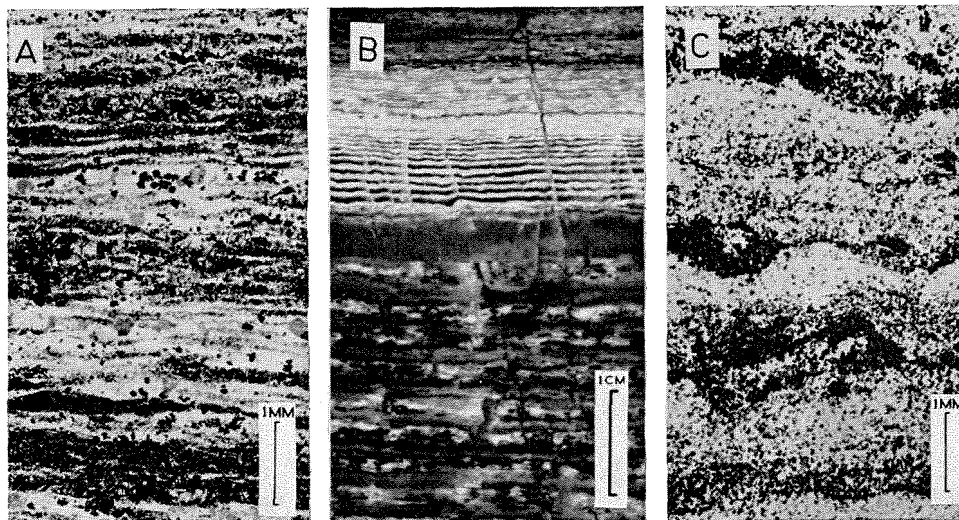


Figure 24. Some unusual varieties of microband expression in cherts from the Dales Gorge Member and the Woongarra Volcanics.

A. Coarse microbanding ($t = 2.2$ mm) in the core of a macule from MB1 (Trendall, 1966a; Trendall and Blockley, 1968, p. 51 and Plate 28) at 286 feet drilling depth in Hole 73 at Wittenoom Gorge. The dark streaky lenticles which define the iron-rich part of each microband consist largely of jaspery hematite platelets and cellular hematite while the lighter streaks in the iron-poor part are of ferrostilpnomelane. There is minor carbonate and magnetite, while apatite prisms are just visible in the iron-rich parts; texturally similar apatite is illustrated from another chert in greater detail in Figure 35E.

B. Polished surface of microbanded chert mesoband in tuffs of the Woongarra Volcanics 53 feet below the top of the formation on the east side of the gorge at Woongarra Pool. The microbanding, which is defined by textural variations in the chert, has an interval of about 4 mm in the lower part and decreases to about 0.2 mm upwards toward the edge of the mesoband, which has total thickness of 75 mm.

C. Microbanding defined by fine-grained siderite in a chert mesoband ($T = 25$ mm, $t = 1.5$ mm, $n = 17$) from chert-siderite of the S6 macroband of the Dales Gorge Member at 490 feet 11 inches in Hole 51 at Wittenoom Gorge, equivalent to about 159.0 feet on the type section. The asymmetric distribution of the siderite, giving an appearance like that of graded bedding, is unusual.

microbands in each group (stripe) and the mean microband intervals are marked in the Figure; it is apparent that the group darkness or lightness is not purely a function of microband interval. Each microband (Figure 25B) is defined by a thin, slightly wavy, concentration of finely granular hematite, which may be weakly divided into three or four laminae. In the slide illustrated, magnetite and stilpnomelane are present as well as the pervasive quartz mosaic of the chert, which here has an average grain diameter of about 0.01 mm. It is variations in the concentration of hematite which principally define the darkness or lightness of the groups.

The striping of Figures 25A and B is less regular than much of that elsewhere in the striped facies. A more typically regular example is figured in Figure 25C. In this rock there is also a greater contrast in interval between the light and dark stripes, so that whereas the microbands can be individually counted in the light stripes they are difficult to distinguish in the dark ones. This tendency, for an antipathetic variation of microband interval in light and dark stripes, is illustrated in Figure 26A-C. The contrast is such that the light stripes virtually

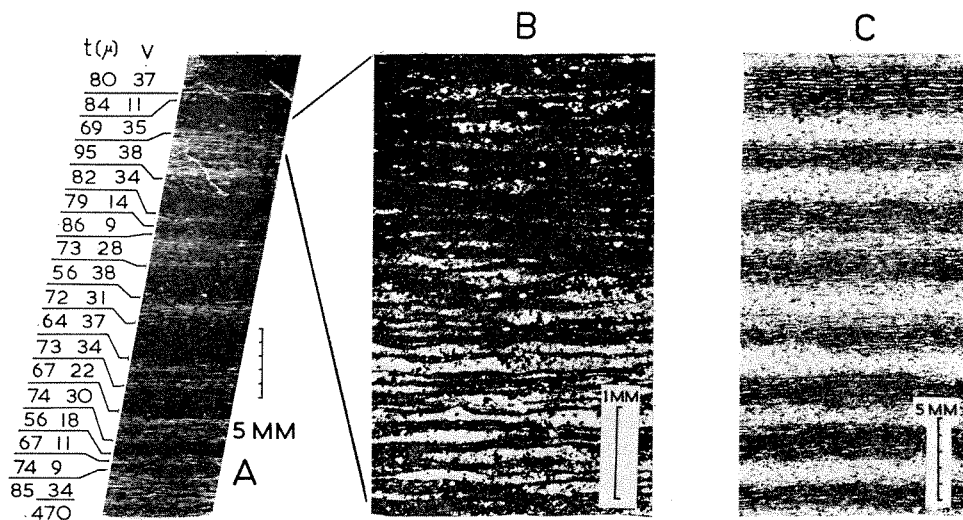


Figure 25. Photographs illustrating microband textures in the striped facies of the Weeli Wolli Formation.

A. Thin-section showing alternating light and dark stripes, the number of microbands (n) in each stripe, and the mean microband interval (t) in millimetres for each stripe. From a sample collected in cliffs on the southeast bank of Marillana Creek (lat. 22° 44'S, long. 119° 06'E); position within the formation is uncertain.

B. Larger scale photograph of part of the same thin-section used in A, showing the rather wavy microbands with a very small interval. The boundary between a light and a dark stripe falls centrally in the photograph.

C. Another example of the fine texture within stripes of the striped facies, in which the striping is more characteristically regular. From a sample collected in cliffs on the southeast bank of Marillana Creek about ½ mile west of Cajubut Bore (lat. 22° 47'S, long. 119° 08'E).

have the status of chert mesobands, while the dark stripes, with their indistinct microbanding, occupy the textural position of chert-matrix.

Outside the striped facies of the Weeli Wolli Formation multiple microband groups are rare, but occasional instances have been seen in chert-matrix of the Marra Mamba Iron Formation, and in an unusual structure in some magnetite and chert-matrix mesobands of the Dales Gorge Member. In the BIF11 macroband of the type section, at 286.1 feet, the chert-matrix is not homogeneous, but consists of several magnetite-rich layers about 2 to 3 mm thick separated by thinner quartz-rich layers. The striking regularity of this arrangement strongly resembles that of the Weeli Wolli Formation striped facies.

MARGINAL AND INTERNAL MICROBAND RELATIONSHIP

The behaviour of microbanding in laterally discontinuous, or podded, cherts is important for later interpretation, and is illustrated here in some detail.

In chert pods whose breadth:thickness ratio is greater than about 3:1 microbanding is laterally continuous from the pod into the enclosing chert-matrix. This is well illustrated in the example from the Weeli Wolli Formation in Figure

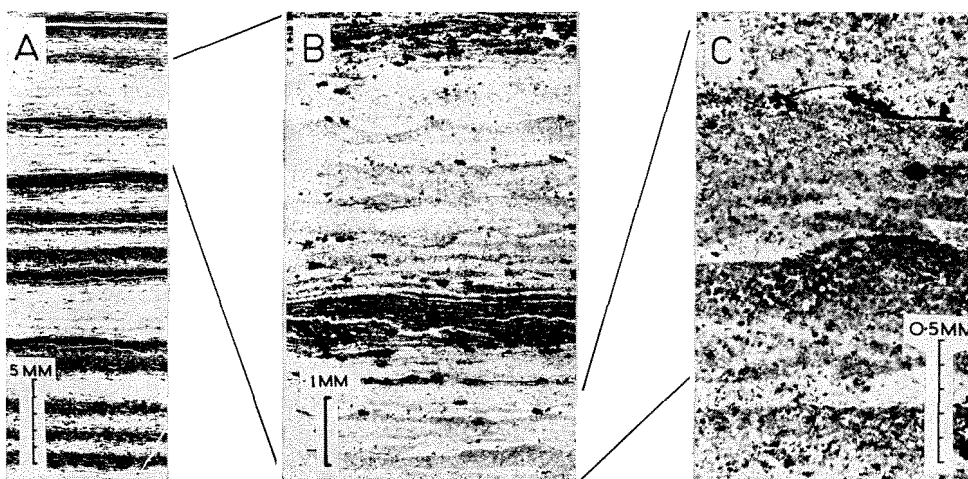


Figure 26. Further photographs illustrating microband textures in the striped facies of the Weeli Wolli Formation.

A. The distribution of stripes in striped facies iron formation from the east bank of Weeli Wolli Creek about $1\frac{1}{2}$ miles downstream from Weeli Wolli Springs (lat. $22^{\circ} 55'S$, long. $119^{\circ} 12'E$). The thin pale chert-like stripes are pink.

B. Enlarged photograph of part of the same thin-section, showing the coarse microbanding in the pale stripes ($t = 0.5$ mm) and the very fine microbanding in the dark stripes ($t = 0.05$ mm). The roughly 10 times difference in microband interval between light and dark stripes contrasts strongly with the slight difference between the light and dark stripes in Figure 25A.

C. Further enlargement of the microbands in the light stripes. Note the asymmetric graded appearance (compare Figure 24C) and the local accumulation of the very fine-grained hematite, which mainly defines the microbands, into globular concentrations.

27A. In the Dales Gorge Member the transition is more commonly as in Figure 27B, in which there is general continuity of lamination, but regular microbanding is not clearly defined in the chert pod. Another example from the Dales Gorge Member appears in Figure 28A. Where the breadth:thickness of the chert pod is about 2:1 or less, as is common in, for example, the Joffre Member and the Marra Mamba Iron Formation, there is normally some degree of discontinuity at pod edges. A transitional case appears in Figure 28B, where continuous microband traces occur at one level but become discontinuous as the edge of the chert pod is followed round. The thickness ratio between stratigraphically equivalent chert and chert-matrix at pod margins varies between about 3:1 and 20:1, with a usual average of about 7:1. In general the transition is, as illustrated in Figures 27 and 28, comparatively abrupt, and there exists no gradational material between the chert of the pod and its enclosing chert-matrix.

Although microbanding is normally concordant with the margins of continuous chert mesobands there are exceptions to this. The textural details of marginal discordance are identical with those of a type of microband behaviour commonly associated with the internal discontinuities or irregularities of microbanding which are laterally persistent within many chert mesobands (see Figure 15). This behaviour is illustrated in Figure 29A, which is a larger scale

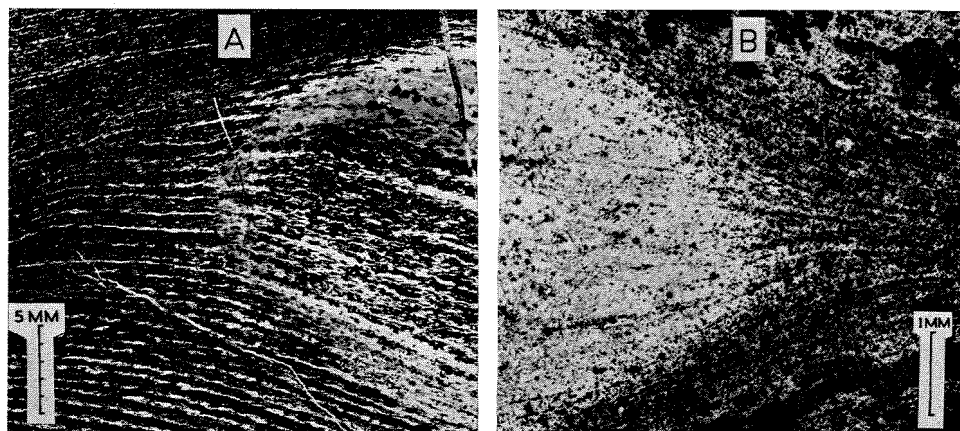


Figure 27. Examples of the textural relationships of laterally discontinuous (podded) cherts.

A. Edge of chert pod (a cross-pod; see Chapter 6) from the Weeli Wolli Formation in a cliff on the southeast bank of Marillana Creek about $1\frac{1}{2}$ miles northwest of Cajubut Bore (lat. $22^{\circ} 47'S$, long $119^{\circ} 08'E$). The coarse microbanding is defined by cloudy concentrations of hematite 'dust' less than 1 micron in diameter, but this surface specimen is, to some extent at least, affected by surface weathering, and it is only to the texture that attention is drawn.

B. Edge of chert pod from the BIF2 macroband of the Dales Gorge Member at 645 feet 11 inches in Hole 40 at Wittenoom Gorge, equivalent to 79.5 feet on the type section (Figure 5). The fine lamination of the chert-matrix on the right clearly passes smoothly into the chert on the left, even though this is not clearly microbanded. The chert-matrix here contains quartz, minnesotaite, magnetite, siderite, hematite and riebeckite, in approximate order of abundance.

photograph (and reversed by the microscope) of the lower right-hand part of Figure 30C. From right to left in the photograph five successive iron-rich parts of microbands, defined by hematite, coalesce into a single hematite-rich unit which, should its thickness exceed a millimetre, must be called a chert-matrix mesoband. In such textural situations it is typical that, as illustrated, the very characteristic streakily discontinuous hematite of the chert microbands (Figure 21B) disappears as the microbands join, and each microband is represented by between 3 and 6 fine *continuous* hematite laminae apparently equivalent to those which are discernible, but discontinuous, in the chert. The assumption from this textural observation is that any dark hematite-rich internal discontinuity of a microbanded chert which possesses the very fine lamination shown by that of Figure 29A may result from the lateral coalescence of several microbands.

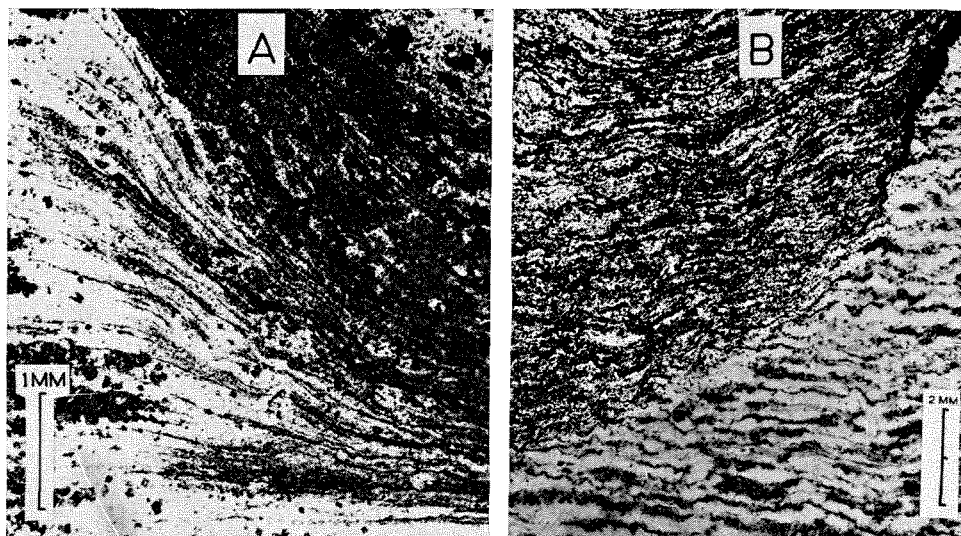


Figure 28. Further examples of the textural relationships of laterally discontinuous cherts.

A. Continuity of chert microbanding (left) and chert-matrix lamination (right) in a partially podded chert mesoband in BIF2 of the Dales Gorge Member, from 580 feet 3 inches in Hole 46 at Wittenoom Gorge, equivalent to 81.9 feet on the type section (Figure 5). Note that part of the chert mesoband runs continuously across the lower edge of the photo. The dark minerals in the chert are ankerite (comparatively coarse), stilpnomelane and jaspery hematite, while siderite and magnetite are the main constituents of the chert-matrix other than quartz.

B. Marginal texture of a thick podded white chert of the Joffre Member at 344 feet in Hole 47 at Wittenoom Gorge, about 298 feet above the base of the member. The microbanding is closely similar to that already shown in Figure 23B. There is general continuity between chert-matrix lamination and chert microbanding in the lower part of the figure, but the upper part of the junction is discordant, and is marked by a thin vein of riebeckite (black). Microbands are defined mainly by ankerite and riebeckite in the chert, while the dark minerals in the strongly laminated chert-matrix are hematite, magnetite and riebeckite, in approximate order of abundance.

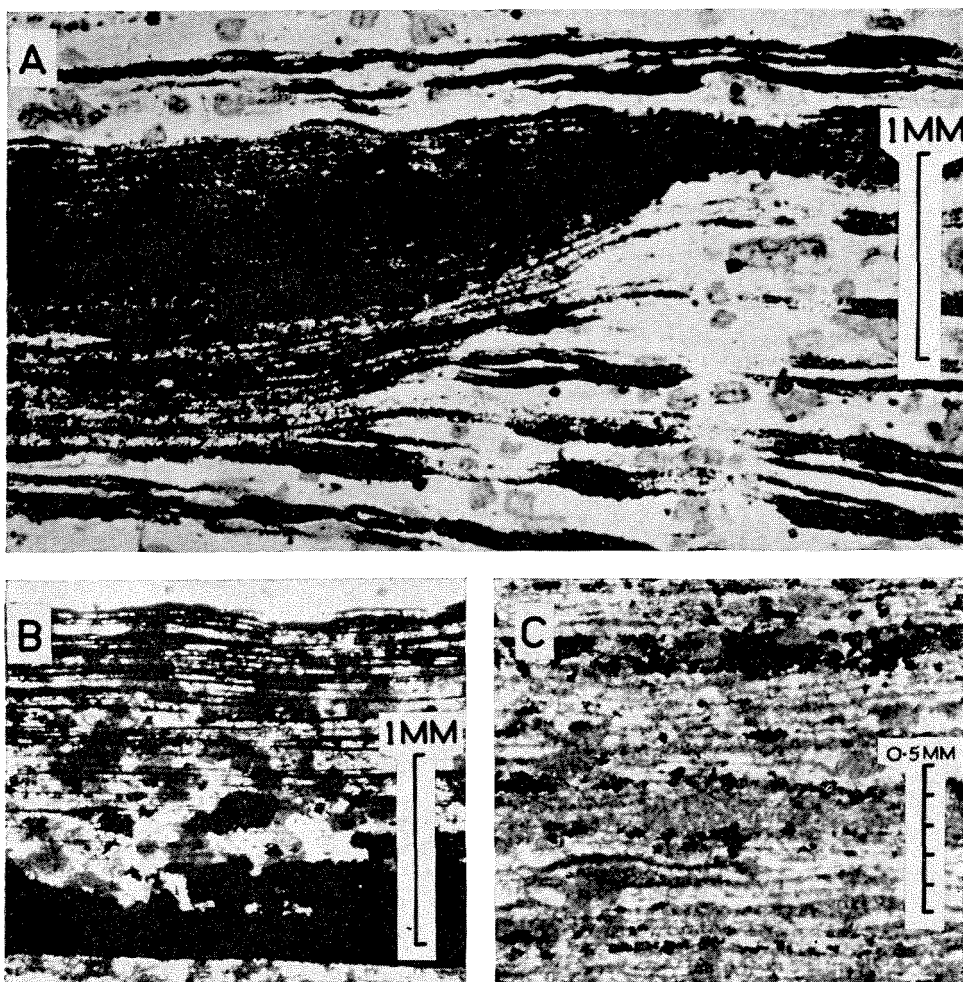


Figure 29. A. Detail of microband textures in a microbanded chert mesoband in the BIF2 macroband of the Dales Gorge Member at 586 feet 4 inches in Hole 51 at Wittenoom Gorge, equivalent to precisely 77.05 feet on the type section (Figure 5). The tendency for vertical superimposition of thin and thick sections of the hematite laminae defining the microbanding is clearly shown; see text for description of other features which are illustrated. Most of the matrix of this 'chert', and all the ankerite-like rhombs are in fact fine-grained stilpnomelane; see 'Notes on paragenetic evidence'.

B. Fine laminae defined by hematite in ankerite mosaic at the margin of a chert mesoband in BIF2 of the Dales Gorge Member at 645 feet 6 inches in Hole 40 at Wittenoom Gorge, equivalent to 79.95 feet on the type section (Figure 5).

C. The typically fine lamination of siderite of chert-siderite in the S13 macroband of the Dales Gorge Member at 319 feet 2 inches in Hole 51 at Wittenoom Gorge, equivalent to about 324.7 feet on the type section... The lamination is defined almost entirely by different grain-sizes of siderite, although a very little quartz, stilpnomelane and ankerite are also present. The strings of small magnetite octahedra present here are most untypical of chert-siderite.

This type of texture is normally present also wherever one or more microbands meet and fuse with the margin of continuous chert mesoband as a result of a very slight fluctuation in thickness; for example at the lower edge of the chert in Figures 30A and B. Fine lamination, defined by dusty hematite, is present at the edges of some chert mesobands where there is no apparent coalescence of microbands (Figure 29B). It often lies within a thin marginal selvage of ankerite mosaic.

LATERAL CONTINUITY OF MICROBANDING

The lateral distance over which the physical continuity of structures as small as microbands can actually be observed is obviously restricted; a satisfactory demonstration of greater continuity depends on whether they can be correlated, like any other strata, between distant samples of any chosen mesoband. Subject to limitations imposed by the textural features just described such correlation is not difficult, and has been achieved in surface samples of cherts in macroband BIF0 of the Dales Gorge Member from Dales Gorge and from James Point, 185 miles apart. In Figure 30 three thin-sections of a single chert mesoband (type section 77.05 to 77.15 feet) from BIF2 demonstrate the difficulties involved.

A primary difficulty for any microband correlation is the usual lack of significant microband interval variation in any single chert; this is analogous, on a smaller scale, with the difficulty of mesoband correlation where the Calamina cyclothem is strongly developed. For convincing subjective correlation some distinctive sequence of thickness changes is essential, the more irregular the better. Most microband sequences do not have these, and the number of mesobands within which correlation, even if it existed, could be demonstrated, is thereby severely restricted. Given sufficient irregularity for potential lateral identification, distant correlations must be made with constant awareness that internal finely laminated hematite-rich discontinuities may be represented laterally by groups (of uncertain size) of microbands, and that microbands may coalesce locally with the chert margins; simple correlation by counting microbands from the margin is therefore, if apparently successful in terms of irregularities, rather lucky.

The microbanding in the part of the chert mesoband shown in Figure 30C is divisible into three groups of 9 to 12 microbands by two dark discontinuities. The lower of these is apparently easily recognisable in Figure 30A, and the upper one less obviously so. In both A and C, microbands plainly coalesce with the lower discontinuity across the slide. In Figure 30B the upper continuity seems clearly correlative with that of C, and diverges into its component microbands in the photograph. In B the lower discontinuity may be supposed to be represented by the broad group of rather compressed microbands, while an additional discontinuity is present 3 to 4 microbands from the lower edge. If attention is now given to the microbands between the two main discontinuities, whose correlation appears at least possible, a central rather thin hematite layer can be identified in A, B, and C with a greater than average thickness of chert

separating it from its neighbours. Its correlation is suggested by dotted lines, and the resulting correlation of neighbouring microbands is shown by solid black lines for 5 microbands up and 6 microbands down. This lowest microband has abundant thick hematite laminae and lies just above the lower discontinuity in A and C. There is not enough irregularity here for a confident assertion of correlation, and the example is provided to illustrate both the possibilities and the difficulties of correlation.

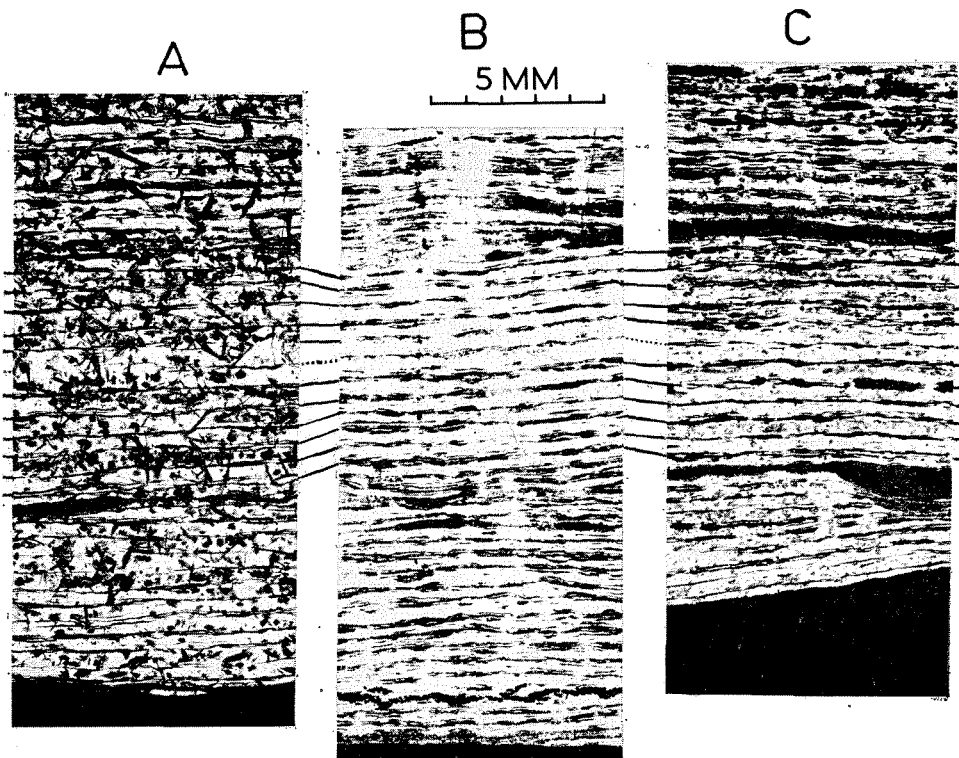


Figure 30. Photographs of part of the same chert mesoband from the BIF2 macroband of the Dales Gorge Member in three different drillholes, to illustrate problems in the lateral correlation of microbands; see text for discussion and type section position. The locations are as follows:

A. Drilling depth 648 feet 3½ inches (base of chert) in Hole 40 at Wittenoom Gorge (Plate 6).

B. Drilling depth about 251 feet in Hole JG1 at Junction Gorge (Figure 66).

C. Drilling depth 586 feet 4 inches in Hole 51 at Wittenoom Gorge. The cores from which A and B were cut are illustrated in Figure 7C. Note the significantly different mineral composition of the three cherts. All have the microbanding defined by hematite, but in A there are needles of riebeckite and ankerite rhombs (see Figure 60A), B has little other than quartz and hematite, while in C much of the apparent 'chert' and ankerite-like rhombs are stilpnomelane.

NON-MICROBANDED CHERT

A gradation exists between microbanded cherts of the type just described, with clearly defined and very regular microbanding, through similar cherts in which there is variably irregular internal lamination (Figure 41B), to cherts with barely distinguishable lamination or none at all. This condition is particularly common in chert pods (Figures 27B and 40B) but occurs also in continuous chert mesobands. The roughly 23 per cent of non-microbanded cherts in the total of 282 chert mesobands reported in Table 4, includes all cherts, including podded cherts, in which the microbanding is not characteristically regular, and sufficiently clearly defined for separate identification of the microbands.

Petrographically, cherts without clear microbanding tend to have a smaller total quantity of the same iron-bearing minerals as those defining the microbanding of microbanded cherts. These include hematite, stilpnomelane, siderite, ankerite, magnetite, and riebeckite, all comparatively fine-grained and distributed at random in the chert.

CHERT-MATRIX

The present use of the name chert-matrix to apply throughout the Hamersley Group iron formations to material texturally equivalent to that first described as QIO in the Dales Gorge Member (Trendall, 1965a) has already been noted. Chert-matrix in thin-section is illustrated, *inter alia*, in Figures 27, 28, 37A, 40, 41, 43C, 47, and 60B. It is impossible to list and describe separately all the possible minor textural variations of this material. The main constituent minerals are quartz, magnetite, hematite, stilpnomelane, ankerite, and siderite. Any or all of these may co-exist in a single mesoband, and the proportions of each are widely variable. The two main textural features of chert-matrix are that all component minerals are relatively fine-grained, with similar habits to those which they possess in the cherts, and that in contrast with the normally distinct separation into two components, as in the microbanding of the cherts, there is a general homogeneity of distribution. There is, however, a variable degree of fine lamination along the stratification (distinct in Figures 28B and 43C; more vague in Figures 27B and 40B). Apatite (Figure 35F) and riebeckite are common minor constituents.

MAGNETITE

Magnetite mesobands consist essentially of closely-packed plates of magnetite about 0.1 to 0.2 mm thick and at least ten times as wide. Usually there is at least 5 to 10 per cent. by volume of interstitial quartz, hematite, stilpnomelane, or other minor minerals, and the content of interstitial hematite mosaic, in particular, often exceeds 40 per cent. It is difficult to assess the proportions of these two minerals macroscopically, and the abundance of thin black magnetic mesobands in fresh core gives a misleading impression of magnetite content. In thin-section the platy structure of bands richer in magnetite is often concealed by superimposition of adjacent plates; the structure which is typical in all magnetite

mesobands is splendidly displayed in Figure 46, where a magnetite mesoband has been naturally opened up into its component layers by the growth of fibrous quartz.

STILPNOMELANE

Mesobands consisting mainly of stilpnomelane are usually thin and comparatively rare in BIF macrobands of the Dales Gorge Member. The thicker (1 inch to 2 feet) stilpnomelane tuffs of the Joffre Member (page 78) are more appropriately included in the later description of shales. In the Dales Gorge Member stilpnomelane mesobands occur preferentially in the mixed groups of the Calamina cyclothem, where their likely presence contributes to the naming of the group.

In thin-section there is normally a structurally continuous groundmass of clear, pale green, fine-grained stilpnomelane in which individual crystal boundaries are not sufficiently clearly defined for the total fabric to be clearly discernible. In some bands a random arrangement is suggested by a complete absence of bulk pleochroism, while in others a dark green colour when the band is parallel to the vibration direction indicates a preferred orientation along the bedding. Others again have a texture consisting of a complex interlocking pattern of rosettes, somewhat resembling that of massive riebeckite (Figure 56A, Chapter 7). Commonly associated minerals are magnetite, invariably in simple octahedra about 10 to 50 microns in diameter, very finely granular (about 20 microns) siderite, and riebeckite. In one stilpnomelane mesoband of the Dales Gorge Member (analysis 6 of Table 12, Chapter 5) riebeckite occurs as an overgrowth over cores of a paler amphibole pleochroic in brown and green.

A type of stilpnomelane mesoband of which no other example has yet been found was reported and illustrated by Trendall (1966b, Figure 2; the depth appears there wrongly as 582 ft. 1 in. instead of 852 ft. 1 in.). This band lies about 3 feet below the S2 macroband. It is (in Hole 51) about 2 inches thick, and consists largely of an aggregate of a brown stilpnomelane, with minor quartz and feldspar, in which lines of fine magnetite define irregularly curved and rounded fragments resembling those of a tuff. This mesoband is exceptional also, for the Dales Gorge Member, in the colour of the stilpnomelane (see Sheet silicates, further below).

It is characteristic of some of the thicker stilpnomelane mesobands, that for a short distance above and below them stilpnomelane appears in the textural position of the more usual minerals of the adjacent chert and chert-matrix mesobands (see Notes on paragenetic evidence, page 127).

CARBONATE

As shown in Table 4, carbonate mesobands do not form an important proportion of the Dales Gorge Member, and they are no more abundant in other iron formations. There are two varieties: siderite and ankerite. Mesobands of siderite are usually thin and consist of homogeneous fine-grained siderite with no

textural irregularity. In the Dales Gorge Member they occur mainly in the mixed group of the Calamina cyclothem, and there appears to be a complete intergradation with the similarly occurring mesobands of stilpnomelane. Ankerite mesobands are more coarsely granular, and are intergradational with the type of coarsely microbanded chert illustrated in Figure 21A and C, by increase in the thickness of the ankerite parts of each microband until an ankerite mosaic comprises the bulk of the mesoband.

MISCELLANEOUS

Petrographically, mesobands classed as miscellaneous by macroscopic inspection of core differ from chert-matrix only in their possession of some textural irregularity defined by coarse granularity of some component mineral or minerals. All the constituent minerals of chert-matrix may be present, with the same wide range of proportions, but if one or more of these are patchily and coarsely crystalline in such a way as to destroy almost all sign of internal lamination parallel to the banding, then we do not call it chert-matrix. They are typically associated, in the mixed group of the Calamina cyclothem, with small spheroidal nodules (page 159 and Figure 41), as in Figure 13.

IRON FORMATION WITHOUT MESOBANDING

Only two rocks of the Hamersley Group classified as iron formation by the definition accepted here (page 26) are not also mesobanded, at least in part. These are the striped facies of the Weeli Wolli Formation and the fine-grained black flaggy iron formation of which the Boolgeeda Iron Formation mainly consists. The striped facies of the Weeli Wolli Formation is, however, clearly microbanded, and the textural details of the microbanding were described under the appropriate heading above. No demonstrably unweathered material of the striped facies is available, and it is not yet known whether the hematite and quartz which together define the observed microbanding are the sole minerals in deeper material; no further petrographic description is therefore given here.

In thin-section the typical non-mesobanded rock of the Boolgeeda Iron Formation has a structurally interconnected groundmass of quartz mosaic of average grain diameter about 10 to 30 microns, much like that of a typical chert mesoband of other iron formation. However, it differs in having, abundantly scattered through it, carbonate crystals from 0.05 mm downwards (the larger ones euhedral and the smaller ones rounded), magnetites from about 0.07 mm down to 0.01 mm across (invariably in simple octahedra), stilpnomelane flakes and riebeckite prisms, both the last of the same generally small grain-size. All these minerals lie more or less at random within the chert, except that the magnetites are sometimes vaguely concentrated along darker lines defining the bedding. Commonly, also, lines of hematite dust of sub-micron grain size, with about an interval of 25 microns between each line, cross the chert, but do not usually have

great lateral persistence. It is evident from Table 16 that in spite of the absence of mesobanding, this rock is chemically close to typically mesobanded iron formation of the Dales Gorge Member. This similarity is reflected in the petrographic appearance, which is somewhere between chert-matrix and chert.

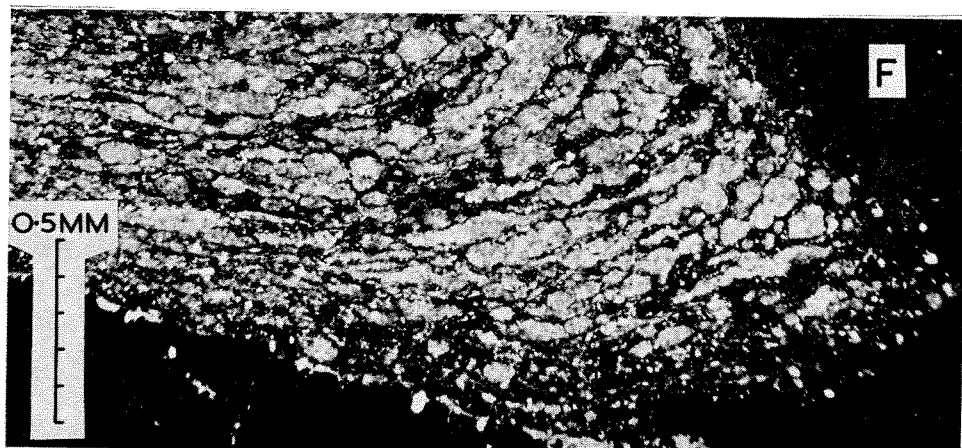
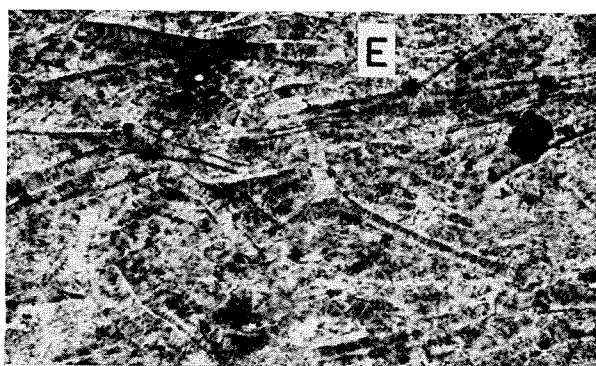
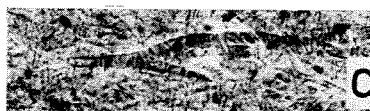
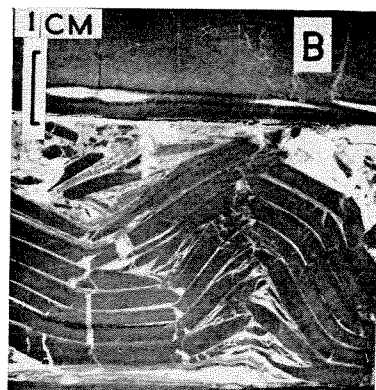
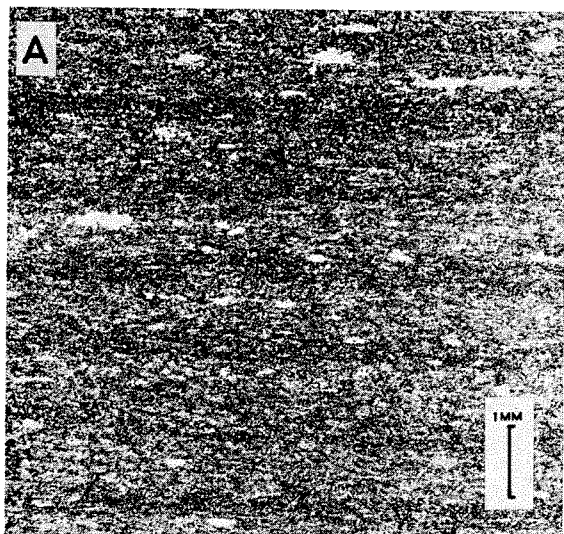
PETROGRAPHY OF THE S MACROBANDS OF THE DALES GORGE MEMBER, AND SOME RELATED ROCKS

SHALE

While our main attention was directed to iron formation, shale is so closely associated with this, especially in the Dales Gorge Member, that its petrography could not be ignored. Our comparatively superficial examination of this shows that more detailed work is needed, and the following paragraphs consist of a summary account of the petrographic range observed in some 70 thin-sections and polished mounts, followed by special attention to some features which, as will appear in later discussion (Chapters 9 and 10), are particularly relevant to the iron formations.

Sheet silicates (including stilpnomelane, biotite and chlorite), carbonates (including siderite, ankerite, dolomite, and calcite), quartz, feldspar, pyrite, carbon, magnetite, tourmaline, hematite, apatite, zircon, and chalcopyrite are the observed constituent minerals, in approximate order of abundance. There is a wide range in the proportions of these. Commonly, either stilpnomelane or chlorite is the dominant mineral, and a fine-grained (flakes 5 to 20 microns long) aggregate of either or both forms the main structurally continuous body of the rock. Although the small grain-size precludes accurate observation of individual grain shape and orientation, there is a wide range in bulk pleochroism, suggesting a complete gradation between perfectly random arrangement and strong preferred orientation along the bedding.

The more granular minerals—carbonates, quartz, and feldspar—occur mainly in subhedral to anhedral, equant grains evenly distributed through the sheet silicate matrix. Siderite is the most abundant carbonate, and has a characteristic inter-relationship with the sheet silicate flakes, in which each single grain is criss-crossed at random to give a trellis-like pattern. Pyrite occurs most abundantly in one or other of two forms: lines of abundant cubes and pyritohedra 5 to 10 microns across, and as layered, lenticular, or rounded nodular masses of solid pyrite of uncertain structure. Complex spherical aggregates of pyrite often hollow, and about 30 to 50 microns in diameter, are not uncommon in some shales, but this and other minor forms form a very small proportion of the total. Carbon is usually in a fine, dusty form of uncertain mineral status; it is probably not graphite. It is often associated with the finer variety of pyrite. Magnetite and chalcopyrite are rare; only a few small crystals of each have been seen in polished mounts, and apatite and zircon also occur rarely, in shales which are largely composed of stilpnomelane.



The stratification of shales in thin-section is highly variable. In some slides there is no major heterogeneity, and only a fine streakiness defines the bedding. In others there is an alternation of laminae 0.2 to 2 mm thick defined by abrupt changes in the proportions of the component minerals. Two forms of stratification are worth special attention.

The first of these is defined by thin lines of fine pyrite, with or without associated carbon, arranged in a continuous elongate anastomosing mesh-work, in which the individual 'meshes' are up to 0.5 mm long (along the bedding) and about 0.05 mm thick (across it). In one slide from the Mount McRae Shale illustrated in Figure 31F the fortuitous juxtaposition of a spherical pyrite nodule immediately above a pyrite sheet has apparently preserved part of such a shale from compaction. In the shale so preserved each 'mesh' assumes a rounded form 0.1 to 0.2 mm across, and the impression is that these shapes may represent primary depositional globules of the shale (see also p. 288).

A second common type of stratification in shales is illustrated in Figures 31A and B. It consists of a very regular sequence of laminae within the thickness range 1 to 3 mm, defined by slight changes in depth of colour, mostly controlled by a thin dark concentration of carbon or pyrite, or both together. There is only rarely any textural suggestion of asymmetric grading in these laminae, and their definition is often quite subtle. In any one sequence the thickness of successive laminae varies very little. Where stress has caused some late splitting of the shale this often emphasizes the existence of such laminae, which may otherwise be hard to detect (Figure 31B).

Concordant and transgressive veins of fine-grained stilpnomelane are common in some shale, and those which are concordant are often marked by slickensides.

Figure 31 (opposite). Some petrographic features of Hamersley Group shales.

A. Thin and even lamination defined by preferential concentration of pyrite and carbon in a matrix of chlorite, feldspar and carbonate in the Mount McRae Shale at 370 feet 5 inches in Hole Y1 at Yampire Gorge, about 41 feet below the top of the formation. The pale patches elongate along the bedding are potassic feldspar, presumably diagenetic.

B. Laminations about 2.5 mm thick in stilpnomelane-rich shale of the S11 macroband of the Dales Gorge Member at 251.7 to 251.9 feet in Hole Y3 at Yampire Gorge, approximately equivalent to 275 feet on the type section. The deformation, probably quite soon after deposition, has here split the shale and emphasized the regularity of the lamination, which would not otherwise be conspicuous.

C, D and E. Volcanic shards preserved in stilpnomelane in the shales of S macrobands of the Dales Gorge Member; all three photographs are at the same scale, indicated in D. C is from the S13 macroband at 320 feet 0½ inches in Hole 51 at Wittenoom Gorge (see Trendall, 1966b, Figure 1), equivalent to about 323.5 feet on the type section. D and E are both from the S3 macroband at 560 feet 7 inches in Hole 51 at Wittenoom Gorge, equivalent to about 85.8 feet on the type section.

F. Globulate bodies in the Mount McRae Shale apparently preserved from compaction in the re-entrant angle between a spheroidal diagenetic pyrite nodule (upper right) and a similar flat sheet of pyrite in the bedding (lower edge). The slide is 2 inches below that illustrated in A, and the mineral composition is similar.

The structure in Figure 31B similarly shows pale green stilpnomelane filling in the volumes between the splintered shale laminae.

In general, no individual crystal of normally fine-grained shale has the appearance of a clastic particle. The frequently random texture of sheet silicate flakes seems more likely to result from post-depositional recrystallisation, while the common trellis-work of flakes in and across the more granular minerals, in particular carbonates, is difficult to see as a depositional texture. Some shales though, are markedly different in possessing a distinct clastic texture, defined not by grains of recognisably clastic material, but by dark 'ghost' outlines within fine-grained material with the same mineral composition as the normal shale. The shapes so defined, by linear concentrations mainly of dusty carbon and pyrite, and by a wide range of minor textural and compositional variations, vary in scale from the coarsely clastic breccias in the S4 and S7 macrobands (p. 64), down to thin, often graded, beds between about $\frac{1}{4}$ -inch and 3 inches thick. It is emphasized that in none of these are the 'fragments' recognisable as other than fine-grained texturally defined aggregates of the same minerals that are present throughout the shales.

Some among these 'clastic' layers have, clearly defined within fine-grained stilpnomelane, the angular curved and globular shapes typical of glass fragments in many tuffs; the bands of ferristilpnomelane in the Joffre Member (p. 78) are typical of these. Also obviously of volcanic derivation are the shard bands described by LaBerge (1966a). Trendall (1966b, Figures 1 and 2) gave details of the occurrence of these in the S13 macroband. They are sharply defined layers of clear stilpnomelane within normal shale, usually less than $\frac{1}{2}$ -inch but up to 2 inches thick, which are composed of close-packed aggregate of glass shards all replaced transversely or axiolitically by stilpnomelane. In most thin-sections (Figures 31C, D, and E) only a few of the transected fragments show the typical shard shapes, but there is little doubt of the validity of the identification. It is noteworthy that the three-armed shards in Figures 31D and E have their vertical arm pointing upwards. The simple interpretation is that shards broken out of close-packed spherical bubbles may contain parts of four bubbles, and have an effectively tetrahedral shape, which will settle with one face facing downward.

In thin-section the limestone which locally appears in the equivalent stratigraphic position of shale in some 8 macrobands of the Dales Gorge Member has an even calcite mosaic of average grain diameter between 0.1 and 10 mm, usually with some interstitial stilpnomelane. An analysis of the rock appears as analysis 1 of Table 16. Most of the recognisable textures described within shale, including graded clastic bands, are clearly traceable as 'ghosts' which are defined, without structural regard for the grain boundaries of the comparatively coarse calcite, by subtle textural variations often more easily perceptible by the naked eye than by the microscope in thin-sections. Stylolites are often developed in such calcite.

Another mineral which has clearly grown diagenetically at a fairly late stage is potassic feldspar. This occasionally occurs in crystals up to 0.1 mm across (Figure 31A) whose complex shape and included carbon leave no doubt of their crystallisation in place. Stumpy subhedral tourmalines mainly between 5 and 10 microns long, but up to 100 microns, are very abundant in some shales. Their diagenetic growth is indicated both by their random orientation and by the presence, in the globulate texture of Figure 31F, of tourmalines which cross between globules.

Preliminary X-ray study of selected shales by Mr. N. L. Marsh at the Government Chemical Laboratories confirmed the mineral identifications that had been made optically, but drew attention also to the quantitative importance of feldspar in some shales (see Table 15, Chapter 5), and indicated the presence of much montmorillonoid in some samples, presumably misidentified as chlorite under the microscope and so described in the preceding descriptions. Chlorite was also confirmed, however, and further work on separated sheet silicates of the shales is needed for more accurate mineral identification, and the relation of mineral species to stratigraphic position.

CHERT-SIDERITE

The mesoband distribution of chert and siderite in chert-siderite is clearly shown in Figure 6, in the parts of the type section of the Dales Gorge Member between about 404 and 409 feet, and 413 and 416 feet. The textural features typical of microbanding in these cherts, defined entirely by carbonates, rather than by iron oxides or silicates, has already been described above, and illustrated in Figure 22. Podding is well developed in these cherts, and the rather abrupt termination of a chert is shown in Figure 28A. Typical podding was also illustrated by Trendall (1966b, Figure 3). Stylolitic contacts between cherts and the neighbouring siderite are typical of this material.

In thin-section the siderite part of chert-siderite consists basically of thin laminae of very finely granular siderite whose exact crystal structure is difficult to distinguish. Each lamina is separated from those adjacent by either more coarsely granular siderite, or by ankerite, or by quartz. Any of these minerals may be accompanied by some stilpnomelane, and hematite is also sometimes present, and very exceptionally magnetite (Figure 29C). The interval between laminae is typically about 25 to 50 microns, but may be much coarser, and approach the normal microband interval of, for example, the cherts of the BIF macrobands of the Dales Gorge Member, but it is always far short of the microband interval of the accompanying cherts of the chert-siderite.

The usual even laminations of the siderite are commonly interrupted by irregular lenticles of fine siderite, or by strikingly spherical siderite bodies up to 0.1 mm in diameter. The laminations always flow evenly and continuously around these interruptions, with appropriate thickness compensation. Other bands

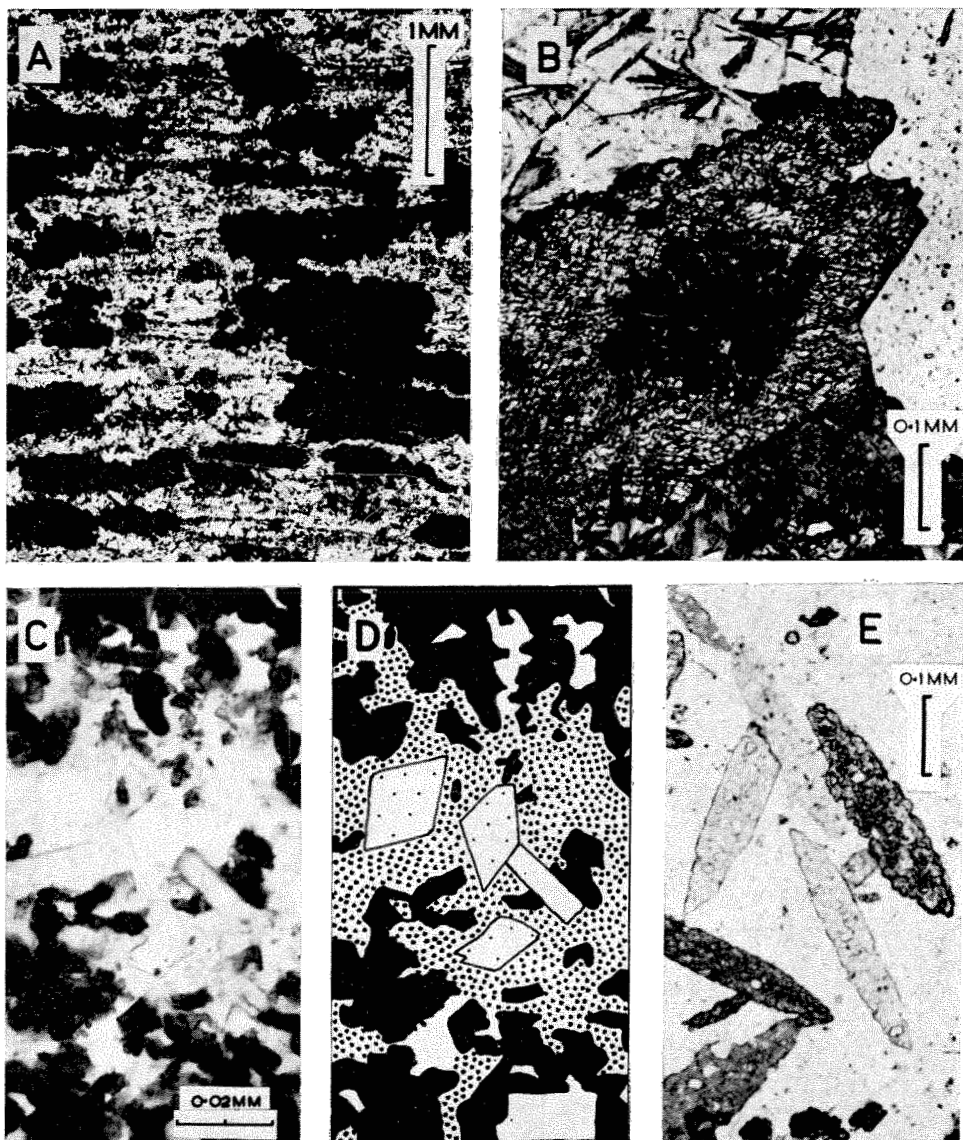


Figure 32. Selected petrographic features of magnetite and carbonate occurrence in iron formations.

A. Plates (extended octahedra) of magnetite in a chert mesoband of the BIF2 macroband of the Dales Gorge Member at 580 feet 10 inches in Hole 46 at Wittenoom Gorge, equivalent to exactly 81.3 feet on the type section (Figure 5). The tendency for vertical superposition of plates is characteristic, and resembles the vertical arrangement of the swells and gaps in hematite-defined microbands (Figures 21B and D, and 29A). This sometimes gives rise to a coarsely speckled macroscopic appearance in core; this is locally used in the northern Cape Province iron formations of South Africa for stratigraphic correlation of cherts.

up to about an inch thick have a ghost clastic texture, sometimes graded, defined in fine siderite and ankerite in much the same way that the clastic bands in the shales are defined by stilpnomelane.

MINERALOGY

QUARTZ

Quartz is by far the most abundant mineral of the iron formations (very roughly 40 per cent by weight, 60 per cent by volume), and its even, close mosaic, with an average grain diameter rarely departing outside the range 5 to 30 microns, forms the main structurally continuous element of both chert and chert-matrix mesobands. It is therefore surprising that little is known of either its shape or crystallographic fabrics. A petrofabric analysis of 200 grains of a single chert mesoband from the Dales Gorge Member with average grain diameter about 30 microns showed an almost random arrangement of c-axes, but with a slight girdle in the plane of the banding. Finer cherts are impossible to analyse optically. A characteristic feature of the mosaic in almost all cherts is that the individual grains appear under high magnification to extinguish in irregularly curved shapes, but we do not know to what extent this is due simply to grain overlap or whether the grain shapes are genuinely complex and curved.

The main departure of quartz from this typically even and fine mosaic is in a variety of situations where it increases abruptly in grain-size. Examples are in the internal 'cracks' of chert pods with septarian structure (Figure 40B), in the cores of macules (Trendall, 1966a, Plates 37 and 38), and in cross-cutting vertical veins and other types of brittle fracture (Figure 44A). Less sudden increases in grain-size take place in some chert mesobands where the micro-banding is defined by grain-size changes (Figure 22C).

Fibrous quartz (known to miners as 'quartz fibre') is a form of quartz which is usually either in concordant veins along the bedding, often marginal to crocidolite, or in the cores of minor folds, or, rarely, in discordant veins. It is illustrated, inter alia, in Figures 46, 47, 58, 59 and 60. The name is applied

B. Platy ankerite in a chert from the chert-siderite of the S6 macroband of the Dales Gorge Member at 491 feet 5½ inches in Hole 51 at Wittenoom Gorge, equivalent to about 158.4 feet on the type section. The rhomb-shaped core, which apparently served as a nucleus for the later growth of the tabular plate, has a slightly higher refractive index than the remainder of the crystal.

C and D. Siderite, ankerite and dolomite co-existing in chert-matrix of the Joffre Member at about 511 feet in Hole 47 at Wittenoom Gorge, about 131 feet above the base of the member. The textural arrangement of the three carbonates (stained in C) is shown in D, where solid black is siderite, close stipple ankerite, and open stipple dolomite. The remaining material is largely quartz, riebeckite (a small prism radiates from the central dolomite rhomb on a 'bearing' of 135°) and a sheet silicate of uncertain identity.

E. Thinly tabular ankerite plates at a high angle to the (horizontal) bedding in chert from the chert-siderite of the S6 macroband of the Dales Gorge Member at 491 feet 3½ inches in Hole 51 at Wittenoom Gorge, equivalent to about 158.7 feet on the type section.

from its convincingly fibrous macroscopic appearance but it cannot be teased out like crocidolite and in thin-section (Figure 58B) consists of a coarse elongate mosaic usually parallel to subparallel with abundant enclosed fibres of riebeckite. It is uncertain to what extent the present structure may have annealed from an originally genuinely fibrous state, but the strictly inaccurate name is retained because of its aptness in the field.

Very occasionally the entire mosaic of a small thickness of BIF may be elongate across the bedding, as though instead of a local dilation to form fibrous quartz there had been a uniformly distributed expansion in the same direction that this would have taken. Even less commonly there is an elongation of the quartz mosaic parallel to the bedding. The significance of both these quartz textures is not clear.

CARBONATE MINERALS

Some features of carbonate occurrence appear in Figures 21, 22, 23, 24, 28, 29, and 30, and are described in the relevant text. Later illustrations of special aspects of carbonate occurrence include Figures 35, 36, 41, and 61. The names ankerite, siderite, dolomite, and calcite are used in descriptions in various parts of this bulletin. Our purposes here are to justify these names to summarise the distribution of the different species, and to illustrate (Figure 32) some further points of likely significance for future carbonate studies in the iron formations.

It is characteristic of virtually all samples of Hamersley Group iron formations unaffected by recent surface 'weathering' that more than one carbonate mineral is present; commonly three (Figures 32C and D) and exceptionally four, different carbonates co-exist in small samples. Chemical analyses, even of single mesobands, are therefore of limited determinative use, and staining in thin-section is necessary to supplement the limited optical criteria which can be used for the confident recognition of different carbonates in complex textural associations (e.g. Trendall, 1965c).

Alizarin Red S in hot alkali (Friedman, 1959) is the most broadly diagnostic stain. After a rock slice is prepared for mounting it is placed, smoothed face uppermost, in a boiling solution of 30 per cent NaOH with the stain. After one minute the slice is carefully removed with tongs, washed immediately under running hot water, and dried on a hotplate before mounting, stained side down, and grinding to standard thickness. Extra care is necessary in the last stages of grinding since adhesion is weaker than that of an unstained rock surface. Under the microscope calcite is not stained, dolomite appears pink, ankerite pale orange-brown, and siderite very dark brown. The reactions for calcite and dolomite were checked by tests on material from analysed material in the Survey mineral collection. The problem of arriving at the exact compositions of the stained ankerite and siderite (using this as a general name for Fe-rich FeMg carbonate) is described below.

For any of the analyses of Tables 11 to 16 in Chapter 5 a theoretical average carbonate composition is is, with certain limitation, calculable. Stilpnomelane and riebeckite are the only two other minerals above to accommodate Mg, and to a lesser extent Ca. If the content of these minerals is fairly low in relation to the total carbonate CaO and MgO may be directly allocated to carbonate, and the remaining CO₂ satisfied by FeO, without serious error. In the analyses of single mesobands, in Tables 12 and 13, it can be ascertained by direct inspection that there is only a small content of these silicate minerals. For the analyses of Table 11 an indication of riebeckite content is given by Na₂O, and of stilpnomelane by K₂O and Al₂O₃, but the MgO/K₂O or CaO/K₂O ratios for stilpnomelanes (Table 16) are so variable that no reliable partition can be made in this way.

The results of 30 of such calculations, for all suitable analyses reported in Chapter 5, appear in Figure 33. Most of the BIF analyses of Table 11 fall centrally between the ankerite—dolomite and the siderite—magnesite lines, in a field where no single carbonate is stable. The individual mesoband analyses

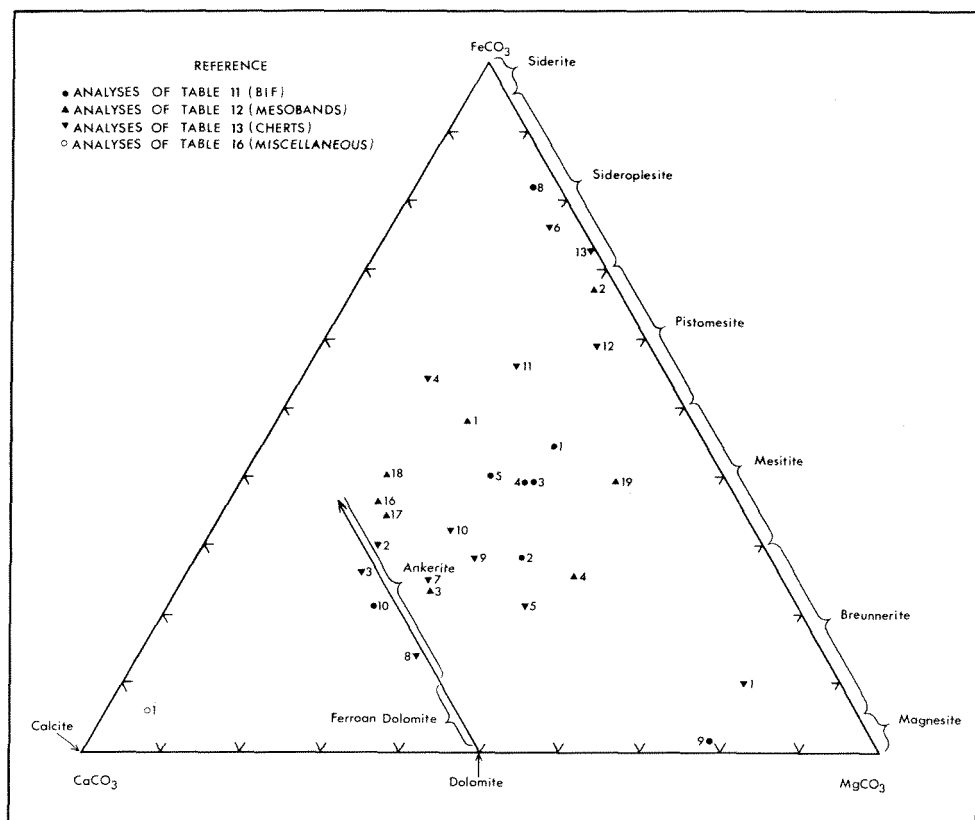


Figure 33. Triangular diagram showing the calculated molecular proportions of various analysed carbonates and carbonate-bearing materials from iron formations of the Hamersley Group. See text for discussion.

of Table 12 and 13 fall partly in the same area and partly towards its two mineralogical bounding lines: dolomite — ankerite and magnesite — siderite. Through any given point in this central area there is a family of straight lines intersecting these two boundaries at alternative pairs of ankerite and siderite compositions, with the relative quantitative proportions of ankerite and siderite shown by the ratios of the distances to each boundary from the point. These proportions are constant for any one point (analysis), whatever the variations in composition of the two constituent carbonates. With due allowance for density changes it is easy to calculate the expected modal proportions of the two carbonates contributing to a central analysis. These will vary slightly according to the relative amounts of Fe allocated to the ankerite and siderite, but the variation is quite small. For analyses 4 to 13 inclusive of Table 13 (single chert mesobands with no significant riebeckite or stilpnomelane) the modal proportions of ankerite and siderite were determined by point counter. No other carbonate was present. The actual stained surface of the slide was used for this, with the slide upside-down on the stage, to avoid errors due to the large refractive index difference between chert and carbonate. The modes measured are compared with calculated modes in Table 10.

TABLE 10. COMPARISON OF CALCULATED* AND MEASURED CARBONATE PROPORTION IN TEN CHERT MESOBANDS OF THE DALES GORGE MEMBER

Analysis No. in Table 13	Siderite as percentage of carbonate	
	Calculated	Measured
4	40	49
5	33	45
6	92	98
7	13	4
8	0	0
9	25	27
10	25	23
11	64	69
12	87	97
13	100	100

* Assuming an equal Fe: Mg ratio in both carbonates of any one mesoband up to a maximum of 7:3 in ankerite: thus, for most of the mesobands, a tie-line whose extension passes through the CaCO_3 apex of the compositional triangle is used.

When allowance is made for some real variation between the analysed samples and the thin-sections used, the general correspondence between the measured and calculated values is satisfactory, and allows the following conclusions to be drawn: (1) the staining colours accepted as diagnostic of ankerite and siderite are valid, (2) analyses 6, 12, and 13 of Table 13 show that there is

a significant proportion of magnesium in the siderite, and that this varies between mesobands, and (3) analyses 2, 3, and 8 of Table 13 shows that there is a variation in ankerite composition between mesobands. From analyses 1 of Table 12 and 9 of Table 11 (Figure 33) it could be supposed that the range of siderite—magnesite compositions extends down to breunnerite or even magnesite, but both these points are probably affected by allocation to carbonate of CaO present in stilpnomelane, with a consequently unreal appearance of paucity in iron. Although a thorough investigation of co-existing carbonate compositions by electron microprobe is needed it seems likely that most 'siderite' in Hamersley Group iron formations is sideroplesite or pistomesite, and that the ankerite has a correspondingly wide range of composition.

These two minerals are the common carbonates of the iron formation, with ankerite normally in euhedral rhombs between 0.2 and 0.5 mm in diameter and the accompanying siderite finer in grain-size by a factor of about 5. A continuous even mosaic of ankerite with about the same grain-size often lies along the margin of chert mesobands, in a zone about a millimetre wide. An unusual variety of ankerite common in chert mesobands of chert-siderite is the tabular form illustrated in Figure 32, B and E. Plates about 0.05 mm thick (parallel to the c-axis) and 0.4 mm wide lie at random within the chert. One example with a small central rhomb of uncertain composition appears in Figure 32B; presumably the tabular habit is a response to conditions obtaining later during diagenesis than those during rhomb growth.

Some ankerite rhombs in cherts, particularly hollow rhombs (page 95), appear to approach a ferroandolomitic composition at their margins, judging by stain colour only. Apart from this, only three situations where dolomite occurs in Hamersley Group iron formations have been noted. Firstly, it may occur in association with any fibrous quartz, as single elongate anhedral crystals among the quartz and parallel with its elongation (Figures 46, 47, and 60C). Secondly, small rhombs of dolomite are often scattered evenly through stilpnomelane-rich shales and in chert-matrix (Figure 32C and D). Thirdly, dolomite is a constituent of the 'tails' of ambient pyrite (page 127).

Calcite occurs within Hamersley Group iron formations only as secondary limestone in the associated shales (pages 64 and 114) and very rarely with a similar status in the immediately adjacent iron formation (Figure 37D). In both types of occurrence it forms an even and rather coarse mosaic, with an average grain diameter from 0.1 mm up to about 10 mm.

HEMATITE

Martite (hematite after magnetite) does not occur in core samples of iron formation, although it is a common constituent, with goethite, of the derived iron ores, and of other secondary material (MacLeod, 1966). This summary is therefore confined to those textural varieties of hematite whose restriction to iron formation unaffected by comparatively recent surface processes ensures that they formed during the normal course of mineralogical evolution of the iron

formation associated with burial due to continued deposition. There are three main varieties: jaspery platelets, cellular octahedra, and platy mosaic. The third is by far the most important in quantity, but the others are very distinct minor forms whose elucidation is not yet achieved, and could be important for interpreting early diagenetic stages (page 272). All three forms tend to occur in close mutual association in defining the microbanding of many cherts (Figures 21B, 29A, and 30), but in chert-matrix the platy mosaic usually occurs alone, while jaspery platelets may occur on their own in a variety of situations.

Jaspery platelets are platelets 2 to 10 microns in diameter, and much less than 1 micron thick, which lie at random within quartz. They are so called because their presence causes a red or pink colouring of the chert, and they are the sole cause of such colouring in unoxidised iron formation. It is not certain whether the common, and probably secondary, redness of many surface chert samples can be caused by platelets, since many red surface cherts are coloured by very finely granular hematite dust without evident platy form. Jaspery platelets are triangular, discoid, or symmetrical hexagonal in areal shape, but are most typically hexagonal with three alternate sides about half the length of the others. They are usually closely packed together but not in contact, so that their centres are separated by about the platelet diameter. In cherts whose quartz mosaic is coarser than the average (30 microns) the platelets are often absent along grain boundaries, to give a speckled appearance under low power due to the cloudy interior of each separate quartz grain.

The name cellular hematite is applied in this bulletin to isolated, roughly equant, single crystals usually 1 to 10 microns but up to 20 microns in diameter, which usually lie in chert with jaspery platelets but are surrounded by clear haloes with a width 1 to 3 times the diameter of the central crystal. Cellular hematite is illustrated in Figure 34. Each crystal is pitted with small rounded (quartz-filled) 'holes' whose inner surfaces have a high lustre. The holes often extend to the margins and have a crudely radiate zonal arrangement. Where their edges are not punctuated in this way, their faces are recognisably octahedral, particularly when a three-dimensional view can be obtained by using an oil-immersion objective in incident light. Anisotropic reflectivity is only recognisable

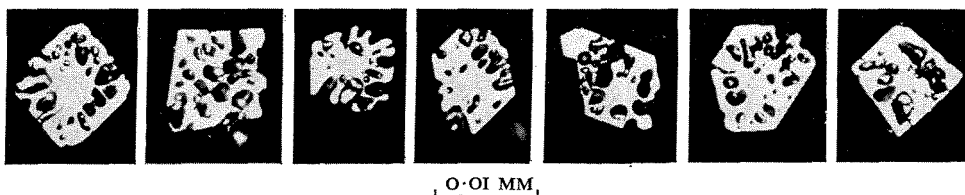


Figure 34. Photomicrographs, taken in incident light, of cellular hematite 'octahedra' from a finely microbanded chert of the BIF4 macroband of the Dales Gorge Member at 526 feet 8 inches in Hole 51 at Wittenoom Gorge. The 'holes' are in fact filled with quartz; the oil-immersion objective used shows up their glossy inner walls.

on the larger examples, but all have the typical white appearance of hematite and are a clear blood-red colour in thin-section. It is possible that some consist of maghemite.

Where cellular hematite is abundant in the defining hematite of a micro-banded chert, the total effect is of a pattern of mottling caused by the abundance of centrally dotted clear rings within the cloudy mass of jaspery platelets. It has already been noted that a comparable pattern appears in Figure 23A, but defined in stilpnomelane. Attention was focussed on this texture by Spencer and Percival (1952), and Percival (1967) illustrated examples from India and the Hamersley Range area side-by-side. We think it possible that this texture may be produced by secondary weathering, and the example from the Hamersley Range illustrated by Percival may have originated in this way. However that may be, we suggest (with Dr. Percival's concurrence) that the name 'Percival texture' be applied to it, without prejudice to its origin, on which more work is needed. Percival texture is a common, but erratically distributed feature of finely microbanded cherts of the Dales Gorge Member and of red cherts of the Joffre Member. Exceptionally, cellular hematite may be dotted abundantly through the normally iron-poor component of the microbanding, and may not be associated with jaspery platelets.

Coarser plates and mosaic of hematite form by far the greatest volume of the hematite of the iron formations. In the defining hematite of chert micro-banding there is often a more or less continuous meshwork of irregularly interlocking anhedral plates rarely wider than 0.05 mm and about or thicker than 0.01 mm. In chert-matrix there is a greater tendency for the plates to be distributed individually, but in general all hematite of the iron formation is fine-grained and anhedral to subhedral.

A very rare textural variety of hematite is a sieved form in which comparatively coarse (0.1 to 0.2 mm) single crystals have a skeletal form and enclose rounded close-packed quartz blebs about 20 microns across: that is, of the same order of grain-size as the chert.

MAGNETITE

In contrast to hematite, magnetite in the Hamersley Group iron formations is normally perfectly euhedral relatively coarse-grained, and texturally invariable. It occurs within chert and chert-matrix mesobands, but its main bulk occurs in magnetite mesobands. It forms perfectly formed octahedra usually about 0.2 mm across, but varying between 0.05 and 0.5 mm. These may be simple, but more commonly there is some degree of lateral extension, by the development of additional octahedral faces on the upper and lower surfaces, so that a final plate-like shape is attained, on the surfaces of which are innumerable small apical projections of octahedra, and there is structural continuity throughout. Such 'extended octahedra' are illustrated in Figure 32A. In the field, when fresh iron formation is broken along magnetite mesobands (as is common), the reflections from adjacent differently oriented plates outline their areal shapes as

the rock is turned in the hand; it is then apparent that really they form an irregularly sutured mosaic pattern with average plate diameters commonly up to 2 to 3 centimetres.

Magnetite occurs occasionally, like quartz, in a coarse form in unusual structural situations. It occurs in this way in macule cores and in crosscutting vertical veins (Figure 40A).

SHEET SILICATES

A more thorough study of the sheet silicates of Hamersley Group iron formations is needed. This account is limited to an indication of our conventionally accepted nomenclature, a review of the few confirmatory analyses available, and most important, an emphasis of the importance of sheet silicates in defining the chemical character of each major stratigraphic unit of iron formation.

Although a greater variety of sheet silicates is present in the associated shales only two occur in the iron formations: stilpnomelane and minnesotaite. Before chemical analyses were available to us it was more or less conventionally accepted in thin-section that the name minnesotaite was applied to colourless talc-like flakes of high birefringence, the name ferrostilpnomelane to highly birefringent flakes pleochroic from α — very pale green to $\beta = \gamma$ — clear green, and the name ferristilpnomelane to similarly birefringent flakes pleochroic from α — medium red-brown or golden yellow to $\beta = \gamma$ — dark brown or brownish-green. The later chemical confirmation of these identifications is discussed further below.

The stratigraphic restriction of each of these three minerals within the five major stratigraphic units of iron formation within the Hamersley Group is as follows:

Marra Mamba Iron Formation. Minnesotaite is the common and characteristic sheet silicate of the bulk of the iron formation. Ferristilpnomelane is equally characteristic of the intercalated shale bands.

Dales Gorge Member. Ferrostilpnomelane is the common and characteristic sheet silicate of the BIF macrobands. Minnesotaite occurs in minor amounts at restricted levels. Ferristilpnomelane is almost unknown.

Joffre Member. Ferristilpnomelane is the common and characteristic sheet silicate of both iron formation and stilpnomelane (shale) bands. Ferristilpnomelane has not been seen and minnesotaite is extremely rare.

Weeli Wolli Formation. Not known, no fresh material available.

Boolgeeda Iron Formation. Stilpnomelane of uncertain oxidation state but apparently chemically distinct from that either of the Joffre Member or Dales Gorge Member.

The Mount Sylvia Formation is not regarded as a major iron formation unit for present purposes; the early discussion in Chapter 3 is relevant here. The Whaleback Shale Member has the typical ferrostilpnomelane of the Dales Gorge Member.

Only two confirmatory analyses of minnesotaite are available. Analysis 2 of Table 16 is of apparently pure fibrous minnesotaite from the Dales Gorge Member. Its rather equal proportions of FeO and MgO place it as an intermediate form between talc and minnesotaite but we do not know whether this represents a genuine isomorph or whether there is interlamination of both minerals. Analysis 6 of Table 16 is of a minnesotaite-rich chert; disregarding the expected excess of silica the iron content is similar to that of the originally described mineral (Gruner, 1944), but is considerably oxidised.

Although structural formulae have been calculated for all relevant analyses reported in this bulletin, we do not think these merit publication and comparative discussion until more complete information is available on separated and purified minerals. A fairly accurate assessment of the composition of Dales Gorge Member ferrostilpnomelane is given by analyses 5, 6, and 7 of Table 12 and analysis 3 of Table 16. The mean weight ratio $\text{Fe}^{3+}/\text{Fe}^{2+}$ is 0.23. The best indication of Joffre Member stilpnomelane comes from analysis 4 of Table 16. The weight ratio $\text{Fe}^{3+}/\text{Fe}^{2+}$, at 0.90, is significantly greater, as would be expected from its distinctively different pleochroism. However, the ferristilpnomelane of Marra Mamba Iron Formation shale, given as analysis 7 of Table 16, is very much greater, and this mineral has a characteristically different pleochroic scheme again. The observed close correspondence between pleochroism and chemical composition in the limited number of available analyses, coupled with the absolute consistency of pleochroism within the stratigraphic units listed above, justifies, we believe, the conclusion that sheet silicate compositions are consistently different between the major stratigraphic units.

Some further relevant discussions appear in Chapter 5.

APATITE

Some idea of the phosphate mineral content of Hamersley Group iron formations is given by the analyses of Tables 11 and 12 (Chapter 5). So far as we are aware this is entirely as apatite, which occurs in a variety of textural situations whose significance is uncertain. The more important of these are shown in Figure 35, and are briefly described below.

Figure 35F shows the most abundant forms of apatite, as amoeboid anhedral aggregates in chert or chert-matrix. The total apatite content of some mesobands may reach about 30 per cent (Figure 35B), and the mineral is always anhedral when thus abundant. Figures 35A and C show two common euhedral forms of apatite. That in Figure 35A is typical of much apatite in the chert of BIF macrobands, while that of Figure 35C is more characteristic of chert mesobands in chert-siderite. The two forms, one globular and one elongate, shown in Figure 35D and E are of interest in that they occur thus preferentially in streaks along the bedding, possibly with some primary depositional significance. That in Figure 35E, in particular, occurs in one half only of the coarse microbanding of its enclosing chert, and of all the forms illustrated is most likely to reflect primary distribution.

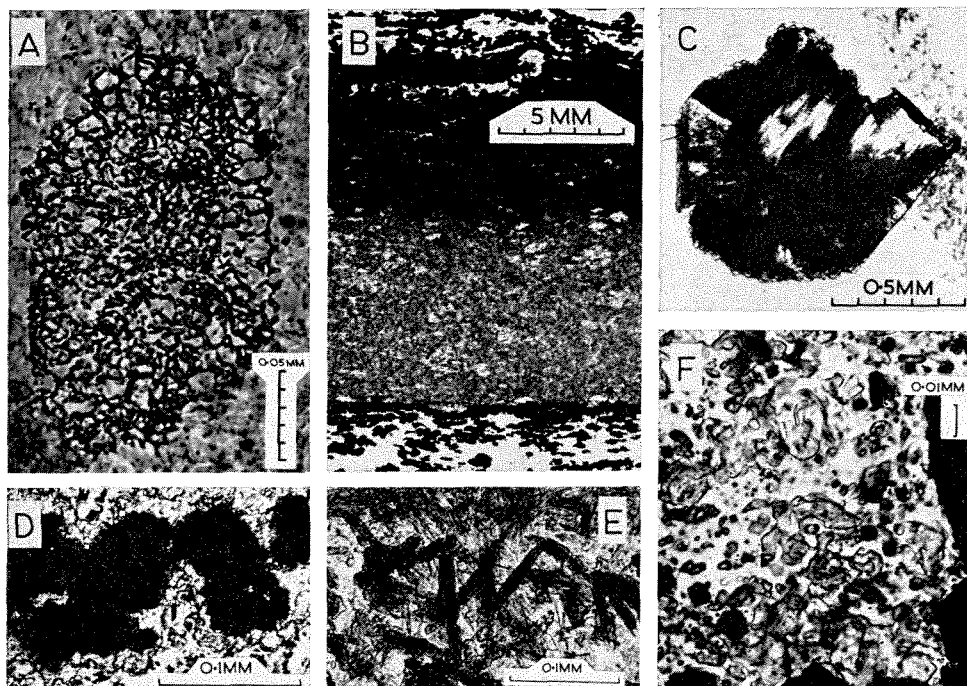


Figure 35. Photomicrographs of various modes of occurrence of apatite in the Dales Gorge Member.

A. Skeletal euhedral apatite crystal in a microbanded chert from the waste dump of the Colonial mine at Wittenom Gorge. The stratigraphic position must be close to the Upper Seam in the BIF2 macroband of the Dales Gorge Member. The crystal shown is in oblique section of a short hexagonal prism. Each 'hole' in the apatite network is an individual quartz crystal of the matrix chert.

B. Mesoband at about 344 feet 7 inches in Hole 51 at Wittenom Gorge, consisting largely of an aggregate of amorphous apatite (the grey material forming the upper part of the lower half of the photograph). This is in a mixed group of the Calamina cyclothem where it is exceptionally clearly developed in the BIF12 macroband, at 297.05 on the type section (see Figure 13A). The paler patches in the apatite consist of ankerite and minnesotaite, and there are also a few scattered magnetite octahedra.

C. Well-formed apatite in a chert of the chert-siderite of S10 and 407 feet 9 inches in Hole 51 at Wittenom Gorge, approximately equivalent to 242 feet on the type section. The internal pattern of dark lines parallel to the crystal face is typical.

D. Globular apatite in a microbanded chert mesoband of the BIF2 macroband at about 500 feet in Hole 22 at Wittenom Gorge, equivalent to 77.9 feet on the type section (Figure 5). Each apatite crystal has a clear rim and a cloudy brown rounded core.

E. Cigar-shaped apatites lying at random in a microbanded chert of the BIF6 macroband at about 485 feet in Hole 51 at Wittenom Gorge, equivalent to about 165 feet on the type section. Closely similar apatite appears in the coarsely microbanded chert illustrated in Figure 24A.

F. Anhedral amoeboid apatite in chert of BIF2 at 648 feet 0½ inches in Hole 40 at Wittenom Gorge, equivalent to 77.45 feet on the type section (Figure 5). The small irregular blobs are the commonest forms of apatite.

PYRITE

Pyrite in the iron formations occurs, outside the associated shales, mainly as rather coarse masses similar to the coarsely nodular forms of the shales (p. 111). Its typically coarse occurrence is well illustrated in Figure 37D. Trendall (1966a) previously noted its occurrence at the crests of riebeckite swells at Dales Gorge. The significance of this texture is discussed under 'Notes on petrogenetic evidence'.

Locally in iron formation near S macrobands in the Dales Gorge Member pyritohedra or cubes of pyrite about 20-50 microns in diameter occur in chert-matrix with comet-like tails indicating movement through the rock. The phenomenon is that described by Tyler and Barghoorn (1963) as ambient pyrite. Dolomite, quartz, and potassic feldspar comprise the tail minerals, derived from the passage of the pyrite through quartz, ankerite, and stilpnomelane.

FELDSPAR

Potassic feldspar in ambient pyrite tails is one of the few occurrences of this very minor mineral. It occurs also in shales (Figure 31A) and abundantly in the unusual black porcelanite of the Joffre Member (p. 78, and analysis 5 of Table 16).

CARBON

LaBerge (1967) described skeletal carbonaceous bodies from Dales Gorge Member chert, probably at about 348.8 feet on the type section, in BIF13. We have seen these bodies also in chert from the Marra Mamba Iron Formation at Kungarra Gorge. They seem to represent the only free carbon in iron formations of the Hamersley Group.

BARITE

A few small (0.4 mm) skeletal grains of barite, rather like the skeletal apatite of Figure 35A, have been noted in a white chert mesoband from the Joffre Member.

NOTES ON PARAGENETIC EVIDENCE

INTRODUCTION

It is almost impossible to see or describe some rock textures defined by a structural inter-relationship between constituent minerals without drawing a commonsense conclusion that these crystallised in some definite sequence. Particularly obvious examples are where there is an evident pseudomorph of one mineral by a fine-grained random aggregate of another, or where there is a euhedral diagenetic overgrowth on a grain having an internal ghost with a normal clastic shape; there is a gradation between these examples and other situations where it is more or less conventional to interpret a certain texture in a certain way without any firm justification, such as the tendency to accept any clean euhedral crystal face as later than a neighbouring anhedral mosaic.

There are a variety of such situations in Hamersley Group iron formation, and they are given in these notes without the strict adherence, which we try to maintain elsewhere in this bulletin, to the presentation of facts in one place and their interpretation in another. Insufficient evidence of this sort is available to trace clearly a universally applicable sequence of phases during which different mineral assemblages were stable. There are at least four reasons for this: (1) the sequence of mineral growth cannot safely be assumed to have been the same throughout the iron formations, still less between such different types as chert-siderite, shale, and normal iron formation, (2) some minerals evidently remained stable over long periods, and cannot therefore be accurately fixed in time, (3) each small volume of iron formation can be expected to have passed sequentially through several stages, all of which may have left some trace in existing textures; through minor differences from place to place different stages may be missing in different samples, and correlation between them may be uncertain, and (4) interpretation of some textures is in turn dependent on the genetic hypotheses presented in later discussion (Chapter 9). However, these notes summarise the available evidence in a form that may ultimately form the basis of a complete interpretation.

It should be emphasized here that no texture of any existing mineral in the present iron formations suggests to us that it results from primary deposition.

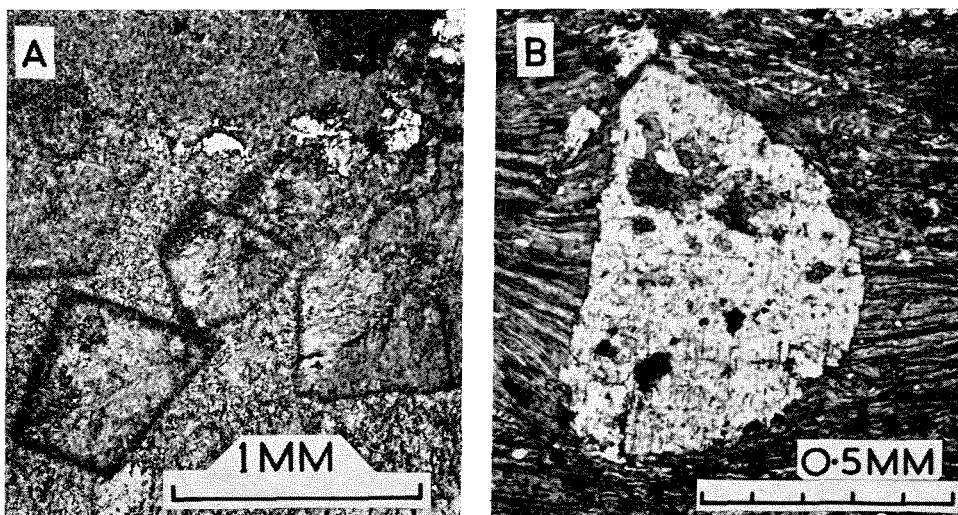


Figure 36. Textural evidence of paragenesis in the Dales Gorge Member.

A. Rhomb-shaped areas defined by texturally oriented stilpnomelane within a more random stilpnomelane mesh in the S13 macroband of the Dales Gorge Member at about 318 feet in Hole 51 at Wittenoom Gorge, equivalent to 326.8 feet on the type section.

B. Subhedral ankerite in finely laminated stilpnomelane in a thin stilpnomelane meso-band between cherts in the BIF2 macroband at about 648 feet 0 inches in Hole 40 at Wittenoom Gorge, equivalent to 77.5 feet on the type section (Figure 5). Included material within the ankerite is stilpnomelane, riebeckite and magnetite.

With a few exceptions mentioned below, there is a notable absence of any compaction effects, such as the fracture of early-formed minerals, and the general impression is that compaction, which we believe to have been extreme (Chapter 9) was successively taken up by the complex sequence of recrystallisations to which these notes bear witness.

NOTES

It is convenient to discuss the inter-relationship of carbonates first, then iron oxides, then silica and silicates, and to conclude with the 'accessory' minerals and a brief reference to riebeckite and the fibrous minerals.

The growth sequence dolomite-ankerite-siderite in shale is suggested by Figure 32C. Clearly the euhedral dolomites grew first, and it is unlikely that a second carbonate would grow independently while the dolomite was exposed, so presumably it was sheathed in ankerite before the appearance of the siderite, and possibly the ankerite was partly resorbed during the growth of this, to cause its rather unusual anhedral habit. The sequence ankerite-siderite is supported also by the common texture of chert in chert-siderite (Figure 22B). There the larger euhedral ankerite rhombs are truncated at the thin lines defining the microbanding, which are partly defined by an abundance of smaller siderites, presumably growing concurrently with the same solution that is corroding the ankerite. And yet the texture is equivocal, in that the ankerites seem to enclose the small scattered siderites of the chert, which were thus already present before the ankerite. Both the inclusion of small siderites by ankerite rhombs, and the obvious surrounding of ankerite rhombs by coarse late siderite are common features. Coupled with the marginal tendency towards dolomite of some ankerite rhombs the general impression from this evidence is that carbonate compositions did not follow a single consistent trend.

The dolomite associated with fibrous quartz is of a much later growth, and the secondary calcite associated with some shales (p. 114) may be assumed to be much later than the bulk of both ankerite and siderite, though its time relationship with the fibrous minerals is unknown.

The most reasonable explanation of Percival texture in hematite seems to be that the central crystal represents an aggregation of iron which was formerly distributed through its clear surrounding halo in the same even fashion as that of the jaspery platelets. Although precise limits of size and distribution are difficult to fix for the platelets a simple volume calculation shows that quantitatively this interpretation is viable without more extensive rearrangement of iron. Where cellular hematite occurs with an aggregate of platy mosaic there is often a circular quartz-filled gap separating the former from the latter; the appearance here is of a later development of the platy hematite, and if the mechanism of cellular hematite growth already suggested is true, the time sequence 'jaspery platelets → cellular hematite → platy mosaic' appears valid for the three main hematite forms. Rhombs of ankerite quite commonly enclose lines of

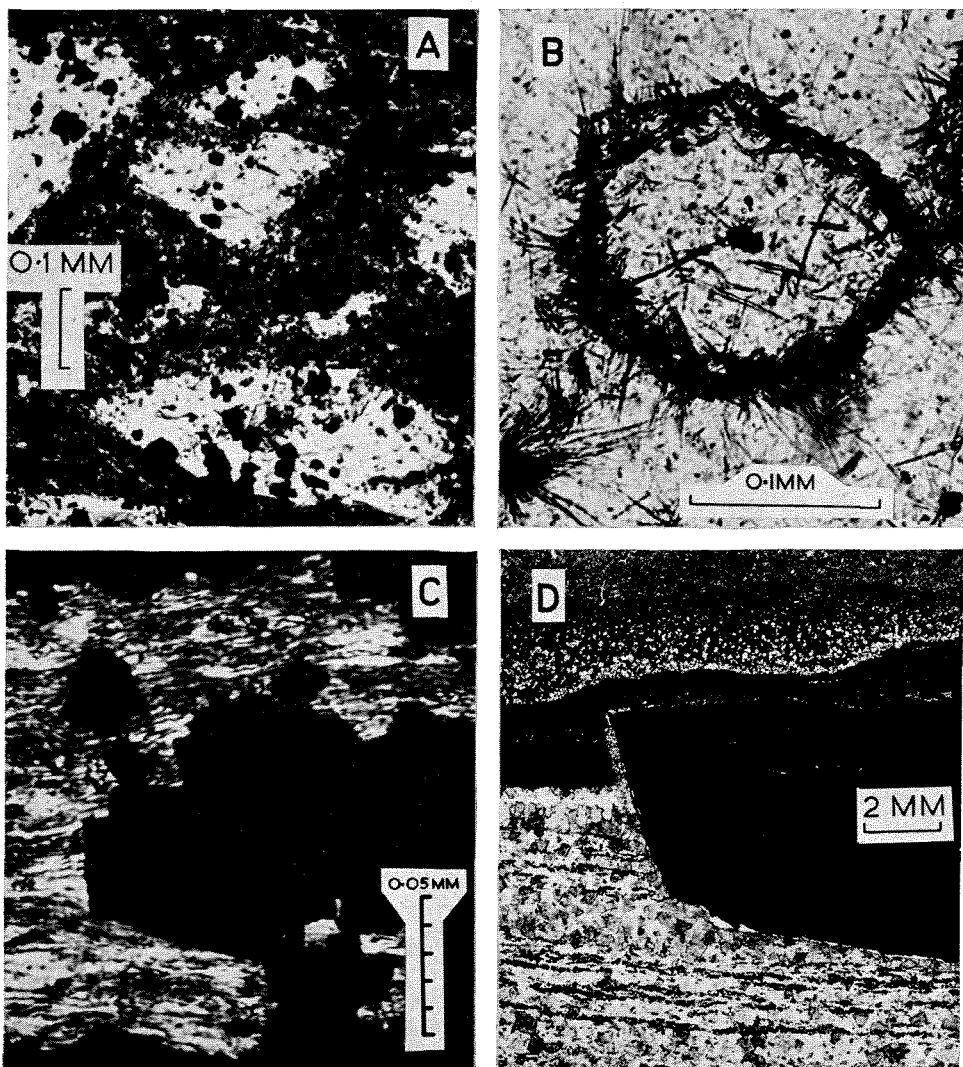


Figure 37. Further textural evidence of paragenesis in the Dales Gorge Member.

A. Rhomb-shaped areas of quartz with some magnetite, hematite and carbonate in a matrix consisting mainly of stilpnomelane and carbonate, in a chert-matrix mesoband in the BIF2 macroband at 478 feet 2 inches in Hole 33 at Wittenoom Gorge, equivalent to about 80.2 feet on the type section. Although one of the upper 'rhombs' has its expected proportions, the lower one has an unusually flat shape.

B. Finely fibrous riebeckite forming a crudely rhomb-shaped sheath in a matrix (inside and outside) of chert in a chert mesoband from the waste dump of the Colonial mine at Wittenoom Gorge. Stratigraphic position uncertain, but close to the Upper Seam, in BIF2. In another adjacent chert mesoband forming part of the same sample an exactly similar sheath of riebeckite surrounds rhombs of ankerite.

cellular hematite defining microbanding, to give some inter-relationship with carbonates. The rare sieved form of hematite (p. 123) seems to have grown along grain boundaries after the quartz mosaic was defined.

Magnetite is perfectly euhedral, and wherever it occurs it cuts sharply across textures present in neighbouring minerals (Figure 37C), whether defined in quartz, stilpnomelane, hematite, or carbonate. It may not always be certain that it is always therefore later, but this may rather indicate its extreme stability, once formed. However, it is not difficult to see the effects of stress on the larger plates (Figures 46, 47, and 57) and the conventional interpretation of hematite-magnetite relationships wherever the two are associated is that magnetite grew after hematite mosaic, the latest form of hematite.

Quartz has demonstrably replaced carbonate in several situations. The hollow ankerite rhombs (p. 95) seem unlikely to have grown in this way, and their cores must be assumed to have been replaced after formation. The reason for this is uncertain, but it seems most likely that the cores had a different composition. Quartz pseudomorphs after carbonate rhombs appear in Figure 37A, and the encircling fringe of riebeckite in Figure 37B not only resembles a carbonate rhomb in shape but is of a type commonly occurring around ankerite rhombs in chert. In the former example it appears that slight compression of the carbonate shape may have occurred during replacement. In many cherts it is only by careful examination under high power that the presence of optically aligned carbonate blebs in patches which were evidently continuous rhombs can be detected.

In spite of all these examples, if a perfectly euhedral carbonate rhomb in anhedral quartz mosaic is interpreted in an analogous way to euhedral magnetite in hematite mosaic, the carbonate must be supposed to be the later. In some sense this may be true, since it is possible that the ankerite grew in silica at some time before this acquired its present crystal structure.

Stilpnomelane is another mineral for whose growth at different times there seems to be evidence. The best interpretation of the texture in Figure 36B is that the ankerite grew later than the stilpnomelane matrix, and replaced it, and that there was slight further compaction after the ankerite grew. In Figure 37C a similar relationship is shown between magnetite and stilpnomelane. Yet in

C. Discordance of stilpnomelane arranged parallel to the bedding against euhedral magnetite, in a magnetite mesoband of BIF2 at 645 feet $4\frac{1}{2}$ inches in Hole 40 at Wittenoom Gorge, equivalent to about 80.1 feet on the type section (Figure 5). The appearance of magnetite growth without structural disturbance of adjacent minerals is typical.

D. Coarse pyrite cutting discordantly across the mesobanding in a sample from the waste dump of the Colonial mine at Wittenoom Gorge. Exact stratigraphic position uncertain, but from comparison within the mine a position close to the junction of BIF0 and S1 is likely. There appears here to have been either slight compaction after pyrite crystallisation or a slight increase in volume associated with pyrite growth. The lower part of the pyrite cuts across a carbonate-rich microbanded chert mesoband. The thin dark mesobands above it would be classified (Chapter 3) as miscellaneous, while the material just appearing at the top of the photograph is a coarse calcite mosaic probably belonging to S1.

Figure 36A stilpnomelane clearly replaces carbonate rhombs, and examples can be found of almost complete pseudo-morphing of a microbanded chert by fine-grained stilpnomelane (Figure 30C). Late fibrous stilpnomelane also occurs (see farther below) as well as stilpnomelane in vertical veins in the Joffre Member. The mottled stilpnomelane of the microbanding in Figure 23A is texturally mimetic of the common Percival texture of hematite (p. 122), and presumably replaces the hematite in this instance, since the various forms of hematite involved are in interpretable crystal forms, while this is not true of the stilpnomelane. Stilpnomelane also occurs rarely in the sieved form described for hematite. Coupled with the evident textural similarity of the stilpnomelane and hematite in Figure 21A and C and 21B and D respectively, it appears that hematite and stilpnomelane have some special replacement inter-relationship. Trendall (1965a) previously supposed that stilpnomelane was earlier, since it typically occurs in more coarsely microbanded chert, but the evidence from Percival texture suggests that in some situations, at least, hematite was the earlier.

It is difficult to deduce any simple time relationship for apatite from the varieties of occurrence described. Using a similar argument for the skeletal apatite as was applied to sieved hematite it would be supposed the apatite of Figure 35A was a late form whose structure was controlled during growth by the already crystallised chert. However, the crystals of Figures 35C and E seem early, while the significance of the amoeboid form in Figure 35F is unknown.

The coarse pyrite locally present in iron formation is normally sharply transgressive and evidently late. In the example in Figure 37D we hesitate to attribute the sloping banding above the pyrite to further (post-pyrite) compaction, in an analogous way to the interpretation of Figure 36B. Firstly, the structure is asymmetric, the lower (calcite) part showing no structural disturbance; secondly, at least some pyrite is post-riebeckite, which we later argue to be effectively post-compactional. The structure in Figure 37D may be due to either deformation or local disturbance due to pressure of pyrite growth.

All paragenetic relationships of riebeckite textures (pp. 192 to 212) indicate that its growth was late. Riebeckite consistently transects early structures (e.g. microbanding, Figures 30A and 60A), grows on or around earlier minerals (Figures 40A and 60D), is never bent, broken, or corroded, and was still locally crystallising during folding (p. 210). The time relationship of the massive form to magnetite is argued in detail in Chapter 11, and also the time relationship of the various fibrous minerals. It is certain that quartz, stilpnomelane, minnesotaite, and riebeckite were all able, in various suitable situations, to grow in this form very late in the history of the iron formations, but it is not entirely clear what the significance of this is for the earlier and less stressed diagenesis of the iron formations.

CHAPTER 5

Chemical composition of the iron formation

GENERAL

We report here 67 new analyses (48 complete and 19 partial) of various materials from the Hamersley Group; one new analysis of Fortescue Group shale is also reported. Five previously published analyses from the Hamersley Group are also listed for convenience of reference, as well as one analysis carried out 60 years ago but not so far published. All the new analyses are by staff of the Western Australian Government Chemical Laboratories. The materials were selected for analysis for various reasons during our study. Rather than retrace in chronological order the original purpose of each analysis we attempt a more rational display of these data by their arrangement into the following five groups, based on the type of material analysed:

Iron formation (Table 11: 13 analyses, 12 new).

Individual mesobands, complete analyses (Table 12: 19 new analyses).

Individual mesobands, partial analyses (Table 13: 17 new analyses).

Riebeckite and crocidolite (Table 14: 7 analyses, 2 new).

Shales (Table 15: 12 new analyses).

Miscellaneous (Table 16: 7 new analyses).

These groups form the subsequent headings of this chapter. Beneath each heading we list the nature of the materials analysed, summarise the objectives of the work, and indicate what we see as the salient features of the results; but in conformity with our separation of factual evidence from discussion we avoid comment here on more theoretical aspects of the interpretation of these analyses, and draw attention instead to the parts of other chapters where this is done. In Table 17 some calculated compositions compiled from analyses reported in the earlier Tables are set out.

ANALYSES OF IRON FORMATION (TABLE 11)

MATERIAL

The analyses set out in Table 11 are of the following material:

1. Brockman Iron Formation, Dales Gorge Member, BIF2 macroband. Drillhole 28 at Wittenoom (Plate 6). Drilling depth 587 ft. 5 in. to 489 ft. 11 in.; approximate type section equivalent 81.45 to 78.95 feet. Government Chemical Laboratories No. 6588/64.

2. Brockman Iron Formation, Dales Gorge Member, BIF2 macroband. Drillhole 33 at Wittenoom (Plate 6). Drilling depth 477 ft. 3½ in. to 479 ft. 11 in.; approximate type section equivalent 81.45 to 78.95 feet. GCL No. 589/64.

3. Brockman Iron Formation, Dales Gorge Member, BIF2 macroband. Drillhole 40 at Wittenoom (Plate 6). Drilling depth 644 ft. 1 in. to 646 ft. 6½ in.; approximate type section equivalent 81.45 to 78.95 feet. GCL No. 6590/64.

4. Brockman Iron Formation, Dales Gorge Member, BIF2 macroband. Drillhole 46 at Wittenoom (Plate 6). Drilling depth 580 feet. 8½ in. to 583 ft. 1½ in.; approximate type section equivalent 81.45 to 78.95 feet. GCL No. 6591/64.

TABLE 11. ANALYSES OF IRON FORMATION OF THE HAMERSLEY GROUP

	1	2	3	4	5	6	7
Stratigraphic position	Brockman Iron Fm. (Dales Gorge Member)	Brockman Iron Fm. (Dales Gorge Member)	Brockman Iron Fm. (Dales Gorge Member)	Brockman Iron Fm. (Dales Gorge Member)	Brockman Iron Fm. (Dales Gorge Member)	Brockman Iron Fm. (Dales Gorge Member)	Brockman Iron Fm. (Dales Gorge Member)
SiO ₂	46.86	47.57	47.85	44.86	51.44	58.05	n.dtm.
Al ₂ O ₃	0.43	0.08	0.33	0.14	1.54	0.24	n.dtm.
Fe ₂ O ₃	24.68	27.01	25.96	29.25	20.12	19.85	42.42
FeO	17.19	14.47	15.15	15.58	14.41	12.79	22.37
MgO	2.58	2.47	2.49	2.30	2.13	1.86	4.50
CaO	1.49	2.17	1.85	1.89	2.74	1.60	2.06
Na ₂ O	0.16	0.23	0.12	0.19	0.24	1.28	n.dtm.
K ₂ O	0.10	0.16	0.11	0.11	0.12	0.10	n.dtm.
H ₂ O ⁺	0.57	0.56	0.68	0.46	0.37	0.90	0.77
H ₂ O ⁻	0.08	0.10	0.17	0.09	0.07	0.10	0.12
CO ₂	5.81	4.99	5.11	5.13	6.81	2.71	2.18
FeS ₂	n.dct.	0.07	0.07	0.05	0.10	0.14	n.dct.
TiO ₂	0.05	0.03	0.03	0.02	n.dtm.	<0.01	n.dtm.
P ₂ O ₅	0.25	0.22	0.19	0.24	n.dtm.	0.47	0.86
MnO	n.dtm.	n.dtm.	<0.01	n.dtm.	n.dtm.	0.04	n.dtm.
Total	100.25	100.13	100.11	100.31	100.09	100.13	PA
Fe ³⁺	17.25	18.88	18.15	20.45	14.06	13.88	29.65
Fe ²⁺	13.36	11.25	11.78	12.11	11.20	9.94	17.39
Total Fe	30.61	30.13	29.93	32.56	25.26	23.82	47.04
Fe ³⁺ /Fe ²⁺	1.29	1.68	1.54	1.69	1.26	1.40	1.71
Analyst ¹	JRG	JRG	PH,MBC	JRG	MBC	JRG	JRG

NOTES—

1. The following is a key to analysts' initials appearing in Tables 11–16:

MBC—M. B. Costello; JRG—J. R. Gamble; PH—P. Hewson; RWL—R. W. Lindsey; RSP—R. S. Pepper; AJS—A. J. Sims.

5. Brockman Iron Formation, Dales Gorge Member, BIF2 macroband. Drillhole 28 at Wittenoom (Plate 6). Drilling depth 586 ft. 2.5 in. to 586 ft. 10.4 in.; approximate type section equivalent 82.55 to 81.85 feet. G.C.L. No. 6604/64.

6. Brockman Iron Formation, Dales Gorge Member, BIF2 macroband. Drillhole 46 at Wittenoom (Plate 6). Drilling depth 579 ft. 5.25 in. to 580 ft. 1.6 in. after removal of about 0.6 in. of crocidolite from the sample; approximate type section equivalent 82.55 to 81.85 feet. GCL No. 6605a/64.

TABLE 11 (continued)

	8	9	10	11	12	13
Stratigraphic position	Brockman Iron Fm. (Dales Gorge Member)	Brockman Iron Fm. (Joffre Member)	Brockman Iron Fm. (Joffre Member)	Boolgeeda Iron Fm.	Boolgeeda Iron Fm.	Brockman Iron Fm. (Dales Gorge Member)
SiO ₂	29.60	51.63	40.61	53.63	49.19	51.54
Al ₂ O ₃	0.13	1.14	0.99	4.74	1.94
Fe ₂ O ₃	2.71	16.87	21.45	29.44	27.87	41.62
FeO	36.58	17.68	17.51	3.24	12.08	6.05
MgO	3.51	3.47	2.94	2.15	2.51	0.29
CaO	0.89	0.05	3.38	<0.01	1.28
Na ₂ O	0.08	0.16	0.26	0.08	0.45	0.03
K ₂ O	0.23	2.67	1.34	1.77	0.93	0.03
H ₂ O ⁺	1.02	1.40	0.98	3.42	0.53	0.40
H ₂ O ⁻	0.05	0.10	0.08	0.95	0.09	0.07
CO ₂	24.75	4.83	10.04	0.03	2.52
FeS ₂	n.dct.	n.dct.	n.dct.	n.dct.	n.dct.	0.07
TiO ₂	0.01	0.07	0.07	0.24	0.09
P ₂ O ₅	0.36	0.02	0.23	0.11	0.39	0.13
MnO	0.27	0.04	0.24	0.09	0.23
Total	100.19	100.13	100.12	99.89	100.10	100.23
Fe ³⁺	1.89	11.79	14.99	20.58	19.48	29.09
Fe ²⁺	28.43	13.74	13.61	2.52	9.39	4.70
Total Fe	30.32	25.53	28.60	23.10	28.87	33.79
Fe ³⁺ /Fe ²⁺	0.07	0.86	1.10	8.17	2.07	6.19
Analyst	JRG	RSP	RSP	PH	PH	H. P. Rowledge

2. Throughout Tables 11-16:
n.dtm. — not determined.
n.dct. — not detected.
n.rep. — not reported.

7. Brockman Iron Formation, Dales Gorge Member, BIF12 macroband. Partial analysis of mixed group of Calamina cyclothem. Drillhole 51 at Wittenoom (Plate 6). Drilling depth 344 ft. 10 to 11½ in.; type section equivalent 296.55 to 296.65 feet. GCL No. 9382/66.

8. Brockman Iron Formation, Dales Gorge Member, S13 macroband. Chert-siderite. Drillhole 51 at Wittenoom (Plate 6). Drilling depth 319 ft. 0 to 3 in.; type section equivalent 325 to 324.75 feet. GCL No. 9383/66.

9. Brockman Iron Formation, Joffre Member, Drillhole 47 at Wittenoom. Drilling depth 363 ft. 5 in. to 364 ft. 5 in. About 280 feet above the base of the member. GCL No. 11655/67. R2657 of G.S.W.A. rock collection.

10. Brockman Iron Formation, Joffre Member. Drillhole 47 at Wittenoom. Drilling depth 511 ft. 0 in. to 512 ft. 6½ in. About 130 feet above the base of the member. GCL No. 11656/67. R2658 of G.S.W.A. rock collection.

11. Boolgeeda Iron Formation. Cliffs at east side of south entrance to Woongarra Gorge (lat. 22° 53'S; long. 117° 06'E). About 320 feet above the base of the formation. Green shaly iron formation. GCL No. 11659/67. R2661 of G.S.W.A. rock collection.

12. Boolgeeda Iron Formation. Cliffs at east side of south entrance to Woongarra Gorge (lat. 22° 53'S; long. 117° 06'E). About 270 feet above the base of the formation. Massive dark magnetite-rich iron formation. GCL No. 11600/67. R2662 of G.S.W.A. rock collection.

RESULTS

The only iron formation worth chemical analysis is fresh material unaffected by recent surface 'weathering'. Either drill-core or surface samples from deep gorges must therefore be used. Representative bulk samples of iron formation from natural gorge exposures are almost impossible to obtain, since the tougher mesobands split out and the softer material is easily lost. Consequently the only analyses reported here are of drill-cores from the Dales Gorge and Joffre Members of the Brockman Iron Formation and of surface samples of the non-mesobanded part of the Boolgeeda Iron Formation. We have seen no unweathered material from the Mount Sylvia or Weeli Wolli Formations, and no adequate bulk sample of the Marra Mamba Iron Formation could be collected at Kungarra Gorge where it is best exposed.

Analyses 1 to 4 are of exactly equivalent stratigraphic sections, but varying between 29 and 31½ inches thick, from four different drillholes at Wittenoom Gorge. For these, and all other core analyses reported, an accurately sawn rectangular prism of cross section about ½-inch by ¼-inch was taken longitudinally from the core and completely ground before splitting for analysis. These analyses were intended (in 1964) to test the range of chemical variation in laterally separated samples of the same stratigraphic thickness. They demonstrate that variation is small, but our present knowledge of the enormously greater lateral

extent of such recognisable stratigraphic intervals lessens their interest. We have not been able to make similar comparisons on a regional scale, for lack of fresh material.

Analyses 5 and 6 are also of stratigraphically equivalent BIF, slightly higher than 1 to 4 in the same macroband. The 7.9 inches used for analysis 5 is equivalent to the 8.35 inches of analysis 6, except that from this latter thickness 0.7 inches of crocidolite was removed and analysed separately (Table 14: 1); the calculated total composition of the 8.35 inches is shown as analysis 1 of Table 17. Also in Table 17, in column 4, is shown the average of analyses 1 to 6 of Table 11. This is the closest estimate we can give of the total composition of the BIF2 macroband of the Dales Gorge Member, and, by subjective extrapolation, of all the BIF part of the member. The accuracy of this estimate is discussed further beneath the following heading.

Analysis 7 of Table 11 is of the mixed group of the Calamina cyclothem where this is very regular, and with thin mixed groups between thick chert-magnetite groups (Figure 13A). It was requested because a thin band of massive apatite is here present (Figure 35B). The high P_2O_5 compared with any other analysis reported in this chapter is therefore expected. The high total iron content is relevant to discussion in Chapter 9.

Analysis 8 is of chert-siderite from the Dales Gorge Member, and is useful for identification of the siderite (sideroplesite: see pages 118 to 121, and Figure 33).

The average of analyses 9 and 10 of the Joffre Member, appears in column 5 of Table 17. Both these constituent analyses show, to variable degrees, the same similarities to, and differences from, all the analyses of the Dales Gorge Member, and chemical comparison between the two members is best made by reference to columns 4 and 5 of Table 17.

The two most striking resemblances about such a comparison lie firstly in the general quantitative similarity of all the major and most of the minor constituents, and secondly in the comparative paucity of materials: silica and iron oxides account for well over 80 per cent of both members. There appear to be two main differences which are also consistently different within the contributing analyses of the two averages, and which are not due to random fluctuation of trace constituents. One is the difference in oxidation state: the ratio of ferric to ferrous iron is consistently and significantly higher in the Dales Gorge Member. The other is the much higher content of stilpnomelane in the Joffre Member, clearly reflected by the two minor constituents Al_2O_3 and K_2O . An adequate Al_2O_3/K_2O ratio and $(Al_2O_3 + K_2O)$ content for ferrostilpnomelane of the Dales Gorge Member is given by the mean of analyses 5, 6, and 7 of Table 12 and analysis 3 of Table 16. These figures are 2.11 and 5.97 per cent respectively. The same parameters for Joffre Member stilpnomelane, from analysis 4 of Table 16, give values of 0.37 and 7.73 per cent. Stilpnomelane is the only mineral with

an important content of either constituent, so that the $\text{Al}_2\text{O}_3/\text{K}_2\text{O}$ ratios of columns 4 and 5 of Table 17 provide a check on whether the different stilpnomelane values already given are representative of all the stilpnomelane of each member. These ratios, 3.83 for the Dales Gorge Member and 0.53 for the Joffre Member, are of the expected order of size. The $(\text{Al}_2\text{O}_3 + \text{K}_2\text{O})$ values of columns 4 and 5 should then, also using the stilpnomelane values already given, show the total stilpnomelane by weight in each member. The values are 9.7 per cent in the Dales Gorge Member and 39.6 per cent in the Joffre Member. Although stilpnomelane mesobands make up only about 1.9 per cent by weight (2.3 per cent by volume: Table 4) of the Dales Gorge Member there is about 15 per cent of stilpnomelane by weight in chert-matrix (from analysis 4 of Table 12) and the figure of 9.7 is of the right order, though probably rather high. The analytical evidence therefore indicates that there is roughly four times as much stilpnomelane in the Joffre Member as the Dales Gorge Member.

The average of analyses 11 and 12 of Table 11, of the Boolgeeda Iron Formation, appears in column 6 of Table 17. There is a striking general similarity to both the Dales Gorge and Joffre Members, in both major and minor constituents; and again there is a significant difference in the ratio of ferric to ferrous iron in contrast to a total iron content which, within the sampling limitations, is effectively identical to that of both the Brockman Iron Formation BIF members. The Boolgeeda average is notably lower in CO_2 , which, as would be expected, involves a smaller CaO content, and contributes to the lower FeO . MgO , although about equal to the Dales Gorge Member, is less than the Joffre Member, in spite of the high stilpnomelane content indicated by Al_2O_3 and K_2O . Optically the stilpnomelane of the Boolgeeda Iron Formation resembles that of the Dales Gorge Member, but it is always fine-grained, and there are no separate analyses of it. The average $\text{Al}_2\text{O}_3/\text{K}_2\text{O}$ ratio of the Boolgeeda Iron Formation, 2.47, is much closer to that of the Dales Gorge Member than the Joffre Member, but if a similar proportion of $(\text{Al}_2\text{O}_3 + \text{K}_2\text{O})$ in the Boolgeeda Iron Formation stilpnomelane is assumed then the theoretical stilpnomelane content of the formation, 78.6 per cent is obviously absurd. We prefer to suggest, therefore, either that the stilpnomelane of the Boolgeeda Iron Formation has a much higher $(\text{Al}_2\text{O}_3 + \text{K}_2\text{O})$ content than that of the Brockman Iron Formation members, or that there is a proportion of sericite among the sheet silicate content of the Boolgeeda; this has an $(\text{Al}_2\text{O}_3 + \text{K}_2\text{O})$ content of the order of 40 per cent, and little would be needed to produce the observed result.

The final BIF analysis, 13 of Table 11, is of interest as a demonstration of the effect of surface weathering. Carbonate is leached out, together with its constituent CaO and most of the MgO , but the FeO is oxidised, together with at least part of the magnetite. In this sample there was evidently no loss of iron (indeed, loss of CO_2 probably raised the total iron), but the ratio of ferric to ferrous iron was greatly increased.

**COMPLETE ANALYSES OF INDIVIDUAL MESOBANDS
FROM THE DALES GORGE MEMBER OF THE
BROCKMAN IRON FORMATION (TABLE 12)**

MATERIAL

The analyses set out in Table 12 are of the following material:

1. BIF2 macroband. Composite sample of all chert mesobands with a microband interval greater than about 0.8 mm (mean 1.1 mm) in the stratigraphic interval equivalent to about 84.5 to 81.5 feet on the type section. Taken from Drillholes 28 (584 ft. 1½ in. to 587 ft. 5 in.), 33 (473 ft. 9 in. to 476 ft. 3 in.), and 46 (577 ft. 8½ in. to 580 ft. 8½ in.) at Wittenoom. GCL No. 6581/64.

TABLE 12. COMPLETE ANALYSES OF INDIVIDUAL MESOBAND TYPES FROM THE DALES GORGE MEMBER OF THE BROCKMAN IRON FORMATION

	1	2	3	4	5	6	7
Mesoband type	Coarsely micro-banded chert	Finely micro-banded chert	Podded chert	Chert-matrix	Thin Green	Thin Green	Thin Green
SiO ₂	74.71	48.41	66.08	35.74	43.39	45.15	43.17
Al ₂ O ₃	0.19	0.16	0.19	0.81	3.65	4.19	3.62
Fe ₂ O ₃	0.46	14.86	1.60	35.43	6.76	7.23	7.06
FeO	8.99	19.00	8.68	19.71	23.32	21.92	23.99
MgO	2.08	3.44	3.28	2.41	8.85	8.57	8.28
CaO	3.39	0.55	6.45	1.31	0.03	0.20	n.dct.
Na ₂ O	0.03	0.07	0.09	0.19	0.69	0.77	0.67
K ₂ O	0.08	0.17	n.dct.	0.12	1.79	1.84	2.08
H ₂ O ⁺	0.57	0.81	0.21	0.58	7.38	6.73	7.42
H ₂ O ⁻	n.dct.	0.06	0.12	0.12	2.20	2.61	2.25
CO ₂	9.22	12.57	12.90	3.68	1.80	0.13	1.27
TiO ₂	0.01	0.06	0.09	0.05	0.04	0.29	0.07
P ₂ O ₅	0.01	0.05	0.45	0.09	0.22	0.12	0.16
MnO	0.04	0.06	0.04	n.dtm.	0.03	n.dtm.	n.dtm.
Total	99.78	100.27	100.18	100.24	100.15	99.75	100.04
Fe ³⁺	0.32	10.39	1.12	24.77	4.73	5.05	4.93
Fe ²⁺	6.99	14.77	6.75	15.32	18.13	17.04	18.65
Total Fe	7.31	25.16	7.87	40.09	22.86	22.09	23.58
Fe ³⁺ /Fe ²⁺	0.04	0.70	0.17	1.62	0.26	0.30	0.26
Analyst	PH	PH	RSP	JRG	RSP	MBC	PH

2. BIF2 macroband. Composite sample of the central and evenly micro-banded part (interval 0.33 mm) of the same thick chert mesoband from Drillholes 28, 33, 40, and 46 at Wittenoom (Plate 6). Type section equivalent of sample exactly 81.25 to 81.30 feet. GCL No. 6582/64.

3. BIF2 macroband. Composite sample of all chert pods in the stratigraphic interval equivalent to 81.5 to 78.5 feet on the type section. Taken from Drillholes 28 (587 ft. 5 in. to 590 ft. 2 in.), 33 (476 ft. 11 in. to 480 ft. 0½ in.), 40 (644 ft. 0 in. to 647 ft. 1 in.), and 46 (580 ft. 8½ in. to 583 ft. 3 in.) at Wittenoom (Plate 6). GCL No. 6585/64.

4. BIF2 macroband. Composite sample of chert matrix in the same interval and same drillholes as analysis 3, preceding. GCL No. 6586/64.

TABLE 12 (continued)

	8	9	10	11	12	13
Mesoband type	Thin Green	Thin Green	Thin Green	Thin Green	Thin Green	Thin Green
SiO ₂	30.03	45.26	24.76	32.49	37.87	28.75
Al ₂ O ₃	2.87	1.69	1.88	2.42	2.85	1.12
Fe ₂ O ₃	4.86	8.24	5.69	4.92	5.20	9.89
FeO	30.01	21.60	32.93	29.44	23.36	27.87
MgO	8.79	7.55	8.55	8.70	12.37	10.83
CaO	0.17	0.79	0.04	0.05	n.dct.	n.dct.
Na ₂ O	0.54	0.55	0.40	0.52	0.70	0.88
K ₂ O	1.11	1.17	0.86	1.08	1.31	0.92
H ₂ O ⁺	3.69	5.52	3.42	3.86	5.14	4.07
H ₂ O ⁻	1.03	0.72	0.81	1.02	1.09	0.64
CO ₂	16.34	6.73	19.44	15.35	9.82	14.58
TiO ₂	0.35	0.13	0.10	0.09	0.09	0.08
P ₂ O ₅	0.08	0.10	0.28	0.31	0.42	0.48
MnO	n.dtm.	0.07	0.15	0.14	n.dtm.	n.dtm.
Total	99.87	100.12	100.25 ¹	100.39	100.22	100.11
Fe ³⁺	3.40	5.76	3.98	3.44	3.63	6.91
Fe ²⁺	23.33	16.79	25.60	22.88	18.16	21.66
Total Fe	26.73	22.55	29.58	26.32	21.79	28.57
Fe ³⁺ /Fe ²⁺	0.15	0.34	0.16	0.15	0.20	0.32
Analyst	MBC	RSP	RSP	RSP	JRG	JRG

¹ Includes SO₃ 0.33, BaO, 0.61.

5. BIF2 macroband. Stilpnomelane-rich mesoband about 2 mm thick at about 586 ft. 0½ in. depth in Drillhole 28 at Wittenoom (Plate 6). Type section equivalent 82.75 feet. GCL No. 6592/64.

6. Same mesoband as analysis 5, at about 475 ft. 10½ in. depth in Drillhole 33 at Wittenoom (Plate 6). Type section equivalent 82.75 feet. GCL No. 6593/64.

7. Same mesoband as analyses 5 and 6, at about 579 ft. 3 in. depth in Drillhole 46 at Wittenoom (Plate 6). Type section equivalent 82.75 feet. GCL No. 6594/64.

8. BIF2 macroband. Stilpnomelane-siderite mesoband about 10 mm thick at about 587 ft. 4½ in. depth in Drillhole 28 at Wittenoom (Plate 6). Type section equivalent at 81.5 feet. GCL No. 6595/64.

TABLE 12 (continued)

	14	15	16	17	18	19
Mesoband type	Thin Green	Thin Green	Micro-banded chert of chert-siderite	Micro-banded chert of chert-siderite	Micro-banded chert of chert-siderite	Micro-banded chert
SiO ₂	30.19	34.20	86.08	92.98	80.69	53.26
Al ₂ O ₃	1.96	2.30	0.13	0.12	0.08	n.dct.
Fe ₂ O ₃	13.20	8.58	0.29	0.20	0.63	35.56
FeO	25.87	24.55	4.25	2.12	6.37	8.14
MgO	10.62	11.07	0.80	0.45	0.99	0.71
CaO	0.33	n.dct.	2.67	1.29	3.17	0.30
Na ₂ O	0.53	0.86	0.04	0.04	0.04	0.19
K ₂ O	1.13	1.16	0.10	0.08	0.18	0.06
H ₂ O ⁺	4.75	4.61	0.46	0.23	0.76	0.33
H ₂ O ⁻	0.92	1.53	0.13	0.13	0.18	0.05
CO ₂	10.27	10.63	4.68	2.27	5.92	1.65
TiO ₂	0.01	0.01	0.02	0.03	0.02	0.01
P ₂ O ₅	0.48	0.66	0.14	0.12	0.46	0.09
MnO	0.09	0.10	0.11	0.05	0.16	0.01
Total	100.35	100.26	99.90	100.11	99.65	100.36
Fe ³⁺	9.23	6.00	0.20	0.14	0.44	27.93
Fe ²⁺	20.11	19.08	3.30	1.65	4.95	6.33
Total Fe	29.34	25.08	3.50	1.79	5.39	34.26
Fe ³⁺ /Fe ²⁺	0.46	0.31	0.06	0.08	0.09	3.93
Analyst	JRG	RSP	JRG	JRG	JRG	RSP

9. Same mesoband as analysis 8, at about 477 ft. 3 in. depth in Drillhole 33 at Wittenoom (Plate 6). Type section equivalent 81.5 feet. GCL No. 6596/64.

10. Same mesoband as analyses 8 and 9, at about 644 ft. 0½ in. depth in Drillhole 40 at Wittenoom (Plate 6). Type section equivalent 81.5 feet. GCL No. 6597/64.

11. Same mesoband as analyses 8, 9, and 10, at about 580 ft. 7½ in. depth in Drillhole 46 at Wittenoom. Type section equivalent 81.5 feet. GCL No. 6598/64.

12. BIF2 macroband, stilpnomelane-siderite mesoband about 3 mm thick at about 588 ft. 11¾ in. depth in Drillhole 28 at Wittenoom (Plate 6). Type section equivalent 79.9 feet. GCL No. 6599/64.

13. Same mesoband as analysis 12, at about 478 ft. 10¾ in. depth in Drillhole 33 at Wittenoom (Plate 6). Type section equivalent 79.9 feet. GCL No. 6600/64.

14. Same mesoband as analyses 12 and 13, at about 645 ft. 7½ in. depth in Drillhole 40 at Wittenoom (Plate 6). Type section equivalent 79.9 feet. GCL No. 6601/64.

15. Same mesoband as analyses 12, 13, and 14, at about 582 ft. 2 in. depth in Drillhole 46 at Wittenoom. Type section equivalent 79.9 feet. GCL No. 6602/64.

16. Dales Gorge Member, S3 macroband. Chert mesoband in chert-siderite. Drillhole 51 at Wittenoom (Plate 6). Drilling depth 559 ft. 7 to 9 in.; approximate type section equivalent 86.65 to 86.85 feet. GCL No. 9384/64.

17. S13 macroband. Chert mesoband in chert-siderite. Drillhole 51 at Wittenoom (Plate 6). Drilling depth 319 ft. 8½ to 9 in.; approximate type section equivalent 324.25 feet. GCL No. 9385/65.

18. S13 macroband. Chert mesoband in chert-siderite. Drillhole 51 at Wittenoom (Plate 6). Drilling depth 318 ft. 6 in.; approximate type section equivalent 325.7 feet. GCL No. 9386/65.

19. BIF2 macroband. Finely microbanded chert (interval 0.25 mm). Drillhole 40 at Wittenoom (Plate 6). Drilling depth about 646 feet. Type section equivalent 77.7 feet (in riebeckite). GCL No. 9380/65.

RESULTS

Of these 19 analyses, 1 to 4 come from the same 6 feet of BIF2 in 4 different drillholes, and were made to determine the range in average chemical composition of the main mesoband types initially distinguished in this study; analyses 5 to 15 were made to test lateral chemical variation in thin green mesobands known to be laterally persistent; analyses 16 to 18 are additional chert analyses for comparison of cherts in chert-siderite with those of BIF proper; and analysis 19 is of the chert of the chert-magnetite group of the Calamina cyclothem at a level which is known to consist of massive riebeckite over wide areas.

In column 2 of Table 17 is shown a calculated average of analyses 1, 2, and 3; this is the closest estimate we can give to average chert of the Dales Gorge Member. Using this average, analysis 4 for chert-matrix, and pure Fe_3O_4 for magnetite mesobands, an estimated BIF composition for the Dales Gorge Member can be calculated using the mesoband proportions of Table 4. Such an estimate appears in column 3 of Table 17 for these three mesoband types only, with assumed densities of 2.9 (chert), 3.6 (chert-matrix), and 5.0 (magnetite) for the conversion of volume to weight proportions. Columns 3 and 4 of Table 17 are sufficiently close to suggest that neither is far removed from the truth. The greatest discrepancies between them are in silica and iron. Inclusion of stilpnomelane would bring these closer, but the other assumptions made for calculation of column 3 are so liable to error that further refinement seems unprofitable. For example, the intergradation of chert-matrix and magnetite mesobands makes estimation of averages for both materials highly subjective. In general, the figures in column 3 support the comments already made concerning the chemical contrast between the Dales Gorge Member and other iron formation units.

Much of the original interest of analyses 5 to 15 is now lost as a result of our increased knowledge of the lateral continuity of the mesobanding. By comparison with the total lateral extent separation between the four drillholes used for these analyses is insignificant, and their chief interest lies in the average composition they give for mesobands consisting largely of stilpnomelane.

TABLE 13. PARTIAL ANALYSES OF INDIVIDUAL CHERT MESOBANDS FROM THE DALES GORGE MEMBER OF THE BROCKMAN IRON FORMATION

	1	2	3	4	5	6
Stratigraphic position	BIF12	BIF2	BIF2	S11	BIF12	S6
Microband interval	0.23	0.50	1.12	0.40	0.95
Fe_2O_3	33.06	19.19	n.dtm.	n.dtm.	n.dtm.	n.dtm.
FeO	9.56	3.74	18.26	n.dtm.	n.dtm.	n.dtm.
MgO	1.86	0.72	4.80	0.81	1.26	1.11
CaO	0.41	2.22	15.96	2.14	1.31	0.30
H_2O^-	0.02	0.01	n.dtm.	n.dtm.	n.dtm.	n.dtm.
CO_2	2.60	3.60	24.09	5.59	3.04	6.13
MnO	n.dtm.	n.dtm.	0.12	n.dtm.	n.dtm.	n.dtm.
Fe^{3+}	23.14	13.43
Fe^{2+}	7.43	2.91
Total Fe	30.57 ¹	16.34 ¹	6.47 ²	9.03 ²	7.76 ²
Analyst	RSP	RSP	JRG

¹ Calculated.

² Analysed.

Analyses 1 to 4 and 16 to 19 are used in Chapter 4 (Figure 33) in discussion of carbonate mineral composition, and analyses 1, 2, and 16 to 18 in discussion in Chapter 9 (Figure 72). Analysis 19 is also used in Figure 72 as well as in Chapter 11 (Table 25), and needs no further comment here.

PARTIAL ANALYSES OF INDIVIDUAL CHERT MESOBANDS FROM THE DALES GORGE MEMBER OF THE BROCKMAN IRON FORMATION (TABLE 13)

Although some of these 17 analyses were intended for other purposes they now serve, in various groups, three main functions: 1. the investigation of carbonate mineral composition, 2. the indication of iron content of cherts in relation to microband interval, and 3. the demonstration of a possible derivation of iron in crocidolite. These topics are dealt with further in Chapters 4, 9, and 11 respectively, and no further comment is needed here besides the locations and stratigraphic positions of the samples analysed.

MATERIAL

1. BIF12. From chert-magnetite group of Calamina cyclothem. Drillhole 51 at Wittenoom (Plate 6). Drilling depth 344 ft. 1 in. Type section equivalent 297.4 feet. GCL No. 6583/64.

TABLE 13 (continued)

	7	8	9	10	11	12
Stratigraphic position	BIF4	BIF4	BIF4	BIF4	BIF4	BIF1
Microband interval	1·15	0·63	0·60	0·62	0·61	0·60
Fe ₂ O ₃	n.dtm.	n.dtm.	n.dtm.	n.dtm.	n.dtm.	n.dtm.
FeO	n.dtm.	n.dtm.	n.dtm.	n.dtm.	n.dtm.	n.dtm.
MgO	0·97	1·22	2·08	1·32	1·32	1·10
CaO	1·89	2·48	3·13	2·28	1·27	0·29
H ₂ O ⁻	n.dtm.	n.dtm.	n.dtm.	n.dtm.	n.dtm.	n.dtm.
CO ₂	3·40	3·82	6·57	4·75	5·54	3·47
MnO	n.dtm.	n.dtm.	n.dtm.	n.dtm.	n.dtm.	n.dtm.
Fe ³⁺
Fe ²⁺
Total Fe	6·41 ²	17·20 ²	8·04 ²	15·6 ²	22·9 ²	21·8 ²
Analyst

² Analysed.

2. BIF2. From chert-magnetite group of Calamina cyclothem. Drillhole 40 at Wittenoom (Plate 6). Drilling depth 647 ft. 0 in. Type section equivalent 81.3 feet. GCL No. 6584/64.

3. BIF2. Carbonate-rich chert. Drillhole 33 at Wittenoom (Plate 6). Drilling depth 474 ft. 3½ to 4½ in. Type section equivalent about 84.5 feet. GCL No. 9379/65.

4. S11. Chert-siderite chert. Drillhole 51 at Wittenoom (Plate 6). Drilling depth about 375 ft. Type section equivalent about 271 feet. GCL No. 1622/66.

5. BIF12. Drillhole 51 at Wittenoom (Plate 6). Drilling depth 334 ft. 0¼ to 0½ in. Type section equivalent about 310 feet. GCL No. 1623/66.

6. S6. Chert-siderite chert. Drillhole 51 at Wittenoom (Plate 6). Drilling depth 504 ft. 1 to 2 in. Type section equivalent about 148 feet. GCL No. 1624/66.

7. BIF4. Drillhole 51 at Wittenoom (Plate 6). Drilling depth 521 ft. 11½ in. to 522 ft. 0 in. Type section equivalent about 132 feet. GCL No. 1625/66.

8. BIF4. Drillhole 51 at Wittenoom (Plate 6). Drilling depth 527 ft. 0 to 0½ in. Type section equivalent about 127 feet. GCL No. 1626/66.

9. BIF4. Drillhole 51 at Wittenoom (Plate 6). Drilling depth 526 ft. 8 to 8½ in. Type section equivalent about 127.3 feet. GCL No. 1627/66.

TABLE 13 (continued)

	13	14	15	16	17
Stratigraphic position	BIF1	BIF2 Upper Seam	BIF2 Upper Seam	BIF2 Upper Seam	BIF2 Upper Seam
Microband interval	0·48	0·56	0·45	0·50	0·59
Fe ₂ O ₃	n.dtm.	0·80	0·72	1·05	0·16
FeO	n.dtm.	2·91	1·83	2·00	2·90
MgO	1·21	0·81	0·50	0·33	0·98
CaO	n.dct.	1·22	1·02	0·27	1·82
H ₂ O ⁻	n.dtm.	n.dtm.	n.dtm.	n.dtm.	n.dtm.
CO ₂	4·82	3·35	2·50	1·10	4·43
MnO	n.dtm.	n.dtm.	n.dtm.	n.dtm.	n.dtm.
Fe ³⁺	0·56	0·50	0·73	0·11
Fe ²⁺	2·26	1·42	1·55	2·25
Total Fe	18·3 ²	2·82 ¹	1·92 ¹	2·28 ¹	2·36 ¹
Analyst	RSP/RWL	RSP/RWL	RSP/RWL	RSP/RWL

¹ Calculated.

² Analysed.

10. BIF4. Drillhole 51 at Wittenoom (Plate 6). Drilling depth 528 ft. 11 to 11½ in. Type section equivalent about 125 feet. GCL No. 1628/66.

11. BIF4. Drillhole 51 at Wittenoom. Drilling depth 531 ft. 4½ to 5 in. Type section equivalent about 123 feet. GCL No. 1629/66.

12. BIF1. Drillhole 51 at Wittenoom (Plate 6). Drilling depth 593 ft. 2½ to 3 in. Type section equivalent about 54 feet. GCL No. 1630/66.

13. BIF1. Drillhole 51 at Wittenoom (Plate 6). Drilling depth 595 ft. 10 to 10½ in. Type section equivalent about 51 feet. GCL No. 1631/66.

14. BIF2. Colonial mine. Chert associated with Upper Seam. Type section equivalent about 70 feet. R2451 of G.S.W.A. registered rock collection. GCL No. 4731/66.

TABLE 14. ANALYSES OF RIEBECKITE (INCLUDING CROCIDOLITE) FROM THE HAMERSLEY GROUP

	1	2	3	4	5	6	7
Material	Crocidolite	Massive riebeckite	Crocidolite	Crocidolite	Crocidolite	Massive riebeckite	Crocidolite
SiO ₂	53·66	53·52	53·10	51·86	51·94	45·51	52·85
Al ₂ O ₃	0·08	0·41	0·88	0·03	0·24	0·78	0·18
Fe ₂ O ₃	17·73	17·72	16·95	20·26	18·93	26·05	18·55
FeO	14·67	16·26	17·54	14·84	15·25	15·07	14·95
MgO	4·54	3·63	3·13	3·26	3·94	2·49	4·64
CaO	0·23	0·08	0·52	0·49	0·40	0·11	1·07
Na ₂ O	5·01	5·57	6·21	6·12	6·00	5·43	5·97
K ₂ O	0·07	0·05	0·14	0·28	0·26	0·05	0·05
H ₂ O ⁺	2·81	2·63	} 1·66	1·97	2·67	3·50	2·77
H ₂ O ⁻	0·33	0·32		0·68	0·72	1·24	0·22
CO ₂	0·57	n.dct.	n.rep.	0·02	nil	0·03	0·23
FeS ₂	0·02	n.dtm.	n.rep.	n.rep.	n.rep.	nil	n.rep.
TiO ₂	0·02	n.dct.	n.rep.	0·03	0·01	nil	n.rep.
P ₂ O ₅	0·36	0·20	n.rep.	0·05	nil	nil	n.rep.
MnO	0·07	0·01	n.rep.	0·01	0·01	nil	tr.
Total	100·17	100·40	100·13	99·90	100·37	100·26	100·48
Fe ³⁺	12·41	12·40	11·85	14·18	13·25	18·23	12·98
Fe ²⁺	11·40	12·64	13·63	11·54	11·85	11·71	11·62
Total Fe	23·81	25·04	25·48	25·72	25·10	29·94	24·60
Fe ³⁺ /Fe ²⁺	1·09	0·98	0·87	1·23	1·12	1·56	1·12
Analyst	JRG	RSP	E. S. Simpson	J. N. Grace	J. N. Grace	Not known (E. S. Simpson?)	D. G. Hiscock and others

15. BIF2. Colonial mine. chert associated with Upper Seam. Type section equivalent about 70 feet. R2452 of G.S.W.A. registered rock collection. GCL No. 4732/66.

16. BIF2. Colonial mine. Chert associated with Upper Seam. Type section equivalent about 70 feet. R2452 (different mesoband to analysis 15) of G.S.W.A. registered rock collection. GCL No. 4733/66.

17. BIF2. Colonial mine. Chert associated with Upper Seam. Type section equivalent about 70 feet. GCL No. 4734/66.

ANALYSES OF RIEBECKITE (INCLUDING CROCIDOLITE) (TABLE 14)

MATERIAL

Of the six existing analyses of riebeckite from the Hamersley Range area only analyses 1 and 2 are newly reported here; the derivation of the material for all 6 analyses is:

1. Crocidolite. Mesoband about 0.6 inches (15 mm) thick in BIF2. Drill-hole 46 at Wittenoom. Drilling depth 590 ft 1 to 1½ inches. Type section equivalent 82.25 feet. GCL No. 6605b/64.

2. Massive riebeckite. BIF 2 (adit-roof riebeckite). Drillhole 22 at Wittenoom (Plate 6). Drilling depth about 500 feet. Type section equivalent 77.7 feet. GCL No. 9381/65.

3. Crocidolite. This is the analysis, carried out by E. S. Simpson in 1908, of the first crocidolite sample (No. 8508) brought to the Geological Survey of Western Australia on 18/3/1908; it has not been previously published. Its location is not known.

4. Crocidolite. Reproduced from Simpson (1930). Locality given as Mount Margaret. Probably Upper Seam Crocidolite Horizon of BIF2; see Chapter 7.

5. Crocidolite. Reproduced from Simpson (1930). Locality given as Weeli Wolli. Stratigraphic position unknown; see Chapter 7.

6. Massive riebeckite. Reproduced from Finucane (1939). Locality given as Yampire Gorge. May be from either of the two Riebeckite Horizons of the Dales Gorge Member.

7. Crocidolite. Reproduced from Hodgson (1965a). Locality given as "Hamersley Range" in Hodgson (1965b). Probably Upper Seam fibre from the Colonial mine.

RESULTS

A detailed examination of the range of chemical variation in riebeckite from the Hamersley Range area did not form part of our study. From the data of Table 14 we conclude firstly that there is no significant compositional difference between massive riebeckite and crocidolite, secondly that the compositional range

is small, and thirdly that the crocidolite compositions reported seem close to those of the northern Cape Province (Pomfret) area of South Africa, reported by Hodgson (1965b).

ANALYSES OF SHALES (TABLE 15)

MATERIAL

The analyses set out in Table 15 are of the following shales:

1. Brockman Iron Formation, Dales Gorge Member, S14 macroband. Dark green shale. Drillhole 51 at Wittenoom (Plate 6). Drilling depth 292 feet. Type section equivalent about 355 feet. GCL No. 6578/64.

TABLE 15. ANALYSES OF SIX SHALES FROM THE HAMERSLEY GROUP AND ONE SHALE FROM THE FORTESCUE GROUP

	1	2	3	4	5	6
Stratigraphic position	Brockman Iron Fm.	Brockman Iron Fm.	Brockman Iron Fm.	Brockman Iron Fm.	Mt. McRae Shale	Mt. McRae Shale
SiO ₂	50.38	41.70	49.85	41.58	80.90	75.50
Al ₂ O ₃	12.66	6.89	13.44	5.86	5.14	10.30
Fe ₂ O ₃	1.24	24.10	7.42	2.02	1.26	1.23
FeO	11.89	2.43	4.91	21.72	0.24	0.89
MgO	3.19	3.67	3.55	3.95	tr.	0.47
CaO	0.18	0.60	0.07	2.99	0.06	0.07
Na ₂ O	0.11	0.31	0.12	00.7	0.08	0.13
K ₂ O	9.93	0.52	8.43	5.02	1.75	3.53
Li ₂ O	0.27	n.rep.	0.25	n.rep.	0.04	0.11
H ₂ O ⁺	1.71	7.97	3.08	2.88	3.24	4.05
H ₂ O ⁻	0.89	10.45	2.60	0.69	0.46	0.08
CO ₂	1.86	0.16	n.dct.	12.64	n.dtm.	n.dtm.
C	0.74	0.15	1.88	n.rep.	0.70	n.dtm.
FeS ₂	4.15	0.47	3.59	n.rep.	n.rep.	n.rep.
SO ₃	0.08	n.rep.	0.11	n.rep.	5.24	3.66
TiO ₂	0.43	0.40	0.44	0.19	0.72	0.20
P ₂ O ₅	0.09	0.25	0.12	0.15	tr.	0.13
MnO	0.18	n.dtm.	0.03	0.38	tr.	0.02
Total	99.98	100.07	99.89	100.14	99.83	100.37
Fe ³⁺	0.87	16.87	5.19	1.41	0.88	0.86
Fe ²⁺	9.24	1.89	3.82	16.88	0.19	0.69
Total Fe	10.11	18.76	9.01	18.29	1.07	1.55
Fe ³⁺ /Fe ²⁺	0.09	8.93	1.36	0.08	4.63	1.25
Analyst	RSP	MBC	RSP	RSP	AJS	MBC

2. Brockman Iron Formation. Dales Gorge Member, S11 macroband. Dark green shale. Drillhole 51 at Wittenoom (Plate 6). Drilling depth 371 feet. Type section equivalent about 267 feet. GCL No. 6579/64.

3. Brockman Iron Formation, Dales Gorge Member, S11 macroband. Black fissile shale. Drillhole 51 at Wittenoom (Plate 6). Drilling depth 370 feet. Type section equivalent about 268 feet. GCL No. 6580/64.

4. Brockman Iron Formation, Whaleback Shale Member. Drillhole 47 at Wittenoom. Drilling depth 655 ft. 7 in. to 658 ft. 2½ in. About 200 feet above the base of the member. R2659 of G.S.W.A. registered rock collection. GCL No. 11657/67.

TABLE 15 (continued)

	7	8	9	10	11	12
Stratigraphic position	Mt. McRae Shale	Mt. McRae Shale	Mt. McRae Shale	Mt. McRae Shale	Mt. McRae Shale	Jeerinah Formation (Fort- escue Group)
SiO ₂	39·61	39·46	33·75	28·54	28·47	72·65
Al ₂ O ₃	9·96	6·04	8·93	7·76	7·02	0·53
Fe ₂ O ₃	8·78	14·56	5·65	9·34	13·04	9·54
FeO	13·01	17·50	13·17	20·30	12·96	n.dct.
MgO	8·24	6·24	9·50	8·08	8·25	0·08
CaO	0·96	0·11	6·95	4·96	4·39	0·26
Na ₂ O	0·30	0·50	0·07	0·34	0·28	0·11
K ₂ O	2·71	1·42	0·13	0·76	0·80	0·39
Li ₂ O	n.rep.	n.rep.	n.rep.	n.rep.	n.rep.	n.rep.
H ₂ O ⁺	6·76	7·03	5·74	7·56	6·42	4·70
H ₂ O ⁻	1·03	2·25	0·23	1·24	1·60	1·40
CO ₂	1·26	0·23	9·82	7·46	6·48	n.dct.
C	0·60	0·97	1·05	1·44	1·38	16·70
FeS ₂	6·30	3·55	4·92	1·78	8·51	1·26
SO ₃	n.rep.	n.rep.	n.rep.	n.rep.	n.rep.	0·67
TiO ₂	0·59	0·27	0·37	0·32	0·30	0·48
P ₂ O ₅	tr.	0·01	0·03	0·17	0·17	n.dtm.
MnO	0·03	0·04	0·05	0·07	0·03	n.dtm.
Total	100·14	100·18	100·36	100·12	100·10	99·77
Fe ³⁺	6·14	10·18	3·95	6·53	9·12	0·38
Fe ²⁺	10·11	13·60	10·24	15·78	10·07	0·00
Total Fe	16·25	23·78	14·19	22·31	19·19	0·38
Fe ³⁺ /Fe ²⁺	0·61	0·75	0·39	0·41	0·91
Analyst	JRG	JRG	JRG	JRG	JRG	MBC

5. Mount McRae Shale. White shale. About 2 miles north Hamersley homestead. R92 of G.S.W.A. registered rock collection. GCL No. 8535/63.
6. Mount McRae Shale. White shale. About 5 miles south of Weeli Wolli Spring. R645 of G.S.W.A. registered rock collection. GCL No. 8542/63.
7. Mount McRae Shale. Dark green shale. Drillhole Y1 at Yampire Gorge (Plate 8). Drilling depth 356 ft. 0 to 3 in. About 27 feet below top of formation. GCL No. 9501/66.
8. Mount McRae Shale. Black shale. Drillhole Y1 at Yampire Gorge (Plate 8). Drilling depth 365 ft. 0 to 9 in. About 36 feet below top of formation. GCL No. 9502/66.
9. Mount McRae Shale. Dark green shale. Drillhole Y1 at Yampire Gorge (Plate 8). Drilling depth 370 ft. 4 to 6 in. About 41 feet below top of formation. GCL No. 9503/66.
10. Mount McRae Shale. Black shale. Drillhole Y1 at Yampire Gorge (Plate 8). Drilling depth 378 ft. 10 in. to 379 ft. 1 in. About 50 feet below top of formation. GCL No. 9504/66.
11. Mount McRae Shale. Black shale. Drillhole Y1 at Yampire Gorge. Drilling depth 384 ft. 6 to 10 in. About 56 feet below top of formation. GCL No. 9505/66.
12. Jeerinah Formation (Fortescue Group). Black shale. From spoil heap of Bloom Well (lat. $21^{\circ} 52'S$; long. $117^{\circ} 39'E$). GCL No. 6603/64.

RESULTS

Two of these analyses, 5 and 6, are of material affected, to an unknown extent, by surface weathering. The sulphate, present as alunite, is presumably derived by breakdown of sheet silicates by sulphuric acid derived from original pyrite. It is uncertain whether the silica and alumina differ much from their initial values. All the remaining four analyses are of fresh material. It is plain that the wide variation in major constituents of all twelve analyses (SiO_2 28.47 to 80.9; Al_2O_3 0.53 to 14.56; K_2O 0.13 to 9.93) makes it essential that at least ten times the number must be obtained before a systematic idea of shale composition can be obtained. The analyses from the Brockman Iron Formation do give some help with mineral identification, and are referred to in this context in Chapter 4. A mean of analyses 1-4 and 7-11 is used, with reservation, in Chapter 9, while the general significance of the results reported is discussed in Chapter 10.

MISCELLANEOUS ANALYSES DIRECTED MAINLY TOWARDS MINERAL IDENTIFICATION (TABLE 16)

MATERIAL

The analyses of Table 16 are of the following material:

1. Brockman Iron Formation, Dales Gorge Member, S3 macroband. Drillhole 28 at Wittenoom (Plate 6). Drilling depth 584 ft. 5 in. Type section equivalent about 85 feet. GCL No. 6587/64.

2. Brockman Iron Formation, Dales Gorge Member, BIF11 macroband. Drillhole 51 at Wittenoom (Plate 6). Drilling depth about 355 feet. Type section equivalent about 286 feet. GCL No. 9387/65.

3. Brockman Iron Formation, Dales Gorge Member, S10 macroband. Drillhole 51 at Wittenoom (Plate 6). Drilling depth about 405 feet. Type section equivalent about 244 feet. GCL No. 10900/64.

4. Brockman Iron Formation, Joffre Member. Base of cliffs at first pool below Joffre Falls. R2660 of G.S.W.A. registered rock collection. GCL No. 11658/67.

TABLE 16. MISCELLANEOUS ANALYSES DIRECTED MAINLY TOWARDS MINERAL IDENTIFICATION

	1	2	3	4	5	6	7
Material	Limestone represent- ing shale	Minneso- taite	Ferro- stilp- nomelane	Ferri- stilp- nomelane	Black porcel- lanite	Chert + minneso- taite	Stilp- nomelane shale
SiO ₂	n.dtm.	56.73	45.54	44.04	65.54	67.38	42.53
Al ₂ O ₃	n.dtm.	n.dct.	4.75	2.10	11.54	0.04	5.26
Fe ₂ O ₃	6.58	2.39	2.90	18.49	4.22	10.90	25.54
FeO	7.22	20.06	25.38	18.55	4.58	16.52	5.09
MgO	1.54	16.81	7.75	6.52	1.20	2.16	7.20
CaO	39.87	0.03	0.04	<0.01	<0.01	<0.01	<0.01
Na ₂ O	n.dtm.	n.dtm.	0.82	0.26	<0.01	<0.01	0.75
K ₂ O	n.dtm.	n.dtm.	1.96	5.63	11.43	0.31	2.37
H ₂ O ⁺	n.dtm.	3.83	8.46	3.66	0.91	2.39	7.44
H ₂ O ⁻	0.09	0.06	1.56	0.41	0.12	0.11	1.37
CO ₂	34.99	n.dtm.	0.28	0.32	0.21	0.07	0.04
C	n.dtm.	n.rep.	n.rep.	n.rep.	n.dtm.	n.dtm.	0.19
FeS ₂	n.dtm.	n.rep.	n.rep.	n.rep.	0.09	0.04	0.28
TiO ₂	n.dtm.	n.dtm.	0.26	0.03	0.08	0.02	1.80
P ₂ O ₅	n.dtm.	n.dtm.	0.44	<0.01	0.33	0.36	0.28
MnO	n.dtm.	n.dtm.	0.13	0.01	<0.01	<0.01	0.02
Total	90.29 (PA)	99.91	100.27	100.02	100.25	100.30	100.16
Fe ³⁺	4.61	1.67	2.03	12.94	2.95	7.63	17.88
Fe ²⁺	5.61	15.59	19.73	14.42	3.56	12.84	3.96
Total Fe	10.22	17.26	21.76	27.36	6.51	20.47	21.84
Fe ³⁺ /Fe ²⁺	0.82	0.11	0.10	0.90	0.83	0.59	4.52
Analyst	RSP	JRG	JRG	PH	RSP	RSP	RSP

5. Brockman Iron Formation, Joffre Member. West side of Joffre Gorge (Joffre Creek) at lat. 22° 22'S, long. 118° 17'E. GCL No. 3489/68.

6. Marra Mamba Iron Formation. Kungarra Gorge. GCL No. 3490/68.

7. Marra Mamba Iron Formation. Kungarra Gorge. GCL No. 3491/68.

RESULTS

Analyses 2, 3, 4, 6, and 7 are concerned with the identification of sheet silicates, and their interpretation was given in Chapter 4 (pp. 124 to 125). Analysis 1 was referred to on page 114 and analysis 5 on pages 78 and 127.

TABLE 17. MISCELLANEOUS CALCULATED COMPOSITIONS

	1	2	3	4	5	6	7
	BIF plus crocidolite (8.87 wt. per cent 1 of Table 14 with 91.13 wt. per cent of 6 of Table 11)	Average chert of BIF2 in Dales Gorge Member (1, 2 and 3 of Table 12)	Theoretical BIF of Dales Gorge Member from Meso-band analyses	Average BIF of Dales Gorge Member (1, 2, 3, 4, 5 and 6 of Table 11)	Average Joffre Member (9 and 10 of Table 11)	Average Boolgeeda Iron Formation (11 and 12 of Table 11)	Analysis 2 of Table 15; re-calculated without carbonate
SiO ₂	58.05	63.06	41.09	49.37	46.08	51.41	59.36
Al ₂ O ₃	0.24	0.18	0.29	0.46	1.06	3.34	8.36
Fe ₂ O ₃	19.85	5.64	28.22	24.44	19.14	28.65	2.88
FeO	12.79	12.22	18.59	14.90	17.56	7.66	17.04
MgO	1.86	2.93	2.09	2.30	3.21	2.33
CaO	1.60	3.46	2.10	1.95	1.71	0.64
Na ₂ O	1.28	0.06	0.08	0.37	0.21	0.26	0.10
K ₂ O	0.10	0.08	0.07	0.12	2.00	1.35	7.17
H ₂ O ⁺	0.90	0.53	0.42	0.59	1.19	1.98	4.11
H ₂ O ⁻	0.10	0.06	0.06	0.10	0.09	0.52	0.98
CO ₂	2.71	11.56	6.84	5.08	7.42	1.28
FeS ₂	0.14
TiO ₂	<0.01	0.05	0.04	0.03	0.07	0.16
P ₂ O ₅	0.47	0.17	0.11	0.27	0.12	0.25
MnO	0.04	0.02	0.14	0.16
Total	100.13	100.00	100.00	100.00	100.00	100.00	100.00
Fe ³⁺	13.89	3.95	19.74	17.11	13.40	20.06
Fe ²⁺	9.94	9.50	14.45	11.59	13.68	5.95
Total Fe	23.83	13.45	34.19	28.70	27.08	26.01
Fe ³⁺ /Fe ²⁺	1.40	0.42	1.37	1.48	0.98	3.37

Structures in the iron formations

INTRODUCTION

Few of the structures with which this chapter is concerned are, as would normally be expected, the consequence of folding and faulting long after deposition. Owing to the peculiar early post-depositional history of the iron formations, which will later be argued (Chapter 9), many of their present lithological features are, to an exceptional degree, due to early post-depositional stress, rather than to any direct para-depositional control. As a consequence, it is difficult to separate those structures which are tectonic in the generally accepted sense from earlier but nonetheless stress-controlled structures. For descriptive purposes it has been convenient to describe together here all those structures which are defined by departure from the theoretical ideal of a continuous sequence of planar mesobands of even thickness, of which for the purposes of Chapter 3 the iron formations were taken to be composed.

CHERT PODDING, AND RELATED STRUCTURES

DEFINITIONS AND CLASSIFICATION

Trendall (1965a, p. 62-3) described concordant chert lenticles in the banding of the Dales Gorge Member with an elongation between 2:1 and 6:1, and separated laterally by gaps about half their length; he called this 'podding' or 'pinch-and-swell structure'. A special form of podding was later called cross-podding (Trendall, 1966a), without closer definition of the earlier term. We now recognise that discontinuous bodies of chert have a range of shapes, and that the term 'pod' may not everywhere be an apt one; but it seems best to retain it here, and to define a *chert pod* as a chert body within the iron formation which appears, in vertical cross section, to be discontinuous laterally. The constituent chert is then called *pod chert* and the phenomenon *chert podding*. The term *podded chert* implies former continuity of the separate pods; such inferences are left for discussion in later chapters, although the name is included here for completeness.

The division of chert pod types used here for descriptive purposes is based on a classification by areal shape of pods in the Dales Gorge Member; indications are given of its application outside this member.

RANDOM PODDING

Random podding is the commonest type of podding in the BIF of the Dales Gorge Member. It is so named because in areal shape the chert pods have irregular amoeboid forms (Figure 38B), with no consistent direction of elongation. Random pods are most typically present in the mixed groups of the Calamina cyclothem, but also occur in chert-magnetite groups (Figure 38A). Chert pods have the same order of thickness as non-podded chert mesobands (Table 4), and in most natural vertical exposures the displayed parts are elongate

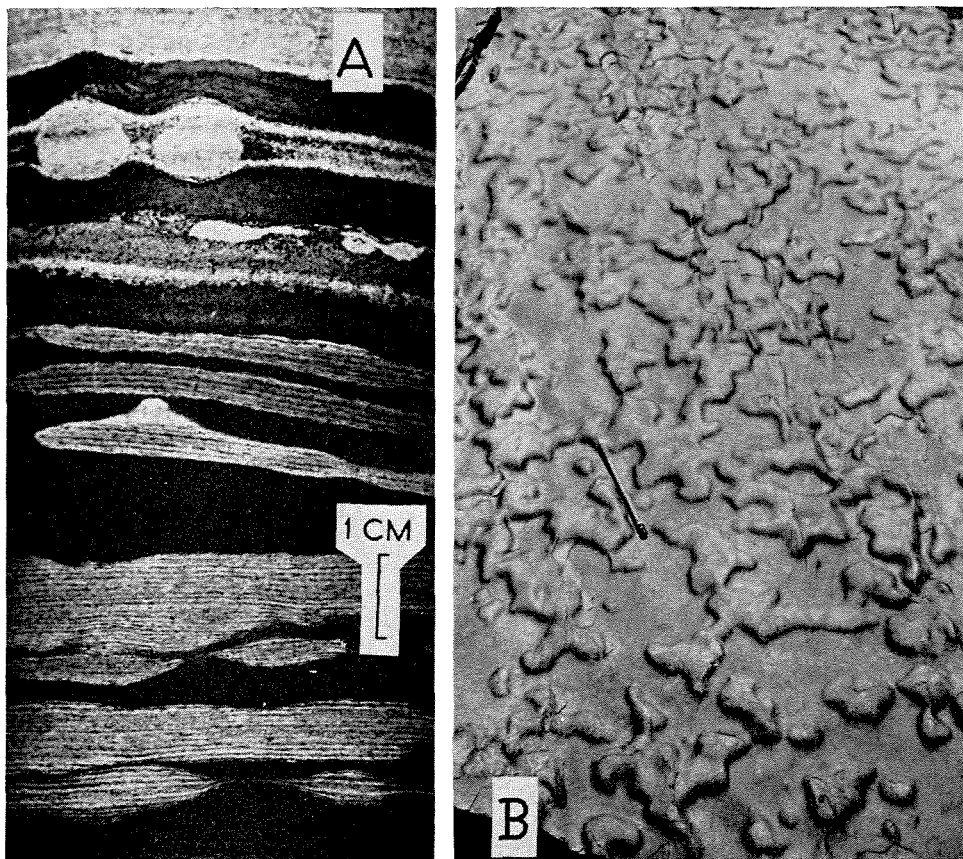


Figure 38. A. Podded cherts in a chert-magnetite group of the BIF0 macroband of the Dales Gorge Member at 33.0 to 33.3 feet of the type section core (Trendall and Blockley, 1968, Plate 28). The uppermost part of the core shows small spheroidal nodules, and appears also in Figure 13B. Note the appearance of lateral microband truncation in the two lowermost pods; in detail these would show the continuity illustrated in Figure 27.

B. Top of a fallen block of BIF in the BIF13 macroband of the Dales Gorge Member in the cliff on the eastern side of Wittenoom Gorge, at the upstream end of the large permanent pool on the eastern side of the gorge about 2 miles upstream from the old Wittenoom mine buildings. The iron formation has split along the banding just above a randomly podded chert, and the areal shape of the random podding is clearly displayed. The pen is 6 inches long.

along the banding roughly between 2:1 and 6:1. It is obvious from Figure 38B that apparently discontinuous chert pods in such exposures are often parts of an almost continuous sheet. Such sheets tend to occur in groups of 3 or 4 enclosed in chert-matrix as representatives of the mixed group of the Calamina cyclothem. Where several such sheets are closely superimposed the pods in each tend to be compensated by gaps in the sheets above and below, and vice versa; this is in interesting contrast with cross-podding. The amoeboid forms of Figure 38B appear to develop where the area of pods is about equal to the area of voids. Wherever the pod area greatly exceeds the void area, or vice versa, these amoeboid shapes are not developed, and in their stead appears either a pattern of perfectly circular voids in a chert, or discontinuous and perfectly circular pods; that is, the less abundant of the two components is restricted within circles.

Petrographically, pods resemble non-podded cherts; the termination of microbands in microbanded chert pods was illustrated in Figures 27 and 28. More frequently than in non-podded cherts there is a tendency for the microbanding to be poorly defined, and a characteristic development of concentric structure is described further below. As may be expected from Figure 38B, vertical sections which pass across narrow necks display all gradations between complete discontinuity and perfect continuity. Where there is merely a thinning of the chert mesoband the apparently truncated marginal microbands pass into the adjacent chert-matrix in a way exactly like those at pod margins; this is illustrated in Figure 38A.

Outside the Dales Gorge Member random podding is present in the Joffre Member, the Marra Mamba Iron Formation, and in the BIF parts of the Mount Sylvia Formation. It has not been seen in the Weeli Wolli Formation, but cannot be taken to be absent, because of poor exposure. The general lack of clear mesobanding in the Boolgeeda Iron Formation precludes its existence there.

CROSS-PODDING AND RELATED TYPES

This term was introduced by Trendall (1966a) for groups of chert pods, resembling cross-bedding in their arrangement, at Dales Gorge. Cross-podding has since proved to be a common feature of both the Dales Gorge and Joffre Members of the Brockman Iron Formation and of the Weeli Wolli Formation.

In suitable vertical cross sections the chert pods of cross-podding closely resemble random pods in their proportions, petrography, and in their marginal microband relationship to the enclosing chert-matrix. In the Dales Gorge Member cross-pods are confined to the mixed groups of the Calamina cyclothem, where their development in any area is dependent on the local strength of the northeast or duplicate structures (see below, in this chapter). The diagnostic differences are: firstly, that in plan cross-pods are linear, and normally elongate in a northeasterly direction; secondly, that cross-pods have an oblique relationship with the banding of the adjacent iron formation, and thus of the enclosing chert matrix; and thirdly, that cross-pods often occur in superimposed piles or groups of some kind. These points are further expanded and illustrated below.

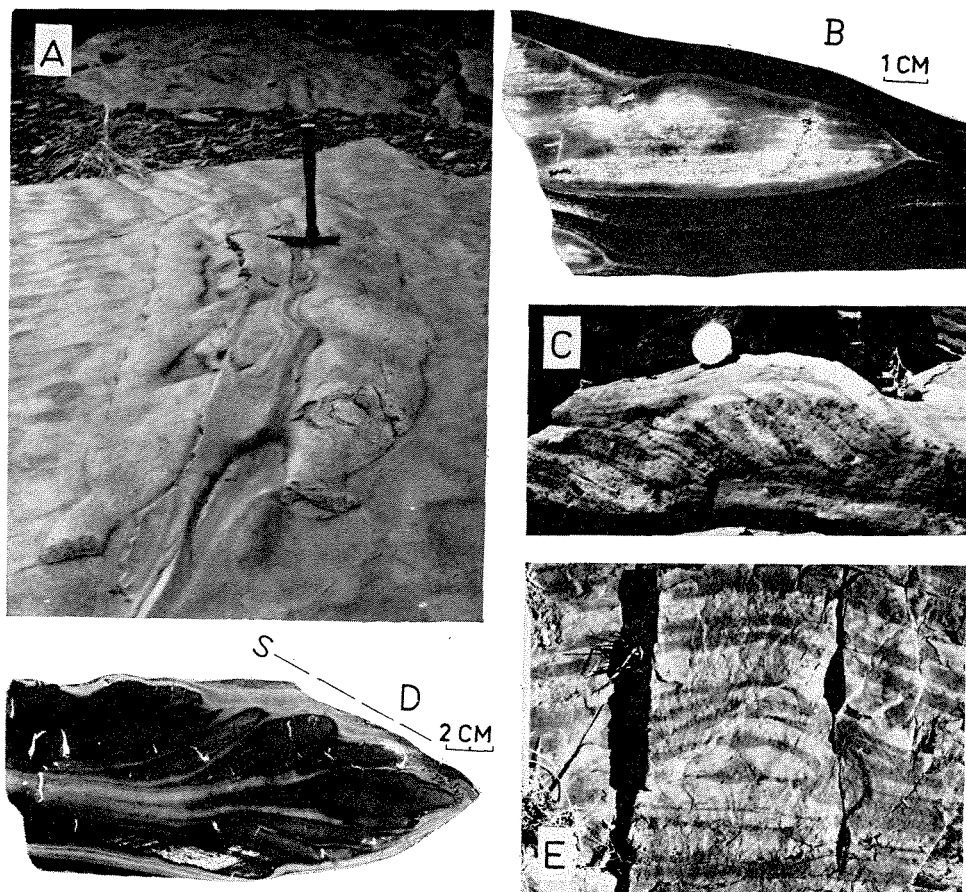


Figure 39. A. The photograph shows a stripped banding surface in the Joffre Member of the Brockman Iron Formation at the north (downstream) end of the pool at the foot of Joffre Falls (lat. $22^{\circ} 24'S$; long. $118^{\circ} 16'E$). A complex cross-podding ridge curves sinuously to the southwest away from the observer, flanked on each side by bolster-like cross-pods, on the more westerly of which the hammer rests. Internally, this cross-pod would be obliquely microbanded, like that illustrated in B.

B. Looking on a bearing of 35° at a cut and smoothed vertical surface across part of a cross-pod from BIF2 of the Dales Gorge Member at the old mine in Yampire Gorge, at a stratigraphic level equivalent to about 75 feet on the type section (Figure 5). Note the westerly relative dip of the microbanding within the chert, so that the microbanding is concordant with the lower surface but has an apparently discordant relationship with the upper contact with the enclosing chert-matrix.

C. Well-developed cross-podding in the Marra Mamba Iron Formation at the northernmost crocidolite occurrence at Kungarra Gorge (Plate 12). The photograph was taken looking in a southeasterly direction, but the direction of the whole structure curves sharply towards the northeast as it is followed laterally, so that this structure has an opposite sense to that of B. The lens cap has a diameter of 45 mm.

The example in Figure 39A, from the Joffre Member, shows the characteristic northeasterly elongation of cross-pods. The sinuous trend is particularly characteristic of cross-pods in this member; in some places wavy pods anastomose to give an elongate reticulate pattern. Larger cross-sectional dimensions of the pods (up to about 18 inches wide and 9 inches thick) are also typical of the Joffre Member in comparison with those of the Dales Gorge Member. In the outstanding exposures of the Joffre Member at Joffre Falls cross-pods are almost entirely confined to white chert groups of the Knox cyclothem, and are often superimposed in successive cyclothem in a remarkable way. The terminating planes of the structures (e.g. the surface 'S' in Figure 39D and the sloping surface to the left of the hammer in Figure 39A) continue obliquely across the mesobanding, and are associated with a similar cross-pod in each cyclothem. Thus each successive cyclothem upwards has its cross-pod offset to the northwest, and the common terminating plane of all the structures appears as a narrow vein of chert-matrix dipping at about 30° to the southeast, obliquely across the nearly horizontal mesobanding.

The oblique relationship with its banded matrix, which gives cross-podding its name, is shown by Figure 39B; it is apparent also in Figure 27A, which is from the termination of a cross-pod rather than a random pod. The obliquity may be defined, as in this example, solely by the microbanding within the pod; it is just as common for the obliquity to be defined by the arrangement of the cross-pods in a group, as in the examples originally figured by Trendall (1966a, Figure 26 and Plate 39) from the Dales Gorge Member. A fine example of this type appears in Figure 39C. An unusual variety of cross-podding, in which the similarly elongate pods have a radiating, palmate arrangement in vertical cross section instead of a simple oblique structure, is illustrated in Figure 39D; this type has been seen only in the Joffre Member. A further variety, from the Yandicoogina Shale Member, in which there is virtual symmetry about a central vertical plane, appears in Figure 39E. Figure 39C, D, and E all show well the tendency for superimposition of cross-pods, in contrast with the compensatory offsetting of random pods.

D. Looking along a bearing of 20° at a cut and smoothed vertical surface across a type of cross-podding restricted to the Joffre Member of the Brockman Iron Formation. It consists of a group of thin white chert mesobands which expand and terminate with a palmate arrangement. Farther along the banding (to the right, or east, in this case) the same chert group usually reappears with a similar structure, but reversed as a mirror-image. The example comes from close to the foot of Joffre Falls. The direction marked S is referred to in the text. In structures of this type it is the dominant chert dip, in this case the westerly dip of the upper cherts, which conforms with the regional sense of accompanying cross-pods of normal type.

E. Looking southwest down the dip of a group of chert mesobands in the Yandicoogina Shale Member of the Brockman Iron Formation at Woongarra Gorge (lat. 22° 52' 30"S, long. 117° 07' 30"E). This unusually symmetrical irregularity is common in this member at this locality, and it appears to be a structure of the same kind as cross-podding, but lacking any preferred lateral sense. The stratigraphic thickness illustrated is 14 inches.

OTHER TYPES OF PODDING

Podding is a common and characteristic feature of the Marra Mamba Iron Formation. Unlike the usual thin biconvex lenses of the Dales Gorge Member the chert pods of the Marra Mamba Iron Formation are frequently rounded in shape with diameters often of 1 to 3 inches and occasionally up to a foot. Such pods resemble, in parts of the formation, strings of misshapen potatoes; these readily weather out from their enclosing chert-matrix, and a surface rubble of rounded chert pods up to the size and proportions of a curling stone is a useful indicator of the weathered outcrop of the formation. In the rare fresh exposures (e.g. Kungarra Gorge, lat. $22^{\circ} 47'S$, long. $116^{\circ} 58'E$; the Hardey River gorge at lat. $22^{\circ} 43'S$, long. $117^{\circ} 31'E$) it is clear that even in nodules whose width is less than their vertical thickness the fine laminations of the chert-matrix still pass evenly into the chert. These pods of the Marra Mamba Iron Formation are in different places consistently elongate both along and across the axial direction of regional folding, and locally at Kungarra Gorge (stratigraphically just above the main deposit on Plate 12) the pods have a spectacularly elongate reticulate pattern in an intermediate direction (70°). But unlike the cross-pods of the Dales Gorge Member there appear to be no associated characters typical of pods running in the different directions, and the classification into random pods and cross-pods is therefore not here extended to those of the Marra Mamba Iron Formation.

Chert pods elongate along the axial direction of the regional folding are also present in the Dales Gorge Member; locally in the chert-siderite part of the S macrobands. But elsewhere these cherts are randomly podded, and those elongate along the fold axial direction do not at present justify classification as a distinct chert pod type. Other discontinuous chert bodies, such as the discoid forms noted under the heading Pseudofossils below, are also forms of chert pods which do not presently fall clearly into a complete system of classification; more work is required before a more satisfactory basis for division of the various pod types grouped here as 'other types', and which are neither random pods nor cross-pods, can be suggested.

PETROGRAPHY OF PODS: CONCENTRIC AND SEPTARIAN STRUCTURE

It was noted above that pod chert is closely similar to that of chert mesobands in petrography. Pod chert may be either non-microbanded, or microbanded, and in the latter case may possess almost any of the features of microbanding already described. However, chert pods have two petrographic features not found elsewhere. The first of these is clearly illustrated in Figure 40A and B. Figure 40A illustrates a microbanded random pod with three very distinct concentric textural zones, through all of which the microbanding continues. The very faintly microbanded random pod which is shown in Figure 40B show little trace of concentric zoning in ordinary light, but with crossed nicols, as in the Figure, four zones defined by varying grain-size of the chert are apparent.

At the outer edge of the third zone, counted inwards, gradually expanding 'cracks', defined by much more coarsely granular quartz, extend inwards in a zigzag manner, and coalesce to enclose sharply angular 'fragments' of fine chert in the core. This septarian structure is most markedly developed in chert pods of the Marra Mamba Iron Formation, where some spheroidal forms have stellate systems of 'cracks' occupied either by coarsely crystalline calcite or quartz.

SMALL SPHEROIDAL NODULES

Structures in the BIF macrobands of the Dales Gorge Member, with many features in common with the concentrically zoned chert pods just described, and yet sufficiently different not to be appropriately called chert pods, are here called small spheroidal nodules. These nodules are mostly between 0.5 and 2.0 cm in diameter, and consist either of structureless chert, concentrically zoned chert and carbonate, or of carbonate only. In nodules whose outer parts consist of chert this is commonly stained pink by hematite dust. Their shape is typically spheroidal (Figure 41A; Figure 13A), but they are also commonly either lenticular, elongate at right angles to the banding, or bowl-shaped, with an upward-facing depression (Figure 13A); these latter give lunate concave-upward cross sections. Spheroidal nodules occur typically in chert-matrix of the mixed group of the Calamina cyclothem, or in the structureless mesobands classified as 'miscellaneous' on p. 49, in the same position in the cyclothem. But they may occur within micro-banded cherts of the mixed groups (Figure 41B), or in morphologically transitional positions where a ghost-like mesoband in chert-matrix of the mixed groups

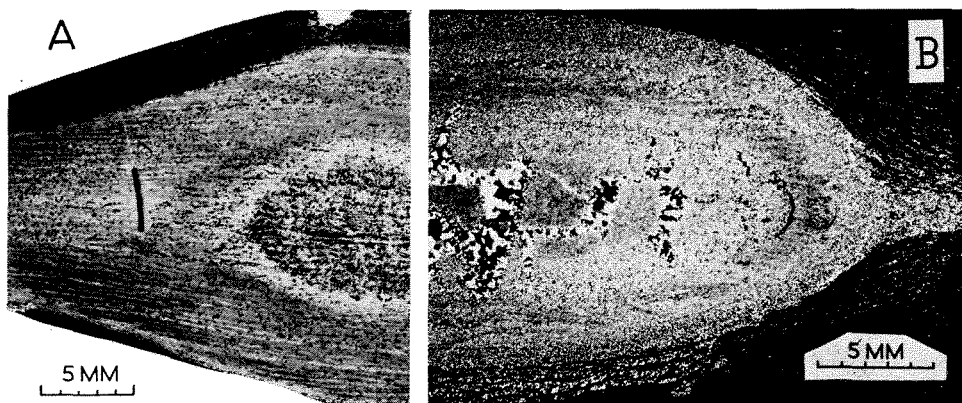


Figure 40. Concentric structures in chert pods of the Dales Gorge Member.

A. Pod from the BIF4 macroband at 525 feet 11 inches in Hole 51 at Wittenoom Gorge, equivalent to about 124 feet on the type section. The three differently coloured zones, through all of which the microbanding persists, are defined by slight variations in jaspersy hematite, carbonate and riebeckite contents. The discordant black line is magnetite in a vertical vein (see later in this chapter), which is sheathed by finely fibrous riebeckite (see 'Notes on paragenetic evidence', in Chapter 4).

B. Pod from the BIF4 macroband at 532 feet 11 inches in Hole 51 at Wittenoom Gorge, equivalent to about 117 feet on the type section. The concentric zones are here defined largely by variations in quartz texture, as described in the text.

is present (Figure 38A). In any situation where nodules occur in a laminated (chert-matrix) or microbanded (chert) groundmass these forms of layering expand to pass smoothly above and below the nodules, but in the equatorial parts of the nodules they are discordantly truncated against the nodule rim (Figure 41A). In field exposures of BIF macrobands of the Dales Gorge Member where the Calamina cyclothem is present it is often made more conspicuous by the striking appearance of bedding surfaces where spheroidal nodules have had their concentric structure etched out by weathering. (Figure 41C).

MACULES

This term was introduced by Trendall (1966a, p. 76) and defined as "an abrupt local thickening of a limited stratigraphic thickness of b.i.f., usually involving a restricted upward and downward bulge of a thick flat-modified chert mesoband into the adjacent levels". With subsequent nomenclatural changes

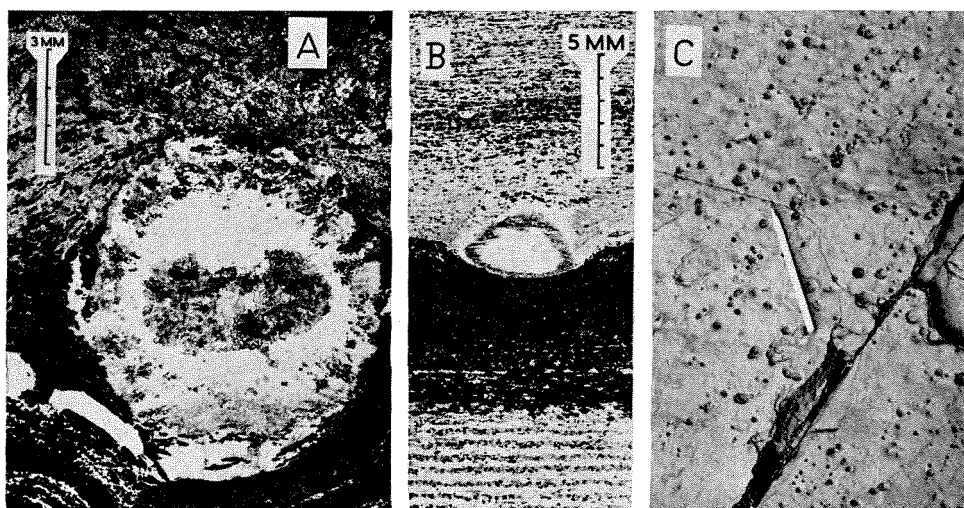


Figure 41. Small spheroidal nodules in the Dales Gorge Member.

A. Photomicrograph of a typical nodule in the mixed group of the well-developed Calamina cyclothem of BIF12 at 344 feet 7 inches in Hole 51, equivalent to 297.2 feet on the type section (see also Figure 13A). The ankerite rim and core, separated by cherty quartz, are typical. Note on the left, the sharp truncation, against the nodule, of the fine lamination of the enclosing chert-matrix.

B. Small nodule at the base of a chert mesoband of the mixed group of a weakly developed Calamina cyclothem of BIF2 at 645 feet 4 inches in Hole 40 at Wittenoom Gorge, equivalent to about 80.15 feet on the type section (Figure 5). The clearly microbanded chert at the bottom of the photograph is that illustrated in Figures 21A and C. There is no carbonate in this nodule, which is defined, apart from its shape, by a marginal rim rich in jaspery hematite, in a way similar to the chert pod illustrated in Figure 40A.

C. The typical exposed surface appearance of nodules like that of A, on a banding surface in Dales Gorge (see Trendall, 1966a) just above the second maculate band, in BIF1, equivalent to about 51.7 feet on the type section. The pen is 6 inches long, and points on a bearing of 20°.

adopted for this bulletin, macules may be redefined as nodule-like thickenings of groups of mesobands in the BIF macrobands of the Dales Gorge Member, usually the chert-magnetite group of the Calamina cyclothem.

The splendidly exposed macules in BIF1 at Dales Gorge were fully described and illustrated, with others, by Trendall in the reference above; only a brief summary is therefore given here, together with photographs of typical examples (Figure 42). Macules have a central core (either cylindroidal, tubular, or bowl-shaped) composed mainly of coarsely crystalline quartz; the core is always circular in plan, and usually about 6 inches both in diameter and depth (thickness). It has very coarse microbanding, which may only be detectable after sectional sawing and smoothing. The outer edges of the core are more or less sharply and discordantly defined; immediately outside them the microbanding of the enclosing cherts is less than that of the core, but still above the normal thickness, into which it grades smoothly, with the mesoband thickness, about one core diameter farther outwards. Macules tend to be restricted to specific levels (or *maculate bands*); in BIF1 at Dales Gorge there are four main maculate bands near the base of the macroband, spaced evenly at intervals of about 18 inches. In areal distribution, within each such maculate band, the macules are evenly and randomly distributed, without apparent relation to any other structure.

Several morphological similarities with both chert pods and small spheroidal nodules are apparent from this summary description, and justify their grouping

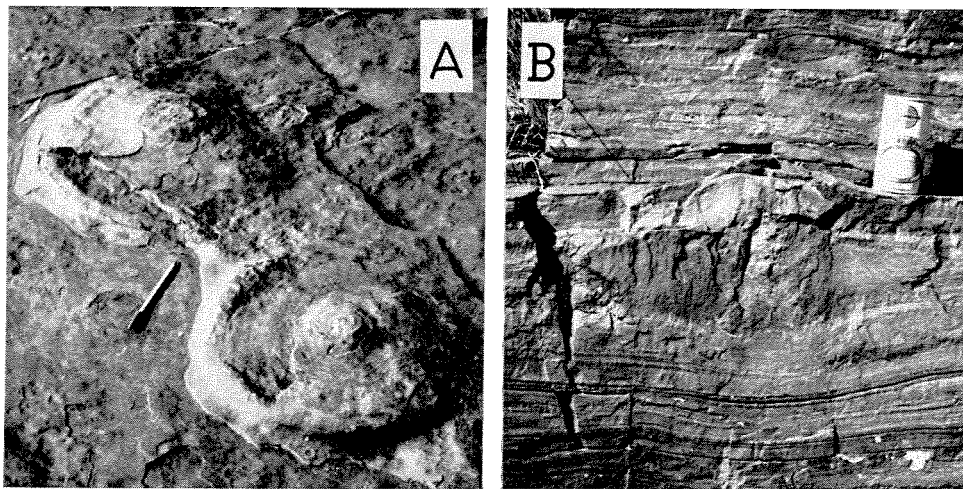


Figure 42. The field appearance of macules in the Dales Gorge Member.

A. Upper surface of discoid macules in MB2 at 190 feet in Dales Gorge (see Trendall, 1966a, for explanation of location). MB2, the second maculate band, is at about 51.2 to 51.6 feet on the type section. The macules illustrated consist mainly of riebeckite.

B. Vertical section through a macule in MB1 at 1,285 feet on the north side of Dales Gorge. MB1, the first maculate band, is at about 48.5 to 49.1 feet on the type section. The dark colour of the inner part of the macule is due to riebeckite. See also Figure 53.

under this heading. Such features in common as the frequent upward concavity of both macule cores and spheroidal nodules is a striking point. However, there seems to be a real difference between these structures, and it seems unlikely that they are simply the opposite size extremes of a continuously gradational range of intermediate structures.

PSEUDOFOSILS

Edgell (1964) described, from the Brockman Iron Formation, a range of internally laminated bodies which he regarded as silicified algal (stromatolitic) growths. With more extensive knowledge of fresh core it is now certain that there is no question of near-surface silicification being responsible for the cherty composition of these bodies (Edgell, 1964, p. 242), although much of Edgell's material is undoubtedly chemically modified by surface weathering. Edgell also described medusoid impressions and concentrically ridged structures, one of which was later figured by Halligan and Daniels (1964, Plate 24). During the course of our studies a reassessment of Edgell's material, in the light of further collection, was carried out from a palaeontological viewpoint. We concur with the conclusions of this work (M. Walter, University of Adelaide, unpublished manuscript, 1968) that none of the forms described by Edgell from the Brockman Iron Formation are of organic origin. We regard both *Collenia brockmani* Edgell and the examples of *Collenia kona* Twenhofel described by Edgell, which bear little resemblance to the paratype, as microbanded chert pods. Walter figures a number of structures related to the chert pods and other structures already described above. They are representative of a great variety of minor structures defined by modifications and irregularities of the mesobanding, which are not further described here.

NORTHEAST AND DUPLICATE STRUCTURES: REGIONAL ORIENTATION

In the initial description of cross-podding (Trendall, 1966a, p. 79) it was made clear that cross-podding at Dales Gorge was only one of a number of closely related structures, grouped as *duplicate structures* and characterised by precise and regular repetition at 5-foot intervals measured in the banding at right angles to their northeasterly trend (Figure 53); they included duplicate corrugations, riebeckite swells, associated minor structures, and the cross-podding ridges and troughs caused on exposed bedding surface by underlying, or stripped, cross-pods respectively.

Detailed descriptions of all these structures are not repeated in this bulletin. In summary, the duplicate corrugations at Dales Gorge are open corrugations of all bedding surfaces (mesoband boundaries) in the BIF0 and BIF1 macro-band, with a wavelength of 60 inches and an amplitude of 1 to 2 inches. The crestal planes are in places vertical, but more often they dip to the southeast;

the fold forms thus defined by the asymmetrically superimposed corrugations then control the position, within each fold, of cross-podding and other structures, and cause their regular duplication in sympathy with the corrugations. All the duplicate structures have a northeasterly trend which is locally sinuous; bifurcation of corrugations takes place rarely.

There are at least 800 regular lateral repetitions of the Dales Gorge duplicate structures, across 4,000 feet, and their full extent is unknown, through limitation of exposure. We have found no other locality in the Hamersley Range area where duplicate structures are so spectacularly displayed. However, component structures such as cross-podding are widespread. There is in many places some degree of regularity in the lateral repetition of cross-podded structures, but nowhere does it approach the perfection of Dales Gorge, and the name duplicate structures thus seems inappropriate for use elsewhere. We therefore propose the general term *northeast structure* to cover all those structures which contribute to the duplicate structure at Dales Gorge, and which are also present away from Dales Gorge, with the same general trend but without duplication. Duplicate structure is thus a specially symmetrical variant of northeast structure.

Cross-podding is the only northeast structure which can be observed over a wide area, since it is sufficiently characteristic for recognition in small and weathered exposures. It also has two measurable directions: its elongation direction in plan, and the dip of its constituent pods in vertical cross section at right angles to the elongation. This second direction may be more conveniently recorded as the sense of the dip in a direction normal to the elongation, to eliminate the effects of subsequent folding. Both directions are shown on Plate 3, from which it is apparent that the name northeast structure is appropriate, since this trend persists regionally without apparent relationship either to folding or to the stratigraphic thickness of the Dales Gorge Member.

All cross-podding directions shown on Plate 3 represent a large number of observations in the immediate vicinity. At an early stage of the recording of these observations it seemed that the pods dipped northwesterly throughout the quadrangle between Mount Frederick, Mount Bruce, Mount Lockyer, and Wittenoom, as opposed to a southeasterly dip further west along the range, but more extensive work destroyed this apparent simplicity and led to the local discovery of opposite dip senses within a single cliff exposure. However, it does appear that the common situation is of broad areas of consistent dip sense; observations are not sufficiently close to delineate the shapes of these areas.

No distinction is made in Plate 3 between cross-pod observations in the Brockman Iron Formation or the Weeli Wolli Formation since, so far as our observations go, the pod slopes are concordant between different stratigraphic levels in a restricted area.

There are few observations in the southern part of the area of Plate 3, since it is increasingly difficult to see and interpret cross-pods with confidence in the more strongly folded iron formation.

Although regional rippling and cross-podding are not normally well developed together in one exposure, examples have been seen in the Dales Gorge Member in the upper part of Wittenoom Gorge. In all of these it is the regional rippling which is affected by the presence of the cross-podding. In some the regional rippling dies away over cross-podding ridges, in others the wavelength changes abruptly over the ridges to less than half that on the adjacent bedding surfaces, while one example of bodily involvement of a cross-pod in a regional ripple was found.

REGIONAL RIPPLING

Throughout the northern part of the Hamersley Range area, where the regional folding is broad and open, a common local feature of bedding surfaces (mesoband boundaries) in the Dales Gorge Member is the presence of crenulations resembling asymmetric ripple marks. Their trend is parallel to the axial direction of the regional folds, and the name *regional rippling* is here proposed for them.

The general appearance and asymmetry of regional ripples of a common order of size are shown in Figure 43B and C; it is clear from their cross-sectional form that they are penetrative puckers of the mesobanding with sloping axial planes, and not para-depositional ripple marks. Regional ripples vary very widely in size from very fine surface striae, through those illustrated by MacLeod (1966, Figure 17) to what are effectively minor folds with amplitudes of about a foot and wavelengths of several feet. In the one bedding surface two or more distinct scales of rippling may co-exist.

Regional ripples often persist for several feet above and below their plane of strongest development, but each individual ripple tends to die out vertically (Figure 43A), and may or may not be replaced by others. Regional rippling is patchy in both vertical and lateral distribution. For example, it is scarcely detectable in the fine exposures of BIF0 and BIF1 at Dales Gorge but is strongly developed on these levels at Wittenoom. At Junction Gorge it is well developed in BIF16, but is not usually conspicuous therein in other areas. Regional rippling is not completely confined to the Dales Gorge Member, but is not easy to detect in other iron formations.

In vertical cross section across their axial direction regional ripples often have chert pods just below or above which fit into their concavities. It seems likely that the form of the rippling in such situations was controlled in its initial development by the prior existence of an irregularity in the mesoband structure.

The elongation and direction of asymmetry of regional rippling are shown on Plate 3; the indicated directions of steepest slope are opposite to the directions of axial plane dip. Indications of asymmetry represent the assessment of many observations in the vicinity since, not only are other ripple-like structures locally present with regional ripples (see further below in this chapter), but in some areas ripples are almost symmetrical, and the judgment of sense must be made from

the scattered asymmetrical ripples among them. Plate 3 shows that, along the main Hamersley Range Syncline, the regional rippling follows the axial fold direction, with the steep ripple faces consistently dipping south, both on the southward-dipping north limb and on the northward-dipping south limb of the syncline; the ripples thus maintain a constant orientation across the syncline. This relationship also holds true over smaller folds within the syncline. In the thickest part of the Dales Gorge Member, around Mount Brockman, and farther south, the regional rippling is largely symmetrical, while in most of the remaining parts

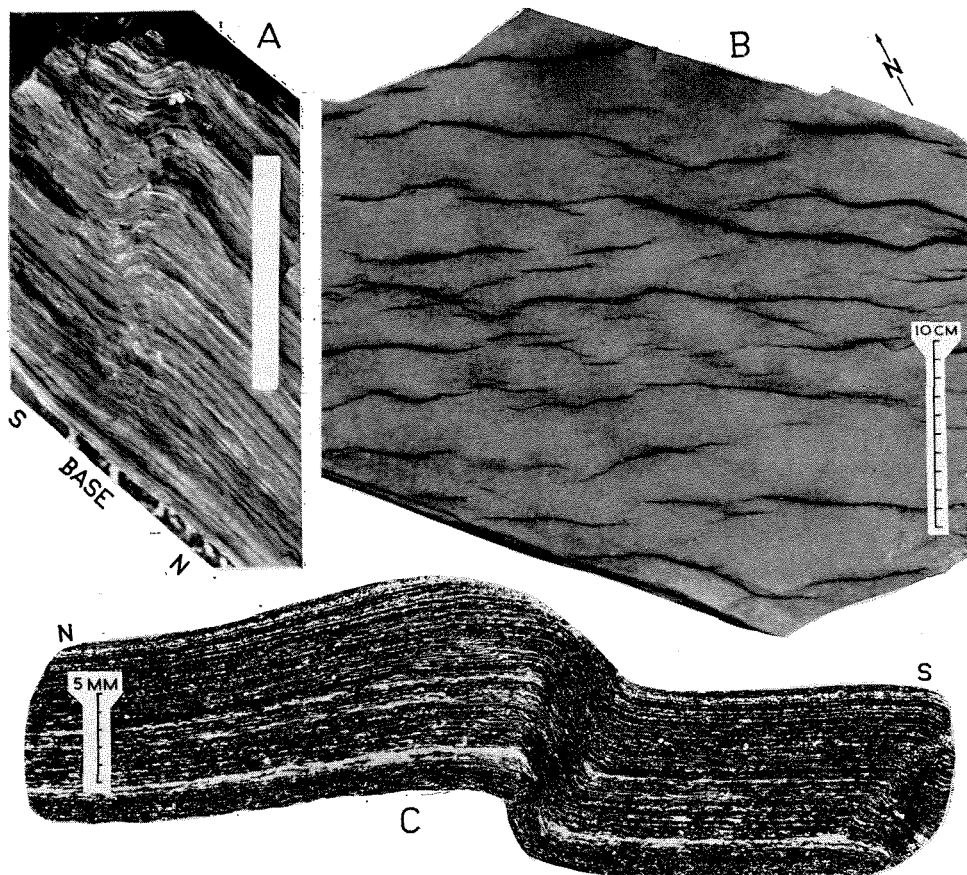


Figure 43. Regional rippling in the Dales Gorge Member, illustrated by examples from the BIF13 macroband in Wittenoom Gorge at the head of the large permanent pool on the western side of the gorge about $2\frac{1}{2}$ miles upstream from the old Wittenoom mine buildings.

A. Looking westerly, showing vertical variation in intensity of a single large ripple. The photograph is in fact of a block fallen from a known position in the cliff; the banding here is effectively flat. The scale is 25 cm long.

B. Looking vertically down (north point marked) at ripples of the common order of size, showing the resemblance to ripple mark.

C. Thin-section, looking easterly, cut from chert-matrix involved in the rippling illustrated in B.

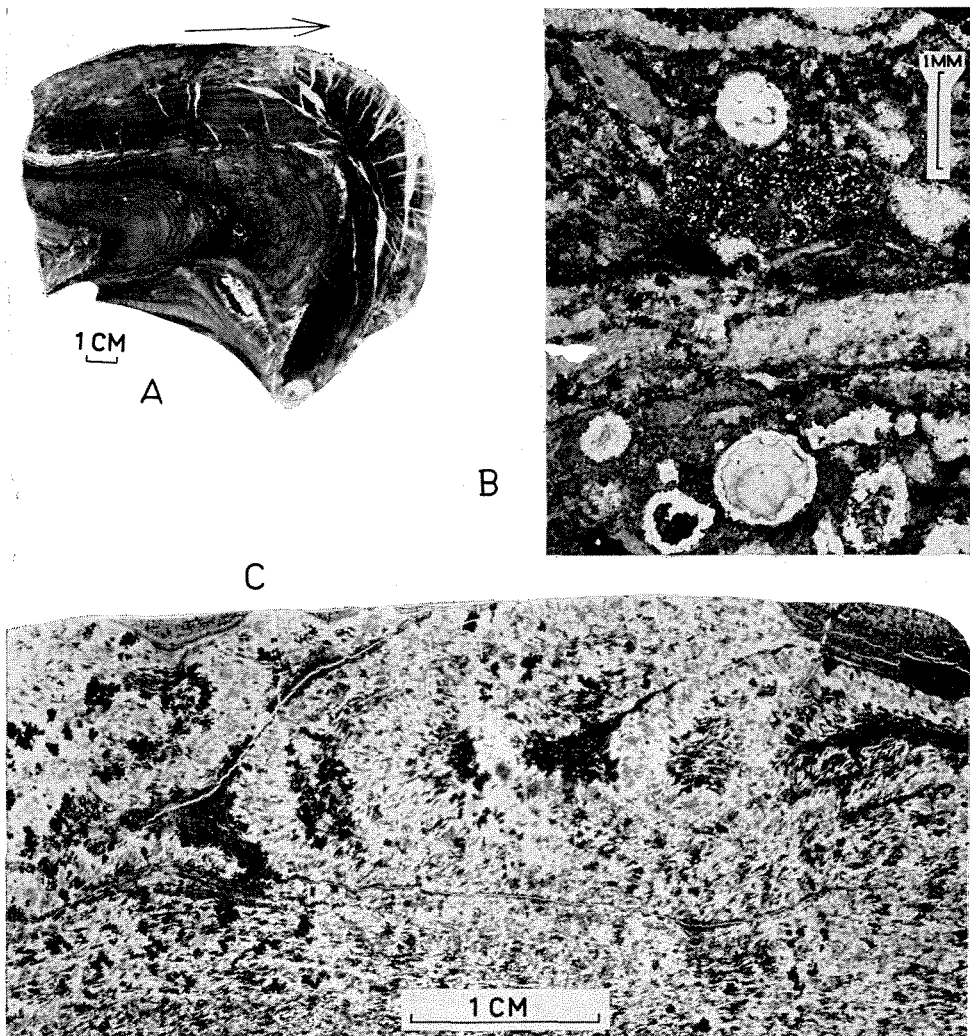


Figure 44. Slumping and related structures in the Weeli Wolli Formation and in the Dales Gorge Member.

A. Looking west-southwest at a cut and smoothed surface of contemporaneously slumped BIF of the Weeli Wolli Formation from a cliff on the southeast bank of Marillana Creek about $1\frac{1}{2}$ miles northwest of Cajubut Bore (lat. $22^{\circ} 47'S$, long. $119^{\circ} 08'E$). The arrow shows the presumed direction of collapse, which is consistent with that of regional rippling. The chert mesobands appear to have been in a critical mechanical state, since there is local fracture (at the bottom of the sample and in the quartz-filled tension gashes around the crest) although most of the deformation is plastic.

B. Thin-section of the breccia in the S4 macroband of the Dales Gorge Member (see 'Macrobands S1-16', Chapter 3), which probably originated by early post-depositional collapse. The spheroidal bodies, composed of concentric arrangements of ankerite, quartz, feldspar and stilpnomelane, often spherulitic, have been suggested (LaBerge, 1966a) to be

of the outcrop area folding is too intense to distinguish regional ripples from minor puckering of the bedding surfaces, which is clearly related, in intensity and structural sense, to the major fold structure of the immediate areas.

SLUMPING AND RELATED COLLAPSE STRUCTURES

Various structures which appear to be due to disruption or distortion during or before compaction are included here. They are widely distributed over the outcrop area but, with the exception of the breccia in the S4 macroband of the Dales Gorge Member, are nowhere conspicuous or abundant. That they are not of tectonic origin, in the accepted sense, is suggested by their apparent lack of correlation with other signs of deformation, by their restriction in vertical and lateral extent, by their general conformity with the supposed bottom slope of the Hamersley Basin (Chapter 10), and by a commonsense assessment of their shape. They are, in their extreme expressions, divisible into 'plastic' and 'brittle' forms, but many are intergradational.

Plastic deformation, or slumping, of mesobanding in iron formation has been noted in the Weeli Wolli Formation at Marillana Creek, and in the Dales Gorge Member at Fortress Gorge, Wittenoom Gorge, and Point James. An example of this type of deformation at Marillana Creek appears in Figure 44A; it clearly took place when the physical state of the chert made it susceptible to brittle fracture if the normal rate of deformation was fractionally exceeded. This slumping is, at the location of the figured example, restricted within a vertical interval of about 2 feet. Similar structures occur in the BIF12 macroband of the Dales Gorge Member on the foreshore at Point James and in BIF3 and BIF14 at Fortress Gorge. In all these instances the mesobanding is more thoroughly broken up, but the separate pieces are each plastically deformed and arranged in positions roughly indicating their original stratigraphic order. The disruption has a comparably restricted vertical stratigraphic range. Similar structures are present in material from the spoil heap of the Colonial mine at Wittenoom Gorge; they must come from either BIF0, 1 or 2 of the Dales Gorge Member. A rather different but related structure was noted in a restricted exposure of BIF1 at Fortress Gorge. A tight recumbent anticline with an amplitude of some 25 feet and a width (perpendicular to the axial plane) of about 6 feet has its axial plane dipping about 5° to the west-southwest, with the axis horizontal and at right angles to this dip direction. The fold therefore faces

of volcanic origin. They seem equally likely to be infilled gas bubbles entrapped during collapse. The slide comes from 535 feet in Hole 51 at Wittenoom Gorge, equivalent to about 111 feet on the type section.

C. Plastic deformation of microbands within a chert mesoband of the BIF7 macroband of the Dales Gorge Member at 457 feet in Hole 51 at Wittenoom Gorge, equivalent to about 189.5 feet on the type section. Note the local development of an axial-plane structure in the deformed microbands.

west-southwest, and it is cut off along its lower boundary by a shaly plane of sliding probably representing S1. The structure thus resembles closely a miniature nappe. Elsewhere in the immediate area the equivalent stratigraphic section shows no anomaly.

Wherever the slump direction of the structures so far described can be determined it is consistent with the bottom slopes postulated in Chapter 10 (p. 280).

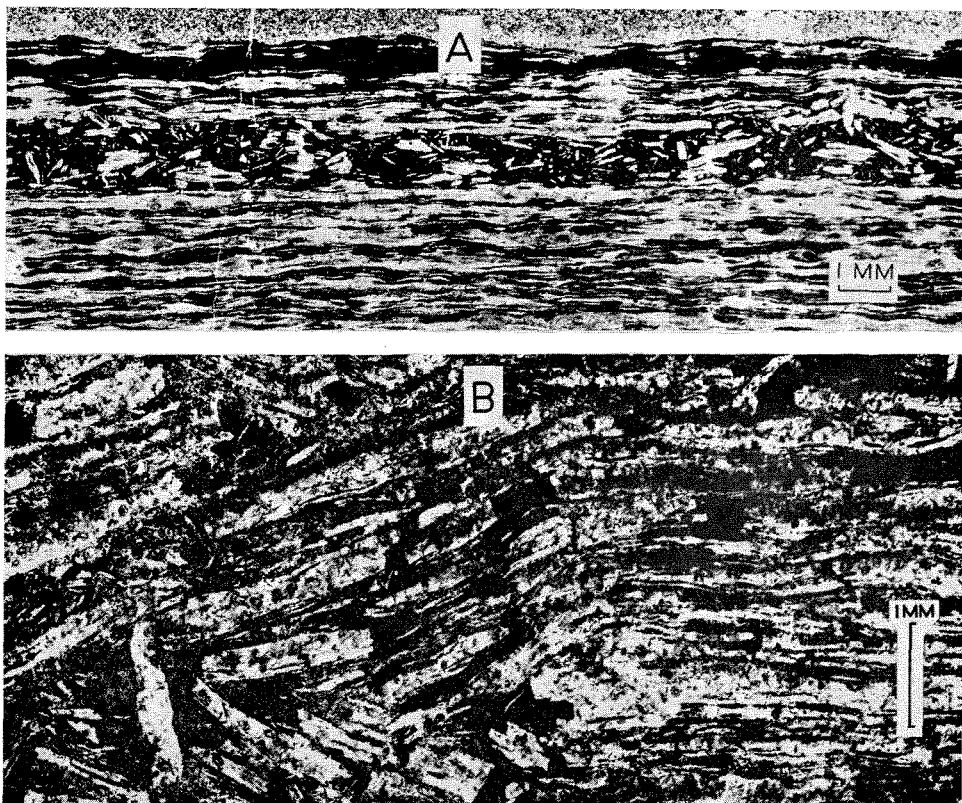


Figure 45. Stratigraphically restricted brecciation of microbanding within chert mesobands of the Dales Gorge Member.

A. Deformation restricted to 3 microbands in a chert of the chert-magnetite group of the Calamina cyclothem in the BIF0 macroband at Dales Gorge, at about 36.85 feet on the type section. This photograph is a larger scale one of part of the thin-section shown in Figure 15D.

B. Larger scale photograph of a similar structure, but showing slight stratigraphic transgression, in a microbanded chert mesoband in BIF2 at 510 feet 11 inches in Hole 27 at Wittenoom Gorge, equivalent to 78.6 feet on the type section (and represented there by massive riebeckite).

The breccia within the S4 macroband of the Dales Gorge Member, described in Chapter 3 (p. 64), seems closely comparable with slump structures in the BIF macrobands. Its bent and vaguely defined fragments (Figure 44B) broadly resemble material from the adjacent laminated shale. A probably related structure from the S11 macroband of the Dales Gorge Member appears in Figure 31B. Slump structures within the Mount McRae Shale are present at Calamina Gorge and Dales Gorge, at least. Like those of the iron formations they are restricted within stratigraphic intervals of only a few feet.

Plastic deformation of microbanding within a chert mesoband that has still retained its continuity is known from one borehole core only (Figure 44C). Apart from the scale difference its similarity to the larger folding of Figure 44A is evident. Brittle disruption of chert on a small scale is probably a fairly widespread phenomenon, but is not easily detectable in the field. It mainly affects only a few microbands within a thick chert mesoband of the chert-magnetite group of the Calamina cyclothem, and produces a thin and broadly concordant layer of elongate and sharply angular microband fragments in a dark hematitic matrix (Figure 45A). Locally it may be discordant (Figure 45B) but is closely restricted both vertically and laterally. This restriction, and the evident delicacy of the process, jointly suggest that it should be grouped here with the other early modifications of the stratification.

MINOR FOLDS WITH FIBROUS MINERALS IN THE NORTH

During mapping of the asymmetry of regional rippling over the main Hamersley syncline it was noted that occasional 'ripples' are present on the southward-dipping north synclinal limb, oriented in a structural sense *opposed* to that of the great majority; their steeper, shorter limbs slope northwards, with a southerly dipping axial plane. Vertically sawn north-south faces prepared from such 'ripples' show that they differ structurally from true regional rippling in that regional ripples are asymmetric plastic puckers, while the opposed ripples are associated with brittle fracture and splitting of the magnetite mesobands, with growth of fibrous minerals in the steeper, thickened, limbs of the puckers. A typical example of this type of fold appears in Figure 46. It was later found that these small folds, whose regional axial orientation, size range, and general field appearance closely resemble regional ripples, are also present on the northward-dipping southern limb of the main Hamersley Syncline, but there have the *same* asymmetry as the regional rippling; their axial planes dip north.

Thus in the north and south limbs of the main Hamersley Syncline the axial planes of the minor folds with fibrous minerals dip in opposite directions, and in both cases inwards towards the main axial plane; they are, in contrast with regional ripples, consistent with the stress to be expected in the two limbs of the

syncline. This concordant relationship with the main regional folding holds south of the Hamersley Syncline at least over the syncline of which Mount Bruce forms the northern (south-dipping) limb, but at the Brockman Syncline and farther south it is not certain to what extent the small folds with fibrous minerals described here are, in principle or in practice, distinguishable from the similar folds described under the following heading.

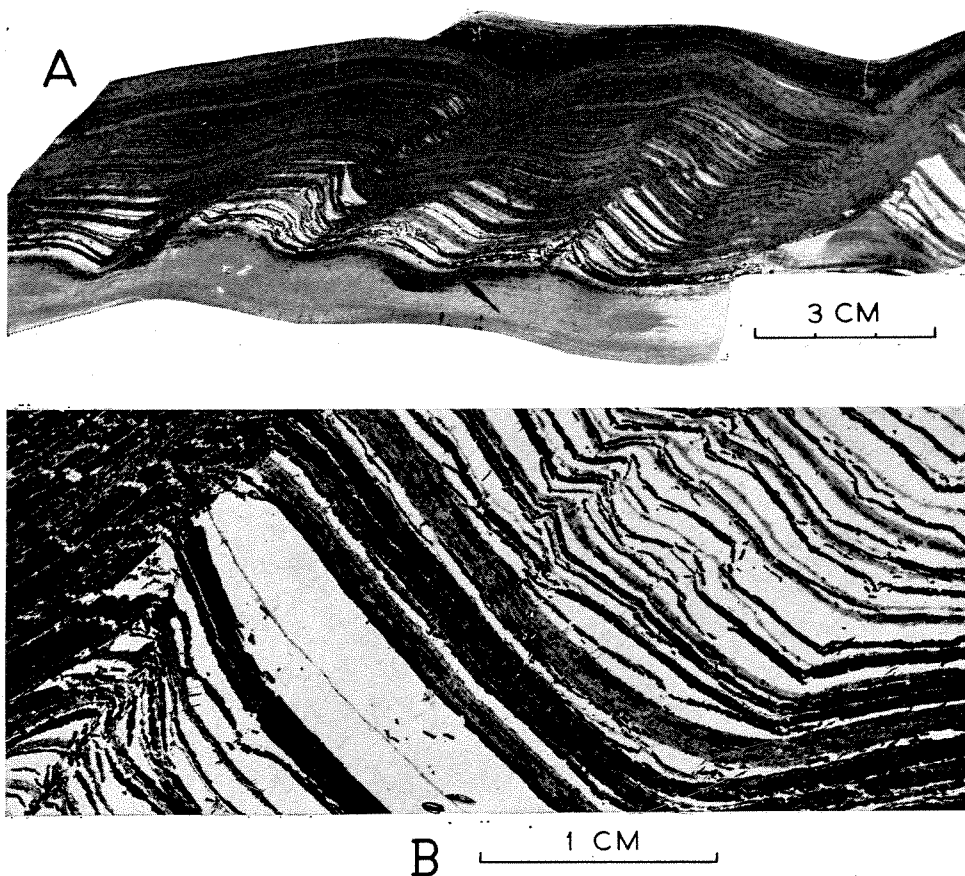


Figure 46. Minor folds with fibrous quartz from the Dales Gorge Member (exact stratigraphic position uncertain) on the north face of Mt. Bruce. The photograph in A is of a vertical north-south cut and smoothed surface, while B is an enlarged photograph of a thin-section from the same specimen. In both photographs the observer is looking in a westerly direction along the regional strike. The dip at Mount Bruce is low and to the south, so that it lies on the north limb of a syncline, and the sense of these folds is thus consistent with that expected. In A a microbanded chert mesoband forms the lower edge of the specimen, and the folds are best developed in the magnetite mesoband above it, in which the laminar structure of the magnetite is emphasized and displayed by the growth of quartz.

Quartz is by far the most common fibrous mineral of these folds; it is fibrous in the sense described in Chapter 4. Riebeckite also occurs commonly, either alone as slip-fibre (page 211) or in association with quartz. Stilpnomelane also occurs very rarely.

Although these folds, which resemble regional rippling in all respects except orientation relative to the Hamersley Syncline and the association with fibrous mineral growth, occur in the same area as regional rippling and have the same

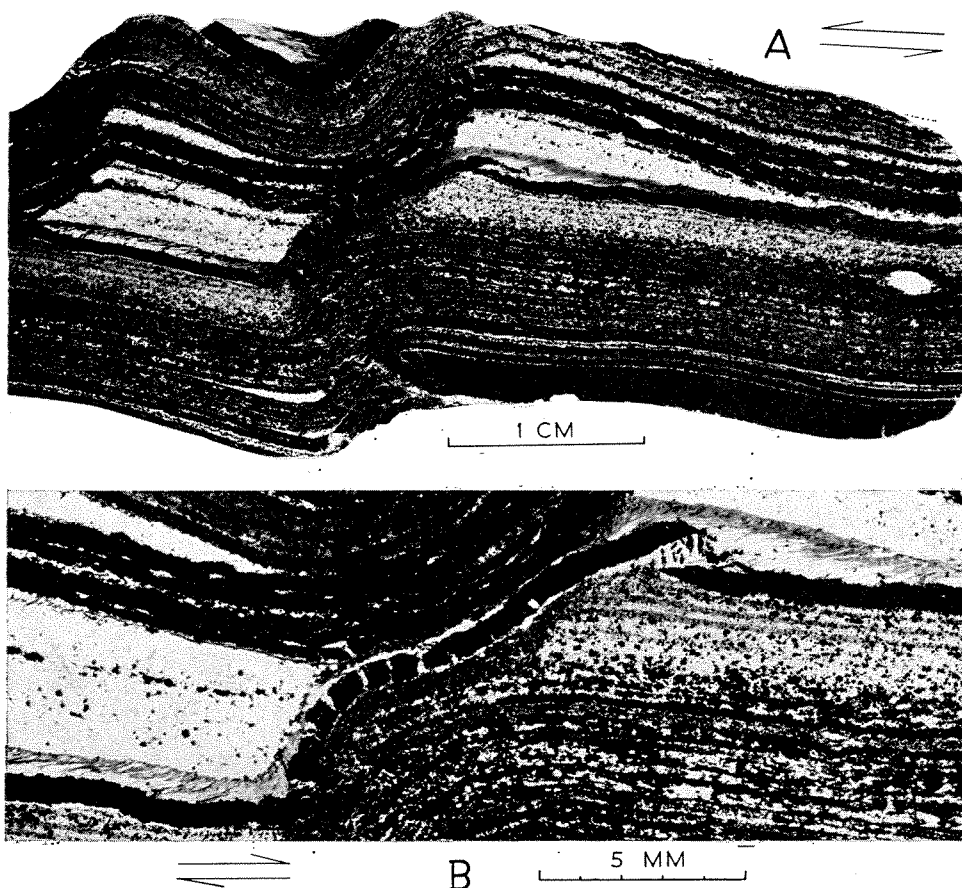


Figure 47. The relationship between regional rippling and stress-controlled growth of fibrous minerals ('stress-reversal'; see Chapter 11). A and B are photographs, at different scales, of two thin-sections from the same 'ripple' in the BIF13 macroband of the Dales Gorge Member, at the same locality as the examples shown in Figure 43. In both photographs the observer is looking in a westerly direction along the ripple axes, and the bedding is almost flat. In A the positions of the short steep and long gentle limbs of the regional ripples suggest the initiating stress shown by the arrows. In B the structure suggests that the ripples were later pushed in the opposite direction (again shown by arrows), so that the lower ripple crest was squashed in by the trough over-riding it from the south; this is consistent with the growth of the fibrous quartz and riebeckite during this reversed movement.

axial trend, they are rarely present together; the distribution of the fibrous mineral folds is restricted and patchy, and often occurs where regional rippling is inconspicuous. However, an apparent example of their mutual relationship is shown in Figure 47. In the structure shown regional ripples on the northern limb of the Hamersley Syncline have apparently been modified by a later stress in a sense consistent with that of the small folds with fibrous minerals; the modification is associated with both growth of fibrous quartz and riebeckite and with brittle fracture of magnetite laminae which were plastically bent during the formation of regional ripples. This structure is regarded as an important clue to the origin of crocidolite and is discussed further in Chapter 11 (page 312). It is possible that these folds have not uncommonly formed in this way from previously existing regional rippling.

MINOR FOLDING IN THE SOUTH

The major regional folds of the Hamersley Group in the southern part of the Hamersley Range area, for example the Wyloo Anticline and Turner Syncline, are much tighter than those in the north, and all iron formations within them are to varying degrees affected by minor folding and puckering clearly relatable to the main folds (Halligan and Daniels, 1963). These structures are penetrative, in the sense that the effects of the causative stress appear throughout any thin-section prepared from these areas, although often they are very slight; at Woongarra Gorge, for example, they locally take the forms of a slight axial plane alignment of riebeckite in the Boolgeeda Iron Formation and of green biotite in the Woongarra Volcanics. In the mesobanded iron formations there is usually in these southern areas some degree of macroscopically visible surface striation or puckering parallel with these penetrative structures and their associated minor folds.

We do not know whether there is a continuous gradation between these southern minor folds and the small folds with fibrous minerals in the north or whether they belong to distinct phases of structural development whose effects may become separable by further work in the central areas.

VERTICAL VEINS

Thin discordant veins cutting steeply across the banding are a general, but rarely conspicuous, structural feature of the iron formations throughout the area. We have not studied these systematically, and here add to the brief notes concerning them in other chapters a few relevant observations which may be useful in future studies.

The veins are mainly about a millimetre thick but vary from about 10 microns up to more than a centimetre. In any restricted locality they tend to have a constant thickness. Quartz is the commonest infilling mineral, but

carbonates, riebeckite, stilpnomelane, and magnetite (Figure 40A) also occur. In the Joffre Member at Joffre Falls abundant thin cross-cutting veins of both stilpnomelane and riebeckite dipping steeply to the north-northeast are a common feature of some chert and chert-matrix mesobands. The infilling minerals are related to the compositions of the mesobands which the veins cross, so that a vein filled by quartz where it crosses a chert may have stilpnomelane where it crosses the adjacent mesoband of chert-matrix, and so on. Thinner veins sometimes stop sharply at both margins of mesobands in which the tensional stress causing them has been accommodated by flow rather than by fracture. In thinner veins the quartz is usually in an even mosaic somewhat coarser than that of the cherts, but in the wider veins it has the fibrous appearance typical of other types of fibrous quartz with the fibre direction across the vein. Like other fibrous quartz, it is in fact quite coarsely crystalline. Short lenticular veins of fibrous quartz running roughly north-south are a widespread structural feature over much of the western half of the outcrop area of the iron formations. Thin-sections from the Dales Gorge Member at Woongarra Pool show that these veins existed before the minor folding associated with the Hardey Syncline, but no other evidence of their time of formation is available.

Riebeckite (including crocidolite) in the iron formations

INTRODUCTION

Since the investigation of blue asbestos was the first purpose of the study whose results are reported in this bulletin, it is appropriate that crocidolite should receive close attention in a discrete chapter. But it would be artificial to separate the geology of crocidolite from that of the chemically indistinguishable forms of riebeckite which are closely associated with it. The preferable (but still artificial) alternative is therefore chosen of, as far as possible excluding reference to riebeckite from the foregoing chapters, although necessary exceptions were made in Chapter 4. Through the joint treatment of all forms of riebeckite this chapter contains much geological information on textural varieties of riebeckite which are of no commercial significance, as well as a great deal of detailed data on crocidolite occurrence included because of its direct economic importance.

FORMS OF RIEBECKITE OCCURRENCE

Miles (1942, p. 16-22), in his description of Hamersley Range riebeckite-bearing rocks, followed previous South African usage (see: Hall, 1918; Peacock, 1928; Du Toit, 1945; Genis, 1961) in classifying his material into 'needle riebeckite', 'mass fibre riebeckite or "potential crocidolite"' and 'cross fibre riebeckite or "crocidolite proper"'. In the following descriptions we divide the textural varieties of riebeckite as follows:

1. *Massive riebeckite* consists almost entirely of a felted mass of interlocking riebeckite fibres. It occurs within iron formation in thick concordant mesobands, and when fresh, is a tough blue homogeneous rock which is highly resistant to mechanical erosion and difficult to break with a hammer. Often, only a few of the joints in the adjacent brittle iron formation continue through the thicker bands of massive riebeckite. Synonyms are listed in the Glossary.

2. *Crocidolite* is the form of the mineral riebeckite whose parallel fibrous structure gives it commercial importance. We agree with Genis (1961) in preferring to limit this name to the economically exploitable form. Other fibrous forms are better described as 'fibrous riebeckite'; crocidolite is thus a term in economic geology, rather than a discrete mineral species. It occurs within iron

formation in concordant mesobands which are up to about 3 inches thick, but which are characteristically discontinuous laterally. The fibre elongation is sub-parallel to the thickness of the mesoband, hence the synonym 'cross-fibre riebeckite'.

3. *Slip-fibre riebeckite* is the term applied to crocidolite-like material in which the fibres are at a low angle to the plane of the banding.

4. *Minor concordant occurrences* of riebeckite include the 'needle riebeckite' of Miles (1942) and others (see Glossary) and a range of other textural varieties of riebeckite which collectively make up only a small fraction of the total riebeckite content of the iron formation. Under this heading are included all occurrences of riebeckite which are neither massive riebeckite, crocidolite, nor slip-fibre, and which do not form discordant veins.

5. *Cross-cutting occurrences* include a few comparatively rare but significant examples where riebeckite occurs in veins discordant to the banding of the iron formation.

Of these five textural varieties the first two together comprise most (subjective minimum estimate 95 per cent) of the total riebeckite in Hamersley Group iron formations; and of these two massive riebeckite is very much more abundant than crocidolite.

VERTICAL AND LATERAL STRATIGRAPHIC DISTRIBUTION OF THE TWO MAIN FORMS OF RIEBECKITE

GENERAL NOTE

Massive riebeckite and crocidolite in the Hamersley Group are confined to the Marra Mamba and Brockman Iron Formations. There is a little riebeckite of other varieties in the Boolgeeda Iron Formation, but both the Mount Sylvia Formation and the Weeli Wolli Formation are virtually free of it, although both contain iron formation otherwise very similar to riebeckite-bearing types in the Marra Mamba and Brockman Iron Formations. At the beginning of this study it was hoped to construct, for each riebeckite-bearing formation or member, a regional block diagram showing the objectively measured vertical and lateral distribution of riebeckite. It is worth setting out initially the three main reasons why this proved impossible:

1. Both massive riebeckite and crocidolite are restricted in their occurrence between narrow stratigraphic limits, of which details are given below. In any one favourable level, broad areas of lesser or greater riebeckite abundance are discernible, but within an area of generally greater abundance the local range of abundance is both wide and erratic. Thus, even in a locality with plentiful data on riebeckite, for example the Wittenoom Gorge area, it is hard to express its concentration by a single accurate and meaningful number although this is,

subjectively and comparatively, 'high'. This factor alone would ensure that a quantitative regional assessment of riebeckite abundance would be enormously time-consuming.

2. Massive riebeckite, quantitatively the most important form, is highly susceptible to chemical weathering, despite its great mechanical resistance. In many outcrop areas it is altered to a hard yellow-brown aggregate of limonite and secondary silica not unlike weathered chert. Any measurement of its abundance in such situations would be unreliable. The same difficulty does not apply to crocidolite, which retains its structure through extreme weathering. The limonitic replacement of crocidolite results in griqualandite, while silicification gives rise to the strikingly chatoyant tiger's eye.

3. The present outcrops of the riebeckite-bearing iron formations in the Hamersley Range area is such that, wherever information about one stratigraphic level is good, information about others is often poor. Thus the concentration of riebeckite in the Marra Mamba Iron Formation is unknown over a broad area of the main Hamersley Range, where concentration in the Dales Gorge Member is well known.

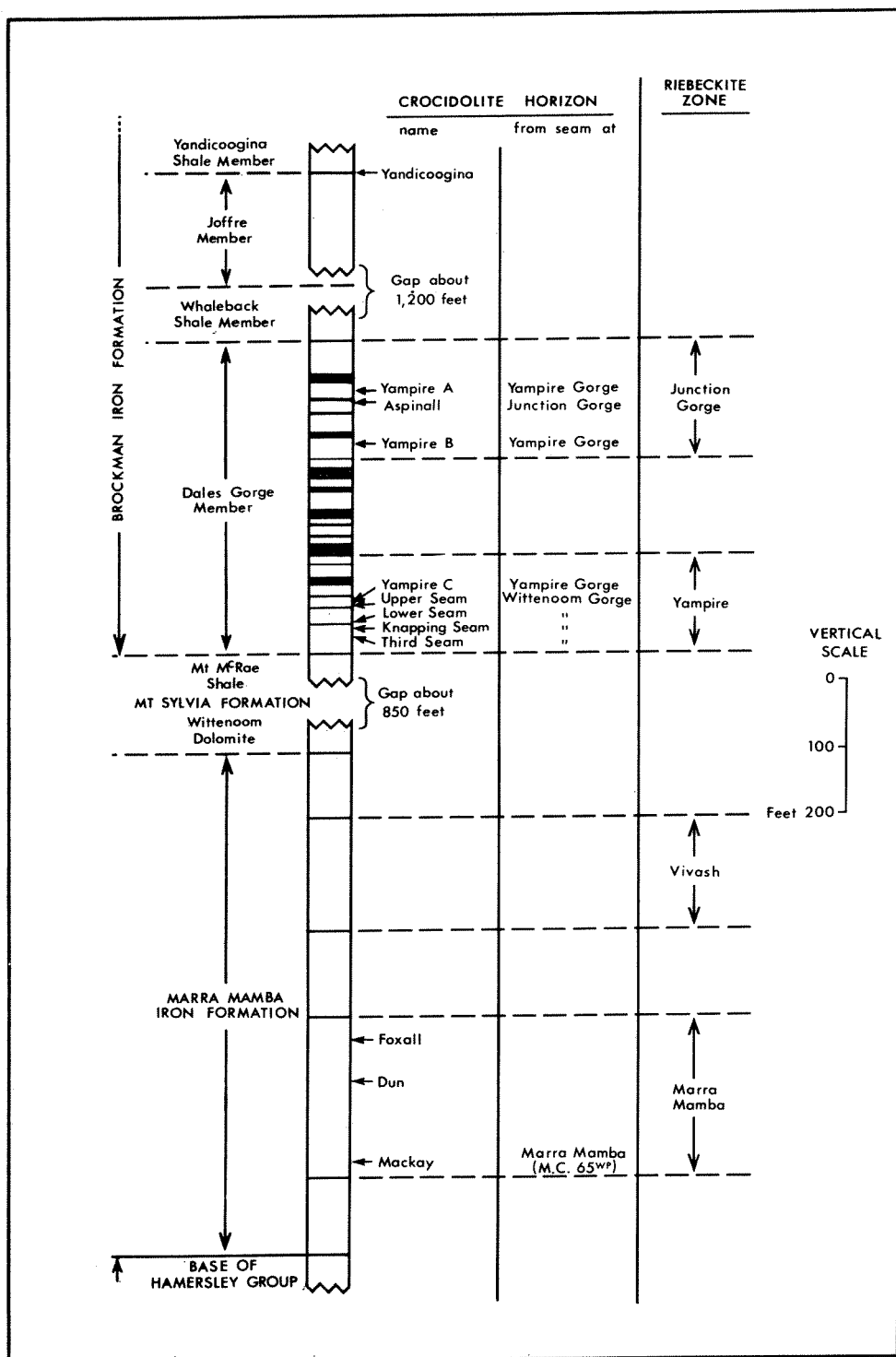
These three factors jointly prevent the presentation of a complete analysis of regional riebeckite distribution; in their light the limitations of the following general account of riebeckite distribution will be appreciated.

VERTICAL DISTRIBUTION OF RIEBECKITE

TOTAL RIEBECKITE: RIEBECKITE ZONES

Although riebeckite in one or other of its minor forms is widely distributed in the Marra Mamba, Brockman and Boolgeeda Iron Formations its two main forms occur with conspicuous abundance at only four restricted stratigraphic levels, or *riebeckite zones* (Trendall, 1965a). Two of these occur in the Marra Mamba Iron Formation and two in the Dales Gorge Member of the Brockman Iron Formation. Their positions are shown in Figure 48. These four zones are herein named for convenience the Marra Mamba, Vivash, Yampire, and Junction Gorge Riebeckite Zones. Since the Australian Code of Stratigraphic Nomenclature (G.S. Aust., 1964, Art. 45) does not provide for this, these names must be regarded as informal, although there are precedents for the use of 'zone' in a comparable way. It should be emphasized here firstly that the boundaries of these zones are somewhat vague, and are not usefully definable with accuracy; and secondly that while riebeckite zones may or *may not* contain riebeckite, in different areas, riebeckite *nowhere* occurs abundantly outside them. Although riebeckite zones are defined by the abundance of riebeckite of all kinds, massive riebeckite forms by far the greatest proportion quantitatively, and the following account of the vertical distribution of massive riebeckite is most relevant to their description.

Figure 48 (opposite). Stratigraphic columns of crocidolite-bearing parts of the Hamersley Group, with positions and nomenclature of crocidolite horizons and riebeckite zones.



Apart from their liability to bear riebeckite it is hard to see any distinctive common characters of the riebeckite zones which are not also present in riebeckite-free parts of the Hamersley Group. The two riebeckite zones of the Dales Gorge Member lie where the S macrobands are comparatively thin and the BIF macrobands correspondingly thick; riebeckite of any kind is rare in the central part of the member, where this situation is reversed. Both the riebeckite zones of the Marra Mamba Iron Formation, and the Joffre Member as a whole, have similar ratios of shale to iron formation. More comparative work is needed to determine whether there exists an optimum value of the ratio for riebeckite development.

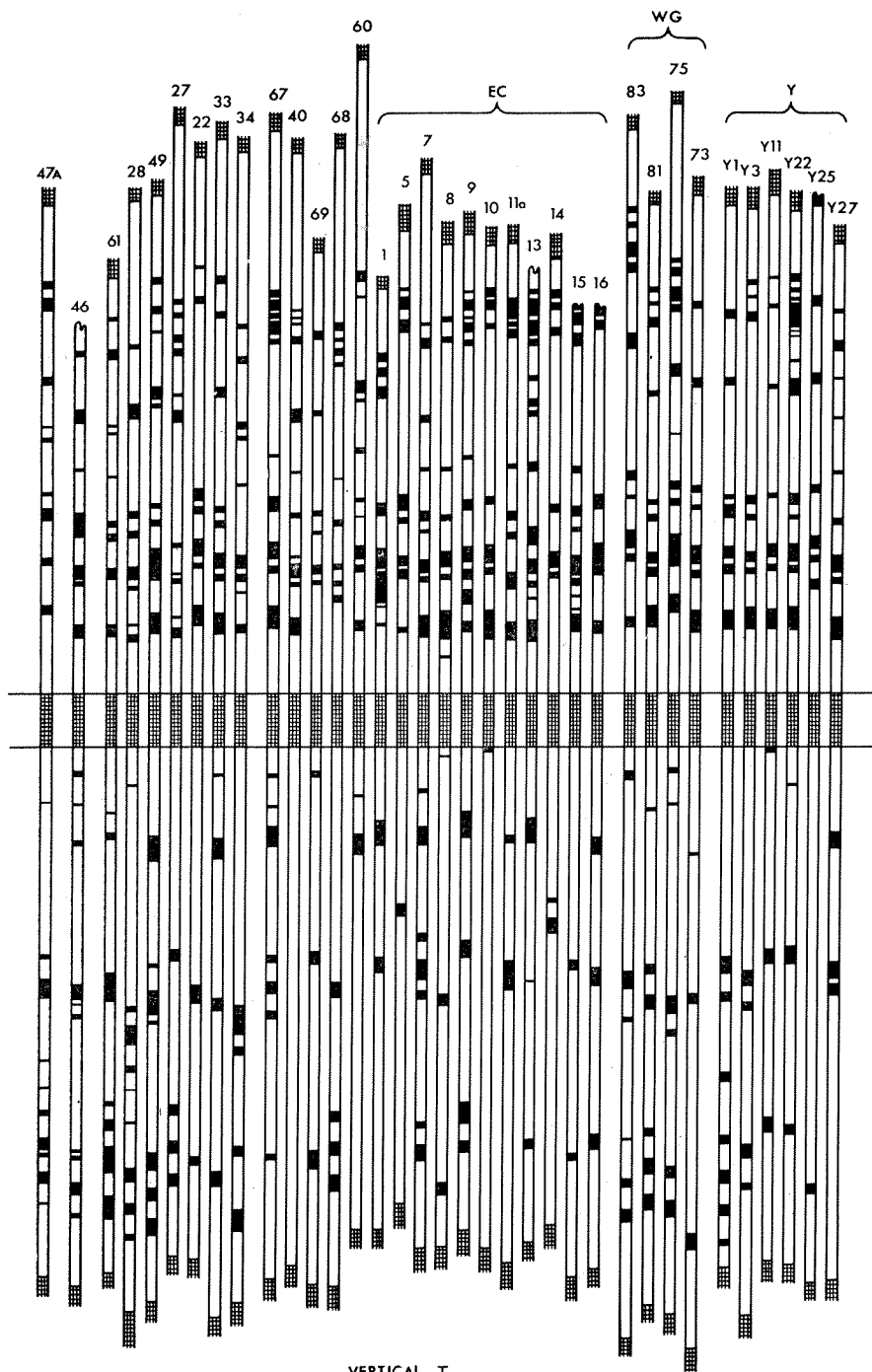
MASSIVE RIEBECKITE

Evidence is presented later in this chapter that mesobands of massive riebeckite are, in the Dales Gorge Member, closely related to the Calamina cyclothems, in that they grade laterally into, and are thus stratigraphically correlative with, the chert-magnetite groups of the cyclothems; it is necessary to anticipate this point for a proper description of the vertical distribution of massive riebeckite within the riebeckite zones. In areas where these zones have abundant riebeckite (see 'Lateral distribution', below) this abundance is expressed by the appearance of massive riebeckite in stratigraphic positions where chert-magnetite groups would otherwise lie. But the appearance takes place according to rules that may be summarised as follows:

1. Not all cyclothems of a macroband are equally liable to be represented by riebeckite. There is a preference for chert-magnetite groups of particular cyclothems; these are the 'riebeckite-prone cherts' of Ryan (see Trendall, 1965a, p. 61).
2. These preferred cyclothems seem to lie in contiguous groups.
3. Some of the preferred cyclothems have greater priority of preference, so that if riebeckite appears anywhere in the zone it almost always appears in their position; among the remainder the choice is random.

These points are illustrated by Figures 49 to 51. In Figure 49 the occurrence of massive riebeckite in macrobands BIF2 and BIF3, in the central part of the Yampire Riebeckite Zone, is shown for 35 drillholes in the Wittenoom and Yampire areas; these are all available holes where these two macrobands were cored completely, or almost completely. Figure 50 is a summary of the information on Figure 49, prepared as described in the caption; the tendency for grouping is clearly illustrated. But comparison of these two figures shows that no single hole contributes to all statistical maxima, and that riebeckite may be completely absent from

Figure 49 (opposite). The distribution of massive riebeckite mesobands in the BIF2 and BIF3 macrobands in 35 drillholes in the Wittenoom and Yampire areas. Locations of the Wittenoom drillholes are given on Plate 6, and of the Yampire drillholes (prefixed by Y) on Plate 9. The general stratigraphic concordance of all the columns, with wide individual variations in detail, is apparent.

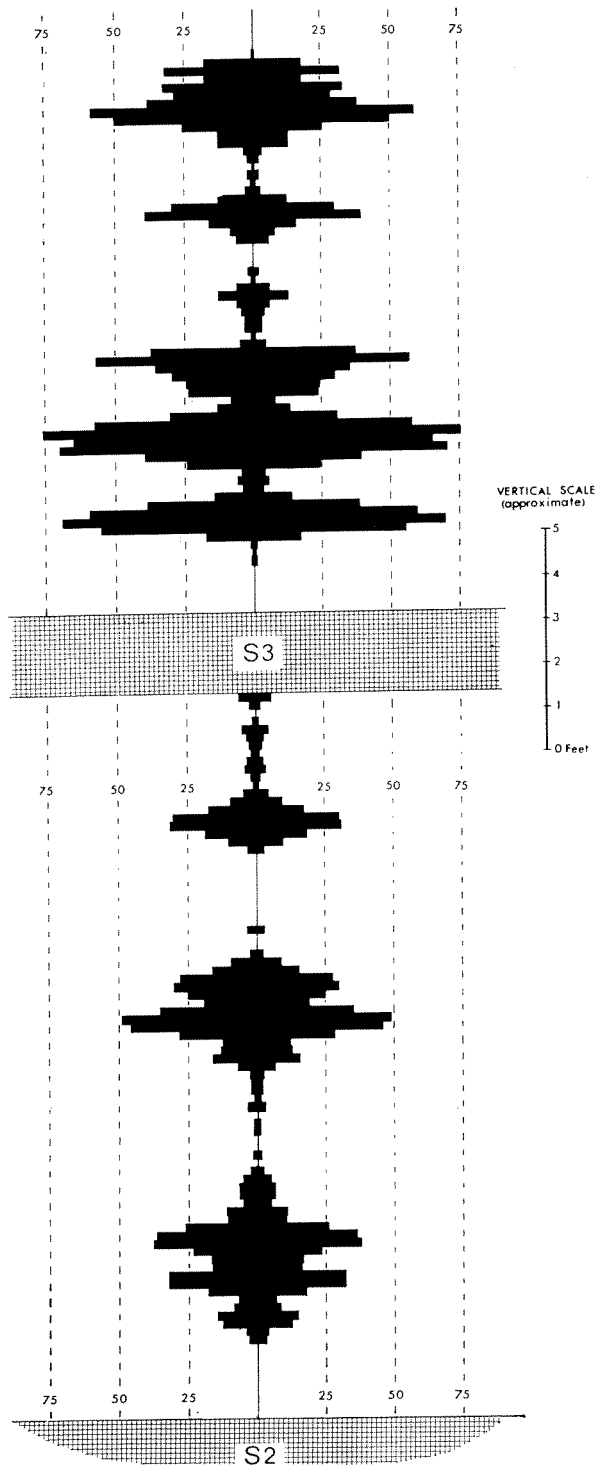


VERTICAL
SCALE | 1 FOOT

a macroband (for example, BIF2 in Hole 40) which has riebeckite mesobands at several levels in nearby holes. The third point is illustrated by Figure 51, in which three cyclothems of BIF2 in which riebeckite is liable to appear, in the interval about 6 to 9 feet below the base of S3 (Figure 49), are compared. Nine holes with five different riebeckite distribution patterns are shown in precise stratigraphic apposition. The main central riebeckite represents a chert-magnetite group with priority of riebeckite appearance; riebeckite never appears above or below it unless riebeckite is present in it, but where riebeckite is present then riebeckite may appear either above, below, or both above and below. This mesoband of massive riebeckite, a useful field stratigraphic marker, forms the roof of the adits of the old mine at Yampire Gorge, and is informally called the 'adit roof riebeckite' (Trendall and Blockley, 1968).

In the outer macrobands of the Yampire Riebeckite Zone there is a steadily patchier appearance of riebeckite, and these two central macrobands adequately illustrate the salient features of vertical massive riebeckite distribution in both the Yampire and Junction Gorge Riebeckite Zones. Exposures of the Marra Mamba Iron Formation are not adequate to determine exactly how its riebeckite zones differ from those of the Dales Gorge Member in this respect. While the general impression is of a similar total quantity of riebeckite, similarly confined to mesobands of the same order of thickness, the Calamina cyclothem is not present, and the details of riebeckite occurrence may be expected to be somewhat different. In the Joffre Member massive riebeckite occurs patchily, and is there equivalent to the red cherts of the Knox cyclothem. We have not studied its stratigraphic distribution closely but our impression is that it is not restricted to any particular zone within the member; no riebeckite zones in it have therefore been named.

Figure 50. Histogram summary of the information given in Figure 49. In the preparation of this figure the graphic log of each of the drillholes used for Figure 49 was either expanded or contracted proportionately to give an equal length on squared paper between the following fixed stratigraphic limits: for BIF2 the top of S1 and the base of S2, and for BIF3 the top of S2 and a selected mesoband above the uppermost riebeckite. For each arbitrary thickness represented by one square of the paper (about 2½ inches actual stratigraphic thickness) the number of squares partly or wholly occupied by massive riebeckite were then counted, and were plotted laterally outwards on both sides of the centre line to give a double histogram. The pecked lines show the percentages of the total available volume at each arbitrary interval which is occupied by massive riebeckite. The tendency for regularity in the intervals between riebeckite mesobands, which is apparent in Figure 49, is thus emphasized in an objective way by compensating for irrelevant variations of macroband thickness.



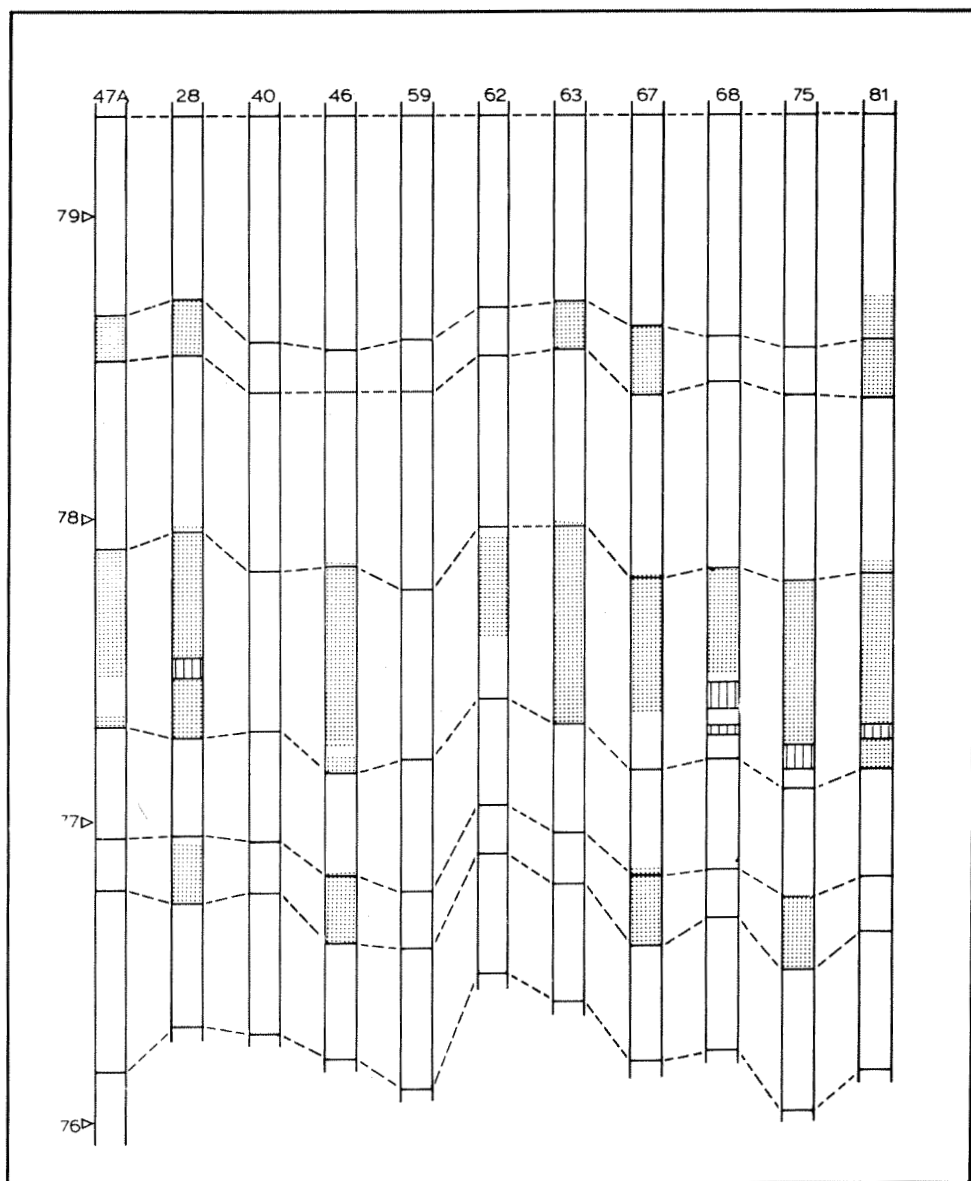


Figure 51. Comparison of massive riebeckite occurrence in the same three consecutive Calamina cyclothems of BIF2, transected in 9 different drillholes in the Wittenoom and Yampire areas. The stratigraphic equivalence of massive riebeckite and the chert-magnetite group of the cyclothem is evident. There is a preference for order of occupation of the permissible riebeckite positions, in that neither the upper nor the lower position may be occupied before the central one; but once this is represented by riebeckite, either of the other two positions may be occupied before the other. Note that this Figure differs from Figure

CROCIDOLITE: CROCIDOLITE SEAMS AND HORIZONS

DEFINITION, NOMENCLATURE, AND STRATIGRAPHIC RELATIONSHIP

Just as riebeckite is closely confined to particular levels of the iron formations, so groups of crocidolite mesobands are mainly confined to still more narrowly restricted stratigraphic levels within the riebeckite zones. If a group of crocidolite bands (mesobands) has locally been mined as a unit, or is, under economic conditions which may reasonably occur, and using existing mining techniques, potentially mineable as such, it is here defined as a crocidolite *seam*; a typical seam has a thickness of about 6 inches to 2 feet and contains about 2 to 20 bands of fibre which comprise between a quarter and a half of the thickness. The stratigraphic interval within which a seam lies we call a crocidolite *horizon*, and define this as a narrow stratigraphic interval in which seams of crocidolite are likely to occur.

We have adapted the seam names that have become established during mining into a rational scheme of horizon and seam nomenclature on stratigraphic lines; these names are also set out in Figure 48. A named crocidolite horizon is a definite narrow stratigraphic interval which bears the same name wherever it exists, regardless of whether or not it contains mineable crocidolite, traces of crocidolite, or no crocidolite whatsoever. If a horizon locally has potentially economic fibre then the fibre forms a seam, which bears a local name applied only to that locally restricted body of crocidolite. A single crocidolite horizon may contain more than one seam, either in one area or at different localities. As displayed in Figure 48, we have used as names for several horizons the seam names currently or formerly used for well developed seams within them.

Although these named horizons are the only levels at which crocidolite of potential commercial interest occurs, thin stringers of crocidolite are present at many levels outside them, but still within the riebeckite zones. We therefore note here an important general relationship between crocidolite occurrence and the small-scale stratigraphic sequence; crocidolite is confined in the Dales Gorge Member either to the mixed groups of the Calamina cyclothem or to the close-packed chert sequences (Table 8). Of these two possible positions the Upper Seam Crocidolite Horizon (see below) is a good example of the second type, while parts of the Yampire C Crocidolite Horizon are of the first kind. A more detailed account of the relationship between crocidolite and the mesoband sequence is given under the heading 'Crocidolite-spatial relationship to iron formation' later in this chapter.

In one exceptional instance a crocidolite horizon—the Yandicoogina Crocidolite Horizon—lies outside a designated riebeckite zone. It follows from the foregoing definitions that this level is exceptional in that crocidolite locally occurs on

49 not only in scale but in the exact stratigraphic equivalence, independently of riebeckite, of the interconnected levels; in Figure 49 the boundaries of the riebeckite mesobands may be stratigraphically transgressive.

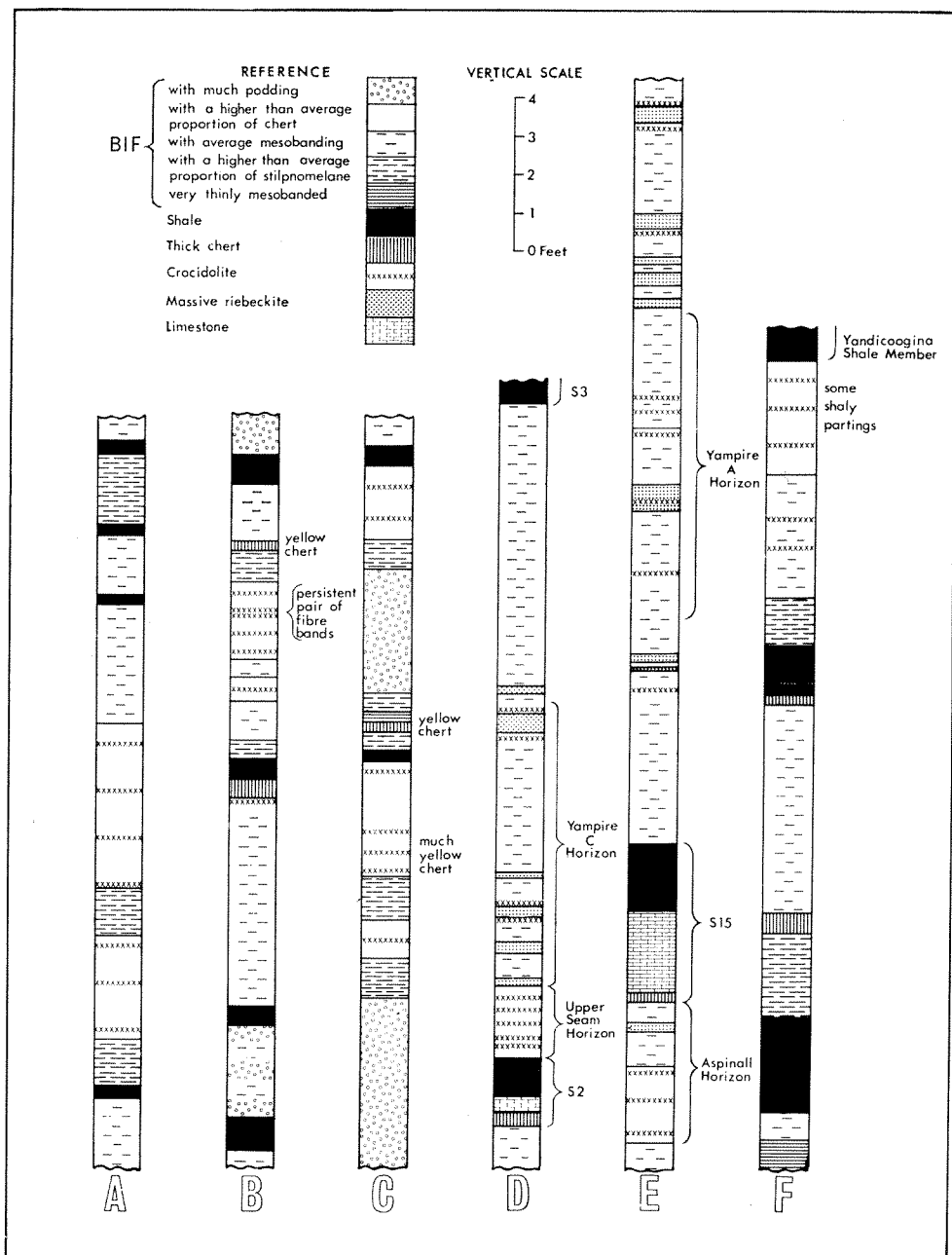


Figure 52. Stratigraphic columns about the main crocidolite horizons of the Marra Mamba and Brockman Iron Formations. A. Mackay Horizon. B. Dun Horizon. C. Foxall Horizon. D. Upper Seam and Yampire C Horizons. E. Aspinall and Yampire A Horizons. F. Yandicoogina Horizon.

it even though it does not form part of a stratigraphic section which in places has exceptionally abundant total riebeckite.

There follow below, in ascending stratigraphic order, more detailed accounts of the salient features of each crocidolite horizon.

MARRA MAMBA RIEBECKITE ZONE

This zone contains three productive horizons, two of which have been named the Mackay and Dun Crocidolite Horizons, after the original discoverers, and the third called the Foxall Crocidolite Horizon after the former State Mining Engineer who first described the workings (Foxall, 1942). Recognition of these horizons is often difficult through poor exposure and deep surface weathering.

Mackay Crocidolite Horizon

This is named from the Mackay Seam on M.C.65^{W.P.}. Its stratigraphic position on this claim is difficult to determine due to incomplete exposure of the section. However, detailed comparisons of its stratigraphy with that of the horizon formerly called by Blockley (1967) the 'A' Horizon, at the eastern end of the Marra Mamba area seem to confirm the earlier tentative conclusion that the two are correlatives. We now accept this correlation and place the Mackay Horizon 120 feet above the base of the Marra Mamba Iron Formation. On M.C. 65^{W.P.} at Marra Mamba the Mackay Horizon contains the most spectacular development of fibre seen in the Marra Mamba Riebeckite Zone, with grades ranging up to 7 inches over a 6-foot seam thickness*. A typical section appears in Figure 52.

The shaly BIF in the middle of the seam is similar to that in the Dun Horizon, but the absence of the twin fibre bands and the different spacing of the surrounding shales serves to distinguish the two horizons.

Dun Crocidolite Horizon

This contains most of the productive seams at Marra Mamba. It is the only horizon recognized at Marra Mamba which has been identified elsewhere in the Hamersley Range. It bears fibre in many places on the Jeerinah Anticline and on the south limb of the Brockman Syncline. The horizon is 260 feet above the base of the formation and is readily recognized by its position in the middle of a sequence of cyclic repetitions of BIF and shale, and by a distinctive internal stratigraphy. A typical section about the fibre horizon is given in Figure 52. The presence of the twin crocidolite bands 6 inches below the 10-inch bed of shaly BIF is characteristic of the Dun Horizon.

* See 'Assay methods', later in this chapter.

Foxall Crocidolite Horizon

This has been worked only on M.C.62^{W.P.} at Marra Mamba, and rarely contains fibre of mineable grade. It lies about 350 feet above the base of the Marra Mamba Iron Formation. A representative section about the horizon appears in Figure 52. In the field, the Foxall Horizon is best recognized by the group of beds immediately overlying the most persistent fibre bands, 13 feet above the base of the section shown. If fibre is absent from the section examined, then confident identification of the horizon is difficult.

Other crocidolite horizons

At Marra Mamba other low-grade seams of apparently small extent have been seen at positions 85 feet and 60 feet below, and 30 feet and 47 feet above the Dun Horizon, and at 35 feet above the Mackay Horizon. Elsewhere on the Jeerinah anticline (e.g. in Serpentine Creek: lat. 22° 21'S; long. 116° 37'E) crocidolite bands have been seen in the Marra Mamba Riebeckite Zone, but the exact stratigraphic positions of these could not be determined.

VIVASH RIEBECKITE ZONE

This lies near the top of the Marra Mamba Iron Formation. It is about 60 feet thick, is about 520 feet above the base of the formation, and contains crocidolite at Vivash Gorge, Horseshoe Creek, Mount Brockman Station and at Jimmawarrada Creek (lat. 21° 48'S; long. 116° 20'E). Due to generally poor exposure, and indefinite stratigraphy, it has not been possible to correlate individual crocidolite horizons between the known outcrops of this zone. Most fibre enrichments within the Vivash Riebeckite Zone are showy, but short-lived. A typical section of an enrichment (Figure 67) may contain 20 fibre bands over a vertical range of 30 feet without having a single seam of mineable grade. Within one or two hundred feet of such a section, the same beds may contain no fibre at all.

YAMPIRE RIEBECKITE ZONE

The Yampire Riebeckite Zone embraces the lowermost six BIF macrobands of the Dales Gorge Member, and is economically the most important zone of the province. Crocidolite has been found at many levels in all six BIF macrobands, but the most important seams are restricted to BIF1 and BIF2. Fibre has been mined from six horizons within the zone, but there are many crocidolite bands of uneconomic grade elsewhere in the section. The general relationship between fibre and lithology is discussed later.

Third Seam Crocidolite Horizon

This is named from the Third Seam at Wittenoom, where it contains up to 1.5 inches of fibre. The horizon bears small amounts of crocidolite in many places in the northern part of the Hamersley Range, but nowhere is it of great economic significance. It is situated about centrally in the BIF0 macroband and is some 12 to 18 inches thick.

Knapping Seam Crocidolite Horizon

This has been worked in the Knapping Seam at Wittenoom Gorge; it is just below the S1 macroband. Where worked it consists of a single mesoband of fibre of variable length which may reach 1.5 inches. Outside the Wittenoom area the horizon is generally barren.

Lower Seam Crocidolite Horizon

This is named from the Lower Seam at Wittenoom Gorge, where it has yielded a considerable amount of crocidolite. Mahlberg's Seam at Dales Gorge is at the top of the Lower Seam Horizon. The horizon takes in the stratigraphic interval between the top of the S1 macroband and the top of MB2, of Trendall (1966a); that is, from about 47 to 51 feet in the type section, an interval of about 5 feet. Seams developed in the horizon normally comprise 10 to 20 bands of fibre spaced over 1.5 to 2.5 feet. The horizon bears crocidolite intermittently from Weeli Wolli Spring to Mount King, a distance of about 85 miles, but economic concentrations within it are restricted to the arc between Wittenoom and Dales Gorge.

Upper Seam Crocidolite Horizon

This contains the Upper Seam of Wittenoom Gorge, from which it is named. It is the most productive of all fibre horizons in the Hamersley Range, having yielded the greater part of the fibre won at Wittenoom and a significant proportion of that from Yampire Gorge, where it contains the 'Lower Seam' of former A.B.A. usage in that area. The horizon is 1½ feet thick and is just above the S2 macroband, between about 69 and 70.5 feet in the type section. Seams within the horizon consist of six to eighteen bands of fibre spread throughout its thickness and totalling up to 4 inches. Crocidolite is known in the Upper Seam Horizon from Junction Gorge to Mount King, a distance of about 60 miles.

Yampire C Crocidolite Horizon

This was first named at Yampire Gorge, and originally included the Upper Seam Horizon and several bands of fibre higher in BIF2. When the correlation with the Wittenoom section became known, the name was restricted to higher bands, and so now includes only that part of BIF2 between the Upper Seam Horizon and the top of the 'adit roof riebeckite' (Figure 51) that is from 70.5 to 78 feet in the type section. At Yampire Gorge, the horizon contains bands of fibre spread over a width of 7 feet, but usually seams within it are restricted to one or two bands adjacent to the adit roof riebeckite. Outside Yampire Gorge crocidolite seams within the Yampire C Horizon have been mined at Dales Gorge, Bee Gorge, Range Gorge and Mount Margaret. The horizon bears fibre mainly in the area between Dales Gorge and Range Gorge, with Mount Margaret an outlying exception.

JUNCTION GORGE RIEBECKITE ZONE

The Junction Gorge Riebeckite Zone embraces the BIF12 to BIF16 macrobands of the Dales Gorge Member. It has been given a variety of names, including

Upper Yampire Series, Upper Yampire Zone, and Upper Riebeckite Zone. As it now appears that the best fibre in it is likely to be found in the eastern part of the Hamersley Range, a name derived from that area is considered appropriate. Crocidolite has been mined from three horizons within the zone and sub-economic fibre has been seen at several other positions within it.

Yampire B Crocidolite Horizon

This contains fibre at Yampire Gorge and includes the whole of the BIF12 macroband. The horizon has been called the Yampire Intermediate Series (Finucane, 1965). Traces of crocidolite are common within the horizon, but fibre of potentially economic grade is rare; even the seam at Yampire being suitable only for surface 'knapping'.

Aspinall Crocidolite Horizon

This is named from the Aspinall Seam at Junction Gorge and occupies the uppermost 4 feet of BIF14. The best fibre developments within the Junction Gorge Riebeckite Zone are in this horizon, which contains intermittent crocidolite between Calamina Gorge and Coondiner Gorge, and thence southward to the Weeli Wolli Anticline.

Yampire A Crocidolite Horizon

This was originally a term applied collectively to the crocidolite bands in BIF macrobands 14-16 at Yampire Gorge. This wide application of the term is unsuitable outside the immediate area of Yampire Gorge and the name is now restricted to a section of BIF15 which has been mined at Yampire Gorge and which commonly bears asbestos elsewhere. The section is from 6 to 14 feet above S15. As with the Yampire C Horizon, the fibre is only present where there is an abundance of massive riebeckite.

Other crocidolite horizons

Within the Junction Gorge Riebeckite Zone crocidolite also occurs at the top and base of BIF13, the base of BIF 14, in BIF 15 outside the defined limits of the Yampire A Horizon, and at about 5 and 16 feet above the base of BIF16. Although any of these horizons may contain local concentrations of fibre totalling some 2 inches, none has been mined, or named by us.

YANDICOOGINA CROCIDOLITE HORIZON

The Yandicoogina Horizon bears fibre in the area drained by Yandicoogina Creek and its tributaries. It is situated at the top of the Joffre Member in an 8-foot thick BIF band just below Yandicoogina Shale Member. A section about the horizon is given in Figure 52.

LATERAL DISTRIBUTION OF RIEBECKITE

MASSIVE RIEBECKITE

Reasons have already been listed for the impossibility of giving a systematic quantitative account of massive riebeckite distribution in each of the four riebeckite zones; the difficulty of expressing the local riebeckite content of any one macro-band is apparent from Figure 49. The following broad regional summary must therefore suffice.

Massive riebeckite occurs in both the Yampire and Junction Gorge Riebeckite Zones of the Dales Gorge Member along the northern part of the main Hamersley Range between about longitudes $116^{\circ} 30'$ and $118^{\circ} 45'E$; roughly from a little west of Silver Grass Peak to Fortress Gorge. At Junction Gorge, further east, two drillholes into parts of the Yampire Riebeckite Zone encountered no massive riebeckite, and none is present in the Junction Gorge Riebeckite Zone at the surface. At each end of this strip, the riebeckite seems to die away gradationally, with a concentration in the Wittenoom—Yampire—Dales Gorge area. Within the Hamersley Range Synclinorium the Dales Gorge Member is usually poorly exposed, and there is little information about massive riebeckite, but along the southern edge of the range riebeckite is either absent or patchily developed, and it does not appear further south. Thus massive riebeckite in the Dales Gorge Member appears to be concentrated in a strip corresponding to a northern zone of intermediate stratigraphic thickness (Plate 3).

In the Marra Mamba Iron Formation massive riebeckite occurs mainly along the flanks of the Jeerinah Anticline.

CROCIDOLITE

REGIONAL DISTRIBUTION: PROVINCES AND SUB-PROVINCES

Potentially, crocidolite may occur anywhere in the outcrop of the two crocidolite-bearing iron formations of the Hamersley Group: the Marra Mamba and Brockman Iron Formations. The area defined by this outcrop is called the Hamersley Crocidolite Province. It is a roughly elliptical area 300 miles long by 100 miles wide, elongated in a west-northwest direction (Plate 4). Within the Hamersley Crocidolite Province there are two distinct sub-provinces to which the bulk of the crocidolite is confined. These sub-provinces are distinguished by their areal separation and probably also by the restriction of crocidolite in each to a different part of the stratigraphic column. The sub-provinces are named, from the principal centre of crocidolite production in each, the Wittenoom Sub-Province and the Marra Mamba Sub-Province.

The economically more important Wittenoom Sub-Province is defined on the north side by the northern face of the Hamersley Range between Mount Pyrtton (lat. $21^{\circ} 53'S$; long. $117^{\circ} 20'E$) and Kalgan Creek. The other boundaries are defined approximately by imaginary lines joining Mount Pyrtton, Mount Stevenson (lat. $22^{\circ} 31'S$; long. $118^{\circ} 03'E$), Juna Downs homestead (lat. $22^{\circ} 53'S$; long.

117° 29'E) and Coondiner Creek. Within this sub-province crocidolite is, as far as is known, restricted to the Brockman Iron Formation, and mainly to the Dales Gorge Member. In the western part of the sub-province, between Mount Margaret (lat. 21° 58'S; long. 117° 51'E) and Wittenoom Gorge, all of the economic fibre is in the Yampire Riebeckite Zone. From Wittenoom Gorge to Yampire Gorge, crocidolite has been mined from both the Yampire and Junction Gorge Riebeckite Zones, but east of Yampire Gorge, all of the significant fibre lies in the upper part of the Dales Gorge Member or in the Yandicoogina Horizon. From east to west the crocidolite thus favours successively lower parts of the succession. The northern boundary of the sub-province is a physical one; there is no further outcrop of the Brockman Iron Formation to the north. The southern boundary, although ill-defined, roughly follows a trend of 300°, which is that of the regional folding and of the long axis of the Hamersley Basin.

The Marra Mamba Sub-Province embraces the Jeerinah Anticline, the Brockman Syncline and the northern part of the Turner Syncline. The northern limit of the sub-province is defined by the southern scarp of the Hamersley Plateau between Serpentine Creek (lat. 22° 15'S; long. 116° 35'E) and Mount Sylvia (lat. 22° 18'S; long. 117° 37'E). The other boundaries of the province are defined approximately by a line joining Mount Sylvia, Mount Tom Price, Mount Jope, Mount Wall, Duck Creek homestead and thence following Duck Creek and Serpentine Creek back to the northern edge of the sub-province. In this second sub-province, all of the significant crocidolite deposits are in the Marra Mamba Iron Formation. Zoning is not as marked as in the Wittenoom Sub-Province, but most deposits in the northern part are in the Marra Mamba Riebeckite Zone, while in the southern part, most are in the stratigraphically higher Vivash Riebeckite Zone. There appears to be no definite relationship between the boundaries of the Marra Mamba Sub-Province and any tectonic trend. Possibly though, any such trend would remain unrecognised due to the comparatively small area of outcrop of the Marra Mamba Iron Formation in the sub-province and the consequent difficulty in obtaining a complete picture of the crocidolite distribution.

Crocidolite is rarely seen outside the two sub-provinces. A little was found in the Brockman Iron Formation about 6 miles south of Mount Nicholson, at latitude 21° 23'S and longitude 116° 04'E, at James point (lat. 20° 58'S; long. 116° 10'E), at Fish Pool (lat. 23° 07'S; long. 118° 04'E) on Turee Creek. Both of these occurrences are in the Yampire Riebeckite Zone. The Marra Mamba Iron Formation also contains crocidolite at Jimmawarrada Creek (lat. 21° 49'S; long. 116° 20'E).

We believe it likely that the observed presence of fibre in the Dales Gorge Member in one sub-province and in the Marra Mamba Iron Formation in the other represents a mutually exclusive relationship; that is, we doubt whether crocidolite occurs in the unexposed Marra Mamba Iron Formation beneath the crocidolite-bearing Dales Gorge Member in the Wittenoom Sub-Province, and also whether crocidolite was present in that part of the Dales Gorge Member now eroded from above the crocidolite-bearing Marra Mamba Iron Formation of the

Marra Mamba Sub-Province. However, there is insufficient evidence for this to be certain. The view is based partly on the observed tendency for crocidolite to occur in a steadily lower stratigraphic position from east to west along the Hamersley Range, partly on our impression that crocidolite in the Marra Mamba Iron Formation tends to occur in the thickest part of the formation (though poor exposure makes this uncertain), and in the second case partly on the apparent regional correlation between massive riebeckite and crocidolite (further below in this chapter).

LOCAL DISTRIBUTION: ENRICHMENTS AND DEPOSITS

The restriction of crocidolite both vertically to specific horizons and laterally within these horizons to sub-provinces has now been described. Within the sub-provinces themselves crocidolite distribution is also continuously variable. Ignoring the various minor fluctuations, described later in this chapter, an average fibre length for each (say) 100 square feet area of any horizon could be drawn. In practice this cannot be achieved. Our assessment, on the basis of the evidence contained in the later part of this chapter, is nevertheless that such a map would show a complex pattern.

Any area on the imaginary map bounded by a closed isopleth such that there is longer fibre within it than outside we called an *enrichment*; it is a positive distributional anomaly. It is impossible to place useful quantitative limits on the areal size, or bounding value, of an enrichment. A *deposit* is an enrichment which has potential commercial interest; it represents enrichment to a point where a seam, as defined earlier (p. 183), exists at the relevant horizon.

Descriptions of all crocidolite deposits, including available information on lateral distribution of crocidolite, appear below, with a final summary of present knowledge of their shape and size in the Hamersley Crocidolite Province.

DISTRIBUTIONAL INTER-RELATIONSHIP BETWEEN THE TWO MAIN FORMS OF RIEBECKITE AND OTHER STRATIGRAPHIC FEATURES

Riebeckite zones were defined earlier as restricted stratigraphic levels within which either, or both, of the two main forms of riebeckite are liable to occur abundantly. On the regional scale the abundance of total riebeckite in both riebeckite zones of the Dales Gorge Member is broadly sympathetic, and so also is the abundance of crocidolite and massive riebeckite within each zone. However, from preceding descriptions it appears that there are two significant departures from this latter relationship. Firstly, massive riebeckite, in the Yampire Riebeckite Zone at least, extends farther south in the area of the Wittenoom Sub-Province, than crocidolite; it appears patchily along the south face of the Hamersley Range, where crocidolite is virtually absent. Secondly, in both riebeckite zones of the Dales Gorge Member, crocidolite extends farther east in the Wittenoom Sub-Province than massive riebeckite, which is absent from Junction Gorge.

In the Marra Mamba Sub-Province a broad regional sympathy in the distribution of the two main riebeckite forms has a similarly significant degree of local

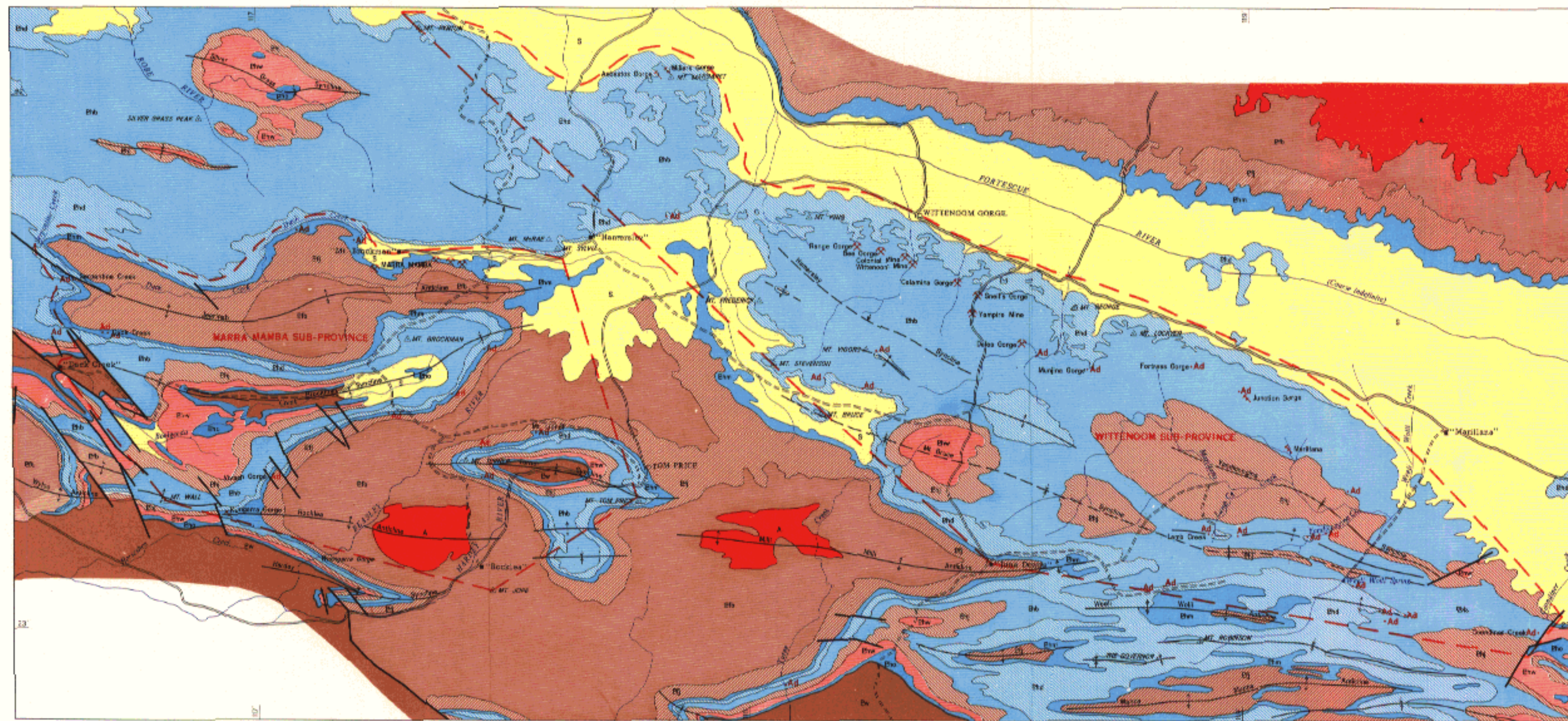
departure. Thus massive riebeckite is rare or absent in the Kungarra Gorge area, in the eastern part of the sub-province, where crocidolite is locally abundant.

Trendall (1965a, 1966a) tested the small-scale distributional inter-relationship of the crocidolite in the Upper Seam Horizon with massive riebeckite and a variety of other parameters, using all available drillholes in the Wittenoom area. No correlation was found between the length of fibre in the Upper Seam (in macroband BIF2) and either: (1) the thickness of BIF2, (2) the combined thicknesses of BIF2 and BIF3, (3) the total thickness of massive riebeckite in BIF2, (4) the total thickness of massive riebeckite in BIF3, (5) the combined thicknesses of massive riebeckite in BIF2 and BIF3, or (6) the ratio of massive riebeckite thickness of BIF2 to that in BIF3. Other correlations tested, all without success, were: (7) the thickness of BIF2 with total massive riebeckite thickness in BIF2, (8) the thickness of BIF3 with total massive riebeckite in BIF3, (9) the combined thicknesses of BIF2 and BIF3 with the combined massive riebeckite thicknesses in BIF2 and BIF3, (10) total massive riebeckite thickness in BIF2 with total massive riebeckite thickness of BIF3, and (11) thickness of BIF2 with thickness of BIF3.

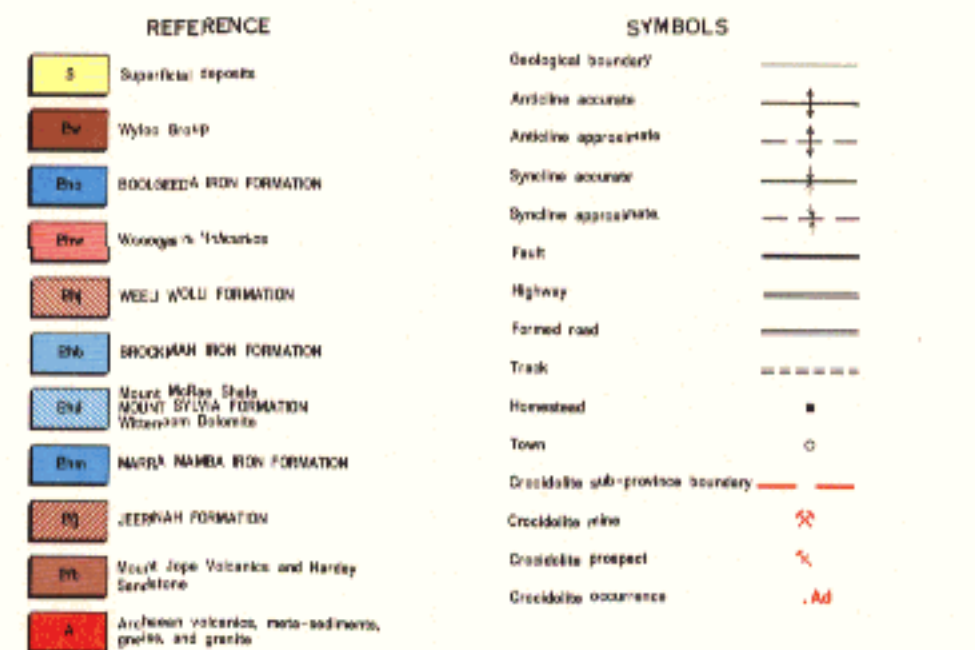
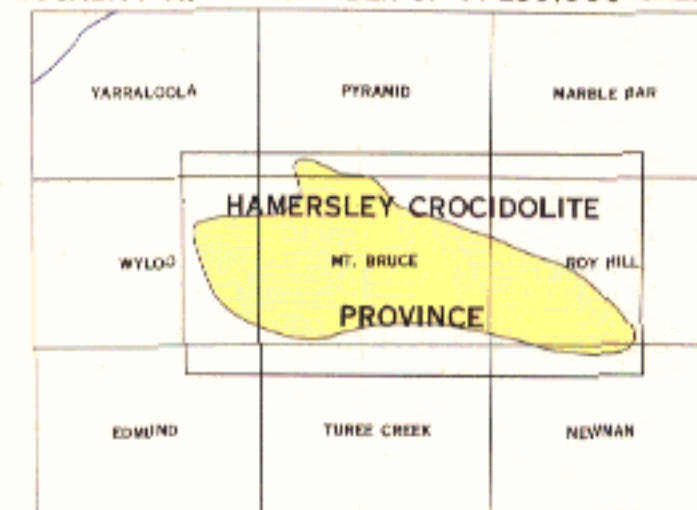
On the other hand an inverse relationship appeared in a correlation of: (12) length of fibre in Upper Seam Horizon with the ratio of massive riebeckite thickness in the upper part of BIF2 to that in the lower part. This final correlation was tested in response to a suggestion by Mr. B. Chapple that, provided any given core was fairly rich in riebeckite, fibre values in the Upper Seam tended to be high if the last riebeckite encountered before the seam in the drilling was more than 2 feet above it. Unfortunately, the scatter in both of this relationship and correlation 12 is so broad as to make both of them useless for practical application, and no significant small-scale relationship between massive riebeckite and crocidolite in drillhole data has yet been detected.

At Dales Gorge the plainly displayed three-dimensional relationship of the two crocidolite forms, in which crocidolite occurs in flat parallel ribbons either alternatively with, or overlapping, massive riebeckite (see further below in this chapter, Figure 53, and also Trendall 1966a) reflects closely the described comparison between their regional and small-scale relationships: the first broadly sympathetic and the second complex with some antipathy. From the relationship at Dales Gorge it would be independently deduced that drillhole data would give erratic results for correlating crocidolite and massive riebeckite quantitatively.

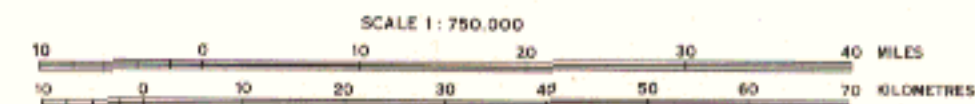
One small-scale example alone can be cited where a qualitative relationship between crocidolite and massive riebeckite is invariable. This is at the 'adit roof riebeckite' of the Yampire C Horizon. Crocidolite has never been seen at this level, either in core or in the field, unless massive riebeckite is present, although massive riebeckite may be present without crocidolite; 'no massive riebeckite, no crocidolite' appears to be an absolute rule in this instance.



LOCALITY MAP AND INDEX OF 1:250,000 SHEETS



GEOLOGICAL SURVEY OF WESTERN AUSTRALIA
GEOLOGICAL MAP
OF
THE HAMERSLEY CROCIDOLITE PROVINCE



PETROGRAPHY AND TEXTURAL RELATIONSHIPS OF RIEBECKITE FORMS

MASSIVE RIEBECKITE

SPATIAL RELATIONSHIP TO IRON FORMATION

It was noted above that massive riebeckite and the chert-magnetite groups of particular Calamina cyclothems are laterally intergradational, and thus stratigraphically correlative. This point was made also in preliminary publications (Trendall 1965a, 1966a). Because the observation has great interpretive significance (Chapter 11), and because initially it seemed contrary to expectations based on published views on the origin of riebeckite in iron formations, we summarise systematically here the evidence for a proposition which is self-evident to any geologist able to spend a day in the field in the Wittenoom—Yampire area.

Evidence for the stratigraphic equivalence of massive riebeckite and chert-magnetite groups of the Calamina cyclothem (formerly 'flat-modified cherts', see p. 60) is of three kinds:

1. Regional comparison of drillholes.
2. Direct observation of intergradation.
3. Ghost textures within massive riebeckite.

These three types of evidence are taken in order below.

Figure 51 adequately illustrates the precise stratigraphic equivalence of massive riebeckite and chert-magnetite groups. The exceptional confidence with which the mesobanding of the BIF macrobands of the Dales Gorge Member can be traced laterally and identified in core, leaves no doubt that, in any drillhole, *either* massive riebeckite *or* the appropriate chert-magnetite group is *always* present at any level where massive riebeckite is likely to occur; *never* are either *both* or *neither* present. The massive riebeckite usually occupies a slightly greater thickness than the mesobands whose place it occupies; from averaged measurements on all available holes the chert-magnetite/riebeckite ratio is about 1:1½.

The expectation from this relationship in drill-core is that a passage from one to the other should somewhere exist. Such passages at Dales Gorge were fully described, but not directly figured, by Trendall (1966a). In the photograph of Figure 53 the main features described by Trendall are illustrated. Parallel strips of massive riebeckite (riebeckite swells) with a flat lenticular cross section are aligned side-by-side, and about 60 inches apart (centre-to-centre), with a northeasterly elongation (see p. 162). They are mainly confined within narrow stratigraphic limits representing chert-magnetite groups of the Calamina cyclothem. The chert-magnetite/riebeckite thickness ratio is here about 1:1.4. The marginal transition from riebeckite to chert-magnetite at the edge of a riebeckite swell is shown more closely in Figure 54. In this instance the riebeckite represents also, at the top, the mixed group of the cyclothem concerned, and continues upwards

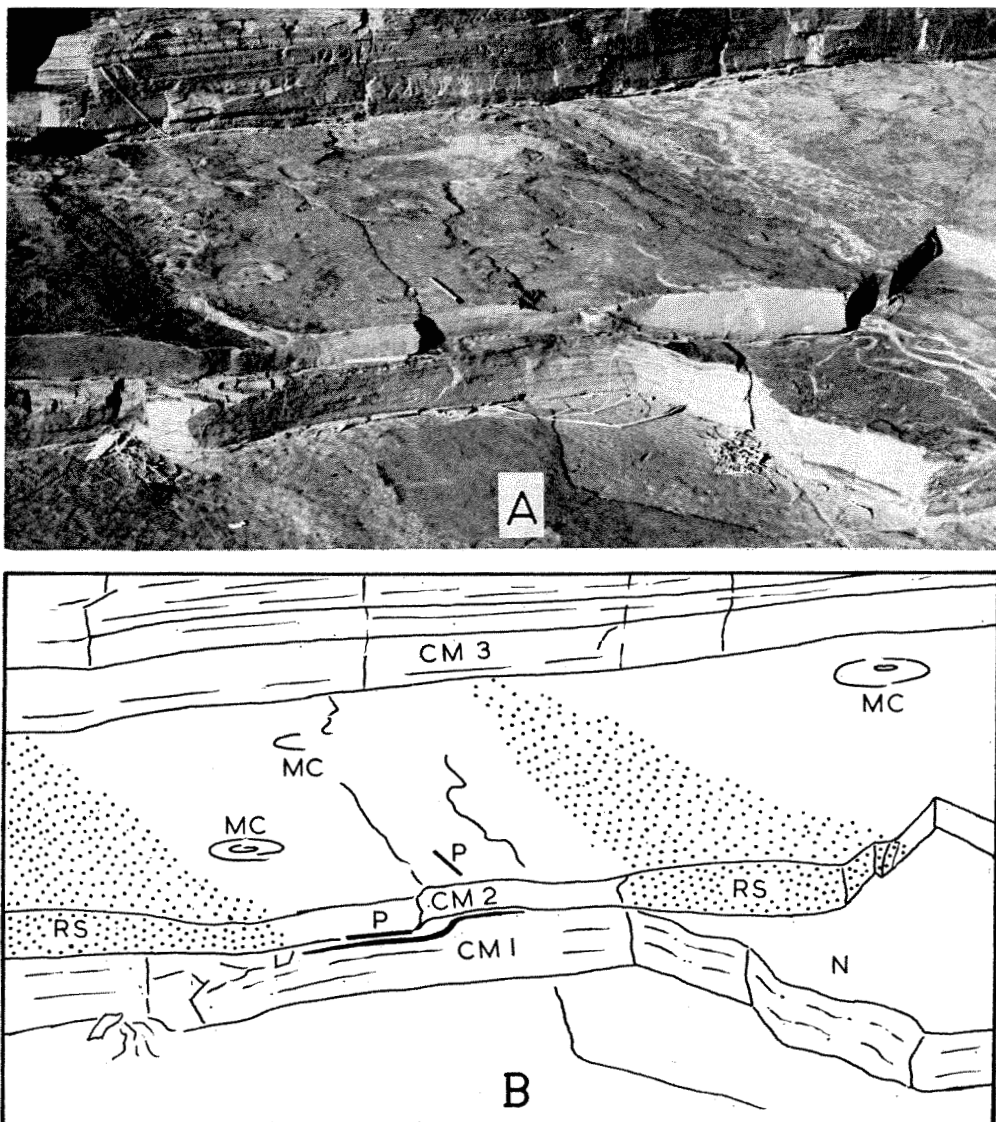


Figure 53. Riebeckite swells and associated structures in Dales Gorge. The photograph in A was taken looking eastwards over the flat gorge floor at 325 feet (see Trendall, 1966a, for exact location significance of this footage). In B a traced sketch of the photograph is provided with identifying letters and symbols. The scale is shown by a central pen and pencil, each 6 inches long and marked by a P in B. The rocks shown are part of the BIF1 macroband of the Dales Gorge Member, between about 50.5 feet (the surface on which the letter B appears) and 53 feet on the type section (Trendall and Blockley, 1968). Three successive chert-magnetite groups of the Calamina cyclothem, marked CM1, CM2 and CM3, appear from below upwards, separated by thin mixed groups with abundant small spheroidal nodules; a typically exposed nodular surface between CM1 and CM2 is marked N. CM2 is the third maculate band (MB3) of Trendall (1966a), and the random distribution of

into the overlying chert-magnetite group, which is represented by riebeckite across the whole width of the photograph. Massive riebeckite also occurs within macule cores in a similar way to its occurrence within riebeckite swells (Figure 42B).

The lateral gradation from massive riebeckite to the virtually riebeckite-free iron formation may take place over several feet or within less than an inch, as in Figure 54. In either case the transition involves a steady appearance of riebeckite in the iron formation without significant disturbance of its textures. Both the mesobanding and some of the internal mesoband textures of the iron formation often continue within the massive riebeckite as barely perceptible differences in colour; such ghost textures are most apparent in cleanly sawcut or cored material, and may often be emphasized by etching with mild acid; where thin magnetite mesobands pass into massive riebeckite there is a much greater thickness differential between the magnetite and its textural riebeckite equivalent than is the case for chert mesobands; the riebeckite ghost is commonly up to four times the thickness of its equivalent magnetite. Riebeckite is not invariably present in duplicate swells of the chert-magnetite group at Dales Gorge. As noted by Trendall (1966a, p. 78-79, and Plate 40) swells may occur without riebeckite. Their existence is important for the interpretation of riebeckite paragenesis, and is referred to in discussion in Chapter 11.

PETROGRAPHY

In thin-sections of standard thickness (0.03 mm) massive riebeckite is semi-opaque, effectively isotropic, and has no optically resolvable crystalline structure. In sections less than about 0.01 mm thick a blotchy texture is often discernible, with poorly defined patches of darker and lighter blue about half a millimetre across, some of which have a vague vertical streakiness (Figure 56A); there is still no clear extinction or crystallinity, although each differently coloured area tends to extinguish as a vague entity. No other mineral is consistently present in massive riebeckite, but the ghost textures equivalent to those of the adjacent iron formation are often emphasized by linearly arranged, small, irregular patches of chert. The boundaries of these are always made indistinct by a fringing felt of riebeckite hairs apparently continuous with the structure of the adjacent massive riebeckite, and protruding from it into, or often across, the chert; the hairs are usually less than 1 micron thick. From these observations massive riebeckite is assumed to consist of comparatively coarse aggregates of very finely fibrous riebeckite with some degree of common orientation, interlocking with neighbouring aggregates in an unknown way.

macules (MC) appears on its top surface. Two riebeckite swells are marked in B by the letters RS, and the dark blue massive riebeckite is stippled. The swells are elongate in a northeasterly direction (the direction of the pencil on the top of CM2), and are 55 inches apart, centre-to-centre. Between these swells, CM2 contains no massive riebeckite, but instead has in the mixed group below it, up to $\frac{1}{2}$ -inch of crocidolite, marked in B as a thick black line below the pen P. The crocidolite thus occurs as a thin flat ribbon elongate in a northeasterly direction.

At Marra Mamba the thicker mesobands of massive riebeckite are sometimes quite coarsely granular, especially in the axial parts of small folds. In thin-section these have blades of well crystalline riebeckite up to 5 mm long, each one of which appears in the slide as a group of several irregular optically continuous pieces interlocking closely with the adjacent crystals.

Where a ghost band in massive riebeckite is identifiable as equivalent to a thin magnetite mesoband in the adjacent iron formation then magnetite may be abundant in the riebeckite. Such magnetite is always sharply euhedral, exactly like that of the iron formation, except that the crystals are separated by riebeckite with the usual texture of massive riebeckite. By gradual decrease in magnetite

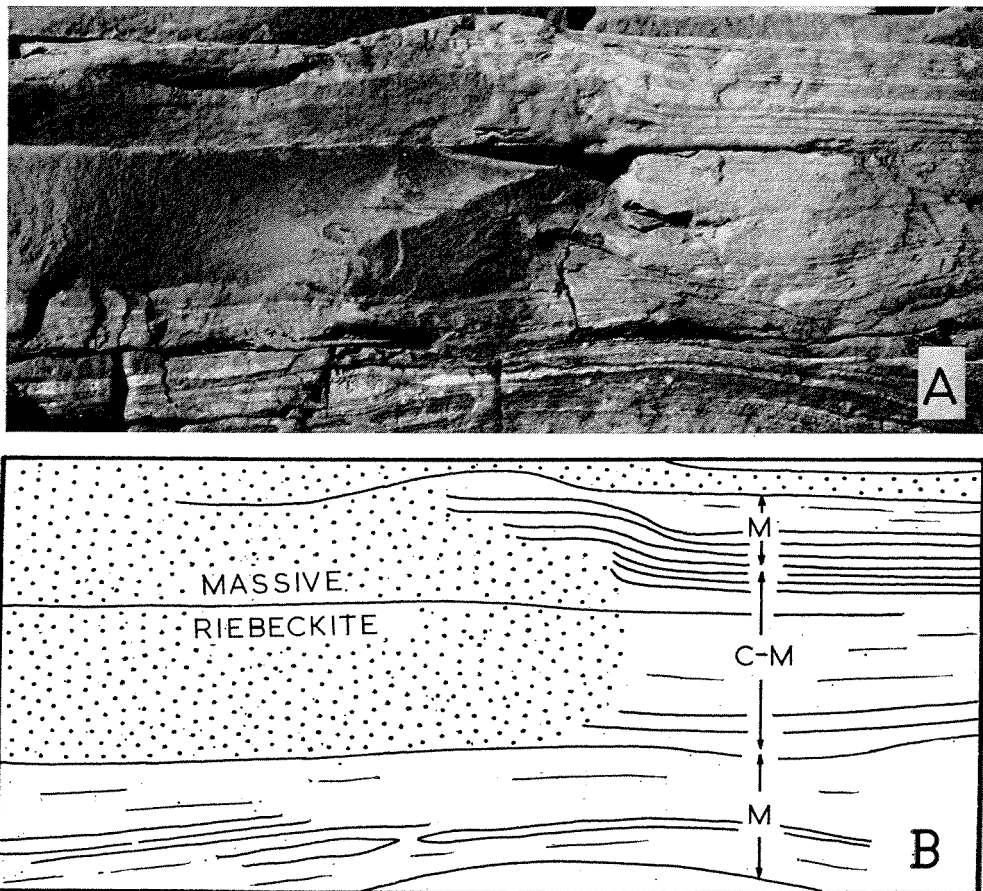


Figure 54. Detail of the lateral passage from the chert-magnetite group of the Calamina cyclothem to massive riebeckite. Photograph taken looking northeastwards at a vertical joint face in Dales Gorge at about 750 feet (see Trendall, 1966a). In B, a traced sketch from the photograph, massive riebeckite is stippled, while M and C-M mark mixed and chert-magnetite groups respectively of the Calamina cyclothem. A total stratigraphic thickness of about 8 inches of BIF1 of the Dales Gorge Member is illustrated between about 50.3 and 51.0 feet on the type section.

content, without change in thickness, such magnetite-bearing ghost bands pass laterally into magnetite-free massive riebeckite, defined as a ghost only by a faint colour difference not usually detectable in thin-section.

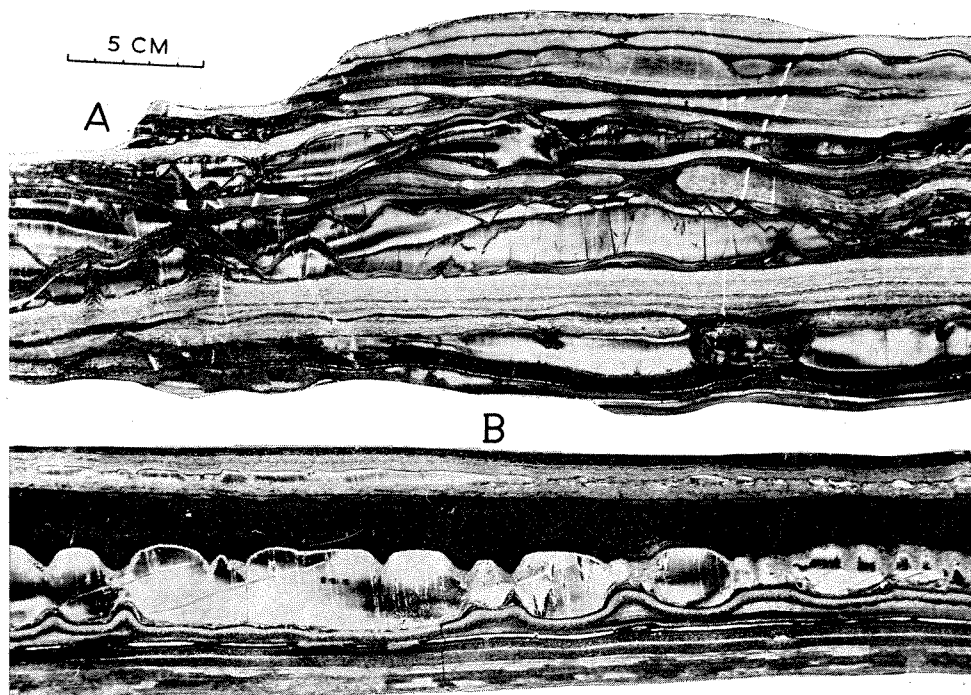


Figure 55. Typical forms of occurrence of crocidolite in the Dales Gorge Member.

A. Typical ore from the Upper Seam of the Colonial mine at Wittenoom. The piece is a grab sample from the outgoing conveyor belt of the mine, and stratigraphic top and bottom are not known. Thin microband chert mesobands are separated by magnetite mesobands in which a variable thickness of crocidolite may be present. Cones, with the chert microbands of some curving into the cores, curved fibre, and magnetite screens are well displayed. This photograph of a cut and smoothed surface was taken through glass with glycerine between it and the rock. This has a generally lightening effect on the cherts, and some of the magnetite. It causes thin cracks across the cherts, caused by blasting, to stand out in white; the thin black lines in the thickest crocidolite mesoband, parallel with the fibre direction, best seen in the right-central area, are quartz intercalations.

B. Typical crocidolite from the mixed group of the Calamina cyclothem. This example is from just below the adit roof riebeckite (see Figure 5) in the BIF2 macroband (Yampire C Crocidolite Horizon) at the old West Australian Blue Asbestos Fibres Ltd. mine at Yampire Gorge. The main central crocidolite mesoband is at above 77.4 feet on the type section. Note the lateral variation in crocidolite thickness, and the cones (or corrugations) projecting into it from both upper and lower surfaces. There is no projection from the lower surface without a corresponding projection from the upper surfaces, but upper surface projections may stand alone. The very dark mesoband above this crocidolite is massive riebeckite with thinner crocidolite associated with magnetite within it. The magnetite appears mainly white because of the lighting conditions used. Below the main crocidolite mesoband there are microbanded cherts and chert-matrix. The observer is looking due east at a vertically cut surface, and the clearly displayed kink bands dip from south to north.

CROCIDOLITE

SPATIAL RELATIONSHIP TO IRON FORMATION

It has already been recorded that crocidolite in the Dales Gorge Member is restricted to two positions in the detailed mesoband sequence: the mixed groups of the Calamina cyclothem and the close-packed chert sequences. This restriction is the basis for the two distinct types of crocidolite occurrence, which are illustrated in Figure 55.

Figure 55A shows a typical piece of Upper Seam ore from the Colonial mine at Wittenoom, and illustrates crocidolite occurrence in a close-packed chert sequence. Crocidolite mesobands about $\frac{1}{4}$ -inch to over an inch thick alternate with groups of two or three thin cherts separated only by thin magnetite mesobands. The separation between the crocidolite mesobands is between about 2 and 4 times their thickness. Six to eighteen crocidolite mesobands over about 18 inches thickness are typical of this seam. Each mesoband fluctuates rapidly in thickness, in sympathy with either podding or waviness of the adjacent cherts; these changes in thickness tend to be antipathetic between adjacent mesobands, in such a way that variations in the total length of fibre in the seam in different vertical transects is negligible compared with variation of the individual mesobands. This total variation in fibre thickness of a seam, or deposit, is best known at Wittenoom, and details are given later in this chapter. We know virtually nothing about the areal shape and range in lateral extent of the individual mesobands in this type of occurrence.

Figure 55B shows, in contrast, the typical occurrence of crocidolite in a mixed group of the Calamina cyclothem. Often, as in the example illustrated, it lies immediately adjacent to the massive riebeckite which represents the neighbouring chert-magnetite group. At the level of this example, as was noted above, crocidolite *only* occurs with massive riebeckite, but at other levels, for example in BIF0 at Dales Gorge, crocidolite may occur sporadically in almost any mixed group of the macroband, even where no massive riebeckite is locally developed in the chert-magnetite groups. In either case it is characteristic of this type of occurrence that instead of being more or less evenly and closely spaced out among thin cherts the individual crocidolite mesobands are grouped at the 6-in. intervals of the cyclothem, either singly or in clusters of two or three. Such mesobands usually have greater lateral continuity than that of those among close-packed cherts, and more even thickness, if the cones and corrugations (described further below) are ignored.

At Dales Gorge the areal shape of at least some mesobands of this type of occurrence in BIF1 was demonstrated to be flat parallel strips, about 3 feet wide and an inch or two thick, elongate indefinitely in a northeasterly direction (Trendall 1966a; our figure 53) in sympathy with the controlling northeast structures (p. 163). Although the same structures are present in a less apparent form at Wittenoom and Yampire Gorge, where they exert at least some control over the crocidolite (Figure 56B), we cannot say how widespread throughout the Hamersley Range area this control is.

The crocidolite mesobands in both types of occurrence have two important features in common in their relationship to the adjacent iron formation: a magnetite mesoband lies on at least one side of each crocidolite mesoband, and each crocidolite mesoband dies out laterally in some observable direction within a few feet at most. The first feature is an invariable association, of which more details are given below the following heading. The second feature is an important difference from the relationship of massive riebeckite to the iron formation. It is a directly observable fact that when a crocidolite mesoband pinches out laterally no other material appears in its place. This is also the expected relationship from detailed correlation between drillholes, in which crocidolite may or may not be present in some magnetite mesobands; but if crocidolite is absent then nothing else is there to represent it. Attention is drawn here to the correlation of Figures 7C and 55B.

The variation in the quantity of magnetite present per unit area in the magnetite mesoband or mesobands adjacent to any crocidolite mesoband does not increase significantly as these are followed laterally beyond the termination of the crocidolite; the presence or absence of crocidolite makes no quantitative difference to the magnetite whatsoever. This point is emphasized here, since it is important for later discussion (p. 300).

STRUCTURAL PETROGRAPHY

In the Wittenoom Sub-Province the simplest possible representation of a single crocidolite band is as a parallel-sided planar sheet concordant with the banding of the enclosing iron formation, with the fibres perfectly parallel and lying normal to the planar extent of the sheet. Component fibres are not resolvable with the optical microscope and in bulk the fibrous aggregate has straight extinction; our work has added nothing to the rather limited published information on the fine structure of crocidolite (e.g. Hodgson, 1965a). The bounding mesobands, above and below, either are both magnetite, or one is magnetite and the other is chert. Although the association with magnetite is invariable this exact geometrical representation is a non-existent theoretical ideal, since it is characteristic of crocidolite mesobands that they exhibit a wide variety of complex structures (Figure 55). These have been described in Western Australian crocidolite by Finucane (1939), Miles (1942), and Trueman (1963); structures in South African crocidolite have been described by, among others, Hall (1918, 1930) and Du Toit (1946). Of all these, Du Toit's account is the most thorough, but none provide a systematic classification of the various structures. The following attempt at such a classification is based on departures from the theoretical ideal with which this paragraph began:

1. Structure defined by lateral thickness variations.
 - A. Total mesoband thickness variation.
 - B. Cones and corrugations.

2. Structures defined by variation of fibre orientation.
 - A. Inclination of straight fibre.
 - B. Curved fibre.
 - C. Mixed fibre.
 - D. Kink bands.
3. Discontinuities in fibre.
 - A. Central parting.
 - B. Planes of fracture.
4. Structures in associated magnetite.
 - A. Internal magnetite screens.
 - B. Marginal disruption of magnetite.
5. Structures defined by, or in, associated quartz.
 - A. Quartz within fibre.
 - B. Marginal fibrous quartz.
6. Miscellaneous structures of uncertain status.
 - A. Dark lines.
 - B. 'Turbulence structure'.

This classification is not a natural one, in that separately grouped structures (for example 1B and 4B) are always closely associated. But it is a convenient one for use in the following short descriptions of these various structures, in which indications of association are given, in which the headings follow the numbering above, and which is accompanied by illustrations of the more important structures.

1A. Total mesoband thickness variation. Our meagre knowledge of the three-dimensional shape of crocidolite mesobands has already been set out under the preceding heading.

1B. Cones and corrugations. These names are applied to abrupt local constrictions in crocidolite mesobands which are often superimposed on the more general variations of thickness. Good examples are present in Figure 55B, and less conspicuous ones in Figure 55A. The constrictions in Figure 55B may result from the transection either of conical marginal protrusions into the crocidolite or of similarly protruding ridges, or corrugations, which in cross section appear structurally identical. In the following paragraphs the descriptions of cones may be taken to apply to corrugations also, unless a specific distinction is made. The areal distribution of cones and corrugations on the lower surface of the thicker crocidolite mesoband of Figure 55B is shown in Figure 56B. Miles (1942, Figures 9 and 10) published good photographs of cones from Yampire Gorge.

Cones may appear on only one side of a mesoband (single cones), or each protrusion may be matched by an equal or a lesser protrusion from the opposite side of the mesoband (both constituting a pair of cones). Single and paired cones are often present together in one mesoband, and where this is so the single cones are almost invariably restricted to one side only (Figure 55B). The single

cones, and the parts of the paired cones on the same side as the single cones, have a structure different from the parts of the paired cones on the side remote from the single cones. Single cones very rarely appear on both sides of a mesoband. The side of a mesoband with single cones is here called the mobile side, and the other the fixed side. The significance of these terms appears in later discussion (Chapter 11). In Figure 55B the mobile side is uppermost in the main crocidolite mesoband. There is no consistent orientation of the fixed and mobile sides of crocidolite mesobands; in those of Figure 55A, where top and bottom are not known, various mesobands have cones on different sides. Wherever crocidolite is present next to massive riebeckite it forms the mobile side, whether it is at the top or the bottom.

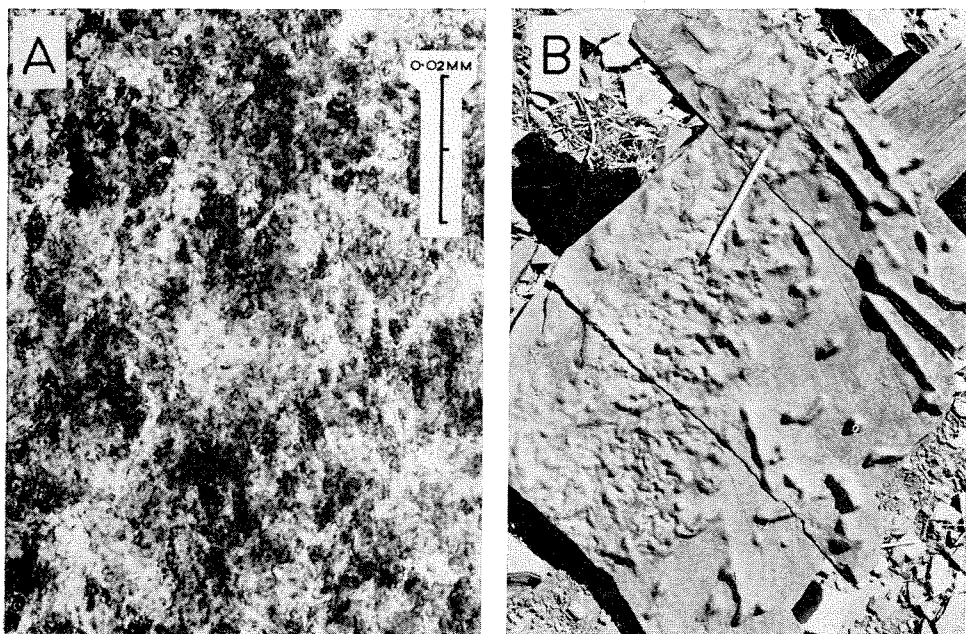


Figure 56. A. Photomicrograph of massive riebeckite from the lower part of the adit roof riebeckite just below 500 feet in Hole 22 at Wittenoom Gorge, equivalent to about 77.6 feet on the type section (Figure 5). Individual fibres of the meshwork are not resolvable, and the only apparent structures are the vague blotchiness on a scale of about half a millimetre, and the local vertical streakiness.

B. Photograph looking vertically down at the top surface of slabs of iron formation split from below the crocidolite mesoband just below the adit roof riebeckite at the old mine in Yampire Gorge (see Figure 55B caption); this is therefore the shape of the lower surface of the crocidolite mesoband. The pencil is 6 inches long and points on a bearing of 30°, roughly parallel to a central division across the slabs between areas of different structural type. At this locality this difference is related to a thinning and thickening of the crocidolite in sympathy with the northeast structural direction; where the crocidolite is thinner the lower surface is highly irregular (northwesterly area in the photograph) and where it is thicker the cones and corrugations are scattered and relatively simple (southeasterly area in the photograph).

The structural features of a typical pair of cones are sketched in Figure 57A. The shape is taken from a thin-section cut from the main mesoband of Figure 55B; photomicrographs of parts of the same thin-section form Figure 57B and C. The cone on the mobile side is characterised by the complexity of the magnetite structure between the crocidolite and the core. In the example illustrated the marginal magnetite mesoband, which in the smooth parts of the upper crocidolite boundary (Figure 55B) is evenly planar, apparently solid magnetite, and about a millimetre thick, curves gently down into the cone and quickly passes into a zone of separate plates and octahedra of magnetite, several millimetres across. The magnetite plates are euhedral, of the normal magnetite mesoband form

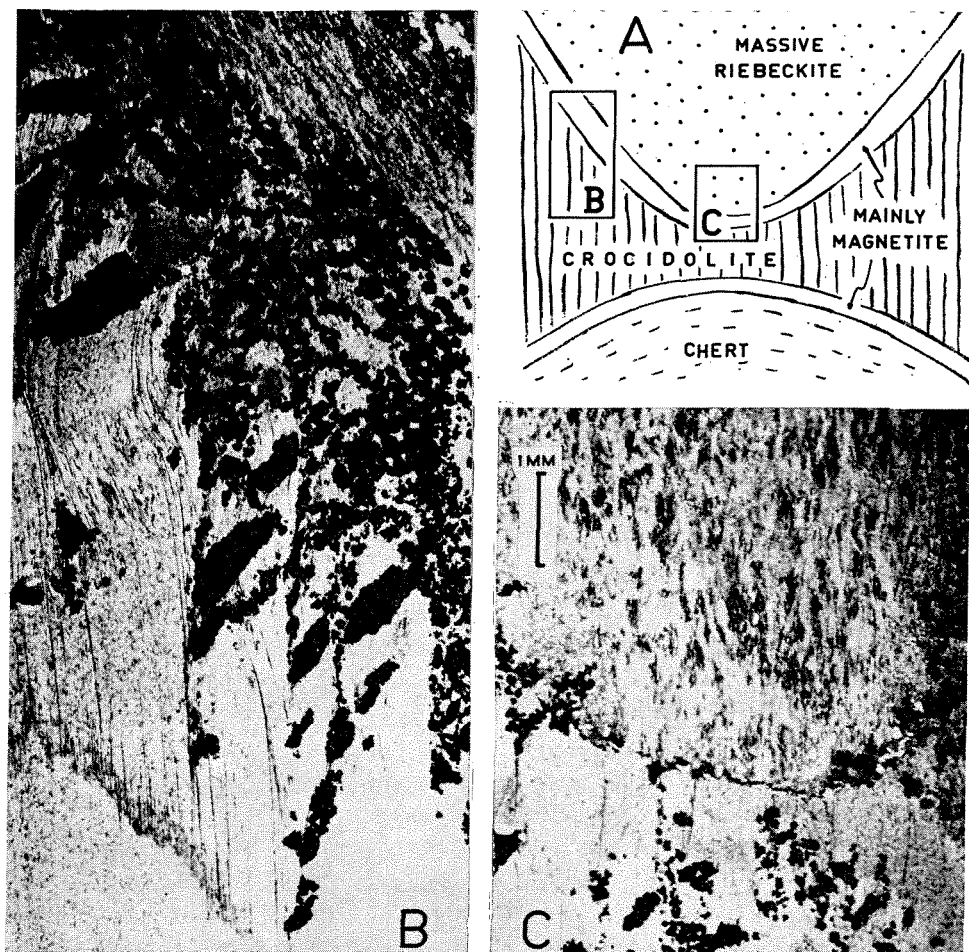


Figure 57. A. Diagrammatic sketch of an opposed pair of cones in a crocidolite mesoband such as that illustrated in Figure 55B.

B and C are photographs of thin-sections of a cone pair from that specimen, and show the marginal interrelationship of massive riebeckite, magnetite and crocidolite. The features illustrated are described in the text.

(Chapter 4). Like the smaller associated octahedra and all other magnetite structurally associated with crocidolite, they have perfect flat faces and sharp edges; there is never any sign of corrosion or departure from a euhedral outline. The plates are arranged in a stepped fashion (see Miles, 1942, Figures 9 and 10), and are offset along planar (actually cylindrical in cones) surfaces along the general direction of the fibre. The slope direction of the plates in Figure 57B is not present in all cones; in many the separate plates are either horizontal, or parallel to the cone edge, but they are always stepped and parallel with each other. The edges of the opposite cone of this pair bend into the fibre in a similar way, but lack this complex imbricate structure, which is confined to one side, the mobile side, of mesobands.

The cores of cones may variously be occupied by an expanded part of the adjacent mesoband, or by different material. Where massive riebeckite lies along the mobile side this invariably expands into the cores. In the example of Figure 57 the uppermost massive riebeckite mesoband has a line of chert patches just above its base, and this curves down into the cone; patches of chert in this line are visible in the top right-hand corner of Figure 57B. Massive riebeckite in cone cores usually has a vertical structure developed in the furthest central extension of the cones (Figure 57C). Expansion into cone cores is more obvious where chert is the adjacent material on the mobile side. It is clearly displayed by the curvature of the microbanding into the cores; examples are clear in Figure 55A. The alternative type of core filling occurs when the adjacent mesoband continues undisturbed across the 'base' of the cone. This has only been seen in the Upper Seam at Wittenoom. The cores then consist of a complex and coarsely crystalline aggregate of quartz, stilpnomelane, riebeckite, dolomite, and apatite, showing no compositional or textural resemblance to any known mesoband type.

In Figure 55B, most clearly on the right-hand side, it is evident that the parts of paired cones on the fixed (lower) side of the main crocidolite mesoband are partly cored by pods of a thin underlying chert.

2A. Inclination of straight fibre. The inclination of the fibres in crocidolite mesobands commonly departs up to 10° from the exact perpendicular to the planar extent of the mesoband (Figure 55B). Greater inclination of straight fibre is rare (see also 'Slip-fibre', later in this chapter).

2B. Curved fibre. Fibre is commonly curved, either consistently in one plane and direction, or in a variety of directions in irregular mesobands (Figure 55A).

2C. Mixed fibre. Crocidolite mesobands very commonly have a mixture of straight and curved fibre; a particularly common form is for the inner part to have straight fibre which curves increasingly at one or both ends.

2D. Kink bands. These are a distinctive form of fibre curvature. In their simplest expression parallel kink bands cross the mesoband at an angle of about 20° . The bands are up to about a millimetre wide, and within them all the fibre is parallel, and evenly kinked so that it dips, in a horizontal mesoband in which the kink bands themselves dip at θ° , at an angle of $(90-2\theta)^\circ$ in the opposite

direction to the bands. Good examples appear in Figure 55B. They die away at the mesoband edges, and the marginal parts of a set of typical kink bands are shown in Figure 58.

In their more complex expression kink bands may vary in orientation both across and along a crocidolite mesoband, and each band may consist, in detail, of a number of subordinate kinks in an echelon pattern. Individual fibres teased from kinked mesobands show no apparant weakness at the kinks.

3A. Central parting. Some crocidolite mesobands have a central plane of discontinuity at which teased fibres break off separately. It is usually rather wavy, and appears in thin-section as a vaguely defined dark line, sometimes with a few small magnetites distributed along it.

3B. Planes of fracture. Some mesobands from Junction Gorge have fibre which is very sharply bent once (unlike kink banding) along a plane sub-parallel to the sides. This bending locally continued to a point (about 90°) of complete fracture of the fibres. The structure is rare.

4A. Internal magnetite screens. Internal 'screens' of magnetite are present in many crocidolite mesobands, and are particularly abundant in those of close-packed chert sequences. They consist of thin sheets of magnetite which branch out obliquely into the crocidolite from the marginal magnetite mesoband and pursue an irregularly zig-zag course laterally through the fibre before terminating either on the same or on the opposite side of the crocidolite mesobands, usually a few inches further along from the start. There are commonly two or three separate screens spaced out across any single cross section of a mesoband in which screens occur, and there may be double this number in exceptionally thick mesobands; mostly, adjacent screens zig-zag in sympathy, but it is possible for one screen to be flat in a part of a mesoband where the neighbouring screen is erratic. Two or more screens may come together within the fibre and either continue as one to the edge, or may redivide before this. Very thin chert pods may be present in association with screens.

The three-dimensional shape of screens is not clearly known, but it may be assumed to be similar to that of mesoband surfaces (Figure 56B). Where magnetite screens rise steeply out of a mesoband edge and return to the same edge after one sharp bend they closely resemble cones; indeed, the screens often consist of separate plates in such situations, although the plates are usually closer than those of cones. Such structures are, in effect, cones with crocidolite-filled cores.

All the described features of screens can be picked out in Figure 55A.

4B. Marginal disruption of magnetite. The disruption referred to here is that of cones; it was described under heading 1B.

5A. Quartz within crocidolite. Thin intercalations of quartz parallel with the fibre direction are a common feature of much crocidolite. They rarely exceed 0.5 mm at the mesoband edge, and usually wedge out across it. They usually occur

in clusters, and form a negligible proportion of the total mesoband volume. Some are present in Figure 55A. Along the edges of these intercalations slivers of bent and broken fibre often project from the crocidolite of the walls into the quartz.

5B. Marginal fibrous quartz. The sense in which quartz is called fibrous in this bulletin was explained in Chapter 4 (p. 117). Fibrous quartz commonly occurs along one or both margins of crocidolite mesobands of the Wittenoom Sub-Province, and is associated in particular with crocidolite in the mixed groups of the Calamina cyclothem. It is usually less than $\frac{1}{4}$ -inch thick (perpendicular to the banding) and may either be of constant thickness or vary in sympathy with puckering of the adjacent mesoband, usually magnetite, so that it resembles the fibrous quartz associated with small folds remote from crocidolite (Figures 46 and 47). The thickness of marginal fibrous quartz is not related to that of the crocidolite against which it lies. Like other fibrous quartz it owes its fibrous appearance, in part at least, to some included fibrous or platy mineral, in this case always riebeckite (Figure 58A). Its contact with the crocidolite may be smooth and sharp or, as in Figure 58, slightly ragged. As also illustrated in that figure, its fibre direction is usually inclined at a low angle to the banding, a direction often attained by steady curvature away from parallelism with the crocidolite at the junction of the two minerals. The actual relatively coarse crystallinity of the quartz, with a tendency for elongation along the fibre direction, is shown in Figure 58B.

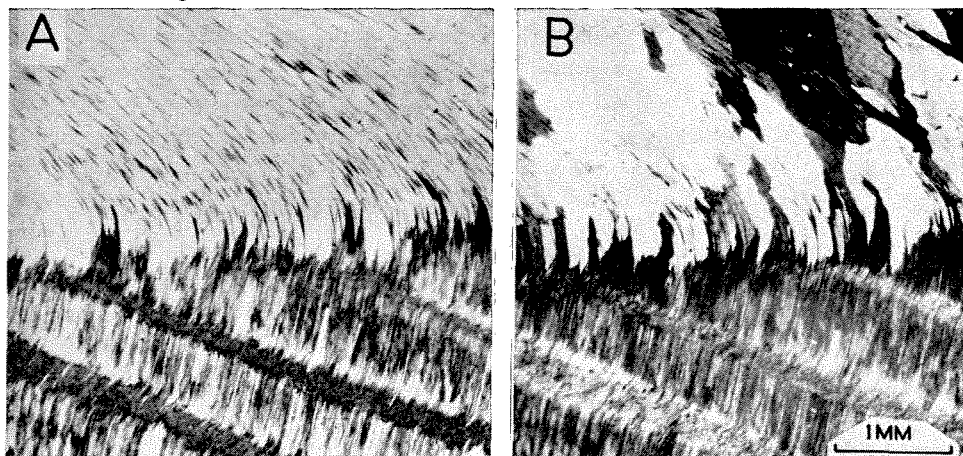


Figure 58. Photomicrographs of the edge of a crocidolite mesoband with marginal fibrous quartz in ordinary light (A) and between crossed nicols (B). This example comes from Yampire Gorge at the old West Australian Blue Asbestos Fibres Limited mine, in BIF2 of the Dales Gorge Member just above massive riebeckite at 73.0 feet on the type section (Figure 5). This is within the Yampire C Crocidolite Horizon. In this photograph the observer is looking easterly at a vertical section and the following points should be noted: the well developed kink bands are in the opposite sense to those of Figure 55B (which are about $4\frac{1}{2}$ feet stratigraphically higher); the fibrous quartz, with its small fibrous riebeckite content, has a stress sense opposite to that of the kink bands (and like that of Figure 47); the fibrous quartz is quite coarsely crystalline (B); there is a ragged but fairly abrupt boundary between quartz and crocidolite.

Marginal fibrous quartz may be involved with adjacent magnetite in complex dislocational structures rather similar to those at the margins of cones in crocidolite, and involving sharp curvatures of the fibre direction; but fibrous quartz never has kink bands, internal discontinuities, or magnetite screens with shapes like those of crocidolite. Only one exception to this last rule has been noted. G. R. Ryan collected from the spoil heap of the Colonial mine a rock with a mesoband of mixed fibrous quartz, minnesotaite, and dolomite. The fibres are $\frac{1}{2}$ -inch long, are straight, and are at right angles to the plane of the mesoband; this rock is discussed in Chapter 11 (p. 304).

6A. Dark lines. Many thin-sections of crocidolite, particularly near cones and corrugations or other irregularities, have dark zig-zag or straight lines running obliquely across the fibre. One such line crosses the lower left-hand corner of Figure 57B. Where two lines intersect one is generally offset by the

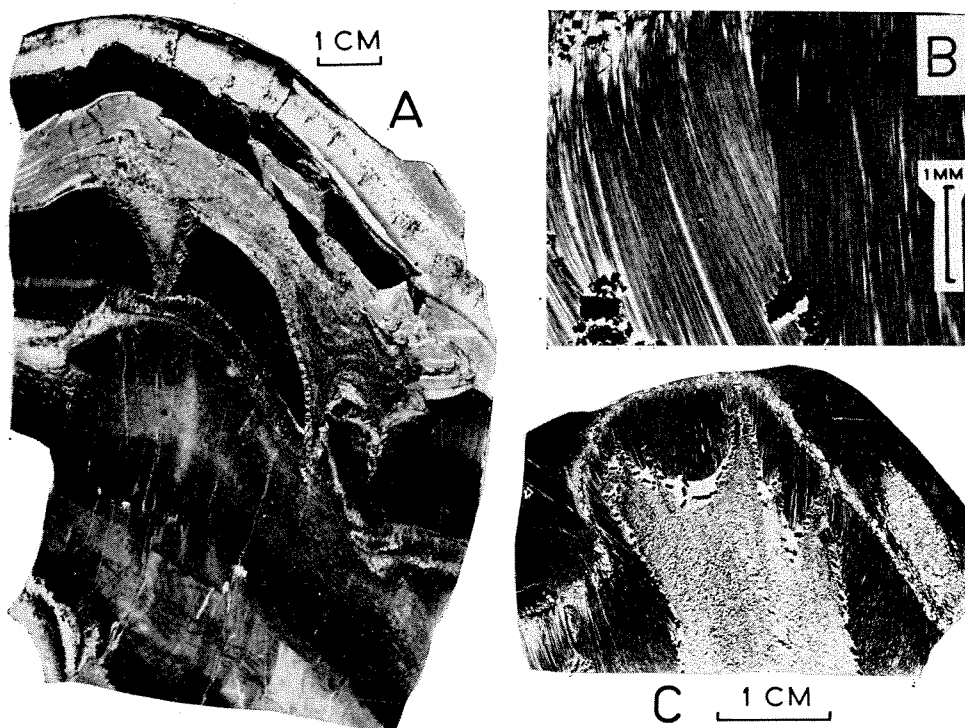


Figure 59. A. Looking westerly along the axis of a small fold in the Marra Mamba Iron Formation (Mackay Horizon on M.C.65W.P.—Plate 11), showing a crocidolite mesoband developed without evident structural relationship to the fold. Cones and (folded) kink bands are developed.

B. Enlarged view of upper left part of fold in C (both oriented as A, and from the same location) showing discordance within crocidolite apparently related to minor folding; this type of structure has never been seen in the structurally simpler Wittenoom Sub-Province.

C. Small fold in the Marra Mamba Iron Formation, with the core occupied by fibrous quartz apparently grown during its development, and after crocidolite growth.

other. It is never easy to see what these lines represent, but they seem most likely to be intersections of the plane of the thin-section with some internal planar discontinuity of the fibre cutting obliquely across the fibre direction at a low angle.

6B. Turbulence structure. This is a structure developed in crocidolite mesobands in which the sides are parallel and the fibre is straight and undisturbed. In such a situation, if any small inward-projecting marginal irregularity of the magnetite is present, the crocidolite inwards from it has a characteristic twisted structure. Among the even fibre on either side this twisted crocidolite resembles a patch of turbulently flowing liquid caused by an obstruction in a moving fluid with otherwise laminar flow.

The foregoing descriptions are applicable to all crocidolite from the Witte-noom Sub-Province, in which the crocidolite horizons have even and relatively gentle dips, and to much of the crocidolite of the Marra Mamba Sub-Province, which occurs in similarly undeformed iron formation. In the crocidolite occurrences at Marra Mamba itself there is often intense minor folding, with steep axial planes and very gently dipping axes along the regional fold direction. Most of the structures already described are present in the crocidolite in these folds (Figure 59); the main differences, and the relationship between the folds and the crocidolite, are summarised as follows:

1. Where crocidolite mesobands are a component of the folded iron formation they continue around the limbs, crests, and troughs of the folds, and do not preferentially thin or thicken in relation to these structural components.
2. Although it is usually curved the fibre has a broadly fan-like orientation in relation to the folds: it is neither parallel with the axial plane nor radial.
3. Kink bands are curved with the folds.
4. There is abundant development of marginal fibrous quartz, but this does not lie at a low angle to the banding, it is arranged, like the crocidolite, in a fanned pattern. The individual plates and octahedra of the magnetite along the crocidolite margins are each separated by quartz in a way exactly similar to the separation of magnetite by riebeckite in the edges of cones, but to a much greater degree. An aggregate of fibrous quartz and magnetite frequently fills the whole core of small folds (Figure 59C).
5. The fan-like orientation of the fibre around folds is accommodated, at least partly, by the development of radial surfaces along which a change of fibre direction is achieved by the discordant truncation of fibre on one or both sides (Figure 59B).

MINOR CONCORDANT FORMS OF RIEBECKITE

ACICULAR RIEBECKITE

Acicular, or needle, riebeckite is illustrated in Figure 60A, which is a larger scale photograph from a different thin-section of the same mesoband shown in Figure 30A. In this form of riebeckite elongate prisms, usually 1 to 3 mm long,

are distributed evenly but sparsely, with a random orientation, throughout the chert. Each prism splits terminally into numerous steadily finer fibres which curve divergently as they die away. Between examples from widely separated localities the size and shape of the riebeckites varies markedly, but they differ little within any one thin-section.

This form of riebeckite is neither common nor conspicuous. The example figured is from a chert which has nowhere been seen to be represented by massive

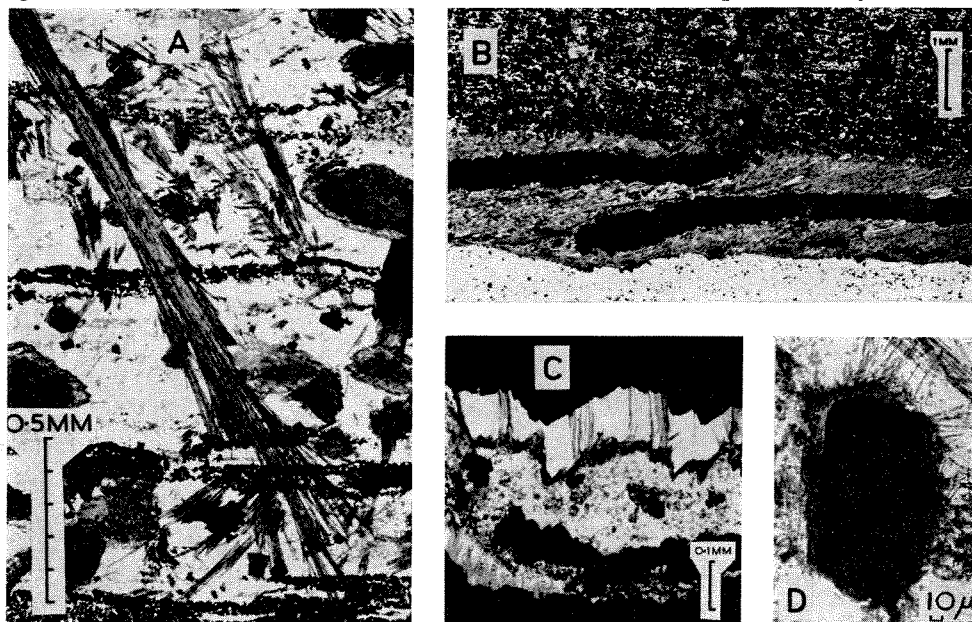


Figure 60. A. Needle riebeckite in a microbanded chert of the BIF2 macroband of the Dales Gorge Member at 648 feet 3 inches in Hole 40 at Wittenoom Gorge, just above 77.05 feet on the type section (Figure 5). The microbands are defined by hematite, and the only other abundant mineral in the chert is ankerite. See text for further notes; this chert is also illustrated in Figure 30A.

B. Slip-fibre in BIF2 of the Dales Gorge Member at about 514 feet in Hole 27 at Wittenoom Gorge, equivalent to about 76.5 feet on the type section. A thin magnetite mesoband marginal to the chert at the bottom of the photograph is displaced along the direction of the slip-fibre. From the topmost point of this 'floating' magnetite a thin discordant vein of randomly fibrous riebeckite cuts upwards through the overlying laminated chert-matrix.

C. Fibrous quartz projecting downwards from a tabular magnetite plate (probably a single crystal) within microbanded chert in the BIF2 macroband of the Dales Gorge Member at 478 feet 8½ inches in Hole 33 at Wittenoom Gorge, equivalent to 80.0 feet on the type section. A little stilpnomelane is interlaminated with the quartz, and along its lower edge there is a fringe of fibrous riebeckite whose shape is generally similar to that of the edge of the magnetite above it.

D. Small magnetite octahedron in chert, sheathed by finely fibrous riebeckite which marginally radiates out into the chert. This example is from a chert mesoband in the BIF2 macroband of the Dales Gorge Member at 646 feet 2 inches in Hole 40 at Wittenoom Gorge, equivalent to 79.3 feet on the type section (Figure 5).

riebeckite, although it seems to lie in the appropriate part of the Calamina cyclothem. We do not know whether acicular riebeckite is confined to cherts which never have massive riebeckite, nor how the lateral and vertical distribution of acicular riebeckite compares with that of either of the two main riebeckite forms. Three points argue that acicular riebeckite is a distinct form in its own right rather than a gradational state between chert and massive riebeckite: (1) the internal absence from massive riebeckite of any parts well enough crystalline to represent internal prisms of the order of size of acicular riebeckite, (2) the absence of acicular riebeckite in association with visible transitions between chert-magnetite groups and massive riebeckite (Figure 54), and (3) the existence of other forms thought to represent a closer textural gradation between massive riebeckite and chert-magnetite (see below).

No part of any riebeckite prism of this form has even been seen to be bent or broken, and its inclusion of the hematite including the microbanding suggests that it is a late material.

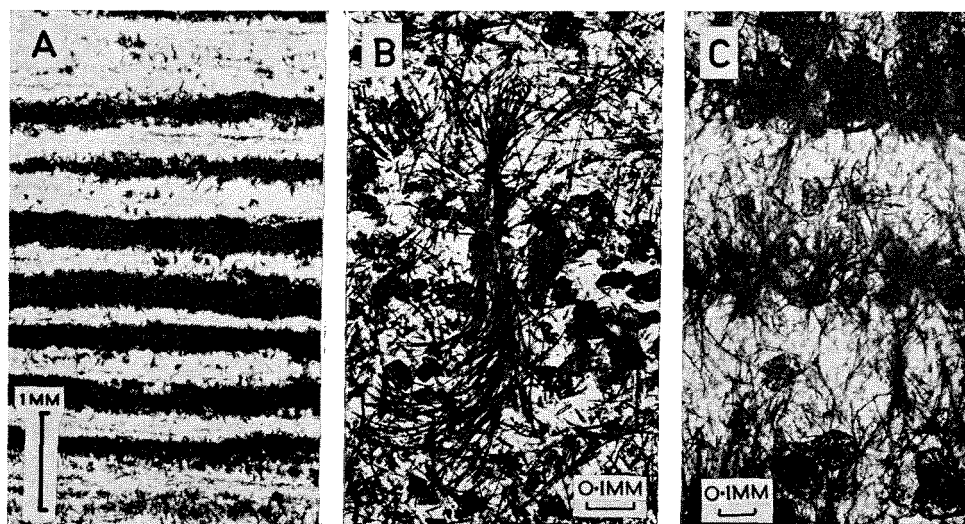


Figure 61. A. Microbanding strongly emphasized by riebeckite in a chert mesoband from the BIF3 macroband of the Dales Gorge Member at 555 feet in Hole 51 at Wittenoom Gorge, equivalent to about 91 feet on the type section. The riebeckite is finely fibrous, and occupies that part of each microband normally richer in ankerite.

B. A single sheaf-like bundle of fibrous riebeckite within chert in the BIF2 macroband of the Dales Gorge Member at 648 feet 2 inches in Hole 40 at Wittenoom Gorge, equivalent to about 77.2 feet on the type section. The axes of such sheaves are commonly, as here, nearly vertical.

C. Feathery riebeckite fibre bundles emphasizing the microbanding in a chert mesoband from the BIF2 macroband of the Dales Gorge Member at 479 feet 3 inches in Hole 33 at Wittenoom Gorge, equivalent to about 79.6 feet on the type section. Ankerite rhombs are also sheathed by fibrous riebeckite.

FORMS GRADATIONAL TO MASSIVE RIEBECKITE

It was noted in descriptions above that the transition between massive riebeckite and its equivalent chert-magnetite group in the Dales Gorge Member is relatively abrupt, so that any appropriate level is represented either by massive riebeckite or by almost riebeckite-free iron formation. Some chert mesobands within the riebeckite zones of the Dales Gorge Member, and throughout the Joffre Member, are liable to bear riebeckite locally in a striking textural form in which the microbanding is emphasized by the presence of riebeckite in one half only of each microband pair (Figure 61A). The riebeckite in this situation is effectively opaque and isotropic, and apparently has the same texture as that of massive riebeckite. It is commonly chert mesobands of the mixed group of the Calamina cyclothem in the Dales Gorge Member, and white cherts of the Knox cyclothem in the Joffre Member, which have this texture. In the Dales Gorge Member cherts it is the carbonate-rich component of the microbanding (Figure 21A) which is riebeckite, and all gradational forms in riebeckite abundance exist. Figure 61C shows the common appearance of a microbanded chert of the mixed group with quite a small total content of riebeckite. It is present in feathery sheaf-like fibrous bundles with a preferred elongation roughly vertical. In the Dales Gorge Member at Woongarra Gorge riebeckite of this type has its elongation vertical and in the axial plane of the Hardey Syncline, the north limb of which is there defined by the steep southerly dip of the banding, so that the riebeckite fibres define a penetrative axial-plane structure.

The thickest central part of each bundle in this form is about 0.1 mm long, and consists of a solid bundle of riebeckite fibres which lacks the optical resolvability of acicular riebeckite. It has no apparent nucleus of any other mineral than riebeckite, although in the example illustrated in Figure 61C the ankerite rhombs are also sheathed by fibrous riebeckite (see Figure 37B, and further below). The typical form of a single sheaf appears in Figure 61B.

Although it is not insisted at this point that this textural variety of riebeckite always represents a gradational stage between chert and massive riebeckite in the sense that it is a halted partial conversion of one to the other, its presence where mixed groups of the Calamina cyclothem pass into massive riebeckite does suggest that this is sometimes so. The origin of massive riebeckite is discussed at length in Chapter 11.

OTHER RIEBECKITE FORMS

Apart from the forms of riebeckite described either under the preceding headings, or to be described beneath the two following, this mineral is liable to occur in a wide variety of situations which have the two common characteristics that: (1) the riebeckite is of small total quantity, and (2) it is in prisms or fibres whose presence or absence does not affect the textural identity of the rock. Riebeckite of this kind may be regarded as having the status of an accessory mineral in an igneous rock. Such riebeckite occurs widely both within and

outside the riebeckite zones, and the following brief summary covers all the iron formation except that of the Weeli Wolli and Mount Sylvia Formations, in which, so far, no riebeckite has been seen.

A thin fringe of riebeckite coating magnetite grains is a widespread but erratically developed feature of almost any mesoband type in which magnetite occurs. (Chapter 4). The magnetite is always euhedral in such occurrences (Figure 60D). Riebeckite of similar appearance is sometimes separated by fibrous quartz from magnetite (Figure 60C). It has already been noted that fibrous riebeckite is also liable to fringe ankerite rhombs (Figure 37B) in a similar way.

In the Boolgeeda Iron Formation scattered prisms of well crystalline riebeckite are locally common, up to 0.5 mm long and stubbier than those of acicular riebeckite. They are subparallel to the bedding or, in strongly folded rocks, to the axial plane of the folds. A little fibrous riebeckite is also present in this formation.

It was noted earlier that the hollow carbonate rhombs which are present in some chert mesobands are occasionally cored by riebeckite.

Although riebeckite is not a common constituent of the shales a single prism of riebeckite appears in Figure 32C, and riebeckite is often present in tuffs of the Joffre Member

CROSS-CUTTING OCCURRENCES OF RIEBECKITE

In the excellent exposures of the Joffre Member at and downstream from Joffre Falls abundant cross-cutting veins mostly 0.1 to 0.2 mm thick dip steeply to the north-northeast, and are locally abundant. Fibrous riebeckite, with the fibres lying along the vein direction, is a common infilling material. The veins may be planar or, where they cross chert mesobands, may follow an erratic course like a vertically disposed stylolite. They are not usually continuous over more than a few inches. Similar riebeckite-filled veins occur rarely in the Dales Gorge Member in association with slip-fibre (see below and Figure 60B).

G. R. Ryan has reported two examples of relatively wide, vertically cross-cutting quartz veins with some riebeckite, one from the Brockman Iron Formation at latitude 22° 40'S, longitude 117° 02' 30"E and one of uncertain stratigraphic position from 5 miles northeast of Juna Downs homestead. The first of these has a width of 0.5 to 0.7 inches and cuts chert-matrix in the specimen collected. Fibrous quartz lying across the plane of the vein is the principal constituent, with a small proportion of fibrous riebeckite in scattered patches. Parallel lines of dusty inclusions within the quartz bear the irregularities of the walls and presumably represent growth stages in the opening of the vein.

SLIP-FIBRE RIEBECKITE

Slip-fibre is commonly associated with crocidolite of the Wittenoom Sub-Province; in the Marra Mamba Sub-Province it is not present at Marra Mamba itself, but its distribution elsewhere is uncertain.

Like true crocidolite, or cross-fibre, it consists of concordant fibrous mesobands with the fibre direction lying at an angle normally less than 20° to the banding (Figure 60B). Although some slip-fibre may exceed this inclination locally, and although some crocidolite may be inclined at an angle less than 70° to the banding (especially where there is marginal curvature), there can be no doubt that slip-fibre and cross-fibre are not simply end-members of a series of fibre types with intergradationally inclined fibre; mesobands of fibrous riebeckite are *either* relatively thick, with the fibres nearly at right angles to their planar extent, *or* they are relatively thin with the fibres at a low angle to their planar extent.

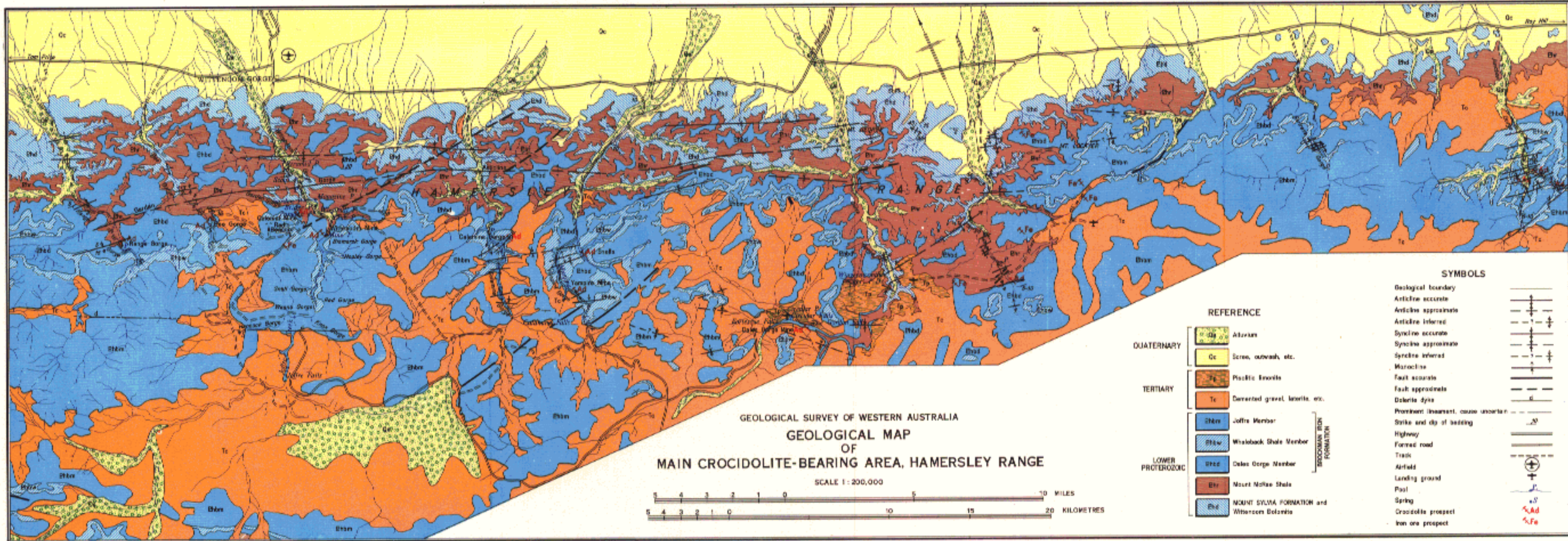
Slip-fibre is confined to the riebeckite zones but not to the crocidolite horizons, and may be developed anywhere in association with thin magnetite mesobands, or with magnetite layers marginal to chert which are below the arbitrary 1 mm thickness limit for macroband status (Chapter 3). It usually occurs in clusters of many thin bands each about a millimetre thick, and rarely exceeding 3 mm, spread over several feet of iron formation. We do not know whether it is preferentially abundant at any particular level.

Slip-fibre is often associated with bending or fracture of the adjacent chert and magnetite (Figure 60B). Where these adjacent mesobands are significantly puckered the structure acquires the status of the small folds with fibrous minerals which are described in Chapter 6.

REGIONAL ORIENTATION OF STRUCTURES IN CROCIDOLITE AND OTHER FIBROUS FORMS

The range of orientation of crocidolite fibre, of its contained kink bands, of marginal fibrous quartz and of associated slip-fibre, were examined in some detail at Junction Gorge, Yampire Gorge, Dales Gorge, and Wittenoom Gorge. The raw data are not here displayed, since their wide scatter and variation between levels, as well as the long distances between recordable exposures in most of these places, make their reading difficult. The following points summarise the salient results:

1. The dip directions of all four structures are preferentially concentrated at right angles to the axial trend of the Hamersley Range Synclinorium; that is, they tend to dip either north-northeasterly or south-southwesterly.
2. The orientation of crocidolite fibre has the widest scatter from this generalisation, and in some exposures its inclination varies so widely both laterally and vertically (between mesobands of a horizon) that no consistent direction is vertical.
3. Kink banding also has a wide scatter, but wherever kink banding has a consistent direction in one mesoband, for example the mesoband below the adit roof riebeckite at Yampire Gorge (Figure 55B) and that about 54 inches farther below it (Figure 57), its strike is closely parallel to the regional folding, and its dip more usually north-northeasterly than south-southwesterly.



4. Fibrous quartz with few exceptions dips south-southwesterly, or due south.
5. Slip-fibre normally has a similar orientation to that of the fibrous quartz.

DETAILS OF CROCIDOLITE DEPOSITS

ASSAY METHODS

The term 'assay' in economic geology usually means the partial chemical analysis of rock for the constituent or constituents of which that rock is regarded as an ore, as a means of determining the total extractable quantity available by mining. In any system of assaying it is necessary to ensure that the assay method is of sufficient accuracy, that the number and positions of samples are properly selected, and that the estimated ore is physically capable of being mined.

Crocidolite seams are assayed by the simple process of measuring the total width of fibre intersected along a line at right angles to the banding. The resultant single assay is expressed as the fibre length in inches over the total length measured; for example, 2.5 inches over 30 inches, meaning that in a seam 30 inches wide there is a total of 2.5 inches of asbestos. Individual fibres less than about a tenth of an inch are usually disregarded, depending on the known capability of the milling processes to be used. In most Western Australian crocidolite it is necessary to mine a width of 3½ feet, and in assays, for example, of both seams of the Colonial mine, assay lengths are understood to be of this width, and are omitted. As the specific gravity of crocidolite is almost the same as that of the host BIF the tonnage of fibre in a seam may be calculated directly from the ratio of fibre lengths to seam width.

From foregoing descriptions of crocidolite distribution it is evident that parallel assays of a single horizon spaced out at small intervals are liable to be widely different. It is impossible to lay down exact rules for assay spacing by which an accurate available tonnage for any given deposit can be ensured. Empirical methods must be applied to each deposit, based on subjective or trial estimation of grade variation within the deposit. Any final estimate must of course be reduced by the supposed extraction efficiency of the mill to be used in processing the ore. Practical assay problems are referred to again in Chapter 12.

DESCRIPTION OF DEPOSITS

WITTENOOM SUB-PROVINCE

WITTENOOM GORGE

At Wittenoom Gorge, two crocidolite deposits were mined and a third indicated by diamond drilling. In each deposit crocidolite of economic grade is present in both the Upper and Lower Seam Horizons. Some fibre was also won from the Knapping Seam Horizon.

Geology

Along the length of Wittenoom Gorge the beds of the Hamersley Group have a gentle southerly dip of the order of 1,000 feet in 7 miles. Just north of Garden Gorge, the beds are buckled upwards to form an anticline which is the most prominent structural feature of the gorge and is named the Garden Gorge Anticline (Plate 6 and Figure 62). This anticline is not counterbalanced by any corresponding synclinal trough; the beds on either side of it simply return to the regional dip. In the core of the anticline, the Mount McRae Shale is thickened from 375 feet to about 430 feet. The thicknesses of the stratigraphic units exposed in Wittenoom Gorge are:

Unit	Thickness (Feet)	Remarks
Joffre Member	650+	Top not present.
Whaleback Shale Member	216	
Dales Gorge Member	459	Average from drilling.
Mount McRae Shale	375	Thickens on anticline.
Mount Sylvia Formation	150	
Wittenoom Dolomite	500	Base not exposed.

The lower part of the Wittenoom Dolomite consist of medium-bedded dolomite with rare beds of black chert and some shale. In the upper 400 feet of the exposed section there is a transition through dolomitic shales to a sequence consisting mainly of shale and chert with siltstone and minor dolomite. The Mount Sylvia Formation is not well-defined at Wittenoom. The two lower bands of iron formation, normally so characteristic of the unit, are represented by ferruginous chert beds which can only be distinguished from other cherts in the sequence by their greater thickness. The top-most member of the formation, Bruno's Band, does not have its normal bold outcrop though it can be easily detected upon close examination. Its outcrop forms part of an irregular cliff-face exposure of dark, indurated shales, quite different from its normal, sharp, step-like expression. At Wittenoom the Mount McRae Shale attains its greatest known

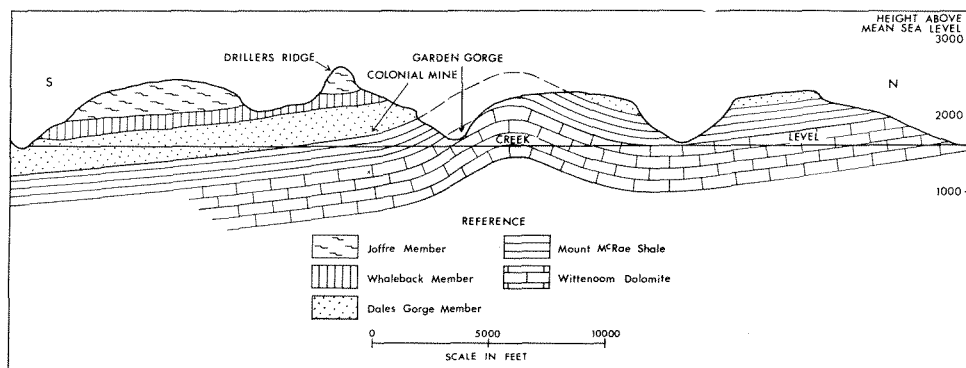
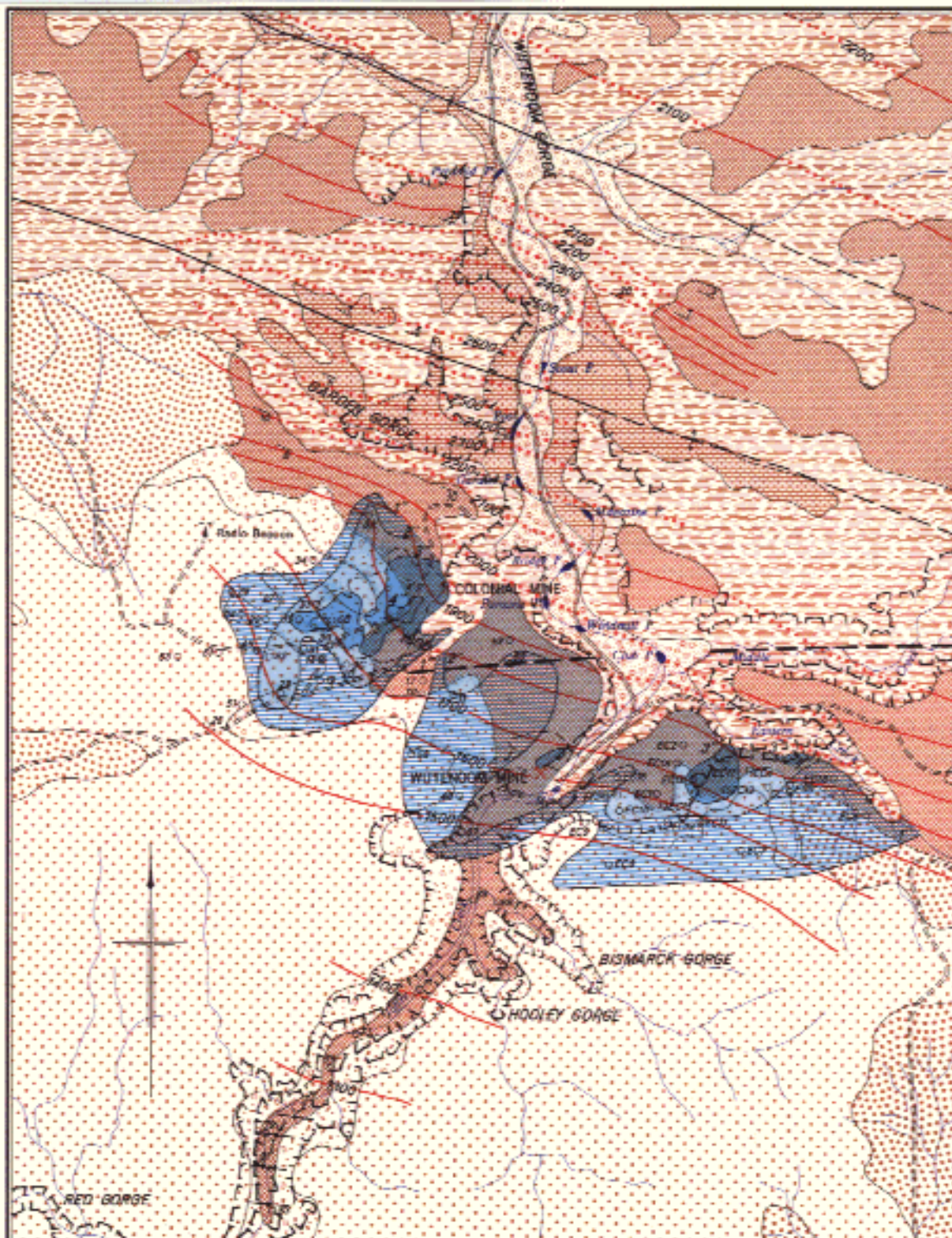
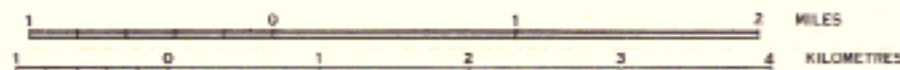


Figure 62. Vertical north-south section showing the geological structure of the Hamersley Range at Wittenoom Gorge.



GEOLOGICAL SURVEY OF WESTERN AUSTRALIA
GEOLOGICAL MAP OF WITTENOOM GORGE
SHOWING
STRUCTURAL CONTOURS AND FIBRE CONCENTRATIONS

SCALE 1: 50,000



REFERENCE

QUATERNARY	Alluvium
TERTIARY	Colliery, canga, and durian
	Joffre Member
	Whaleback Shale Member
PROTEROZOIC	Dalke Gorge Member
	Mount McRae Shale
	Wittenoom Dolomite

SYMBOLS

Geological boundary	—
Fault approximate	- - -
Syncline	~ ~ ~
Anticline major	~ ~ ~
Anticline minor	~ ~ ~
Strike and dip of bedding	— 20°
Structural contour on base of BROCKMAN IRON FORMATION (Datum is Mean Sea Level)	— 2500 —
Interpolated structural contour on base of BROCKMAN IRON FORMATION (Horizon eroded)	- - - 2300 - - -
Isopleth of cassidolite grades in Upper Seams	— 2° —
Outline of underground workings	- - -
Diamond drillhole with designating number	0.20
Creek	~ ~ ~
Escarpment	~ ~ ~
Adit Portal	~ ~ ~
Formed road	—
Track	- - -

thickness of 375 feet. It contains, 150 feet below its top, a prominent 6-foot thick chert bed which forms a good marker horizon. Twenty-five feet above this chert there is a 10-foot thick bed of massive dolomite, and the upper 80 feet of the formation consists of ferruginous chert and banded iron formation. The topmost BIF unit contains the 'bed of holes'.

The macrobands in the Dales Gorge Member are clearly defined, both in cliff exposures (Figure 4) and in the cores of numerous diamond drillholes. The Whaleback Shale Member is well exposed in Bismarck Gorge and near the mouth of Red Gorge. Fifty feet above the base of the member there is a 15-foot thick bed of podded chert which is characteristic of the member over a wide area. The top of the Whaleback Shale Member is difficult to determine in natural exposures, but is well defined in the core of Drillhole 47A. Between Red Gorge and Joffre Falls there are excellent exposures of the lower part of the Joffre Member.

From Plate 6 it can be seen that the three crocidolite deposits at Wittenoom are higher-grade areas within a zone of moderate fibre enrichment following the southern hinge line of the Garden Gorge Anticline. In each deposit the fibre is enriched in both the Upper and Lower Seam Horizons, though the Upper Seam is usually the richer. The three deposits are known as the Colonial mine, the Wittenoom mine, and the Eastern Creek prospect. Their locations are shown on Plates 5 and 6.

Colonial Mine

The Colonial mine is situated in Colonial Gorge, a northern branch of Western Gorge which itself is incised by an east-flowing tributary of Joffre Creek. Between the years 1937 and 1946 the deposit was worked from benches in Western Gorge and on the southeast side of Colonial Gorge (see Finucane 1939, Plate 1). In the mid 1950s, Australian Blue Asbestos Pty. Limited developed the prospect as a deep mine, using methods described in Chapter 8. In the early period of deep mining no separate production figures are available, since the fibre produced was treated along with that from the Wittenoom mine. Recorded production from the Colonial mine, after the closure of the Wittenoom mine, is about 130,000 tons of which about two-thirds came from the Upper Seam and one-third from the Lower Seam.

Upper Seam. The deposit in the Upper Seam contains two irregular-shaped areas averaging more than 3 inches of fibre over the seam width, each with a central core averaging more than 4 inches, and both within a halo of lower grade material averaging from 2 to 3 inches, which constituted the bulk of the seam mined. The boundaries of the ore body as stoped are irregular and poorly defined and apparently depended upon a combination of grade and distance from the haulage ways, rather than any single geological criterion. Except for an elongation in the dip direction the ore body has no linear features in the plane of the seam. The Upper Seam was stoped for about 3,000 feet down the dip and for 2,000 feet along the strike. The total area of stoping (including pillars left for support) is about 4.5 million square feet. Within the stopes, the seam averaged 3.17 inches of fibre over an average width of about $1\frac{1}{2}$ feet, or 17 per cent of

the total rock. However, as the seam was stoped to a width of 42 inches to permit access, the actual proportion of fibre in the mined ore was about $7\frac{1}{2}$ per cent.

Lower Seam. The shape of the enrichment in the Lower Seam is not well known. Due to their low grade, large areas of the seam were not developed, and no complete picture of the distribution of its fibre content can be obtained. The better parts of the seam averaged from 3 to $3\frac{1}{2}$ inches and the average grade was 2.58 inches, or 6.1 per cent of the rock mined. In some sections of the mine the first maculate band consists of massive riebeckite, which sufficiently increased mining and milling costs to make the extraction of the adjacent fibre unpayable, and so caused some areas, which contained fibre normally of ore grade, to be left intact.

Wittenoom Mine

The Wittenoom mine is situated on the west side of Wittenoom Gorge close to the point where the base of the Dales Gorge Member dips below creek level. Early work consisted of benching the outcrop of the seam on the sides of the gorge, but in 1946 Australian Blue Asbestos Pty. Limited started a deep mine on the deposit. When the mine was abandoned the workings extended for 1,600 feet into the side of the gorge, along the strike of the seam, and for some 1,200 feet up the dip direction. It is estimated that about a third of the mine's production of about 20,000 tons of crocidolite came from the Lower Seam and about two-thirds from the Upper Seam.

The Upper Seam was stoped over an area of about 1.3 million square feet, with an estimated 30 to 40 per cent left as pillars. The grade of the seam averaged about 2.1 inches of fibre, but varied from about 3.0 inches in a small area near the eastern side of the ore body to about 1.5 inches at the western end of the stopes. There is no discernible pattern to the enrichments within the seam.

The Lower Seam was stoped out over an area of about 600,000 square feet and it too averaged about 2.1 inches of fibre, with a range of from about $1\frac{1}{2}$ inches to $2\frac{3}{4}$ inches.

An east-northeast trending fault, passing through the northern side of the mine workings, displaces the seam a few feet. In places this fault forms the limit of the stoping, as the fibre in the seam beyond it was found to be 'dead' (oxidized sufficiently to be too brittle for commercial use).

Eastern Creek

The crocidolite enrichments which form the Eastern Creek prospect crop out in the east side of Wittenoom Gorge and the southern cliff-edge of the Eastern Creek. The deposit was tested by 20 diamond drillholes in 1965 and 1966 and shown to consist of two areas of higher grade fibre in the Upper Seam and one in the Lower Seam. The westernmost enrichment in the Upper Seam is probably an extension of that worked in the Wittenoom mine immediately across the gorge (see Plate 6). Between the western and eastern enrichments the Upper Seam Horizon contains low fibre values of only $1\frac{1}{2}$ inches. Excluding the poor zone, the Eastern

Creek prospect has an area of about 10 million square feet and is estimated to contain 225,000 tons of crocidolite in the Upper Seam with an average grade of 2.8 inches. Reserves in the Lower Seam are less reliably estimated at 40,000 tons averaging 2.3 inches. Assuming that in mining, 10 per cent of the seam would be left as pillars, and that mill recovery would be 70 per cent (the approximate ratios for the Colonial mine), then the total recoverable reserves of fibre would be about 160,000 tons. The Eastern Creek prospect is therefore larger than the Colonial mine, but of lower grade.

Treatment of assay data

The assay plans of the Upper and Lower Seams within the Colonial mine offer the most detailed information locally available on the shape of crocidolite enrichments within a seam. Accordingly, the information was analysed with the following aims:

1. to determine the shape of the enrichments;
2. to relate enrichments to local structure;
3. to obtain an average grade for each seam and for the whole mine;
4. to examine the possibility of either a sympathetic or an antipathetic relationship between the Upper and Lower Seams; and
5. to find the extent of the variation of fibre length within a seam.

Shape of enrichments. Early inspection of the assay plans indicated that any attempt to contour the individual assays would be meaningless; the local variations in fibre length within the seams were obviously erratic and would mask any overall trend. In order to minimise the local variations, the assays within each 100 x 100 feet square of the mine grid were averaged, and these averages were used in determining the shape of the enrichments. Experiment showed that the best picture of the shape of the fibre enrichments was obtained by shading the squares according to their average fibre value. Plate 7 shows the variations in fibre values within the Upper Seam.

Relationship of fibre enrichment to local structure. On Plate 7 the grade of the Upper Seam is accompanied by its structural contours. While the longest fibre seems to be confined to areas of least dip there is no immediately apparent connexion with structure. The minor folds trending west-southwest, whose presence is revealed in the area only by these structural contours, seem unrelated to fibre grade.

Average grade of seams. An average of all 18,548 samples within the Upper Seam was calculated at 3.23 inches. However, this result is probably biased upwards; the better parts of the seam being more intensively sampled. The mean of the averages obtained for each of the 734 100-foot squares is considered a closer estimate of the grade of the seam, as it weights each sample by the area it represents; this mean is 3.17 inches. The mean for the Lower Seam obtained in the same way is 2.58 inches, and for the whole mine 3.00 inches.

Relationship between seams. To test whether the fibre lengths in the Upper and Lower Seams varied together or were independent within the mine, their average grades within each 100-foot square were plotted against one another. The distribution of the points (Figure 63) suggests a slight tendency for sympathetic variation, but the departure from a random distribution of points is very slight.

Extent of variation of fibre length within a seam. Frequency distribution plots of groups of assays within the mine showed that the fibre lengths within the Upper Seam had an approximate normal distribution about the mean. Consequently it is possible to use the methods of statistical mathematics to measure the amount of variation within the seam. (The Lower Seam was less suited for this treatment as large gaps exist between stoped areas and assay data is sparser). The best parameter of the variation within the seam is the standard deviation*.

For the 18,548 samples taken in the Upper Seam, the standard deviation is 0.895 inches, or 27 per cent of the mean value (3.23 inches). However, as

* Definitions of the standard deviation and discussion of its use may be found in any text-book of statistical mathematics. We find the explanation of Moroney (1965) particularly clear.

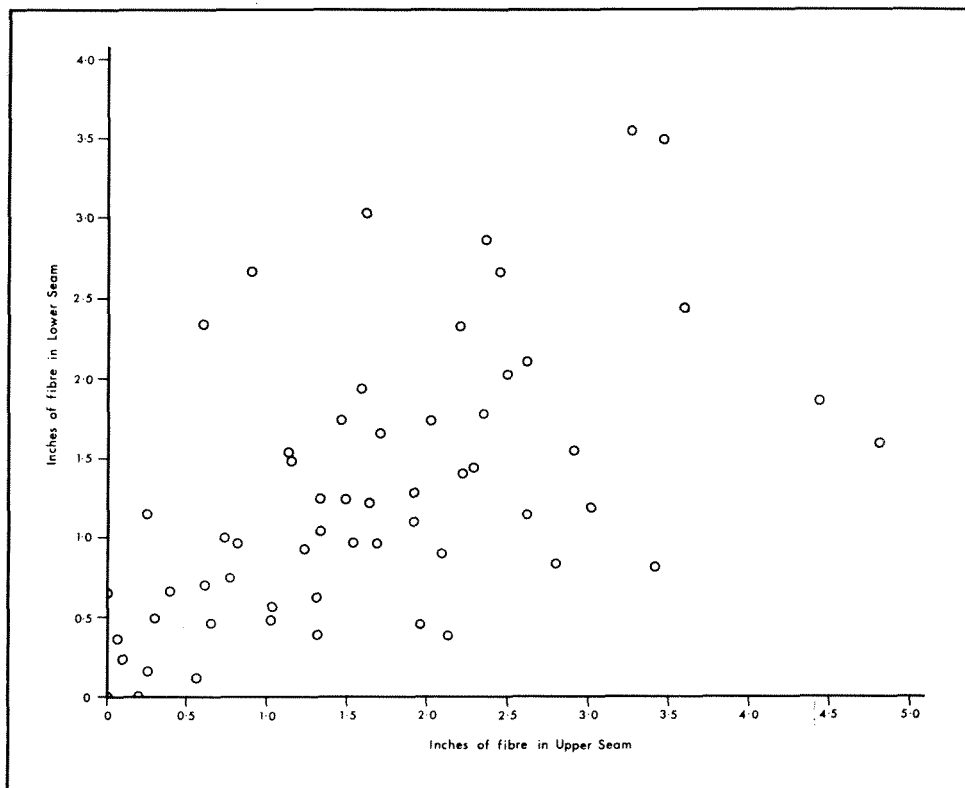


Figure 63. Scatter diagram showing the grade relationship between vertically super-imposed samples of the Upper Seam and the Lower Seam in the Colonial mine at Wittenoom Gorge.

there is a total variation in grade throughout the seam, this does not give a true picture of the local variation, i.e. variation within a part of the seam having 'uniform' grade. To determine this, the standard deviations of all samples within each of several blocks of 9 or 12 100-foot squares were determined. Each block of squares was chosen to lie in an area of about uniform grade and to include about 300 assays. The fibre length variations are shown by the histogram in Figure 64. The standard deviations range from 16.6 per cent to 22.4 per cent of the mean. It seems therefore, that within a small part of the seam having a

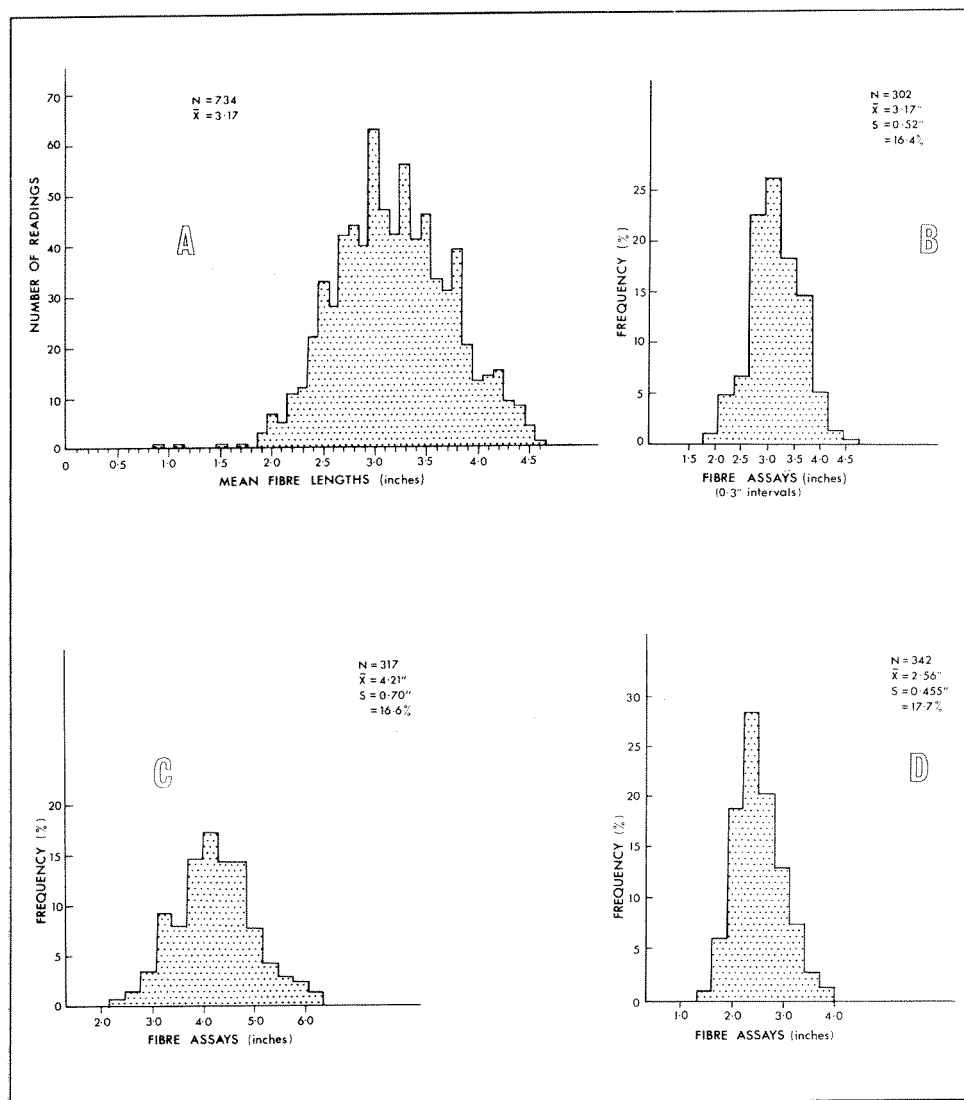


Figure 64. Histogram showing distribution of assay values in the Upper Seam at the Colonial mine.

reasonably uniform grade, two-thirds of all assays fall within 20 per cent of the mean value and 95 per cent within 40 per cent of the mean value. The significance of this result for testing crocidolite seams by diamond drilling is discussed in Chapter 12.

Diamond drilling

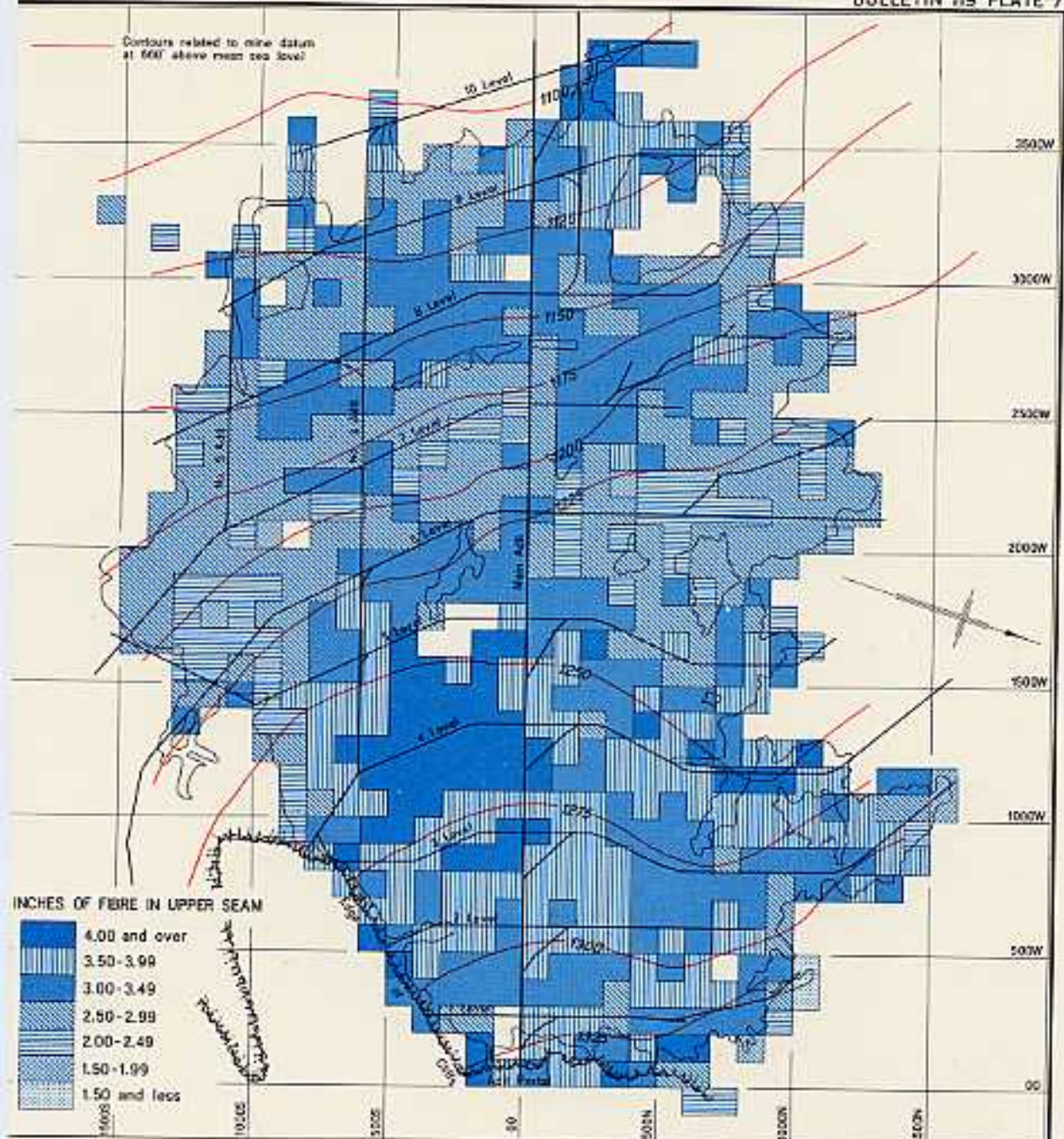
From 1961 to 1966, the Australian Blue Asbestos Pty. Limited company drilled 64 holes in the Wittenoom area. Of these, four were abandoned before intersecting the fibre horizons. Thirty of the holes were sited to test the seam beyond the immediate limits of the Colonial and Wittenoom mines, 20 were laid out to test the Eastern Creek prospect, and 14 were 'wildcat' holes. Of the 30 holes drilled in the vicinity of the Colonial and Wittenoom mines, 18 were apparently aimed to test the extension of the Colonial ore body down the pitch of the flexures which were assumed to exercise some control on the fibre enrichment. Seven of the remaining holes were sited between the two mines to test the intervening ground, and the rest were scattered about the periphery of the area, apparently as scout holes. At Eastern Creek, most of the holes were laid out approximately on a grid at intervals of about 700 or 800 feet, although the rough terrain prevented the grid spacing from being exact. As the drilling progressed, some holes were placed between those on the grid in order to close the gap in the more critical parts, and others were placed well outside the grid area, apparently with the hope of proving large reserves of ore quickly. Most of the wildcat holes were drilled in the bed of Wittenoom Gorge, where access was comparatively easy. Many of these were sited on small anticlines, as in the absence of other guides to ore location, the concept of a structural control on anticline crests was used as a basis for exploration. Other wildcat holes such as Hole 46 near Bee Gorge and MC 1 near Middle Creek were located on the general area of crocidolite outcrops, but their exact positions were governed by available access rather than geology. Hole 47 was sited to test the plunge extension of the Colonial ore body at a point about 5 miles from the mine.

The results of the diamond drilling are shown in Table 18, and the locations of the holes are given on Plates 5 and 6. Most of the Eastern Creek holes, and some of the earlier holes at the Colonial mine struck better grade fibre, but otherwise the drilling programme had little success. None of the wildcat holes intersected significant fibre, although Hole 47 gave valuable stratigraphic information.

YAMPIRE GORGE

At Yampire Gorge about 1,000 tons of crocidolite were mined from workings scattered along a 3½-mile length of the gorge, and from tributaries such as Snell Gorge and Denis Gorge. Most of the fibre came from the Yampire mine, at the south end of the workings, but the proportion of the total production contributed from each locality or seam is not known. The Yampire crocidolite deposits have been previously described by Forman (1938) and by Finucane (1939, 1964, 1965).

Contours related to mine datum
at 600' above mean sea level



GEOLOGICAL SURVEY OF WESTERN AUSTRALIA

PLAN OF COLONIAL MINE

SHOWING

FIBRE GRADES AND STRUCTURAL CONTOURS OF THE UPPER SEAM

SCALE 1 INCH TO 600 FEET

600 300 0 600 1200 1800

Mine data from plans by Australian Blue Asbestos Pty. Ltd.

TABLE 18. SUMMARY OF RESULTS OF DIAMOND DRILLING IN THE WITTENOOM GORGE
AREA

Hole No.	R.L. ¹ collar	R.L.	Upper Seam assay (inches)	Lower Seam assay (inches)	Reason for drilling	Core ² logs	Remarks
6A	1568	1125	3·47	3·48	Testing extension of Colonial Mine	
7A	1501	1164	0·80	2·67	” ” ”	
8A	1579	1217	2·80	” ” ” Assay may include Yampire C Horizon Fibre oxidized.
9C	1539	1121	2·50	2·03	” ” ”
10	1497	1142	0·93	1·23	” ” ” Fibre oxidized.
11	1554	1145	1·96	” ” ” Fibre oxidized.
12B	1508	1117	2·04	0·90	” ” ” Lower Seam oxidized.
14	1543	1088	1·70	1·65	” ” ”	
15	1575	1093	3·60	2·44	” ” ”	
17	1531	1142	0·61	0·70	” ” ”	
19	1534	1082	1·64	1·21	” ” ”	
20	1598	1046	1·81	1·28	” ” ”	
22	1547	1038	2·02	1·73	” ” ”	
26	1573	939	1·03	0·56	” ” ”	G.S. G.S. Lower Seam oxidized.
27	1607	1087	1·68	0·96	” ” ”	
28	1623	1024	1·02	0·48	” ” ”	
29	1634	1019	1·33	1·04	” ” ”	
30	1556	1107	2·63	2·10	” ” ”	
31	1604	1076	1·63	3·03	” ” ”	
33	1614	1124	1·34	1·28	” ” ”	

Hole No.	R.L. ¹ collar	R.L.	Upper Seam assay (inches)	Lower Seam assay (inches)	Reason for drilling				Core ² logs	Remarks
34	2104	1194	0·40	0·66	”	”	”			
40	1·13	1·53	”	”	”			
49	1851	1021	1·36	0·62	”	”	”			
51	1567	990	0·74	1·00	”	”	”		Lower Seam oxidized.
56	1·40	1·24	”	”	”			
59	2·62	1·14	”	”	”	G.S.		
60	1·46	1·73	”	”	”	G.S.		
61	2018	1001	0·26	0·16	”	”	”	G.S.		
62	1769	1025	2·27	1·43	”	”	”	G.S.		
63	0·20	Nil	”	”	”	G.S.		
Test Pit	988	2·40							
46	Weak	Wildcat	Bee	Gorge	Base Upper Seam intersected at 592 feet.
47	Wildcat	G.S.	Abandoned in BIF3 macroband.
47A	1625	375	0·30	0·50	”	G.S.	
	(approx.)									
WG 67	1042	906	2·45	2·66	”	G.S.	
WG 68	1063	861	0·65	0·46	”	G.S.	
WG 69	1021	870	0·10	0·24	”	G.S.	
WG 71	1036	833	0·77	0·75	”	G.S.	
WG 73	1045	782	0·82	0·96	”	G.S.	
WG 75	1061	734	0·57	0·12	”	G.S.	
WG 77	1066	”	Abandoned.
WG 79	”	Abandoned.
WG 81	0·06	0·61	”	G.S.	Base Upper Seam at 308' bore depth.
WG 83	Nil	Nil	”	G.S.	Base Upper Seam at 377' bore depth.

EC 1	1484	1063	2·36	2·85	To test Eastern Creek prospect	G.S.	
EC 2	1478	1162	0·50	1·15	" " "	G.S.	Fibre oxidized.
EC 3	1607	1151	3·42	0·82	" " "	G.S.	
EC 4	1590·6	1213	2·80	0·84	" " "	G.S.	
EC 5	1576	1203	2·14	0·38	" " "	G.S.	2·68"/10" in Yampire C Horizon.
EC 6	1487	1164	1·33	0·38	" " "	G.S.	
EC 7	2036	1002	1·15	1·49	" " "	G.S.	
EC 8	1827	916	1·54	0·97	" " "	G.S.	
EC 9	1573	926	0·60	2·33	" " "	G.S.	
EC 10	1554	990	3·26	3·54	" " "	G.S.	
EC 11	1671	1045	1·95	0·46	" " "	G.S.	
EC 12	1503	1137	4·44	1·86	" " "	G.S.	
EC 12A	1137	4·82	1·58	" " "	G.S.	Wedged from EC 12.
EC 13	1567	1000	1·87	1·10	" " "	G.S.	
EC 14	1633	1176	2·23	1·40	" " "	G.S.	Core of Upper Seam badly broken.
EC 15	1530	1033	2·35	1·77	" " "	G.S.	
EC 16	1536	1055	1·59	1·93	" " "	G.S.	
EC 17	1556	1202	2·50	1·27	" " "	G.S.	Core of Upper Seam broken.
			(est.)					
EC 17A	3·02	1·18	To check EC 17	G.S.	Wedged from EC 17.
EC 18	1524	1227	Nil	0·65	To test Eastern Creek prospect	G.S.	Core weathered.
EC 19	1540	1129	2·81	1·54	" " "	G.S.	
EC 20	1545	1030	2·20	2·32	" " "	G.S.	
MC 1	1540	To test fibre enrichment south of Middle Creek	Abandoned.
		(approx.)						

NOTES—¹ Elevations referred to Mine Datum 660 feet above mean sea level.

² G.S. in this column means logs on file at Geological Survey of Western Australia.

Geology

The part of the stratigraphic succession exposed in Yampire Gorge is very similar to that at Wittenoom Gorge. It extends from the Wittenoom Dolomite to the Joffre Member of the Brockman Iron Formation, and differs from the Wittenoom section mainly in the clearer definition of the Mount Sylvia Formation and in the absence of the massive dolomite bed in the Mount McRae Shale.

In the vicinity of the crocidolite workings, the Dales Gorge Member is folded into a broad syncline which takes the Yampire Riebeckite Zone below creek level over much of the gorge. Near Snell Gorge workings there are some very gentle folds with dips of no more than one or two degrees on opposing limbs. The Yampire mine is on a gentle dome (see Plate 9). Half a mile south of the Yampire Mine there is an abrupt, south-dipping monocline which carries the Dales Gorge Member below creek level, and locally steepens the dip to 50° or 60°.

The principal seams worked at Yampire Gorge are in the Yampire A, Yampire C, and the Upper Seam Horizons. A very small amount of mining was done on a seam in the Yampire B Horizon.

The Yampire A Horizon bears from 1 inch to 3½ inches of fibre over an area of about one square mile. The fibre is spread over a stratigraphic interval of from 3½ to 8 feet, but is usually concentrated about a prominent riebeckite bed 8½ feet above S15 to form a seam of from 2 to 4 bands within a space of 4 to 6 inches. This seam contains an average of about 1½ inches of fibre, reaching 3 inches in Snell Gorge. Workings on the Yampire A Seam extend for 2¼ miles along Yampire Gorge and spread into Snell Gorge and Denis Gorge.

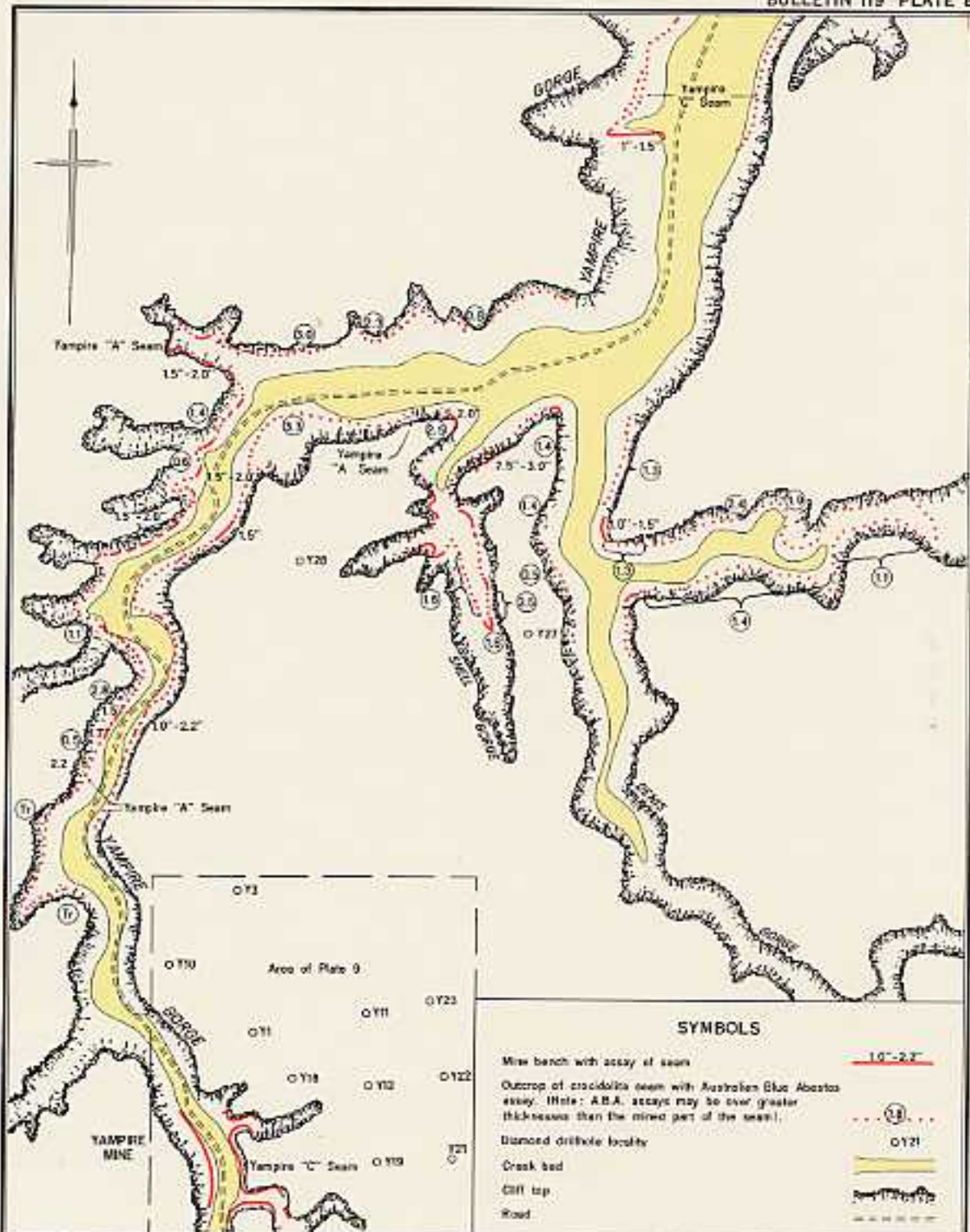
The Yampire B Horizon has from 1½ to 2½ inches of fibre spread over 3 to 8 feet. It has been worked only in one place, in Snell Gorge, where apparently a single band of asbestos within it was mined.

The Yampire C Horizon is exposed at the southern and northern ends of the workings. In the central part it is taken below creek level by the broad syncline which is the principal structural feature of the local geology. The seam is richest at the southern exposure, having up to 4 inches of fibre spread over 7 feet. In the northern outcrop where it has been worked on Hancock's Benches, it contains from 1 to 1½ inches of fibre. Mostly the worked seam comprises a single mesoband of fibre on either side of the adit roof riebeckite. In the Yampire mine it contains further fibre bands between these and the Upper Seam Horizon.

The Upper Seam Horizon has fibre wherever it is exposed. It has been worked only in the Yampire mine where its average grade was between 1½ and 2½ inches. As at Wittenoom, the seam consists of a number of fibre bands within an 18-inch interval.

Yampire mine

The Yampire mine was abandoned in 1946 after attempts to work it profitably had failed. The productive seams were in the Yampire C and Upper Seam Horizons of the Yampire Riebeckite Zone. In some benches the two horizons were



GEOLOGICAL SURVEY OF WESTERN AUSTRALIA
 PLAN OF YAMPRIE GORGE SHOWING CROCIDOLITE WORKINGS

SCALE 1: 25,000

1 0 1 MILES

Topography from aerial photograph Roy 168 & No. 3070

worked together on a 9-feet high face, from the top of the S2 macroband to the top of the adit roof riebeckite. On other benches the Yampire C Horizon was worked alone, and in many places, only the fibre bands adjacent to the adit roof riebeckite were mined. The benches extend along both sides of Yampire Gorge for about 1,800 feet and reach into two side gorges. They straddle a gentle dome which takes the seam 50 feet above creek level at the centre of the workings. West Australian Blue Asbestos Fibres N.L. carried out a little underground mining on the seam, but obtained most of their fibre from the benches. Where worked, the Yampire C Horizon contains an average of 2.4 inches of crocidolite over $5\frac{1}{2}$ feet, and the Upper Seam Horizon, 2.1 inches over $1\frac{1}{2}$ feet. In the richer sections the fibre content of the two horizons totalled 5 to 6 inches, over 9 feet, or about 5 per cent of the rock. In the Yampire C Horizon there are several bands of massive riebeckite which undoubtedly contributed to the milling difficulties experienced by the former operators.

Diamond drilling by Australian Blue Asbestos Pty. Limited indicates that the grade of the seam falls off rapidly to the east of the workings. No testing was done to the west of the mine but the seam is poorer on the west side of the gorge than on the east, and possibly the fibre content decreases rapidly in that direction too. From the results of diamond drilling and cliff sampling at the Yampire mine, we estimate the following crocidolite reserves:

Yampire C Horizon: 50,000 tons of fibre in a seam averaging about 1.3 inches over a seam width of 1 to 7 feet.

Upper Seam Horizon: 50,000 tons of fibre in a seam averaging 1.6 inches over a width of 1 to 2 feet.

Lower Seam Horizon: 40,000 tons in a seam averaging about 2.0 inches over 3 feet.

Of the reserves in the Upper Seam Horizon, about 15,000 tons are available in a seam averaging better than 2 inches of fibre overall. The reserves in the Lower Seam Horizon are calculated from drillhole data only; there are no supporting cliff samples.

Snell Gorge workings

It should be noted here that the 'Snell's workings' of Finucane (1939) are part of the present Yampire mine. The workings in what is now called Snell Gorge were described by Finucane as 'Johnsons Benches'.

The workings in Snell Gorge follow the Yampire A Seam for about half a mile upstream until the horizon dips beneath creek level. Individual benches range from 10 to 300 feet in length, and the total length of all benches in the gorge is about 1,900 feet. The mined parts of the seam are not appreciably richer in grade than the rest; the selection of sites apparently depended as much on access and the overburden ratio as on the fibre grade. The average grade of the seam varies from about 1 inch to 3 inches along the length of the gorge.

Denis Gorge

In Denis Gorge the Yampire A Seam was benched in two places on the eastern side of the gorge. The northernmost benches run intermittently for about 400 feet along the cliffs and the seam exposed on them averages from 1 to 1½ inches. On the other bench, the seam has been mined over a length of 100 feet and averages about 1 inch.

Hancock's benches

At the position of Hancock's benches, the lower part of the Dales Gorge Member reappears on the northern limb of a broad syncline. Crocidolite is again present in both the Yampire C Horizon and in the Upper Seam Horizon but is of lower grade than at the Yampire mine. The Upper Seam Horizon contains about 1½ to 2½ inches of fibre and the Yampire C Horizon from 1¼ to 2 inches. Narrow benches run for 600 feet up a small tributary gorge.

Other workings

From Fig Tree Soak southwards, the Yampire A Seam was benched at intervals for 2¼ miles along Yampire Gorge. The benches are widely scattered and the seam was worked only where it was more accessible and needed little work to remove the overburden. In length the benches range from 10 feet to 250 feet, and total about 1,800 feet. On most the seam averages about 1½ inches over 4 to 6 inches.

Diamond drilling

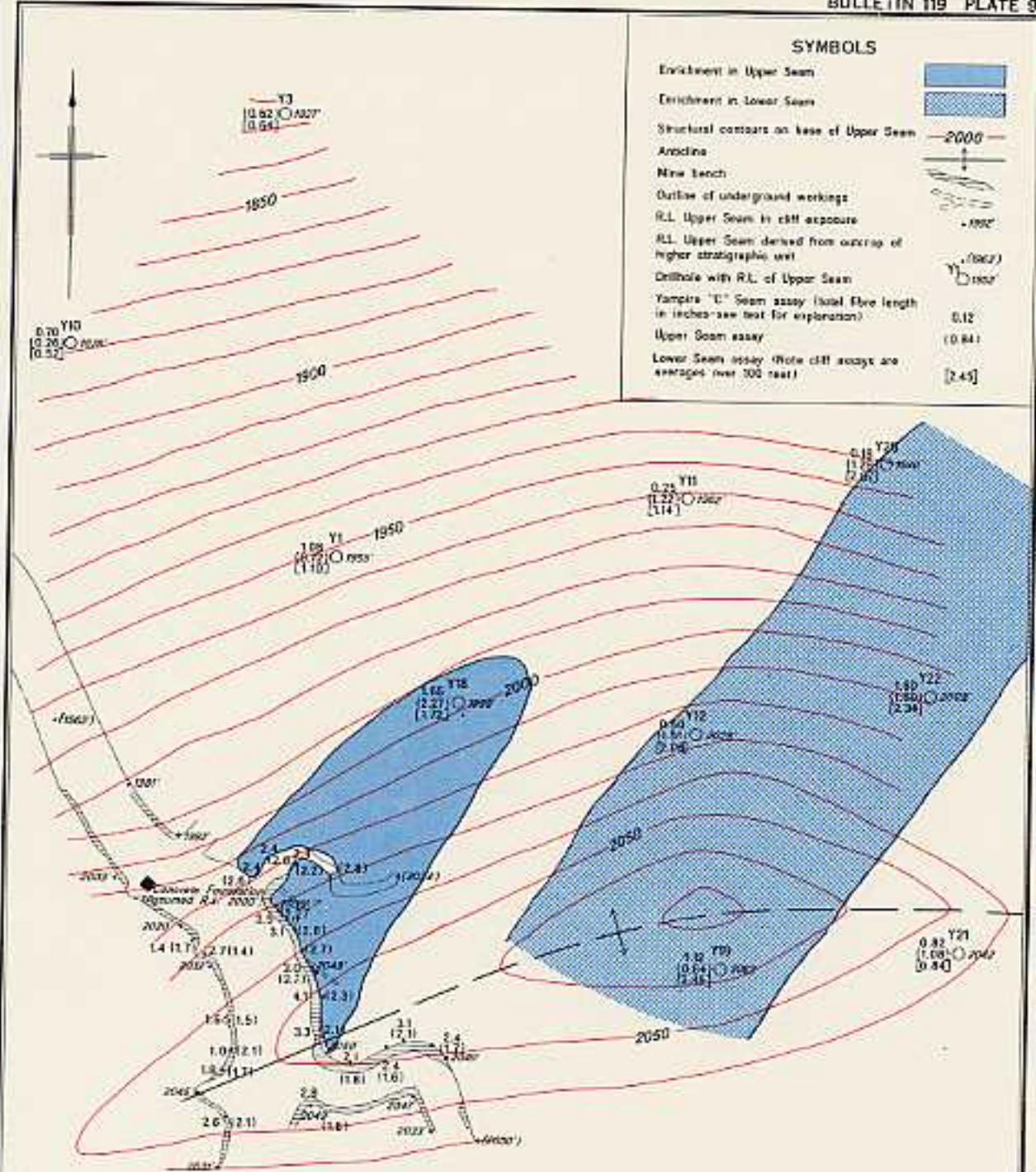
In 1964, Australian Blue Asbestos Pty. Limited, with financial assistance from the Western Australian Government, drilled 12 holes in the Yampire Gorge area. Ten of the holes were in the vicinity of the Yampire mine, and two were near Snell Gorge. Of the first group of 10, only one hole, Y18, intersected significant fibre in the Upper Seam Horizon, and only four, Y12, Y19, Y22, and Y25, showed more than 2 inches of crocidolite in the Lower Seam Horizon. The Yampire C Horizon had encouraging values only in holes Y18 and Y22.

Neither of the holes near Snell Gorge intersected promising fibre. The locations of the 12 holes are shown on Plate 8 and the details of the seams intersected are given in Table 19.

DALES GORGE

In the vicinity of the crocidolite workings, Dales Gorge is a 350-foot deep vertical-sided defile cut into the duricrust of the Hamersley Surface and the underlying iron formation of the Dales Gorge Member. The trend of the gorge is nearly parallel to the strike of the gently-dipping beds, and only the lower part of the Dales Gorge Member, from the base to BIF9, is exposed. Superimposed on the gentle southerly dip of the iron formation are very slight cross-folds trending about northeast and having wavelengths of several hundred feet and amplitudes of only a few feet.

At Dales Gorge crocidolite was mined from three seams, which were called by Finucane (1939) the Top Seam, the Mahlberg Seam, and the Main Bottom



GEOLOGICAL SURVEY OF WESTERN AUSTRALIA

PLAN OF YAMPIRE MINE AREA

SHOWING

LOCALITIES OF DIAMOND DRILLHOLES, STRUCTURAL CONTOURS, AND FIBRE ENRICHMENTS

SCALE 1:8,000

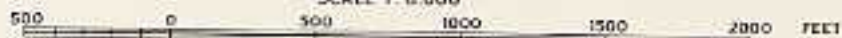


TABLE 19. DETAILS OF DIAMOND DRILLING AT YAMPIRE GORGE

Hole No.	Collar ¹ R.L.	Fibre horizons intersected with assays ^{2 3}					R.L. ¹ Upper Seam Horizon	Remarks
		Yampire A	Yampire B	Yampire C	Upper Seam	Lower Seam		
Y 1	2208	1·08 (10)	0·72	1·10 (8)	1953	Knapping Seam Horizon has 0·46" fibre and Third Seam Horizon 0·70" over 5".
Y 3	2265	2·29 (15½)	0·02	0·62	0·64	1827	
Y 10	2254	0·70 (6)	0·26	0·52	1878	
Y 11	2168	0·55 (½)	1·21	1·14	1962	
Y 12	2168	0·20	1·51	2·08	2029	
Y 18	2189	1·65 (1)	2·27	1·72	1998	Knapping Seam Horizon has 0·3" fibre.
Y 19	2193	0·12 (4)	0·64	2·45	2061	
Y 21	2202	0·82 (5)	1·08	0·84	2042	
Y 22	2206	1·60 (¾)	1·60	2·34	2008	
Y 25	2186	0·18	1·28	2·07	1840	
Y 27	1·96 (11)	3·95 (11½)	0·82 (5)	1·34	1·42	Upper Seam 480 feet down hole. Yampire B Horizon 380 feet down hole.
Y 28	0·62 (8)	2·46 (12½)	

NOTES—¹ Reduced levels related to an assumed datum of 2000' at the concrete foundation shown on Plate 9. They are approximately equivalent to height above mean sea level.

² Core logs of all Yampire drillholes are held by the Geological Survey of Western Australia.

³ Assays are in inches throughout; figures in brackets show stratigraphic thickness covered by the assay, in feet, where this is less than the total horizon thickness.

Seam. Figure 65 shows the distribution of workings in the gorge. The Top Seam is in the Yampire C Horizon and comprises two bands of fibre, one on either side of the adit roof riebeckite, the lower band being the more persistent. The seam averages about 1 inch in aggregate fibre length and was mined in a small way at only two places along the gorge.

The Mahlberg Seam is $4\frac{1}{2}$ feet above S1, and at the top of the Lower Seam Horizon. It consists of a single lenticular band of fibre just below MB2 of Trendall (1966a). The lenses of fibre are in the troughs of well-developed duplicate structures (Chapter 6) and have the clearest relationship to structure of any crocidolite in the Hamersley Range area. Individual lenses are about 2 feet long and are spaced regularly at 5-foot centres. They are from 1 to $2\frac{1}{2}$ inches thick in the centre and in plan they follow the troughs to the limit of the local exposure. Due to this lenticular habit, about half of the area of the seam is barren and its average grade is quite low despite maximum fibre lengths of up to $2\frac{1}{2}$ inches within each lens.

The Mahlberg Seam was worked at the northwestern end of Dales Gorge and in the tributary containing Circular Pool. It was benched at intervals for about 1,800 feet in the main gorge and for 180 feet in the tributary. The longest single bench runs for 1,200 feet along the southern side of Dales Gorge. The workings are mainly on the floor of the gorge where the seam had only a thin cover of overburden.

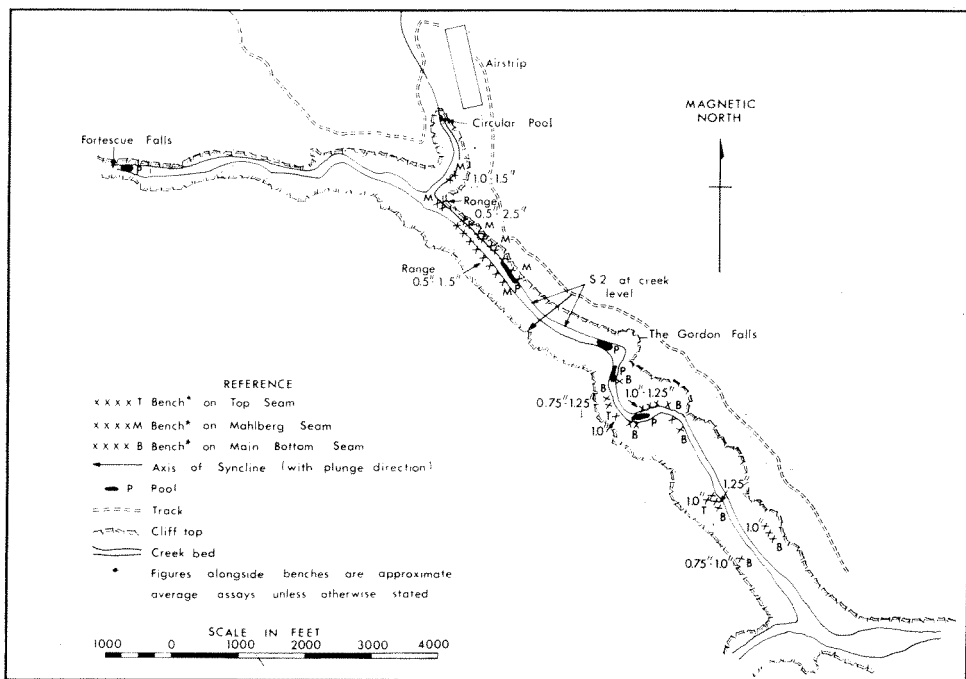


Figure 65. Map of the crocidolite workings at Dales Gorge.

The Main Bottom Seam is 10.3 feet below S1, at about 33.5 feet on the type section. It consists of two antipathetic fibre bands on either side of a 4-inch thick chert band. Two thinner bands of fibre which are sometimes present a few inches below these, have not been mined. Each of the two main bands may reach $1\frac{1}{2}$ inches in thickness, but owing to their almost perfectly antipathetic relationship, never do so in the one place. A single band of fibre called the "Stringer", sometimes present $2\frac{1}{2}$ feet above the Main Bottom Seam, was worked in at least one place. The Main Bottom Seam has been benched intermittently over a distance of $\frac{3}{4}$ -mile downstream from The Gordon Falls, but most of the 1,400 feet of benching was done within a space of 1,000 feet at the western end of the workings. As a Yampire Gorge, the former miners chose their bench sites for ease of access or mining rather than for a high fibre content in the seam.

BEE GORGE

Bee Gorge is about 4 miles west of Wittenoom Gorge and cuts the same stratigraphy. The most pronounced structure is a continuation of the Garden Gorge Anticline, the southern limb of which brings the Dales Gorge Member down to creek level. The crocidolite workings at Bee Gorge are on the Yampire C Horizon and are located on the south flank of the Garden Gorge Anticline. One group of benches is in the main gorge, and there is another group extending for about 250 feet along the southern edge of a small eastern tributary. In the main gorge the individual benches are short and widely spaced, but in the eastern tributary the benches are almost continuous. Fibre production from Bee Gorge is unknown, but is certainly small.

In most places, the seam consists of one band of fibre just above the adit roof riebeckite band. There is little fibre in the lower part of the Yampire C Horizon and the Upper Seam Horizon is mostly barren, although the Lower Seam Horizon, 28 feet below the benches, does bear some crocidolite. Locally, on a small monocline, a seam is developed in the BIF3, 5 or 6 feet above S3. Both BIF2 and BIF3 contain much massive riebeckite.

Australian Blue Asbestos Pty. Limited drilled one hole, 46, about one mile south of the workings. Only 'weak' fibre values were recorded.

RANGE GORGE

The Range Gorge crocidolite deposits are situated about 7 miles west-northwest of the Colonial mine. Access is by way of a dogger's track which branches from the Wittenoom—Tom Price road 10.6 miles from Wittenoom townsite and leads to the workings about $6\frac{1}{2}$ miles upstream from the mouth of the gorge. There is no record of the quantity of fibre produced from Range Gorge, but the small size of the workings make it certain that this was small.

The geological section at Range Gorge is similar to that at Wittenoom and the most conspicuous of several west-trending folds is again the Garden Gorge Anticline. On the south limb of the anticline there is a sharp monocline which

brings the base of the Brockman Iron Formation from near the hill-tops down to creek level. Crocidolite was worked in the Yampire C Horizon at the foot of this monocline.

The principal workings are in a small eastern tributary of the main gorge where the seam has been benched for a distance of 150 to 200 feet at a height of about 100 feet above creek level. Another group of benches in the main gorge starts a few hundred feet south of the confluence of the eastern tributary and extends for 300 feet down-dip to creek level. In this section, the dip of the seam is 8° southerly.

The seam worked at Range Gorge consists of one or two bands of fibre next to the adit roof riebeckite band, and contains no more than $1\frac{1}{2}$ inches of knapping fibre. Crocidolite is also present (but has not been worked) in the Upper Seam Horizon, in a seam 7 or 8 feet above the S3 macroband, and in the BIF12, where this is exposed in the gorge one mile south of the workings. There are boulders of crocidolite in the alluvium upstream from this position and it is likely that these come from the Yampire A Horizon, although the exposures of this horizon which were examined contained no fibre.

CALAMINA GORGE

A small but unknown quantity of crocidolite was knapped from a seam in the Aspinall Horizon cropping out at creek level in Calamina Gorge (lat. $22^{\circ} 17'S$, long. $118^{\circ} 25'E$), 11 miles southeast of Wittenoom. The band mined is 2 feet below S15 and immediately below a 6-inch band of massive riebeckite. It is from one to $1\frac{1}{2}$ inches thick. Further fibre bands are present in BIF14 below the mined seam and assays of the complete fibre-bearing section range from 1.6 inches over 6 inches to 3.5 inches over 193 inches. Near the old working, BIF macrobands 12 and 15 contain uneconomic quantities of crocidolite.

ASBESTOS GORGE

The workings in Asbestos Gorge are 3 miles southwest of Mount Margaret trigonometrical station (lat. $21^{\circ} 57'S$, long. $117^{\circ} 50'E$). Access is by way of a track leading south from Nelson Well into a large gorge west of Mount Margaret. The last mile of the route, up the tributary known as Asbestos Gorge, can only be travelled on foot or horseback.

Three seams were worked in Asbestos Gorge, all in the Yampire Riebeckite Zone. The lowermost of these is 6 feet below S2 and consists of one band of fibre averaging about 1 inch in length. It has an unusual abundance of cone structure. The middle seam is in the Yampire C Horizon and comprises one impersistent band of fibre immediately below the adit roof riebeckite band. Where mined, it contains about 1 inch of asbestos. The uppermost seam is $5\frac{1}{2}$ feet above S3 and is made up of 1 band of fibre averaging about half an inch in thickness.

Most of the mining at Asbestos Gorge was on the lowermost seam, which was knapped over a distance of 200 feet along the sides and bed of the gorge.

The seam in the Yampire C Horizon was knapped over a few feet only, and a little readily broken fibre was taken from the uppermost seam. The mining method used seems to have been simple knapping with only a little use of explosives. It is stated that the cobbled fibre was lowered over the waterfall in buckets and carted out of the gorge on the backs of donkeys.

MILLER'S GORGE

Miller's Gorge is cut into the north side of Mount Margaret and is best reached by following a track running southeasterly from Forrest Well for 6 miles, and then travelling across country to the gorge. The workings are 1 mile north of the trigonometrical station and 200 feet above creek level. Here the larger production came from the Yampire C Horizon, which was benched for about 40 feet. The grade of the seam averaged about 1 inch. The seam 6 feet below S2 contains up to 1½ inches of crocidolite, but was barely touched by the former miners. The fibre was lowered to the bed of the gorge by means of a flying fox.

JUNCTION GORGE

The Junction Gorge crocidolite prospect (lat. 22° 33'S, long. 119° 01'E) was first reported to the Mines Department by S. Aspinall in 1964. However, Foxall (1938) mentions that "good floaters of long fibre have been found as far eastward as 30 miles from Yampire Gorge" and it is likely that Junction Gorge was one such locality. Junction Gorge is situated about 50 miles east-southeast of Wittenoom Gorge and is reached by following the Wittenoom—Roy Hill road from Wittenoom for 52 miles and then turning southward along a rough track.

Three mineral claims have been pegged on two of the better-grade fibre occurrences in the gorge; the northern two claims, M.C.s 321 and 322 by A.B.A. and the southern claim, M.C.329 (now expired) by S. Aspinall.

Geology

At Junction Gorge (Plate 10) the Brockman Iron Formation is gently folded about axes trending 100°. The creeks have cut down to about the average level of the BIF16 macroband, but more of the Dales Gorge Member, down to BIF12, appears in anticlines, and the Whaleback Shale Member comes down to creek level in synclines. The hills traversed by the gorge are capped by the Joffre Member, with slopes consisting of the Whaleback Shale Member. Consequently the Dales Gorge Member is exposed in 'windows' on structural highs in the topographically lower parts of the area. North of the fibre prospects the Dales Gorge Member is brought to the surface by the regional dip, but its exposure is strongly weathered and consists mainly of canga and duricrust.

The principal fibre occurrences at Junction Gorge are in the Aspinall Horizon, 2 to 6 feet below the S15 macroband. Fibre also develops in BIFs 12, 13, 15 and 16, but is always of low grade and small extent.

The Aspinall Horizon crops out intermittently over an area measuring 10,000 feet easterly and 6,000 feet northerly. Most exposures of the horizon in this area show at least some fibre, and potentially mineable seams exist in three localities,

here named the Aspinall prospect, A.B.A. prospect, and Western prospect respectively.

Aspinall Prospect (M.C.329^{W.P.})

At the Aspinall prospect (Figure 66) the Aspinall Seam is exposed on both sides of the gorge up to 50 feet above creek level. The better grade crocidolite is on the eastern side of the gorge where aggregate fibre lengths reach 5 inches, average $3\frac{1}{2}$ inches over about 150 feet, and 1-2 inches over a further 400 feet. The exposure on the western side of the gorge contains less fibre, but the seam still assays 2 to $2\frac{1}{2}$ inches over a length of 1,000 feet. To the north of the prospect, the Aspinall Horizon can be traced along the western side of the gorge, but its asbestos content is low. Southwards, it dips beneath creek level, but re-emerges on another anticline 1,500 feet away where it contains 2 inches of fibre.

A.B.A. Prospect (M.C.321^{W.P.} and 322^{W.P.})

The A.B.A. prospect consists of an exposure of the Aspinall Horizon on the east side of the gorge. The seam can be traced for 600 feet along a low, east-west cliff. Owing to the effects of bedding dip and topography, the seam dips beneath creek level at either end of the outcrop. The deposit is about 200 feet south of an anticlinal axis, and the seam dips 5° - 10° southerly. A few spot assays on the seam averaged 1.6 inches.

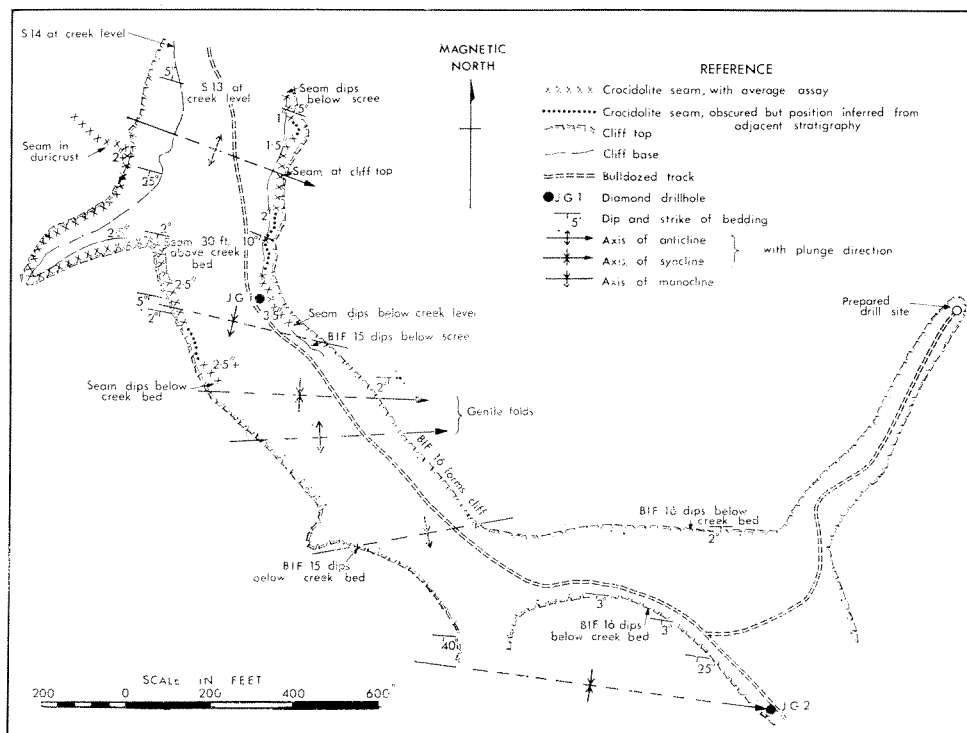
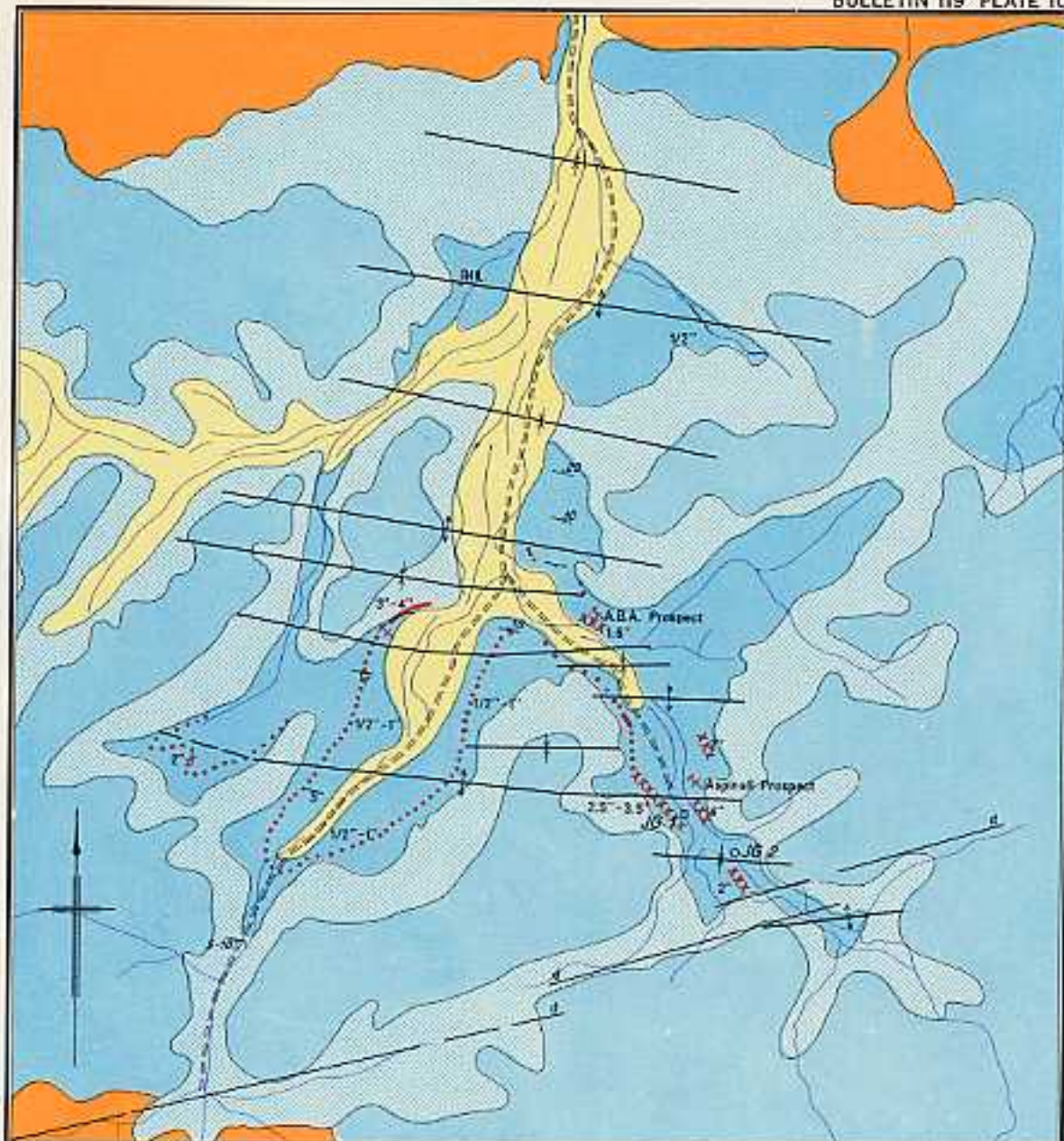


Figure 66. Map of the crocidolite occurrences at Aspinall prospect, Junction Gorge.



GEOLOGICAL SURVEY OF WESTERN AUSTRALIA
 GEOLOGICAL MAP OF JUNCTION GORGE SHOWING OUTCROP OF ASPINALL SEAM
 SCALE 1:40,000



Western Prospect

The Western prospect is situated about 3,700 feet west of M.C.321. In it, the Aspinall Horizon is exposed in two places 500 feet apart. It carries $3\frac{1}{2}$ inches of fibre in one outcrop and $1\frac{1}{2}$ inches in the other. Between the outcrops the horizon is obscured by scree.

Other exposures

Midway between the A.B.A. and Aspinall prospects, the horizon contains 2 inches of fibre just below the duricrust on the east side of the gorge.

In another branch of Junction Gorge, and about 8,000 feet west of M.C.321^{W.P.}, a small enrichment on the Aspinall Horizon contains 2 to $2\frac{1}{2}$ inches of fibre. Its main interest is that it lies on the same anticline as the Aspinall prospect.

Diamond drilling

Australian Blue Asbestos Pty. Limited drilled two holes at Junction Gorge (Figure 66). The first, JG1, was sited on the Aspinall prospect at the foot of the cliff showing the best values in the Aspinall Seam. The object of the hole was to test the Yampire Zone vertically below long fibre in the Junction Gorge Riebeckite Zone. The hole encountered fibre in the Yampire C Horizon, the Upper Seam Horizon, and the Lower Seam Horizon. Details are tabulated below:

<i>Horizon</i>	<i>Drill depth</i>				<i>Inches fibre</i>
	<i>From</i>		<i>To</i>		
	<i>(ft)</i>	<i>(ins)</i>	<i>(ft)</i>	<i>(ins)</i>	
Yampire C	250	10	252	8½	0.40
Upper Seam	256	5½	257	7	0.79
Lower Seam	275	9	277	10	0.43

Hole JG 2 was sited 1,600 feet southwest of JG 1 on the axis of a syncline. It intersected fibre in BIF16 and in the Aspinall Seam, but did not reach the interesting horizons in the Yampire Riebeckite Zone. Details of the intersections are:

<i>Horizon</i>	<i>Drill depth</i>		<i>Inches fibre</i>
	<i>(ft)</i>	<i>(ins)</i>	
BIF16	87	2	0.40
	92	9	1.30
Aspinall Seam	147	$3\frac{1}{2}$	0.81
	to		
	148	$6\frac{1}{2}$	

COONDINER GORGE

The Coondiner Gorge crocidolite prospect (lat. $23^{\circ} 01'S$, long. $119^{\circ} 35'E$) was discovered in about 1963. It is reached by following a track from Poonda Outcamp to the mouth of the gorge and thereafter by negotiating the creek bed. Access is difficult as the terrain is rough. The fibre was found where the Dales Gorge Member is exposed on an anticline in a deep tributary gorge which cuts

through the section from the lower part of the Joffre Member to BIF11. This seems to be the only outcrop of the Dales Gorge Member in the locality.

The main seam is in BIF13, six feet below S14. It contains up to 3 inches of patchy fibre on either limb of the anticline, though the seam is barren on the crest of the fold. There are also two thin but regular bands of fibre in the upper part of BIF14.

The deposit as exposed does not constitute an ore body, but there remains the possibility of extensions along the anticline, and the potential of the Yampire Riebeckite Zone below.

MARILLANA PROSPECT

The Marillana prospect (lat. 22° 39'S; long. 119° 05'E) is located on a northern tributary of Marillana Creek. Access is by way of a station track from Weeli Wolli Creek to the confluence of the tributary and then via the creek bed which is negotiable by 4-wheel drive vehicle in the dry season. The fibre seam lies in the Yandicoogina Horizon.

In the vicinity of the deposit, the Brockman Iron Formation has a slight regional dip to the south, superimposed on which are gentle folds. The gradient of the creek is about the same as the dip of the beds, so very little of the stratigraphy is exposed. The higher ground is occupied by the Yandicoogina Shale Member while the creek is incised into the upper 30 or 40 feet of the Joffre Member. Most of the fibre occurrences are on anticlines, but as these also give the best exposures of Yandicoogina Horizon, it is difficult to establish any association between structure and fibre enrichments.

At the Marillana prospect the seam is exposed almost continuously for about 500 feet on the western bank of the creek. It contains an average of 0.8 inches of crocidolite with a maximum of 1½ inches. Often the seam consists only of one band of fibre, and where this averages from 1 to 1½ inches, it has been worked as a knapping seam.

About 3,500 feet south-southwest of the prospect, another exposure of the horizon contains up to 2½ inches of crocidolite, but as the seam is patchy, past workings on it were restricted to a little knapping. Several other exposures of the Yandicoogina Horizon in the drainage basin of Marillana Creek contain up to 1 inch of fibre while other outcrops are barren.

LAMB CREEK

The original discovery of fibre here was made by G. R. Ryan in 1965, at lat. 22° 49'S, long. 118° 55'E. It is located in a gorge on a small tributary of Lamb Creek, itself a branch of Marillana Creek.

Access is via a station track leading from a yard on Marillana Creek to a pool on Lamb Creek 1½ miles north of the deposit. Thereafter, it is possible to drive along the ridges to within 300 yards of the find.

In the original find up to 3 inches of crocidolite occur in an interval of 11 feet within the BIF0 macroband of the Dales Gorge Member. The best section

is within the interval from 27 to 29 feet above the base of the unit, where up to 1½ inches of fibre is concentrated in five bands.

The asbestos is located on the northern limb of a large anticline. Most other exposures of BIF0 are on the crest of the structure, and contain only a little fibre.

Further work in the area revealed fibre bands in the Lower Seam Horizon and the middle of BIF16. The best aggregate fibre lengths in these horizons are 1½ inches and 2 inches respectively, but both occurrences are of small extent and it is unlikely that they will be of economic interest.

The discoveries at Lamb Creek are important because they demonstrate that crocidolite approaching ore grade can be found in the Dales Gorge Member away from the north face of the Hamersley Range.

MINOR OCCURRENCES

There are many occurrences of blue asbestos in the Wittenoom Sub-Province which are of little economic importance and some about which little is known. Some of these are described below:

Fortress Gorge

The crocidolite in Fortress Gorge is situated about 52 miles southeast of Wittenoom at latitude 22° 32'S, longitude 118° 51'E. A dogger's track branching from the Wittenoom—Meekatharra road 47 miles from the former town leads into the gorge but stops short of the fibre occurrences. The first report of asbestos in this gorge was made by Mr. Aspinall in 1964 who found the fibre while trapping wild dogs.

Two significant deposits are known in the gorge. The first, about 4.7 miles from the main road, is situated high in a cliff on the western side of the gorge. Here 3 to 4 inches of fibre occur in the Yampire A Horizon 10 feet above S15, while a further 1½ inches lie immediately above the same unit. Across the gorge the same horizon contains 2 inches of crocidolite. Elsewhere in the gorge, only traces to 1 inch of blue asbestos or quartz fibre occupy this position.

The second of the two deposits is about half a mile upstream from the first. It comprises a seam 2 feet thick occupying the interval from 11 to 13 feet above the base of BIF16 and containing 1½ to 2 inches of fibre where exposed for about 100 feet on the crest of an anticline. Only small amounts of crocidolite were seen in other exposures of the same horizon within the gorge.

In one exposure of BIF14, 2 inches of fibre occur in the Aspinall Horizon, but other outcrops contained only traces. While bands of fibre were seen in BIFs 12, 13, and 15, none exceeded one inch in width, and they are not regarded as significant.

Weeli Wolli Spring

At Weeli Wolli Spring a little crocidolite has been seen in the Yampire Riebeckite Zone, particularly in BIF macrobands 0 and 1. Similar occurrences are known where the Dales Gorge Member is exposed on the north-dipping limb of the Weeli Wolli Anticline. Similar occurrences are known over a distance

of about 20 miles west, and 5 miles east of the spring, but in none does the aggregate fibre length exceed one inch. The low grades of the exposed fibre horizons, and the deep weathering prevalent in the region, has discouraged systematic prospecting.

Devan's prospect

The first applications for mining tenements for crocidolite in Western Australia were made by Messrs. Devan and Nelson of Marillana Station in 1929. The applicants submitted samples of their find to the Government Chemical Laboratories and the results are recorded by Simpson (1930). The deposit was described as being 8 miles south-southeast of Weeli Wolli Spring on the west side of the highest hill on the watershed of the Weeli Wolli and Mindi Mindi creeks. Despite several searches, the site of these claims was not located during the current investigation. In two localities which answer to the prospectors' description, up to 1½ inches of fibre were seen in the Aspinall Horizon. Most of this was in one band which is characterised over a wide area by sharp kink bands. No fresh crocidolite was seen, and the source of the material submitted for analysis was not located.

The original sample is preserved in the Government Chemical Laboratories (No. S1108) and comprises three pieces of fibre. Two of the pieces are of fresh crocidolite obviously broken from the one band, and with fibre lengths of from 1.2 to 1.4 inches. The third piece is more weathered and may have been broken from a boulder in scree or alluvium. It has fibre 1.7 inches long. In the two fresh pieces the fibre is attached to a ¼-inch thick mesoband of pink chert at one end and to a thin band of chert-matrix at the other. There is a thin layer of fibrous quartz between the crocidolite and the chert-matrix. None of the fibre shows any sign of kink banding, which is surprising in view of its reported locality.

Munjina Gorge

In Munjina Gorge at latitude 22° 32'S, longitude 118° 41'E the beds of the Hamersley Group have a slight regional dip to the south, superimposed on which are very gentle folds trending about east-west. Several small faults at 250° disrupt the beds, but the most prominent structure is a monocline which locally steepens the dips to about 30° south, bringing the Dales Gorge Member from hill-top level to the floor of the gorge.

South of the monocline, the bedding is almost flat over a wide area, and the tops of low cliffs forming the sides of the gorge follow the same stratigraphic horizons, BIF4 and BIF5, until eventually all exposure is obscured by duricrust. A small anticline causes the top of BIF0 to reappear about a mile south of the monocline.

Crocidolite is present in several horizons within the Yampire Riebeckite Zone, the best concentrations being in the Third Seam, Lower Seam, Upper Seam, and Yampire C Horizons, and at the top of BIF3. Other bands of fibre were noted

in BIF0, BIF3, and BIF4. No more than about 1 inch of fibre was seen in any one seam.

MARRA MAMBA SUB-PROVINCE

MARRA MAMBA DEPOSITS

At Marra Mamba, five deposits of crocidolite were worked in a narrow belt extending from 3 miles west to 9 miles east of Mount Brockman Station homestead (lat. 22° 18'S, long. 117° 17'E). Marra Mamba is 80 road miles from Wittenoom Gorge and 210 miles from Point Samson, the closest port. Repair of an old road through Caliwinga Gorge could reduce the distance to Point Samson to 145 miles. The crocidolite workings are in a range of hills about 2 miles south of the southern edge of the Hamersley Plateau. The seams are exposed in small ravines cut by north-flowing tributaries of Duck Creek.

The first mining tenement at Marra Mamba was pegged in 1931. Intermittent mining of the deposits between 1933 and 1942 produced 57.6 long tons of fibre. All of the fibre was won from shallow pits and benches; there are no deep openings on the field. Foxall (1942), Finucane (1964 and 1965), and Blockley (1967) have described the Marra Mamba crocidolite deposits. MacLeod and others (1963), de la Hunty (1966), and MacLeod (1966) have related the occurrences to the regional geology.

Geology

The crocidolite at Marra Mamba is in the Marra Mamba Riebeckite Zone and seams have been worked in the Mackay, Dun, and Foxall Crocidolite Horizons within the zone. The Vivash Riebeckite Zone is not exposed in the area of the deposits, but is known to contain fibre some 5 miles west of Mount Brockman homestead.

Marra Mamba lies on the north limb of the Jeerinah Anticline, and the beds have an average dip of 10° north. Minor folds are common and mapping has revealed two types. Folds of the first, and probably earlier type, trend between 260° and 290°. They may change direction and usually die out within a short distance along strike. Crumpling is common in the limbs and the north-dipping limbs are often the steeper. The folds are therefore in the reverse sense to normal drag folds on the north limb of the Jeerinah Anticline. These folds may appear abruptly in evenly dipping strata and usually only a small area is involved in the folding. It seems that the rocks were incapable of transmitting stresses over any great distance during folding. The second and more intense type of folds control the form of the outcrop and trend at 300°. Their south-dipping limbs are the shorter, indicating a normal drag-fold relationship to the Jeerinah Anticline. Many folds can be traced for several thousands of feet and folding is present in wide belts, suggesting that the causative stresses were transmissible through a considerable body of rock. Both these sets are of a larger order of size than the small folds already described in dealing with crocidolite structures earlier in this chapter. The relationship between the folds of different sizes is not clear; the problem

is an expression of the common phenomenon of continuous size variation in folding of Hamersley Group iron formation, mentioned in Chapter 2.

Most faults at Marra Mamba strike either northwest or northeast and have little displacement. Some contain dolerite dykes. Towards the eastern end of the area shown on Plate 11 a west-northwest trending fault displaces the beds several hundred feet laterally, and is the only large fault known in the area.

Dun prospect (M.C.s 61^{W.P.}, 43^{W.P.} and 21^{W.P.})

First pegged by G. and A. Dun in 1937, this deposit was later worked by L. G. Hancock and S. L. Hancock to yield 47.55 tons of fibre. The prospect is the most easterly of those worked at Marra Mamba and the productive seam is in the Dun Horizon. Mining was restricted to the northern part of the outcrop where the seam contains up to 2½ inches of fibre over 2 feet. Benches extend continuously for 500 feet along the eastern side of the gorge and intermittently for the same distance on the western side.

The Dun Horizon was also mined in another branch of the gorge 1,200 feet to the southeast. Here benches extend 250 feet along the cliffs on the western side of the ravine. Fibre grades range from 2 to 3 inches over 2 feet.

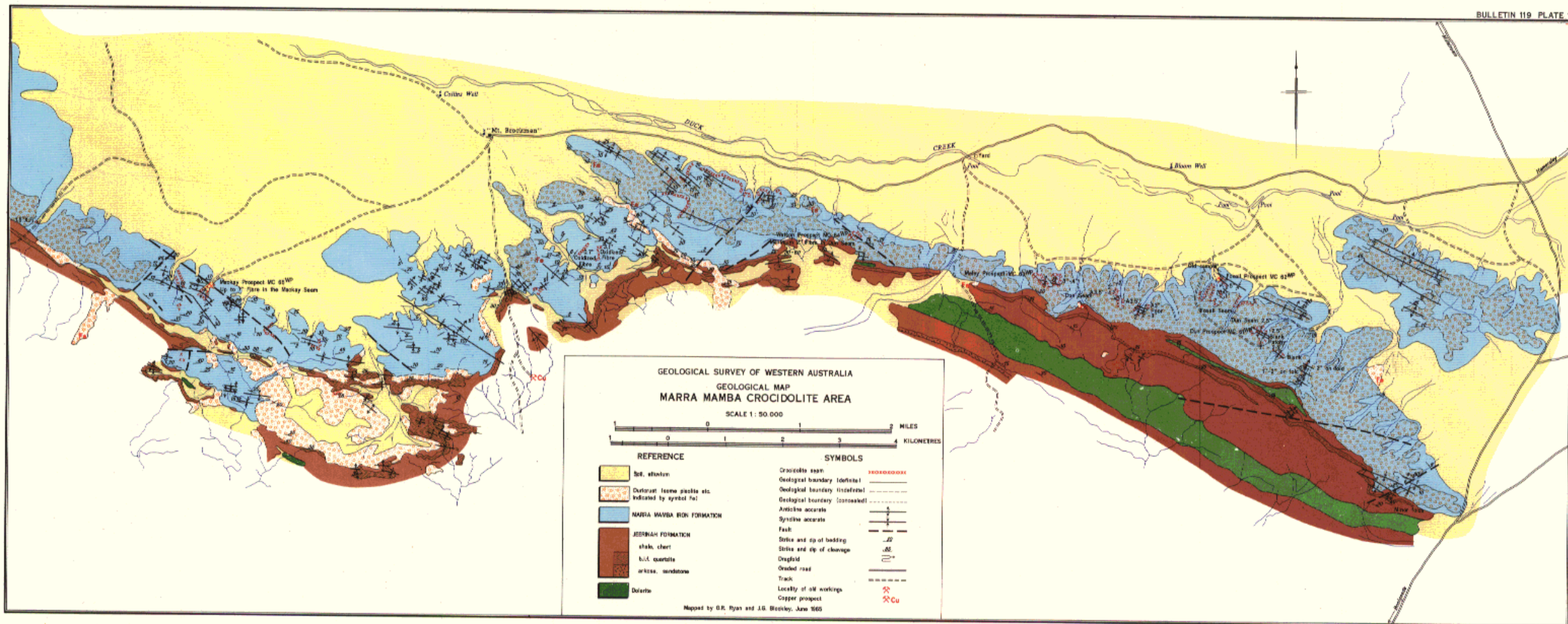
There is little evidence for structural control of the crocidolite distribution on these claims, although the fibre is largely restricted to the more steeply dipping beds.

Foxall prospect (M.C.s 62^{W.P.} and 41^{W.P.})

Mining on M.C.62^{W.P.} was restricted to a spectacular fibre enrichment in the Foxall Horizon where this is exposed over a distance of 150 feet on a low bluff. The seam still contains fibre where it dips northwards below creek level, but south of the workings the fibre content is low and erratic. The horizon was traced for some thousands of feet in adjacent gorges, but no further mineable seams were found. Foxall (1942) quotes an assay from the seam as 9 to 10½ inches over 8 to 8½ feet. However, the average is nearer 5 inches over 10 feet. Recorded production from this seam is 0.15 tons. The enrichment is on the northern limb of an anticline at a place where the dip steepens from 15° north to 30° north.

Maley's prospect (M.C.s 63^{W.P.} and 42^{W.P.})

The area of Maley's prospect includes two gorges, each containing workings on the Dun Horizon. In the western gorge, the seam was benched for about 250 feet along its outcrop. The workings start at creek level and extend southwards along the cliffs on the eastern side, where the grade of the seam ranges up to 3 inches of fibre over 2 feet. To the south of these benches, the horizon is nearly barren for 350 feet but values improve again on a monocline. Oxidized fibre can be traced eastwards from the southern end of the exposure into the next gorge. Here, the seam has been mined on the eastern side of the gorge with the diggings extending intermittently for 500 feet along the outcrop. Fibre values of 3 to 4 inches over 2 feet are common, and the seam is still of good tenor where it dips below creek level. Another seam 30 feet above the Dun Horizon was also benched over a short distance. The richer seams on Maley's



prospect are located on the more steeply dipping parts of gentle monoclines. Total recorded production is only one ton of fibre, but the extent of the workings suggests that considerably more was produced.

Watson's prospect (M.C.s 64^{W.P.} and 39^{W.P.})

On M.C.64^{W.P.} the Dun Horizon can be traced for about 800 feet along the cliffs, but contains significant fibre only where it has been mined at the head of the gorge. The seam contains no more than 2 inches of fibre over two feet, and production from the deposit is only 4 tons. A fault passing close to the benches has displaced the seam a few feet vertically. Any relationship of fibre to structure is obscured by lack of exposure south of the workings.

Mackay's prospect (M.C.s 65^{W.P.} and 40^{W.P.})

Mackay's prospect contains the only workings on the Mackay Horizon. The horizon can be traced for about 1,000 feet along the gorge, but contains asbestos only on the limbs of an anticline of the 'reverse-drag' type (p. 237). The seam has been benched on the western side of the gorge on both limbs of the anticline, and on a spur on the eastern side of the gorge. Fibre grades reach 7 inches over 6 feet on either side of the anticline's crest, but decline appreciably further from the fold axis. Despite the richness of the seams only 4.9 tons of crocidolite have been produced from the prospect. Foxall (1942, p. 44) gives the reason for this as discoloration of the fibre due to oxidation.

Other deposits

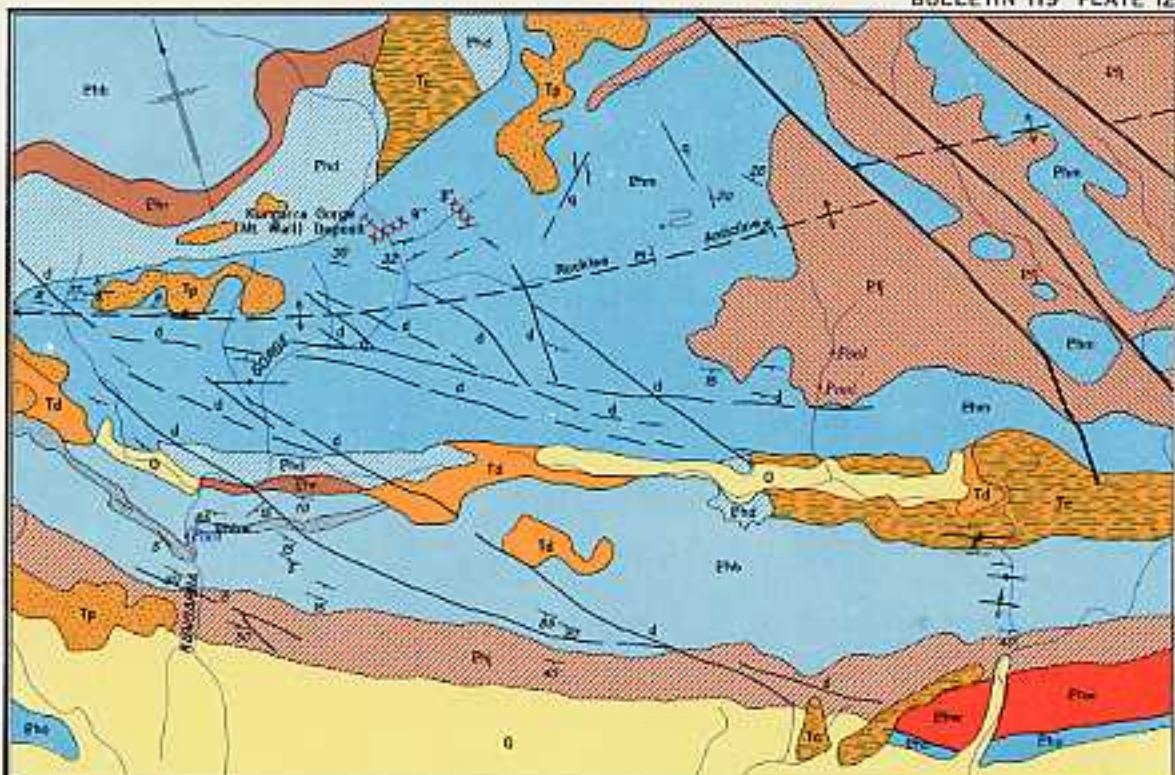
Between M.C. 62^{W.P.} and M.C. 64^{W.P.}, the Mackay Horizon is exposed in three gorges. In some outcrops it contains up to 4 inches of fibre in a seam 2 feet thick, but no fibre has been mined from it here, possibly because of the difficulty of separating the crocidolite from the cherty host rock.

KUNGARRA GORGE PROSPECT

The Kungarra Gorge (or Mount Wall) crocidolite prospect (lat. 22° 47'S, long. 116° 58'E) is about 10 miles east-southeast of Mount Wall. It is exposed in a gorge formed by one of the tributaries of Horseshoe Creek and lies about 3 miles upstream from the point where this tributary emerges from the range. The most suitable access to the mouth of the gorge is by way of the bed of Horseshoe Creek where this crosses the Rocklea—Wyloo road 10 miles west of Cheela Springs. There seems to be no likelihood of putting in a road to the prospect along the gorge, for in many places this is choked by house-sized boulders and obstructed by waterfalls. Any road constructed to the fibre deposit would have to approach from the north along the top of the range. The prospect has never been pegged, but is believed to have been found by Mr. Barrett-Lennard, of Mount Stuart Station.

The crocidolite lies in the Vivash Riebeckite Zone of the Marra Mamba Iron Formation where this is folded into a broad, faulted, west-plunging anticline. Dips are gentle near the prospect, but steepen rapidly to the south in the overlying formations.





GEOLOGICAL SURVEY OF WESTERN AUSTRALIA
GEOLOGICAL MAP
KUNGARRA GORGE AREA

SCALE 1:60,000

1 0 1 2 3 MILES

REFERENCE	
QUATERNARY	Q Alluvium
TERTIARY	Tc Collierian
	Td Duricrust
	Tp Pisolite
PROTEROZOIC	Ehc BOOLEDEGA IRON FORMATION
	Zfw Woongarra Volcanics
	WJF WIDEI WOLLI FORMATION
	Phb BROCKMAN IRON FORMATION
	Pshw Whiteback Shale Member
	Psh Mount McRae Shale MOUNT SYLVIA FORMATION
	Pnd Wimmeroo Dolomite
	Pnw MAYHA MAMBA IRON FORMATION
	Pj JEEPINAH FORMATION

Mt. Bruce Superficial

SYMBOLS

Geological boundary	—
Fault	—
Anticline approximate with plunge direction	—
Minor anticline	—
Minor syncline	—
Monocline	—
Strike and dip of bedding	—
Small folds, with plunge	—
Crinoid stem with approximate assay	XXX 3"
Dolerite dyke	d
Quartz vein	q
Creek	—
Prospect	—

Mapped by G.R. Ryan 1965

A stratigraphic section measured about the deposit is shown in Figure 67. Outcrop is masked over most of the area by duricrust, canga, and pisolite, and exposures are confined to the gorges. Dolerite dykes occupy many of the steeply dipping fractures which cross the area in a general northeasterly direction.

Crocidolite occurs in several places, but the best exposure is at the locality indicated in Plate 12, just above a small pool and waterfall. Here fibre bands are spread throughout a stratigraphic interval of 32 feet, but most lie in the lower 15-foot section. One assay of the whole fibre-bearing section gave $12\frac{1}{2}$ inches over 32 feet, and five A.B.A. assays of the richer part averaged 9.5 inches over 15 feet. The best seam within this averaged 4.6 inches over $4\frac{1}{2}$ feet. Figure 67 shows the distribution of fibre bands and average values within this section.

North of the exposure the lower fibre bands dip beneath creek level, but the higher bands pinch out before dipping into the floor of the gorge. To the south, the fibre-bearing section becomes rapidly poorer, until at 300 feet south of the pool, only $1\frac{1}{2}$ to 2 inches of crocidolite remains. Several hundred feet southwest of the principal locality, fibre is again developed in the favourable section where exposed near the tops of the cliffs. In this outcrop, the zone contains from 5 to 7 inches of crocidolite and fibre is still present where the seam dips beneath cover to the west.

The Kungarra Gorge crocidolite occurrence is the best untested prospect in the Marra Mamba Sub-Province. In its favour is the length over which the asbestos crops out, the large amount of fibre in the favourable zone, and the down-dip potential to the north and west. Against the prospect are its remoteness and inaccessibility, and the large stratigraphic interval over which the fibre is distributed.

VIVASH GORGE DEPOSIT

The deposit at Vivash Gorge (lat. $22^{\circ} 43'S$, long. $117^{\circ} 02'E$) is particularly inaccessible, and of poor quality. It consists of a number of thin bands spread over about 10 feet in the Vivash Riebeckite Zone and totalling no more than three inches. However there are some folds in the host rock, and further deposits could be present. Outcrop is generally very poor and further search would be seriously hampered.

OTHER OCCURRENCES IN THE MARRA MAMBA SUB-PROVINCE

Brockman Syncline

The Marra Mamba Iron Formation was examined in several places along the southern and eastern side of the Brockman Syncline, from a point almost due south of Boolgeeda Camp. In most places the host rock dips steeply and uniformly and contains only traces of fibre. Only at the locality south of the camp was any substantial amount of fibre seen, and even here no economic deposit was found. Several bands of fibre are present in the Vivash Zone, with traces in the Marra Mamba Zone and at the top of the formation.

Figure 67 (opposite). Stratigraphic section through the Kungarra Gorge crocidolite deposit.

Turner Syncline

Traces of crocidolite are common in the eastern part of the Turner Syncline where the Marra Mamba Iron Formation is steeply and uniformly dipping. The only enrichment found was at Mount Lionel, where several inches of fibre are present on the limb of a small fold. The shoot is small and is apparently the only one in the locality.

Duck Creek

A little fibre was found in the Marra Mamba Riebeckite Zone in a gorge (lat. 22° 25'S, long. 116° 41'E) about 8 miles northeast of Duck Creek homestead. Some thin bands of fibre were also seen in the Vivash Riebeckite Zone between here and Duck Creek. Boulders of crocidolite have been found in Duck Creek upstream from its junction with the Serpentine Creek, but the source of these has not been traced. However, many tributaries of Duck Creek dissect the Marra Mamba Iron Formation between Serpentine Creek and Marra Mamba, and almost any of these could have brought the crocidolite boulders into the main stream. Even so, the exposure of the Marra Mamba Iron Formation on the western nose of the Jeerinah Anticline has potential and warrants further prospecting.

Serpentine Creek

A seam containing about 1 inch of fibre in two bands is exposed in the upper part of the Marra Mamba Riebeckite Zone where this is cut by Serpentine Creek (lat. 22° 21'S, long. 116° 37'E), 10 miles north of Duck Creek Station homestead. The exact position of the fibre in relation to the defined crocidolite horizons within the zone is not known. No other blue asbestos was found in the locality.

Marra Mamba west

About 5 miles west-northwest of Mount Brockman homestead there are several deposits of crocidolite in the Vivash Riebeckite Zone. They occur on the nose of an east-plunging anticline and all are oxidized and apparently of small size. However, some spectacular enrichments are present, the best seen containing 9 inches over a width of 30 feet. This resembles the Kungarra Gorge deposit, but no exact correlation could be made. In another section there is up to 6 inches of oxidized fibre over 8 feet. Where these enrichments can be traced along strike they die out quickly.

Owing to their small size these occurrences have little economic potential, except, perhaps, as a source of tiger's eye.

Mount Tom Price

Crocidolite, or tiger's eye, has been reported from the Marra Mamba Iron Formation where this is crossed by the road from the mine to the township; the report has not been confirmed.

CROCIDOLITE OCCURRENCES OUTSIDE THE TWO SUB-PROVINCES

Crocidolite has been found in three localities outside the two sub-provinces in which most of the deposits lie. Two of these occurrences are in the Dales Gorge Member of the Brockman Iron Formation, and one is in the Marra Mamba Iron Formation. These occurrences are described below in approximate order of size.

JIMMAWURRADA CREEK

A very small, discontinuous seam of oxidized fibre crops out on the north bank of Jimmawurrada Creek (lat. $21^{\circ} 48'S$, long. $116^{\circ} 20'E$), about 6 miles east-southeast of Deepdale homestead. The seam lies at the top of the exposure of the Marra Mamba Iron Formation, probably in the Vivash Riebeckite Zone. It is of little interest as a source of blue asbestos, but has yielded some tiger's eye, and has been pegged for that reason.

MOUNT NICHOLSON

Crocidolite was found during the regional mapping of the Yarraloola Sheet on an un-named hill (lat. $21^{\circ} 22'S$, long. $116^{\circ} 06'E$) about 5 miles due south of Mount Nicholson. Originally quartz fibre and oxidized crocidolite were found at the top of BIF2 in the Dales Gorge Member. Subsequently, some more oxidized fibre was seen a few feet above the base of the BIF0 macroband. The fibre is neither abundant nor extensive in either horizon, although a small quantity of tiger's eye could be won from the locality.

FISH POOL

Fish Pool (lat. $28^{\circ} 07'S$, long. $118^{\circ} 04'E$) is situated on Turee Creek where this cuts the Brockman Iron Formation on the northern side of the Turee Creek Syncline. A good section of the Dales Gorge Member is exposed on the eastern side of the gorge, and in this, traces of crocidolite were seen in the BIF0 macroband, 32 feet above the base of the member. This fibre has no economic interest.

JUNA DOWNS

Daniels (1966, p. 21, and personal communication) reports the presence of crocidolite in the Marra Mamba Iron Formation, a few miles south of Juna Downs homestead. Only about 4-inch of fibre is present, and the locality was not visited by us.

SUMMARY OF RELATIONSHIP BETWEEN CROCIDOLITE AND STRUCTURE

Throughout the Hamersley Crocidolite Province there is no constant, unequivocal relationship between crocidolite deposits and mappable geological structures. In some places fibre deposits may be loosely associated with folding, but this seldom holds for all of the deposits in any area, and the nature of the association is locally variable.

In the Marra Mamba Iron Formation, blue asbestos is present mainly on the limbs of small folds superimposed on the regional dip, with the better enrichments commonly on the regional down-dip side of the folds. Where the Marra Mamba Iron Formation dips uniformly and lacks these small folds, then crocidolite is generally absent. This relationship is of little use in prospecting the formation for crocidolite, for even in its most productive parts, many folds contain no fibre.

The relationship between fibre and folding in the Brockman Iron Formation is less obvious. In the eastern part of the Wittenoom Sub-Province, crocidolite is most commonly found on the limbs of open folds. Areas where the folding is tighter normally bear only traces of fibre. In other places, such as Dales Gorge, where the formation is almost horizontal, there is no demonstrable relationship between crocidolite and structure.

Possibly the most significant association of crocidolite with structure is at Wittenoom Gorge where three enrichments lie on the south limb of the Garden Gorge Anticline. The deposits are in a narrow belt defined by the southern hinge-line of the fold; that is, by the line along which the beds flatten to the gentle regional dip after crossing the anticline. The crocidolite seams worked at Bee Gorge and Range Gorge occupy similar positions on the same structure. At Range Gorge, the change of dip from steep to flat is emphasised by a monocline superimposed on the south limb of the anticline. The asbestos workings are at the foot of the monocline where the dips flatten from 15° to 5° . A minor crocidolite occurrence at Munjina Gorge is in a similar position on another south-facing monocline.

At Yampire Gorge there is an apparent strong association between the seam worked at the Yampire Mine and the crest of the anticline which it straddles. However, the trend of the fibre enrichment, as determined from diamond drilling, does not follow the axis of the fold, but veers across it at about 45 degrees. It is evidently coincidental that the fibre seam occupies the crest of the fold in the present cliff exposures.

In the Colonial mine at Wittenoom Gorge the ore bodies are in a zone of minor flexuring trending at 250° . These flexures trending across the strike of the regional folding may be due to a crimping of the beds on the concave side of a bend in the Garden Gorge Anticline. The correspondence between fibre values and the flexures is only a broad one and does not hold in detail. The two other ore bodies known at Wittenoom are similar in grade to the Colonial mine, but are not associated with flexures of the bedding.

Crocidolite mining in Western Australia

HISTORY OF MINING

The presence of crocidolite in Western Australia was first reported to the Mines Department in March 1908 by Herbert Soanes, the prospector who had a year or two earlier developed the chrysotile deposits at Soanesville in the Pilbara System to the north of the Hamersley area, to pioneer asbestos mining in the northwestern part of the State. Despite this successful history of prospecting, and the evidence of a specimen submitted to the Government Geologist, there was some doubt about Soanes' report. At the time he refused to disclose the locality of the deposits and this apparently led to the belief that his specimen had originally come from South Africa. Consequently, the discovery was not officially recognised. Soanes, who was still mining chrysotile at Soanesville, did not pursue the matter.

In 1911, after the Soanesville mine had closed down, and again in 1916, Soanes applied for a concession to prospect for crocidolite in Western Australia. He outlined in his first application a scheme in which, if granted prospecting rights over several hundred square miles of country, he would undertake prospecting and development to prove several million tons of fibre. His letter then continues: "When this part of the Scheme has been completed, it is proposed to then endeavour to command from £50,000 to £100,000 with a view to doing certain development work, carrying out extensive and costly Experiments Abroad, and which I believe will if successful, absorb quite 1,000,000 tons per annum, thereby involving the securing of large Contracts."

"Subject to this portion of the Scheme meeting with success, I estimate that little short of £1,000,000 working Capital would be required to build from 150 to 200 miles of substantial Tramway, install a COLOSSAL PLANT which would be found necessary to handle such immense tonnage, and which would be required to compensate such an absolutely necessary outlay of Capital." His later application also added a tidal power station to the scheme.

This ambitious proposal was greeted with some scepticism from Soanes' contemporaries, especially as crocidolite then had little commercial value. But the State Mining Engineer, A. Montgomery, was inclined to favour the scheme, although perhaps accepting its feasibility with a little seasoning. In a note on the file he wrote "(Soanes) is a person of extraordinary ambitious schemes which have to be severely discounted to reduce them to a residuum of practical workability. On the other hand he has the true enthusiasts' power of persuasion, and has

therefore perhaps a better chance of getting financial assistance for his projects than a man of less sanguine temperament." Montgomery recommended that Soanes be allowed 1,000 square miles in which to prospect for crocidolite on terms which were very similar to those governing the granting of Temporary Reserves today. He argued that as the mineral had no commercial value, the State had nothing to lose by granting such a large area and indeed stood to profit if Soanes could establish an industry based on crocidolite. The application was however rejected on the grounds that the area requested was too large and that there was some doubt about Soanes' ability to raise the money necessary for his scheme.

Looking back now, it seems reasonably certain that Soanes could not have realised his ambitious project. At that time all available labour and capital was being used to fight the Great War. There is little doubt though that in promoting his ideas, Herbert Soanes would have given considerable publicity to the crocidolite deposits and perhaps hastened their eventual development by several years. That Soanes knew of a deposit of crocidolite in the Hamersley Range there can be little doubt. His description of it to Montgomery as extending "in a flat-lying layer over a large area of ground" fits the blue asbestos deposits on the north side of the Hamersley Range and is hardly likely to have been invented by him. At any rate, Soanes' plausibility was sufficient for Montgomery to mention crocidolite in a Mines Department publication of the time (Woodward & Montgomery, 1917, p. 28).

Soanes' correspondence with the Mines Department ended in 1918 and in the following decade, crocidolite receives only an occasional mention in the files. In 1921, two samples were sent to the Government Geologist for determination. The first was submitted by H. A. Hall of Mount Florance Station who gave the locality as Mulga Downs Station. The second specimen came from L. de Souef of Roebourne, who reported it as coming from the Hamersley Range. In that year, Wilson (1922) wrote "Specimens of crocidolite, said to have come from the Hamersley Ranges, have been exhibited in Perth, but no deposit has yet been officially examined." It was not until 1929 that the first mining tenements were taken out on a blue asbestos deposit. These were pegged in 1929 by Messrs. Devan and Nelson of Marillana Station, but were allowed to lapse without any fibre having been produced. The leases were located about 9 miles southeast of Weeli Wolli Spring.

Official credence was given to the Hamersley crocidolite in 1930 when E. S. Simpson (1930, p. 38-40) reported on specimens from Mount Margaret and Weeli Wolli Spring. In 1933 MacKay and Party produced a small parcel from Marra Mamba which realised £40 per ton. Within a few years however, buyers were offering up to £75 per ton for top-grade fibre and when the news of this spread a minor rush took place. Foxall (1942, p. 39) estimated that 150 to 200 men poured into the field. Production during this period (1937-38) was mainly of long fibre, the demand for which was limited, and soon the market was

over-supplied and prices fell. In addition, a shortage of shipping, and the distance of the markets, caused long delays in payments, which the generally undercapitalised miners could not sustain. Mining at this time was limited to surface exposures, from which the fibre was won by benching (Figure 68). About 500 tons of crocidolite are estimated to have been produced. The deposits worked included those at Wittenoom Gorge, Yampire Gorge, Dales Gorge, and probably those at Bee and Range Gorges. Following the fall in prices, most of the leases passed into the hands of companies and subsequent mining was confined to the deposits at Yampire Gorge, Wittenoom Gorge, and Marra Mamba.

The leases at Yampire, which had first been worked by L. Snell, were taken over by the Asbestos, Molybdenum and Tungsten Co. Ltd. This company erected a small plant on the deposit in 1939, and produced asbestos intermittently from 1940 to 1942. After a period of idleness West Australian Blue Asbestos Fibres Limited bought the leases, improved the mill, and mined crocidolite in the period from 1944 to 1946. Most of the fibre was still being won from benches on the sides of the gorge, but the company did start some underground work. The company quickly ran into financial difficulties and eventually closed down the mine after a flood had wrecked the mine plant. No further asbestos has been won from Yampire Gorge, although the leases have been held almost continuously since 1946 by other parties.

The early 'Wittenoom Gorge' leases were worked by L. G. Hancock and W. McLarty and were located in the branch now known as Colonial Gorge. In 1938, Hancock and McLarty formed a company called Australian Blue Asbestos Mines No Liability which took over these leases. Meanwhile, Hancock had pegged a seam exposed in the main trunk of the gorge, then called Joffre Creek, which has since become known as Wittenoom Gorge. In partnership with E. A. Wright, he formed the L. G. Hancock Asbestos Company to work the new claims. By 1942 it was obvious that more capital was needed and the partners approached the Colonial Sugar Refining Limited company, which had previously expressed interest in obtaining blue asbestos for their Building Materials Division. C.S.R. bought a controlling interest in the L. G. Hancock Asbestos Company in 1943 and formed the company Australian Blue Asbestos Pty. Limited to develop the leases. This development resulted in the opening of the Wittenoom mine on the site of Hancock's original claim in Joffre Creek. The Wittenoom mine stayed in production until about 1956. In 1953, the company had started to develop the Colonial mine on the seams exposed in Colonial Gorge, and when the Wittenoom mine was closed, all the plant was transferred to the new site. The Colonial Mine (Figure 69) was worked until 1966, when it was closed down due to lack of ore reserves and high production costs.

From 1947 to 1966, the Australian Blue Asbestos Pty. Limited company was the sole crocidolite producer in the field. Apart from its leases at Wittenoom Gorge it held ground covering the deposits at Yampire Gorge, Calamina Gorge, Bee Gorge, Range Gorge, Junction Gorge, and Marra Mamba. Although it

worked none of these, it did carry out a programme of Government subsidised diamond drilling to test the Yampire, Junction, and Bee Gorge deposits.

The Marra Mamba deposits were reopened by Hancock in 1940-41. Hancock then sold them to the Lionel Chrysotile Asbestos Limited Company, a sister company to West Australian Blue Asbestos Fibres Limited, of Yampire Gorge. This company announced plans to build a plant at Marra Mamba, but these did not eventuate. No crocidolite has been won from Marra Mamba since 1941.

The sorry review of crocidolite mining in Western Australia since the late nineteen-thirties is that, although the value of the product has averaged over \$200 per ton, no company has been able to maintain profitable operations. It is clear that cheaper production methods will have to be found if the industry is to be restarted. At the time of writing, A.B.A. have sold their leases to Hancock and Wright, who have outlined a scheme to reopen the blue asbestos mines as part of a giant industrial complex involving, among other things, the construction of a railway to the coast. The wheel of progress has turned a full circle since Herbert Soanes departed from the scene.

Crocidolite production in the Hamersley Range to the end of 1966 was 152,466.74 tons valued at \$33,496,664.98, making blue asbestos the State's fourth most valuable mineral product after gold, coal, and iron ore. During its most flourishing years, the industry supported the largest inland town in the north of the State and the facilities provided for it have helped the tourist industry and greatly assisted the later search for iron ore in the Hamersley Range.

Table 20 lists the annual productions of crocidolite by the various operators engaged in the industry.

MINING METHODS

The various methods used to mine blue asbestos, from the crudest knapping of an exposed seam to complex stoping hundreds of feet underground, have all been governed by two principal characteristics of the seams, their typical

TABLE 20. ANNUAL PRODUCTION OF CROCIDOLITE IN WESTERN AUSTRALIA

Year	Mining Centre	Producer	Crocidolite
			long tons
1933	Marra Mamba	Mackay and party	4.90
1937	Yampire Gorge	Snell, L.	20.10
	Wittenoom Gorge	McLarty and party	14.00
1938	Mt. Lockyer ¹	Bright, C.	2.65
	Dales Gorge	Snell, L. and Mahlberg, A.	26.65
	Yampire Gorge	Snell, L.	29.45
	Yampire Gorge	Walker, E.	9.05
	Wittenoom Gorge	McLarty and party to 30/6/1938; Australian Blue Asbestos Company N.L. from 1/7/1938 ¹	54.45

¹Probably from the Dales Gorge deposit

TABLE 20 (continued)

Year	Mining Centre	Producer	Crocidolite
1939	Wittenoom Gorge	Australian Blue Asbestos Company N.L. ²	24·00
1940	Marra Mamba	Watson, K.	4·00
	Yampire Gorge	Asbestos, Molybdenum & Tungsten Co. Ltd.	355·00
	Wittenoom Gorge	Hancock, L. G.	·50
1941	Marra Mamba	Hancock, S. (M.C.61)	2·00
	Marra Mamba	Hancock, S. (M.C.62)	·15
	Marra Mamba	Maley, M.	1·00
	Marra Mamba	Hancock, L. G. (M.C.61)	45·55
	Yampire Gorge	Wright, E. A. M.	3·65
	Wittenoom Gorge	Wright, F. W. M.	·67
1942	Yampire Gorge	Asbestos, Molybdenum & Tungsten Co. Ltd.	10·00
	Yampire Gorge	Wright, E. A. M.	73·85
1943	Yampire Gorge	Wright, E. A. M.	93·00
	Wittenoom Gorge	Hancock, L. G.	47·55
	Wittenoom Gorge	Walters, I.	41·00
1944	Wittenoom and Yampire Gorges	West Australian Blue Asbestos Fibre Limited ²	32·24
	Wittenoom Gorge	Walters, I.	24·00
	Wittenoom Gorge	Australian Blue Asbestos Pty. Limited	217·25
1945	Wittenoom and Yampire Gorges	West Australian Blue Asbestos Fibre Limited...	598·88
	Wittenoom Gorge	Australian Blue Asbestos Pty. Limited	388·32
	Wittenoom Gorge	Walters, I.	4·10
1946	Wittenoom and Yampire Gorges	West Australian Blue Asbestos Fibre Limited	117·57
	Wittenoom Gorge	Australian Blue Asbestos Pty. Limited	247·99
1947	Wittenoom Gorge	Australian Blue Asbestos Pty. Limited	888·99
1948	Wittenoom Gorge	Australian Blue Asbestos Pty. Limited	607·30
1949	Wittenoom Gorge	Australian Blue Asbestos Pty. Limited	1,155·87
1950	Wittenoom Gorge	Australian Blue Asbestos Pty. Limited	1,018·41
1951	Wittenoom Gorge	Australian Blue Asbestos Pty. Limited	1,392·61
1952	Wittenoom Gorge	Australian Blue Asbestos Pty. Limited	2,940·09
1953	Wittenoom Gorge	Australian Blue Asbestos Pty. Limited	3,795·40
1954	Wittenoom Gorge	Australian Blue Asbestos Pty. Limited	3,793·67
1955	Wittenoom Gorge	Australian Blue Asbestos Pty. Limited	4,344·42
1956	Wittenoom Gorge	Australian Blue Asbestos Pty. Limited	7,285·97
1957	Wittenoom Gorge	Australian Blue Asbestos Pty. Limited	11,104·87
1958	Wittenoom Gorge	Australian Blue Asbestos Pty. Limited	11,887·10
1959	Wittenoom Gorge	Australian Blue Asbestos Pty. Limited	14,680·17
1960	Wittenoom Gorge	Australian Blue Asbestos Pty. Limited	12,921·59
1961	Wittenoom Gorge	Australian Blue Asbestos Pty. Limited	14,086·59
1962	Wittenoom Gorge	Australian Blue Asbestos Pty. Limited	15,616·95
1963	Wittenoom Gorge	Australian Blue Asbestos Pty. Limited	11,094·57
1964	Wittenoom Gorge	Australian Blue Asbestos Pty. Limited	10,614·14
1965	Wittenoom Gorge	Australian Blue Asbestos Pty. Limited	9,279·94
1966	Wittenoom Gorge	Australian Blue Asbestos Pty. Limited	11,464·57
Total			152,466·74

²Not Australian Blue Asbestos Pty. Limited of later years.

cliff-face exposures, and their flat-lying attitudes. The steep cliffs tried the early miners' ingenuity in finding precarious footholds from which to attack the seams, and also afforded him a rapidly increasing overburden ratio which severely limited the amount of fibre he could win from any one exposure. When companies took over from the small operators, they were faced with the problem of adapting methods used for soft-rock coal mining to the extraction of the flat asbestos bodies from their hard, brittle, iron formation host. That these adaptations were not entirely satisfactory, is attested by the subsequent history of the mines.

SURFACE MINING METHODS

The earliest and simplest mining method was to knap fibre from the outcrops of the seam with, perhaps, a little blasting to loosen the surrounding rock. Unless, as at Dales Gorge and Mount Margaret, a wide area of the seam was exposed on the floor of a gorge, the amount of fibre that could be won in this way was quite small.

Benching involved blasting off the overburden in a succession of vertical faces, leaving the seam exposed on the floor of the bench, from where it could be mined either by spalling or further blasting. The method worked best where the seam consisted of closely spaced bands of fibre which could easily be broken from the floor after the removal of the overburden. It was probably less efficient where fibre bands were spread over several feet, as at Yampire Gorge, and a considerable amount of hand-picking was needed to sort the crocidolite from



Figure 68. Abandoned surface bench working of crocidolite on the north side of Snell Gorge (Plate 8). The steep gorge sides severely limit the mineable bench width. The view is in a southwesterly direction with the western side of Yampire Gorge in the distance.

the mullock. As the benches advanced into the hillsides, the amount of overburden to be removed from the seams increased to a point where the operation became uneconomic (Figure 68). In most localities where 1½ to 2 inches of fibre were being mined in a seam, the benches were abandoned when the height of overburden reached about 6 to 8 feet, but at the Yampire mine, where the fibre was richer, the economic limit of overburden was about 15 feet. Benches varied in width according to the steepness of the cliff faces in which they were cut. On very steep cliffs, some benches were only 2 feet wide, but in most places, widths of from 5 to 10 feet were usual. The widest benches were cut at the Yampire mine and reached about 25 feet. Waste rock from benching was easily disposed of by shovelling or bulldozing it over the edge of the bench.

UNDERGROUND MINING METHODS

Underground mining was practised on only three asbestos deposits in the Hamersley Range, the Colonial and Wittenoom mines in Wittenoom Gorge, and the Yampire mine in Yampire Gorge. The methods used were mainly based on the bord and pillar principle, but some long-wall mining was done in the Colonial mine in the last few years of its life. The earliest bord and pillar system was pioneered at the Wittenoom mine and followed at Yampire. It consisted of breaking the seam up into lozenge shaped blocks by two sets of parallel drives intersecting each other at about 120°. The individual blocks were then mined by stripping, apparently until it was considered unsafe to remove any further ore. Examination of the mine plans shows that a large proportion of the ore was left as pillars.

The second variation of the bord and pillar system was practised mainly at the Colonial mine, although it had been used in the later work done on the Wittenoom mine. Keats (1965) gives a full description of the method used at the Colonial mine (Figure 69) and only a brief summary is necessary here. The mine was laid out on four elevations (Figure 70): the main or No. 1 adit, 40 feet or so below the Lower Seam and driven parallel to the dip of the bedding; the haulage ways spaced at about 400 feet intervals along this adit and 20 feet above it; and two levels of stopes on the Lower and Upper Seams. Access to the haulage ways from the main adit was gained by curved turn-outs, graded at 1:10, and by vertical man-ways. The haulage ways were parallel to the strike of the seams and connected to the stopes by man-ways and ore chutes. Chutes with storage bins were situated in the haulage ways vertically above the main adit, which had a conveyor belt running along it to transport ore to the mill. Stopping was preceded by driving headings between adjacent ore chutes, and by excavating a chamber to accommodate a scaper at the top of each ore chute. Mining proceeded from the headings by advancing 24-foot wide 'filtches' spaced so as to leave 10 feet of ore between each to act as support for the back. When the filtches had advanced far enough, they were connected so as to leave 10-foot square pillars spaced 24 feet apart. Stope heights were kept at 40 inches to minimise the amount of barren rock which had to be milled along with the narrow seams. The

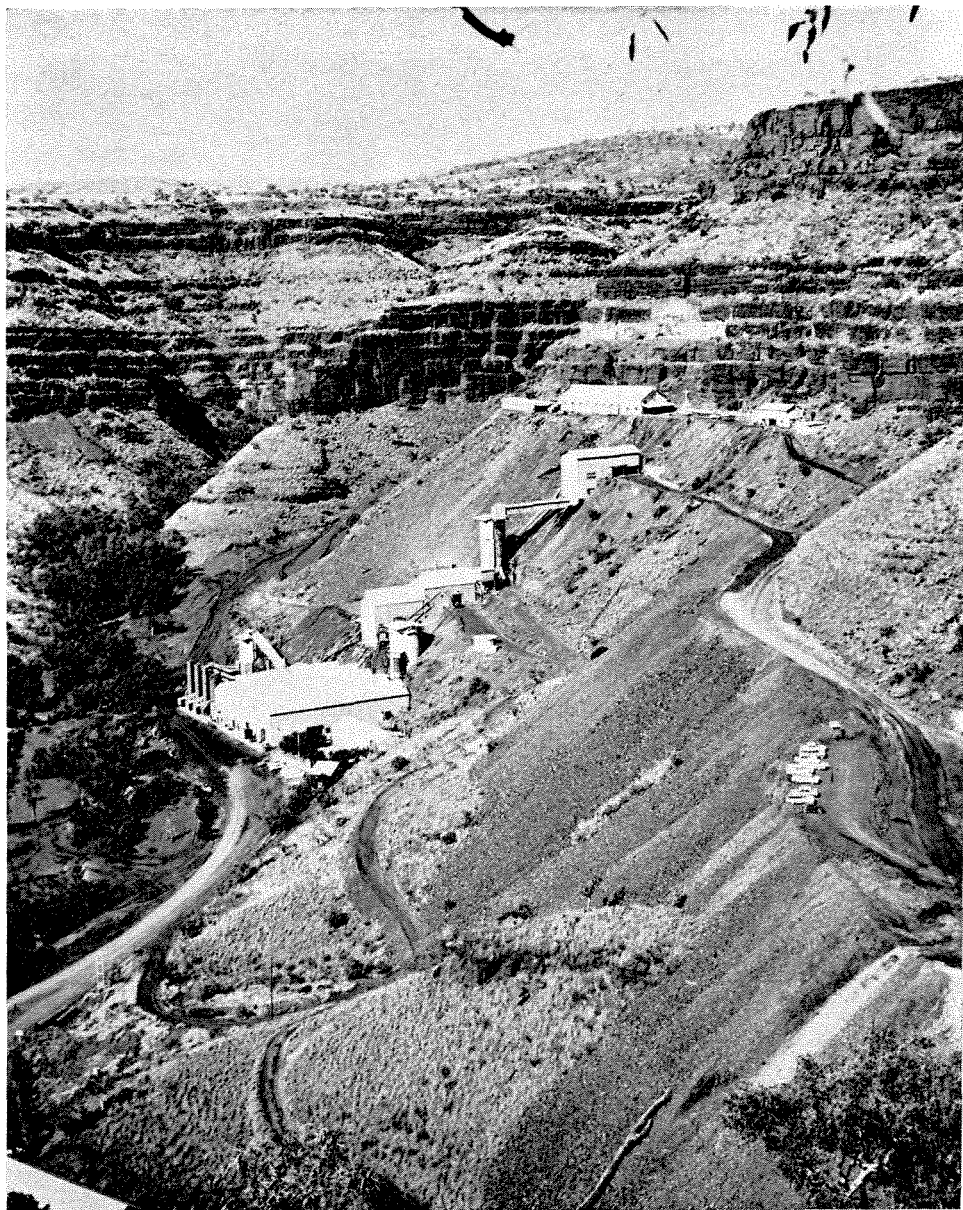


Figure 69. View of the Colonial mine at Wittenoom Gorge from the north (Plate 6). The mine service building and main adit entrance are on the uppermost level, at the base of the Dales Gorge Member of the Brockman Iron Formation. In the cliffs above this level macrobands S1, S2, S3, S4 (thicker), and S5 (thin) can be counted easily, while S6 lies at the base of a steep grassy slope. The macrobands can also be traced in the far cliffs of the gorge, particularly by comparison with Figure 4. Farther down the slope from the mine entrance primary and secondary crushers are followed by the mill. The roof of the administrative offices and workshops appear in the lower left-hand corner, with the waste dumps above them on the right.

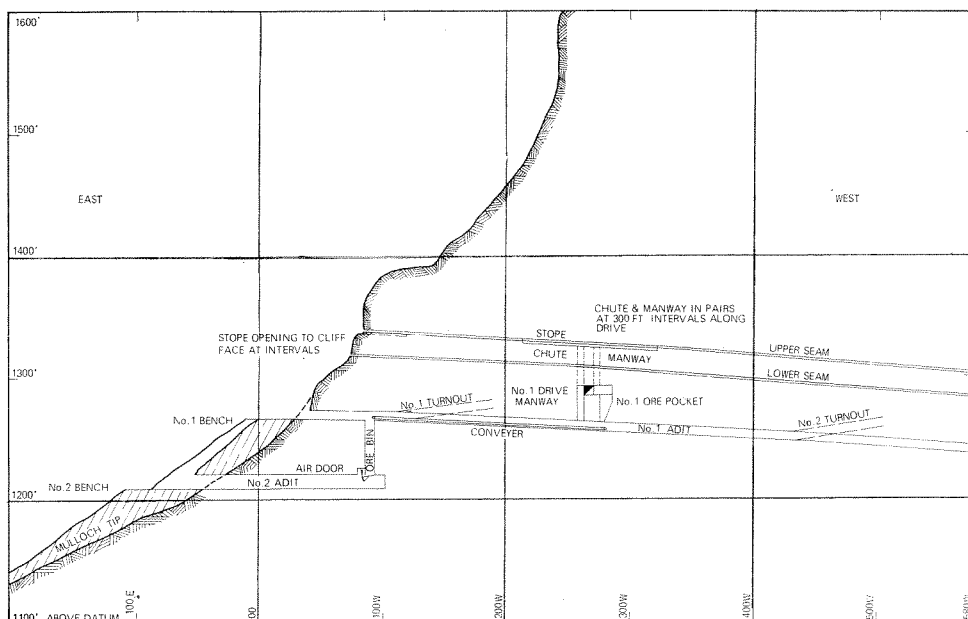


Figure 70. Cross-section of the Colonial mine, showing layout of workings.

broken rock was shovelled back from the face and dragged to one of the ore chutes by a scraper. Once in the chute it was fed into rail cars and carted along the haulage ways to an ore bin above the main adit. From here the rock was fed on to the conveyor belt and taken to the mill as required. All of the rock broken in the mine was removed in the same manner, the waste being intercepted at the start of the milling circuit and carted to a mullock dump, or to extend the bench at the mine portal.

This method of mining had several disadvantages. The low height of the stopes, together with the associated problem of poor ventilation, made working conditions uncomfortable, and meant that high wages had to be offered to obtain and keep labour. Again, because the rock sent to the mill contained, on the average, more than 50 per cent of waste from above the seam, haulage and milling costs were disproportionately high. The method meant leaving about 12 per cent of the ore behind as pillars and so reduced the overall production of the mine. Another disadvantage became evident in 1961, when a large section of the stope on the Lower Seam collapsed, the iron formation proving too brittle to be supported indefinitely by pillars.

The failings of the bord and pillar method led to trials of two long-wall stoping techniques. In the first of these, the stope roof behind the working face was held by three rows of steel supports designed on the principle of the screw jack. As the face advanced, the hindmost row of supports was taken out and transferred to the front, allowing the stope to collapse behind and keeping the

support near the working area. The method allowed full extraction of the ore body and forestalled the possibility of future collapses, but did not alleviate the problems caused by the low stope heights. It ran into difficulties when the pressure of the overlying rocks became too great to allow the rear row of supports to be extracted, and when the back of the stope refused to collapse gently, but cracked along joints and caved abruptly. For some months before the close of the Colonial mine, the Australian Blue Asbestos Pty. Limited company experimented with another long-wall mining method which offered to solve most of the problems met with in the older techniques. The method was explained to us by Mr. R. Graham, formerly underground manager for A.B.A. and now with Hancock and Wright.

Basically the new method consists of two operations. In the first, the 5-foot interval of waste rock above the seam is broken out and used as back-fill to support the stope behind the face. Following this, the lower 2 feet containing the fibre seam is mined out and sent to the mill. Mr. Graham thinks that both operations can be done in the one round of blasting and firing, if different firing patterns and explosives are used in the upper and lower sections of the face, and the charges in the upper part exploded a fraction of a second before those in the lower part. The effect of the multiple explosion is to throw the upper 5 feet well back from the face packing the broken rock firmly against the pre-existing fill, but merely to shatter the lower 2 feet, leaving it sitting close to the face, from where it can be readily hauled to the mill. By increasing the height and safety of the stopes, and by reducing the amount of waste rock which has to be carted and milled, this method seems capable of increasing the efficiency of any future crocidolite mining venture. Mr. Graham anticipates that it will be used if the Eastern Creek deposit is mined.

HEALTH HAZARDS

Possible danger to human health is currently an important factor which affects the marketing economics of crocidolite. McNulty (1968) reports that from June, 1958, 103 men who worked at Wittenoom have developed pneumoconiosis. The disease was more common in mill-workers than in miners, developing more quickly and after shorter periods of exposure to the asbestos dust. Of the 16 men who died from the disease, 14 were mill workers and 2 were miners. These figures indicate the need to reduce the dust hazard in any future crocidolite mining operation, particularly in the milling process.

Origin of the iron formation

INTRODUCTION

The hypotheses for banded iron formation presented here are new. Because they evolved over several years in close step with the acquisition of the data which they inter-relate, it was difficult for us in preparing this bulletin to isolate interpretation from fact. The mental effort required for this separation, into different chapters, has clarified our own appreciation of the problem, but the wide separation of this discussion from the evidence recorded earlier may cause difficulty in reading.

Under 'origin' are included all those earlier processes (derivation, transport, deposition, diagenesis) which contributed to the final existence of banded iron formation in the Hamersley Basin, in much its present state, but before modification by stress associated with the end of the basin's development. It is difficult in these rocks to distinguish between late, stress-controlled, diagenesis and the early effects of externally imposed ('tectonic') stress; indeed, we doubt whether such a distinction is valid, but for present purposes it has been useful to discuss the effects of stress in the following chapter, and also to deal separately with most aspects of riebeckite in Chapter 11. In the present chapter emphasis is placed on the internal evidence from the iron formations themselves; some evidence relevant to iron formation origin which is itself reliant on an interpretation of the total development of the Hamersley Basin is more appropriately discussed in Chapter 10.

Finally we reiterate two guiding principles used in this discussion: firstly, we try to break the main problems into smaller component problems for individual discussion; secondly, we restrict discussion as much as possible to the Hamersley Basin iron formations. A comparison of some other basin by Trendall (1968) gives references to comprehensive reviews by several authors of iron formation problems in general.

REVIEW OF THE PROBLEMS

That banded iron formation presents problems at all is because, above all other sedimentary rocks, no aspect of its origin is self-evident in commonsense or uniformitarian terms. Nowhere is there available for study a basin in which alternate thin layers consisting largely of silica and magnetite are in process of deposition; nor is there any reasonably close analogy, where minor chemical or physical

changes could be expected to result in the deposition of a rock body like the Dales Gorge Member. It is not surprising that for at least two decades in north America it was thought to be lava, nor, that during a later period in Western Australia it was thought to be a sheared fault infilling (see Nomenclature, p. 25). This absence of a firm foundation of commonsense acceptance makes it necessary to argue the origin of the Hamersley Group iron formations step-by-step from whatever evidence seems most significant, within a framework of limitations governed more by other available evidence relevant to the surface environment 2,000 m.y. ago than by everyday experience.

We emphasize firstly the striking lateral continuity of stratigraphic detail (p. 65 to 68 and 106 to 107, Figures 7 and 15; Trendall and Blockley, 1968), and secondly the absence of any marked variation in mesoband composition over the depositional area. These features together indicate that although at no time during iron formation deposition were currents strong enough for bottom disturbance, the material was spread more or less evenly over the whole basin; we conclude that this material must have been distributed either in solution or colloidal suspension. The additional fact that (in spite of a low temperature history, p. 294) there is no sign of clastic granularity in these generally fine-grained rocks supports this conclusion.

We are dealing, then, with chemically or colloiddally deposited material, and there are four general problems to be resolved in its origin:

1. *Derivation*: where was the material before it became involved in the processes leading to its incorporation in iron formation?
2. *Transport*: if it was not in the basin, how was it carried into it?
3. *Deposition*: how, why, and in what form was the material thrown out of solution or suspension?
4. *Diagenesis*: does the present iron formation represent the deposited material, or were there important changes after deposition?

We emphasize next the peculiar total chemical composition of the iron formations (Chapter 5). This material, whatever its derivation, represents a chemical differentiate from its source. A fifth main problem thus arises:

5. *Differentiation*: how and when did the material of the iron formations become isolated from its parent material?

Differentiation may have occurred during any one, or in any combination, of the four main genetic stages. The purpose of the following discussion is to show to what extent our evidence can answer these five main questions for the Hamersley Group; its results are summarised at the end of the chapter. However, these problems are so closely inter-related that it is not convenient to discuss each sequentially under a separate heading, and the course of the discussion is determined by the chain of evidence which is critical for our interpretation. We therefore emphasize finally the extreme chemical contrast between adjacent mesobands. It is a basic difficulty in any simple chemical hypothesis of deposition that material approximating first to silica and then to magnetite should be supposed to have come out alternately from the same body of water. Although suitable

controlling mechanisms have been proposed (Alexandrov, 1955; Sakamoto, 1950) these are not related to the textural details of an actual iron formation. In this discussion an alternative interpretation of the deposition of the Hamersley Group iron formation is developed whose principal feature is the attribution to diagenesis of much of the present vertical chemical heterogeneity.

SIGNIFICANCE OF MICROBANDS

An explanation of microbands is required; their striking regularity, even thickness, and lateral continuity seem most consistent with their interpretation as seasonal, possibly annual, varves. The only reasonable alternatives are either that they are Liesegang bands developed in a colloidal sediment, or that they are primary but reflect some other time rhythm. Liesegang bands which are continuous over 20,000 square miles are, of course, unusual; but so is primary stratification. Liesegang bands have not been described with over a hundred thin alternations of even thickness; but some microbanded cherts have many more than this. Liesegang bands with the complex internal textures of microbands (Chapter 4) have yet to be recorded. Liesegang bands characteristically increase in width away from the reacting surface; microbands show no sign of this. The possibility of a Liesegang origin for microbanding is not completely excluded by these points, but the last three argue strongly against it.

If microbands are primary depositional features, the annual seasons seem to be the only modern climatic rhythm of sufficient contrast, energy, and regularity to control rhythmic precipitation consistently over such a great area. The diurnal rhythm has sufficient regularity, and potentially wide contrast, but firstly it is doubtful whether it could produce the necessary quantitative chemical effect on a basin of this size, and secondly a daily significance of microbanding would imply (if our subsequent hypotheses are accepted), a depositional rate of the order of 6 years (of the present number of days) per foot of iron formation; this seems fast in a basin with only a gentle distributing circulation.

Microbanding is remarkably similar in scale and texture, though not in composition, to various Phanerozoic varves (e.g. Anderson & Kirkland, 1966, Plates 1-4), and for the remainder of this discussion we accept microbands as varves. The same suggestion was made by Cullen (1962) for the 'internal lamination' (texturally equivalent to our microbanding) of cherts in the Griquatown Stage banded iron formation of South Africa.

RELATIONSHIP OF MESOBAND TYPES: THE BASIC HYPOTHESIS

It was shown in Chapter 3 that although the microband interval typically varies within only narrow limits in any one chert mesoband the range in microband interval between different mesobands is comparatively wide. Consider now a hypothetical stratigraphic situation in which a chert mesoband with $T = 12$ mm and $t = 0.8$ mm ($n = 15$) is overlain by a chert-matrix mesoband 3 mm thick,

which is itself overlain by another chert with $T = 20$ mm and $t = 0.4$ mm ($n = 50$). Such a wide contrast in between adjacent cherts would probably be hard to find in practice, but situations very close to this in principle are sufficiently common for it to serve as a valid basis for discussion. If microbands are varves, what does it represent?

In the simplest reading of the sequence, 15 years, during each of which 0.8 mm of (compacted) material was precipitated, were followed by some unknown event responsible for the chert-matrix, which was succeeded by 50 years during each of which only half of the previous annual quantity of (compacted) material was laid down. Even supposing that a satisfactory explanation of the chert-matrix were advanced, this type of deposition, in which a process giving a constant annual increment stops and starts at erratic intervals, each time with a possible change in that increment, seems to represent unconvincingly spasmodic behaviour for any natural environment.

The first step in an alternative hypothesis for this succession, which includes an explanation of the chert-matrix, is based on the continuity of microbanding between chert and its laterally adjacent chert-matrix in discontinuous cherts (Figures 27 and 28, and relevant text). A simple interpretation of this relationship is that the chert was once continuous laterally, and that the neighbouring chert-matrix was formed by the compaction of a greater thickness of microbanded chert which was formerly there. If this chert-matrix next to chert pods was formed by the compaction of chert the second step in the hypothesis follows easily: *all* chert-matrix was derived from the compactional modification of chert. If this order of compaction is acceptable, it is easy to suppose also, as a third step, that cherts with a small t were derived by compaction of cherts with a large t ; it is a logical consequence of this that all cherts must then be assumed to be derived from material with a microband interval greater than that of the thickest known microbanding, which is about 5 mm.

Our alternative interpretation of the hypothetical mesoband sequence described above is now as follows: for an unknown period probably longer than 100 years an annual increment of precipitate at least 5 mm thick was precipitated. The first 15 layers, laid down in the first 15 years, were subsequently compacted to an average thickness of 0.8 mm. The last 50 layers were compacted to an average thickness of 0.4 mm. The intervening group of layers, whose exact number is not known, were more radically compressed, to such a degree that their primary layering is not now distinguishable. Assuming a chert to chert-matrix thickness ratio of about 7:1 (p. 103) some 21 mm of chert are represented by the 3 mm of chert-matrix, and if that had a microband interval within the common range (Figure 10) then it may represent some 20 to 100 years; although this cannot now be certain, some relevant evidence is discussed further below.

The subjectivity of the distinction between chert-matrix and magnetite mesobands makes it possible to extend the hypothesis, and to suggest, as a fourth step, that all of the three mesoband types (chert, chert-matrix, magnetite) which together constitute 90 per cent of the volume of the BIF macrobands in the Dales

Gorge Member were derived by increased compaction and diagenesis of an evenly, regularly, and comparatively coarsely varved parent precipitate. This hypothesis was first proposed by Trendall (1965a) and in a later summary (Trendall, 1966a) was called the basic hypothesis.

The advantages of the basic hypothesis, apart from the fact that it accommodates all the listed textural details of microbanding, are firstly that it requires precipitate of comparatively credible chemical composition, particularly in regard to iron content, and secondly that it requires less drastic changes of depositional chemistry in time. Its main disadvantage has been the difficulty of explaining the origin of mesobanding by it: why and how do different varve sequences respond to compaction so differently, or even the same varve sequence in different places? A possible explanation follows.

SIGNIFICANCE OF MESOBANDING

The lateral continuity of stratigraphic detail, and the absence of evidence for primarily discordant contacts, suggest that during iron formation deposition a thin skin of precipitate accumulated over the basin floor each year, without pause, for immense periods of time, if the basic hypothesis is valid. Under these conditions a feasible control for the proposed differential reaction of microband groups to compaction seems to lie in slight primary chemical or physical differences, controlled in their turn by changes in the depositional environment. That these different reactions take place in groups, rather than at random, shows that these environmental changes must have had at least some regularity, while the mesoband cyclicity of the Calamina and Knox cyclothem indicates an even greater regularity. We examine now some microband sequences to see how reasonably these are capable of interpretation as the result of cyclic climatic variation during deposition.

The 470-varve sequence of the slide illustrated in Figure 25, A and B is of interest here; although the groups defining the light and dark stripes have no immediately conspicuous regularity it is clear from the numbers in successive stripes that a span of 30 to 38 years has some special significance. It is noteworthy that the mean microband thickness of the stripes varies independently of their lightness or darkness which is controlled by hematite content; it could be that there are here two independent climatic rhythms. In the sequence of Figure 25C the rhythm is more regular, and also of the order of 30 years, although the microbands of the dark stripes cannot here be clearly enough differentiated for accurate counting. The control of the climatic variation reflected by this rhythm is not relevant for immediate discussion. The question is discussed later, and for present purposes the rhythm is called a second-order rhythm, in a sense akin to that of Anderson (1966), but with a broader range—a multiple of years less than one hundred.

But mesobanding is not developed in these varve sequences. The further sequence from the striped facies of the Weeli Wolli Formation in Figure 26 closely

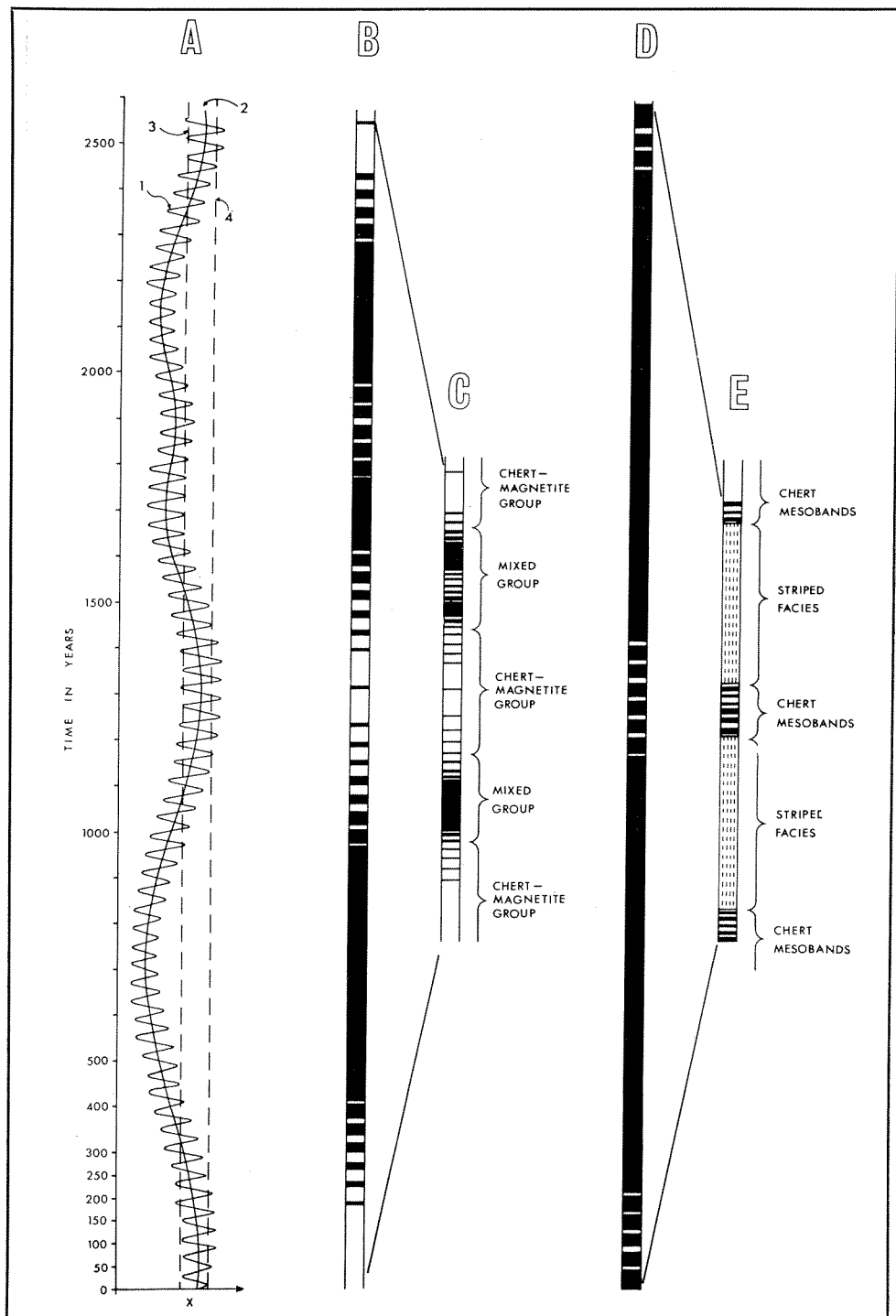


Figure 71. Diagrams illustrating a possible cyclic climatic control of mesobanding; see text for further explanation.

resembles those of Figure 25, except that, as was noted, the light stripes with thicker microbanding are, in effect, thin chert mesobands, while the microbanding in the dark stripes is antipathetically compressed. It was noted also that the cyclic appearance of such cherts bears a strong resemblance to the Knox and Calamina cyclothems. The salient points of a hypothesis which accommodate all these features, including the Calamina cyclothem, are:

1. Superimposed on the annual, seasonal, climatic cycle which controlled the varving of the parent material (destined to become either microbanded chert, chert-matrix, or magnetite) there was a second-order climatic variation most conspicuously reflected in the striped facies of the Weeli Wolli Formation.

2. A threshold value for some climatic factor existed, above which compaction was disproportionately inhibited; the varved material deposited at times when the second-order cycle raised this factor above the threshold became microbanded chert, while that deposited below the threshold was liable to compactional collapse.

3. Compaction of the varved parent material deposited below the threshold was intensified in proportion to the abundance of potential chert immediately adjacent.

4. Superimposed on the second-order cycle was a longer climatic cycle, or possibly a double cycle, of the order of 1,000 to 3,000 years (a 'fourth-order cycle', in the sense of Anderson, 1966).

This hypothesis is illustrated in Figure 71, of which an explanation follows: In the diagram of Figure 71A the abscissa represents some unspecified factor of mean annual climate (x); numerical value and sense are irrelevant. The ordinate represents time. The line marked 1 represents the second-order rhythm, here shown arbitrarily as 40 years, and the line marked 2 shows fourth-order fluctuations of the 40-year mean. The pecked line marked 3 represents a threshold value for x such that all varved material deposited at times when x is above it, is highly resistant to compaction, and may become chert, while material deposited when x is below it, will be severely compacted, to chert-matrix or magnetite. The column marked B in the same figure shows the depositional (stratigraphic) result of these suggested climatic and depositional conditions, black indicating material liable to extreme compaction, and white showing potential chert.

The column marked C represents B after compaction, with 80 per cent of the black material removed and 20 per cent of the white material. The suggested equivalence to the parts of the Calamina cyclothem is indicated on the figure, and this column should be compared with the expressions of the cyclothem in Figure 13. The postulated climatic curves of Figure 71A show, in the lower part, a simple fourth-order cycle of period about 1,300 years, while the same cycle in the upper part has an intermediate central irregularity superimposed. This is a possible mechanism for the absence (Figure 13A) or presence (Figure 13B) of chert mesobands in the mixed groups of the Calamina cyclothem.

The column marked D in Figure 71 shows the stratigraphic result of the climatic curve of A if the threshold for inhibition of compaction were raised to the line marked 4 (or alternatively if the whole curve moved down relative to a stationary threshold). Depositional material is marked as in column B. The possible course of compaction of D is shown by column E. On the assumption (3, above) that the varved deposit tends to compact evenly in the absence of potential chert the continuous thick black parts of D are assumed to have compacted to the same average extent as the change from B to C; the smaller mixed black and white parts of D are assumed to have compacted in the same proportions used in constructing C from B. Column E, as a result, closely resembles parts of the Weeli Wolli Formation: the row of dots in E represent the paler stripes of the striped facies, corresponding to second-order cycle peaks on the climatic curve, while the intervening alternations between chert and chert-matrix represent the type of material in Figure 25C.

The significance of the earlier record (p. 91) of 70 stripes or mesobands in a single alternation from white chert to red chert and back to white chert in the Weeli Wolli Formation is now clear. It gives an indication of the number of second-order cycles in a fourth-order cycle, and thus of the total length of the latter: 70 x 30 to 40, or roughly 2,000 to 3,000 years.

The assumption has been implicit in discussion so far that this fourth-order cycle in the Weeli Wolli Formation has the same control as the Calamina and Knox cyclothems, and that all three may be regarded as different expressions of the same controlling environmental rhythm. But in Chapter 3 separate names were applied to these cyclothems because they occur in different members of the Brockman Iron Formation, and differ from each other to the same degree that these members are characteristically different in lithology and petrography. Thus in the Knox cyclothem thin red and white cherts alternate sharply within the typically homogeneous and blue-grey chert-matrix of the Joffre Member (Figure 19B), whereas the Calamina cyclothem of the Dales Gorge Member has the rather different chert-magnetite and mixed groups (Figure 13); the average thickness of the Knox cyclothem is about 7 cm, whereas the mean thickness of the 55 Calamina cyclothems of Tables 6 and 7 is 14 cm (0.56 feet). These differences apart, both the red cherts of the Knox cyclothem and the cherts of the chert-magnetite group of the Calamina cyclothem:

1. are liable to be represented completely by massive riebeckite,
2. have relatively fine microbanding,
3. are coloured red or pink even in fresh core material,
4. have internal irregularities in microbanding (of the type illustrated in Figure 30),
5. are rarely podded or cross-podded.

The white cherts of the Knox cyclothem and the cherts of the mixed group of the Calamina cyclothem have in common that they:

1. are rarely represented by riebeckite,
2. are relatively coarsely microbanded,

3. do not normally carry hematite.
4. are liable to podding.

These striking resemblances between the cherts of the two parts of both cyclothems certainly support the possibility of their common control. But since the varves supposed to have been present in the material now represented by chert-matrix cannot now be counted, the duration of neither of the cyclothems is capable of direct determination, as in that of the Weeli Wolli Formation. However, a chemical argument, given below the following heading, suggests independently that the Calamina cyclothem, at least, is sufficiently close to a fourth-order cycle in length for a provisional assumption that the counted length of the Weeli Wolli chert alternation may also be that of both of the named cyclothems of the Brockman Iron Formation.

IRON/SILICA RELATIONSHIP IN THE BASIC HYPOTHESIS

If the basic hypothesis is accepted it is evident that in the change from micro-banded chert to chert-matrix, there is a large relative increase in total iron content (Table 12, analyses 1-4). Let it be supposed, therefore, that under the chemical conditions of diagenesis, iron remained stable in each microband, and that the relative increase in iron was achieved by removal of other more mobile constituents, chiefly silica. If each microband pair then had the same initial composition, there should be an inverse quantitative relationship between microband interval and total iron content in all microbanded cherts. A number of microbanded cherts were analysed to test this relationship, and several cherts originally analysed for other purposes proved suitable for inclusion in the study. In all, 22 analyses are available of cherts with known microband intervals (Table 12, analyses 1, 2, 16-19; Table 13, analyses 1, 2, 4-17). The composite analyses among these have equivalently averaged intervals. These analyses are plotted in Figure 72, together with a composite analysis of Dales Gorge Member chert-matrix, analysis 4 of

The four analyses of chert associated with crocidolite (Table 13, analyses 14-17) are discussed separately in Chapter 11. Of the 18 remaining analyses only 3 do not fall within the area between the pecked lines. The general trend of this area is precisely the type of curve which would be produced by steady reduction of microband thickness by removal of the constituents other than iron; these must represent the lighter and bulkier part of each microband. The single analysis of chert-matrix at the lower end of the area is so placed on the assumption of a 7:1 reduction of microband interval in its formation from material assumed to have had originally the interval of its associated cherts. When allowance is made for the several varied assumptions made in forecasting such a relationship, the degree of adherence to the indicated area of Figure 72 seems to lend support to the basic hypothesis.

Each point of Figure 72 represents, independently of the microband interval of the chert, a determination of the total iron content per microband, which should

be constant on the assumptions made. The values given for the 18 relevant analyses (excluding chert-matrix and cherts associated with crocidolite) appear in Table 21, in order of microband interval. Again, considering the varied assumptions made, and possible errors, the scatter of values is sufficiently small for the mean, 22.5 mgm Fe per microband per square centimetre area, to be taken seriously. In particular, this figure can be used to calculate a mean depositional rate for iron formation knowing only the total iron content, and thus to estimate the duration represented by the Calamina cyclothem. Taking a figure of 30 per cent total Fe for the Dales Gorge Member (Table 17, analyses 3-4), with a density of 3.3, the iron formation contains 0.99 gm of iron per cubic centimetre, and each cm of iron formation represents 44 years. Thus a Calamina cyclothem of 14 cm would represent 616 years.

This estimate differs by a factor of about 4 from the 2,000 to 3,000 years suggested for a complete cyclothem in the Weeli Wolli Formation, but the possible variables are so many that the correspondence must at present be considered

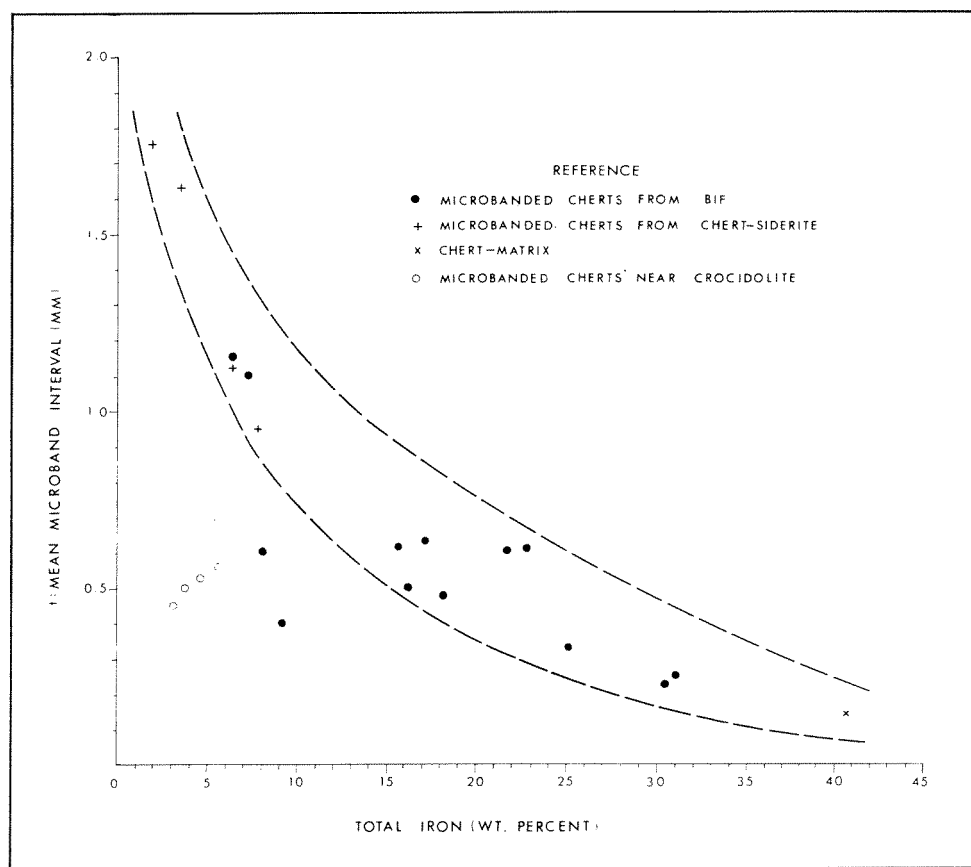


Figure 72. Graph showing the relationship between total iron content and microband interval in some microbanded chert mesobands of the Dales Gorge Member.

TABLE 21. COMPARISON OF MICROBAND INTERVAL AND TOTAL IRON CONTENT OF 22 CHERT MESOBANDS OF THE DALES GORGE MEMBER

5	2	3	4	5	6
Table	Analysis	Microband interval	Total Fe	Calculated density	Milligrams Fe per microband per cm ²
		mm	Wt. percent		
12	17	1.75	1.79	2.62	8.2
12	16	1.63	3.50	2.65	15.1
13	7	1.15	6.41	2.71	20.0
13	4	1.12	6.47	2.71	19.6
12	1	1.10	7.31	2.74	22.0
		(mean)			
13	6	0.95	7.76	2.73	20.1
12	18	0.69	5.39	2.68	10.0
13	8	0.63	17.2	2.96	32.1
13	10	0.62	15.6	2.92	28.2
13	11	0.61	22.9	3.10	43.3
13	9	0.60	8.04	2.75	13.3
13	12	0.60	21.8	3.07	40.2
13	2	0.50	16.3	2.93	23.9
13	13	0.48	18.3	2.98	26.2
13	5	0.40	9.03	2.76	10.0
12	2	0.33	25.2	3.15	26.2
12	19	0.25	31.2	3.33	26.0
13	1	0.23	30.6	3.32	23.3
Mean of column 6 = 22.5 mgm					

satisfactory. It is possible that the basic hypothesis must be modified to envisage actual variation of total iron deposition during the course of a cyclothem. Table 21 gives some evidence for this, in that the mean of column 6 for the 9 cherts with thickest microband intervals, is 21.9 mgm, while that for the 9 cherts with thinnest microband intervals is 25.8 mgm. Also, as will be argued in Chapter 11 for the cherts close to riebeckite, and as is testified by any mineral reconstitution involving iron, *some* degree of iron mobility must be envisaged during diagenesis; and loss of iron from the system during diagenesis will lead to a misleading low value for cyclothem duration by the method used here.

THE CONTROL OF COMPACTION

In proposing a climatic control of compaction as the main cause of both mesobanding and cyclic mesoband sequence the problem remains of determining

the exact mechanism of the control. It was previously suggested (Trendall, 1966a) that phosphate content may be an important control of compaction in both chert podding and macule formation, but additional analyses reported by M. R. Walter (University of Adelaide, unpublished manuscript, 1968) have cast doubt on the general applicability of this. Certainly in the case of podded cherts there was no single factor controlling podding which was dependent solely on time, since a podded chert is a group of microbands, deposited over the same time interval, which have reacted differently to compaction in different places. At present, no satisfactory suggestion for compaction control can be made, and the problem must await more detailed chemical work. In particular, it would be useful to find one or more mesobands which are, in three different areas, continuous, podded, and completely compacted.

The existence of gradually less clearly microbanded cherts, with complete gradation to non-microbanded cherts (p. 108), suggests that non-microbanded cherts may originate by destruction of microbanding within a chert mesoband without compaction; this may give a useful clue for further work on compaction control.

PHYSICAL STATE OF THE PRECIPITATE

After discussion of chemical changes during diagenesis, it may seem most relevant to deal with the original composition of the precipitate, but it is convenient to note beforehand the available evidence for its physical state. From previous discussion we suppose that the iron formations originated as colloidal precipitate of some form; we have yet to discuss either the nature and derivation of the precipitated material or the reason for its precipitation. On the other hand we have argued firstly that each microband pair represents the result of one year's precipitation, and secondly that the precipitate was capable of extreme compaction. We now assume that, to possess this unusual capability, the precipitate was in some gel form, with a very high water content. The textural details of the microbanding, given in Chapter 4, may be expected to yield some information about the nature of this material.

An initial unknown is the position within the basin at which the material nucleated. It may have grown out of chemical solution in place on the basin floor, or it may have aggregated in some particulate form close to the water surface, with a subsequent gravitational descent to the floor.

Attention is first directed to Figure 29A, and its interpretation in the light of the basic hypothesis. It is supposed from this that the left-hand parts of each of the central group of microbands represent compacted representatives of what now appear as the right-hand parts. It is consistent with the basic hypothesis that the difference in compaction between the two sides of this group of microbands is taken up largely by reduction of the thickness of the chert component of each microband pair. The most reasonable explanation of the continuity of the constituent hematite laminae of the iron-rich part of each microband on the left,

contrasted with discontinuous laminae on the right, seems to be that these laminae were originally continuous throughout, and that the initial compaction had the effect of preserving this continuity, while in the uncompacted chert the laminae were subject to some later disturbance which produced their characteristic lateral variation (Figure 21B). If this interpretation is correct then the iron-rich part of each varve was itself composed of several very thin and evenly deposited layers. The obvious textural resemblance between the laminated stilpnomelane of coarsely microbanded ('primitive') cherts (Figure 21C) and the hematite of finely microbanded ('flat-modified') cherts (Figure 21D) speaks for the continuous existence of this phenomenon throughout the course of the Calamina cyclothem. The precipitation of part of each microband as a number of separate thin sheets is consistent also with the unusual microbanding from the Boolgeeda Iron Formation shown in Figure 23C, where 8 or 9 continuous dark laminae form the iron-rich part of each microband.

However, elsewhere among the Hamersley Group iron formations microbanding occurs not only with no trace of this internal lamination but with indications of an entirely different texture. The 'graded' structures in Figure 26C, in chert from the Weeli Wolli Formation, and Figure 24C, from the Dales Gorge Member, show no sign of lamination, and conversely the typically laminated microbanding never shows any tendency towards grading. The microbanding in Figure 26C seems to have vaguely globular concentrations of hematite texturally reminiscent of the globulate structure of some shales (Figure 21C). The streakiness of the very coarse microbands of Figure 24A is suggestive of an intermediate type between perfectly laminated and perfectly globular material in the original material of the microbands. The streaks there are less continuous than in the compacted parts of normal microbanding (e.g. Figure 29A), and the texture continues through both parts of each microband.

It is reasonable to suppose that the very finely laminated structure (hematite in ankerite) quite commonly present at chert margins (Figure 29B), and possibly also the lamination in the siderite of chert-siderite at about the same scale (Figure 29C), both originated by preservation of a primary lamination by early compaction in the same way as is suggested above for that of the left-hand part of Figure 29A.

In summary, there seems to be evidence in microband textures both for an originally coarsely globulate structure of the precipitate, in which case the globules may be assumed to have formed at some high level in the basin and settled to their final resting place, and for an initially laminated structure, in which case the material may either have settled in a very fine form or may actually have accreted in place on the basin floor. This latter mechanism has been suggested as an annual process for example, in nodular manganese-rich accretions on the floor of the Baltic Sea (Winterhalter, 1968).

In either case, it will be argued below the following heading that the material was light, and able to permit the free passage, across the stratification, of very

large quantities of water. We suppose therefore that the material was particulate, at least on the colloidal scale, and that both microbanding and its internal lamination where this existed, were defined by differences in particle composition, so that neither was destroyed by the passage of interstitial water. Neither the origin of the internal laminations which are commonly present in microbanding, nor that of the less common 'graded' structure, are known.

CHEMICAL COMPOSITION AND EVOLUTION OF THE PRECIPITATE: A MODIFIED HYPOTHESIS

We suppose that, in bulk, the chemical composition of the original precipitate approximated closely, at least insofar as the more stable constituents are concerned, to the existing bulk composition of the iron formation. This supposition may be contrasted with a type of hypothesis in which the original material is chemically unlike the present iron formation, and at some subsequent time is systematically and consistently converted into it (e.g. Lepp and Goldich, 1964). Our proposal cannot be proved; it is a judgment derived largely from the following three points:

1. It is argued, beneath the following heading, that the total weight of iron in the sediments of the Hamersley Basin makes the case for the direct addition of this element from some extraneous source very strong, since the disposal of excess materials, if it were derived by weathering of the older Pre-Cambrian crust, represents a formidable (in our view insurmountable) bulk problem in terms of practical geological processes. When the total bulk of the Hamersley Group iron formations is considered, similar quantitative problems confront any hypothesis involving significant post-depositional changes of chemical composition. When faced with the necessity of introducing, and later removing, tonnages of any material of the general order of those in Table 23, it seems simpler to take the present iron formation composition at its face value, unless some strong positive evidence suggests otherwise.

2. In spite of their range in lithology, the chemical compositions of the various iron formation units of the Hamersley Group are, as far as the available information goes (Table 17), remarkably uniform. A similar uniformity of bulk chemical composition, coupled with even more varied lithology, exists among iron formations of the Lake Superior area and the Cape Province of South Africa (Trendall, 1968). If iron formation began with some composition different from what it now possesses, then the subsequent course of alteration might be expected to vary with different lithologies, and the environmental differences which these imply.

3. It seems reasonable to expect, in any rock which has undergone important chemical modification since deposition, a degree of lateral heterogeneity due to local variation of fluid movement and the factors controlling it. This is found in the local secondary alteration of shale to limestone in the Dales Gorge Member (p 64 and 110), and typically in the secondary growth of nodular chert in limestone.

These three factors suggest that the original precipitate contained much the same stable materials as the present iron formations. The arguments do not apply to the alkali metals, whose transport in solution is easy and whose total bulk is comparatively small, or to carbon dioxide, which is even more mobile; nor is it implied that a good deal of rearrangement within the precipitated constituents may not have taken place within the rock after deposition. A possible modification of the basic hypothesis in the light of these chemical suppositions is now discussed.

The basic hypothesis supposes that iron-bearing and silica-rich varves are, after deposition, compacted differentially in groups to form mesobanding, the general trend of the chemical changes during compaction being given by an upper left to lower right passage along the curve of Figure 72. In this simple concept iron-rich chert-matrix is supposed to have lost, among other things, a great deal of silica, finely microbanded chert rather less silica, and coarsely microbanded chert least silica. But from all these materials the silica lost must be disposed of, and this can only be achieved by re-solution and return upwards to the waters of the basin in the simultaneously expelled water. There are two objections to this. Firstly, if coarsely microbanded precipitate contained as much silica per microband as the more coarsely microbanded cherts now preserved, then passage of water through this necessarily rather dense material would be difficult in sufficient bulk to remove the theoretically required amount of silica; secondly, it is hard to see why silica just precipitated on the basin floor should shortly afterwards be redissolved in the interstitial water, and taken right back to the same silica-saturated water from which it was precipitated.

Both objections may, to some extent, be overcome by a modification of the basic hypothesis. Let it be again supposed that 22.5 mgm of iron were deposited annually (Table 21), but let it be supposed also that the other major iron formation constituents were deposited in equal annual increments in their appropriate proportions to this quantity of iron. From the average iron formation composition of Table 17 (columns 4, 5, and 6) there would be deposited per square centimetre of the basin, each year, in each future microband:

					mgms
SiO ₂	40
Fe ₂ O ₃	20
FeO	10
CO ₂	4
					—
Total	74
					—

Assuming these oxides to be in some form with an effective average density or 3 they would occupy about 0.025 cc. It has already been suggested that each microband had a depositional thickness of about 5 mm. Each cubic centimetre of wet precipitate thus had 0.05 cc of material other than water, of which the

remaining 0.95 cc was presumably composed, to give a bulk density of 1.1, of the following approximate composition:

		Wt. per cent	mgm/year/cm ²
SiO ₂	8	40
Fe ₂ O ₃	4	20
FeO	2	10
CO ₂	1	4
H ₂ O	85	476

This percentage of water includes combined and interstitial water. A possible assumption is that half of the water was combined in the particulate gel, while half was interstitial, and occupied about 48 per cent of the total volume; but there is no present evidence to prefer one allocation to another. The modified hypothesis now supposes that, on burial, each varve group was subjected to increasing pressure. Virtually all were compacted, but some reacted abruptly, at an unknown level, to give the sharp break in the present iron formation represented by the transition from chert to chert-matrix. We suppose that during this transition a proportion of the silica was redissolved and streamed upwards through the less compacted and highly porous overlying material. The difficulty of explaining this re-solution is set aside for discussion in the following paragraph. We suppose that any less-compacted material bathed by the ascending silica-rich

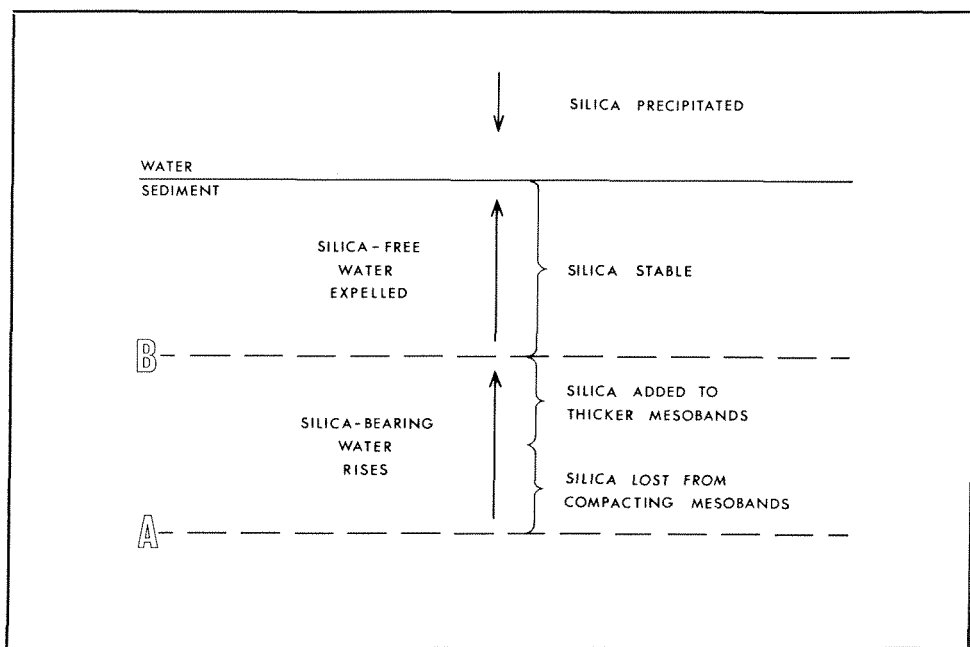


Figure 73. Diagram illustrating the suggested movement of silica during the diagenesis of iron formation.

water is then able to absorb more silica, to raise its silica content per microband above that originally deposited. The passage of this water may be responsible for the partial rearrangement of the internal lamination of some microbands, noted in discussion above. The suggested process is shown very diagrammatically in Figure 73. The first objection to the operation of the basic hypothesis is now overcome, since the nature of the material suggested would allow large-scale passage of fluid without, as it were, the process of stifling itself with the sheer bulk of its own silica.

The second objection still remains, although it is less severe, since it is no longer proposed that silica must be carried, in solution, right back to the region of its precipitation. Instead a zone of change in silica stability is suggested, between levels A and B in Figure 73. It is not possible to be certain of the reasons for this change, but three suggestions may be made:

1. As is emphasized below the next heading, we make no suggestions of the combined chemical form of the precipitated material whose bulk composition we have set out. Clearly, another constituent which could be removed in upward-streaming water during compactional diagenesis is CO_2 (see later heading: 'Significance of chert-siderite'). It is possible that, according to the nature of the precipitated material, CO_2 may be lost at a higher level than silica, whose stability may be affected by consequent Eh/pH change.

2. A biochemical agency is at least possible as a control of precipitation in the basin (Chapter 10). It is possible that the zone AB of Figure 73 represents the depth of burial below which the chemical balance of silica is not subject to biological (photosynthetic) control.

3. It is not certain that the silica of the precipitate was in an uncombined, or simply hydrated, form. The source of the soda during formation of riebeckite, which formed variously (see Chapter 11) by metasomatic replacement of chert at a fairly late stage of compaction, and by growth (as crocidolite) in concordant dilational veins, is unknown, but its local abundance in an available form cannot be doubted. If the initial precipitate was, wholly or partly, sodium silicate then it is possible that the breakdown of this under a specific pressure of burial liberated both silica and soda simultaneously. Eugster (1967) has described the formation of chert from sodium silicate (magadiite) in the evaporitic beds of Lake Magadi, in Kenya. Colloidal sodium silicate is known to be pressure-sensitive, and while this suggestion is highly speculative, it opens interesting possibilities for exploratory experimental work.

As a final note on this modified hypothesis, in which silica *redistribution*, rather than *selective removal*, accompanies compaction, it is appropriate to show how available data give some quantitative basis for the hypothesis. In Table 22 all analyses of Table 21 for which SiO_2 figures are known are recalculated in terms of SiO_2 per microband. Neighbouring analyses of Table 21 are averaged, and chert-matrix (4 of Table 12) is included with an assumed microband width based on average thickness ratio to chert. This Table shows that, if the modified

TABLE 22. SILICA CONTENT PER MICROBAND IN SOME CHERTS AND IN CHERT-MATRIX

1	2	3	4	5	6
Material (column No. of Table 12)	SiO ₂	Calculated density	SiO ₂ per cc.	Microband interval	SiO ₂ per microband per cm ²
	Wt. percent				(milligrams)
Mean of 16 and 17	89.53	2.64	2.36	1.69	399
1	74.71	2.74	2.05	1.10	226
18	80.69	2.68	2.16	0.69	149
Mean of 2 and 19	50.84	3.24	1.65	0.24	40
4	35.74	3.50	1.25	(0.15)	19

hypothesis is true, (1) chert of microband interval 0.24 mm still has its original amount of silica, (2) chert-matrix has lost about half of its silica, and (3) coarsely microbanded chert may be enriched by a factor of ten above its initial silica content.

MINERALOGY OF DIAGENESIS

As has already been noted, we offer no opinion on the precise chemical combination of the oxides whose proportions in the initial precipitate have been set out. There are three reasons for this. Firstly, we believe that all minerals in the existing iron formation are secondary, and that little can be deduced about their parent materials from their present textures; secondly, we see no useful purpose in speculative suggestions unsupported by the results of a successful demonstration that precipitation of the suggested material is possible in the laboratory under conditions reasonably assumable to be those of the basin; and thirdly, we think that work in this field is more appropriately conducted by colloid chemists than by geologists.

Our knowledge of the mineralogy of diagenesis is therefore confined to the paragenetic evidence already given in Chapter 4; with one exception, no significantly paracompaactional stage is represented in this evidence, and it can be taken to apply to reorganization at deeper levels than those with which discussion has so far been concerned in this chapter. Only two points additional to the evidence of Chapter 4 need to be made here: the significance of the $\text{Fe}^{2+}/\text{Fe}^{3+}$ ratio, and that of cellular hematite.

Although the data are not separately tabulated, it is apparent that in the chemical progress of the genetic hypothesis suggested, there is a steady increase in $\text{Fe}^{3+}/\text{Fe}^{2+}$ ratio from coarsely microbanded chert to chert-matrix, from about

0.05 to about 3 (Tables 12 and 13, and Figure 72). This rather surprising tendency towards oxidation rather than reduction after burial is correlated with a decrease in relative carbonate content, as would be expected from the paragenetic evidence, but the source of additional oxygen is not clear, and it may be either that a proportion of ferrous iron returns to the basin or that there is a redistribution of iron between the mesoband types in the same way as silica. Thus the apparent change in oxidation state using the interpretation of the basic hypothesis may be illusory.

Cellular hematite is a puzzling phenomenon which seems to give some guide to the type of work which may elucidate the earlier chemistry of diagenesis. The 'octahedra' illustrated in Figure 34 have a mean *cavity* volume of 31 per cent. They may reasonably be supposed to represent pseudomorphs of an earlier iron mineral, and it may therefore be that the total amount of iron in each octahedra is that of this parent crystal. An octahedral form of $\text{Fe}_2\text{O}_3 \cdot 4\text{H}_2\text{O}$ has been described by Thiessen and Köppen (1931). But this has a density of 3.0 to 3.1, and the hematite resulting from a direct conversion would occupy only 28 per cent of the original volume. However, if it is supposed that $\text{Fe}_2\text{O}_3 \cdot \text{H}_2\text{O}$ formed the original octahedron a conversion to hematite would give a volume of about 70 per cent. This compares well with the present volume of the octahedra, but no cubic form of $\text{FeO} \cdot \text{OH}$ is known (Bernal and others, 1959). The point made here is that future work on the mineralogy of diagenesis must take account of forms not described from the present natural environment.

DERIVATION OF THE IRON

In whatever form, and by whatever mechanism, iron was precipitated from the waters of the depositional basin, it must have been supplied to those waters from some earlier source. In the previous literature of iron formation two main proposals for this source have been made: weathering of the surface rocks of the catchment area of the basin, and vulcanicity of some sort within or close to the basin itself. These two suggestions have been aptly called the 'from-above' and 'from-below' theories by Oftedahl (1958). A third hypothesis, whereby iron is concentrated within a basin by re-solution and circulation, is favoured by Borchert (1960), and may be termed the 'from-within' theory.

One of us (Trendall, 1965b) argued earlier, for the Brockman Iron Formation only, that the total originally deposited quantity of iron in it was so great as to make it virtually impossible, in terms of practical geological processes, to weather enough crustal material to supply the iron and simultaneously to dispose of all the excess materials, in particular aluminium. Therefore, it was argued, extra iron must have been supplied by some means other than weathering.

It is now possible to extend this form of argument to include all the sedimentary rocks of the Hamersley Group, and to set limits of uncertainty to some of the required parameters which cannot be precisely determined. In our description of the type section of the Dales Gorge Member (Trendall and Blockley, 1968,

p. 50) we gave a minimum depositional area of the Dales Gorge Member of 20,000 square miles, and of the Marra Mamba Iron Formation 33,000 square miles. The lower formations of the Hamersley Group have a crudely crescentic outcrop, and if deposition of the whole group was continuous between the horns of the crescent (Plate 2), the Hamersley Group may have been deposited over some 50,000 square miles.

For the purpose of further discussion, the estimate of 33,000 square miles is used, except that as all subsequent figures are in metric units a rounded figure of 100,000 square kilometres is accepted; this is subject to an unavoidable error of about ± 45 per cent, discussed further in Chapter 10. In metric units an average Hamersley Group sediment thickness of 1,200 metres (4,000 feet) is reasonable (Chapter 3), to give a volume of 120,000 cubic kilometres.

Using the approximate average volume proportions of Table 3 (rounded to iron formation 70, shale 20, dolomite 10) and average densities of 3.2, 2.6, and 2.85 the weight proportions of the different sediment types in the Hamersley Group are: iron formation 73.6 per cent, shale 17.1 per cent, and dolomite 9.3 per cent. Accepting now a composition of Hamersley Group iron formation based on an average of columns 4, 5, and 6 of Table 17, a shale composition based on the average of analyses 1-4 and 7-11 of Table 15, and for dolomite the theoretically pure mineral composition, the following average composition for Hamersley Group sediments is obtained, recalculated to 100 per cent and ignoring water and minor constituents:

SiO ₂	45.72
Al ₂ O ₃	2.81
Fe ₂ O ₃	20.79
FeO	12.90
MgO	4.64
CaO	3.65
Na ₂ O	0.27
K ₂ O	1.50
CO ₂	7.72

From the volume estimate already given, and using an average density of 3.05, the total weight of Hamersley Group sediments originally deposited was 36.6×10^{13} metric tons. In column 1 of Table 23 is shown the consequent total weight of each metal, using the average composition already suggested. The more significant figures there are 9.4×10^{13} metric tons of iron (about a hundred million million metric tons) compared with 0.6×10^{13} metric tons of aluminium: the weight ratio of Fe/Al is 15.7. An estimate of the likely composition of the catchment rocks of the Hamersley Basin, based on present day areal proportions in the adjacent Archaean 'shield' proved previously (Trendall, 1965b) to be close to Sederholm's (1925) average Precambrian of Finland. This was therefore used for columns 2 and 3 of Table 23. In column 2 the constituent weights of metals in Finnish Precambrian crust are shown for a total metal weight of 20.5×10^{13} metric tons, the same as that of the Hamersley Group. A comparison

TABLE 23. TOTAL ORIGINAL METAL AND SILICON CONTENT OF HAMERSLEY GROUP SEDIMENTS, AND COMPARISON WITH METAL CONTENT OF AVERAGE PRECAMBRIAN CRUST (ALL FIGURES IN UNITS OF 10^{13} METRIC TONS)

	1	2	3	4	5	6
	Hamersley Group sediments	Precambrian crust for total of Hamersley Group	Precambrian crust for Hamersley Group iron	Oxide weights of column 3	Excess of column 3 over column 1	Precambrian crust for Hamersley Group silicon
Si	7.7	12.5	86.2	184.4	78.5	7.7
Al	0.6	3.1	21.1	39.9	20.5	1.9
Fe	9.4	1.4	9.4	12.5	0.8
Mg	1.1	0.4	2.8	4.6	1.7	0.2
Ca	1.1	1.0	6.6	9.2	5.5	0.6
Na	0.1	0.9	6.2	8.4	6.1	0.6
K	0.5	1.2	8.1	9.8	7.6	0.7
Total	20.5	20.5	140.4	268.8	119.9	12.5

of columns 1 and 2 demonstrates clearly the gross chemical imbalance in the direct equation of Hamersley Group sediments with eroded crust. In column 3 the constituent metal weights are shown if sufficient average crust is used to supply all of the Hamersley Group iron. In column 4 the approximate oxide weights of these metals are given; from the total it may be seen, assuming a density of about 2.7 (2.7×10^9 metric tons per cubic kilometre) that close to one million cubic kilometres of average crust are needed to supply sufficient iron for the Hamersley Group. In column 5 are shown the excess metal weights between columns 2 and 3; these represent the total weight of metals (120×10^{13} tons—about 6 times the weight deposited) which must be disposed of if the Hamersley Group is to be derived by weathering from an older Precambrian terrain.

The stiltstones and greywackes of the overlying Wyloo Group seem to present no unusual features chemically, which suggests that the land from which they were derived was not blanketed by a thick aluminous sheet. Either, therefore, more than twice as many tons of aluminium as there were tons of iron deposited must be supposed to have been removed from the area completely, or the 'from-below' theory for the derivation of the iron must be preferred to the 'from-above', or weathering, theory. Records of present volcanic supply of iron to the surface (Behrend, 1936; Zelenov, 1958; Miller and others, 1966; Butuzova, 1966) coupled with abundant evidence of constant volcanic activity in the area of the basin, seem jointly to remove any possible objection to the derivation of most of the iron, at least, within the Hamersley Group from such a source.

Column 6 of Table 23 shows the metal and silicon content of sufficient average Precambrian crust to supply all the silica of the Hamersley Group sediments. The only significant excess material there which is not now present in the Hamersley Group is 1.3×10^{13} metric tons of aluminium; the 0.5×10^{13} metric tons of sodium and 0.2×10^{13} metric tons of potassium are easily disposable in solution, while all other metals are deficient. We still see the difficulty of disposing of this quantity of A2 without evident trace as a good argument against the destruction of even this much (about 10^5 cubic kilometres) crust by weathering for the derivation of the silica of the iron formations. Silica is a common associate of fumarolic volcanic activity, and a supposition that both of the major and probably all the minor constituents of the iron formations were provided by volcanism within the basin would remove the necessity of proposing a rather complex combination of two genetic processes, for one of which there is no positive evidence.

SIGNIFICANCE OF CHERT-SIDERITE

Chert-siderite is invariably associated with shale, either in the S macrobands of the Dales Gorge Member or in the Whaleback Shale and Yandicoogina Shale Members. We therefore now prefer the first of the two alternative genetic hypotheses given by Trendall (1966b): chert-siderite represents iron formation in which the normal course of diagenesis was modified by an abundance of water and carbon dioxide trapped by the relatively impermeable shale. The similarity of its chemical composition (analysis 8, Table 11) with normal iron formation (column 4, Table 17) in all respects other than CO_2 supports this interpretation; it is apparent also that the Whaleback Shale Member (analysis 4, Table 15) is chemically a mixture of chert-siderite and normal shale (e.g. analysis 3 of Table 15).

The abundance of stylolitic contacts argues for an abundance of available water to assist solution, and it is possible to interpret the exceptionally fine lamination typical of the siderite (Figure 29C) as another example of the fortuitous preservation of the component laminations of the microbands; but this cannot be proved.

In the following chapter, therefore, a depositional environment for chert-siderite different from that of the iron formation is not argued.

SUMMARY

We now summarise the progress which has been made during the preceding discussion towards answering the 5 basic problems of iron formation listed in the opening part of this chapter.

1. *Derivation:* where was the material before it became involved in the processes leading to its incorporation in iron formation?

Answer: it was probably almost entirely beneath the ground surface.

2. *Transport*: if it was not in the basin, how was it carried into it?

Answer: the massive transfer of material from below the ground surface can only be by some form of volcanic activity, but there is no evidence in the iron formations themselves to indicate the exact form of this; it is discussed fully in the following chapter.

3. *Deposition*: how, why, and in what form was the material thrown out of solution or suspension?

Answer: although the exact chemical form of the precipitated material is uncertain, it is likely that, in bulk, its content of stable materials was much like that of the present iron formation; evidence for its precise physical state is difficult to interpret, but its proneness to extreme compaction leaves little doubt that it was in some water-rich colloidal form; the material was precipitated through seasonal control of basin conditions.

4. *Diagenesis*: does the present iron formation represent the deposited material, or were there important changes after deposition?

Answer: no constituent mineral of the existing iron formation is primarily precipitated; different layers of the annually varved primary precipitate compacted to different degrees, but all suffered extreme modification and complete recrystallisation.

5. *Differentiation*: how and when did the material of the iron formations become isolated from its parent material?

Answer: presumably by some deep magmatic process, possibly associated with the sinking of the basins, but we have no evidence on this.

Development of the Hamersley Basin

THE BEGINNING OF THE BASIN

Before the deposition of the Fortescue Group the Archaean rocks of the area had been eroded to a plain, above which rose scattered groups of parallel ridges only a few hundred feet high. These were formed by the steeply dipping metasediments and metavolcanics separating the broad granite domes, and they followed the sinuous patterns of their strike. The partly exhumed pre-Fortescue Group landscape is strikingly displayed around Nunyerry (about $21^{\circ} 30'S$, $117^{\circ} 50$ to $55'E$; see map of Kriewaldt and Ryan, 1967) and north of Nullagine (about $21^{\circ} 30'S$, $120^{\circ} 05'E$; see map of Noldart and Wyatt, 1962). At both these places along the main northern unconformity of the Fortescue Group its basal lavas clearly lapped around and finally engulfed ridges of metamorphic rocks closely similar to those common in the existing topography; it seems likely that much of the present landscape of the Archaean rocks north of this unconformity is very close to its appearance at the opening of Fortescue Group time. The direction of drainage over the plain immediately before basin formation is unknown, as are the amount of material which was stripped off, the present location of that material, and the time taken for the erosion.

In the area of the Mount Bruce 1:250,000 sheet the lowermost part of the Fortescue Group consists of some 4,000 feet of sandstone, locally arkosic, calcareous conglomeratic and quartzitic, with some interbedded basalt (de la Hunty, 1965). This predominantly clastic material was presumably derived by further erosion of the Archaean rocks, with transport of the derived material inwards towards a central area of initial depression, since in this region the Fortescue Group has its thickest development, of 14,000 feet (Figure 2). The 7,000 feet of basic lavas and pyroclastic rocks which succeed these basal sandstones in the Mount Bruce area are broadly equivalent to the volcanic rocks which in most places mark the beginning of the Fortescue Group; but detailed correlation within the group is difficult, and beyond an impression of consistently greatest depression in the Mount Bruce Sheet area, with a steadily widening spread of the vulcanicity over the outcrop area (Plate 2), it is difficult to reconstruct the inter-relationship of local events in the Fortescue Group.

Pillow-form basalts, rippled-marked, pisolitic, and cross-bedded water-laid tuffs, and interbedded limestones with *Collenia*, are all common in the Fortescue Group. Many of the flood basalt flows are of great lateral extent. Taken together, these features suggest that during the main Fortescue Group vulcanicity

the whole surface of the accumulating material was almost flat, with local shallow lakes. The sources of this vast quantity of volcanic material is not known. Kriewaldt and Ryan (1967) believe that the Cooya Pooya Dolerite may represent one vent, and dolerite dykes cutting Archaean rocks may represent other sources, but it remains unknown whether the Fortescue Group material came from a great number of small vents or from a few grouped centres.

However that may be, the rate of sinking in late Fortescue Group time seems to have outpaced the supply of volcanic material, since the comparatively great lateral stratigraphic variability of the main volcanics of the group is not present in the uppermost shale, which is recognisably correlative throughout the outcrop area. This fine black pyritic lutite which immediately and conformably underlies the Hamersley Group has, as Kriewaldt and Ryan (1964) noted, more affinity with the stable conditions of the Hamersley Group, which are discussed below.

DEPOSITIONAL ENVIRONMENT OF THE HAMERSLEY GROUP

THICKNESS CONTROL OF IRON FORMATION

In any good example of a geometrically simple basin associated with localised long-term crustal depression, such as the Michigan Basin of north America, it is evident that formational isopachs will have the same general form as both structural contours on the sub-basin surface and isopleths of equal depression; any local depression of the sediment surface corresponding to locally greater depression of the floor is likely to become filled in by the normal processes of clastic sedimentation. But it is less easy to see this as a necessity with iron formation deposition, for two main reasons.

Firstly, the genetic hypothesis proposed for iron formation supposes that, on average, the initial precipitate has suffered 95 per cent compaction: the present thickness represents only 5 per cent of that of the precipitate. It may therefore be asked whether this may not be as dependent on compactional differences as on differences of depositional thickness. With the first basic hypothesis this was certainly a problem, but an additional advantage of the modified hypothesis of Chapter 9, not mentioned there, is that the final thickness of the iron formation must be dependent on the amount of stable material in the precipitate; none of the major constituents is completely lost after deposition, and the final compacted thickness will be independent on their relative redistribution.

Secondly, it is uncertain exactly what factors control the amount of precipitate laid down at any given point. Only if this is directly related to the depth of water can it be assumed in a chemical precipitate not liable to lateral rearrangement that its isopachs also reflect the general form of isopleths of equal depression. For the moment we do make this assumption, but it is a point whose speculative status should be borne in mind in later discussion.

SIZE, SHAPE, AND STRUCTURE OF THE BASIN

The Dales Gorge Member is the only stratigraphic unit of the Hamersley Group for which a reliable isopach map is available, and we therefore discuss this first as representative of Hamersley Basin conditions. With the assumption just noted, the isopachs of Plate 3 may be taken to represent the general form of the bottom of the Hamersley Basin in Dales Gorge Member time. The changing pattern of the isopachs illustrated in Figures 16 to 18 may also reflect minor changes in the evolution of the basin during this period. It seems from Figure 16 that when deposition of the Dales Gorge Member began the basin varied little in depth over wide areas. Later, between the deposition of the S4 and BIF 11 macrobands, deepening occurred about two centres, one at Mount Bruce and the other at Mount Stevenson. The final stage in the deposition of the member was accompanied by deepening of the basin along a line joining these two centres, to give the shape that characterises the isopach map of the whole member.

That the general form for the basin suggested by Dales Gorge Member isopachs follows closely the general distribution of depression during Fortescue Group time supports the validity of the noted assumption. Although thickness data for the remainder of the Hamersley Group are less adequate we have already noted that the Marra Mamba Iron Formation seems to be thickest a little south of Mount Brockman, and so far as our recorded information (Chapter 3) goes, it seems likely that Plate 3 reflects a stable pattern of isopleths of equal depression in the area from the first initiation at the start of the Fortescue Group until the top of the Hamersley Group.

Given this general structural form it remains to determine its exact shape and limits, and evidence for these is unfortunately sparse. Only in the Wyloo anticline area (Plates 3 and 4) does the Hamersley Group stratigraphy show gross departure from its normal lateral continuity (Chapter 2) and the proximity of a shoreline may be assumed; but it is also possible that this anticlinal area was an anomalously stable tectonic 'high' during basin sinking and that Hamersley Group deposition extended much farther south. There is little evidence for or against this proposition, but some relevant evidence for extent may be given by the easternmost exposures of the Hamersley Group (Plate 2).

We have worked little in this area and are dependent on previous descriptions (Chapter 1). The area was mapped before the definition of the Mount Bruce Supergroup, and MacLeod and de la Hunty (1966, p. 7) have set out the stratigraphic equivalence as on the opposite page. Since the top of the Carawine Dolomite is not exposed, and the base of the present Hamersley Group is not easily definable within the Lewin Shale, it is not possible to deduce much from thicknesses, but it is certain that the equivalent of the Marra Mamba Iron Formation is both thinner and lithologically different from the main part of its outcrop in the Hamersley Range area; it is known also that the Carawine Dolomite has *Collenia*, and we find the suggestion of Mr. L. E. de la Hunty (pers. comm.), that these eastern representatives of the Hamersley Group are relatively shallow-water representatives laid down on a marginal shelf of the main basin, one which

fits well with our Plate 3. MacLeod (1966, p. 42) has referred to this area as a separate 'Oakover-Davis Basin', but we would prefer to regard it as a separate structural subdivision of the Hamersley Basin.

It would be possible to postulate such a marginal shelf roughly encircling the whole area of Plate 3. However, there is no positive evidence for this, and some points seem to suggest otherwise. Firstly, the Dales Gorge Member appears to be thickening at its northwesternmost measurable point on the coast, and this area may represent a former oceanic connexion; this point is discussed again below. Many continental reconstructions place this Western Australian coast, for independent reasons, against the Singhbhum iron formations of India, and the possibility of some connexion between the two must be considered. Although it is too speculative yet to be given great weight as evidence in the interpretation of the Hamersley area, it does add a further suggestion of a break in any marginal shelf in the Point James area.

Secondly, the slope asymmetry of the isopachs to the north and south of the deepest trough of the basin seems to be significant. The influence of this asymmetry on riebeckite distribution is discussed in Chapter 11. It must be envisaged as a possibility that the nature of the marginal parts of the basin differed to the north and south. The available evidence on these points is simply inadequate, and as a basis for continued discussion it is accepted that although the Hamersley Basin had the general shape suggested by Plate 3, and a marginal shelf probably lay along the northern and eastern parts, the edges lay some limited but unknown distance beyond the existing outcrop areas. For the purpose of quantitative discussion in this bulletin, a rounded estimate of 100,000 square kilometres is acceptable, with a likely error of ± 45 per cent.

Group	Formation	
	Mount Bruce Sheet (de la Hunty, 1965)	Balfour Downs Sheet (de la Hunty, 1964)
Lower part of Hamersley Group	Wittenoom Dolomite	Carawine Dolomite
	Marra Mamba Iron Formation	} Lewin Shale
Fortescue Group	Jeerinah Formation	
	Mount Jope Volcanics	Little De Grey Lava and Tum- biana Pisolite

DEPTH, CIRCULATION, AND IRON CONTENT OF WATER

We have argued that all present irregularities of the primary microbanding of the iron formations are the result of compressional diagenesis, and we see no evidence in the iron formations for post-depositional and pre-burial disturbance of the precipitated material. We have argued also that this was extremely light, and particulate, and it may therefore be assumed to have had little cohesive strength. It thus appears that the floor of the basin was beyond the reach of disturbance by waves, and, with the proviso implied in the possible existence of an algal raft (see further below in this chapter), its depth may be taken to have been at least 50 and possibly 200 metres (Kuenen, 1950, p.228).

This is one of the two main arguments for depth. The other runs as follows: (1) apart from thickness differences, there is little apparent difference in lithology or composition in any one stratigraphic thickness of iron formation over the whole of the presently observable part of the basin; (2) therefore all parts probably had a similar environment and were laid down in water of the same order of depth; (3) but there was probably at least some bottom slope towards the most rapidly sinking central part of the basin; (4) even if this were as little as 1 : 1,000 there would be a depth differential of 100 metres between centre and edges; (5) therefore some figure above this is a minimum depth estimate for iron formation deposition.

A water depth for Hamersley Group iron formation of 150 to 250 metres would conform with the 'shallow inland seas' or 'epeiric seas' of Kuenen (1950), and may be accepted as a basis for continued discussion. A third argument for a minimum depth, based on the circulation needed to distribute 74 mgm per cm² of material annually in the basin without involving current speeds too fast for stability of the precipitate, is not significant in the light of later parts of this chapter.

Iron is the least soluble of the major constituents of the iron formation, and we have proposed that 22.5 mgm of it were deposited annually per square centimetre of the basin area. It is interesting to examine quantitatively the possibility of the deposition of this from a superincumbent column of water 200 metres high. The amount of iron that can reasonably be supposed to have been held in solution is uncertain. Given suitable atmospheric conditions (discussed later in this chapter) a concentration of 10 to 20 ppm is reasonable (Gruner, 1922). Thus the water over each square centimetre of the basin would contain between 200 and 400 mgm of iron, and the annual precipitation of some 5 to 10 per cent of this would be enough for iron formation deposition. The quantitative problem of its annual renewal still remains, and of the process by which, effectively, a column of water about 10 to 20 metres high, is chemically 'processed' to release its iron; it is possible that annual overturn of part or all the basin water must be invoked to achieve this.

A single example based on an arbitrary choice of values is used to illustrate the first problem. Suppose at some initial state of some chosen square centimetre of the basin the column of superincumbent water is 200 metres deep, with a

concentration of 15 ppm of iron, so that it contains 300 mgm of iron. During the first year 25 mgm are precipitated, to leave a concentration of 13.75 ppm. If circulation were confined to the upper part of the basin, complete replacement of the uppermost 100 metres of water at this concentration by water with 16.25 ppm of iron would restore the initial average concentration. Currents of 1 metre per second in the upper part of the basin would be adequate for this, and the required velocity would be reduced if a higher concentration of iron in the replenishing current is assumed.

It is possible that evaporation is an important factor in iron replenishment. Under modern desert conditions over 3 metres annual evaporation is possible (Wisler and Brater, 1959, p.203). If the same assumptions are made as in the previous paragraph, after 25 mgm of iron are precipitated and 3 metres of water are evaporated, the new concentration, in the remaining 197 metres of water, is 14 ppm. If this water is made up by the simple addition of 3 metres at a concentration of 83 ppm the original concentration and depth are again restored. This is considerably less than the 220 to 325 ppm iron content of the Iur'eva River, described by Zelenov (1958).

Given a source within the basin of fumarolic water with a high concentration of iron, there does not seem to be any great difficulty, using a combination of evaporative loss and slow circulation, in maintaining a concentration of 10 to 20 ppm throughout the basin. The second problem, the mechanism of iron precipitation is discussed beneath the following heading. The greater potential solubility of silica (Gruner, 1922) makes its quantitative distribution less difficult than that of iron, and it is not discussed separately.

POSSIBILITY OF AN ALGAL RAFT

One possible objection to the genetic and environmental hypothesis so far proposed lies in the high degree of regularity of much microbanding: if the supply of iron was volcanic, and if the control of the precipitating mechanism was climatic, the action of both these together might be expected to produce a deposit lacking the striking long-term and short-term regularity that characterise much of the iron formation. A possible solution to this difficulty is that the surface of the basin was covered, partly or entirely, by a floating layer of algae. The suggestion has three simultaneous points in its favour.

1. By acting as a quantitative biochemical buffer between some simple climatic factor (?sunshine) and the basinal chemistry an algal layer able to tolerate the suggested range of iron concentrations may provide an equal annual precipitation regardless of a relatively spasmodic supply. The problem of climatic regularity still remains, and is discussed later.

2. The interposition of a biochemical process may overcome the difficulty of finding any climatic factor which is likely by itself to affect the basinal chemistry sufficiently to provide the chemical contrast between the two parts of the microbands.

3. An algal raft may be a contributory cause of the apparent absence of any influence by waves or weather on the light and incoherent precipitate.

WAS THE BASIN CLOSED OR OPEN?

Although it was suggested that the general form of the basin is reflected by the isopachs of Plate 3, the possibility of some external oceanic connexion was also noted. This uncertainty is part of the more general problem of when, in the evolution of the earth, a single globally interconnected body of surface water began to exist to a degree approaching that now obtaining. This is not the place for a full discussion of this problem; it is enough to state that the existence of a single world-wide ocean 2,000 m.y. ago cannot be assumed with confidence, and that any positive evidence from the Hamersley Basin for the connexion of its water with some larger external body is as welcome for the support it gives to the existence of such a body as it is for the light it throws on the Hamersley Group.

The best evidence on this point seems to lie in the general impression of stability in all controlling parameters of iron formation deposition if the conditions of deposition already suggested are valid. If there was only a limited variation of basin depth throughout the several million years necessary for the deposition of, say, the Joffre Member, then connexion of the basin water with a larger reservoir is a more credible mechanism for effecting this than the chance balance of a variety of potentially unrelated factors. If iron and silica were brought to the basin by fumarolic volcanic activity then this was probably one source of water. As far as the surrounding land was concerned, it was either desert (as is suggested later), in which case there was evaporative water loss, or there was drainage into the basin. Whatever the total water balance it seems remarkable that climate and volcanic activity together could have produced an approximate hydrological equilibrium in a closed basin for many millions of years.

What effect a gross increase in water depth would be likely to have on deposition is uncertain, except that extreme dilution of iron content by pure water would presumably have halted iron formation deposition; it is more predictable that complete desiccation would have produced some recognisable stratigraphic effect. There is no discontinuity in the Hamersley Group which can convincingly be interpreted in either way. Either, then, a delicate water balance was maintained in a closed basin, or there was a connexion with a larger body of water which acted as a surge tank to smooth out fluctuations of supply and evaporation. Problems of balance in the basin still remain, however, and are discussed again under the heading 'Material balance in the basin'.

Assuming some external connexion for the Hamersley Basin it is reasonable to suppose, on grounds other than the isopach evidence already discussed, that this was limited, and chemically restrictive. One of us (Trendall, 1968) has shown that the difference between, for example, the Lake Superior and Hamersley iron formations, are at least as striking and significant as their resemblances. If some common depositional environment is to be sought for Precambrian iron formations,

it may be that local basinal restriction (envisaged by James, 1954, for Lake Superior), coupled with inevitable locally distinctive characteristics of depositional environment, may satisfactorily account for these differences.

VULCANICITY

Although volcanic activity became less important at the Fortescue—Hamersley boundary, evidence for continual episodic volcanic activity throughout the deposition of the Hamersley Group is irrefutable. Stilpnomelane-rich shales with relict shards or other recognisable volcanic debris are present in at least the Mount McRae Shale, the Dales Gorge Member and the Joffre Member, while if stilpnomelane is itself taken as evidence of volcanism the assumed incidence is very much higher. However, we are reluctant to equate stilpnomelane and volcanism, since the common presence of stilpnomelane mesobands would imply a volcanic cyclicity in unison with the Calamina cyclothem. We think this unlikely, but to indicate the possibility, and a need for further work, we have placed a question mark against a tectonic control for the Calamina cyclothem in Table 24.

Apart from the fact that they are indeed lavas, and that the undisturbed Boolgeeda Iron Formation rests on them via transitional tuffs, the precise manner of emplacement of the Woongarra Volcanics is not known. Their great lateral extent, with a recognisable internal stratigraphy, suggests that they were extruded over a very flat surface in a very mobile form. Their stratigraphic conformity above and below makes it unlikely that the basin was lifted up for their sub-aerial extrusion and dropped again for the deposition of the later iron formation. Apart from the fact that the process would need to be performed twice, to account for their interstratified iron formation, successive regional uplifts and depressions over 200 metres would be expected to be accompanied by other evidence of basinal disturbance. We therefore suppose these lavas to have been emplaced sub-aqueously, and suggest that the enforced acceptance of this by the evidence of general stability of the basin may also be welcome as a potential explanation of lateral mobility.

Further stratigraphic study is urgently needed, both of the Woongarra Volcanics and of the various tuffs of the iron formations, to provide evidence for the direction of derivation and source or sources of all the volcanic material of the Hamersley Group. Virtually none is available, and it remains to discuss here whether the suggested relationship between volcanic activity and iron derivation is compatible with any possible reconstruction of the basin.

If the basin had an area of 100,000 square kilometres, in which 22.5 mgm of iron per square centimetre were deposited each year, then 22.5×10^6 metric tons of iron were laid down annually during iron formation deposition. Zelenov (1958) records a *single river* flowing off the volcano Ebeko, on Paramushir Island in the Kurile Islands, which is estimated to carry 35 to 50 tons of iron daily to the sea. From Zelenov's (1960, Figure 1) map of the distribution of active vulcanicity in the Kurile Islands, it is easy to imagine that this figure could well

be increased by the necessary factor of about 10^3 to bring it up to the level required for iron formation deposition in the Hamersley Basin. It remains to see whether a site for volcanic activity on this scale can be found in a reconstruction of the basin; the site will be the more credible if: (1) it is over younger rocks, to explain its apparent present absence, (2) it is associated with an area of tectonic instability, (3) it is nevertheless reasonably close to the basin, and (4) there is some other evidence of penecontemporaneous volcanic activity.

A site satisfying all these requirements seems to lie along the western side of the outcrop of the Hamersley Group (Plate 2). The Hamersley Group is separated from the overlying Wyloo Group to the west by a zone with abundant complex faulting. Although it is virtually certain, from the impression of discordance along this zone in Plate 3, that Hamersley Group rocks there underlie the Wyloo Group, they are not exposed. This zone is close to and parallel with a smooth northern extension of the major curvilinear fault zone which runs north-south some 20 to 100 miles inland to the east of the western coast of Western Australia. This line, marked in its southern part by the Darling Fault, follows the eastern edge of the Phanerozoic Perth and Carnarvon Basins, and has been intermittently active at least since late Precambrian time. The Wyloo Group to the west of the western edge of the Hamersley Group contains a variety of contemporaneous volcanic rocks. At June Hill extensive volcanics are interstratified with the Ashburton Formation and there is a thick development of the Cheela Springs Basalt Member in the general area north of the Wyloo anticline (Daniels and Halligan, 1968). Farther north, in the area of the Yarraloola 1:250,000 Sheet, Williams (1966) has described volcanic rocks within the Duck Creek Dolomite, as well as quartz-feldspar porphyries intrusive into both the Fortescue Group and Hamersley Group (Woongarra Volcanics and Wittenoom Dolomite). All these occurrences, by indicating a continuing concentration of localised volcanism in this area, support the possibility of volcanic activity there during Hamersley Group deposition.

It is therefore proposed that the principal source of material for the Hamersley Group iron formations lay in a belt of fumarolic volcanic activity to the west of the basin; this may itself have formed a separating ridge from the open ocean, if such existed, in a manner closely analogous to the present separation of the Okhotsk Sea from the Pacific Ocean by the Kurile Islands.

CONDITIONS ON THE SURROUNDING LAND

It is apparent from discussion so far that the conditions on the land around the Hamersley Basin were such that little or no terrestrial debris was transported into the basin, and virtually none at all for long periods of iron formation deposition. Two contrasted explanations are conventionally available for this: either there were no rivers because the surrounding area was desert, or the existing rivers were so sluggish as to be incapable of carrying a significant undissolved load.

There seems to be little uniformitarian support for the second hypothesis. All existing large rivers, however gentle their slope to the sea, appear to carry mud into it, and have, without exception, deltas built up from this transported debris. It may be argued against this that much of this transport may be effected in periods of flood, when velocities were well above normal, but seasonal differences of flow are as likely to have occurred in the Precambrian also.

It seems a fair generalisation that offshore from the existing continents sea floors are always muddy unless there is scour by currents. This is unacceptable for the process of iron formation deposition proposed, and the hypothesis of a desert shore for the basin is consequently preferred. In effect, the Hamersley Group iron formations are suggested in our hypotheses to be evaporites, and the environmental similarities with, in particular, Permian and Triassic varved evaporites, in many features other than basin chemistry, are striking.

Acceptance of a desert environment for the Hamersley Basin holds an additional advantage for its interpretation. No single parameter of modern temperate climate approaches the quantitative regularity of much microbanding, and it has already been suggested that an algal raft may have helped to produce regularity by acting as a biochemical buffer. In a desert climate, total annual receipt of solar energy might be expected to vary little year by year. We therefore see the regularity of microbanding as contributory support both for a desert environment and for our general genetic hypothesis.

COMPOSITION OF THE ATMOSPHERE

The composition of the Precambrian atmosphere is not known with sufficient confidence for this to be used as a main argument for or against any depositional hypothesis for iron formation; on the contrary, if a hypothesis seems sufficiently well founded on other evidence to demand a particular atmospheric composition, then this is admissible as evidence for that composition. The problem in relation to iron formation has been reviewed by Gross (1965), James (1966), and Govett (1966), and specific aspects have been discussed by Trendall (1966c). Our suggested basinal iron concentration range of 10 to 20 ppm seems most easily accomplished with a low pH, and a high carbon dioxide partial pressure is the simplest supposition for its achievement. Until more evidence is forthcoming to refute the possibility of an atmosphere relatively rich in carbon dioxide during deposition of the Hamersley Group we accept it as the most likely explanation for the proposed iron content of the basin. The suggestion is entirely in accord with the effusion of vast quantities of acid (CO_2 saturated) water as part of the same volcanic activity that supplied the iron and silica.

CONTROLS OF STRATIGRAPHY

So far in this chapter the likely depositional environment of the iron formations has been the main topic. It remains to discuss the meaning of the stratigraphy at all scales, in particular by answering two questions: (1) how did the depositional environment of the other main sedimentary rock types of the

Hamersley Group (shale and dolomite) differ from that of the iron formation, and (2) what mechanism caused the change from one environment to another? Any suggested answers to these questions should take into account the fact that the changes of environment were relatively sudden and infrequent: the large-scale stratigraphic divisions of the Hamersley Group are, on the whole, clearly defined and internally homogeneous, in contrast to a possible thinly interstratified random sequence of the different sediment types. This description does not apply, though, to the Dales Gorge Member, whose macrobands (Figure 3) represent conspicuous and rather regular shaly intercalations in iron formations. A further main question is therefore: (3) what were the controls of macrobanding, and similar minor sedimentary rhythms? Finally, some answer is needed to the enquiry: (4) why are the five major stratigraphic units of iron formation (Marra Mamba Iron Formation, Dales Gorge Member, Joffre Member, Weeli Wolli Formation, Boolgeeda Iron Formation) recognisably different?

One possible interpretation of the major stratigraphic shale units of the Hamersley Group would be that there was an influx of clastic detritus to the basin from erosion of the surrounding land. Transport by rivers would suggest a major climatic change, if the suggested environment for iron formation deposition is accepted; addition of wind-blown dust to the basin is certainly possible without any drastic climatic change, but a secular change from a consistently windy to a consistently calm environment seems unlikely to take place abruptly and access of large quantities of dust may involve bulk problems in its derivation. However, at least five points suggest that the shales may not result from clastic sedimentation in the conventional sense, but are colloidal precipitates of a different composition; other features of the shales independently prove a degree of volcanic derivation and a stronger circulation of the basin water.

The five points which argue against normal deposition as clastic silt for Hamersley Group shales are: lateral stratigraphic continuity, absence of evident debris, globulate texture, possible varves, and chemical composition. The lateral stratigraphic continuity of at least some shales (for example, that in the upper part of the S3 macroband of the Dales Gorge Member; see Trendall & Blockley, 1968, Plate 29) only a few inches thick is equal to that of equivalent thicknesses of iron formation, and can be recognised over at least 10,000 square miles. This seems to preclude any form of deposition involving physical distribution of debris by currents over the basin floor; the material must have been carried in colloidal form or in solution over the basin, and must have then settled evenly over a long period. The absence of any minerals which are clearly recognisable as the deposited particles, and the presence of much crystalline stilpnomelane and feldspar (for example) which is texturally diagenetic, lend support to the suggestion of deposition in some much more finely divided state; whether the coarse breccias of S4, S7 and S16 (p. 64) are of volcanic or slump origin (p. 114) is uncertain, but whatever their genesis there is no doubt that they are untypical of the shales as a whole, and can be explained without appeal to current transport of coarse

terrigenous debris. The curious globulate structure of Figure 31F, grading as it does into a common compacted shale texture, can very reasonably be interpreted as the expression of deposited balls of flocculated colloidal material. The very regularly laminated shales illustrated in Figure 13, A and B, closely resemble described sedimentary varves, and may be an indication that seasonal modification of basin chemistry is a depositional mechanism that did not cease to operate during the time now represented by shale.

Fifthly, the distinctive chemical composition of the shales argues against their normal clastic origin. It was noted in Chapter 5 that the diversity in composition of analysed shales indicates the need for more data, and this discussion is necessarily cursory. The five available analyses of unweathered Mount McRae Shale (7-11 of Table 15) are sufficiently similar to be considered as a group. The main differences of this group from normal clastic shales (Pettijohn, 1956, p. 344) are: (1) a lower SiO_2 content by a factor of about 0.6, (2) lower Al_2O_3 by about 0.5, (3) higher total iron by about 5.0, (4) higher MgO by about 2.5, (5) lower K_2O by about 0.4, and (6) a significant content of FeS_2 . The carbon content and colour of these samples of Mount McRae Shale could qualify them for classification as black shales, but it is noteworthy that of the representative carbonaceous shales selected by Pettijohn (1956, p. 362) all still differ in the same way in the 6 listed features, except one 'graphitic slate' associated with Precambrian iron formation in the Iron River district of Michigan; this has higher pyrite and carbon and lower MgO , but is otherwise sufficiently similar to suggest that close matches could be found in the Mount McRae Shale. The analysed shale from the Jeerinah Formation (12 of Table 15) is remarkable in that it is essentially a carbonaceous chert with some iron-bearing sheet silicate and remarkably low alumina and potash. It is a black, fissile, friable rock. It is not unlike the siliceous Mowry shale (Cretaceous) of the Black Hills region of America, described by Rubey (1929), as far as silica content is concerned, but is notably richer in iron and carbon, and poorer in alumina. Other comparable analyses come from the Miocene Monterey formation of California, including some almost as poor in alumina (Bramlette, 1946, p. 13). In view of subsequent suggestions in this discussion it is worth noting that a volcanic contribution of material (especially silica) has been suggested for both these formations, by the authors quoted. The three analysed shales from the Dales Gorge Member (1-3 of Table 15) show the most remarkable variation. While analysis 2 is evidently fairly pure stilpnomelane (cf. analyses 3, 4 and 7 of Table 16), analyses 1 and 3 show almost double the Al_2O_3 , half the total iron and pyrite contents comparable with those of the Mount McRae Shale. The alumina content is still slightly below that of normal clastic shales, however, and probably reflects a high content of both potassic feldspar and an aluminous chlorite. In summary the shales of the Hamersley Group appear to have distinctive chemical compositions comparable variously with other shales associated with Precambrian iron formations and with Phanerozoic shales of volcanic derivation.

The shard bands described and illustrated in Chapter 4 are clearly of direct volcanic origin, and they invariably occur in association with shale not bearing shards; there is a suggestion here of some link between the two. While there is no special reason for greater vulcanicity to be associated with a long-term climatic change of the kind necessary for erosional addition of clastic material for shale, it is possible that greater vulcanicity directly affected the supply and nature of dissolved material in the basin. The cross-bedding in limestone after S1 shale at Dales Gorge and Yampire Gorge shows that, unlike periods of iron formation, currents of sufficient strength to redistribute bottom sediment were present locally and rarely during shale deposition.

On the basis of all the evidence we suggest that the environment of shale deposition was controlled jointly by increased volcanic activity and tectonic instability, both associated with crustal adjustment in the development of the basin. The latter probably modified the connexion of the basin with the open ocean, and via this mechanism affected simultaneously both the circulation and chemistry of its water. Thus no climatic change is postulated, and seasonal control of chemistry continued to act as a mechanism of precipitation during some periods of shale deposition. The exact chemistry of deposition is unclear, but the initial precipitate form was probably globules of silicate colloid.

Periodic direct addition of airborne ash to the basin resulted in thin layers of glass shards which were probably replaced by stilpnomelane during or soon after their fall into the water. Available potassium in the waters of the basin is suggested by this reaction. The even thickness of shard layers shows that there was negligible current concentration of this fine ash during its slow descent through the water. It seems unlikely too that at the time of its fall an algal raft existed on the basin surface, and it is possible that the killing of this by the initiating vulcanicity of the shales which bear shard bands may have contributed to the free carbon by its descent and decay on the basin floor.

On the other hand we find the opposite situation, where the amount of volcanic activity markedly decreased, and in particular the supply of iron to the basins was cut off, a very credible interpretation of the depositional environment of the Wittenoom Dolomite. At this time, the basin was sufficiently stable, and the intensity of vulcanicity sufficiently slight, for calcareous algae to flourish in the shallow parts of the basin in the northeast, while dolomite was precipitated, again without sensible change of climate, in the main basin.

Concerning the second question asked at the start of this discussion (what mechanism caused the changes of environment?) we can give no satisfactory answer, except to say that our suggestion of a volcanic influence is consistent with the common stratigraphic restriction of volcanic rocks to well defined levels; this implies that a fairly abrupt start and stop of long periods of vulcanicity is not unique to the Hamersley basin. It is the third question (what controlled macrobanding?) that might provide some clue to an answer for the second. Sedimentational cyclicity of the order of thickness of macrobanding (but not necessarily of time) is best known elsewhere in the cyclothem of the American and European

Carboniferous. Bott and Johnson (1967) have argued that the control of these was intermittent tectonic basin subsidence, caused by the intermittent abrupt yield of a plastic asthenosphere with finite yield strength in response to increasing stress resulting from erosional transfer of material to the basin from surrounding highlands. The application of this explanation to macrobanding would imply that the first cause of shale deposition was more rapid sinking of the basin through abrupt yield of the mantle in response to whatever steady long-term forces were the ultimate cause of the whole basin. The associated vulcanicity affecting the depositional environment more directly would be a reasonable corollary of this tectonic adjustment.

TABLE 24. PRIMARY CONTROL OF VARIOUS ORDERS OF STRATIFICATION IN IRON FORMATIONS OF THE HAMERSLEY GROUP

Order of stratification	Primary control	
	Astronomical	Tectonic
Microbanding 	x	
Mesobanding 	x	
Striped facies of Weeli Wolli Formation	x	
Calamina = Knox cyclothem 	x	?
2-3 foot rhythm of Joffre Member 		x
Macrobanding of Dales Gorge Member		x
Major shale/BIF alternation 		x
Beginning and end of group 		x

We now approach the fourth question: why are the five major units of iron formation recognisably and consistently different? This difference is expressed by several aspects of lithology (Chapter 3), to some extent in chemical composition (Table 17, and relevant text), quite strikingly in mineralogy (Chapter 4—Sheet silicates), and to some extent in structure (Chapter 6). It may be summarised in an assertion that no geologist with a thorough field acquaintance with the Hamersley Group would fail to identify which of the five major units of iron formation he was standing on, if he were carried blindfold to an exposure showing a clean section over twenty vertical feet. We cannot adequately answer this question, and we make only two points relevant to it, one here and one later under the heading 'The end of the basin' (p. 294). If the Calamina and Knox cyclothem

are the same in the sense that they have the same cyclic climatic control, we find it difficult to conceive that any difference in the nature of this climatic cycle is the main cause of the different expression of the cyclothems in the Dales Gorge and Joffre Members. We believe, therefore, that after the period of vulcanicity and accelerated sinking represented by the Whaleback Shale Member, the whole chemical balance of the basin was permanently changed in some way, and remained in its new state until changed again in the period marked by the Yandicoogina Shale Member; but we cannot at present guess at the nature or control of the change.

Almost all controls of surface sedimentational environments originate within the earth, and are tectonic, or outside the earth, and are astronomical; usually, there is some buffer mechanism acting as a secondary control. Table 24 summarises the result of discussion here and in Chapter 9 of the nature of the primary control for the various scales of stratification in the Hamersley Group.

POST-DEPOSITIONAL EFFECTS OF BASIN DEVELOPMENT

EARLY STRUCTURES IN THE IRON FORMATION

The post-depositional diagenetic development of mesobanding and of pods was described in Chapter 9. The purpose here is to discuss their development in relation to the structural development of the basin and to the other structures described in Chapter 6.

Trendall (1965a, p.85) suggested previously that the duplicate structures at Dales Gorge, including cross-podding, were formed by gentle downslope slumping from east-southeast to north-northwest down the bottom slope of the depositional basin. It was then believed that: (1) such a direction was consistent with the isopach pattern of the Dales Gorge Member, and (2) regional rippling was a tectonic feature related and axial to the gentle folds of the main Hamersley Range. Our further work has now shown that: (1) the consistent direction of duplicate structures (now more generally northeast structures) at many levels shows no regional relationship to Dales Gorge Member isopachs (Plate 3), (2) isopachs of different levels of the Dales Gorge Member show local variations, and cannot be accurately relied upon to give an exact indication of bottom slope at a particular moment (Figures 16 to 18), and (3) regional rippling is structurally and genetically unrelated to the folds of the Hamersley Range.

We now suggest alternatively that it is the regional rippling which represents gentle downslope slumping of the iron formation. We suggest that it occurred at some (unknown) depth in the buried iron formation as a natural response to steady increase in slope as the basin sank. The strike and asymmetry of regional rippling (Plate 3) are perfectly consistent with this interpretation, particularly since some degree of isopach discordance could be attributed to local discrepancies between isopach trend and post-burial slope trend due to slight differential irregularities in sinking. This interpretation of regional rippling is consistent also with

its tendency for symmetry in the central parts of the basin, and with Dallmus's (1958) demonstration that the sinking of a basin produces compression, not tension, so that inward gravitational slumping at high levels will be continuously augmented by outward compressional stress at lower levels.

We take the formation of regional rippling as the structural event resulting from basin development which marks the time limit of our concern in this chapter. The various slump structures described in Chapter 6 formed either simultaneously or (the more brittle-looking ones) slightly later. Later events are particularly relevant in crocidolite growth, and are discussed in Chapter 11. It is with the earlier events that we are concerned here. The fallacy of Trendall's (1966a) belief that regional rippling was tectonic invalidates also his reliance on that fact to prove it to be younger than the duplicate structures. However, the observed relationship of these two structures at Wittenoom Gorge (p. 164) confirms that this is the correct time sequence, and an explanation of northeast structures is required.

This is a problem to which we have found no satisfactory solution at all. It may still be proposed that they are a different kind of gravitational slump, formed earlier and at a higher level, but their strikingly consistent regional orientation argues against this; and why are they so distinct from, instead of directionally and geometrically intergradational with, regional rippling? We accept, though, that the comparative flatness of the basin floor, which has already been argued, and the even deposition over it, make it likely that random pods, apparently unaffected by a gravitational component, were the earliest structures to develop within the compacting precipitate, probably synchronously with mesobanding itself. We also see macules (as did Trendall, 1966a, on the Dales Gorge evidence) as structures formed before cross-pods, but we have no evidence of the relative ages of random pods and macules; they may be contemporaneous.

The presence of varying types of concentric structures in random pods (Figure 40) itself suggests a possibility of a genetic connexion with small spheroidal nodules, which are often concentrically zoned (Figure 41). Now that extreme selective compaction has been argued on independent evidence in the mixed groups of the Calamina cyclothem it is easy to see these nodules, which are characteristically present there (Figure 13), as remnants of random pods in which all traces of stratification have been destroyed.

Thus a general time sequence of random pods, macules and related structures, followed by northeast structures, followed by regional rippling and slumping is established. It should be understood that this sequence applies only to a restricted level. Regional rippling may be forming at that level concurrently with both northeast structures at a higher level and random podding at a higher level still, while on the basin floor precipitation is simultaneously taking place of colloid destined later to pass successively through all these stages. For the later structures dealt with in Chapter 11, this is less likely to be true, and minor folds with fibrous minerals, for example, probably formed simultaneously over a great vertical thickness.

This time sequence gives clues both to the type of mechanism which should be sought for the northeast structures and to the reasons for their apparent uniqueness in geological literature. The number of times when a light, incoherent, sheet of gel about 100,000 square kilometres in extent lay stably and receptively on the earth's surface for at least thousands of years must be few, and the forces needed to impose northeast structures on it may have been quite small. Forces due to geomagnetism, seismicity, earth tides, and rotational instability have been suggested to us in discussion, but there is as yet no adequate answer for northeast structure origin.

THERMAL HISTORY OF THE HAMERSLEY GROUP

The Hamersley Group has nowhere undergone regional metamorphism. Trendall (1966b) argued previously from the evidence of Hoering that no part of the Brockman Iron Formation had reached a temperature above 160°C. Since then Grubb (1967) has successfully synthesized fibrous riebeckite at 35°C, and Mr. R. Becker and Dr. R. N. Clayton (University of Chicago; pers. comm.) have carried out oxygen isotope analyses. Both these lines of evidence support the view that the evolution of the Hamersley Basin was not accompanied by heating of the sediments to temperatures above those associated with ordinary geothermal gradients.

THE END OF THE BASIN

The Hamersley Basin was essentially an elliptical area of surface depression in which the amount of depression decreased uniformly outwards from a fixed central area of maximum sinking. Sedimentary basins of comparable simplicity are known from the Phanerozoic; the Michigan basin (Cohee and Landes, 1958, Figure 2) is the best example with a similar order of size. It is not known how or why such basins develop; in this section the closing events in Hamersley Basin development are discussed in the light of some published suggestions concerning these basic problems.

It has already been argued that the lateral stratigraphic uniformity of the iron formations across the basin floor indicates a similar order of depth over a wide area, and also that the extent of the Woongarra Volcanics makes it likely that they were extruded over a rather flat surface. The close stratigraphic restriction of the Weeli Wolli Formation dolerites seems to support this general concept of even, stable, steady sinking of the basin. Clearly this cannot go on for ever, and some point must be reached where the basin can be said to be 'full'.

Dallmus (1958) showed from an empirical study of basin evolution that round or elliptical areas of crustal subsidence ('primary dynamic basins') tend to have a subsidence limit which is reached when the original floor is planar. Thus no basin is truly concave, it is an area of lesser convexity than the geoid. The greatest thickness of the Hamersley and Fortescue Groups together in the central part of their basin is about 22,350 feet, or 6.81 kilometres. The required

diameter for a basin with a planar basement floor at this depth is 300 kilometres, subtending an angle of $2^{\circ} 42'$ at the earth's centre. This is quite an acceptable figure for the Hamersley Basin, and gives a theoretical basin area of about 7×10^4 square kilometres, compared with the 10×10^4 figure used in earlier discussion above.

It is instructive to apply Dallmus's proposal to the Fortescue Group and Hamersley Group separately; some justification for this can be argued from the much greater present outcrop area of the Fortescue Group and from their contrasted sedimentational regimes. The resultant diameters are then 241 kilometres for the Fortescue Group and 188 kilometres for the Hamersley Group. Although these figures are small, we suggest that there is a real possibility of a contraction of the main area of subsidence during the Fortescue—Hamersley transition, and that this gave rise to the fringing shelf whose Hamersley Group sediments are now preserved in the northeastern Oakover—Davis area. However that may be, there is a strong suggestion from Dallmus's proposals that during the deposition of the upper parts of the Hamersley Group the basin was becoming full. We attribute the great spread of the Woongarra Volcanics to the flattening associated with this fullness, and suggest the possibility also that the very different lithology of the Boolgeeda Iron Formation, at least, is in some way indicative of the senility of the basin.

This possibility has important consequences, since it supports an interpretation of Wyloo Group deposition as something totally different in kind from that of the Fortescue and Hamersley Groups; this is an interpretation suggested, but not proved, by the present restricted outcrop of the Wyloo Group. Figure 74 illustrates very diagrammatically our suggestion of Wyloo Group deposition in a marginal downwarp along the southern side of the stable and completed Hamersley Basin. The abundant clastic deposition of the Wyloo Group must entail a simultaneous climatic change. This is discussed below the next heading.

The subsequent folding of the Wyloo and Hamersley Groups together in the southwestern part of the Hamersley Group outcrop took place at a stage when riebeckite growth was still possible in the Hamersley Group iron formations (p. 306). However, as far as the purposes of this chapter are concerned the evolution of the Hamersley Basin reached its final phase of development at the beginning of Wyloo Group time, and considerations of deformation which are relevant in crocidolite, in particular, are discussed in Chapter 11.

MATERIAL BALANCE IN THE BASIN

The existence of basins of clastic sedimentation with great thicknesses of shallow-water sediments has long been recognised, and it has been presented as a puzzle that a delicate balance appears to have been maintained between rate of sinking and supply of infilling material. This is difficult to see as a problem. Firstly, if a basin sinks it cannot be filled by clastic material unless there is a corresponding uplift of at least some of the adjacent land; and unless such uplift materially outpaces the rate of erosion (there is a natural balance here in that

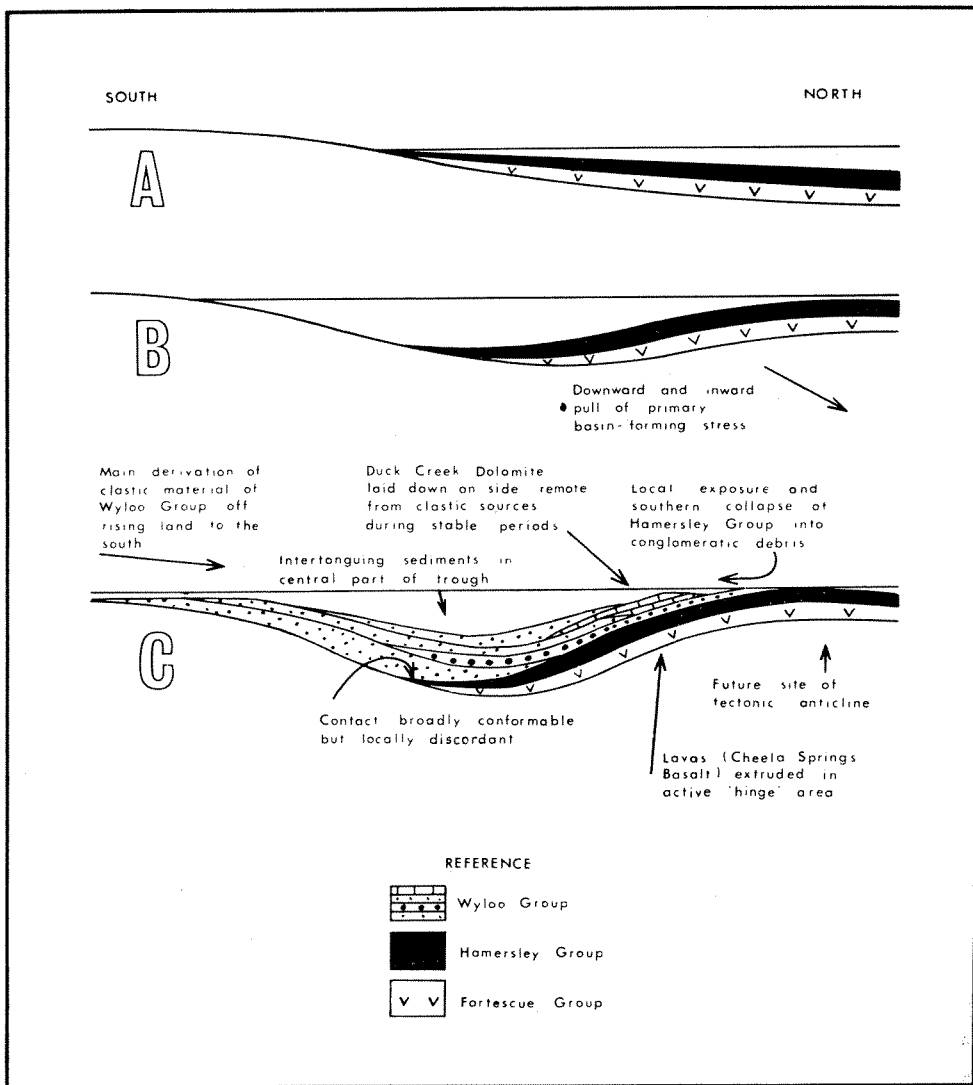


Figure 74. Sketch cross-sections, not to scale, showing the development of the depositional trough of the Wyloo Group.

A. The southern edge of the basin at the end of Hamersley Group deposition; the basin cannot sink further, but the primary cause still acts beneath the central area farther north.

B. The resultant inward stress is accommodated by a marginal downwarp around the southern edges of the basin; in the central parts some fine silty sediment spreads conformably over the Boolgeeda Iron Formation.

C. Wyloo Group deposition is accomplished mainly by erosion of rising land to the south, but these sediments intertongue with slides of conglomeratic debris from some areas of Hamersley Group rocks exposed over the precursors of the future anticlines; other features of this interpretation appear on the cross-section.

higher relief tends to intensify erosional agencies) the basin *can* only be filled in at about the speed at which it sinks. Secondly, unless there is local uplift, or some other form of material transfer (discussed below), the sinking of a basin would imply an increase in the diameter of the earth. Bott (1964) formalised this concept, and gave it a more precise geophysical expression, although it had been implicit for many years in geological text-books (e.g. Holmes, 1945, p.381; de Sitter, 1956, p.447). Bott (1964) however, regarded erosion of the uplifted land and deposition of the sunken basin as joint *causes* of the uplift of the mountains and the sinking of the basin. This can only seem to be true if investigation is begun when both already exist, and Bott passed lightly over the greater problem of their initiation.

The sinking of the depositional basins of the combined Fortescue and Hamersley Groups, with a thickness of over 22,000 feet, seems unlikely to have been accompanied by a proportional uplift of any adjacent land. Firstly, the resultant mountainous topography would be expected to create a local climate able to make its effect visible in the stratigraphy of the basin, even if the immediate shores were desert. Secondly, the great bulk of the Fortescue Group, at least, is indisputably not terrigenous, and if complementary and proportional uplift occurred, then the derivation of this immense amount of material would create a difficult bulk problem. This second point suggests a simple solution: there was no compensatory uplift of the land adjacent to the depositional basin of the Fortescue Group because the direct upward transfer of material from below the sinking basin removed the necessity for any lateral compensation in the mantle. We believe the same to be true for the Hamersley Group, and find the concept entirely consistent with our proposed depositional model. But as soon as subsidence took place without a quantitatively equivalent release of volcanic material to the surface, as in the Wyloo Group, then there was a complementary rise of part of the land. The same argument used above in this paragraph now applies in reverse. Certainly the influx of clastic material in the Wyloo Group represents a climatic change, but we see this as caused by the rise of mountains farther south, rather than by any astronomical factor.

That many factors necessary for iron formation deposition still existed in Wyloo Group time is indicated by the local presence of iron formation (p. 134), but the basic stability which is an integral part of the environmental reconstruction here suggested could only have existed in relatively brief periods of quiescence during the terminal upheaval represented by the Wyloo Group.

The implication of these suggestions is that a first cause exists of initial basin depression which is independent of surface processes. It is possibly a stationary centre of convective downflow in the mantle, but this is purely speculative. However, we believe that this study of the Hamersley Basin justifies the following general conclusions:

1. There exists some unknown primary cause of stationary basin formation which is independent of isostatic readjustment.
2. This acted in a similar way 2,000 m.y. ago as during the Phanerozoic.

3. The sinking of a basin as a result of this primary cause must be accompanied by compensatory movement of material from beneath.

4. There are two possible mechanisms for this: (a) proportional rise of the adjacent land, and (b) direct compensatory upflow of volcanic material.

5. The sinking of the depositional basin of the Fortescue and Hamersley Groups was compensated by the second process; that of the Wyloo Group was compensated by the first process.

SINKING RATE AND TIME SPAN OF THE BASIN

If it is accepted that: (1) the likely time range of the Calamina cyclothem is 1,000 to 3,000 years, (2) the depositional rate of those parts of the Dales Gorge Member where the Calamina cyclothem is well developed is representative of all other iron formation in the Hamersley Group, (3) other lithological types in the Hamersley and Fortescue Groups had about the same average depositional rate as iron formation, and (4) sinking of the basin kept pace with deposition, then the depositional basin of the Fortescue and Hamersley Group took between 45 and 135 m.y. to reach its final depth of 22,350 feet, with an average sinking rate of 2,000 to 6,000 years per foot. When the uncertainty of all these preconditions is taken into account, the correspondence with the approximate time span suggested by isotopic dating (200 m.y.: p. 31) is surprisingly close. Although two corresponding pieces of weak evidence don't add up to one piece of good evidence, a comparison of this with the average maximum rate of Cambrian to Cretaceous sedimentation (1,458 years per foot: Hudson, 1964), and also with some individual Phanerozoic basins (Appalachian geosyncline: 7,500 years per foot), suggests that the existing data on basin sinking rates do not permit any confident assertion that these have altered consistently since the depression of the Hamersley Basin.

Origin of riebeckite (including crocidolite) in the iron formations

REVIEW OF THE PROBLEMS

The origin of riebeckite in the iron formation is neither a single nor a simple problem; we therefore set out beforehand, as a guide to the structure of the following discussion, the main questions concerning riebeckite to which it has been the purpose of our work to provide answers. These questions are concerned largely with massive riebeckite and crocidolite, the former because it forms the great bulk of total riebeckite and because its chemical identity and physical association with crocidolite make its origin of high potential significance in studying that of crocidolite, and the latter because of its economic importance. For each type separately the following enquiries are relevant:

1. *By what main process* did it come to occupy its present position?
2. *When* did it form both in relation to the genetic and diagenetic scheme for iron formation outlined in Chapter 9, and in relation to the events in basin evolution discussed in Chapter 10.
3. *What controlling factors* governed its present limited vertical and horizontal distribution, both regionally and on a local scale?

These are not the only questions that it is possible to ask, nor are they the only ones discussed in this chapter; but they jointly outline in a direct form the main problems.

MASSIVE RIEBECKITE

BASIC ARGUMENT FOR GENETIC PROCESS

The information on vertical stratigraphic restriction of massive riebeckite, and its structural relationship to the enclosing BIF, given in Chapter 7 (see especially Figures 49 to 54 and relevant text) may be diagrammatised as shown in Figure 75A. The salient features of this diagram are that a thickness 'a' of BIF, often a chert-magnetite group of the Calamina cyclothem, passes gradationally into a greater thickness 'b' of massive riebeckite, with continuity of internal structure; this thickness difference is compensated by less marked differences above and below, so that between 'cc' and 'dd' there is no difference, and the lateral change between 'ee' and 'ff' may take place over a few inches.

The simplest interpretations of such relationships are *either* that one material represents an altered or replaced form of the other, *or* that both were derived from a common parent. While it is not logically impossible that a linear boundary on the basin floor separating different chemical precipitates remained stationary for some thousands of years, the concept strains credulity to a point where it seems unnecessary to pursue it; sedimentational differences as a main genetic process are therefore discarded, and a choice must be made between the three diagenetic possibilities: (1) BIF is altered massive riebeckite, (2) massive riebeckite is altered BIF, and (3) BIF and massive riebeckite are alternative derivatives of a common parent different from either. The time relationships which are important for choice between these are discussed below.

EVIDENCE FROM TIME RELATIONSHIPS

The first of the alternatives listed is discarded on the following two grounds. Firstly, all petrographic evidence of riebeckite paragenesis indicates that it is a later mineral (p. 132 and 192 to 212): riebeckite consistently transects early structures (e.g., microbanding, Figure 60A), grows on or around earlier minerals, (Figure 60D), is never bent, broken or corroded, and was still locally crystallising during folding (p. 210). Secondly, it is hard to imagine selective replacement of riebeckite compositionally emphasizing subtle structural differences, and negligible compositional differences, in the 'ghost' banding (p. 193) to form contrasted magnetite and chert mesobands; it is a commonsense criterion of replacement in geological interpretation that a tendency towards structural and compositional homogeneity is usual.

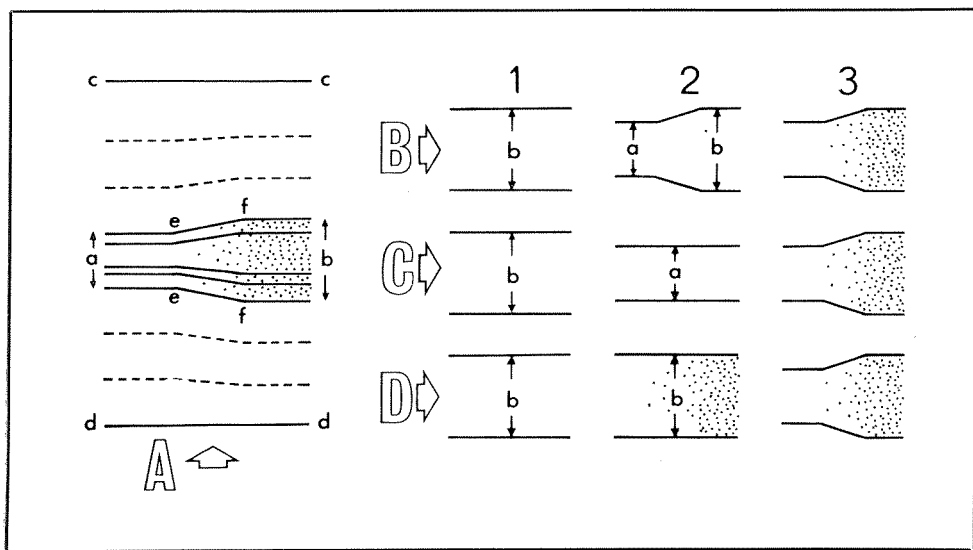


Figure 75. Diagrammatic stratigraphic relationship of massive riebeckite and iron formation, and three theoretically possible sequences in its development; see text for further explanation.

Consequently, either massive riebeckite is replaced BIF, or both formed from a common parent. In distinguishing between these two remaining possibilities it is important to determine first the time relationship between massive riebeckite and compaction.

In the right-hand part of Figure 75 the columns 1, 2, and 3 represent a time sequence of three alternative possibilities in the rows B, C, and D. In B an original thickness, 'b', of material is locally compacted and the uncompacted part is, in column 3, replaced by riebeckite. In row C the same original thickness is uniformly compacted, in column 2, and subsequently replaced by riebeckite, with expansion, in column 3. In row D an original layer of material, again of thickness 'b', is partially converted to riebeckite, and compaction follows in 3. In all three rows columns 1 and 3 are diagrammatically identical.

The sequence in row C is discarded on the grounds that subsequent swelling of a riebeckite body should show evidence of distension at the sides as well as the top and bottom, with minor folding or fracture of the adjacent BIF. No such structures are ever present. Rows B and D are the remaining alternatives. As critical evidence for the choice between them we use the presence at Dales Gorge (p. 193; and Trendall, 1966a, p. 79-82 and Plate 40) of duplicate swells which may or may not contain riebeckite: if this occurrence typifies the general process then we conclude that replacement by riebeckite preferentially affects those parts of some chert-magnetite groups of the Calamina cyclothem which have compacted less than the average, and that row B represents the correct sequence of events. This conclusion is supported by the frequency of riebeckite replacement in the uncompacted part of macules (p. 193, Figure 42B; see also Trendall, 1966a). It agrees also with the expectation that with the sequence in row D some marginal fracture or bending of riebeckite should be present; and there is none.

The significance of this for the nature of the parent material may now be taken up. It has just been shown that, at the time of formation of riebeckite (between columns 2 and 3, Figure 75) the material about to become riebeckite certainly differed to some degree, by virtue of its lesser compaction, from its adjacent stratigraphically equivalent material. In this sense, therefore, the parent age of the two final materials was not common; but to what extent, at the time of column 2, either material, of thickness 'a' or 'b', was like existing BIF, is still not resolved. The transition of magnetite mesobands into massive riebeckite seems to give a clue here.

It was shown that thin magnetite mesobands may be represented within massive riebeckite variously by a much greater thickness of texturally distinct massive riebeckite or by massive riebeckite with abundant disseminated magnetite. In the latter case the magnetite shows no sign of resorption or corrosion (p. 210); the magnetite-riebeckite relationship is similar in this respect in crocidolite mesobands (p. 201), while fibrous riebeckite growing around isolated and perfectly euhedral magnetite octahedra in chert is common (Figure 60D). In all these

instances magnetite physically associated with riebeckite growth contributed nothing to the riebeckite and apparently remained stable during its growth. We therefore suppose that where magnetite mesobands are represented within massive riebeckite by riebeckite alone then the parent material for this was not magnetite, and that the magnetite of the BIF and the equivalent riebeckite of the massive riebeckite formed from some common parent material. It is possible to correlate the growth of magnetite in the adjacent BIF with the compaction from 'b' to 'a' between columns 1 and 2 of Figure 75B, but there is no specific evidence for this. There must be reason other than the preoccupation of iron by magnetite for the prevention of riebeckite growth in the more strongly compacted chert-magnetite groups, since magnetite never takes up all the iron in such groups, and the local presence of magnetite within riebeckite shows that the remainder of the BIF was still liable to be converted to riebeckite.

In summary, the evidence suggests that massive riebeckite and its laterally equivalent BIF represent different derivatives of a common parent material, but (1) their development was not synchronous, in that the parent material was already modified in such a way as to prevent riebeckite growth before riebeckite formed, (2) it is uncertain at what point in the evolution of BIF from the undifferentiated parent the possibility of riebeckite replacement was excluded, and what the controls of this exclusion were, and (3) lesser compaction did not *necessarily* involve riebeckite formation, it only permitted the possibility of riebeckite growth to remain.

The nature of the parent material can only be guessed at, and has already been discussed at a more appropriate point in Chapter 9. The present treatment of the time relationships of massive riebeckite continues below with a consideration of its time relationship to the structural development of the iron formation.

Firm evidence for this is meagre. Preceding discussion fixes the formation of massive riebeckite at a fairly late stage of compaction and after the development of duplicate structures; this was previously indicated by Trendall (1966a, Figure 29). The next stage marked by a distinct structure is the formation of regional rippling. Although some weakly developed corrugations on massive riebeckite mesobands within the Junction Gorge Riebeckite Zone in the upper part of Wittenoom Gorge could be interpreted as regional rippling, and have the typically north-dipping axial planes, no really well developed association of regional rippling and massive riebeckite has yet been seen. We assume that crystallisation of riebeckite would effectively 'set' the BIF and inhibit the formation of regional rippling. The simplest interpretation of the available evidence is therefore that massive riebeckite formed just before and overlapped with the start of regional rippling; but it must be borne in mind that good exposures of massive riebeckite surfaces are not common, and that at Dales Gorge, where exposures are exceptionally fine, regional rippling is nowhere conspicuous. More intensive examination of suitable areas is therefore desirable.

It will be shown later in this chapter that crocidolite probably formed after massive riebeckite and before the minor folds with fibrous minerals. Although no

direct evidence for the time relationship of massive riebeckite and these small folds is available they would not be expected to affect massive riebeckite which had already formed. Formation of massive riebeckite before the minor folds with fibrous minerals is therefore fairly certain, if our later interpretation of crocidolite is valid, with probable formation before regional rippling.

CHEMICAL EVIDENCE

Two of the analyses listed in Chapter 5 are of stratigraphically equivalent massive riebeckite and BIF (chert-magnetite group of the Calamina cyclothem). Both come from the 'adit roof riebeckite' (Figures 5 and 56A), which is only rarely represented by chert, and both are also from boreholes in the Wittenoom area (locations are on Plate 6). These two analyses are reproduced side-by-side in Table 25, together with total iron data, theoretical densities, and iron content per unit volume.

From these latter figures it follows that, if the total iron content of the equivalent BIF-riebeckite thickness remains unchanged during later diagenetic stages, as suggested to be likely on p. 263 to 265, then a thickness ratio of

TABLE 25. COMPARISON OF STRATIGRAPHICALLY EQUIVALENT BIF AND MASSIVE RIEBECKITE

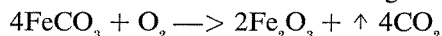
	BIF ¹	Riebeckite ²
SiO ₂	53.26	53.52
Al ₂ O ₃	0.41
Fe ₂ O ₃	35.56	17.72
FeO	8.14	16.26
MgO	0.71	3.63
CaO	0.30	0.08
Na ₂ O	0.19	5.57
K ₂ O	0.06	0.05
H ₂ O ⁺	0.33	2.63
H ₂ O ⁻	0.05	0.32
CO ₂	1.65
P ₂ O ₅	0.09	0.20
MnO	0.01	0.01
TiO ₂	0.01
Total	100.36	100.40
Fe ³⁺	24.87	12.39
Fe ²⁺	6.33	12.64
Total Fe	31.20	25.03
D (calculated)	3.38	3.3
Fe (gm/cc)	1.05	0.826

¹ See column 19 of Table 12.

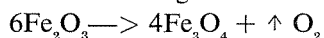
² See column 2 of Table 14.

1 : 1.28 should exist between the BIF and riebeckite. In the holes from which the material was selected for analysis the equivalent thicknesses are 6.6 and 10.2 cm, giving a ratio of 1.54, but in other holes the equivalent riebeckite thickness, which may be taken to have the same chemical composition, varies down to at little as 7.2 cm, so that the expected 1 : 1.28 ratio is within the extreme limits of observed riebeckite thickness variation, and close to the average (p. 193) of 1 : 1.4.

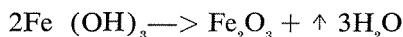
The hypothesis that iron is relatively immobile during diagenesis thus seems to receive some support, and it is useful to examine, for these two analyses, the effect of supposing that the riebeckite reflects the composition of the BIF at an earlier stage of its chemical evolution. The main disparities between these two analyses, in terms of constituents per unit weight of total iron, are in soda and magnesia; the ratio of ferric to ferrous iron is the only other major difference. Now it was shown that the general paragenetic sequence of iron minerals is from carbonate to hematite to magnetite. If, just before riebeckite crystallisation, about half the iron was ferric and in hydroxide gel, and half ferrous in carbonate, then the latter may have been oxidised in the BIF according to the equation:



The CO_2 passed upwards and out of the rocks in solution, and ferric oxide crystallised as hematite in the BIF. The oxygen was derived from lower stratigraphic levels, where hematite was breaking down as follows:



This lower hematite was additionally derived from the breakdown of ferric hydroxide gel.



The water may be supposed to have assisted in the general upward and outward transport of material from the rocks.

Thus, in terms of the previous discussion of textural evidence, it can be supposed that at the time of riebeckite formation the parts of the present riebeckite equivalent to the existing magnetite mesobands consisted of thick ferric hydroxide gel, which formed, in the BIF, first hematite and later, as the pressure increased with depth of burial, magnetite. The iron in the chert mesobands was in carbonate, which also supplied magnesia for the riebeckite; this was removed with the soda (the possible derivation of which was discussed earlier) in solution as the carbonate broke down to release its iron for hematite. In the BIF of Table 25 about half of the total iron must be in magnetite, so that unless subsequent breakdown of magnetite is assumed (a phenomenon for which no textural evidence exists), it seems certain that in this instance no magnetite was present before massive riebeckite in the volumes which riebeckite now occupies.

DISTRIBUTIONAL CONTROLS

The problem of massive riebeckite distribution may be considered as two interlinked problems; firstly, why it exists where it does, and secondly, why it does not exist elsewhere. This dual approach is emphasized because a deceptively

simple answer could be found for the first, but the second is both more puzzling and of greater promise for future study. As a starting point for both it may be taken that if, in a given volume of BIF, all the constituents of riebeckite are present, pressure and temperature are suitable, and reaction is possible in the environment, then riebeckite will form. These three points are taken in reverse order below.

Firstly, factors that could prevent riebeckite growth where all constituents are present at proper pressure and temperature are the absence of ample water for mobility of constituents, and the prior formation of stable minerals. It appears from textural evidence that, once formed, magnetite never contributes iron to riebeckite. Secondly, concerning temperature and pressure, it may be supposed that there are lower limits of both for riebeckite crystallisation. Grubb (1967) has grown fibrous riebeckite at 35°C and 50 bars, which are more realistic conditions than those with which Ernst (1960) was concerned in previous syntheses, but the actual pressures and temperatures needed for riebeckite growth in Hamersley Group iron formation cannot yet be closely estimated. Thirdly, from the earlier discussion of chemistry it is clear that there is little chemical difference between massive riebeckite and its adjacent BIF. The possible derivation of the soda was discussed in Chapter 9; as all the other constituents of riebeckite are still abundant in the iron formation, the possibility that its presence or absence was a control of riebeckite formation is very real.

Thus if riebeckite is *not* now present in BIF it may be concluded either that: (1) soda was not available at the appropriate time, (2) the proper pressure was not reached, (3) the necessary temperature was not reached, (4) magnetite, or some other stable material, had already used all the available iron, (5) insufficient water was available, or (6) some other unknown factor inhibited its growth. These various possibilities for control are now discussed in relation firstly to regional distribution and secondly to small-scale distribution.

From previous discussion of basin development (Chapter 10) and from the regional distribution of massive riebeckite (p. 192) it is clear that on a broad scale all the necessary conditions for massive riebeckite formation were satisfied in a strip along the northern part of the basin, parallel to its axis, and in an area of intermediate stratigraphic thickness (Plate 3). The northern edge of this strip is of course defined by the edge of outcrop for the Dales Gorge Member, but this does not apply to the Marra Mamba Iron Formation, and in any case it must be supposed that towards the basin edge pressures and temperatures must ultimately fall below the required minimum, for lack of burial depth. There are two main problems in this broad distribution: (1) what factor controls the southern edge of the strip? (2) why is there no corresponding strip along the southern side of the basin?

No confident answer can be given for the first question, but it may be assumed that the pressure and temperature were adequate. However, as discussed earlier (Trendall, 1966a, p. 86-7), towards the basin centre the pressure gradient may have been relatively steeper than the temperature gradient, so

that neither water nor soda or both were expelled before the BIF was hot enough for riebeckite to form. No fresh material is available from the deeper parts of the basin, and these possibilities must remain speculative until petrographic evidence is forthcoming about possible minor differences in diagenesis in the Boolgeeda—Mount Brockman area.

The second question raises further problems. The asymmetry of the Hamersley Basin about its main axis is expressed in two main ways: by the presence of the Wyloo Group on only the south side, and by the steeper isopach gradient on the south (Plate 3; p. 69). The absence of a southern zone of massive riebeckite is another such expression, and it is reasonable to look for some connexion. It was noted earlier that at Woongarra Gorge a penetrative axial-plane alignment of riebeckite fibres in cherts of the Dales Gorge Member is present (p. 210). Up to at least that stage, therefore, *some* soda must have been present in these rocks, and also enough water for mobility of its constituents. If pressure and temperature during earlier diagenesis were comparable with those on the opposite side of the basin, as may reasonably be supposed, and if soda were present, then either prior magnetite formation or some unknown factor must have been responsible. But magnetite never takes *all* the available iron; it is concluded that the regional controls of massive riebeckite growth are not fully understood. The solution of this point will probably contribute evidence concerning the problem of the original distribution of the Wyloo Group.

Turning to the small-scale distribution of massive riebeckite within the area where it is regionally abundant, along the main Hamersley Range, it has already been shown, in the discussion of time relationships, that in a single chert-magnetite group of the Calamina cyclothem the development of massive riebeckite is closely related to compaction: the less compacted material retained its option to form riebeckite, but was not bound to do so. In such situations as that of Figure 53 absence of soda was certainly not the reason for inhibition of riebeckite growth in the more compacted BIF between the riebeckite swells, since crocidolite later (see discussion further below) grew immediately beneath it; but, at Dales Gorge at least, crocidolite did not grow near uncompacted riebeckite-prone levels where riebeckite is absent (Trendall, 1966a, Pl. 40: MB3). There is thus a suggestion here that, given suitably uncompacted BIF, availability of soda is the controlling factor for riebeckite growth. The growth elsewhere (e.g. Junction Gorge, p. 188) of crocidolite without massive riebeckite does not refute this argument, since no comparable northeast structures elsewhere provided such a fine local guide to relative compaction.

Little can be said in discussion of vertical riebeckite restriction on the scale on which the riebeckite zones are defined, except to recall that the ratio of shale to iron formation may be significant (p. 178). Whatever the original content and distribution of soda (see Chapter 9, p. 271) in the iron formations the impression given by the distribution of riebeckite within its area of regional abundance is that at the time of massive riebeckite formation soda was already restricted in both its distribution and mobility; but as with the major regional

distribution, the nature and relative importance of its distributional controls are not fully understood.

CROCIDOLITE

BASIC ARGUMENT FOR GENETIC PROCESS

It was shown in Chapter 7 that if crocidolite mesobands are locally absent from any stratigraphic position where they are elsewhere present then they are not, as with massive riebeckite, represented by some other material; this conforms with the commonsense expectation from the typically pinched out terminations of crocidolite mesobands that may be seen wherever crocidolite occurs. This important and absolute difference in the stratigraphic relationships of the two main forms of riebeckite necessitates a different form of the argument for origin.

The initial possibilities for crocidolite origin are: (1) crocidolite is sedimentary material, perhaps chemically or physically modified, or both, and (2) crocidolite formed within the BIF after deposition. Although there is no decisive evidence to refute absolutely the first possibility it can be shown that, if crocidolite is depositional, there must firstly have been a degree of physical redistribution of material unknown elsewhere in geology, and secondly the parent sediment must have differed completely, in regional distribution, from any other component of the Hamersley Group.

The patchy areal distribution of crocidolite on all scales is not matched in known sedimentary material but the possibility of a depositional control could not in the Hamersley Crocidolite Province be discounted for much of the irregularity. However, belief in a primary depositional control is strained beyond a reasonable limit by the flat parallel strips of crocidolite between the riebeckite swells at Dales Gorge (Figure 53; and Trendall, 1966a). In the Cape Province of South Africa vertically superimposed crocidolite enrichments obviously related to both anticlines and synclines occur in a way not demonstrable in Western Australia. Even if it were supposed that the synclines developed from minor hollows in the basin in which the parent material of crocidolite accumulated the same explanation cannot be applied to the anticlinal enrichments. It seems impossible to accept that the potentially crocidolite-forming material knew where both anticlines and synclines were to develop later. However, it can be acceptably argued, even for South Africa, that lateral rearrangement during folding, with extreme bedding-plane mobility, modified the primary sedimentary distribution to its present form. The argument would carry more conviction if examples of quantitatively comparable mechanical behaviour could be found in other sedimentary rocks; there are none recorded.

Even if small-scale thickness fluctuations of crocidolite mesobands are attributed to post-depositional redistribution the regional distribution of crocidolite within the Hamersley Group is still difficult to account for by primary deposition. If the equivalence of massive riebeckite and BIF is accepted then the regional

lateral continuity of all mesobands of the Dales Gorge Member *except crocidolite* has been demonstrated. It is a reasonable supposition that the same continuity is present throughout the iron formation. We are reluctant to accept that, in a basin whose interpretation must be based on a concept involving the steady accumulation of thin annual basin-wide skins of chemical precipitate over millions of years of stability, thin layers of sediment of a uniquely different type are likely to have been deposited in various different sharply restricted irregular areas of the basin at sporadic intervals with no other sign of unusual events.

If the second possibility—that crocidolite formed within the BIF after deposition—involves fewer distributional or other anomalies then it should be accepted; this possibility is now examined.

It may be supposed that crocidolite fibres grew along their length. Consequently, *either* they grew in some suitable medium which previously filled the space now occupied by the crocidolite, *or* the existing crocidolite mesobands opened with the crocidolite as it grew. The shapes of fractured magnetite laminae in marginal cone structures indicates disruption along the fibre direction (Figure 57); if any material other than crocidolite previously existed in its position it must have been similarly fibrous. There is no evidence for any fibrous precursor of crocidolite, and the simplest hypothesis, if crocidolite formed within the BIF after deposition, is therefore that crocidolite grew concurrently with the dilation of the mesobands which it now occupies.

An hypothesis of crocidolite growth along a previously existing magnetite mesoband is consistent, if the materials for growth are found from solution (p. 309), with the absence of evidence for resorption or corrosion of magnetite (p. 201), and also of any quantitative relationship between crocidolite and its accompanying magnetite (p. 199). Crocidolite mesobands now have a close parallel with other fibre growth situations such as the fibrous quartz (often with some riebeckite) in the opened limbs of the minor folds in Figure 46, and in the apparently opened fibrous quartz and riebeckite layers in Figure 47; indeed, the fibrous or acicular growth of minerals across an opening vein is so commonly accepted in geological interpretation that examples could be multiplied indefinitely. Dilational growth of crocidolite seems also to account perfectly for its highly erratic distribution on a small scale, and removes the awkward necessity for redistributing some unknown parent with exceptional mechanical properties.

Cones and corrugations in crocidolite are now interpreted as points or lines where the magnetite has failed to dilate. Rather than suppose these points or lines to have had some primary difference it seems more plausible to suppose that crocidolite growth was initiated at seeding points with a random areal distribution, and that lateral spread of dilation steadily wedged outwards from these to give discrete 'cells' of fibre growth. It may then be supposed that wedging becomes less effective where two such 'cells' meet along a line, since the last magnetite plate to be lifted is wedged from both sides, and must be broken away horizontally, without initial tilting; a mechanically naive comparison may be drawn with the

inflation of a flattened rubber inner tube with a sticky inside surface. If the materials on the two sides of such a growing mesoband have different mechanical properties, so that one behaves less competently, it is clear that if there is wedging between them cones will be preferentially formed on that side, while if both sides have equal competence the cones will be symmetrical; the names fixed and mobile sides (p. 200) were suggested for this reason. The typical internal magnetite screen forms in crocidolite may easily be generated by an extension of this hypothesis involving simultaneous growth in many layers of a laminated magnetite mesoband.

The dilational hypothesis also provides no difficulties for the hypotheses of iron formation development set out in Chapter 9. We would expect, in a stratigraphic situation like that of Figure 55A, that if the crocidolite were depositional, its presence would have had some influence on the diagenesis of the enclosing BIF; and there is no sign of this. In addition, we find it reasonable to expect that the two main forms of riebeckite—massive riebeckite and crocidolite—should, with their sharply contrasted textures and stratigraphic relationships, have developed by equally contrasted processes; we therefore accept the dilational growth of crocidolite as a basis for subsequent discussion. One argument for a depositional origin—the stratigraphic restriction of crocidolite—is argued against in discussion further below.

CHEMICAL EVIDENCE FOR IRON DERIVATION

If crocidolite growth during dilation is accepted, then, unlike massive riebeckite, all the constituents must have moved into the present volume occupied by crocidolite from the adjacent BIF during fibre growth. The two major constituents of riebeckite are silica and iron. Our earlier diagenetic hypothesis involves an assumption of iron stability, and to be consistent with this we must show that enough iron would have been available close to existing crocidolite without large-scale migration. Silica and water have already been supposed to have been abundantly available during diagenesis, and magnesia is sufficiently abundant in the BIF to present no problems of availability if enough iron can be found. Soda availability is a separate problem, which was discussed earlier.

It was noted in Chapter 4 that the chert mesobands closely associated with crocidolite in worked seams are often red, and poor in carbonate (p. 99). Analyses of four such mesobands appeared as analyses 14-17 of Table 13 in Chapter 5; assuming a mean density of 2.7 for these, their mean total iron content is 0.11 gm/cc, and their mean microband interval is 0.53 mm. The mean total iron content of the nine microbanded cherts of Figure 72 with microband intervals falling between 0.4 and 0.7 mm is 14.95 weight per cent, or 0.48 gm/cc assuming a mean density of 3.2; their mean microband interval is 0.53 mm. Crocidolite contains about 0.85 gm/cc of total iron. Thus if the typical red and carbonate-poor chert mesobands close to present crocidolite were originally of about mean iron content for their microband interval, then they could have provided 0.37 gm of iron per cc for the growth of crocidolite; and for any given vertical

thickness of crocidolite the contained iron could have been obtained from about $2\frac{1}{2}$ times this thickness of adjacent chert. For any crocidolite horizon of the Hamersley Group there is thus no reason to suppose that a dilational origin of the fibre need have involved migration of iron derived from the breakdown of carbonate in chert over more than a foot at most. Breakdown of carbonate may also be expected to have released adequate magnesia for the crocidolite.

EVIDENCE FOR TIME RELATIONSHIPS

In the preceding discussion of massive riebeckite it was argued that at least some magnetite is likely to have formed later than it. The invariable association of crocidolite with magnetite, which demonstrably exists whether or not crocidolite occurs with it (p. 274), seems overwhelming evidence in favour of the growth of crocidolite after the magnetite; the evident fracture of magnetite by the growing crocidolite, already noted, is satisfying but redundant confirmation. The expectation is therefore that crocidolite formed after massive riebeckite. The stressed structure of riebeckite within marginal cone structures of crocidolite mesobands adjacent to massive riebeckite (p. 202 and Figure 57C) confirms this expectation.

The marginal fibrous quartz which is commonly associated with Hamersley Range crocidolite is most credibly interpreted as a later growth than the crocidolite (p. 312); almost insuperably so where it occurs on both sides of the crocidolite. Its general orientation concordantly with the fibrous quartz of the minor folds makes it a reasonable supposition that the two grew contemporaneously. Crocidolite may thus be placed in time after regional rippling and all preceding events and also after massive riebeckite growth and magnetite development, but before minor folds with fibrous quartz. A hypothesis is developed below which is based on this time sequence, and accommodates also certain other features of crocidolite to which attention is first drawn.

THE STRESS-REVERSAL HYPOTHESIS FOR CROCIDOLITE GROWTH

The hypothesis outlined here was developed to account for the crocidolite of the Wittenoom Sub-Province; its applicability to the Marra Mamba Sub-Province is discussed after its presentation. Although it is based on the relative position of the growth of crocidolite in time, which has just been argued, it is framed also to take into account the following three points: (1) the regional distribution of crocidolite in the Dales Gorge Member, (2) the contrast between the broad association of crocidolite with massive riebeckite on the one hand, and on the other hand the apparent absence of any close interdependence in the occurrence of the two forms, and (3) the comparatively long and straight fibres of crocidolite, which seem to indicate growth in a relatively stress-free environment, in spite of evidence of strain before and after crocidolite growth. Figure 76 illustrates the following explanation of the hypothesis.

The elongate tilted rectangle in Figure 76A represents a vertical north-south section through the Dales Gorge Member, across the future position of the main Hamersley Range Synclinorium to the south of Wittenoom, at the stage when regional rippling was forming (Chapter 10, p. 292 to 294). The vertical pecked line marks the future position of the axial plane of the syncline, and the arrows show the sense of the stress which formed the regional rippling. 'P' is a point in the northern limb of the future synclinorium where crocidolite later forms. Although this rectangle is diagrammatic it may be taken to represent a horizontal distance of some 30 miles with a thickness of 500 feet.

In Figure 76B the same section is represented at a stage during formation of the Hamersley Range Synclinorium, whose axial plane is again marked by the vertical pecked line. The former stress sense of the regional rippling is here indicated by pecked arrows, while the stress to be expected within each limb of the syncline as a result of its formation is shown by solid arrows. In the southern limb the later stress has the same sense as the first; but in the northern limb the later stress is in the opposite sense to that of the regional rippling. It is suggested that the second stress is related to the minor folds with fibrous minerals, and that crocidolite grew, necessarily only in the northern limb of the synclinorium, at a time when the two stresses were equal and opposite. Thus crocidolite grew at a 'flat spot' during reversal of stress. This stress-reversal hypothesis is illustrated

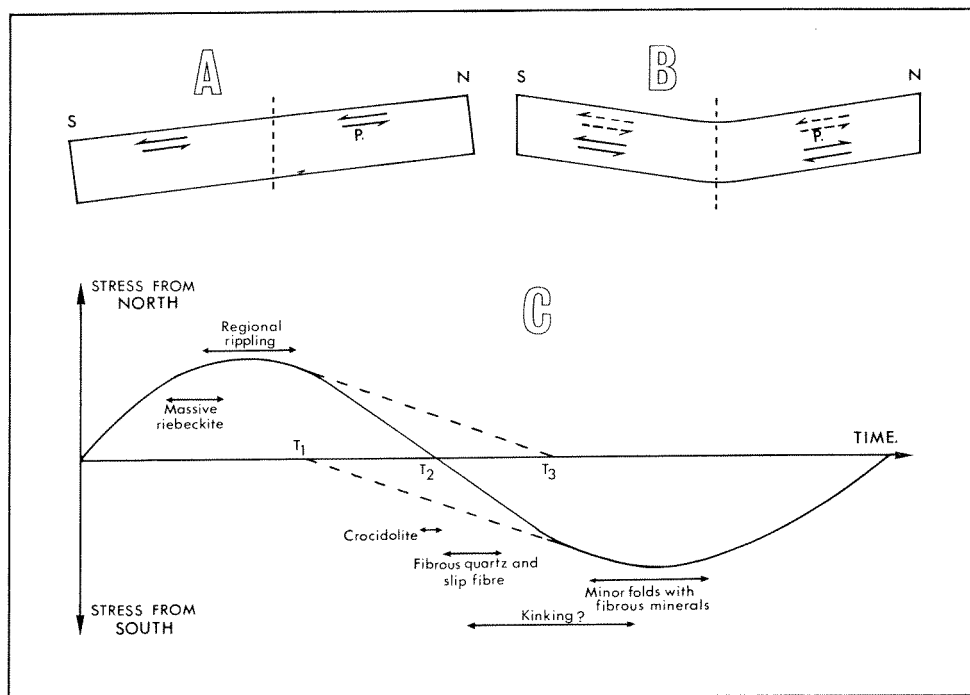


Figure 76. Diagrams illustrating the stress-reversal hypothesis of crocidolite growth; see text for further explanation.

more fully in Figure 76C, which represents the stress history near the point 'P' of Figure 76, A and B; an explanation of this diagram follows.

The solid sinusoidal line in Figure 76C represents the development in time of the effective laterally directed stress in a north-south sense around the point 'P'. The origin is taken as the moment of deposition, when stress is almost nothing. As the sediment is progressively more deeply buried beneath later material, it dips more steeply towards the deeper parts of the basin, and regional rippling develops, as described in Chapter 10. As the iron formation becomes more rigid the effective lateral stress from the north gradually declines and becomes negligible at T3. This increasing rigidity permits the transmission through the rock of stress associated with the folding, which is assumed to begin at time T1. The interval between T1 and T3 represents a period when declining gravitational stress from the north is steadily compensated by increasing tectonic stress from the south, so that at T2 the two are exactly equal. It is important for the stress-reversal hypothesis that at this time (T2) although the effective lateral stress is nil the rock at 'P' is not in an equivalent state to one which is subject to no stress from either side; it is being pushed equally from both sides, and can obtain relief (since it is confined on both east and west) only by vertical extension. *Crocidolite grows during this period as a means of achieving such relief.*

With increasing tectonic stress, from the south, the steady growth of vertical crocidolite is halted, but the growth of oblique fibrous minerals continues in the marginal fibrous quartz of crocidolite mesobands, in separate occurrences of slip fibre and fibrous quartz, and finally in the minor folds with associated fibrous minerals. The stress-reversal hypothesis is well illustrated by Figure 47. There the regional rippling has evidently been driven back on itself, with continued diagenetic destruction of chert, and cracking and buckling of the more rigid magnetite. Indeed, from evidence of this kind it is evident that stress-reversal is more than a hypothesis; the identification of the point of reversal with crocidolite growth, however, is incapable of such vivid and direct demonstration in a single photograph.

The strikingly fibrous macroscopic appearance of fibrous quartz, together with its frequent blue colour caused by a small concordant fibrous riebeckite content, together make it appear that the quartz may represent a late replacement of previously existing fibrous riebeckite. It is worth emphasizing the evidence against this, and in favour of the alternative hypothesis that this quartz grew as quartz. This is two-fold: firstly (Figure 58), where fibrous quartz borders crocidolite the contact between them is always fairly sharp and across the fibre length (the assumed direction of growth); secondly (also Figure 58, page 205) several structures common in crocidolite are almost never present in fibrous quartz, although it would be reasonable to expect their preservation during replacement. The only exception to this second point is a rock from the spoil heap of the Colonial mine (p. 205), which shows crocidolite-like structures, but is mineralogically distinct, and is probably, unlike normal fibrous quartz, a secondary replacement of crocidolite.

DISTRIBUTIONAL CONTROLS

In addition to the regional stress history required by the stress-reversal hypothesis for crocidolite growth it is evident that several of the basic prerequisites for massive riebeckite growth are also required for crocidolite, and are therefore potential controlling factors of distribution. The pressure and temperature must again be above some (unknown) minima, all the chemical constituents must be present, and the conditions must be such that reaction is possible; prior growth of magnetite mesobands is an additional prerequisite.

For control of large-scale distribution the absence of crocidolite from the deeper parts of the basin is possibly attributable to an unsuitable stress history, since no other fold comparable with the Hamersley Range Synclinorium exists between it and the central axis of the basin. However, in a similar way to the distribution of massive riebeckite, equivalent conditions for crocidolite growth, including stress-reversal, could be expected along the southern side of the basin in the north-dipping limbs of synclines (for example the Turner Syncline). That crocidolite does not occur in the southern part of the basin suggests that, as with riebeckite, some unknown factor related to the asymmetry of the basin has inhibited its growth. It seems reasonable to assume that this factor was the same for both crocidolite and massive riebeckite, which has already been discussed; and the same factor could have applied to the central part of the basin.

Whatever conditions were responsible for the asymmetric distribution of crocidolite between the northern and southern parts of the basin the stress-reversal hypothesis accounts for its restricted distribution in relation to structure in the northern part. The more southerly extent of massive riebeckite, as far as the southern part of the Hamersley Syncline, is a discrepancy in the generally sympathetic distribution of the two types which fits the hypothesis well. Both the horizontal and vertical distributional controls of crocidolite growth within the generally favourable area indicated by the hypothesis now remain to be discussed; these include the small-scale controls which govern the existence, shape and grade of crocidolite ore-bodies.

The virtual restriction of both massive riebeckite and crocidolite in the Wittenoom Sub-Province to the two riebeckite zones of the Dales Gorge Member argues for at least one controlling factor in common for their vertical distribution at this scale; it has already been stated in discussion of massive riebeckite that this factor is uncertain, but that a likely one is availability of soda. Within the riebeckite zones the preferential restriction of crocidolite within narrow stratigraphic limits has been described in detail (Chapter 7); and it was also noted that minor and local control is exerted by the Calamina cyclothem. We assume initially that, given the possibility of stress relief by crocidolite growth in the Dales Gorge Member, the obvious vertical heterogeneity of mechanical properties caused by minor variations in details of the mesoband sequence will ensure that one or more levels will preferentially dilate to allow crocidolite growth: a stretched chain will break at its weakest link. We cannot say why the crocidolite horizons

are the weakest link in the Dales Gorge Member but we can assert confidently that the detailed lateral stratigraphic continuity of the member is such that, if they are the weakest link in one place, they will be similarly so elsewhere. We therefore see no argument for a depositional origin of crocidolite in its close stratigraphic restriction.

Given an area of the Dales Gorge Member which is subjected, as though in a vice, to lateral compression from opposite sides, and given that relief may be found by consequent dilation at one or several of a few specified levels within the member, it remains to consider what factors control the local occurrence or non-occurrence of dilation: why does crocidolite not occur evenly over the entire area within which, under the stress-reversal hypothesis, conditions favour crocidolite growth? Although we cannot answer this question completely we believe that the points raised below are relevant guides to a final solution, and that they suggest provisionally acceptable answers to some puzzling details of crocidolite distribution.

The plain rectangle of Figure 77A represents the northern limb of the Hamersley Range Synclinorium at the time of crocidolite formation; that is, the right-hand half of Figure 76B at the time T2 of Figure 76C. The opposing forces are suggested by arrows, and the pecked line represents a crocidolite horizon before crocidolite growth. It would not be expected that stress relief would come by

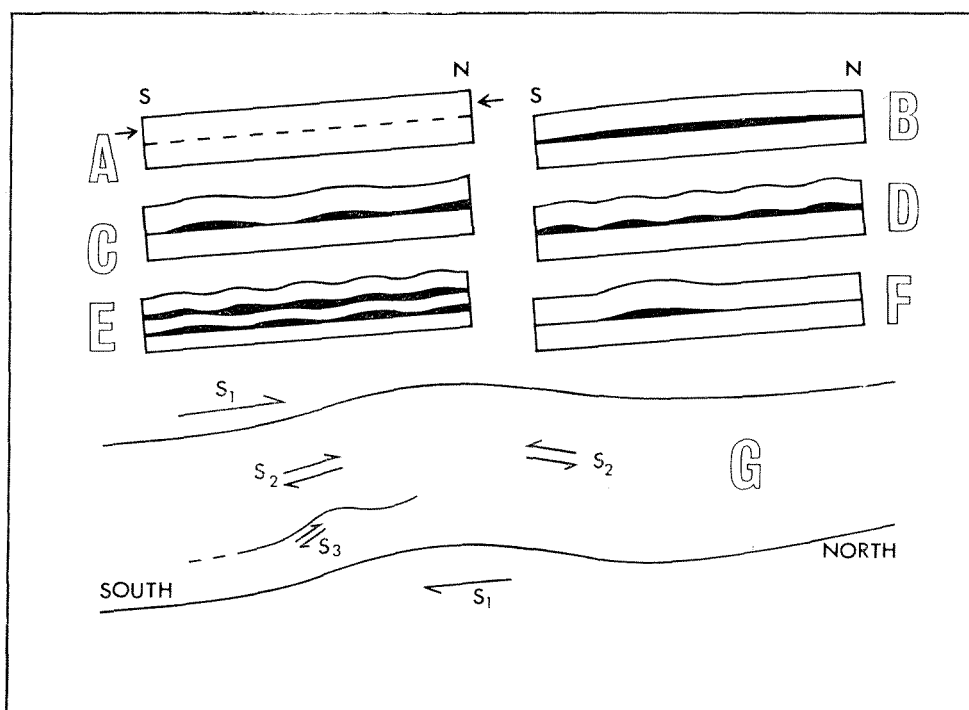


Figure 77. Diagrams illustrating the structural control of crocidolite growth; see text for further explanation.

simple arching over about 15 miles, the approximately north-south span involved, as shown in Figure 77B, but that buckling of the form of Figure 77, C or D, would take place; however, for most geologists this expectation follows more from geological 'intuition' based on such familiar structural analogies as Jura-type folding than from acquaintance with the theoretical mechanical reasons why an arch of these proportions is unlikely. Ramberg and Stephansson (1964; particularly Figure 3) investigated an analogous problem experimentally, and provided an equation expressing the expected fold wavelength in terms of the thickness and mechanical properties of the upper block, various constants, and the density of the fluid material of the lower block, on which in their model the upper block was assumed to float; it is noteworthy that the magnitude of the compressive stress was not a factor for elastic plates.

Ramberg and Stephansson's (1964) models involved only homogeneous elastic and viscous plates. Ramberg (1964) later discussed the effect of compression on a composite pile of layers with contrasted rheological properties and showed (his Figure 16) that several orders of fold could be produced both simultaneously and successively according to the magnitude of the compressive force and the differing mechanical properties of the layers. Assuming two crocidolite horizons separating three blocks of mechanically differing iron formation the response could be of the type shown in Figure 77E. Ramberg (1964, p. 333) concluded part of his discussion with the words "in view of the virtually infinite possibility of variations, modifications of the pattern in order to suit special geologic structures are best left to the reader". Even if the Dales Gorge Member had perfect lateral homogeneity at the time of crocidolite growth a purely theoretical adaption of Ramberg's calculations to it would be impossible, for several reasons. Firstly, knowledge of the mechanical properties of the Dales Gorge Member at that time is completely speculative. Secondly, the compression of the stress-reversal situation is not evenly and externally applied, as suggested by the arrows of Figure 77A; it is a balance of two rather differently applied forces. The southward force, the down-dip gravitational component, acts both penetratively on every part of the rock, and by mechanical transmission through it. Thus a small piece of, say, a magnetite mesoband at point 'P' of Figure 76B is both pulled down by its own weight (and hence southwards according to the mechanical properties of the adjacent mesoband below and the strength of the contact between them) and pushed by the upslope iron formation. This second part of the force obviously increases downslope. The northward force, on the other hand, is due to inter-layer friction during folding, and has no independently penetrative component; it relies on continuous contact of particles for its transmission.

In spite of these complexities for theoretical analysis of the stress-reversal situation in the Dales Gorge Member we believe that the type of response to compression discussed by Ramberg is the best available foundation for a theory of localisation of crocidolite within the generally favourable northern limb of the Hamersley Range Synclinorium; some other factors affecting the relative simplicity of such fold patterns as those of Figure 77, C, D, and E are now discussed.

Apart from the inevitable minor departures from geometrical perfection present in any geological structure, the starting point of Figure 77A, the northern limb of the Hamersley Range Synclinorium at T2 of Figure 76C, already had significant irregularities in its layering. Northeast structures, locally variable in their expression and distribution (Chapter 6), were already present (Chapter 9); on a small scale the influence of these on crocidolite growth is vitally important (Figure 53; Trendall, 1966a). Regional rippling was also in existence, and was even more variable in distribution (Chapter 6); it had made the possibility of a perfectly symmetrical response even less likely. As a final example of pre-existing irregularity, we point out the presence of massive riebeckite; effectively structurally reinforced sheets of erratic distribution. We assume that more extreme local responses, controlled by one or more of these irregularities, could give isolated relief, as in Figure 77F, which could relieve the compressional stress for some distance on either side.

We have already noted that the co-existence of a wide range of fold scales in the Hamersley Range area is normal (p. 34). To this extent the representation of the Hamersley Range Synclinorium by a simple form of Figure 76B, and thus Figure 77A, is misleading. Figure 77G is a more realistic but still diagrammatic representation of part of the northern synclinal limb. S1 represents the regional stress caused by the folding; S2 and S3 are the local stresses associated with two contained folds at successively smaller scales. The total resultant stress at any point is the sum of all the component stresses of the folds to all scales within which the point lies. In Figure 77G the northward S1 stress may exceed the southward gravitational component, but crocidolite may nevertheless grow on the northern limb of the smaller anticline, when the stress S2 produces the exact balance needed for crocidolite growth. If the regional S1 stress were elsewhere less than the southwards stress then crocidolite growth could be expected on the south anticlinal limb, where S1 is augmented by S2. This is an explanation for the common association of crocidolite with structure, but with a variable relationship to the structure in detail (p. 243). This feature, present but not outstandingly well displayed in the Hamersley Range area, is well known in the Cape Province crocidolite area of South Africa.

One other feature of horizontal distributional control remains to be mentioned: variation along the axial direction of the controlling structures. Attention was drawn earlier (p. 34) to the common axial discontinuity of all folding of the area. We assume that this must be controlled by slight obliquities of stress directions at one or more phases of structural development. In effect this would produce, instead of axially continuous structures of the type shown in Figure 77, D and E, two obliquely interfering sets of such structures, with consequent formation of axially discontinuous bodies of crocidolite. This feature does not effect the general course of the preceding discussion.

We thus believe that, although the stress-reversal hypothesis adequately accounts for the development of crocidolite on a broad scale, the details of its distribution within the generally favourable area are controlled by a complex

structural response of the iron formation to the opposed stresses. We expect the distributional regularity or irregularity of the resultant crocidolite to reflect exactly the regularity or irregularity of the regional structure. For the Hamersley Range area we believe that the actual situation is too complex for effective theoretical analysis, and that the practical use of structure to forecast and locate crocidolite ore must be an empirical process. The practical application of this empirical approach to ore search in the Hamersley Range area is discussed in the following chapter, but prior discussion of some theoretical aspects follows immediately.

SOME CONSEQUENCES OF THE HYPOTHESES PROPOSED

One consequence of our hypotheses has just been set out, but its importance justifies emphasis by reiteration: we expect a strong correlation between crocidolite and structure, but we cannot forecast the exact nature of the correlation other than empirically. Some additional consequences of potential practical use are now discussed.

Firstly, we would expect the correlation with structure to be quantitative as well as qualitative. If it were empirically established in some area that a particular crocidolite horizon tended to be enriched on the north limbs of anticlines, then large anticlines should be more enriched than smaller ones. The quantitative relationship should also hold on a regional scale, and any north-south strip about a mile wide across the north limb of the Hamersley Range Synclinorium in the Wittenoom—Yampire area should contain about the same amount of crocidolite. Another aspect of the same consequence is that in any large structurally homogeneous area of crocidolite occurrence ore bodies are likely to be of about the same area and tonnage; rich bonanzas of crocidolite can never be expected in any area where known ore bodies are all of comparable grade, unless some conspicuously anomalous local structure is present. But if the regional shape of a large controlling fold changes, then changes in enrichment can be expected. For example, the Hamersley Range Synclinorium south of the Wittenoom—Yampire area (in a vertical north-south section along roughly longitude $118^{\circ} 20'$) tends to have a simple shape with a more definite central axis than its equivalent in the Mount Margaret area (in a similar section along $117^{\circ} 30'$), where it consists of a number of continuous corrugations of about equal status, with no clear central axis of the synclinorium. The lower crocidolite values in the Mount Margaret area (Chapter 7) may be related to this difference.

Secondly, it is instructive to consider the possible situations where, as in the Dales Gorge Member, there are a number of superimposed crocidolite horizons in the regionally favourable area. On the smallest vertical scale, the single horizon, it is evident that over a small area of constant dip (a few square yards) the stress conditions would be constant, and it is not therefore surprising that individual crocidolite mesobands sympathetically pinch and swell, to give comparatively little variation in total fibre length in any vertical section through a seam in this situation.

We consider now a situation, which we emphasize to be initially theoretical, where three crocidolite horizons, called X, Y, and Z in order of increasing depth, exist in a potentially favourable crocidolite area. An empirical relationship with a regularly repeated structural pattern is established and most enrichments are of equal grade in all horizons. If a favourable structure for enrichment is then located in an immediately adjacent area, we would expect the total grade of all three horizons to be maintained. Thus if X were drilled to, and proved to have 3 times the normal fibre length, we would forecast low grades at the Y and Z horizons; conversely, if X were barren, we would predict greater than average enrichment at one or both of the lower horizons. If, however, the apparently favourable structure lay in an area at some distance (relative to the regional structure controlling stress-reversal) from the known area of measured enrichments, no deductions from inspection of the uppermost level could be made, since the empirically determined local expectation of ore need not apply.

Three theoretical possibilities for two neighbouring horizons X and Y, appear in the left-hand part of Figure 78. In the topmost of these three diagrams there is sympathetic dilation of X and Y in response to local structurally controlled stress. If vertically superimposed assays of X and Y are plotted against each other, they fall along the line 'a' in the diagram of the right-hand part of the figure. In the central diagram of the three on the left exactly the same dilation occurs, but only in X. Vertically superimposed assays of these two horizons fall along the abscissa of the right-hand diagram, or, if the situation is reversed, with dilation in Y only, along the ordinate. A more complex situation appears in the lowermost left-hand diagram. Here there is sinusoidally antipathetic dilation

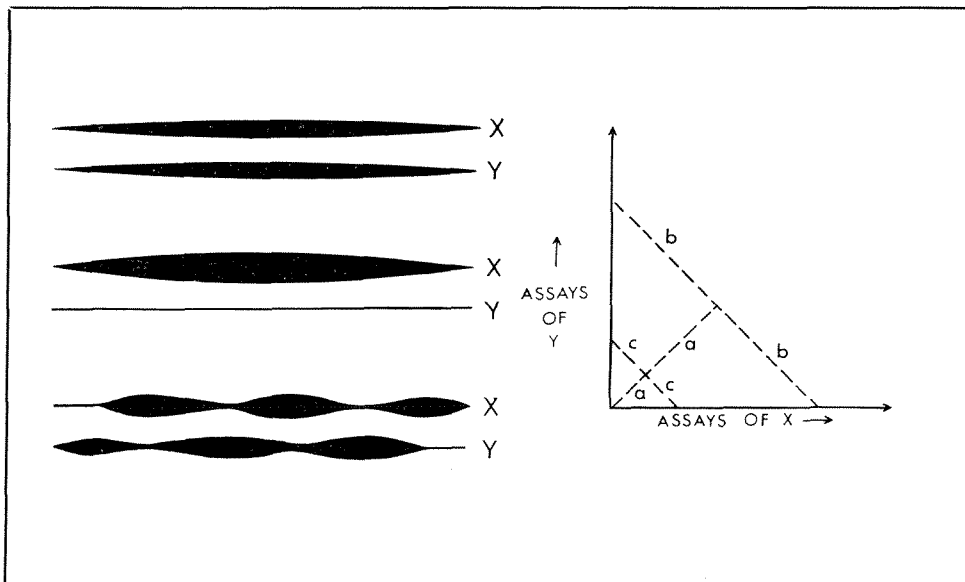


Figure 78. Diagrams illustrating the theoretical inter-relationships of vertically superimposed crocidolite enrichments; see text for further explanation.

in X and Y about the same basic shape of the top diagram; the same total dilation is represented in all three diagrams. Assuming the enrichments of the lowermost diagram to be circular in plan then any group of vertically superimposed assays at the same distance from the centre of the ore body fall along lines sloping like 'b' and 'c' of the right-hand diagram; 'b' nearer, and 'c' farther, from the centre.

Since all these conditions may exist in different parts of an enrichment caused by a complex structure, it is not surprising that, although the assays of the Upper and Lower Seams at the Colonial mine at Wittenoom most closely approach the pattern of 'a' (Figure 63), they show no close correlation; especially since there are no available data in the same area for the other crocidolite horizons of the Dales Gorge Member, which would all, in our hypotheses, be expected to show mutual inter-dependence.

The practical applicability of the theoretical discussion in the preceding paragraphs depends mainly on the relative scale of structure and enrichment; for a structure to be confidently identified as the control of any enrichment (and unless this is done the association is useless as an exploration tool) the enrichment must have the same order of scale as the structure, and possess an invariable geometric relationship with it. For example, within any seam the individual mesobands pinch and swell antipathetically, and the controls for this must be sought in variations of the same order of size in the enclosing BIF; but the structural control for the existence of the seam must be sought at a larger scale. An example of such a scale might be the enrichments at the combined Yampire C and Upper Seam Horizons at Yampire Gorge and the Wittenoom area. At Yampire, the Yampire C Horizon is, where enrichment exists, preferentially enriched over the Upper Seam, but the reverse is true at Wittenoom. It is useless here to study the enrichment at either of these restricted levels and look for a constant structural control; none will be found. On the broadest possible scale, the origin of regional enrichment along the north face of the Hamersley Range must be sought in a structure of the appropriate size, and it was in that way that the stress-reversal hypothesis came to be set up. The practical empirical use of the crocidolite-structure association in exploration must include an appreciation of the scale factor.

APPLICATION OF THE STRESS-REVERSAL HYPOTHESIS OUTSIDE THE WITTENOOM SUB-PROVINCE

The crocidolite occurrences of the Marra Mamba Sub-Province do not immediately lend themselves to interpretation by the stress-reversal hypothesis. It was nevertheless noted earlier that in the main group of deposits at Marra Mamba fibre distribution is variably related to local structure, so that its broad applicability in some modified form seems not unlikely. For example, crocidolite formation might be possible by stress-reversal on both limbs of any large syncline in a body of iron formation, if the fold were initiated at an appropriate diagenetic stage, so that inward gravitational stress down the limbs when the material was plastic could later be opposed by the outward internal fold stresses as the rocks

became sufficiently rigid for their transmission; in effect, the developing basal slope on which regional rippling in the Wittenoom Sub-Province was formed, is replaced in this modification by the developing slope of the fold limbs themselves.

The Marra Mamba deposits *could* certainly be thus interpreted, and there are enough differences between it and the Wittenoom Sub-Province deposits to make a difference of this degree credible: for example, regional rippling is not present in the Marra Mamba Iron Formation, the fibre at Marra Mamba was folded after growth, and if crocidolite growth was everywhere approximately coeval (p. 293) then all the Marra Mamba crocidolite grew under a load at least 300 bars above that of the Wittenoom Sub-Province, and at a temperature an unknown amount higher.

We believe, however, that the generally poor exposure of the Marra Mamba Iron Formation in the Marra Mamba Sub-Province precludes any present possibility of either proof or disproof of hypotheses of this kind. No attempt at an isopach map for the Marra Mamba Iron Formation can yet be attempted, nor can a reliable picture of regional fibre distribution be obtained. In summary, while a modified form of the stress-reversal hypothesis for crocidolite could be applied to the Marra Mamba Sub-Province, and no evidence is present there to invalidate it, we prefer that the hypothesis should stand or fall by the much more detailed evidence available from the better exposed and known Wittenoom Sub-Province.

COMPARISON WITH SOUTH AFRICAN CROCIDOLITE DISTRIBUTION

It has been our deliberate policy in this discussion of crocidolite to rely wherever possible on evidence from the Hamersley Range area, but a few references have already been made to South African evidence, where, in the specific aspect under discussion, it seemed obviously relevant and helpful. We do not wish to abandon this policy now by embarking on a detailed comparison with South African crocidolite occurrence; but at a stage of our work when the main form of our own hypotheses had just been established one of us (A. F. T.) was able to visit South Africa, armed with the stress-reversal hypothesis, to make a broad assessment of its applicability there. That such close similarity does exist between the Hamersley Range area of Western Australia and the northern Cape Province of South Africa, not merely in crocidolite distribution but in broad geological evolution, is an additional reason for the insertion here, against our stated policy, of the following brief comparative notes. The comparison is made by reference to the map of Cilliers and Genis (1961, Figure 1).

Crocidolite is mined in the Cape Province from iron formation of the Lower Griquatown Stage, whose outcrop forms a narrow north-south belt some 300 miles long. It is convenient in the first place to restrict comparison to the central part of this belt, between latitudes 27° and 29° South, from about 30 miles north of Kuruman to about 10 miles south of Griquatown. If the map of this part of the belt were rotated 70° anticlockwise, so that the north point lay along the present 70° bearing, regional geological comparison would become most compelling. From roughly north-northeast to south-southwest in the Hamersley Range area, and

from east to west in the northern Cape Province, the following features appear successively:

1. An older Precambrian (c.3,000 m.y. granites) floor of granitoid and steeply folded metasedimentary rocks (the Pilbara block of Western Australia; not shown on Cilliers and Genis' map, since it lies farther to the east).

2. Unmetamorphosed Precambrian sediments, somewhat older than 2,000 m.y., resting unconformably on this older floor and dipping gently off it (the Fortescue Group in a southerly direction in Western Australia; the Black Reef and Dolomite Series in a westerly direction in South Africa).

3. Conformable iron formation, with crocidolite, higher in the same sedimentary sequence, and likewise gently dipping (the Hamersley Group southerly in W.A.; the Lower Griquatown Stage westerly in S.A.).

4. A broad syncline in these rocks (Hamersley Range Synclinorium of W.A.; Dimoten and Ongeluk-Witwater Synclines of S.A.—the central plunge culmination of both these structures, along the south branch of the Fortescue River and west of Danielskuil respectively, is an interesting additional detail of the comparison).

5. Across this syncline a more tightly folded belt of the same sediments, incorporating higher sediments and volcanics (Wyloo Group of W.A.; Middle and Upper Griquatown Stages of S.A.) and re-exposing the lower sediments in anticlines (Rocklea and Milli Milli Anticlines of W.A.; Maremane Anticline of S.A.).

6. Iron formations enriched to major hematite ore bodies in the folded area (Mount Tom Price, W.A.; Sishen, S.A.).

7. Comparatively undisturbed and much younger Precambrian sediments (largely sandstones) lying unconformably over the older rocks of the folded area (Bangemall, Bresnahan, and correlated groups in the southern part of the area in W.A.; Waterberg System of the Langeberg in S.A.).

It is the synclines of point 4, above, that are important for comparison of crocidolite in the two areas. Just as significant crocidolite growth in the Dales Gorge Member of Western Australia is confined to the northern limb of the Hamersley Range Synclinorium so in the Kuruman—Danielskuil area productive mines are almost all confined to the eastern limbs of the Dimoten—Ongeluk-Witwater Synclines; Bestwell, Doornfontein, and Mimosa, the only three mines on the western limb, are now closed. The paleogeography of the depositional basin of the Griquatown Stage is not known, and regional rippling is not clearly developed, so that the existence of an early stress from the east cannot be proved; but throughout the Lower Griquatown Stage of the Kuruman—Danielskuil area there is minor folding indicative of the expected stress from the west on the eastern limb of the major syncline. Locally this stress has folded the crocidolite after its growth, as would be expected from Figure 76C.

The crocidolite occurrences at the northern and southern extremities of the outcrop of the Lower Griquatown Stage are less obviously analogous with any in Western Australia. The southernmost group of mines, between Leelykstaat and Carn Brae on Cilliers and Genis' map, lie in an area of more intense folding

probably related to its position at the termination of the belt. On present knowledge of this area it is impossible to judge confidently to what extent crocidolite distribution is related to any developmental stage of the present complex structure. On the other hand the mines in the north, Heuningsvlei and Pomfret, lie in a very gently dipping iron formation in an area whose regional structure is hidden by the overlying Kalahari sand.

In the central area, where comparison is very close, it is interesting to speculate also whether the apparently low crocidolite potential of the Asbestos Hills, east of the Ongeluk-Witwater Syncline, is not related to the different shape of this fold compared with the Dimoten Syncline, to the east of which is a belt of high regional potential. This would be analogous to the apparent regional difference in crocidolite potential between the eastern and western parts of the northern limb of the Hamersley Range Synclinorium, noted above. However that may be, the application of the stress-reversal hypothesis to the Cape Province certainly suggests that deeper continuity of crocidolite ore-bodies westwards beneath the Dimoten Syncline, at the stratigraphic level where they are now mined comparatively near the surface, cannot be expected.

Economic applications of this study

EXPLORATION

PRINCIPLES

Crocidolite is one of the easiest minerals for which to prospect in outcrop. Its distinctive blue colour and fibrous texture serve to identify it on sight, and seams, when discovered, may be assessed by simple measurement of their asbestos content without recourse to analytical laboratories. The resistance of the fibre to oxidation is such that it is one of the last minerals in its host rock to be weathered, and boulders may be carried many miles downstream from their source, and still be fresh and readily recognisable. Many of the blue asbestos deposits were originally discovered by pastoral workers or dingo trappers who had little knowledge of minerals or prospecting methods. The prospective crocidolite seeker needs physical stamina and a fondness for rock climbing rather than a profound knowledge of mineralogy.

Most blue asbestos deposits in the Hamersley Range area have been found by tracing 'floaters' (pieces broken from the outcrop and carried downhill or downstream) to the outcrop of the seam. This method is quite effective where the seam has been dissected below the limit of surface oxidation of crocidolite and during this investigation, several old prospects whose whereabouts were recorded only vaguely, were relocated by this means. On deeply weathered, undissected terrain, the method does not work so well; oxidized crocidolite is harder to recognise and much less durable than the fresh fibre. In such places, remnants of tiger's eye or griqualandite in the scree may lead to an oxidized seam, the blind outcrops of which are usually marked by an abundance of tiger's eye in the overlying duricrust.

We think it safe to state that all of the significant outcrops of fresh crocidolite in the Hamersley Range area have now been located. Further surface prospecting in deeply weathered country may find seams whose outcrops are oxidised, but such prospecting is only likely to be fruitful if directed by knowledge of the geological controls of the mineral.

In contrast to surface prospecting, exploration for blind bodies of crocidolite is difficult, and the chief tools of the exploration geologist are of little use. Crocidolite shows only subtle relationship to mappable geological structure. Geochemical methods have no application, since crocidolite and massive riebeckite

are not chemically distinguishable. There is no known geophysical method of detecting crocidolite, although some techniques could conceivably be used to assist in stratigraphic mapping. Massive riebeckite within the stratigraphically favourable zones is a useful regional guide to crocidolite, but there is no invariable relationship between the two which could serve as a direct guide to ore. Commercial deposits of blue asbestos are surrounded by a wide halo of sub-economic grade fibre which usefully indicates areas in which to confine intensive prospecting or exploration. In the Dales Gorge Member, these halos may be several miles across, but in the riebeckite zones of the Marra Mamba Iron Formation, they extend only for a few hundreds or thousands of feet from the worked deposits.

The stress-reversal hypothesis, proposed in the previous chapter to explain all of the known features relating to the growth and presence of crocidolite in the banded iron formations of the Hamersley Range area, has yet to be put to the test of predicting new deposits. By its premises, crocidolite grows in zones where the early, gravitational force acting from the north on the semi-consolidated iron formation is exactly counterbalanced by a later tectonic force from the south. It seems logical to assume that the equilibrium between the two would be attained in zones running in a direction parallel to the bisectrix of the angle between them. In fact, the forces are almost opposed and the zones of stress relief could be expected to trend at 90° to both, that is west-northwest. Evidence for such a trend is seen in the alignment of the crocidolite deposits in the Wittenoom Gorge area, where the Eastern Creek, Wittenoom and Colonial deposits lie on a line which, when extended, passes close to the old mines at Bee Gorge and Range Gorge. Other less conclusive examples of this trend are the Snell Gorge and Calamina Gorge workings in the Yampire A Horizon, the workings in Dales Gorge and the Yampire mine in the Yampire Riebeckite Zone, and the occurrences at Junction Gorge and Fortress Gorge in the Junction Gorge Riebeckite Zone. At Marra Mamba the known fibre occurrences at the eastern end of the area lie on a straight line passing through the workings on M.C.s 61 and 62, and trending about northwest.

Mapping of crocidolite deposits has shown that enrichments are often concentrated on slight changes of dip within the beds. We believe these may be the remnants of early folds or flexures which influenced the localisation of the fibre growth. Such control could be exercised in two ways: first by tensional opening of the bedding planes on the dip changes when the direction of movement was reversed, and second as a result of the rapid variation of the gravity sliding component over such a dip change, and the consequent likelihood that somewhere during this change it will exactly equal the tectonic stress, thus giving the required conditions for fibre growth.

An expected corollary of the stress-reversal hypothesis is that the favourable positions for fibre growth will occur about evenly spaced centres, and so a regular repetition of crocidolite deposits within a favourable area could be anticipated. We believe that this has been the situation in some South African mines, but in the Hamersley Range too little development has been done to determine if such a

geometric repetition exists. Certainly the Colonial, Wittenoom and Eastern Creek deposits lie at about equal distances apart, but more examples are needed to show if the relationship is valid.

EXPLORATION IN NEW AREAS

At our present state of knowledge of the geological controls of blue asbestos, we have no way of predicting whether or not an untested area of Marra Mamba or Brockman Iron Formation will contain crocidolite. However, we can say with fair confidence, that the area will have a much better chance if it is in one of the two crocidolite sub-provinces described in Chapter 7, and that any significant fibre present will be in one of the riebeckite zones defined in that chapter.

The first and vital step in appraising a new area is to examine the best available exposures of the riebeckite zones. If no fibre is found in a very short time, then the area is best disregarded. Should the preliminary inspection reveal some fibre, then more thorough prospecting is required and every accessible outcrop of the fibre-bearing horizon should be examined. Special attention should be given to places where the horizon is affected by flexures which may be earlier than the later tectonic folding: for example, monoclines which face the wrong way to the tectonic drag-folds. If commercial-grade asbestos is located during this stage of the programme, some drilling may be necessary to evaluate the deposit. This should be confined to any structure found favourable for asbestos enrichment, or if no such structure is apparent, then on a line trending approximately west-northwest through the occurrence. Even though no commercially promising fibre is found by prospecting, a widespread, consistent distribution of fibre within a horizon may indicate the presence of completely blind ore bodies which could be found by drilling. At this stage we feel that such wild-cat drilling is not warranted, there being many places where drilling could be better used to test known prospects.

EXPLORATION IN AREAS WITH KNOWN DEPOSITS

In looking for fibre in areas with known deposits, the first step should be a stratigraphic study to determine the number and relationship of the fibre horizons present. This should be followed by mapping to determine any structural relationship of the fibre, and if possible, any geometric or linear relationships shown by the occurrences. Any predictions based upon this mapping should be tested by diamond drilling. As shown in the next section, at least two holes should be drilled to test each prediction. Drillholes should be sited high enough in the stratigraphic succession to ensure that they will intersect all of the crocidolite horizons. A structural contour map is of great assistance in this, although the preparation of these can be time consuming, and we have found them of little assistance in determining structural controls of the fibre. When testing deposits in the Dales Gorge Member, drillholes are best sited in the Whaleback Shale Member to ensure that all fibre horizons are intersected without involving a large excess of drilling to reach them. Obviously local conditions of topography and

geological structure will determine the exact positions of the holes, and it may happen that it will be impracticable to drill in a spot judged to be favourable from geological or geometric considerations.

AREAS RECOMMENDED FOR FURTHER EXPLORATION

The following areas are believed to warrant further exploration if the economics of crocidolite mining improves in the future. The first two areas contain widespread crocidolite, but have yielded no economic deposits to date, a failing that may be due to remoteness and lack of thorough prospecting. Any work in them should start with regional exploration. The remaining areas all contain crocidolite deposits which have been worked or seriously considered as workable propositions. Further exploration would involve drilling.

WEELI WOLLI ANTICLINE

At the eastern end of the Weeli Wolli Anticline, the Aspinall Horizon contains widespread fibre which may be a halo around higher grade deposits. Unfortunately the Dales Gorge Member is deeply weathered in this area, and its position is often obscured by colluvium, but a few exposures of the upper part exist in the deeper creeks around the margins of the anticline. The area also contains the elusive Devan's prospect which may, from the appearance of fibre samples from it, be in a difference horizon.

DUCK CREEK

Crocidolite is known from several places within the Marra Mamba Iron Formation where this is exposed on the western end at the Jeerinah Anticline. Duck Creek and its tributaries have cut a number of gorges into the host formation, and regional scale prospecting could best be done by examining each of these. The country is largely inaccessible to vehicles.

WITTENOOM GORGE AREA

The line of fibre occurrences extending from Eastern Creek to Range Gorge is the prime target for future exploration. Most cliff exposures of the Yampire Riebeckite Zone along this line were examined during the current investigation, but in many places, drilling is the only means of testing the zone. The deposits follow the southern limb of the Garden Gorge Anticline and it must be assumed that this structure has exercised some control on the fibre enrichments. Accordingly, drillholes should be spaced along the lower hinge line of the south limb of the anticline at about 500 feet intervals so as to intersect the horizons where the beds flatten to the south. The 500 feet spacing is to ensure that at least two intersections are obtained of any reasonable-sized deposit (about 100 feet in diameter). The Garden Gorge Anticline can be traced from Dales Gorge to the east, to beyond Range Gorge to the west, and may possibly join with an anticline noted about $1\frac{1}{2}$ miles south of Mount King. However, the distance over which exploration is warranted is about 13 miles, from Calamina Gorge to a mile

or two west of Range Gorge. The eastern limit is controlled by topography; east of Calamina Gorge the favourable part of the structure influences the crocidolite horizons only where the Dales Gorge Member is preserved on high bluffs close to the Tertiary surface and where any crocidolite is likely to be oxidized. West of Range Gorge, the regional fibre content of the Dales Gorge Member is quite low, decreasing to almost nothing near Mount King. We conclude from this that Range Gorge is near the western edge of the broad halo that surrounds the deposits in the Wittenoom Gorge area, and that no exploration is justified for more than about two miles to the west of it.

YAMPIRE GORGE

Two possibilities for future exploration exist at Yampire Gorge. The more obvious one is to follow a west-northwesterly trending line both ways from the Yampire mine, testing it at intervals by drilling. Such a programme would entail a high element of risk, first because there is no geological structure to help in selecting drill sites (the anticline at the Yampire mine is a small, local structure which cannot be followed far from the vicinity of the workings), and secondly because the sizes of the likely targets, as indicated by the extent of the better fibre at the Yampire mine, are small in relation to the cost of finding them.

Another line of investigation at Yampire Gorge is suggested by the similarity of the monocline half-a-mile south of the old workings to the steep southern limb of the Garden Gorge Anticline, and the consequent possibility that it has a like influence on the position of crocidolite enrichments. On our present knowledge of the area, we feel that this possibility is worth testing by drilling. While more speculative than the first, the second prospect has the advantage that preliminary drillholes could be sited near existing roads and tracks, hence cutting drilling costs. If the early holes gave encouraging results, then the prominent monocline would provide good geological control for further sites.

The widespread fibre in the Yampire A Horizon to the north of the Yampire mine, may be part of a halo surrounding concealed enrichments. Only one enrichment is known on this horizon: on the point separating Snell Gorge and Denis Gorge, and here there are sufficient cliff exposures for the prospect to be assessed as being too small for commercial exploitation.

JUNCTION GORGE

Future exploration recommended at Junction Gorge falls logically into three phases, each successively more speculative than the last. The first and obvious project is to evaluate the known deposits at Junction Gorge, and particularly the Aspinall prospect, a venture requiring diamond drilling in the hills on either side of the gorge. The second project is a search for further enrichments in the Aspinall Horizon which is well enough exposed for careful mapping and sampling to yield information on any geometric repetition of the enrichments. The mappable geological structures are thought to be younger than the fibre, and to have no

control over its distribution but it may be significant that the two highest grade occurrences fall on a line trending west-northwest.

The third line of investigation at Junction Gorge is the most speculative, but in the long term, could be the most productive. It is to test the hypothesis that fibre enrichments in different horizons lie vertically above one another by drilling the Yampire Riebeckite Zone vertically beneath the enrichments in the Aspinall Horizon. The best way to do this would be to extend all drillholes sited to test the Aspinall Horizon down to BIF0. Australian Blue Asbestos Pty. Limited drilled one hole to test the Yampire Riebeckite Zone and found uneconomic, but still encouraging, fibre values in the Upper and Lower Seam Horizons.

MARRA MAMBA

At Marra Mamba there is scope for proving a number of small, but relatively high grade deposits within a small area. It is possible that the fibre from these deposits could be treated at one central plant owned by a company, and the actual mining done by tributors or parties of contract miners as in South Africa. The first step in exploring for fibre at Marra Mamba is to evaluate at least one of the known deposits if its size and grade are sufficient to justify the search for similar bodies. The most suitable areas for this initial work are M.C.'s 61 and 63, on both of which the Dun Seam contains 2 to 2½ inches of fibre over several hundred feet, and on each of which the seam is still carrying fibre where it dips beneath creek level. Any holes drilled to test the Dun Seam should be extended to intersect the Mackay Horizon 120 feet below. If the results of the drilling are encouraging, then exploration should be extended to other localities where the Dun Horizon is known to contain fibre, for example in the area to the west of M.C. 64.

MUNJINA GORGE

In Munjina Gorge (p. 236) the Yampire Riebeckite Zone bears fibre in several horizons where it is exposed on the steeper part of a south-facing monocline. Although no crocidolite of direct economic interest is exposed, the general abundance of crocidolite and massive riebeckite throughout the section makes the area an interesting one. This prospect is a speculative one, but could be tested cheaply by one or two holes drilled from the bed of the gorge.

EVALUATION OF DEPOSITS

In the past, evaluation of crocidolite deposits has been done by combined outcrop sampling and diamond drilling. Due to the variable fibre contents of blue asbestos seams, these methods are not entirely satisfactory, but except for expensive underground development, no better way has been devised. In this section it is proposed to discuss the methods used, the reliability that can be placed on them, and procedures of calculating ore reserves from the results.

METHODS

Outcrop sampling, usually done where the seam is exposed in a cliff face, consists of measuring the total length of fibre in the seam at selected intervals along the exposure. The sampler should select the sample intervals with due regard to the variations shown by a seam, and especially to any regular variation. For example, if an interval of 5 feet, or a multiple of 5 feet, was selected for sampling the Mahlberg Seam at Dales Gorge (p. 226), then it is possible that all readings could be zero, or all could be high, depending whether the samples fell on, or between, the regularly spaced lenses of fibre within the seam. Fortunately, such extreme variations within a seam are rare, but we recommend that in the evaluation of any continuous exposure the sampler should: (1) test the suitability of the interval employed empirically by studying the variation in grade given by progressively increasing and decreasing the interval, and (2) examine the exposure for any sign of periodicity of grade, and allow for its effects if present.

Outcrop sampling can give very detailed information on a small part of a seam, but experience has shown that the results cannot be extended far from the outcrop. We suggest that the grade obtained from outcrop sampling be extended into the deposit for no more than half the outcrop length. In many places in the Hamersley Range, to mine a seam near its outcrop would cause dangerous rockfalls from the overhead cliffs, hence any proposed mining plan would have to allow for most of the seam near the cliff-face to remain as pillars. That is, the recoverable reserves calculated from outcrop sampling would be negligible.

Early diamond drilling in the Wittenoom area using conventional rigs proved unsatisfactory, only a small part of the core being recovered. For their later drilling, Australian Blue Asbestos Pty. Limited used a Schram self-propelled drilling rig capable of being used as a percussion drill or a diamond drill. The practice they adopted was to drill the upper part of the holes with the more economical percussion method and to switch to diamond drilling a short distance above the target horizons. By using water-soluble lubricants and controlling the bit pressures, the drillers obtained nearly 100 per cent core recovery. Details of the methods used are given by Kitching (1965). Drill sites were spaced at 700 to 1,000 feet intervals apart, in a pattern as close to a rectangular grid as the topography would permit. Additional holes were drilled between the original sites when results showed them to be necessary.

RELIABILITY OF DIAMOND DRILLING RESULTS

It can be seen from the previous section that in evaluating a deposit of crocidolite, great significance is attached to individual drillholes, the assay value of each hole being used to represent up to 1 million square feet of the seam. By contrast, a perfectly exposed, reliably sampled cliff section of the seam 500 feet long would represent only about 125,000 square feet of the seam. To gain as much information as possible from each hole, A.B.A. staff made a practice of wedging holes to gain a second intersection of a seam if the first was erratically

high or low in fibre, or if its results were uncertain due to poor core recovery. In assaying a drill-core sample, six vertical lines were drawn at equal intervals around the perimeter of the core, and the length of fibre intersected on each measured. The seam assay was taken as the mean of the six measurements. The uncertainty of applying this assay to a large area of the seam is manifested by the great variation which may be shown even within the circumference of the drill core; in hole EC 3, for example, the six measurements ranged from 0.54 inches to 5.34 inches, averaging 3.42 inches of fibre.

The reliability of one drillhole intersection as an indication of the average grade of the seam is very important. One or two erratically high results may make an uneconomic deposit seem profitable, while an unlucky hole or two striking abnormally low values in a seam may cause a worthwhile prospect to be rejected. The problem is best considered in two parts. The first is to determine the likelihood that, during exploration, a payable deposit may remain undetected because a single drillhole through it intersected fibre grades below some chosen 'cut-off grade' or 'threshold grade' (i.e. the grade above which the intersection is held to be significant). The second part of the problem is to determine how well each hole drilled to evaluate a deposit indicates the average grade of the part of the seam it is assumed to represent. If we consider a drillhole intersection as a single sample chosen at random within the seam, and we know the variation shown by a large number of samples within the seam, then we can use the methods of statistical mathematics to determine the chances of our single drillhole sample being close to the average of the seam, or being erratically high or low. Obviously, no great amount of statistical data will exist for any seam being evaluated, but by using reasonable geological inferences we can apply the statistical parameters derived from a well-sampled deposit to predict the behaviour of the deposit being tested. We have chosen the ore-body on the Upper Seam of the Colonial mine as our statistical type, mainly because it is the best sampled deposit of crocidolite that we have, and because it is considered to be the type of deposit upon which any future mining venture will be based.

The 18,548 assays plotted on the plans of the Upper Seam of the Colonial mine have a normal distribution about their mean value of 3.231 inches* and a standard deviation of 0.895 inches or 28 per cent of the mean. From these parameters we can calculate the chance of any sample taken at random within the ore-body being less than some specified value. For example, the cut-off grade of the ore worked in the Colonial mine was about 2.3 inches and therefore in a drilling programme aimed at proving extensions or repetitions of the Colonial ore body, an intersection of less than 2.3 inches might be assumed to indicate uneconomic fibre. However, the chance of obtaining such an intersection within a deposit similar to the Colonial ore body is about 15 per cent or 1 in 7, so that by ignoring an intersection assaying just under 2.3 inches, the prospector would be taking a 1 in 7 chance of overlooking his target. If he chooses to ignore

* This mean of all samples differs slightly from the average grade of the ore body as calculated on page 215 because it makes no allowance for the spacing of the samples.

TABLE 26. CHANCE OF OVERLOOKING AN ORE-BODY OF AVERAGE GRADE ABOUT 3.23 INCHES BY IGNORING SINGLE ASSAYS LESS THAN SPECIFIED THRESHOLD VALUES

Threshold grade (inches)	Probability (as a percentage)	Probability (as a fraction)
0.50	0.11	1 chance in 1,000
0.75	0.28	1 chance in 360
1.00	0.62	1 chance in 160
1.25	1.32	1 chance in 75
1.50	2.62	1 chance in 40
1.75	4.95	1 chance in 20
2.00	8.38	1 chance in 12
2.25	16.35	1 chance in 6
2.50	23.27	1 chance in 4

only intersections of less than 1.5 inches, his chance of missing a deposit is about 1 in 40, and of less than 1 inch, 1 in 160. Table 26 lists the probabilities of obtaining assays of less than specified values from 0.5 to 2.5 inches. The pros-

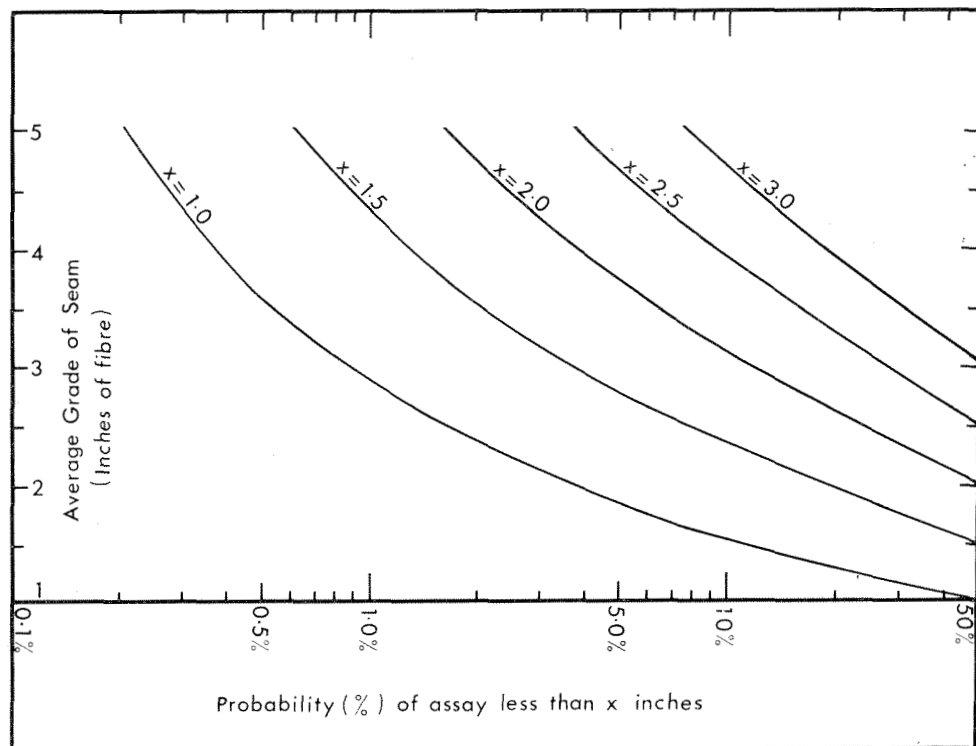


Figure 79. Curves showing the chance of one drillhole intersecting a value of less than some specified threshold grade in any seam averaging between 2 and 5 inches of crocidolite.

pector must select the risk he is prepared to take of missing a prospect, and select his threshold grade accordingly. If he is prepared to take a high risk, he may overlook an ore body, but if he accepts little risk, he will almost certainly be committed to an excessive amount of drilling to check comparatively low-grade intersections.

Table 26 applies only to crocidolite deposits of the same average grade as the Upper Seam ore body in the Colonial mine. It is unlikely that a second deposit would have exactly this grade, but by assuming that the fibre content of any target deposit will have about the same standard deviation (expressed as a percentage of the mean), it is possible to draw the probability curves shown in Figure 79. These curves show the chances of intersecting a value (x) of less than some specified threshold grade, in any seam averaging between 2 and 5 inches of fibre. For example, in a deposit whose average grade is 4 inches of fibre, the chance of getting an intersection of 1.5 inches or less is 1.2 per cent, or about 1 in 85.

In practice the prospector would have to decide the lowest grade he is prepared to work in a deposit, and then use the curves to decide whether any drillhole intersection has a reasonable chance of being within an ore body of this grade. The definition of 'reasonable chance' will depend upon the inherent optimism of the prospector. The rule of multiplication of chances will apply in drilling for crocidolite deposits. If there is 1 chance in 10 that a drillhole intersection will pass through an ore body without recording a significant assay, then the chances of two holes doing this are 1 in 100, and of three holes, 1 in 1,000, and so on.

The problem of determining the reliance that can be placed on drillholes in evaluating an orebody is more complex. We are not simply drawing a line between payable and unpayable deposits as in exploration work, but are trying to determine fairly exact tonnages and grades for separate sections of the deposit. The histograms in Figure 64 show that the standard deviations of samples in small (90,000 to 160,000 square feet) parts of the Upper Seam in the Colonial mine average about 20 per cent. If we apply this figure to the ore body being assessed, it can be shown that each drillhole has one chance in three of being more than 20 per cent in error from the true average of the seam in its vicinity, one chance in seven of being more than 30 per cent in error, and one chance in 20 of being more than 40 per cent out. It therefore seems hazardous to use the results of one drillhole to calculate the tonnage and grade of a part of the seam. Instead, a method should be used which averages the results of several neighbouring drillholes to calculate the grade of each block. If the holes are spaced on a strict grid, then the grade of each grid square could be taken as the average of the intersections at the four corners. If the hole spacings are irregular, then the best method is to divide the area of the deposit into triangles with a hole at each apex, and to assume the grade of each block to be the average of the three intersections at its corners. Care should be taken to arrange the triangles so as not to include in each more than one sample which seems to be erratically high or low.

TABLE 27. ESTIMATED WESTERN AUSTRALIAN CROCIDOLITE RESERVES AND RESOURCES

Locality	Prospect	Seam	Indicated Reserves		Inferred Reserves		Resources	
			Tons	Grade	Tons	Grade	Tons	Grade
Wittenoom Gorge	Eastern Creek	Upper	225,000	2·8"				
	Area in general	Upper					500,000	1·5"
	Area in general	Upper					300,000	2·0"
	Area in general	Lower					600,000	1·5"
Yampire Gorge	Yampire mine	Yampire C	50,000	1·3"				
	Yampire mine	Upper Seam	50,000	1·6"				
	Yampire mine	Lower Seam	40,000	2·0"				
	Yampire mine	Yampire C plus Upper Seam			10,000	3·5"		
	Snell Gorge	Yampire A					300,000	1·5"
Dales Gorge	West end	Mahlberg					25,000	1·0"
	East end	Main Bottom Seam					90,000	1·0"
Junction Gorge	Aspinall prospect	Aspinall Seam			7,000	2·5"		
	A.B.A. prospect	Aspinall Seam			2,500	1·6"		
	Area in general	Aspinall Seam					250,000	1·0"
Marra Mamba	M.C. 61	Dun Seam			13,500	2·0"		
	M.C. 63	Dun Seam			12,000	2·0"		
Totals			365,000		45,000		2,000,000 (approx.)	

CROCIDOLITE RESOURCES

At present, reserves of crocidolite blocked out and proven by accepted mining standards are negligible, amounting to only a probable few thousand tons blocked out on two or three sides in the lower levels of the Colonial mine, and perhaps a few hundred tons blocked out at Yampire Gorge. For technical reasons, it is unlikely that any of this material will be mined. The most reliable information we have on crocidolite reserves are the results of the diamond drilling and close-spaced cliff-sampling done at Eastern Creek and Yampire Gorge. By Australian convention, reserves calculated from such information are classed as *indicated*, and have been shown as such in Table 27. *Inferred* reserves shown in the Table were calculated from cliff exposures which have been mapped and sampled in some detail, but for which there are no supporting drillhole results. Seams cropping out in adjacent gorges were assumed to continue through the intervening ground and the width of the body was taken to be the average of the exposed diameters. Seams exposed in only one gorge were assumed to extend back into the cliff face for one half the distance of the exposed length. Similar principles were used to estimate the crocidolite *resources* of the third column, but the basic information used was derived from regional mapping with relatively few cliff assays and, at Wittenoom, a few diamond drillhole intersections. The main distinction between the three listed categories is that the indicated and inferred reserves are conceivably mineable in the present economic and technological era, but the resources are likely to be exploited only if there is a marked improvement in future mining methods, or if there is a radical change in the economic climate, such as would be produced by national emergency.

Glossary

This glossary includes (1) terms which have been introduced, either in this Bulletin or in preliminary publications, to denote features for which no term existed previously, and (2) terms which have been used in differing senses or forms in the published literature of iron formation; we record our preferred or restricted usage of these. Stratigraphic names are not included here, as they are adequately indexed.

BIF A convenient abbreviation for banded iron formation (q.v.). We prefer this form to b.i.f. or other variants.

B.I.Q. An abbreviation of 'banded ironstone quartzite'; this term was applied by Australian Blue Asbestos Pty. Limited geologists to chert-siderite (q.v.).

Band A discrete stratum with some distinctive features; a band may be a micro-band, a mesoband, a macroband (q.v.), or some other restricted stratigraphic division. It is used in isolation only where its application is unlikely to be misunderstood.

Banded iron formation Iron formation (q.v.) consisting of successive thin layers (mesobands) of fine-grained quartz, iron oxides, carbonates, and silicates in various proportions. See 'Nomenclature', on pages 25 to 27.

Calamina cyclothem A common cyclic sequence of mesoband types in BIF macrobands of the Dales Gorge Member, in which either a single thick chert mesoband with fine microbanding, or a group of such cherts separated by thin magnetite mesobands, alternates repeatedly at regular intervals with a mixed mesoband group of chert-matrix, magnetite, and comparatively thin and coarsely microbanded cherts. These two parts of the cyclothem are referred to as the chert-magnetite group and the mixed group.

Chert Traditionally and strictly chalcedonic silica. Here applied to the compact quartz mosaic of average grain diameter 10 to 30 microns which forms the main groundmass material for most mesoband types in iron formations of the Hamersley Group. Note that *a* chert means a chert *mesoband*.

Chert-magnetite group See Calamina cyclothem.

Chert-matrix Fine-grained dark and relatively iron-rich material separating chert mesobands and surrounding chert pods; so named because it forms the matrix within which chert occurs. The chert-matrix of the Dales Gorge Member was formerly (Trendall, 1965a) called QIO, but the name is here changed so that it may be generally applied to all iron formations of the Hamersley Group. See also page 108.

Chert-siderite A variety of iron formation in which chert mesobands with a characteristic type of microbanding (Figure 22) are scattered within a finely banded matrix of fine-grained siderite (Figure 29C). It occurs typically in the Whaleback Shale Member, and in the S macrobands (q.v.) of the Dales Gorge Member, in the Brockman Iron Formation.

Crocidolite Asbestiform riebeckite of the cross-fibre (q.v.) type suitable for commercial exploitation. Separate fibres of riebeckite within a chert, or other matrix material, should be called fibrous riebeckite, not crocidolite, on grounds of both etymology and first application; we prefer also to exclude the distinctive *slip-fibre* (q.v.) from this name.

Crocidolite horizon See Horizon.

Cross-fibre Asbestiform riebeckite in bands in which the fibre length is sub-parallel to the thickness of the band is known as cross-fibre; it is a synonym for the mined crocidolite, or blue asbestos. The name distinguishes it from slip-fibre and mass-fibre (q.v.).

Cross-podding A locally restricted oblique arrangement either of chert pods with banded iron formation or of microbands with a chert pod. In either case there is a structural resemblance in transverse section to foreset beds of cross-bedding; hence the name. First described by Trendall (1966a, p. 79) in association with duplicate corrugations (q.v.) in the lower part of the Dales Gorge Member at Dales Gorge. The appearance in section is related to the existence of one or more ribbon-like chert mesobands tilted obliquely to the general stratification of

the enclosing iron formation about their long axes, and pinched out along both edges.

Cross-podding ridge A linear ridge on an exposed bedding surface of iron formation caused by the existence a few inches below of cross-podding.

Duplicate corrugations Rectilinear, sub-parallel, open sinusoidal undulations of bedding surfaces in the lower part of the Dales Gorge Member at Dales Gorge were called duplicate corrugations by Trendall (1966a, p. 79). See also p. 162.

Duplicate structure Trendall (1966a, p.78) applied the general term duplicate structure to several closely related structures displayed in the lower part of the Dales Gorge Member at Dales Gorge; their common characteristic is precise and regular repetition (duplication) at small horizontal intervals. Trendall's definition embraced duplicate corrugations, cross-podding, riebeckite swells (q.v.), and various associated minor structures.

Fibrous quartz Many thin quartz mesobands associated with crocidolite, or in areas where crocidolite occurs, often have a fibrous appearance in hand specimen, and can easily be mistaken for cross-fibre or slip-fibre; hence the synonym quartz fibre. In fact such quartz is quite coarsely crystalline.

Flat-modified chert A term introduced by Trendall (1965a) for thick and finely microbanded chert mesobands with, by implication, certain other typical characteristics. Not recommended for continued use; see p. 51 and 60 for further discussion.

Horizon (=Crocidolite horizon) A restricted stratigraphic interval within which crocidolite is known to occur locally; a horizon may, in different places within one area, contain either no crocidolite at all, one or more seams (q.v.), or traces of crocidolite of no commercial interest.

Immaculate band A chert-magnetite group (q.v.) which is not maculate, and consequently not a maculate band (q.v.).

Iron formation Chemical sedimentary rock with a high iron content. See also 'Nomenclature', pages 25 to 27.

Ironstone This term has two distinct usages in geological literature. In South Africa (du Toit, 1954) it is roughly synonymous with banded iron formation. In America (James, 1966) it means the mainly Mesozoic, 'minette', often chamositic, iron-rich sediments, as distinct from the Precambrian banded iron formation. It is not used in this bulletin.

Jasper Red chert, particularly where the colour is not due to very recent surface weathering.

Jaspilite A rock with alternating thin bands of jasper and some other material, usually either black iron oxides or chert of another colour.

Kinking Small, sharp, zig-zag puckering in crocidolite.

Knox cyclothem A cyclic sequence of mesoband types present in the Joffre Member, in which a group of red chert mesobands in chert-matrix alternate with one or more white cherts in chert-matrix; the red cherts are more finely and clearly microbanded than the white cherts.

Lower riebeckite zone Used by Trendall (1965a) for what is called in this bulletin the Yampire Riebeckite Zone. See also Riebeckite Zone.

Macroband The Dales Gorge Member is subdivided into 33 numbered macrobands, which are lithologically distinct stratigraphic units between about 2 and 50 feet thick. Macrobands BIF0 to BIF16, which are composed of banded iron formation, alternate with macrobands S1 and S16 so that BIF1 lies immediately above S1, and so on. The S macrobands consist of shale and chert-siderite facies. The term was introduced by Trendall (1965a); see also Trendall and Blockley (1968), p. 43, and Figure 4.

Maculate band A chert-magnetite group (q.v.) with more or less abundant macules (q.v.). Introduced by Trendall (1966a) to describe four maculate bands, which were called MB1-4, in the BIF1 macroband of the Dales Gorge Member at Dales Gorge.

Macule A term introduced by Trendall (1966a) for a nodule-like thickening of a group of mesobands; spectacularly displayed at Dales Gorge and fully described in the reference cited; see also p. 160 to 162.

Mass-fibre See massive riebeckite.

Massive riebeckite The greater part of the riebeckite which occurs in iron formations of the Hamersley Group does so as thick blue mesobands (q.v.) which consist almost wholly of a randomly felted mass of interlocking fibres of riebeckite. This material is called massive riebeckite; mass-fibre riebeckite, a term which we prefer not to use, has in the past been used synonymously, and miners refer to it simply as riebeckite.

Mesoband Almost all iron formation in the Hamersley Group has, on the hand specimen scale, a conspicuous alternation of differently coloured bands or strata, whose internal variations of composition and texture are negligible compared with their differences in these respects from their immediate neighbours. Such bands are mesobands; they are well displayed by Figures 5 and 6. The term was introduced by Trendall (1965a).

Microband Microbands are regularly repeated laminae of even thickness within chert mesobands of Hamersley Group iron formation. The lamination is normally defined by varying content of some iron-bearing mineral within the chert; an iron-poor and an iron-rich lamina together constitute a single microband. In this exact sense the term was introduced by Trendall (1965a); previous usages by Genis (1961, p.67), Sitler (1963), Gross (1964), and Chakraborty (1966), are now known to us in different senses, but there seems little danger of confusion.

Mixed group See Calamina cyclothem.

n The theoretical number of microbands in a microbanded chert mesoband; obtained by dividing T by t (q.v.), and accepting the nearest whole number. For most cherts the accuracy is about ± 5 per cent.

Needle riebeckite A textural variety of riebeckite occurrence in which scattered needles lie in the otherwise normal chert of a mesoband; contrasted with massive riebeckite (q.v.), cross-fibre (q.v.) and slip-fibre (q.v.). See Figure 30A.

Northeast structure Any one of a number of related structures in the central part of the Hamersley Range area whose common characteristic is a northeasterly trend; includes duplicate structures and cross-podding (q.v.).

Percival texture A textural arrangement of hematite characteristic of many red cherts. Within chert which is generally cloudy with fine-grained hematite 'dust' are scattered blebs or octahedra of iron oxide (possibly hematite, maghemite, or magnetite in different cherts) surrounded by a halo of clear quartz, sometimes spherulitic. The haloes have a usual diameter of about 50 microns, and are often abundantly distributed to give a distinctively speckled appearance in thin-section.

Pinch-and-swirl An alternative name for podding of any type in chert mesobands.

Pod An apparently discontinuous body of chert within iron formation. See Chapter 6 for fuller discussion and related terms.

Primitive chert A term proposed by Trendall (1965a) for chert mesobands in the Dales Gorge Member which have relatively coarse microbanding defined mainly by ankerite; the name implied that it represented an early stage in a continuous diagenetic sequence. Abandoned in this bulletin; see p. 51 and 60.

QIO See *quartz-iron oxide*.

Quartz fibre See fibrous quartz.

Quartz-iron oxide (QIO) A term proposed by Trendall (1965a) for the enclosing material of podded cherts in the Dales Gorge Member. Now replaced by *chert-matrix* (q.v.) as a more general term for use throughout the Hamersley Group.

Random podding Chert pods with no preferred elongation in their areal shapes or distribution. See Figure 38B.

Reef The term used in South African crocidolite mining to denote what we refer to as a seam (q.v.).

Regional rippling A crenulation of bedding surfaces of iron formation in the northern part of the Hamersley Range area. It resembles sedimentary ripple mark and is often parallel to the axial direction of the regional folds; hence the name.

Riebeckite Apart from its standard usage as a mineral name the word is used by miners to refer specifically to massive riebeckite (q.v.).

Riebeckite swells Parallel elongate ribbons of massive riebeckite duplicated laterally at 5-foot intervals at Dales Gorge; they represent thicker stratigraphic equivalents of adjacent and intervening chert-magnetite groups of a particular Calamina cyclothem. Term proposed by Trendall (1966a, p.79) and illustrated here in Figures 53 and 54. They are northeast and duplicate structures (q.v.).

Riebeckite zone A restricted stratigraphic level of iron formation within which riebeckite of any kind is liable to be locally abundant. See p. 176.

Riebeckite-prone chert The chert-magnetite group of a specific Calamina cyclothem (q.v.) which is often represented by massive riebeckite. See p. 178.

S macroband Any one of the 16 macrobands of shale and chert-siderite which separate the 17 BIF macrobands of the Dales Gorge Member.

Seam If a horizon locally contains enough crocidolite to be potentially mineable it is, at that locality, a crocidolite seam.

"Shale" Used by Trendall (1965a) to refer to the S macrobands and their constituent mixture of shale and chert-siderite; now abandoned.

Shale Refers in this Bulletin either to those parts of S macrobands which consist largely of sheet silicates, or, as a stratigraphic term, to formations which have a high proportion of sheet silicate-rich material.

Slip-fibre Asbestiform riebeckite in which the fibres lie at a low angle to the banding of the host iron formation.

Striped facies A lithological variety of iron formation confined to the Weeli Wolli Formation, characterized by a very regular and even striping defined by variations in depth of colour 2 to 5 mm thick. It appears shaly and fissile when weathered.

Swells The chert-magnetite group of some Calamina cyclothems at Dales Gorge thins and thickens laterally so that the lines of greatest thickness lie in the bedding in a north-east direction and 5 feet apart. These thickest parts are usually massive riebeckite, and are riebeckite swells (q.v.); but in places they remain as chert, and are simply swells, or duplicate swells.

T, t T is the total thickness of a chert mesoband, measured in millimetres by dividers to an accuracy of ± 0.2 mm. t is the microband interval of a microbanded chert mesoband, measured by spanning a divider over 10 microbands, if available, to a resultant accuracy of ± 0.02 mm; the accuracy is less if less than 10 microbands are available in the mesoband.

Upper riebeckite zone Used by Trendall (1965a) for what is called in this bulletin the Junction Gorge Riebeckite Zone. See also Riebeckite zone.

Wavy bedding A term used in the Lake Superior area for granule iron formation with irregularly undulating banding (e.g. Aldrich, 1929, Figures 22-4). Used by Ryan and Blockley (1965) to describe coarse podding in Hamersley Group iron formations.

Zone Used only in the combined form 'Riebeckite Zone' (q.v.) in this Bulletin. *Not* equivalent to South African stratigraphic usage.

List of unpublished plans

The following maps and plans relevant to crocidolite are held by the Western Australian Mines Department in Perth, and are listed here for the convenience of persons concerned with future crocidolite exploration.

Held by	Locality	Title or content	Scale	Availability	Ref. No.	Remarks
G.S. *	Regional	Geological map of the Hamersley Asbestos Deposits	10 miles to 1 inch	Transparency	G.S. 8596	Compiled February 1965
G.S.	Regional	Geological map of the Hamersley Asbestos Deposits	10 miles to 1 inch	Transparency	G.S. 9060	Revised December 1966
G.S.	Wittenoom Area	Wittenoom area geological map (Six sheets plus legend)	50 chns to 1 inch	Transparencies		Consists of linephoto compilations with geological boundaries. Covers a greater area than Plate 5
D.B. †	Wittenoom Area	Joffre	1 : 50,000	Published		Topographic map with mineral leases
D.B.	Wittenoom Area	Mulga Downs	1 : 50,000	Published		Topographic map with mineral leases
D.B.	Wittenoom Area	Mount Frederick	1 : 50,000	Published		Topographic map with mineral leases
D.B.	Wittenoom Area	Mount King	1 : 50,000	Published		Topographic map with mineral leases
G.S.	Wittenoom Gorge	General Plan	400 ft to 1 inch	Dyeline		Australian Blue Asbestos Pty. Limited plan
G.S.	Wittenoom Gorge	Diamond drillhole localities Wittenoom Gorge	800 ft to 1 inch	Transparency	9767	General base map completed from A.B.A. plans
G.S.	Wittenoom Gorge	Colonial mine : assay plans of Upper Seam (6 sheets)	60 ft to 1 inch	Dyelines		A.B.A. plans
G.S.	Wittenoom Gorge	Colonial mine : assay plans of Lower Seam (6 sheets)	60 ft to 1 inch	Dyelines		A.B.A. plans
G.S.	Wittenoom Gorge	Colonial mine : averaged assays of Upper Seam (2 sheets)	100 ft to 1 inch	Transparency		
G.S.	Wittenoom Gorge	Colonial mine : plan of Upper Seam	100 ft to 1 inch	Dyeline		A.B.A. plan
G.S.	Wittenoom Gorge	Colonial mine : averaged assays of Lower Seam	100 ft to 1 inch	Transparency		

D.B.	Wittenoom Gorge	Colonial mine : plan of Upper Seam workings (2 sheets)	60 ft to 1 inch	Transparencies		A.B.A. plan
D.B.	Wittenoom Gorge	Colonial mine : plan of Lower Seam workings (2 sheets)	60 ft to 1 inch	Transparencies		A.B.A. plan
G.S.	Wittenoom Gorge	Wittenoom mine : assay plan of Upper Seam (4 sheets)	60 ft to 1 inch	Dyeline		A.B.A. plan
G.S.	Wittenoom Gorge	Wittenoom mine : assay plan of Lower Seam (5 sheets)	60 ft to 1 inch	Dyeline		A.B.A. plan
G.S.	Wittenoom Gorge	Wittenoom mine : mine plan of Upper Seam	80 ft to 1 inch	Dyeline		A.B.A. plan
G.S.	Wittenoom Gorge	Eastern Creek Deposit	400 ft to 1 inch	Dyeline		A.B.A. plan with drillholes and fibre isopleths
G.S.	Yampire Gorge	Diamond drillhole locations : Calamina Gorge—Yampire Gorge	20 chns to 1 inch	Transparency		Traced from A.B.A. plan
G.S.	Yampire Gorge	Sample locations	20 chns to 1 inch	Dyeline		A.B.A. plan showing locations of samples listed on file M51
G.S.	Yampire Gorge	Fibre assays in vicinity of old workings	60 ft to 1 inch	Dyeline		A.B.A. plan
G.S.	Yampire Gorge	Assay plan of Snells (Gorge) workings	500 ft to 1 inch	Dyeline		A.B.A. plan
G.S.	Junction Gorge area	Geological map : Junction and Fortress Gorges	50 chns to 1 inch	Transparency	G.S. 9062	
G.S.	Lamb Creek	Geological map	50 chns to 1 inch	Transparency	G.S. 9139	
G.S.	Marra Mamba	Geological map : Marra Mamba crocidolite area (3 sheets)	20 chns to 1 inch	Transparencies	9140, 9141 & 9142	Contains more detail than Plate 11
G.S.	Marra Mamba	Structural contour map : mineral claims 61 ^{WP} and 62 ^{WP} , Marra Mamba crocidolite area	300 ft to 1 inch	Published	9562	In Blockley, 1967
G.S.	Kungarra Gorge	Geological map : Vivash Gorge—Horse-shoe Creek area	50 chns to 1 inch	Transparency		
G.S.	Kungarra Gorge	Plan of fibre outcrop at Mt. Wall	100 ft to 1 inch	Dyeline		A.B.A. plan
G.S.	Kungarra Gorge	Fibre sections at Mt. Wall area	1 ft to 1 inch	Dyeline		A.B.A. plan

* G.S.—Geological Survey Office.

† D.B.—Drafting Branch

References

- Aldrich, H. R., 1929, The geology of the Gogebic Iron Range of Wisconsin: Wisconsin Geol. Nat. History Survey Bull. 71, 279 p.
- Alexandrov, E. A., 1955, Contribution to studies of origin of Precambrian banded iron ores: Econ. Geology, v. 50, p. 459-468.
- Anderson, R. Y., 1966, Varve calibration of stratification: Kansas State Geol. Survey, Bull. 169, v. 1, p. 1-20.
- Anderson, R. Y., and Kirkland, D. W., 1966, Intrabasin varve correlation: Geol. Soc. America Bull. v. 77, p. 241-256.
- Behrend, F., 1936, Eisen und Schwafel Forende Gasquellen aus den Kameni Inseln, in Santoren der Werdegang eines Insel vulkans und sein Ausbruch, 1925-1928; by Hans Reck, v. 2, Berlin.
- Bernal, J. D., Dasgupta, D. R., and Mackay, A. L., 1959, The oxides and hydroxides of iron and their structural inter-relationships: Clay Minerals Bull. v. 4, p. 15.
- Blockley, J. G., 1967, The crocidolite deposits of Marra Mamba, West Pilbara Goldfield: West. Australia Geol. Survey Ann. Rept. 1966, p. 71-73.
- Borchert, H., 1960, Genesis of marine sedimentary iron ore: Inst. Mining and Metall. Bull. 640, p. 261-279.
- Bott, M. H. P., 1964, Formation of sedimentary basins by ductile flow of isostatic origin in the upper mantle: Nature, v. 201, p. 1082-4.
- Bott, M. H. P., and Johnson, G. A. L., 1967, The controlling mechanism of Carboniferous cyclic sedimentation: Geol. Soc. London Quart. Jour. v. 122, p. 421-436.
- Bramlette, M. N., 1946, The Monterey formation of California and the origin of its siliceous rocks: U.S. Geol. Survey Prof. Paper 212, 57 p.
- Butuzova, G. Y., 1966, Iron ore sediments of the fumarole field of Santorin volcano, their composition and origin: Akad. Nauk SSSR Dokl. v. 168, p. 215-217.
- Chakraborty, K. L., 1966, Ferromagnesian silicate minerals in the metamorphosed iron-formation of Wabush Lake and adjacent areas, Newfoundland and Quebec: Canada Geol. Survey Bull. 143, 34 p.
- Cilliers, J. J. le R., and Genis, J. H., 1964, Crocidolite asbestos in the Cape Province, in The geology of some ore deposits of southern Africa v. II: Geol. Soc. South Africa, p. 543-570.
- Cohee, G. V., and Landes, K. K., 1958, Oil in the Michigan basin, in Habitat of oil, edited by L. G. Weeks: Tulsa, Am. Assoc. Petroleum Geologists, p. 473-493.
- Compston, W., and Arriens, P. A., 1968, The Precambrian geochronology of Australia: Canadian Jour. of Earth Sciences, v. 5, p. 561-583.
- Cullen, D. J., 1963, Tectonic implications of banded ironstone formations: Jour. Sed. Petrology, v. 33, p. 387-392.
- Dallmus, K. F., 1958, Mechanics of basin evolution and its relation to the habitat of oil in the basin, in Habitat of oil, edited by L. G. Weeks: Tulsa, Am. Assoc. Petroleum Geologists, p. 883-931.
- Daniels, J. L., 1966, The Proterozoic geology of the North-West Division of Western Australia: Australasian Inst. Mining Metall. Proc. 219, p. 17-26.

- Daniels, J. L., 1967, Explanatory notes on the Turee Creek 1:250,000 geological sheet, Western Australia: West. Australia Geol. Survey Rec. 1967/7 (unpublished).
- Daniels, J. L., and Halligan, R., 1968, Explanatory notes on the Wyloo 1:250,000 geological sheet: West. Australia Geol. Survey Rec. 1968/9 (unpublished).
- Daniels, J. L., and MacLeod, W. N., 1965, Newman, Western Australia: West. Australia Geol. Survey 1:250,000 Geol. Series Explan. Notes, 24 p.
- de la Hunty, L. E., 1964, Balfour Downs, W.A.: West. Australia Geol. Survey 1:250,000 Geol. Series Explan. Notes, 23 p.
- 1965, Mount Bruce, Western Australia: West. Australia Geol. Survey, 1:250,000 Geol. Series Explan. Notes, 28 p.
- de Sitter, L. U., 1956, Structural geology: London, McGraw-Hill, 552 p.
- du Toit, A. L., 1946, The origin of the amphibole asbestos deposits of South Africa: South Africa Geol. Soc. Trans., v. 48, p. 161-206.
- 1954, Geology of South Africa: Edinburgh, Oliver and Boyd, 611 p.
- Edgell, H. S., 1964, Precambrian fossils from the Hamersley Range, Western Australia, and their use in stratigraphic correlation: Geol. Soc. Australia Jour. v. 11, p. 235-261.
- Ellis, H. A., 1939, The geology of the Yilgarn Goldfield, south of the great eastern railway: West. Australia Geol. Survey Bull. 97.
- Ernst, W. G., 1962, Synthesis, stability relations, and occurrence of riebeckite and riebeckite-arfvedsonite solid solutions: Jour. Geology, v. 70, p. 689-736.
- Eugster, H. P., 1967, Hydrous sodium silicates from Lake Magadi, Kenya: precursors of bedded chert: Science, 157, p. 1177-1180.
- Feldtmann, F. R., 1921, The geology and mineral resources of the Yalgoo Goldfield. Pt. 1, The Warriedar gold-mining centre: West. Australia Geol. Survey Bull. 81.
- Finucane, K. J., 1939, The blue asbestos deposits of the Hamersley Ranges, Western Australia: Aerial Geol. Geophys. Survey North Australia Rept. West. Australia 49, 15 p.
- 1964, The blue asbestos deposits of the Hamersley Ranges: Australasian Inst. Mining Metall. Proc. 211, p. 75-84.
- 1965, Blue asbestos deposits of the Hamersley Ranges: Commonwealth Mining Metall. Australia and New Zealand Cong., 8th Pub. v. 1, p. 156-159.
- Forman, F. G., 1938, The Yampire Gorge crocidolite deposits, Hamersley Range, North-West Division: West. Australia Geol. Survey Ann. Rept. 1937, p. 8-9.
- Foxall, J. S., 1939, Report on Hamersley Range blue asbestos: West. Australia Mines Dept. Ann. Rept. 1938, p. 57.
- 1942, The blue asbestos deposits of the Hamersley Range and their economic importance: West. Australia Geol. Survey Bull. 100, Part II, p. 38-53 (this bulletin includes Forman, 1938 and Foxall, 1939, as Appendices).
- Friedman, G. M., 1959, Identification of carbonate minerals by staining methods: Jour. Sed. Petrology, v. 29, p. 87-97.
- Genis, J. H., 1961, The genesis of the blue amphibole asbestos of the Union of South Africa: University of Cape Town, Ph.D. thesis (unpublished), 146 p.
- Geological Society of Australia, 1964, Australian code of stratigraphic nomenclature: Geol. Soc. Australia Jour., v. 11, p. 165-171.
- Govett, G. J. S., 1966, Origin of banded iron formations: Geo. Soc. America Bull. v. 77, p. 1191-1212.
- Gregory, A. C., and Gregory, F. T., 1884, Journals of Australian Explorations: Brisbane, Govt. Pr.
- Gross, G. A., 1964, Primary features in cherty iron formation: Int. Geol. Congress XXII, Abstract, p. 73.
- 1965, Geology of iron deposits in Canada. Vol. 1, General geology and evaluation of iron deposits: Canada Geol. Survey Econ. Geology Rept. 22, 181 p.

- Grubb, P. L. C., 1967, Asbestos: C.S.I.R.O. Division of Applied Mineralogy Ann. Rept. 1966-67, p. 6.
- Gruner, J. W., 1922, The origin of sedimentary iron formations, the Biwabik formation of the Mesabi Range: *Econ. Geology*, v. 17, p. 407-460.
- 1944, The composition and structure of minnesotaite, a common iron silicate in iron-formations: *Am. Mineralogist*, v. 29, p. 363-372.
- Hall, A. L., 1918, Asbestos in the Union of South Africa: *South Africa Geol. Survey Mem.* 12, 152 p.
- 1930, Asbestos in the Union of South Africa: *South Africa Geol. Survey Mem.* 12, 2nd ed., 324 p.
- Halligan, R., and Daniels, J. L., 1964, Precambrian geology of the Ashburton Valley region, North-West Division: *West. Australia Geol. Survey Ann. Rept.* 1963, p. 38-46.
- Hodgson, A. A., 1965a, Fibrous silicates: *Royal Institute of Chemistry Lecture Series*.
- 1965b, The thermal decomposition of miscellaneous crocidolites: *Mineralog. Mag.*, v. 35, p. 291-305.
- Holmes, A., 1945, *Principles of physical geology*: London, Thomas Nelson & Sons, 532 p.
- Hudson, J. D., 1964, Sedimentation rates in relation to the Phanerozoic time-scale, p. 37-42: *Geol. Soc. London Quart. Jour.* v. 120S, 458 p.
- James, H. L., 1954, Sedimentary facies of iron-formation: *Econ. Geology*, v. 49, p. 235-291.
- 1966, Data of geochemistry, 6th Edition. *Chemistry of the iron-rich sedimentary rocks*: U.S. Geol. Survey Prof. Paper 440-W, 61 p.
- Keats, A. L., 1965, Mining and processing of industrial minerals: *Commonwealth Mining Metall. Australia New Zealand*, 8th, Pub. v. 3, p. 341-367.
- Kitching, J., 1965, Major advance in drilling technique reported from Wittenoom Gorge: *Mining and Chem. Eng. Review*, v. 57, no. 2, p. 11-13.
- Kriewaldt, M. J. B., 1964, Dampier and Barrow Island, Western Australia: *West. Australia Geol. Survey 1:250,000 Geol. Series Explan. Notes*, 24 p.
- Kriewaldt, M. J. B., and Ryan, G. R., 1967, Pyramid, Western Australia: *West. Australia Geol. Survey 1:250,000 Geol. Series Explan. Notes*, 39 p.
- Kuenen, P. H., 1950, *Marine geology*: New York, John Wiley, 568 p.
- LaBerge, G. L., 1966a, Altered pyroclastic rocks in iron-formation in the Hamersley Range, Western Australia: *Econ. Geology*, v. 61, p. 147-161.
- 1966b, Altered pyroclastic rocks in South African iron-formation: *Econ. Geology* v. 61, p. 572-581.
- 1967, Microfossils and Precambrian iron-formations: *Geol. Soc. America Bull.* v. 78, p. 331-342.
- Leggo, P. J., Compston, W., and Trendall, A. F., 1965, Radiometric ages of some Precambrian rocks from the Northwest Division of Western Australia: *Geol. Soc. Australia Jour.*, v. 12 p. 53-66.
- Lepp, H., and Goldich, S. A., 1964, Origin of the Precambrian iron formations: *Econ. Geology* v. 59, p. 1025-1060.
- Low, G. H., 1965, Port Hedland, Western Australia: *West. Australia Geol. Survey 1:250,000 Geol. Series Explan. Notes*.
- MacLeod, W. N., 1966, The geology and iron deposits of the Hamersley Range area, Western Australia: *West. Australia Geol. Survey Bull.* 117.
- MacLeod, W. N., de la Hunty, L. E., Jones, W. R., and Halligan, R., 1963, A preliminary report on the Hamersley Iron Province, North-West Division: *West. Australia Geol. Survey Ann. Rept.* 1962, p. 44-54.
- MacLeod, W. N., and de la Hunty, L. E., 1966, Roy Hill, Western Australia: *West. Australia Geol. Survey 1:250,000 Geol. Series Explan. Notes*, 27 p.
- McNulty, J. C., 1968, Asbestos mining Wittenoom, Western Australia: *Proc. First Australian Pneumoconiosis Conference* 1968.

- Miles, K. R., 1942, The blue asbestos bearing banded iron formations of the Hamersley Ranges, Western Australia: West. Australia Geol. Survey Bull. 100, Part I, p. 1-37. (This bulletin includes Forman, 1938, and Foxall, 1939, as Appendices.)
- Miller, A. R., Densmore, C. D., Degens, E. T., Hathaway, J. C., Manheim, F. T., McFarlin, P. F., Pocklington, R., and Jokela A., 1966, Hot brines and recent iron deposits in deeps of the Red Sea: *Geochim. et Cosmochim. Acta* v. 30, p. 341-359.
- Moroney, M. J., 1965, *Facts from figures*: London, Penguin Books, 3rd ed.
- Noldart, A. J., and Wyatt, J. D., 1962, The geology of portion of the Pilbara Goldfields: West. Australia Geol. Survey Bull. 115, 199 p.
- Oftedahl, C., 1958, A theory of exhalative-sedimentary ores: Stockholm, Geol. For. Förh., v. 8, p. 1-19.
- Peacock, M. A., 1928, The nature and origin of the amphibole asbestos of South Africa: *Am. Mineralogist*, v. 13, p. 241-285.
- Percival, F. G., 1967, Texture of Brockman Iron Formation jaspilite, Western Australia: *Econ. Geology*, v. 62, p. 431-432.
- Pettijohn, F. J., 1956, *Sedimentary rocks*: New York, Harper, 718 p.
- Ramberg, H., 1964, Selective buckling of composite layers with contrasted rheological properties, a theory for simultaneous formation of several orders of folds: *Tectonophysics*, v. 1, p. 307-341.
- Ramberg, H., and Stephansson O., 1964, Compression of floating elastic and viscous plates affected by gravity, a basis for discussion crustal buckling: *Tectonophysics*, v. 1, p. 101-120.
- Richter-Bernburg, G., 1960, Zeitmessung geologischer Vorgänge nach Warven-Korrelation im Zechstein: *Geol. Rundschau*, v. 49, p. 132-148.
- Rubey, W. W., 1929, Origin of the siliceous Mowry shale of the Black Hills region: U.S. Geol. Survey Prof. Pap. 154D, 170 p.
- Ryan, G. R., 1964, A reappraisal of the Archaean of the Pilbara Block: West Australia Geol. Survey Ann Rept. 1963, p. 25-28.
- 1966, Roebourne, W.A.: West Australia Geol. Survey 1:250,000 Geological Series Explan. Notes, 26 p.
- Ryan, G. R., and Blockley, J. G., 1965, Progress report on the Hamersley blue asbestos survey: West. Australia Geol. Survey Rec. 1965/32 (unpublished).
- Sakamoto, T., 1950, The origin of the pre-Cambrian banded iron ores: *Am. Jour. Sci.*, v. 248, p. 449-474.
- Sederholm, J. J., 1925, The average composition of the earth's crust in Finland: Finland Geol. Commission Bull. 70, 20 p.
- Simpson, E. S., 1930, Contributions to the mineralogy of Western Australia, series 5: Royal Soc. West. Australia Jour. v. 16, p. 25-40.
- Sitler, R. F., 1963, Petrography of till from northeastern Ohio and northwestern Pennsylvania: *Jour. Sed. Petrology*, v. 33, p. 365-379.
- Spencer, E., and Percival, F. G., 1952, The structure and origin of the banded hematite jaspers of Singhbhum, India: *Econ. Geology*, v. 47, p. 365-385.
- Thiessen, P. A., and Köppen, R., 1931, Ein kristallisiertes Ferrioxyd-4-Hydrat: *Zeitsch. anorg. Chem.* v. 200, p. 18-22.
- Trendall, A. F., 1965a, Progress report on the Brockman Iron Formation in the Wittenoom—Yampire area: West. Australia Geol. Survey Ann. Rept. 1964, p. 55-65.
- 1965b, Origin of Precambrian banded iron formations (Discussion): *Econ. Geology*, v. 60, p. 1065-1070.
- 1965c, Technique for optical identification of iron-bearing dolomites, a modification and an evaluation: *Canadian Mineralogist*, v. 8, p. 253-255.
- 1966a, Second progress report on the Brockman Iron Formation in the Wittenoom—Yampire area: West. Australia Geol. Survey Ann. Report, 1965, p. 75-87.

- 1966b, Altered pyroclastic rocks in iron-formation in the Hamersley Range, Western Australia (Discussion): *Econ. Geology*, v. 61, p. 1451-1458.
- 1966c, Carbon dioxide in the Precambrian atmosphere: *Geochim. et Cosmochim. Acta* v. 30, p. 435-437.
- 1968, Three great basins of Precambrian banded iron formation deposition: a systematic comparison: *Geol. Soc. America Bull.* v. 79, p. 1527-1544.
- Trendall, A. F., and Blockley, J. G., 1968, Stratigraphy of the Dales Gorge Member of the Brockman Iron Formation, in the Precambrian Hamersley Group of Western Australia: *West. Australian Geol. Survey Ann. Rept.* 1967, p. 48-53.
- Trueman, N. A., 1963, The mineralogy and paragenesis of the crocidolite veins at Wittenoom Gorge, Western Australia: *Australasian Inst. Mining Metall. Proc.* 206, p. 113-122.
- Tyler, S. A., and Barghoorn, E. S., 1963, Ambient pyrite grains in Precambrian cherts: *Am. Jour. Sci.* v. 261, p. 424-432.
- Van Hise, C. R., and Leith, C. K., 1911, The geology of the Lake Superior region: *U.S. Geol. Survey Mon.*, v. 52, 641 p.
- Wadsworth, M. E., 1880, *Bull. Mus. comp. Zool. Harv.* v. 7, p. 1.
- Wells, A. T., 1959, Yarrie—4-mile geological series: *Australia Bur. Mineral Resources Explan. Notes* 16.
- Whincup, P., 1968, Tom Price Water Supply: *West. Australia Geol. Survey Hydro. Rept.* 489 (unpublished).
- Williams, I. R., 1965, Explanatory notes on the Yarraloola 1:250,000 sheet area, Western Australia: *West. Australia Geol. Survey Rec.* 1965/29 (unpublished). Also in press in published Explanatory Notes Series.
- Wilson, R. C., 1922, The asbestos deposits of the Pilbara and West Pilbara Goldfields, North-West Division: *West. Australia Geol. Survey Ann. Rept.* 1921, p. 39-49.
- Winchell, N. H., 1900, The geology of Minnesota, structural and petrographic geology of the Taconic and Archaean: *Minnesota Geol. Nat. History Surv.*, v. 5 of final report.
- Winterhalter, B., and Siivola, J., 1967, An electron microprobe study of the distribution of iron, manganese and phosphorus in concretions from the Gulf of Bothnia, Northern Baltic Sea: *Finland Geol. Soc. Compte Rendus* 229, p. 161-172.
- Wisler, C. O., and Brater, E. F., 1959, *Hydrology*: New York, John Wiley, 408 p.
- Woodward, H. P., and Montgomery, A., 1917, Notes on the useful minerals of Western Australia, and on sale of ores and minerals: *West. Australia Dept. of Mines*.
- Zelenov, K. K., 1958, Leaching and transportation of dissolved iron by thermal waters of Ebeko volcano (Paramushir Island) to the Sea of Okhotsk: *Akad. Nauk SSSR Dokl.* v. 120, p. 1089-1092.
- 1960, Transportation and accumulation of iron and aluminium in volcanic provinces of the Pacific: *Akad. Nauk SSSR Dokl. Ser. Geol.* v. 2, p. 47-59 (English trans.).

Index

- A.B.A. prospect 232
- Acicular riebeckite *see* Riebeckite
- Adit roof riebeckite 180, 187, 192, 229, 303, Figs. 5, 21, 55B, 56A
- Age determination 31
- Algal fossils (*Collenia*) 85, 162, 278, 280, 290
- Alunite 150
- Ambient pyrite 121, 127
- Ankerite 95, 98, 99, 108-111, 115, 118-121, 127, 129, Figs. 22, 28, 29, 30, 32, 36, 60
- Apatite 108, 111, 125, 132, 203, Figs. 24A, 35
- Archaean rocks 278, 279, Pl. 2
- Asbestos Gorge 230, 231
- Asbestos, Molybdenum and Tungsten Co. Ltd. 247
- Ashburton Formation 286
- Ashburton River 21, 23
- Aspinall, S. 231
- Aspinall Crocidolite Horizon 188, 231-233, 235, 236, 326-8, Figs. 48, 52
- Aspinall Seam 188, 232, Tab. 27
- Aspinall prospect 232, 233, 327
- Australian Blue Asbestos Company NL Tab. 20
- Australian Blue Asbestos Co. Pty. Ltd. 28, 41, 73, 215, 220, 225, 226, 229, 233, 327, 329, Pl. 7
- Australian Blue Asbestos Mines NL 247
- BIF (*see also* Banded iron formation) 334
- B.I.Q. 334
- Balfour Downs area 31, 84, 281, Fig. 2
- Band 334
- Banded iron formation,
 - as varved evaporite 287
 - compaction of 258, 261, 272
 - definition 26, 335
 - deposition of 256
 - diagenesis of 255, 268-273, 277, 304
 - interpretation of isopachs 279
 - in Mt. McRae Shale 87
 - in Woongarra Volcanics 92, 93
 - in Wyloo Group 34, 297
 - lateral stratigraphic continuity 256
 - origin 255-277
- Bangemall Group 30, 31, Pls. 1, 2
- Barite 127
- Beasley River 92, Fig. 2
- Beasley River Quartzite 34

Bed of holes	87, 215
Bee Gorge	187, 220, 229, 244, 247, Pls. 4, 5
Bee Hill	84
Biochemical control of precipitation	271
Biotite	111
Bismarck Gorge	73, 215, Pls. 5, 6
Black porcelanite	78, 127, 152, Tab. 16
Bloom Well	150
Boolgeeda (Camp)	241, Pl. 3
Boolgeeda Creek	93
Boolgeeda Iron Formation,	
chemical composition	138, Tabs. 11, 17
description	93
microbanding in	99
outcrop	Pl. 4
petrography	110
riebeckite in	172, 175, 211
sheet silicates in	124
stratigraphic position	34, 36, Fig. 3
thickness	93
Bord and pillar mining	251, 253, 254
Breccias in S4, S7 and S16 macrobands	64, 114, 167, 169, 288, Figs. 14, 44B
Brecciation of microbanding	169, Fig. 45
Bresnahan Group	30, Pls. 1, 2
Bright, C.	Tab 20
Brockman Iron Formation (<i>see also</i> Dales	
Gorge Member, Whaleback Shale Mem-	
ber, Joffre Member, Yandicoogina Shale	
Member),	
crocidolite in	186-190, 213-237, 244
description	41-81
field appearance	Figs. 1, 20
outcrop	Pls. 3, 4
status in Hamersley Group	38-40
stratigraphic position	36, Fig. 3
Brockman Syncline	84, 92, 93, 170, 185, 190, 241, Pl. 4
Bruno's Band	86, 87, 89, 214
Calamina cyclothem,	
chert-magnetite group of	56, 59, 60, 95, 142, 144, 145, 154, 161,
	193, Figs. 7B, 13, 38A
definition	56, 335
description and illustration	55-60, Figs. 6, 13, Tabs. 6, 7
effect on correlation	68
field expression	61, 160, Fig. 19, Tab. 8
microbanding in cherts of	95, 97, 98, Fig. 21
mixed group of	56, 59, 60, 95, 137, 155, 159, 262 Fig. 13
origin of	259 261-263, 285, Fig. 71, Tab. 24
relation to crocidolite	183, 198, 313, Fig. 55B
relation to Knox cyclothem	79, 262, 263
relation to massive riebeckite	178, 180, 193, 195, 209, Figs. 51, 53, 54
relation to minor riebeckite forms	210
Calamina Gorge	64, 169, 188, Pls. 4, 5

Calcite	111, 114, 118, 129, Figs. 33, 37D
Calcrete	25, 85
Caliwunga Gorge	237
Carawine Dolomite	31, 85, 280, 281
Carbon,	
in iron formation	127
in shale	111, 113-115, Fig. 31
Carbonaceous shale,	
Mt. McRae Shale	88
Mt. Sylvia Formation	86
Carbonate minerals (<i>see also</i> Ankerite,	
Calcite, Dolomite, Magnesite, Siderite,	109-111, 118-121, Figs. 21, 22, 23, 24,
Vertical veins)	28, 29, 30, 32, 33, 35, 36, 37, 41, 61
Carnarvon	21, Pl. 1
Cellular hematite	<i>see</i> Hematite
Chalcopyrite	111
Cheela Springs	239
Cheela Springs Basalt Member	286, Fig. 74
Chert (<i>see also</i> Mesobands),	
Boolgeeda Iron Formation	93, 99, Fig. 23C
chemical composition	139-147, Tabs. 12, 13
definition	335
flat-modified	51, 52, 55, 59, Figs. 8, 10, Tab. 5
chert-siderite	129, 145, Tab. 13
Dales Gorge Member	44, 51-55, 139-147, Figs. 21, 22, 32A,
	Tabs. 4, 13
Joffre Member	76, 262
Marra Mamba Iron Formation	82
Mount McRae Shale	88
Mount Sylvia Formation	86
petrography of mesobands	94-108
primitive	51, 52, 55, 59, Figs. 8, 10, Tab. 5
Weeli Wolli Formation	90, 91
Whaleback Shale Member	73, 74
Woongarra Volcanics	99, Fig. 24B
Chert-magnetite group (<i>see also</i> Calamina	
cyclothem)	335
Chert-matrix (<i>see also</i> Mesobands),	
definition	47, 335
Dales Gorge Member	47, Figs. 27B, 28A
Joffre Member	76, Fig. 28B
Marra Mamba Iron Formation	82, 102
Mount Sylvia Formation	86
origin of	257-259
petrography of	108, Figs. 27, 28, 32B, 37A, 40, 41, 43C,
	47, 60B
relation to chert	103, Figs. 27, 28
Weeli Wolli Formation	90, 102
Chert-siderite,	
chemical composition	137, Tab. 11
definition	335
description	61

microband textures in	98, 99, Figs. 22, 29C
petrography	115
position in S macrobands	Fig. 14
significance	276
Chichester Range	84
Chlorite	111, Fig. 31
Circular Pool	228
Clastic texture,	
in chert-siderite	61, 62
in shale	64
Climatic cyclicity	261, 262, Fig. 71
Close-packed chert sequence	61, 99, 183, Tab. 8
<i>Collenia brockmani</i>	162
<i>Collenia kona</i>	162
Colonial Gorge	215
Colonial Mine,	
assays and grade	217-220, 319, 330, 332, Figs. 63, 64, Pl. 7, Tab. 27
other references	198, 213-217, 220, 244, 247, 251, 254, Figs. 55A 69, 70, Pls. 4, 5, 6
Cone structure	see Crocidolite
Coolawanyah	84, Pl. 3
Coondiner Creek	22, 190, Pl. 4
Coondiner Gorge	188, 233
Coondiner Member	89
Cooya Pooya Dolerite	279
Crocidolite,	
association with fibrous quartz	205-207, Figs. 58, 59
central parting in mesobands	200, 204
chemical composition of	147, 148, Tab. 14
cone structure in	199-203, 308, 309, Figs. 55, 56B, 57
corrugations in	199, 200, 308, 309, Fig. 56B
curved fibre	200, 203
dark lines in	200, 206, Fig. 57B
definition	174, 335
derivation of iron for	309, 310
distributional controls	313-317
enrichments	191
evaluation of deposits	328-332
exploration for	323-328
first report in W.A.	245
growth of	308-312, Fig. 77
health hazards	254
inclined fibre	200, 203
kink bands in	200, 203, 204, 207 212 Figs. 55B, 58, 59A
lateral distribution	189-191
lateral mesoband termination	199
magnetite screens in	200, 204, 308-309, Fig. 55
mines	Pl. 4
mining	245-254
occurrences	Pl. 4
orientation of structures	212, 213

origin	307-317
production	248, Tab. 20
Province	Pl. 4
relation to magnetite	199-204, 206, 308, 309
relation to massive riebeckite	191, 192, 203, 310, Fig. 55B
relation to structure	243, 244
relative time of formation	310-312
reserves and resources	334, Tab. 27
stratigraphic status in iron formation	198, 199, 307
stress-reversal hypothesis for growth	310-312, Fig. 76
structures in mesobands	199-207
structure at Marra Mamba	207
Sub-Provinces	Pl. 4
turbulence structure in	200, 207
weathering of	323
Crocidolite deposits,	
Asbestos Gorge	230, 231
assaying of	213
Bee Gorge	229, 248, 324
Brockman Syncline	241
Calamina Gorge	230, 324
Coondiner Gorge	233, 234
Dales Gorge	226-229, Fig. 65, Tabs. 20, 27
definition	191
Denis Gorge	226
Devan's prospect	236
Duck Creek	242
Eastern Creek	215-217, 220, 254, 324
evaluation	328-332
Fish Pool	243
Fortress Gorge	235, 324
Jimmawarrada Creek	243
Juna Downs	243
Junction Gorge	231-233, 248, 324, 327, Fig. 66, Tab. 27
Kungarra Gorge	239-241, Fig. 67
Lamb Creek	234, 235
Marillana	234
Marra Mamba	237-239, 248, 320, 324, 328, Tabs. 20, 27
Millers Gorge	231
Mount Margaret	230
Mount Nicholson	243
Mount Tom Price	242
Munjina Gorge	236, 328
Range Gorge	229, 230, 324
Serpentine Creek	242
Snell Gorge	225, 324
Turner Syncline	242
Vivash Gorge	241
Weeli Wolli Spring	235, 236
Wittenoom Gorge	213-220, 247, 324, Pls. 6, 7, Tabs. 20, 27
Wittenoom Sub-Province	213-237
Yampire Gorge	220-226, 248, 327, Pls. 8, 9, Tabs. 20, 27

Crocidolite horizons,	
definition	183, 335
stratigraphic positions	Fig. 48
Crocidolite seams,	
definition	183, 339
stratigraphic positions	Fig. 48
Cross-bedding	64, 85, Pl. 3
Cross-fibre (definition)	335
Cross-podding,	
Dales Gorge Member	155, 157, Fig. 39B
definition	153, 335
description and illustration	155, 157, Fig. 39
Joffre Member	78, 155, 157, Fig. 39A, D
regional orientation	Pl. 3
relative time of formation	293
Weeli Wolli Formation	155
Yandicoogina Shale Member	Fig. 39E
Cross-podding ridges	162-4, 336
Cyclicality	<i>see</i> Calamina cyclothem, Climatic cyclicality, Knox cyclothem, Whaleback Shale Mem- ber, Wittenoom Dolomite
Dales Gorge	23, 64, 106, 164, 169, 192, 212, 226, Fig. 15, Pls. 4, 5
Dales Gorge Member (<i>see also</i> Calamina cyclothem),	
chemical composition	133-138, 150, 151, Tabs. 11, 16
classification of mesobands	44, 47, 49
crocidolite in	186-190, 213-237, 244, Figs. 48, 52, 53, 55
definition and description	41-72
field expression	72, Figs. 1, 4, 20
lateral stratigraphic continuity	65-68, 106-107
lithology	43-64
macrobands	29, 43, 66, 69, Figs. 1, 3, 4, Tabs. 8, 9
mesoband abundances	50, Tab. 4
microbanding	95, 97-99, 102, 103, 106, 107, Figs. 21, 22, 24, 27, 30
outcrop	Pl. 5
riebeckite in	176, 178, 180, 181, 189-191, 193, 210, 211, Figs. 48, 49, 53, 60, 61
scales of banding	43
sheet silicates in	124, 137, 138
status in Hamersley Group	40, Fig. 3
structures in	153-173
thickness	68-72, Pl. 3
type section	41, Figs. 5, 6
vertical veins in	173
volcanic shards in	Fig. 31C, D, E
Wittenoom Gorge	214, Fig. 62
Dales Gorge Mine	Pl. 5
Dampier	Pls. 1, 2
Dampier and Barrow Island sheet	28
Darling Fault	286

Davis River	84
de Souef, L.	245
Deepdale	22, 92, 243, Fig. 2, Pl. 3
Denis Gorge	220, 224, 226
Devan's prospect	236, 326
Diagenesis	<i>see</i> Banded iron formation
Diamond drilling,	
Junction Gorge	233, Fig. 66
locations and details	Pls. 5, 6, Tabs. 18, 19
Wittenom area	220, 329-332
Yampire area	225, 226
Dolerite dykes	238, 241, Fig. 19, Pl. 5
Dolerite sills	89-91
Dolomite (mineral)	111, 118-121, 129, 203, Fig. 32C, D
Dolomite in Mt. McRae Shale	86-88
Duck Creek	82-84, 88, 190, 237, 242, 326, Pls. 3, 4
Duck Creek Homestead	190, Pl. 4
Duck Creek Dolomite	286, Fig. 74
Dun, G. and A.	238
Dun Crocidolite Horizon	84, 89, 185, 237, 328, Figs. 48, 52
Dun prospect	238
Dun Seam	328, Tab. 27
Duplicate corrugations	336
Duplicate structures (<i>see also</i> Northeast structures)	162, 228, 292-4, 336
Eastern Creek prospect	215-217, 220, 326
Edmund map sheet	Pl. 4
Ethel Gorge	91
Even-bedded BIF	61
Faulting	238
Feldspar	111, 115, 127, Fig. 31
Ferristilpnomelane (<i>see also</i> Stilpnomelane)	124
Ferrostilpnomelane (<i>see also</i> Stilpnomelane)	124
Fibrous quartz	<i>see</i> Quartz
Fig Tree Soak	226
Fish Pool	88, 190, 243
Flat-modified chert	<i>see</i> Chert
Forrest Well	231
Fortescue Group	30, 31, 33, 40, 278, 279, 295, 321, Figs. 2, 74, Pl. 2
Fortescue River	21-24, 31, 32.
Fortress Gorge	167, 189, 235, Pls. 4, 5
Foxall Crocidolite Horizon	186, 237, 238, Figs. 48, 52
Foxall prospect	238
Garden Gorge	214, Fig. 62, Pls. 5, 6
Garden Gorge Anticline	214, 215, 229, 244, 326, 327, Fig. 62, Pl. 5
Giles Point	22, 88, Pl. 3

Globulate structure in shale	113, Fig. 31F
Gordon Falls	Figs. 1, 65
Griqualandite	176, 323
Hall, H. A.	246
Hamersley Basin,	
algal raft in	283, 284
beginning of	278, 279
circulation of water in	282, 283
conditions on surrounding land	286, 287
connexion with ocean	284, 285, 290
currents in	256
depth of water	282, 283
development of	278-298
end of	294, 295
evaporation from	283, 284
iron content of water	282, 283
material balance in	295
shape of	280, 281
sinking rate	298
size of	280, 281
structure of	280, 281
supply of iron to	285, 286
time span of	298
vulcanicity near	285, 286
Hamersley Crocidolite Province	189-191, Pl. 4
Hamersley Exploration Pty. Ltd.	29
Hamersley Group,	
chemical composition	273-276, Tab. 23
depositional environment	279, 292
formal stratigraphic subdivision	36, Fig. 3
igneous rocks in	38, 40
lithological proportions in	40, Tab. 1, 2, 3
metamorphism	294
'natural' stratigraphic subdivision	40, 41
outcrop	Pl. 2
regional variation	30, 31, Fig. 2
relation to Wyloo Group	34
stratigraphy	36-93
Hamersley Plateau	22, 80, 86, 88
Hamersley Range	20-24, 92, 189, Pls. 2, 5
Hamersley Range Synclinorium	34, 35, 189, 212, 311, 313, 315-317, 321, Fig. 20
Hamersley Station	22, 86, Pls. 3, 4
Hamersley surface	23, 24, Fig. 1
Hancock, L. G.	238, 247, Tab. 20
Hancock Gorge	Pl. 5
Hancock's Benches	224, 226
Hardey River	25
Hardey Sandstone	Pl. 4
Hardey Syncline	35, 82, 173, 210, Pl. 4
Hematite,	
cellular	122, 123, 129, 272, 273, Figs. 24A, 34

general	95, 97, 98, 99, 101, 103, 106, 108, 111, 115, 121-123, Figs. 23C, 27B, 29, 30, 37A
jaspery platelets	99, 122, 129, Figs. 24A, 28, 40A
sieved	123, 131
status in paragenesis	129, 130
Hooley Gorge	Pls. 5, 6
Horseshoe Creek	186, 239
Igneous rocks	<i>see</i> Hamersley Group
Immaculate band (defined)	336
Iron,	
average Precambrian crust	275, 276
behaviour in diagenesis	263
content in basin water	282, 283
content in chert mesobands	139-147, 263-265, Fig. 72, Tabs. 12, 13, 21
content of precipitate	269
derivation of	273-276, 285, 286
mobility during diagenesis	304
total in Hamersley Group	275
Iron Formation (defined)	27
Iron formation,	
chemical composition	133-153
definition	26, 336
without mesobanding	110, 111
Ironstone (defined)	336
Isopachs of Dales Gorge Member	68-72, Figs. 16, 17, 18, Pl. 3
Isotopic dating	31
James Point	<i>see</i> Point James
Jasper (defined)	336
Jaspilite (defined)	27, 336
Jeerinah Anticline	35, 84, 185, 186, 189, 190, 237, 242, 326, Pl. 4
Jeerinah Formation	33, 40, 82, 150, 281, Pl. 4
Jimblebar Creek	33, 92, 93
Jimmawarrada Creek	186, 190, 243
Joffre Creek	25, 81
Joffre Falls	75, 79, 80, 157, 173, 215, Figs. 19, 39A
Joffre Gorge	151, 152, Fig. 19
Joffre Member (<i>see also</i> Knox cyclothem),	
chemical composition	136, 151, 152, Tab. 11
crocidolite in	188, Figs. 48, 52
definition and description	75-80
field expression	80
lateral stratigraphic continuity	80
lithology	75-79
mesobanding	76
microbanding	76, 99, Fig. 23A
outcrop	Pl. 5
riebeckite in	180, 210, 211
sheet silicates in	78, 124, 137, 138

status in Hamersley Group	38, 40, Fig. 3
thickness	75, 80
type section	75
vertical veins	173
vulcanicity in	78, 79, Fig. 19C
Wittenoom Gorge	214, Fig. 62, Pl. 6
Yampire Gorge	224
Juna Downs	69, 189, 211, 243, Pl. 4
Junction Gorge	164, 187-189, 212, 231-233, 247, 327, 328, Figs. 7C, 19, 30, 66, Pls. 4, 5
Junction Gorge Riebeckite Zone	176, 180, 187-190, 324, Fig. 48
June Hill	286
Kalgan Creek	38, 91-93, 189
Kink bands	<i>see</i> Crocidolite
Kinking (defined)	336
Knapping Seam Crocidolite Horizon	187, 213, Fig. 48
Knox cyclothem,	
definition and description	78, 79
illustrated	Fig. 19
origin of	259, 261-263, Fig. 71
possible analogue	91
red cherts	78, 79, 262
relation to Calamina cyclothem	262, 263
relation to massive riebeckite	180
white cherts	78, 79, 262
Knox Gorge	Pl. 5
Kungarra Gorge	152, 158, 192, 239, Fig. 39C, Pl. 4
Kungarra Gorge prospect	239, 240, Fig. 67
L. G. Hancock Asbestos Company	247
Lamb Creek	234, 235, Pl. 4
Lewin Shale	31, 84, 280, 281
Liesegang bands	257
Limestone	64, Fig. 14
Lionel Chrysotile Asbestos Limited Com- pany	248
Little De Grey Lava	281
Long-wall mining	251, 253, 254
Lower Seam	187, 215-217, 251, 319, Fig. 70, Tab. 27
Lower riebeckite zone (defined)	337
Lower Seam Crocidolite Horizon	187, 213, 215, 225, 228, 229, 233, 235, 236, 327, Fig. 48
Mackay Crocidolite Horizon	185, 237, 239, 328, Figs. 48, 52
Mackay's prospect	239
Mackay Seam	185
McLarty, W.	247, Tab. 20
Macrobands (of Dales Gorge Member),	
definition and illustration	43, 337, Figs. 1, 3, 4, 20
lateral continuity	66
origin of	290, 291
S	61-64, 98, 111, 338, Figs. 4, 14

Maculate bands	161, 337
Macules	99, 160-162, 293, 294, 337, Figs. 24A, 42, 53
Maghemite	123
Magnesite	119-121
Magnetite (<i>see also</i> Crocidolite)	95, 98, 101, 108-111, 115, 123, 124, 131, Figs. 24A, 27B, 29, 32, 37A, C, 40A, 60
Mahlberg, A.	Tab. 20
Mahlberg Seam	187, 226, 228, 329, Fig. 65, Tab. 27
Main Bottom Seam	226, 229, Tab. 27
Maley, M	Tab. 20
Maley's prospect	238, 239
Manganese Group	30, Pl. 2
Marble Bar	27, Pls. 1, 2
Marble Bar map sheet	28, Pl. 4
Mardie Station	69, 84, 88, Pl. 3
Marillana	Pls. 3, 4
Marillana Creek	167, 234, Fig. 25, 27A
Marillana prospect	234
Marillana Station	236, 246
Marillana Syncline	34
Marra Mamba	83, 185, 186, 196, 237-239, 246, 247, 328, Pl. 4
Marra Mamba Iron Formation,	
chemical composition	152
crocidolite in	185, 186, 190, 237, 243, 244, Figs. 48, 52, 59
definition and description	82-85
field expression	84, 85, Fig. 20
lateral correlation of	31, 84, 281
lithology	82, 83
outcrop	Pl. 4
sheet silicates in	124
status in Hamersley Group	36, 40, Fig. 3
subdivision of	83
thickness	82, 84
type area	82
Marra Mamba Riebeckite Zone	176, 185, 186, 237, 241, 242, Fig. 48
Marra Mamba Sub-Province	189-191, 211, 237-244, 310, 319, 320, Pl. 4
Martite	121
Mass-fibre (defined)	337
Mass fibre riebeckite	174
Massive riebeckite,	
comparative stratigraphic thickness	193, 304, Figs. 54, 74
composition compared with chert	303
definition	174, 337
factors controlling growth	304-307
lateral distribution	189
origin of	299-307
paragenetic relationship	178, 180, 301
petrography	195, 196, Fig. 56A
relation to crocidolite	191, 192, 203, 310, Fig. 55B
relative time of formation	300, 301

stratigraphic status in BIF	193, 195, 299, 300, Figs. 53, 54, 75
vertical distribution	178
weathering	176
Meekatharra	21, Pl. 1
Mesobanding (defined)	43
Mesobands,	
carbonate	44, 48, 109, Tab. 4
chemical composition	139-147, Tabs. 12, 13
chert	44, 51-55, 60, 76, 78, 82, 90-108, 139-147, Figs. 8, 19, 23, 32, Tabs. 4, 12, 13
chert-matrix	44, 47, 82, 108, 140, Figs. 32, 37, Tabs. 4, 12
classification	44, 51-55
crocidolite	183, 198-207
defined	337
in chert-siderite	61, 145, Tab. 13
lateral correlation of	66, 68, Fig. 7B, C
magnetite	44, 47, 108, 109, Fig. 37C, Tab. 4
massive riebeckite	174, 175, 178, 180, 193, 195, Figs. 49, 51, 53
measurement of	49-55, Tab. 4
miscellaneous	44, 49, Tab. 4
origin of	257-259, 261-263, Fig. 71
petrography	94-110
relative abundance of types	Tab. 4
stilpnomelane	44, 47, 49, 109, 141-143, Tabs. 4, 12
thickness	51, Tab. 5
Metamorphism	294
Microband interval	see t
Microbanding,	
asymmetric	99, Figs. 24C, 26C
brecciation of	169, Fig. 45
defined	43, 94, 337
defined by riebeckite	210, Fig. 61A
in chert mesobands	51-55, 73, 95, 97-99, Figs. 7, 21, 22, 23, 24
in chert pods	103, 155, 158, Figs. 27, 38, 39, 40
in chert of chert-siderite	61, 98, 99, Fig. 22A, B
in macules	161, Fig. 24A
laminae within	101, 104, 106, Fig. 29A
lateral continuity	67, 106, 107, Figs. 15, 30
marginal and internal relations	102-106, Figs. 27, 28, 29
multiple grouping	100-102
origin of	257
petrography of	94-99, Figs. 21, 22, 23, 24, 25, 26, 27, 28 29, 30
plastic deformation of	169, Fig. 44C
relation of interval to iron content	263-265
thickness (t)	51-55, Fig. 8
Middle Creek	220
Milli Milli Anticline	Pl. 4
Millers Gorge	230, 231, Pl. 4
Millstream	24, 84, Pl. 3

Mindy Mindy Creek	80, 236
Mindy Mindy Member	75
Mining of crocidolite	<i>see</i> Crocidolite
Minnesotaite	83, 124, 125, Figs. 27B, 35B
Minor folds,	
in the south	172
with fibrous minerals	169-172, 293, Figs. 46, 47
Millstream area	Fig. 2
Mixed group (<i>see</i> also Calamina cyclothem)	337
Montgomery, A.	245, 246
Montmorillonoid	115
Mount Brockman	68, 69, 80, 84, 88, 165, Pls. 3, 4
Mount Brockman Homestead	237, 242, Pl. 4
Mount Brockman Station	186
Mount Bruce	68, 163, 280, Fig. 46, Pls. 3, 4
Mount Bruce map sheet	28, 278, 281, Pl. 4
Mount Bruce Supergroup	30, Pl. 1
Mount Bruce Syncline	Pl. 4
Mount De Courcey	33, 34, 69, Fig. 2
Mount Dempster	69, 86
Mount Farquahar	Fig. 20, Pl. 3
Mount Flora	87, 88, Pl. 3
Mount Florance Station	246
Mount Frederick	69, 72, 163, Pls. 3, 4
Mount George	Pls. 4, 5
Mount Goldsworthy	Pl. 1
Mount Jope	190, Pls. 3, 4
Mount Jope Volcanics	281, Pl. 4
Mount King	187, 326, 327, Pl. 4
Mount Lionel	242, Pl. 4
Mount Lockyer	69, 72, 163, Pls. 3, 4, 5, Tab. 20
Mount Margaret	88, 187, 190, 230, 246, 250, 317, Pls. 3, 4
Mount McRae	86, Pl. 4
Mount McRae Shale,	
chemical composition of	150, Tab. 15
definition and description	86-89
dolomite in	86-88
field expression	89, Figs. 1, 20
lithology	88
outcrop	Pls. 4, 5
petrography	113, Figs. 31A, F
status in Hamersley Group	36, 40, Fig. 3
stratigraphic continuity	88
subdivision	87
thickness	88
Wittenoom Gorge	214
Yampire Gorge	224
Mount McGrath	33, 69
Mount Meharry	22
Mount Minnie Group	30, Pls. 1, 2
Mount Newman	22, 68, 81, 84, Pl. 3

Mount Newman area	Fig. 2
Mount Nicholson	190, 243
Mount Pyrton	189, Pls. 3, 4
Mount Robinson	Pl. 4
Mount Stevenson	189, 280, Pl. 4
Mount Stuart	34, Pl. 3
Mount Sylvia	86, 190, Pls. 3, 4
Mount Sylvia Formation	36, 38, 40, 86, 175, 211, 214, 224, Figs. 3 20 Pls. 4, 5
Mount Tom Price	21, 190, Pls. 2, 3, 4
Mount Turner	Pls. 3, 4
Mount Vigors	Pl. 4
Mount Wall	82, 83, 91, 92, 190, Pls. 3, 4
Mount Wall prospect	239
Mount Whaleback	21, 72-74, 88, Pls. 1, 2, 3
Mount Whaleback Shale Member	72
Mulga Downs Station	246
Mundiwindi	21
Munjina Gorge	236, 244, 328, Pl. 4
n (number of microbands in a mesoband)	52, 53, 55, 337, Figs. 11, 12, Tab. 5
Needle riebeckite (<i>see also</i> Riebeckite, acicular)	174, 175, 337
Nelson Well	230
Newman	21
Newman map sheet	28
Northeast structures	162-164, 292-294, 338, Figs. 53, 56A
Nullagine	278, Pls. 1, 2
Nullagine map sheet	28
Oakover Formation	25
Oakover-Davis Basin	281, 295
Onslow	21, Pl. 1
Ophthalmia Range	21, 22, 33, 85, 86, 88, 91, 92, Pl. 2
Oxygen isotope analyses	294
Paragenetic relations of iron minerals	127-132, 272, 273, Figs. 36, 37
Percival texture	123, 129, 338
Phosphate in iron formation	137, Tab. 11
Pinch-and-swell (defined)	153, 338
Podding (including Pod, Pod chert and Podded chert),	
concentric structure in	158, 159, Fig. 40
definition	153, 338
description	153-159
effect on mesoband correlation	68
in Calamina cyclothem	59
in chert-siderite	115
in Dales Gorge Member	140, Figs. 27B, 28A, Tab. 12
in Joffre Member	Fig. 28B
in Marra Mamba Iron Formation	83, 85
in Weeli Wolli Formation	Fig. 27A

random	78, 154, 155, 293, 294, 338, Fig. 38
relation to microbanding	103, 155, 158, Figs. 27, 38, 39, 40
relative time of formation	292-294
septarian structure in	158, 159, Fig. 40B
significance of	258
Point James	69, 74, 80, 85, 86, 88, 106, 167, 190, 281, Fig. 15, Pl. 3
Point Samson	237
Port Hedland	21, Pl. 1
Port Hedland map sheet	28
Potential crocidolite	174
Pilbara Block	30, 321
Pilbara System	30, 31
Poonda Outcamp	233
Precambrian atmosphere	287
Primary precipitate	266-272
Primitive chert	51, 52, 55, 59, 60, 95, 338, Figs. 8, 10, 11, Tab. 5
Pseudofossils	162
Pyramid (area or map sheet)	28, 93, Pl. 4
Pyrite	111, 113, 114, 121, 127, 132, Figs. 31, 37D
QIO (defined)	47, 338
Quartz,	
fibrous	117, 118, 129, 171, 172, 200, 211, 213, 308, 310, 312, Figs. 46, 47, 58, 59, 60
in shale	111
textural and paragenetic status	95, 97, 99, 101, 108, 115, 117, 118, 131, Figs. 22, 27, 28, 37
with crocidolite	200, 204, 205, Fig. 55A
Quartz-iron oxide	<i>see</i> QIO
Rainfall	24
Random podding	<i>see</i> Podding
Range Gorge	187, 229, 230, 244, 247, 326, 327, Pls. 4, 5
Red Gorge	215, Pls. 5, 6
Red Hill	34, Pl. 3
Reef (defined)	338
Regional rippling,	
defined, described and illustrated	164-167, 172, 338, Fig. 43, Pl. 3
relative time of formation	293, 303
significance of	292, 293
Riebeckite (<i>see also</i> Crocidolite, Massive riebeckite),	
acicular	207-209, Fig. 60A
chemical composition	147, 148, Tab. 14
coating other minerals	211, Figs. 37B, 60D
cross-cutting forms	211
definition	338
distribution in Hamersley Group	175, 176, 178, Fig. 48
distribution relative to stratigraphic features	191, 192
in iron formation	174-244

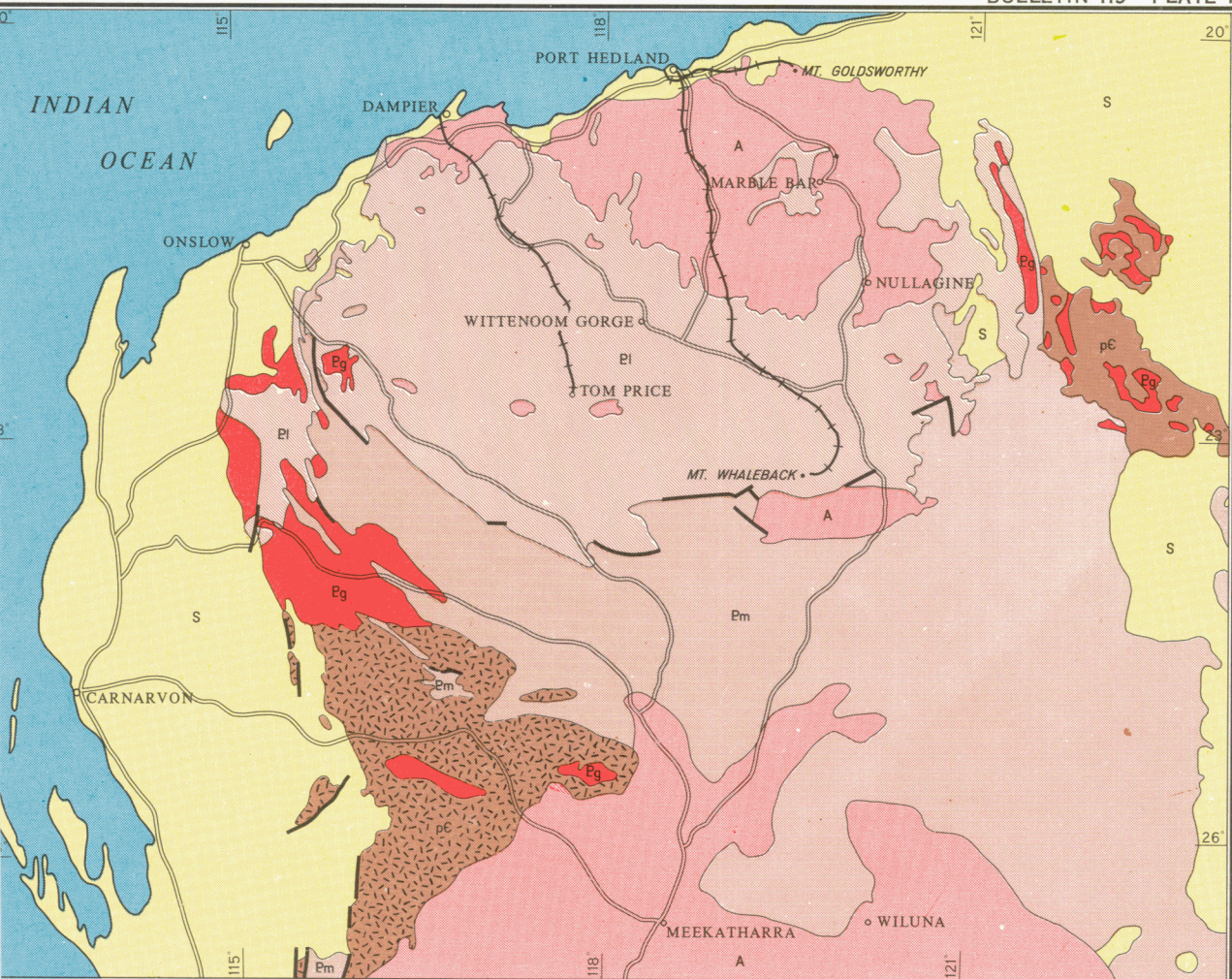
minor forms	207-209, Figs. 60, 61
minor notes	98, 108, 109, 110, Figs. 23, 27, 28, 30, 32, 37, 40
miscellaneous occurrences	210, 211, Figs. 60, 61
origin of	299-322
petrography	207, 211, Figs. 60, 61
in shales	211
slip-fibre	171, 172, 175, 211-213, Fig. 60B
status in paragenesis	132, 209
synthesis	294
Riebeckite swells	162, 193, 195, 338, Fig. 53
Riebeckite zones	176, 178, 338, Fig. 48
Riebeckite-prone chert	178, 338
Rocklea	Pls. 3, 4
Rocklea Anticline	Pl. 4
Rocklea Dome	83
Roebourne	21, Pl. 2
Roebourne map sheet	21, Pl. 2
Roy Hill	21, 31, Fig. 2, Pl. 2
Roy Hill map sheet	28, Pl. 4
S macrobands	<i>see</i> Macrobands
Seam (defined)	183, 339
Septarian structure	<i>see</i> Podding
Serpentine Creek	186, 190, 242, Fig. 20, Pl. 4
Seven Mile Creek	29, 80, 81, 84-86, 88
Shale (<i>see also</i> Jeerinah Shale, Mt. McRae Shale, Whaleback Shale Member, Yandicoogina Shale Member),	
Boolgeeda Iron Formation	93
chemical composition of	148-150, 289, Tab. 15
clastic textures in	114
Dales Gorge Member	61, 64, 148, 149, Fig. 14
definition and description	111-115, 339
deposition of	288-290
globulate texture in	113, 115, 289, Fig. 31F
Joffre Member	75, 78
lamination in	113, 114, 289, Fig. 31A, B
Marra Mamba Iron Formation	83, 84
Mount Sylvia Formation	86
slickensides in	113
volcanic shards in	114, 289, Fig. 31C, D, E
Weeli Wolli Formation	90
Sheet silicates	124, 125
Siderite,	
general	98, 108, 109, 115, 118-121, 137, Figs. 22, 23, 24, 27, 28, 29, 32
spherical bodies in	115
status in paragenesis	129
Silver Grass Peak	189, Pl. 4
Silver Grass Syncline	34, 91, Pl. 4
Slickensides	<i>see</i> Shale
Slip-fibre (<i>see also</i> Riebeckite)	339

Slumping	167, 169, Fig. 44, Pl. 3
Small spheroidal nodules, definition, description, illustration in Calamina cyclothem origin of	159-161, Figs. 38, 41 59, 159-160, Figs. 13, 53 293
Snell, L.	247, Tab. 20
Snell (= Snells) Gorge	220, 224-226, Fig. 68, Pls. 4, 5
Soanes, Herbert	245, 246, 248
Soanesville	245
South Africa	148, 174, 245, 257, 307, 316, 320-322, 324, 328
Stilpnomelane	82, 95, 98, 99, 101, 108-111, 113-115, 124, 125, 131, 132, 137, 171, 173, 203, 290, Figs. 22, 23, 24, 28, 29, 30, 31, 36, 37A, C
Stress-reversal hypothesis	310-312
Striped facies	<i>see</i> Weeli Wolli Formation
Stromatolites	<i>see</i> Algal fossils
Structure, in iron formation regional of Hamersley Range area	153-173, Figs. 38-47 34, 35, 172
Stylolites	85, 114, 115
Swells (defined)	339
T (chert mesoband thickness)	52, 53, 339, Fig. 9, Tab. 5
t (microband interval)	52, 53, 55, 60, 94, 95, 339, Figs. 10, 12, Tab. 5
The Governor	35, Pl. 4
Third Seam	186
Third Seam Crocidolite Horizon	236, Fig. 48
Tiger's Eye	176, 242, 243, 323
Tom Price	21, Pls. 1, 4
Top Seam	226, 228, Fig. 65
Tourmaline	111, 115
Tumbiana Pisolite	281
Turee Creek	243, Fig. 2
Turee Creek Formation	34, 93
Turee Creek map sheet	Pl. 4
Turee Creek Syncline	93
Turner Syncline	84, 172, 190, 242, 313, Pl. 4
Upper Seam	99, 187, 198, 215-217, 319, 330, 332, Figs. 55, 70, Tab. 27
Upper Seam Crocidolite Horizon	183, 192, 213, 215, 224-226, 229, 233, 236, 319, 327, Figs. 48, 52
Upper riebeckite zone (defined)	188, 339
Upper Yampire Series	188
Upper Yampire Zone	188
Varves	257
Vertical veins, carbonates in	173

general	172, 173, 211
magnetite in	173, Fig. 40
quartz in	172, 173
riebeckite in	173
stilpnomelane in	173
Vivash Gorge	186, 241, Pl. 4
Vivash Riebeckite Zone	176, 186, 190, 237, 239, 241-243, Fig. 48
Volcanic shards	<i>see</i> Shale
Walters, I.	Tab. 20
Wanna Munna Anticline	Pl. 4
Water supply	24, 25
Watson, K	Tab. 20
Watson's prospect	239
Wavy-bedding	61, 339
Weano Gorge	Pl. 5
Weathering of iron formation	138, Tab. 11
Weeli Wolli Anticline	84, 188, 235, 326, Pl. 4
Weeli Wolli Creek	236, Fig. 26A
Weeli Wolli Formation,	
definition and description	89-92
field expression	92
lithology	90, 91
outcrop	91, Pl. 4
microbanding	90, 99
riebeckite in	175, 211
slumping in	Fig. 44
status in Hamersley Group	36, 38, 40, 81, Fig. 3
striped facies	90, 95, 100-102, 110, 259-263, 339, Figs. 25, 26
thickness	89, 91
tuff in	91
Weeli Wolli Spring	24, 87-89, 91, 150, 187, 235, 236, 246, Fig. 26A
West Australian Blue Asbestos Fibres NL	225, 248, Tab. 20
Western Gorge	215
Western prospect	232, 233
Whaleback Shale Member,	
chemical composition	149, Tab. 15
cyclicality in	73
definition and description	72-74
field expression	74, Figs. 1, 20
interpretation of	292
Junction Gorge	231
lateral variation	74
lithology	73, 74
microbanding	98, 99
outcrop	Pl. 5
sheet silicates in	124
status in Hamersley Group	36, 40, Fig. 3
thickness	74

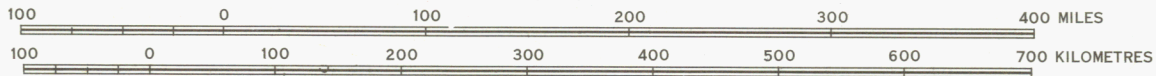
type section	73
Wittenoom Gorge	214, 215, Pl. 6
Wittenoom	21, 69, 74, 78, 85, 163, 164
Wittenoom Dolomite,	
cyclicality in	85
definition and description	85
field expression	Fig. 20
lateral correlation	31, 281
outcrop	35, Pls. 4, 5
porphyry intrusive into	286
significance of	290
status in Hamersley Group	36, 40, 82, Fig. 3
Wittenoom Gorge	214
Yampire Gorge	224
Wittenoom Gorge	23, 41, 64, 73, 87, 88, 167, 213-220, Figs. 4, 15, 21, 27B, 29, 30, 31, Pls. 1, 2, 3, 4, 5, 6.
Wittenoom Mine	215-217, 220, 247, 251, Pls. 4, 5, 6
Wittenoom Sub-Provinncce	189-191, 199, 211, 213-237, 243, 244, 310, 319, 320
Woodie Woodie	85
Woongarra Dacite	36, 92
Woongarra Gorge	74, 81, 91, 93, 172, 210, Fig. 15, Pl. 4
Woongarra Pool	80, 81, 89, 90, 92, 93, 173, Fig. 24B
Woongarra Volcanics,	
age of	31
biotite in	172
definition and description	92, 93
emplacement of	285, 295
in contact with Wyloo Group	34
microbanded chert in	99, Fig. 24B
outcrop	Pl. 4
porphyry intrusive into	286
status in Hamersley Group	36, 38, Fig. 3
xenolith in Weeli Wolli dolerite	91
Wright, E. A.	247, Tab. 20
Wyarma Spring	85, 86, 88
Wyloo	Pl. 3
Wyloo Anticline	33-35, 69, 80, 81, 84, 88, 93, 172, 280, Pl. 4
Wyloo Group	30, 31, 33, 34, 69, 275, 286, 295, 321, Figs. 2, 74, Pls. 2, 4
Wyloo map sheet	28, Pl. 4
Yampire A Crocidolite Horizon	188, 224, 226, 230, 235, 324, 327, Figs. 48, 52
Yampire A Seam	225, 226, Tab. 27
Yampire Gorge	64, 212, 220, 224, Figs. 31, 39B
Yampire B Crocidolite Horizon	188, 224, Fig. 48
Yampire C Crocidolite Horizon	183, 187, 224-226, 228-231, 233, 236, 319, Figs. 48, 52, 58
Yampire C Seam	Tab. 27
Yampire Intermediate Series	188

Yampire Mine	224-226, 244, 247, 251, Pls. 4, 5
Yampire Riebeckite Zone	176, 178, 180, 186, 187, 189-191, 224, 230, 235, 236, 324, 327, 328, Figs. 48, 52
Yandicoogina Creek	74, 75, 80, 81, 188
Yandicoogina Crocidolite Horizon	183, 188, 190, 234, Figs. 48, 52
Yandicoogina Shale Member	40, 80, 81, 89, 157, Fig. 39E
Yandicoogina Syncline	75, 91, Pl. 4
Yarraloola	21
Yarraloola map sheet	28, 243, Pl. 4
Yarrie map sheet	28
Zircon	111
Zone (defined)	339



GEOLOGICAL SURVEY OF WESTERN AUSTRALIA
 REGIONAL GEOLOGICAL MAP
 SHOWING
 SETTING OF MOUNT BRUCE SUPERGROUP

SCALE 1 : 6,000,000

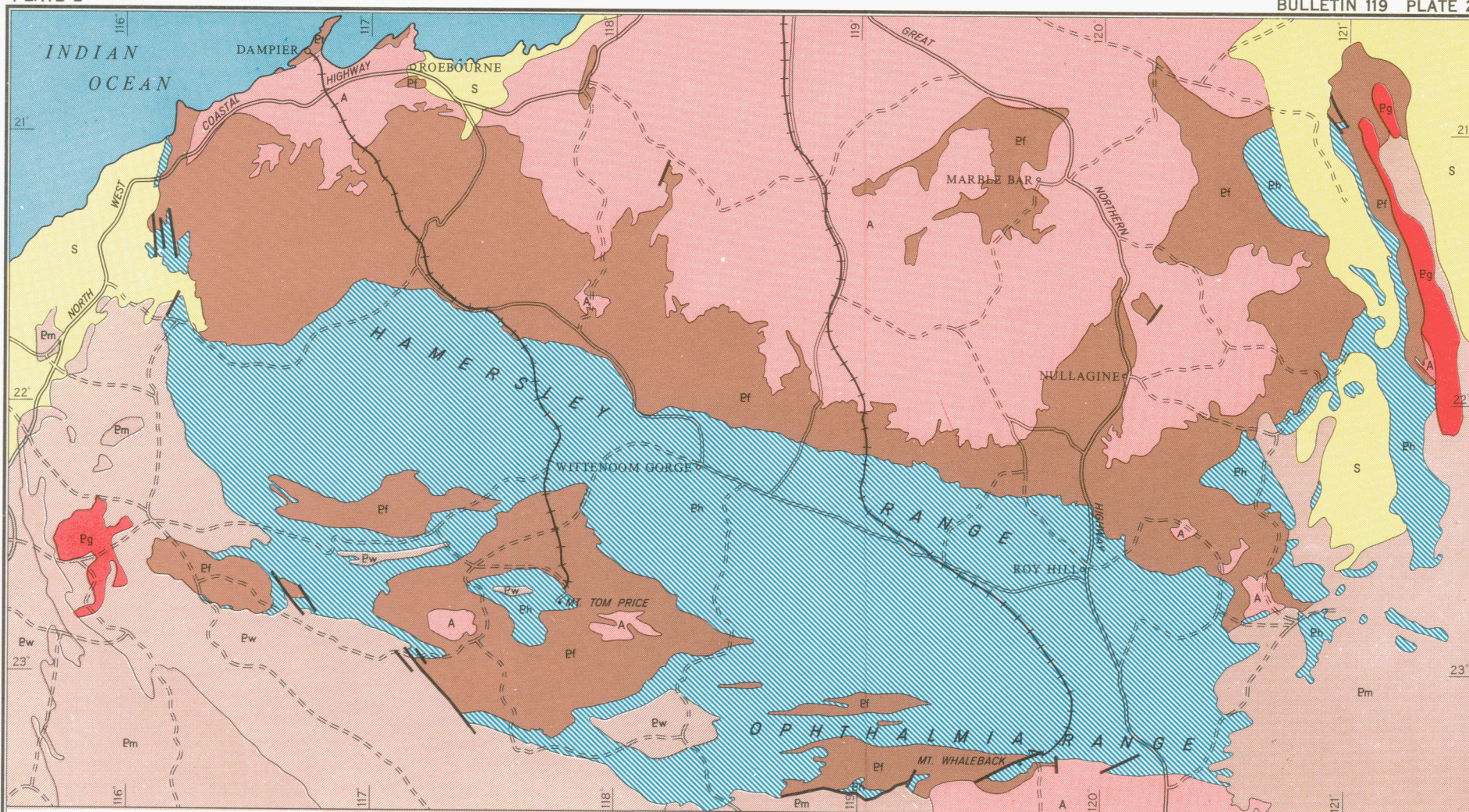


REFERENCE

S	Phanerozoic sediments
Em	Bangemall, Bresnahan and Mount Minnie Groups
El	Mount Bruce Supergroup
A	Archaean
pC	Undetermined (Precambrian)
Pg	Proterozoic Granite

SYMBOLS

Area of high grade metamorphism	
Geological boundary (unconformity or intrusive contact)	
Geological boundary (faulted)	
Road	
Railway	



REFERENCE

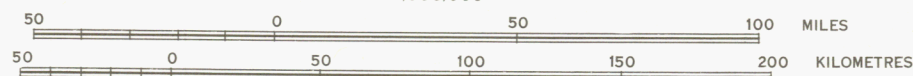
PHANEROZOIC	S	Mesozoic to Recent marine and continental sediments
MIDDLE PROTEROZOIC	Pm	Bangemall, Bresnahan, Mount Minnie and Manganese Groups
LOWER PROTEROZOIC	Pw	Wyloo Group
	Ph	Hamersley Group
	Pf	Fortescue Group
ARCHAEAN	A	Warrawoona Series, Mosquito Creek Series, and GEORGE CREEK FORMATION with granitic intrusives
IGNEOUS ROCKS	Pg	Proterozoic granite intrusive into Wyloo Group

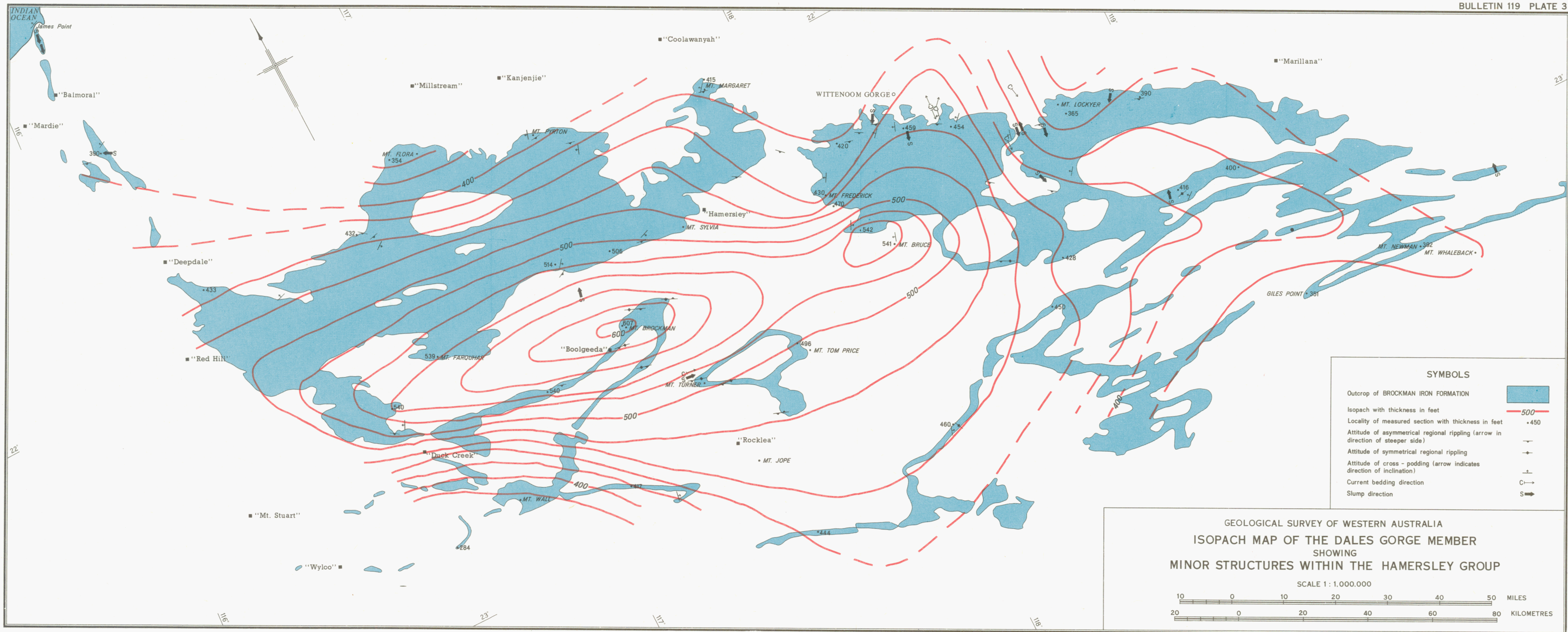
SYMBOLS

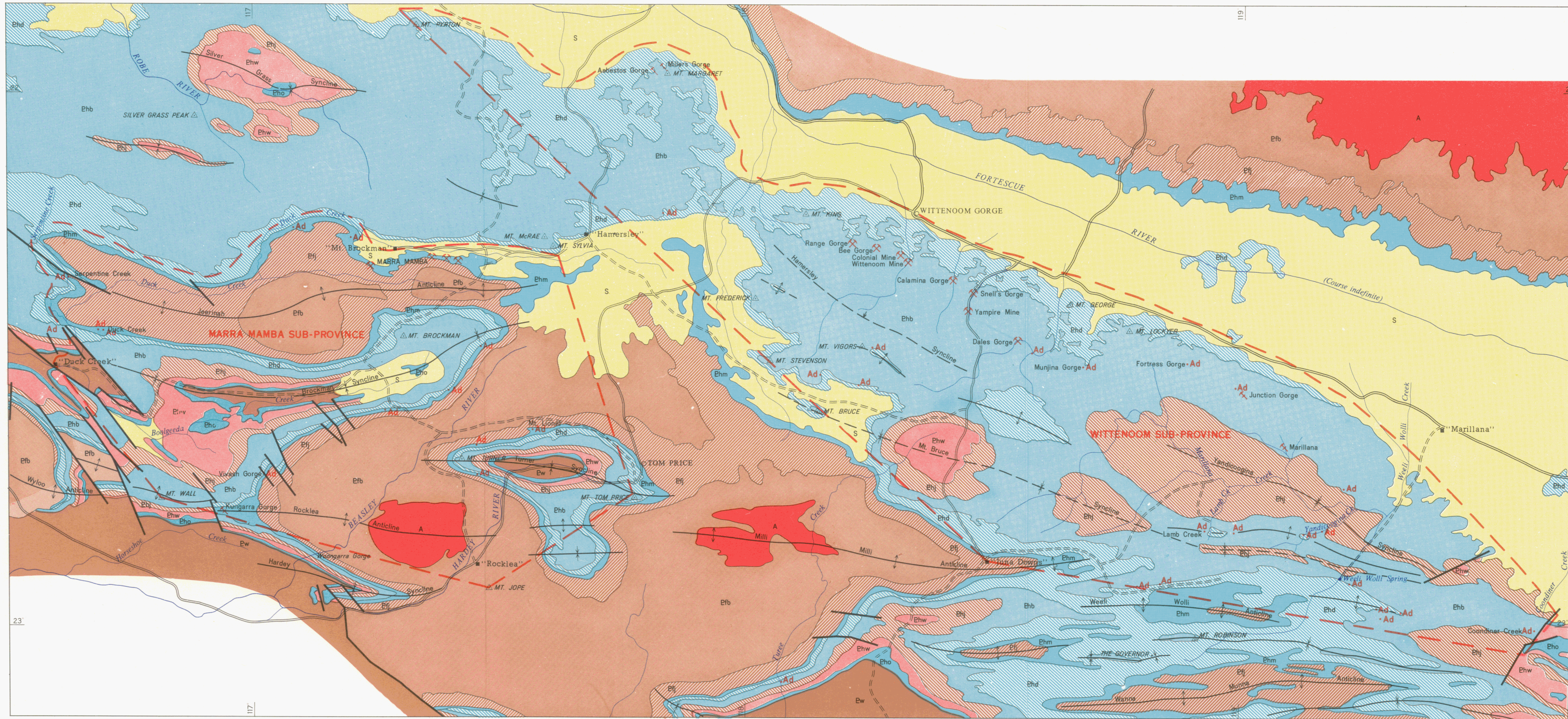
Geological boundary	— — — — —
Fault	— — — — —
Railway	+ + + + +
Highway	== == ==
Formed Road	== == ==
Track	= = = = =

GEOLOGICAL SURVEY OF WESTERN AUSTRALIA REGIONAL GEOLOGICAL MAP OF HAMERSLEY GROUP

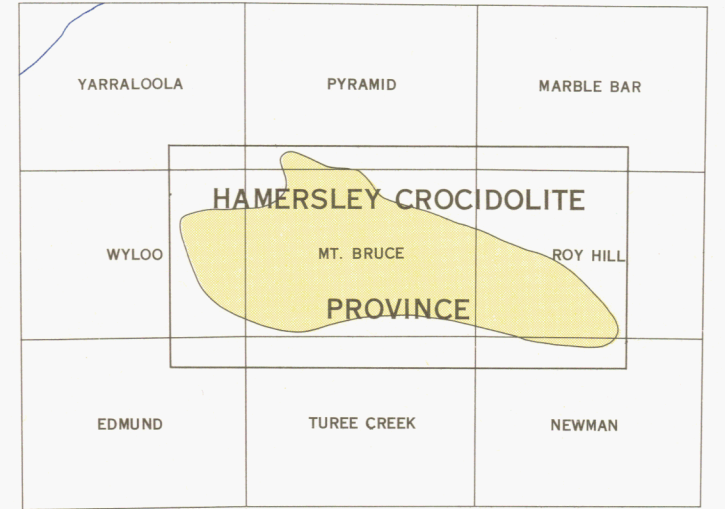
SCALE 1 : 2,500,000







LOCALITY MAP AND INDEX OF 1 : 250,000 SHEETS



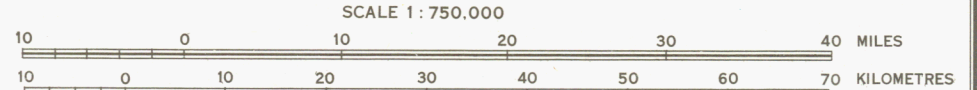
REFERENCE

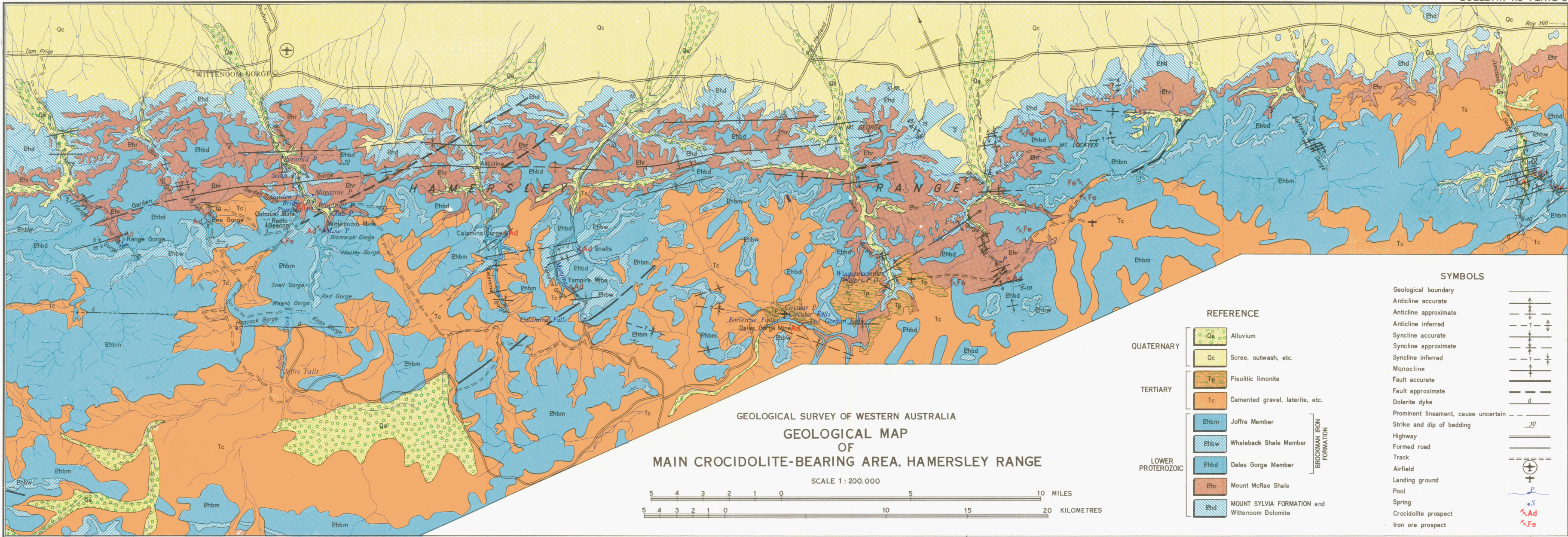
S	Superficial deposits
Ew	Wyloo Group
Eho	BOOLGEEDA IRON FORMATION
Phw	Woongarra Volcanics
Ehj	WEELE WOLLI FORMATION
Ehb	BROCKMAN IRON FORMATION
Ehd	Mount McRae Shale MOUNT SYLVIA FORMATION Wittenoom Dolomite
Ehm	MARRA MAMBA IRON FORMATION
Efi	JEERINAH FORMATION
Efb	Mount Jope Volcanics and Hardey Sandstone
A	Archaean volcanics, meta-sediments, gneiss, and granite

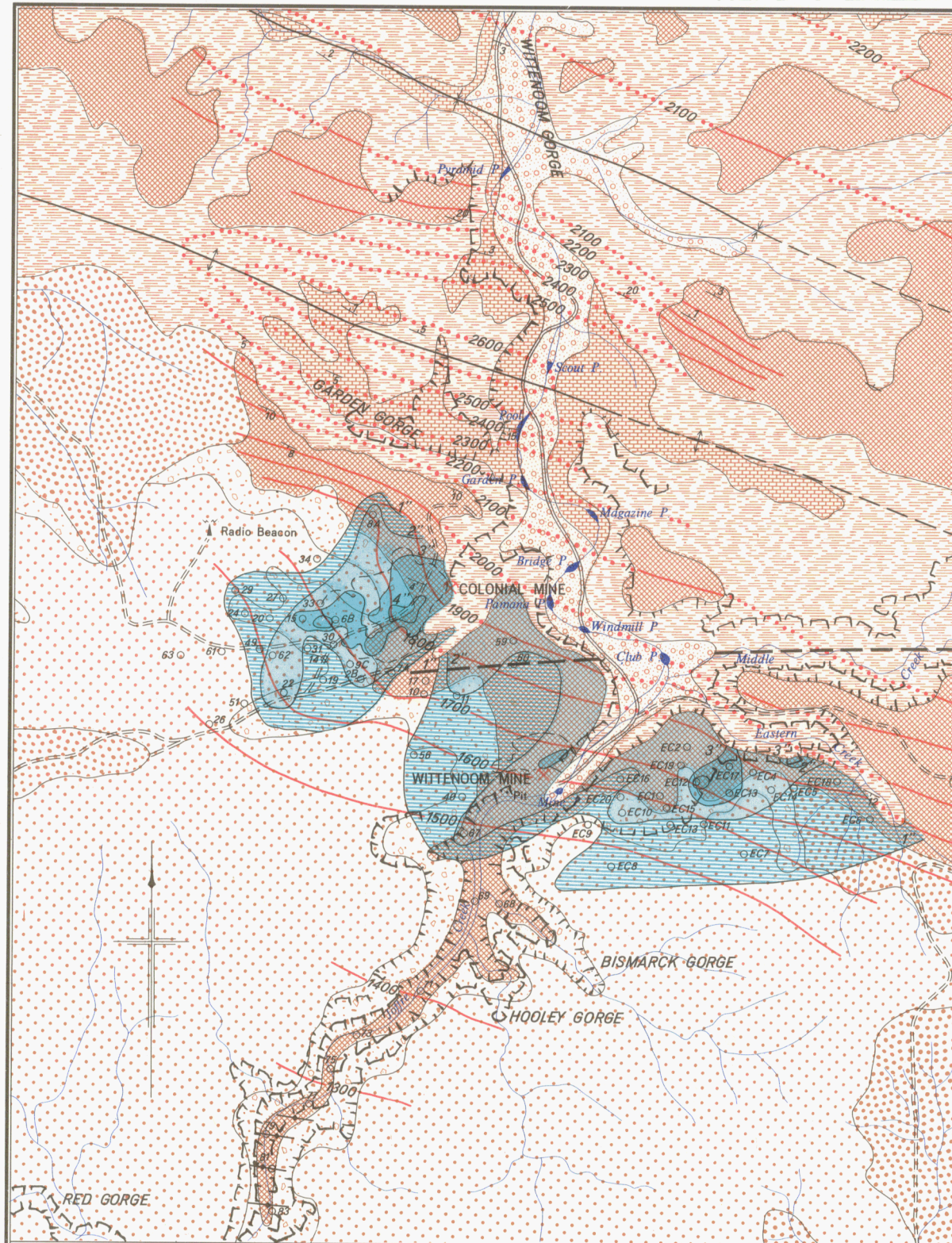
SYMBOLS

Geological boundary	—
Anticline accurate	↕
Anticline approximate	-↕-
Syncline accurate	↕
Syncline approximate	-↕-
Fault	—
Highway	==
Formed road	==
Track	----
Homestead	■
Town	○
Crocidolite sub-province boundary	- - -
Crocidolite mine	⊗
Crocidolite prospect	⊗
Crocidolite occurrence	.Ad

GEOLOGICAL SURVEY OF WESTERN AUSTRALIA
GEOLOGICAL MAP
OF
THE HAMERSLEY CROCIDOLITE PROVINCE

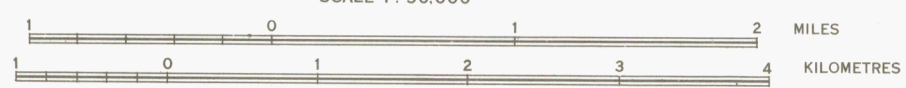






GEOLOGICAL SURVEY OF WESTERN AUSTRALIA
GEOLOGICAL MAP OF WITTENOOM GORGE
SHOWING
STRUCTURAL CONTOURS AND FIBRE CONCENTRATIONS

SCALE 1:50,000



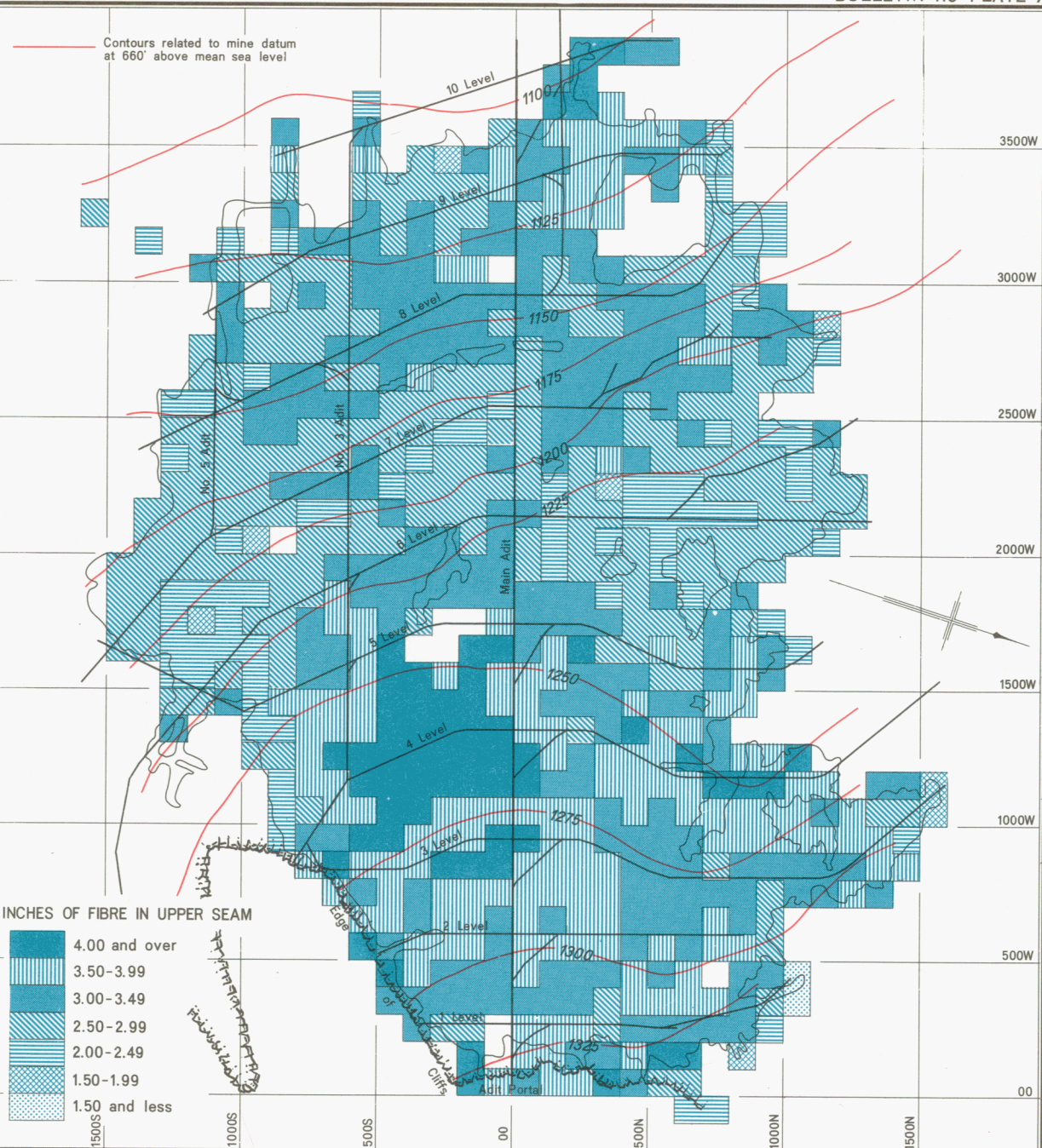
REFERENCE

QUATERNARY		Alluvium
TERTIARY		Colluvium, canga, and duricrust
PROTEROZOIC		Joffre Member
		Whaleback Shale Member
		Dales Gorge Member
		Mount McRae Shale
		Wittenoom Dolomite

BROCKMAN
IRON FORMATION

SYMBOLS

Geological boundary	
Fault approximate	
Syncline	
Anticline major	
Anticline minor	
Strike and dip of bedding	
Structural contour on base of BROCKMAN IRON FORMATION (Datum is Mean Sea Level)	
Interpolated structural contour on base of BROCKMAN IRON FORMATION (Horizon eroded)	
Isopleth of crocidolite grades in Upper Seam	
Outline of underground workings	
Diamond drillhole with designating number	
Creek	
Escarpment	
Adit Portal	
Formed road	
Track	



GEOLOGICAL SURVEY OF WESTERN AUSTRALIA

PLAN OF COLONIAL MINE

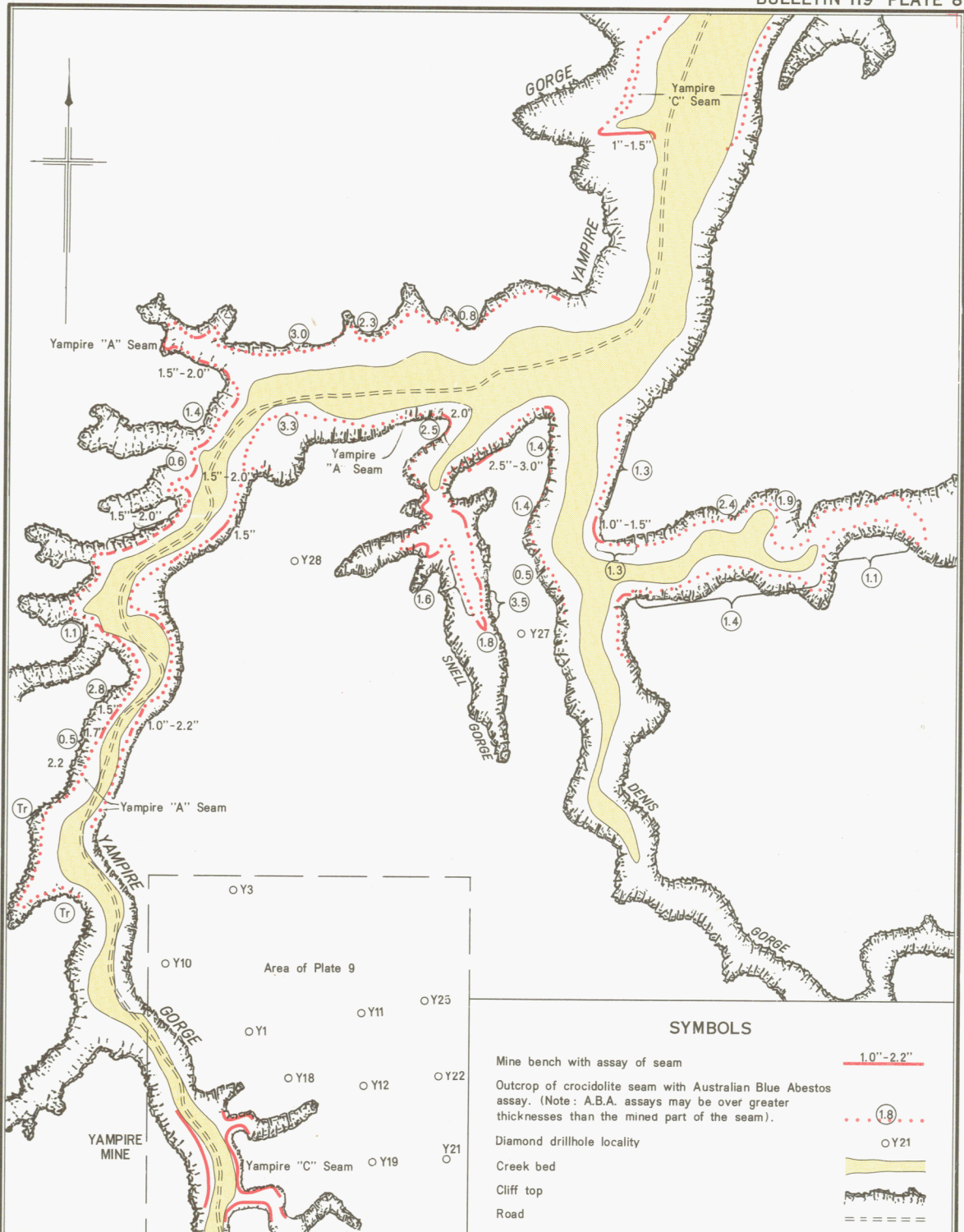
SHOWING

FIBRE GRADES AND STRUCTURAL CONTOURS OF THE UPPER SEAM

SCALE 1 INCH TO 600 FEET

600 300 0 600 1200 1800

Mine data from plans by Australian Blue Asbestos Pty. Ltd.

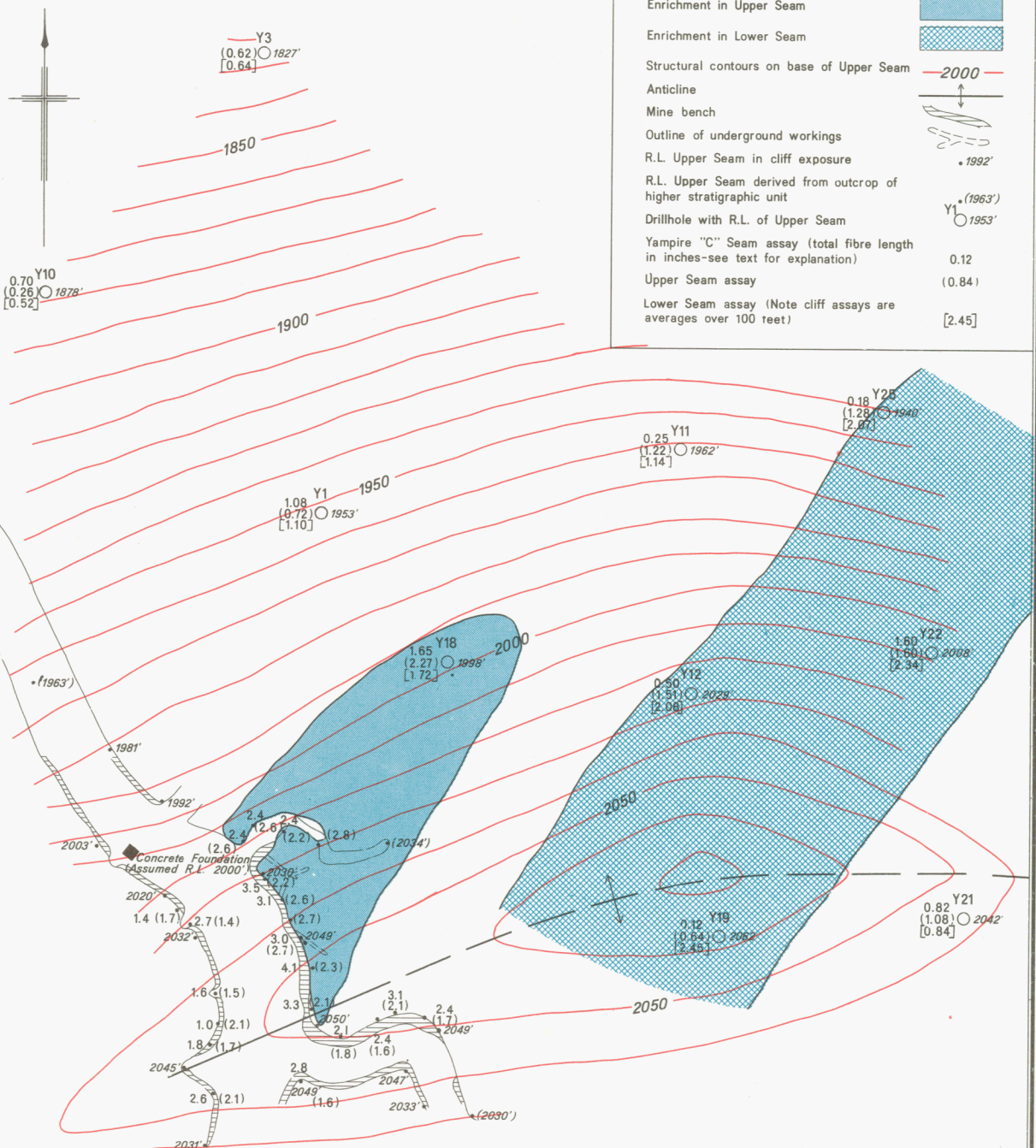


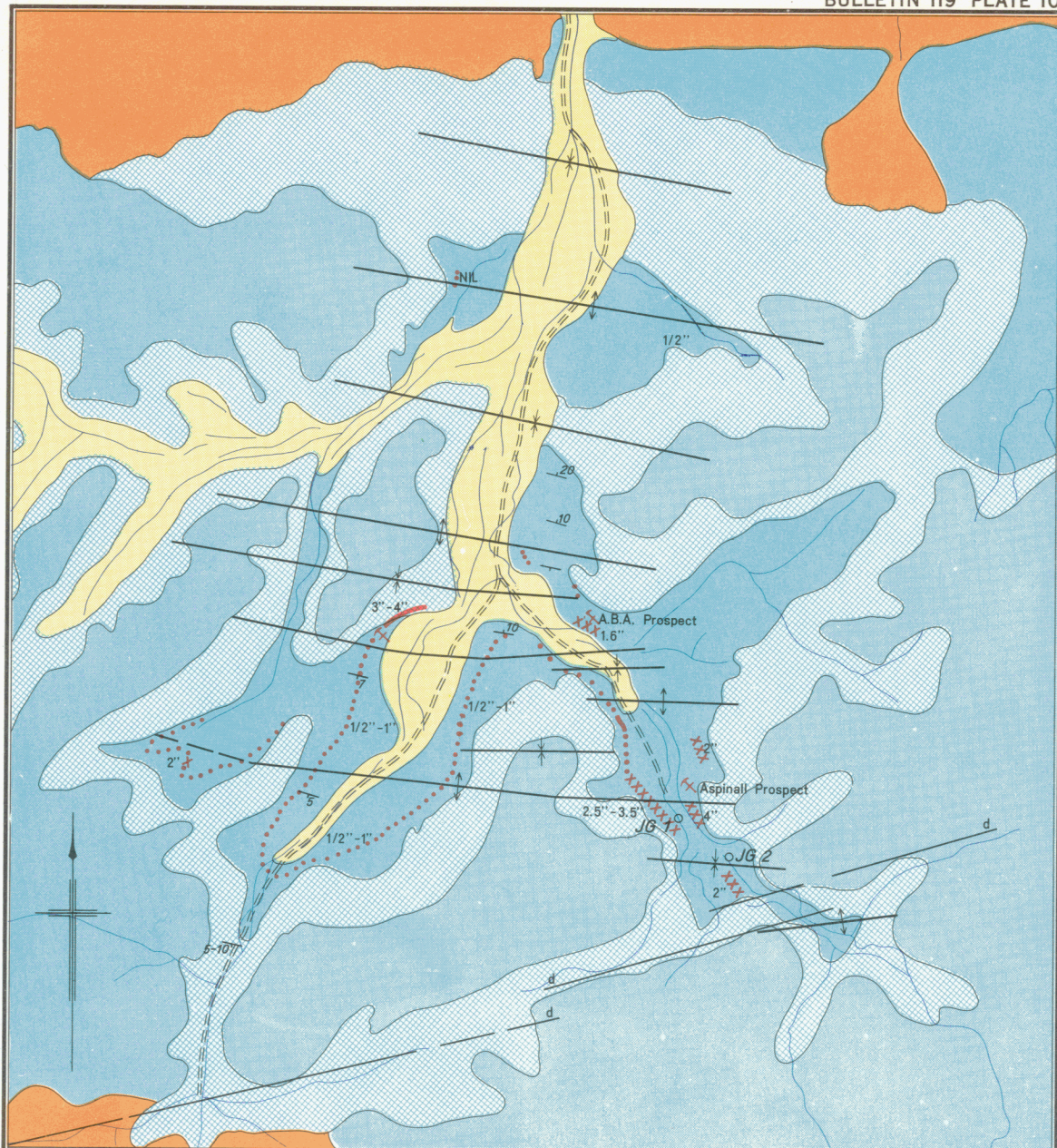
GEOLOGICAL SURVEY OF WESTERN AUSTRALIA
PLAN OF YAMPIRE GORGE SHOWING CROCIDOLITE WORKINGS

SCALE 1 : 25,000

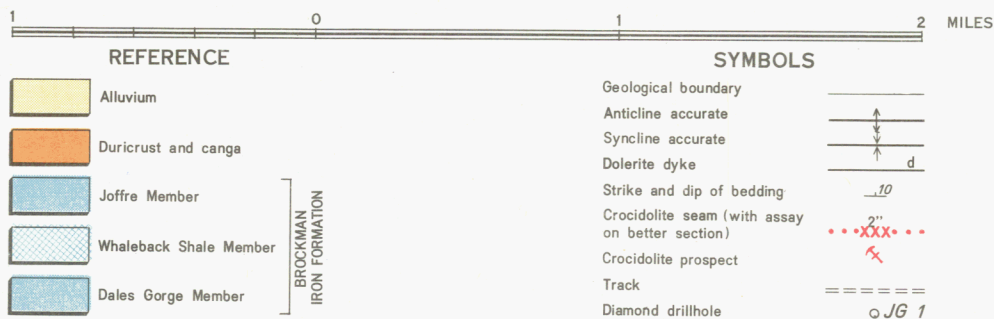
1 0 1 MILES

Topography from aerial photograph Roy Hill 8, No. 5670

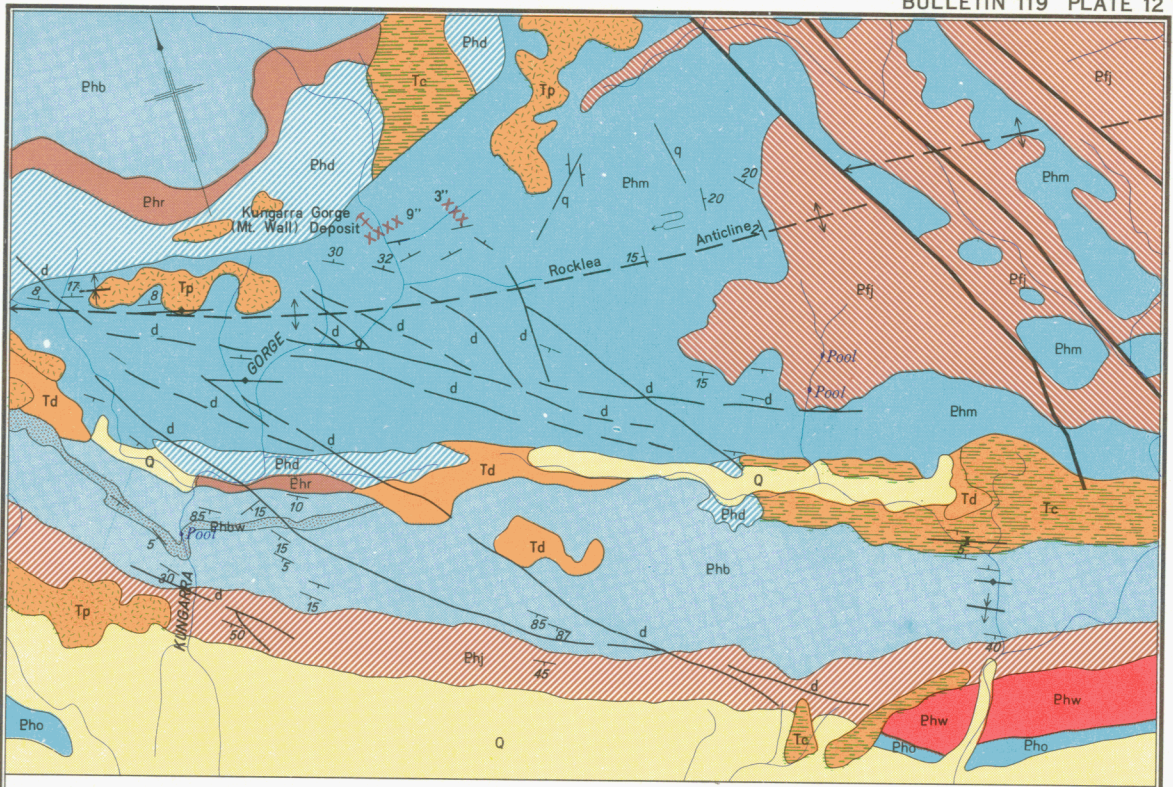




GEOLOGICAL SURVEY OF WESTERN AUSTRALIA
 GEOLOGICAL MAP OF JUNCTION GORGE SHOWING OUTCROP OF ASPINALL SEAM
 SCALE 1 40,000



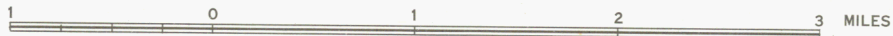




GEOLOGICAL SURVEY OF WESTERN AUSTRALIA

GEOLOGICAL MAP
KUNGARRA GORGE AREA

SCALE 1 : 60,000



REFERENCE

SYMBOLS

QUATERNARY



Alluvium



Colluvium

TERTIARY



Duricrust



Pisolite



BOOLGEEDA IRON FORMATION



Woongarra Volcanics



WEEILI WOLLI FORMATION



BROCKMAN IRON FORMATION



Whaleback Shale Member

Mount McRae Shale
MOUNT SYLVIA FORMATION

WITTENOOM DOLOMITE



MARRA MAMBA IRON FORMATION



JEERINAH FORMATION

Geological boundary

Fault

Anticline approximate with plunge direction

Minor anticline

Minor syncline

Monocline

Strike and dip of bedding

Small folds, with plunge

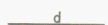
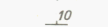
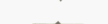
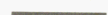
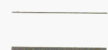
Crocidolite seam with approximate assay

Dolerite dyke

Quartz vein

Creek

Prospect



PROTEROZOIC

Mt. Bruce Supergroup

Mapped by G.R. Ryan 1965